The comparative dynamics of bulk liquid flow and interpolymer diffusion during inkjet ink imbibition in porous coating structures

Taina Lamminmäki

VTT

The comparative dynamics of bulk liquid flow and interpolymer diffusion during inkjet ink imbibition in porous coating structures

Taina Lamminmäki

The comparative dynamics of bulk liquid flow and interpolymer diffusion during inkjet ink imbibition in porous coating structures

Abstract

The focus of this thesis is to establish the timescale of interactions, physical and chemical, during dye-based inkjet ink imbibition into calcium carbonate ($CaCO_3$) pigmented coatings. Comparison is made between conventional offset quality $CaCO_3$ (GCC), and special inkjet qualities in the form of either modified (MCC) or precipitated (PCC) $CaCO_3$ combined with swelling diffusion driving or non-swelling diffusion-inert binder. The selection of pigment is based on the control of pore volume, pore size distribution and connectivity of the coating layer. Pigments containing nano-size pores (intra-particle) are primarily exemplified. The final coating layers display discrete pore size bimodality in relation to the intra-particle and inter-particle pores, respectively. Polyvinyl alcohol (PVOH) is used as the diffusion sensitive binder and styrene acrylate latex (SA) as the bulk diffusion-inert binder. By changing the coating layer structures and using the contrasting binders the roles of liquid diffusion, capillary pressure and permeation flow are clarified both in the short and long timescale imbibition. The wetting force within the finest coating layer capillaries drives the inkjet ink into the porous structure, whilst the viscous drag within the pore structure resists the movement. The nano-size capillaries initiate absorption of the ink vehicle, though typical impact pressure of an inkjet droplet is shown to provide forced wetting. During the subsequent flow, the hydrophilic binder swells, acting to close the smallest pores and reduce the remaining pore diameters. The total pore volume decrease competes with the initial capillarity, reducing absorption rate. The diffusion is shown to have a marked effect on the polar liquid absorption rate into the PVOH-containing coatings over different timescales. The swelling opens the polymer matrix so that the colorant of the ink fits into the binder structure and can either hydrogen bond or become mechanically trapped there on drying. The diffusion coefficient of water in PVOH and on SA latex films is shown to be very similar, despite the difference between bulk diffusion and surface diffusion, respectively. The colorant fixing is enhanced mainly by the ionic interactions between the colorant and coating surface adsorption sites. The anionic colorant fixes under chromatographic separation to the cationic components of the coating layer. There is seen to be an optimal absorption rate beyond which the colorant has insufficient time to translate under the Coulombic attraction potential toward the cationic adsorption sites or to respond to the binder interpolymer matrix diffusion potential. The final print density of a high-speed inkjet printed surface depends on the colorant location in the coating layer and the optical properties of the whole coated paper. Therefore the competing mechanisms of

liquid flow, ab- and adsorption are seen as crucial to developing a high quality print. The intercolour bleeding is additionally dependent on the coating layer capability to absorb enough ink at adequate high absorption rate in competition with colorant spreading on the surface. Spreading can be further curtailed using a cationic surface treatment.

**Liuoksen virtausdynamiikka ja polymeerien diffuusio mustesuihku-
värin asettumisessa huokoisiin päällysterakenteisiin**

Tiivistelmä

Väitöskirjatyön tavoitteena on selvittää vuorovaikutusilmiöiden, sekä fysikaalisten että kemiallisten, aikaskaaloja liukoisen mustesuihku- eli inkjet-värin asettumisessa kalsiumkarbonaattipigmentti-päällysteissä (CaCO$_3$). Vertailuja tehdään perinteisen offset- (GCC) ja inkjet-laadun CaCO$_3$ välillä. Inkjet-puolella on tutkittu sekä modifioitua (MCC) että saostettua (PCC) CaCO$_3$:a, ja sideaineina on käytetty turpoavaa diffuusioherkkää tai ei-turpoavaan diffuusio-inerttiä sideainetta. Pigmentit on valittu siten, että päällystekerroksen muuttujiksi on saatu sekä huokostilavuus, -kokojakauma että -rakenne. Tämä on toteutettu muutamissa päällysteissä siten, että päällysteessä on käytetty nanohuokosia sisältäviä pigmenttipartikkeleita. Tällöin lopullisissa päällysteissä esiintyy bimodaalinen huokoskokojakauma, jossa on sekä partikkelien välisiä että sisäisiä huokosia. Diffuusioherkkänä sideaineena käytetään polyvinyylialkoholia (PVOH) ja diffuusio-inerttinä styreeni-akrylaatti-lateksia (SA). Päällystekerroksen rakenteen vaihtelulla ja erilaisten diffuusioherkkien sideaineiden käytöllä tutkitaan kapillaari- ja permeaatiovirtauksia sekä lyhyen että pitkän aikaskaalan nesteen imeytymisessä. Kostutusvoimat päällysteen pienissä kapillaareissa ajavat inkjet-väriä huokoisen rakenteen sisään, kun taas viskoottinen voima vastustaa liuoksen liikkumista. Inkjet-värin liuotinosan absorptio alkaa nanokoon kapillaareista, tosin inkjet-pisaran aiheuttamaa iskeytymispainetta ei pidä unohtaa tässä yhteydessä. Seuraavassa vaiheessa hydrofiilinen sideaine turpoaa, sulkee pienimmät huokoset ja pienentää jäljellä olevien huokosten halkaisijoita. Kokonaishuokostilavuuden pieneneminen kilpailee alkuperäisten kapillaari-ilmiöiden kanssa hidastaen absorptionopeutta. Työssä osoitetaan, että diffuusiolla on merkittävä vaikutus polaarisen liuoksen absorptionopeuksiin PVOH:ta sisältävissä päällysteissä. Turpoaminen aukaisee polymeerimatriisia siten, että värin väriaineosa mahtuu sideainerakenteeseen ja voi joko sitoutua vetysidoksilla polymeeriin tai jäädä polymeerimatriisin sisään sen kuivuttua. PVOH- ja SA-lateksi-filmin veden diffuusiokerroin on samaa suuruusluokkaa, tosin PVOH:n yhteydessä on kyse massadiffuusiosta ja SA-lateksilla pintadiffuusiosta. Väriaineen kiinnittymistä päällysteen pintaan voidaan parantaa ionisilla vuorovaikutuksilla. Anioninen väriaine sitoutuu kromatografisen erkanemisen aikana päällystekerroksen kationisiin komponentteihin. Tulokset osoittavat, että on löydettävissä optimaalinen värin absorptionopeus, jossa väriaineella on riittävästi aikaa sitoutua Coulombisilla attraktio-voimilla kationisiin ryhmiin tai siirtyä sisään sideainepolymeerin matriisiin diffuusiolla. Nopean tulostuksen inkjetin painojäljen densiteetti riippuu väriaineen sijainnista päällystekerroksessa sekä koko päällystetyn paperin optisista ominaisuuksista.

Liuoksen virtauksen kanssa kilpailevat absorptio- ja adsorptioilmiöt ovat välttämättömiä, jotta saavutettaisiin hyvä painojäljen laatu. Värien välinen sekoittuminen (bleeding) riippuu siitä, miten paljon päällystekerros kykenee absorboimaan väriä ja miten nopeasti väri siirtyy pinnan sisään. Lisäämällä kationista pintakäsittelyainetta päällysteen pinnalle pystytään vähentämään värin leviämistä.

Preface

This thesis work has been done in the School of Chemical Technology, Department of Forest Products Technology of Aalto University during the years 2007–2011. Firstly, I would like to express my sincere gratitude to my supervisor, Professor Patrick Gane, Chair of Printing Technology, Aalto University, and Head of Research and Development, Omya Development AG, Oftringen, Switzerland, who gave me constant and invaluable guidance, and support throughout the work. I am most indebted to him for being always available and responding rapidly with his excellent comments to each of the research papers and the final thesis. Professor Gane also kindly arranged an opportunity for me to use the measuring devices of Omya Development AG and Aalto University for the purposes of this thesis.

The study commenced at Oy Keskuslaboratorio – Centrallaboratorium Ab (KCL) and continued and has been completed after the integration of KCL with VTT Technical Research Centre of Finland. This PhD work benefited from the positive attitude of these two organizations and the instructor of this work, Dr. John Kettle. I would like to express my greatest gratitude to him for being available whenever I needed support. He has always patiently guided me and helped me both in my research and with the English language.

I also wish to thank Dr. Cathy Ridgway, Omya Development AG (Oftringen), for her guidance in the use of mercury porosimetry and microbalance measurement techniques. I also wish to thank all of my co-authors involved in the publications of this thesis.

The data of this thesis work was collected from several projects at KCL and VTT. I would like to take this opportunity to thank my colleagues Anu Ilmonen, Eija Kenttä, Jukka Ketoja, Annaleena Kokko, Jorma Koskinen, Heikki Pajari, Pasi Puukko, Hille Rautkoski, Robert Roozeman, Yingfeng Shen, Asko Sneck and Oleg Timofeev for the many helpful discussions. I also would like to thank Seija Rinkinen and Sinikka Rosenlöf who were both involved in some aspects of the production and analysis of the coated papers.

Last, but definitely not least, I would like to express my deepest gratitude to my family, Seppo and Nina, and to all my friends who gave their support and encouragement during this work.

Espoo, 4.5.2012

Taina Lamminmäki

List of publications

This doctoral thesis is based on seven publications. All publications have been published in peer reviewed journals named below. In all publications the author has been in charge of the experimental plan, and has made the analyses of results and first manuscript. Some of the measurements made on specialist equipment and related model calculations have been performed via the grateful assistance of specialists in the field. The focus of each paper and how they assist the study of inkjet ink imbibition in the coated paper structure is explained in the "Introduction" section to the thesis (Chapter 1).

I   Lamminmäki, T., Kettle, J. P., Puukko, P., Gane, P., Ridgway, C.: Inkjet print quality: the role of polyvinyl alcohol in speciality $CaCO_3$ coatings, Journal of Pulp and Paper Science 35(2009)3–4, 137–147.

II   Lamminmäki, T., Kettle, J., Puukko, P., Ketoja, J., Gane, P.: The role of binder type in determining inkjet print quality, Nordic Pulp and Paper Research Journal 25(2010)3, 380–390.

III   Lamminmäki, T., Kettle, J., Rautkoski, H., Kokko, A., Gane, P.: Limitations of current formulations when decreasing the coating layer thickness of papers for inkjet printing, Industrial and Engineering Chemistry Research 50(2011)12, 7251–7263.

IV   Lamminmäki, T. T., Kettle, J. P., Puukko, P. J. T., Gane, P. A. C.: Absorption capability and inkjet ink colorant penetration into binders commonly used in pigmented paper coatings, Industrial and Engineering Chemistry Research 50(2011)6, 3287–3294.

V   Lamminmäki, T. T., Kettle, J. P., Puukko, P. J. T., Gane, P. A. C.: The chromatographic separation of anionic dye in inkjet coating structures, Colloids and Surfaces A: Physicochemical and Engineering Aspects 377(2011)1–3, 304–311.

VI   Lamminmäki, T. T., Kettle, J. P., Puukko, P. J. T., Ridgway, C. J., Gane, P. A. C.: Short timescale inkjet ink component diffusion: an active part of the absorption mechanism into inkjet coatings, Journal of Colloid and Interface Science 365(2012)1, 222–235.

VII   Lamminmäki, T. T., Kettle, J. P., Gane, P. A. C.: Absorption and adsorption of dye-based inkjet inks by coating layer components and the implications for print quality, Colloids and Surfaces A: Physicochemical and Engineering Aspects 380(2011)1–3, 79–88.

Author's contributions

Author has taken part in the planning of experimental work, developed and refined especially the thin layer chromatography measurement, done part of the actual measurements, analysed the data and based on the results written the first versions of the manuscripts.

Paper I   The coating trial using the SAUKKO device was performed by Seija Rinkinen from OY Keskuslaboratorio – Centrallaboratorium AB (KCL). Anu Ilmonen (KCL) produced the layouts of the printing trial. The mercury porosimetry measurement was made by the guidance of Dr. Cathy Ridgway from Omya Development AG (OMYA).

Paper II   Seija Rinkinen (KCL) measured the capacitance-based absorption (Clara) analysis.

Paper III   Hille Rautkoski (VTT Technical Research Centre of Finland) was responsible for the curtain-coating trial at the Metso Paper, Inc. (Järvenpää), pilot coater, and Seija Rinkinen (VTT) made again the corresponding measurements on the Clara device.

Paper IV   The ToF-SIMS measurement was performed by Jyrki Juhanoja from Top Analytica.

Paper V   Cathy Ridgway (OMYA) measured the pore volume and pore size distribution by mercury porosimetry. Asko Sneck (VTT) arranged the camera system for the TLC measurement and made the gray level determination.

Paper VI   Philip Gerstner (Aalto University) and Kimmo Koivunen (Aalto University) advised how to produce coating tablets. Cathy Ridgway (OMYA) arranged the mercury porosimetry analysis and guided in the measurement of liquid wicking by microbalance. Oleg Timofeev from VTT assisted in the diffusion coefficient calculations.

Paper VII   Robert Rooseman (VTT) assisted in the interpretation of the UV-VIS results and Sinikka Rosenlöf (VTT) measured the Clara results.

Paper II   The base paper grammage was reported wrongly. The grammage was 67 gm^{-2}, not 53 gm^{-2}.

Paper IV   Figure 2 the legend "Cationized PVOH, no additive" should be "Carboxylated PVOH, no additive".

Contents

13

List of symbols

<u>Symbols</u>

Symbol	Description	Number of publication	Unit
A	Area	II, III, VI	m^2
a^*	Colorimetric component in the CIELab orthogonal representation of colour space describing the position along the magenta/ red-green axis	VII	-
b^*	Corresponding colorimetric component on the yellow-blue axis	VII	-
Bo	Bond number, Eötvös number	-	-
c	Concentration	VI	e.g. $(mol)m^{-3}$
C	Capacitance	II, III	F
C^*	Chroma	-	-
d	Thickness of paper	II, III	m
d	Diameter of capillary	VI	m
D	Diffusion coefficient	VI, VII	m^2s^{-1}
g	Gravitational acceleration, $9.81\ ms^{-2}$	-	-
ΔE	Colour change measured with CIELab* values (CIE76)	VII	-
H^*	Hue	-	-
J	Diffusive flux	-	$(mol)m^{-2}s^{-1}$ e.g.
k	Porous medium permeability	III	m^2
k_B	Boltzmann constant, $1.3806503 \times 10^{-23}$	VII	JK^{-1}
l	Length of capillary, characteristic length of fluid flow	III, V	m
L	Paper depth	III	m
L^*	Luminance component in the CIELAB color space	VII	-
m	Mass	VI	kg
$_l$	Liquid phase	V	-
M	Moisture content	VI	%
N	Number of consecutive layers	VI	-

p, P	Pressure	III, VI	bar
q	Particle electrical charge	-	C
Q	Volumetric liquid flux	-	ms^{-1}
s	Solid phase	-	-
r	Internal radius of capillary	III, V, VII	m
R	Radius of ink droplet	-	m
t	Time	II, III, V, VI	s
T	Temperature	VII	°C or K
u, v, w	Velocity (in three Cartesian directions)	-	ms^{-1}
V	Volume of capillary, fluid or droplet	III, V, VI	m^3
v	Vapour phase	V	-
We	Weber number	-	-
x	Position of meniscus	VI	m

Greek letters

Symbol	Description	Number of publication	Unit
γ	Interfacial/Surface tension	V	Nm^{-1}
ε	Material dielectric permittivity	II, III	Fm^{-1}
ε_r	Dielectric constant (relative permittivity)	III	-
$\boldsymbol{\epsilon}$	Amplitude of oscillation	-	m
η	Viscosity	III, V, VII	$kgs^{-1}m^{-1}$ (Pas)
θ	Contact angle	V	°
λ	Distance between atoms	VI	m
ρ	Density	VI	kgm^{-3}
σ	Binder film thickness	VI	m
τ	Time	VI	s
ω	Frequency	III	s^{-1}
μ	Dynamic viscosity	-	$kgs^{-1}m^{-1}$ (Pas)
μ_q	Electrical mobility of a charged particle	-	$m^2V^{-1}s^{-1}$

Abbreviations

Abbreviation	Description
cat.	cationic
CD	Cross-direction
Clara	Capacitance-based penetration measurement
DIGAT	Dynamic inkjet ink absorption time measurement
DSC	Differential scanning calorimeter (calorimetry)
GCC	Ground calcium carbonate
MAX	Maximum
MCC	Modified calcium carbonate
MIN	Minimum
PCC	Precipitated calcium carbonate
polyDADMAC	poly(diallyl dimethyl ammonium chloride)
pph	Parts per hundred
PVOH	Polyvinyl alcohol
SA (latex)	Styrene acrylic latex
SEM	Scanning electron microscopy
Si-oil	Silicon oil
ToF-SIMS	Time of flight secondary ion mass spectrometry
TLC	Thin layer chromatography
UV-VIS	Ultraviolet-visible spectroscopy
UV/NIR/VIS	Ultraviolet-near infrared-visible spectrometry
wt-%	Weight percent

1. Introduction

1.1 Background

The popularity of using high-speed inkjet printing in the printing of products like books, labels, packages, direct mails, transactional mails (bills, statements, cheque books, credit cards and communications from the central government and local authorities), displays and security products, amongst others, has recently shown a large increase (Batz-Sohn *et al.* 2010, Smyth 2010). During the last twenty years, the inkjet printing method and application have developed both in terms of speed and print quality (Smyth 2010, Ward 2010, van Laethem 2003). Even though inkjet is still a minor printing method in terms of total volume in the printing world today, there are forecasts for its strong growth (Smyth 2010). Despite this, there is no commonly accepted or determined speed definition for a high-speed inkjet printing operation, but quite often speeds in excess of 10 m$\cdot$min^{-1} are typically quoted in the emerging digital printing world. The main drawbacks related to inkjet remain, to a large extent, the high cost of inks and substrates, in many cases inferior print quality compared to existing conventional printing methods, and the lack of good product ideas to utilize the full capabilities of variable data printing.

Two ink drop formation techniques are used in high-speed inkjet printing: continuous jetting (CJ) and drop-on-demand (DOD) (Smyth 2010, Svanholm 2007). In both techniques, water-based soluble dyes, aqueous-based dispersed pigment inks, UV-curable inks and hot-melt inks are used. Additionally, in the case of CJ printing, solvent-based inks are also used.

Inkjet suitable papers are generally fine papers, though wood containing newsprint is becoming increasingly common as a substrate for inkjet compatibility. Amongst the woodfree fine grades, categories span surface sized papers, coated papers and photo-quality papers (layer-structure containing media) (Svanholm 2007, Glittenberg *et al.* 2003). The surface-sized grade is a fine paper where the surface has been treated most commonly with starch and/or polyvinyl alcohol (PVOH) (Svanholm 2007). The coated papers traditionally have silica pigments in the receiver and/or top coating layer, with their combination of high porosity micropores and high specific surface area, providing rapid ink drying and high pore volume (Chapman 1997). Different silica-based pigments have also been studied (Hladnik 2004), like precipitated, fumed, colloidal silica and silica gel. Surface

modified calcium carbonate, surface modified clays, colloidal precipitated calcium carbonate, aluminosilicate and zeolite are seen as the most promising alternative pigments for silica (Klass 2007, Malla and Devisetti 2005, Vikman and Vuorinen 2004b, Cawthorne *et al.* 2003, Gane 2001). The most common binder used in inkjet coatings is polyvinyl alcohol (PVOH). This choice is due to the fact that it is one of the few binders providing sufficient surface strength for the adhesion of fine high specific surface area pigments. The binding strength of PVOH depends on the degree of polymerization. Modified PVOH has also been utilized: carboxylic-, sulphonic-, acryl amide-, cationic- and silicone-modified PVOH (Hara 2006, Mowiol 2003). The use of various types of pigments in the inkjet area has enabled the use of some other binders, like polyvinyl pyrrolidone, polyacrylic acid, poly-acrylamide, methylcellulose, cellulose derivatives, gelatin, polyvinyl acetate latex, vinyl acetate ethylene and cationic starch (Nilsson and Fogden 2008, Hara 2006, Malla and Devisetti 2005, Yip *et al.* 2003, Glittenberg and Voigt 2001, Morea-Swift and Jones 2000, Khoultchaev and Graczyk 1999, Lavery and Provost 1997).

Anionic inks are widely used in inkjet applications (Glittenberg and Voigt 2001, Pond 2000). So, a cationic charge of the coating layer components is understood to accelerate the fixing of the colorant part of the ink to the top layer of the coating structure. The cationic charge of the coating layer is usually produced by adding a few percent of poly(diallyl dimethyl ammonium chloride) (polyDADMAC) into the coating colour (Svanholm 2007, Malla and Devisetti 2005, Vikman and Vuorinen 2004b, Morea-Swift and Jones 2000), but other chemical compounds have also been considered for use (von Raven et al. 1988). Further, the pH of the coating layer affects the ionic interactions (Kallio *et al.* 2006, Boisevert *et al.* 2003). Morea-Swift and Jones (Morea-Swift and Jones 2000) and Hamada and Bousfield (Hamada and Bousfield 2009) indicated that the dyes can also be coagulated on the surface, though this method is not widely used but rather applied to pigmented inks by flocculating physically using soluble divalent metal salt, e.g. calcium or magnesium chloride (Varnell 2001).

The interactions between the ink and the substrate depend highly on the ink type used. In the ink setting process, there are different ink-substrate interactions occurring, such as wetting, capillary flow, colorant and vehicle separation, adsorption, diffusion, ink colorant fixing, polymerization and drying (Kettle *et al.* 2010, Yip *et al.* 2003, von Bahr *et al.* 2000, Agbezuge and Gooray 1991). These interactions have a direct effect upon the print quality formation, for example the penetration depth of the colorant affects the print density and print-through, and the ink spreading on/in the paper surface affects the ink colour mixing tendency and bleeding properties. In the optimal ink imbibition condition, the colorant part of the ink adheres to the top layer of the coating, whilst the solvent part (ink vehicle) penetrates deeper into the structure before finally evaporating/drying out of the structure. Thus, during the ink setting there exist many concurrent phenomena both related to the ink colorant fixing and to the vehicle movement.

1.2 Objectives

The first objective of this thesis is to clarify the role of *diffusion*. This is studied in particular during dye-based ink imbibition into model coating structures and components. Due to its increasing popularity as a cost effective alternative to silica pigment, the model structures are based on calcium carbonate coating pigments. Diffusion occurs wherever an interface or concentration gradient is present. Such interfaces can be phase boundaries of the same material, or contacts between materials. Specific cases relevant to the passage of liquid through a porous structure are the liquid-vapour, liquid-solid and liquid-polymer interfaces. Whilst diffusion is generally considered as either a precursor to subsequent mass transport, for example wetting and capillarity, or a progressive surface adsorption process, the interaction of diffusing liquid molecules with polymers is generally overlooked in respect to it being a mechanism for local mass transport. The diffusion of significant volume in the coating structure is exemplified by the use of various polyvinyl alcohols as "diffusion driving" (water diffusive) binders. Contrast is then drawn by comparison to a styrene acrylic latex, chosen as a "less water diffusive" (almost non water-interacting) binder. The behaviours of the studied binders are connected to the different pore structures (porosity and permeability) of the coatings, the polarity of ink vehicle and the ionic charge of the coating, especially its top layer. The research problem is approached by studying the physical properties and ionic charge of the coating structures, and their effects on the inkjet ink penetration by using several absorption measuring methods: these specifically being a capacitance-based measurement (Clara), a microbalance and thin layer chromatography. The final high-speed inkjet print quality was then correlated with the analysed coating layer properties.

The second objective is to determine the relevant *timescales of the various interactions* active during the imbibition of inkjet ink, especially short timescale phenomena. This timescale span is important to define in order to identify the relevance of the various mechanisms in practice, and crucial in deciding the role of diffusion. During this evaluation, the effect of coating layer thickness on the ink penetration was also taken into account, once again determined by capacitance change and mass balance.

1.3 Hypotheses and outline of the work

The main interest in this thesis is concentrated on the physical properties of the coating layer, their effect on network capillary absorption and surface adsorption phenomena, and the role of diffusion during inkjet ink imbibition. The method of study adopts measurements employing model coating layers with known compositions.

The chemical as well as physical properties like permeability, connectivity and porosity of the coating layer control the imbibition of high-speed inkjet ink and the final location of colorant in the coating layer. The structure of the coating layer dominates where and how quickly the inkjet ink penetrates into the layer. However,

the coating structural parameters controlling absorption are very complex. For example, a high void volume, permeable structure enables sufficient penetration of inkjet ink into the structure and thus less inter colour bleeding problems, but at the same time the colorant can penetrate too deeply into the structure and the print density as a result decreases and the print-through problem can appear. Thus, besides the structural properties, the ionic interaction between coating components and the dye-based ink colorant is needed to control the final fixing of the colorant. The surface must have suitable chemical groups which locate in the top layer of the coating structure and the surface area concentration of these groups is crucial.

The role of binder and/or additives in the coating colour is two-fold: affecting the coating structure established by the coating pigment packing and providing a significant portion of the chemical properties of the coating layer in addition to those brought by the coating pigment surface and the polymer species associated with it. The binders also affect the capillary phenomenon and the colorant fixing. The effect of diffusion into the binder matrix, and thus the binder swelling, is generally assumed to have only a slight, or no, role to play at the shortest timescales. However, in this thesis it is proposed that this diffusion plays an important role in inkjet ink imbibition into inkjet coating structures on both the second timescale and even at the shortest microsecond timescale due to its combination with certain pigment structures. The diffusion of ink vehicle and colorant on/into the binder and additive polymer structures starts immediately from the ink droplet arriving at the coating surface and it affects the ink penetration speed in the coating layers. Quite often it is postulated that after about 10 seconds from the ink arrival on the surface, the ink vehicle diffuses into the hydrophilic binder network and the swelling tendency of binders becomes more important (Kumaki and Nii 2010, Hodge *et al.* 1996). However, this is countered by the fact that, in the case of hydrophilic binders and surface polymers, the swelling in the coating layer decreases the amount of the smallest pores and therefore the ink penetration slows down. In addition, the binder swelling reduces the connectivity of the coating layer. The main role of additives in inkjet coatings is to fix the colorant. However, cationic additives in the coating colours can also influence the formation of the coating layer structure.

The hypotheses to be considered are based on the phenomena described in Figure 1, and in particular the competing timescales occurring.
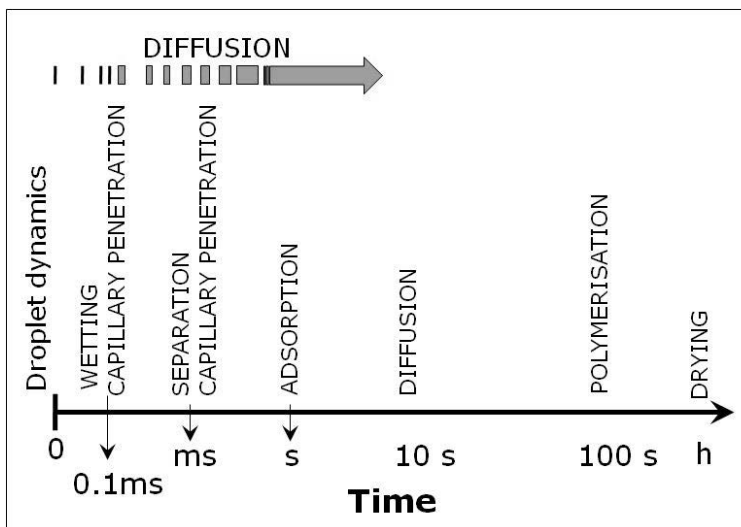
Figure 1. The presumed interaction phenomena in the inkjet ink setting process and their relevant onset timescales (Kettle *et al.* 2010).

> **Hypothesis I** – inter molecular diffusion of the liquid phase of inkjet ink into polymers acts on a sufficiently fast timescale and in sufficient volume to compete with the permeation of ink through coating structures.
>
> **Hypothesis II** – inter molecular diffusion of the liquid phase of inkjet ink into polymers, acting as a colorant carrier, is a competing mechanism to the surface adsorption of ink dye.
>
> **Hypothesis III** – the verity of Hypotheses I and II can be used to design porous coating structures, based on discretely bimodal pore size distributions, using binder and surface charge distribution characteristics to provide rapid fixing of ink colorant optimally close to the coating surface.

In illustrating the timescale selection consideration is given to the positioning of the absorbent binder and surface charge in relation to the pore structure, i.e. when considering porous particulate coating pigments. Such pigments exhibit internal pores (intra-particle) and pores between the particles (inter-particle). The intra-particle pores are designed to be within the nanometre size range (< 100 nm), providing capillarity, whereas the inter-particle pores are larger and interconnected (showing high connectivity) to provide sufficient permeability to allow effective access to the nanopores. Such a structure has a discretely bimodal pore size distribution with its respective parts referring to these intra and inter-particle pore types (Ridgway and Gane 2005). Due to the capillary dynamic during coating drying, soluble binder is drawn into the intra-particle pores, and its distribution is preferentially within these high surface nanopores forming part of the discretely bimodal pore structure. Thus, it is exposed by way of its position to the short time-

scale established interface with the ink vehicle, and, if absorbent to that vehicle by interpolymer diffusion, will take part in, and compete with, the shortest timescale phenomena.

Table 1 shows the main points in respect to the properties of inks and coating layers that affect the inkjet ink imbibition. A deeper study of the variables in a wide range of dye-based ink compositions is considered out of the scope of this study, but the generalities of ink component behaviour nonetheless satisfy the needs of the investigation in hand. The hypotheses of this thesis are therefore able to be challenged based upon combining the experimental observations made and the mechanisms found in the literature regarding the coating component-ink interactions utilized in Figure 1 and Table 1.

Table 1. Suggested major ink and coating layer properties that affect the interaction phenomena in the high-speed inkjet ink (dye- and pigment-based) setting process.

Interaction phe-nomena during inkjet ink imbibition	Ink	Coating layer
Wetting	Impact speed Surface tension Viscosity Density	Topography Surface energy
Capillary flow	Surface tension Viscosity Density Surfactants Vapour diffusion Pre-wetting At high humidity pore condensation	Surface energy Polarity Average pore diameter and pore size distribution Configuration of pores Type of binder and additive
Differential separa-tion of colorant and solvent	Surface tension Viscosity Colorant type Colorant charge Ink type	Surface energy Void volume Average pore diameter and tortuosity Chemical groups (charge)
Adsorption	Surface tension Viscosity Differential surface energies Molecular weight M_w Colorant charge Concentration gradient Solubility/precipitation Nearest neighbour repulsion	Surface area Void volume Average pore diameter and arrangement Surface chemistry Temperature Moisture content Ionic charge
Diffusion	Surface tension Viscosity Molecular weight (M_w)/size of species Concentration differential	Surface energy Temperature Pore connectivity Tortuosity Binder swelling
Drying (= evaporation)	Solvents of ink	Void volume Average pore diameter and pore size distribution Tortuosity Temperature Binder type Thermal conductivity

The thesis summarizes the findings of seven papers: *Paper I* concentrates on the pigment particle size and structure and how these influence the forming of the coating layer structure. At the end of the paper, it is reported how the coated papers are printed with a high-speed inkjet press and the print quality is analyzed. In *Paper II*, different contents of swelling (polyvinyl alcohol, PVOH) and non-swelling (styrene acrylic latex, SA) binder with one modified calcium carbonate are used. The paper is concentrated on the penetration of dye-based ink through the coated papers containing the different binder types and content, and the timescales observed during the inkjet ink penetration. The third paper (*Paper III*) illustrates how the thickness of coating layers affects the ink penetration, and the coatings derived from inkjet and offset coated pigments are compared in respect to the observed penetration of aqueous-based dye. This is then linked to the final ink mixing on the printing press. The penetration mechanisms are further explored using coatings on plastic film. *Paper IV* reports work concentrated on the binders, after film-forming, to identify and quantify their interactive properties with the ink vehicle and dyestuff. The cationic and anionic dye-based ink absorption into the three different polyvinyl alcohols and the styrene acrylic latex are studied by combining with applied cationic and anionic additives. *Paper V* illustrates the effect of coating structure on the liquid and colorant movement when the controlled variables in coating layers are the ionic charge of dispersing agent and the swelling/non-swelling of binder. The same coating structures, as well as two others adopting structured pigments, together with PVOH or SA latex binder are used in *Paper VI*, where the effect of liquid polarity vs. coating layer structure and hydrophilicity is researched. The seventh paper (*Paper VII*) concentrates on the absorption and/or adsorption of the different coating components, the effect of cationic additive application onto the top of the coating layer and its influence on the print quality. Figure 2 shows the interest focus of each paper.
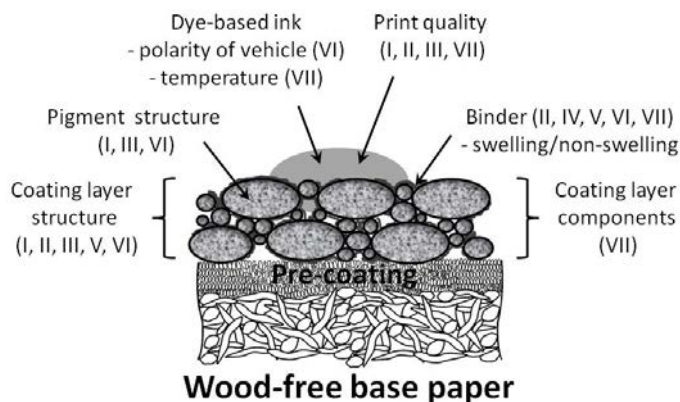
Figure 2. A structural illustration of the individual study focus interests, and in which papers they have been explored more closely. The paper, in which there has been concentration on a certain item, has been pointed out with the respective Roman numbers in brackets.

2. Literature review

In the inkjet ink setting process, we are confronted with different phenomena, like wetting, capillary flow, colorant and vehicle separation, adsorption, diffusion and ink colorant fixing, as the section 1.3 "Hypotheses and outline of the work" emphasized. Kettle *et al.* (Kettle *et al.* 2010) summarizes the knowledge of the inkjet ink droplet setting on the surfaces as well as its imbibition into the structure, and the contribution to that publication from the literature study for this thesis is summarised here. In this chapter, the study concentrates on the most common inkjet inks found in the area of high-speed inkjet printing and how the coating layer properties will affect the imbibition of this class of inks.

2.1 Properties of inkjet inks

The most important components in inkjet inks are the colorant and solvent/diluent. The colorant's fixing and movement on the surface of print media during the ink setting process determines the final print quality formation. The diluent in the ink vehicle is a carrier of colorant and it affects above all the ink viscosity, the droplet formation properties and the final colorant setting. The most common diluents in inkjet inks are water and/or various solvents. Water is used in desktop printers for the home and office market. The ink contains usually many other compounds as additives, which act as surfactants, solubilizers, rheology modifiers, polymer resins, humectants, carriers etc. Table 2 illustrates the main purposes of the ink components and their typical amount found in inks.

The properties of ink affect strongly the ink setting process and the final drying. The most common ink types in inkjet printing are dye-based and pigment-based inks. A dye is a colorant that is completely dissolved in the carrier fluid, and a pigment consists of solid colorant particles in the carrier fluid. In addition, the inks can be classified as aqueous, solvent-based, oil-based, UV-curable and hot-melt/phase change inks (Svanholm 2007).

Table 2. Main components of inkjet inks and their purposes (Pond 2000).

Ink component	Purpose	Amount in the ink, wt-%
Colorant	Gives the ink its primary function as light filter – absorbing light of a particular wavelength band	2–8
Carrier fluid	Dissolves or suspends the colorant	35–80
Surfactant	Lowers the surface tension of the ink to promote wetting	0.1–2.0
Humectant	Inhibits evaporation (miscible with the carrier fluid) and assists to prevent inkjet nozzle build-up	10–30
Penetrant	Promotes penetration of the ink into the paper structure for the purpose of accelerating drying	1–5
Dye solubilizer	Promotes dye solubility in the primary carrier fluid	2–5
Anticockle additives	Reduces the interaction with paper fibres, which otherwise leads to paper cockle and curl	20–50

Agbezuge and Gooray (Agbezuge and Gooray 1991) showed that, after the water-based ink droplet impact, there exists a wetting delay. They used commercial thermal inkjet print heads, where the ink droplet was produced by temperature change in the nozzle. As previously described, at droplet impact the most important variables are ink rheological properties, initial shape and volume, surface tension and viscosity. During the wetting delay, the droplet settles on the surface without much spreading or penetration. Equilibrium contact angle is established so that cohesive forces in the droplet overcome the adhesive forces between droplet and paper, then the paper starts to absorb the liquid volume. The effective driving parameters for absorption related to ink are surface tension, viscosity, contact angle, temperature, and volume, and, in the case of pigment inks, solids content. After this stage, there is droplet spreading and penetration, where liquid and vapour phase diffusion occur. The most important ink properties at this stage are spot shape, volume, viscosity and vapour pressure.

The differences in ink viscosity and surface tension can affect the ink setting process (Rousu *et al.* 2000, Desie *et al.* 2004a). Inkjet inks have very low viscosities, typically < 10 mPas (Girard *et al.* 2006). However, the meaning of viscosity or

its change during the inkjet ink setting process is unclear as it depends on composition as a function of time in the various separation steps.

The demands placed on inkjet inks are shortly described in Figure 3. There are many demands for inks in respect to the printing head and nozzle design as well as from the final print quality side.
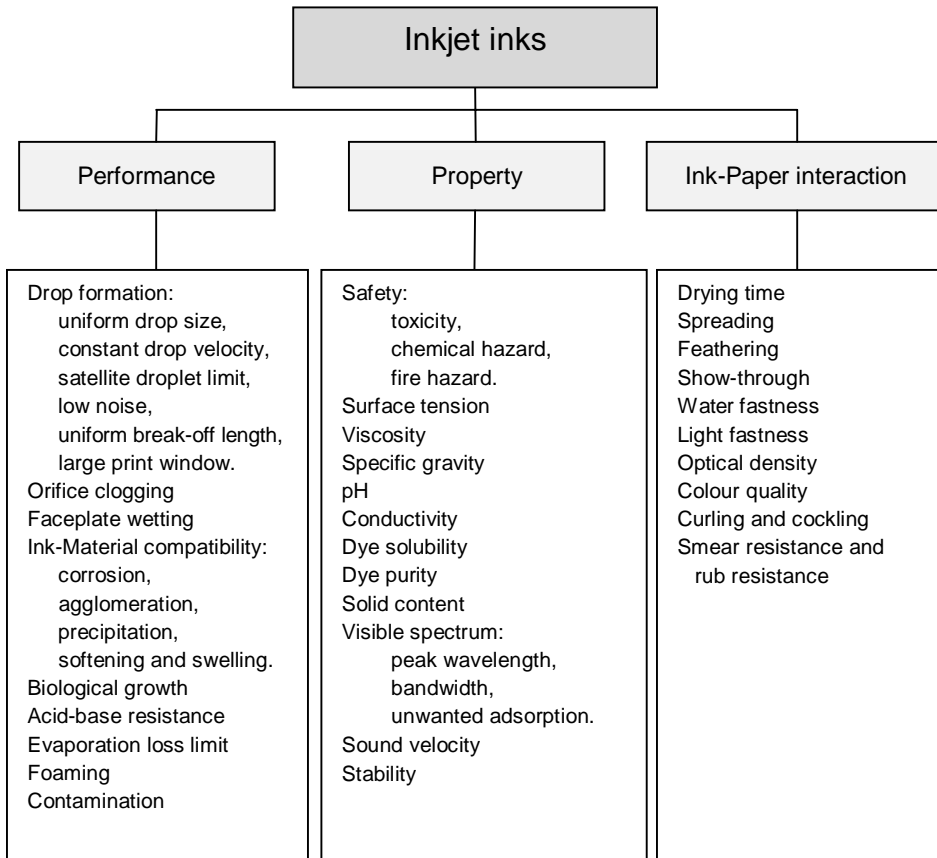
Figure 3. General description of the demands on inkjet inks (Kang 1991).

2.1.1 Water-based soluble inks (dye)

Water-based soluble inks consist of water as diluent and soluble compounds, dyes, as a colorant forming part. Nowadays, there exist different types of dyes on the market. The dyes in inkjet inks can be classified similarly to those found in the textile industry (Sundquist 1985). Water-based soluble dyes are used both in the home and office area, and in high-speed inkjet printing. The classification of color-

ants based on Colour Index International is introduced in Figure 4 and the chemical structure of dyes in Table 3.

1. Nitroso dyes	10. Acridine dyes	19. AminoketonYe dyes
2. Nitro dyes	11. Quinoline dyes	20. Hydroxyketone dyes
3. Azo dyes	12. Methionine and polymethionine dyes	21. Anthraquinone dyes
4. Azo based dyes	13. Thiazol dyes	22. Indigoidic dyes
5. Stilbene dyes	14. Indamine and indophenol dyes	23. Phthalocyanine dyes
6. Carotene dyes	15. Azine dyes	24. Organic natural dyes
7. Diphenylmethane dyes	16. Oxathiane dyes	25. Oxidized base dyes
8. Triacrylmethane dyes	17. Thiazine dyes	26. Inorganic pigments
9. Xanthene dyes	18. Sulphur dyes	

Figure 4. Classification of colorants based on Colour Index (Sundquist 1985, Colour Index 2011).

Table 3. The chemical structure of colorants of different classes (Sundquist 1985, Shore 2011). The chemical structure refers to Figure 4.

Colour class	Chemical structure
Acid dyes (anionic dyes)	1, 2, 3, 8, 9, 15, 21
Azo developer dyes	4
Alkaline colours (cationic dyes)	3, 7, 8, 9, 10, 12, 13, 16, 21
Direct dyes	3, 5, 13, 16, 23
Dispersion dyes	2, 3, 12, 21
Optical brighteners	5
Mordant	3, 21
Oxidation based dyes	25
Pigments	3, 6, 21, 22, 23, 26
Reaction dyes	3, 21, 23
Sulphur dyes	18
Vat dyes	21, 22
Food dyes	24, 21, 22

Typical dyes in inkjet inks are water soluble acid dyes, direct dyes, modified direct dyes, reactive dyes and poorly water soluble dispersion dyes (Lavery and Provost 1997).
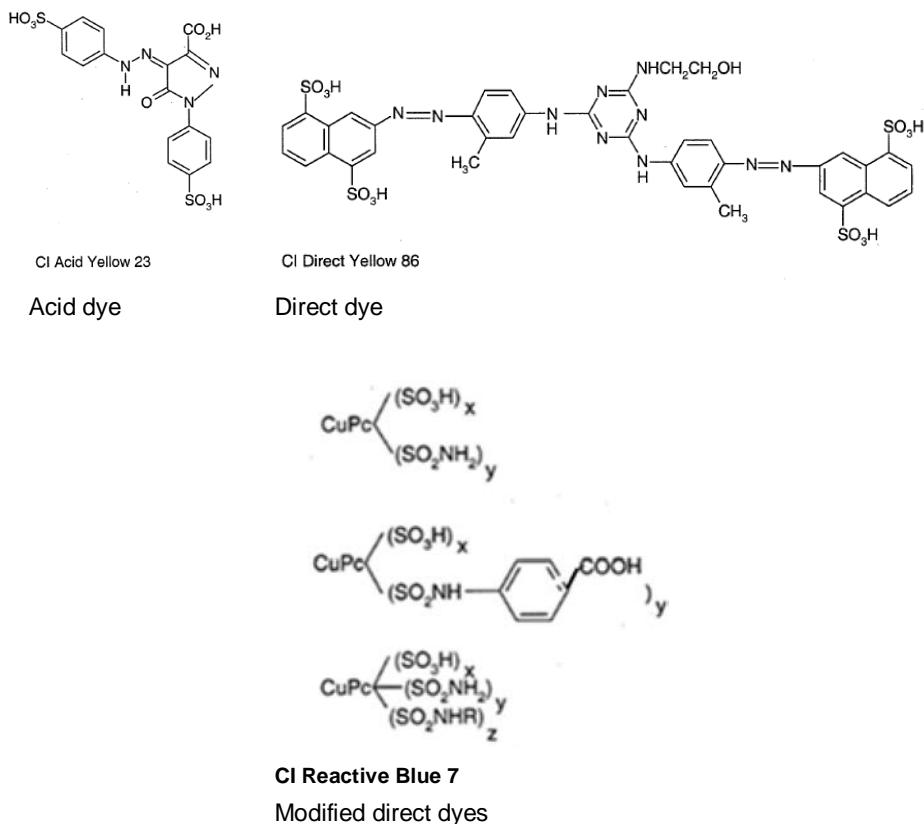
Acid dyes are low molecular weight anionic dyes. The small molecular weight enables the easy movement of dyes deeper into the porous structure of the coating layer and/or fibre network. The molecular structure of acid dyes is azo, antraquinone and triacrylicmethane dyes, and they have one or several sulphonic acid groups. Figure 5 shows an example of acid dye. 1:1 and 1:2 metal complex dyes are also included in the acid dyes. These complexes have metal atoms in the molecular structure (trivalent Co and Cr, and divalent Ni and Cu). The fixing to the fibres/coating structure happens usually with ionic bonds, for example with the ammonium groups and the sulphonic groups of dyes. There can also be hydrogen bonds and van der Waals interactions (Sundquist 1985). In section 2.2.6 "Colorant fixing" the binding mechanisms are described more closely.

Direct dyes have higher molecular weight than acid dyes and therefore they are larger. They have planar aromatic structures. Direct dyes have also better affinity for cellulose fibres and good water-solubility. The brightness of these colorants is not as high as the brightness of acid dyes, but they have better water and light fastness properties (Lavery and Provost 1997). Figure 5 illustrates an example of direct dyes. The direct dyes fix to the fibres/coating structure with ionic and hydrogen bonds and van der Waals interactions. The majority of the direct dyes belong to the family of dis, tris and polyazo dyes (Sundquist 1985).

Modified direct dyes contain added chemical functional groups to improve the interactions between colorants and fibres. The first generation of dyes had sulphonic acid groups. In the second generation dyes, the sulphonic acid groups had become replaced with carboxylic acid groups. These dyes have good solubility in water under alkaline conditions, but they flocculate at lower pH, for example advantageously on the top of the paper surface. The third generation of modified direct dyes have functional groups in their chromophores. These functional groups can improve, for example, water fastness of the printed surface (Lavery and Provost 1997). In Figure 5, the modified direct dyes of all generations are introduced.

Reactive dyes are also water-soluble dyes. There exists a covalent bond between the dye and the fibre/coating structure, and therefore the dye has very good affinity to the surface. However, the colorant fixing usually requires a treatment at elevated temperature or pH, which is quite a demanding requirement for use in inkjet papers (Sundquist 1985, Lavery and Provost 1997).

Dispersion dyes are insoluble in water, but they are solvent-soluble. The dispersion dyes can be used in colloidal liquids such as latex particles, emulsions, microemulsions or surface active agents, forming aggregates (Kang 1991). They are used for hydrophobic substrates, such as polyester (Lavery and Provost 1997). The print quality has good water fastness but the dye can easily block the print engine nozzles.

CI Acid Yellow 23

CI Direct Yellow 86

Acid dye   Direct dye

CI Reactive Blue 7

Modified direct dyes

Figure 5. Examples of acid dyes, direct dyes and modified direct dyes (Lavery and Provost 1997).

2.1.2 Water-based pigment inks

Water-based pigment inks have a diluent part and a colorant part, as in the case of the water-based soluble inks. The colorant part in this case is insoluble pigment. The pigment colorants are a combination of about a thousand molecules, and they are much larger than their dye counterparts, usually less than 100 nm (Bermel and Bugner 1999). The pigment colorants have a platy like structure which have a bound-form remaining as an insoluble crystal structure. The colorant molecule itself has usually similar structure, such as in the case of soluble monomolecular dyes. These pigment inks are used in the dispersion form. The pigments are bound to the paper surface with binders.

The larger size of colour pigments gives a better light fastness of the printed surface (Vikman and Vuorinen 2004b). The rub resistance of the pigment-based inks has been problematic. By a careful binder selection for the inks, the rub-off problem can be reduced. On the other hand, the colorant pigments can form a

rough printed surface (Desie *et al.* 2004a) which causes a non-uniformity in light reflection. Moreover, the colour gamut can be smaller than that of the dyes. However, the cyan, magenta and yellow inks containing small pigment particles (under 50 nm) have significantly greater colour gamut than inks with larger pigment size (Bermel and Bugner 1999).

Red pigments can be, for example, azo pigments or 2,9-dimethylquinacridone pigments. The yellow colours are produced with benzimidazolone or pyridone (Bauer *et al.* 1998). The most common black pigment in inkjet inks is carbon black. The stability of carbon black requires polymeric surfactants which can be problematic in the inkjet nozzle.

All the abovementioned colorants are organic compounds. Inorganic compounds are rarely used, but may include, for example, titanium dioxide.

Desie *et al.* (Desie *et al.* 2004a) showed that the phenomena of the wetting of pigment inks and dye-based inks are very similar, when the droplet volume was 70 pl. However, the absorption behaviour of the inks is different. The pigments of pigment-based ink were shown to form aggregates on the coating layer, and the droplets do not mix together at any stage, even in the situation where the impact delay between the droplets was only 100 ms. They noticed that the pigment ink's dot diameter remains much more constant over time during the wicking process than that of dye-based inks, and, therefore, at the beginning of the pigment cake formation, the Darcy model explains better the ink absorption process (in section 2.2.2 "Liquid penetration into porous coating layers"), in which the controlling permeability is that of the concentrating ink pigment layer. Finally, the pigment particles, with the polymer blend, form a filter cake, and a barrier layer develops, thereby limiting the penetration of carrier liquid into the coating structure. Then the diffusion phenomenon becomes more dominating, and Fick's law describes this latter situation better.

The drying time of aqueous-based inks (70 pl droplet volume) can be longer with pigment inks than dye-based inks on a porous substrate (Desie *et al.* 2004b). The filter cake formation limits water movement into the substrate. The filter cake formation was also detected with solvent-based pigment inks on a microporous receiver in the study of Desie *et al.* (Desie *et al.* 2004b). The composition of the solvent-based inks affects the drying time and it can cause even faster ink penetration than that of the aqueous-based inks. They used "piezo pigment eco-solvent ink" (from Mutoh) that had quite similar viscosity to "piezo dye ink" (water-based). However, the surface tension was somewhat lower, 30.4 mNm^{-1} with the solvent-based ink (piezo dye ink 33.2 mNm^{-1}). On a vinyl substrate, the solvent-based pigment inks had a very long drying time. By increasing the substrate temperature, the drying time could be shortened. The reason behind this is that the diffusion into the vinyl, as used in the substrate, increases (Desie *et al.* 2004b).

2.1.3 UV-curable inks

UV inkjet inks are inks that cure under the influence of ultraviolet light. UV-curable inks consist of monomer, oligomer, photoinitiators, colorant pigment and additives. UV-curable inkjet ink is a rapidly developing technology, and these inks can also be used in the area of high-speed inkjet printing.

UV inkjet inks can be classified into two different types of formulation, depending on the mechanism of photoinitiation, free radical or cationic curing mechanisms. In the conventional free radical curing, the photoinitiators absorb UV-light and form free radicals to initiate the polymerization of monomers and oligomers. This happens immediately under the influence of UV-light, and the result is that the solvent does not penetrate into the substrate (Svanholm 2007). The reaction happens only if the photoinitiators are matched to the spectral output of the lamp. The cationic photo-induced polymerization is a ring opening polymerization process of epoxies or oxetanes initiated by protonic or Lewis acids. Cationic polymerization is a "living" process. The UV exposure starts the cationic polymerization process and it stops once all of the components have been consumed. This process can last up to 24 h (Biry and Dietliker 2006). The roles played by the ink components are:

− The monomers in the UV-curable inks are typically low-viscosity acrylates, like acryl esters, that function as diluents, cross-linkers and performance-property enhancers. They affect the viscosity of the ink, enhance cure speed and improve adhesion to the printed surface. The molecular weight of monomers is lower than oligomers. The viscosity of monomers varies from 5 mPas to 25 000 mPas (Klang and Balcerski 2002).

− Oligomers can have acrylated urethanes, epoxies, polyesters and acrylics. Their amount in the ink is quite low, and they mainly influence the film forming properties and pigment dispersion. Their molecular weight is 1 000–30 000 (Biry and Dietliker 2006). Oligomers determine the physical property formation of the printed surface.

− The UV-curing free radical-generating photoinitiator is selected based on the desired cure speed and the pigments used. The most common photoinitiators are mono- and di-functional monomers. They can be, for example, benzophenone, benzyl dimethyl ketal and 2-hydroxy-2-methyl-1-phenyl-1-propanone (Klang and Balcerski 2002).

− The pigments produce the colours, and additives affect the ink flow, levelling, wetting, cure speed and adhesion (Klang and Balcerski 2002).

100 % of UV-curable inkjet inks are today working in drop-on-demand print heads. However, conventional UV inks have too high viscosity for the typical inkjet, and so this has been specifically adjusted. The viscosity requirement for workable UV inkjet inks is commonly about 10 mPas (Klang and Balcerski 2002). This is achieved by using lower functionality acrylates than in conventional UV inks. The

increase of jetting temperature aids also to lower the viscosity of the inks. The photoinitiators, nonetheless, are similar to those used in conventional UV inks.

In the case of UV-curable inks (40 pl droplet volume), there exists only spreading on the substrate and very little absorption or capillary wicking (Desie *et al.* 2004b). The spreading continues until the equilibrium stage of the droplet has been reached or the UV-curing process has stopped the spreading. Desie *et al.* (Desie *et al.* 2004b) divided the UV ink setting process into three phases. In the beginning there is initial inertial spreading, after that the rearrangement of the droplet geometry, and then the capillary (surface wetting) spreading. The most important property in capillary spreading is the surface tension of ink and the surface energy of substrate. If the ink has much lower surface tension than the surface energy of the substrate, spontaneous spreading continues in a regime of perfect wetting (Desie *et al.* 2004b). If the difference between ink and substrate is small, then the spreading occurs until the equilibrium contact angle has been reached (Desie *et al.* 2004b).

2.2 The wetting and imbibition of inkjet ink

In both the dye-based as well as pigment-based inkjet ink technologies the uptake of liquid (imbibition) is required to provide drying of the print and runnability in the press and post-press handling. The target is to attain sufficient ink vehicle penetration into the substrate with the colorant remaining in the top layer of the substrate to provide good image quality and high print density. If the colorant is transported too deeply into the structure, the print density will decrease and the print-through increase. However, a complete holdout of colorant on the outer surface of the substrate provides no physical or chemically bonded protection for the print, such that the print has poor rub-resistance. To achieve an optimal ink transfer process it is necessary to understand the control parameters involved in the many different interaction phenomena. At any given moment in the imbibition process there are usually one or two dominating phenomena, while the others at that instant have a less important role, manifesting their importance on a prior or subsequent time-scale. Kettle *et al.* (Kettle *et al.* 2010) summarized different ink-substrate interactions such as wetting, capillary flow, colorant and solvent separation, adsorption, diffusion, ink colorant fixing, polymerization (if colorant requires this) and drying.

At the first stage, the inkjet ink droplet arrives onto the paper surface and wets it. The inertia of the droplet affects the ink movement at the substrate surface, initiating forced wetting and top surface pore structure penetration (von Bahr *et al.* 2000, Schoelkopf *et al.* 2000, Agbezuge and Gooray 1991). The droplet settles into the roughness volume of the surface and begins to spread in the *xy*-plane on the surface depending on the surface tension of ink and the surface energy of the structure surface (Desie and Van Roost 2006, Girard *et al.* 2006, von Bahr *et al.* 2000, Agbezuge and Gooray 1991). At the same time the capillary flow into the pore network structure begins, and it competes with the spreading action. The capillary force becomes a dominating phenomenon after the droplet arrives at the surface, and it forces the ink vehicle and mobile components into the structure.

Capillary penetration starts typically after about 0.1 ms from the droplet arriving (Schoelkopf *et al.* 2000, Ridgway and Gane 2002). The chemical properties of the paper surface and inkjet ink strongly affect the capillary flow, and the surfactants in the ink and the coating layer surfaces play an important role here, on the one hand ensuring wetting, but on the other hand frequently exerting a delay whilst the surfactant orients to favour the contact with the polar ink vehicle (water) (Desie and van Roost 2006, Pan and Yang 1996). After a further millisecond, the separation of the ink colorant and vehicle starts and the capillary penetration continues strongly. The most important ink properties at this stage are thought to be the viscosity and surface tension (von Bahr *et al.* 2000). The porosity of the substrate has an effect on the separation of ink vehicle from the colorant, in that the surface area exposed within the pore structure defines the adsorption capacity for colorant at a given interaction potential (Desie *et al.* 2004a, Desie and van Roost 2006, von Bahr *et al.* 2000). After about one second from the droplet arriving, the significance of adsorption onto the coating structure internal surface increases. In parallel, diffusion needs to be considered, which is often thought classically to be only a slow phenomenon. However, in the case of contact with high surface area species, the length of diffusion reduces to the nanoscale, and, over such short distances, molecular motion is rapid. It is this often neglected feature of the imbibition process that is one of the main focus points of this thesis. Finally, the ink dries, a process that can last hours, depending on ink type.

There are also many varieties of inkjet inks, which display other or additional ink setting mechanisms, for example UV-curable inks, that adopt a UV-initiated polymerization mechanism to dry. Unlike nanoscale diffusion, polymerization in practice is a slow phenomenon, and the final drying can take the order of a hundred seconds to complete, although initial polymersiation of the upper ink layer may begin within milliseconds. Incomplete polymerization during the initial exposure to UV light relates to the poor short wavelength penetration properties of UV light and the construction of printers in which a dual exposure is often employed.

2.2.1 Wetting of a surface

When the inkjet ink droplet arrives onto the paper surface the primary spreading of the droplet takes place under the influence of the inertia and surface forces. The dynamic spreading of the droplet is usually simulated by studying the contact angle of the moving wetting line, the dynamic contact angle, θ_d. In the ideal case of liquid wetting, there is a balance of surface tension forces according to the Young-Dupré equation (equation (1)), in which the equilibrium contact angle (θ_{eq}) has a connection to the three interphase surface tensions (Young 1805, von Bahr *et al.* 2000, Girard *et al.* 2006)

$$\gamma_{ls} + \gamma_{lv} \cos\theta_{eq} = \gamma_{sv} \tag{1}$$

where γ_{sv} is the surface tension between the solid surface and vapour interface, γ_{ls} is the surface tension between the solid surface and liquid interface, γ_{lv} is the surface tension between the liquid and vapour interface (Figure 6).
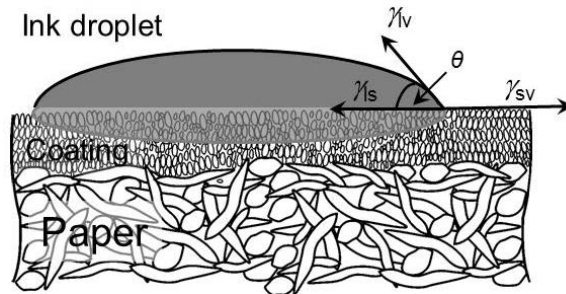
Figure 6. A schematic figure of the ink droplet on the coated paper surface.

When the inkjet droplet arrives at the paper surface, it fills the roughness volume of the surface and begins to spread in the *xy*-planar direction on the surface (von Bahr *et al.* 2003, Desie and van Roost 2006, Girard *et al.* 2006). In the contact angle measurement of coated paper, the roughness of the surface, applied surface modifiers, such as dispersants and tensides, coating pigment crystallite orientation, and adsorbed components from the atmosphere and surroundings all can have an effect on the contact angle identification (Gane *et al.* 1999).

The gravimetric forces can also be involved in the motion of the droplet, for example, in cases where centrifugal forces or large volumes of liquid are involved or when accelerating the droplet before impact. Bond number or Eötvös number (Bo) is a dimensionless number expressing the connection between gravitational acceleration, g, and surface tension forces.

$$Bo = \frac{\rho g r^2}{\gamma_{lv}} \tag{2}$$

where ρ is the density of fluid and r the droplet radius. A high Bond number indicates that the surface tension between the liquid phase, l, and the vapour phase, v, has quite a small effect on the system compared to the gravitational interaction. A low Bond number (typically less than one) indicates that surface tension dominates the process.

In the case of a droplet striking the paper surface and being driven into spreading, the Weber number (We) is frequently relevant

$$We = \frac{\rho v^2 l}{\gamma_{lv}} \tag{3}$$

where l is the characteristic length of the fluid flow, and v the velocity of the droplet. The Weber number is also a dimensionless number describing the fluid kinetic energy flow in respect to its surface tension forces.

Von Bahr *et al.* (von Bahr *et al.* 2003) assumed that the kinetic force caused by the droplet hitting the paper surface transforms into surface kinetic energy. It relates to the formation of the liquid-vapour interface ($_{lv}$) and partly becomes dissipated due to viscous forces. The droplet oscillates for a while, and after that it settles down on the surface reaching the equilibrium stage and the contact angle, θ_{eq}. The contact angle, θ, of the sessile droplet with volume, V, follows equation (4)

$$\theta = \theta_{eq} + \epsilon \exp\left(-\frac{\eta t}{\rho V^{2/3}}\right) \cos\left[\left(\left(\frac{\gamma_{lv}}{\rho V}\right) - \left(\frac{\eta^2}{\rho^2 V^{4/3}}\right)\right)^{1/2} t\right] \qquad (4)$$

where ϵ is the amplitude of oscillation, η dynamic viscosity of liquid, ρ density of liquid, γ_{lv} surface tension of liquid and t time as oscillations damp down.

Equation (4) shows that the viscosity of the ink affects the oscillation, and as the viscosity increases the quicker the droplet settles. The other interesting thing is that the amplitude of oscillations is proportional to the square root of surface tension and decreases with time. Von Bahr *et al.* (von Bahr *et al.* 2003) showed that there is a critical droplet size, d, below which there occurs no oscillation, which might have a meaningful effect in the case of a small inkjet droplet

$$d \approx \left(\frac{\eta^2}{\rho \gamma_{lv}}\right) \qquad (5)$$

If the values of aqueous-based inkjet ink ($\eta = 2 \times 10^{-3}$ Pas, $\rho = 1.05 \times 10^3$ kgm^{-3} and $\gamma_{lv} = 35 \times 10^{-3}$ Nm^{-1}) are taken into account in equation (5), the calculated diameter of the droplet is 110 nm. In inkjet printers, the smallest volume of droplets is today near 2 pl (picolitres) and this corresponds to a droplet diameter of 16 µm. Therefore, it can be concluded that the oscillation has a meaningful influence during the initial droplet contact process.

Von Bahr *et al.* (von Bahr *et al.* 2003) concluded that a droplet oscillation period lasts about 8 ms. In their study, the droplet volume was large, 1–5 µl. However, they measured that the damping occurs much faster than predicted by equation (3). They explained this difference by damping factors such as the contact line friction, internal vortices, and the viscous dissipation in air.

2.2.2 Liquid penetration into porous coating layers

The dynamic spreading and absorption of the inkjet ink droplets on the porous structure has theoretically been approached by using a hydrodynamic model (Alleborn and Raszillier 2004, Desie *et al.* 2004a, Josserand and Zaleski 2003, Gane

2001, von Bahr *et al.* 2000) or a molecular kinetic model (Marmur 2003, von Bahr *et al.* 2000, Hayes and Ralston 1994) as well as their combinations (Schoelkopf *et al.* 2002, Sorbie *et al.* 1995). The hydrodynamic model assumes that the loss of energy during the droplet imbibition is based on the viscous drag within the spreading droplet, whereas in the molecular kinetic model the energy lost derives from the intermolecular interactions between the solid phase and the liquid phase. There are also studies (Desie and van Roost 2006, Tiberg *et al.* 2000), where the effect of diffusion has been combined with these models.

The hydrodynamic model is based on the Navier-Stokes equation (6), where the droplet of the inkjet ink is assumed to be an incompressible Newtonian fluid that has dynamic viscosity, μ, and density, ρ, (Josserand and Zaleski 2003, Alleborn and Raszillier 2004). The equation describing liquid motion assumes that the fluid stress is the sum of terms relating to the pressure and viscosity controlled diffusivity, $-\nabla p + \mu \nabla^2 \vec{u}$, and these are combined to act according to Newton's second law, $\rho\left(\dfrac{\partial \vec{u}}{\partial t} + \vec{u} \cdot \nabla \vec{u}\right)$, considering any other externally acting force, such as gravity.

$$\rho\left(\frac{\partial \vec{u}}{\partial t} + \vec{u} \cdot \nabla \vec{u}\right) = -\nabla p + \mu \nabla^2 \vec{u} + \rho \vec{g} \tag{6}$$

where, $\vec{u} = (u,v,w)$ is the three-dimensional flow velocity vector, t is the time, p is the pressure and $\vec{g} = (0,0,-g)$ the vector of gravitational acceleration if the mass of fluid is big enough to warrant considering its action.

Following the wetting of the surface and the start of capillary pressure the droplet imbibition proceeds. The balance between the wetting force of capillaries and the viscous drag determines the rate of progress. As the viscous drag increases in proportion to the length over which the liquid flows within the structure, and to the inverse of the fourth power of the typical equivalent capillary size (Poiseuille effect, equation (7)), there comes a point when the drag equals the wetting force. The Hagen-Poiseuille equation (called also Poiseuille equation) can be derived from the Navier-Stokes equation (6) in cylindrical symmetry, making the assumption that the liquid undergoes steady laminar flow. The Poiseuille equation thus describes the liquid flow rate in a long capillary (longer than its diameter) under the application of pressure,

$$\frac{\mathrm{d}V}{\mathrm{d}t} = \frac{\pi r^4}{8 \eta l} \Delta p \tag{7}$$

where dV/dt describes the volume flow rate across a given area of the sample of liquid that has shear viscosity η (defined at the respective shear rate) through the effective capillary pipe of radius r and length l, representing this area, under the driving pressure difference Δp.

The permeability of a porous structure is linked to the Poiseuille description of flow through a pipe, where the porous structure is described as having an equivalent hydraulic radius as if it were a simple pipe. The term permeability applies to a saturated structure, in which the liquid is forced through the porous medium under a pressure gradient, ∇p. It can be described by Darcy's law (Darcy 1856, Yip $et\ al.$ 2003, Alleborn and Raszillier 2004), which can also be derived from the Navier-Stokes equation for constant flow rate $(\nabla \vec{u} = 0)$.

$$\vec{u} = -\frac{k}{\eta}\left(\nabla p - \rho \vec{g}\right) \tag{8}$$

If we ignore the action of gravity within a microscopic structure, this reduces to

$$\frac{\mathrm{d}(V\,/\,A)}{\mathrm{d}t} = \frac{k\Delta p}{\eta l} \tag{9}$$

where A describes the area of cross-section of the porous sample perpendicular to the linear flow direction. The term k is the permeability of the porous medium with units of length-squared. In inkjet ink setting, $1/k$ describes the resistance to flow experienced when the wetting front lies deep within the coating structure or when the inertia of the droplet causes penetration into the top layer of the coating.

The Young-Laplace equation (equation (10)) (Young 1805, Ridgway $et\ al.$ 2001, Schoelkopf $et\ al.$ 2000) describes the wetting force, $\pi r^2 p_c$, of a liquid that has contact to the walls of a capillary

$$p_c = \frac{-2\gamma_{lv}\cos\theta_{eq}}{r} \tag{10}$$

where p_c is the Laplace capillary pressure, r the internal capillary radius, γ_{lv} the interfacial tension at the liquid-vapour interface, and θ_{eq} is the equilibrium contact angle (Figure 6).

During inkjet ink imbibition, the liquid phase is transported dynamically in the capillaries, and the position of the liquid meniscus advances with time. At equilibrium flow, the moving position of the wetting meniscus, $x(t)$, in the capillaries can be described by the Lucas-Washburn equation (equation (11)) in which the Young's pressure is balanced with the Hagen-Poiseuille flow resistance (Washburn 1921, Desie $et\ al.$ 2004a and 2004b, Marmur 2003, Gane 2001, Ridgway $et\ al.$ 2001, Lundberg $et\ al.$ 2011).

$$x(t) = \left[\frac{r\gamma_{lv}\cos\theta}{2\eta}\right]^{1/2}\sqrt{t} \tag{11}$$

where θ is the dynamic contact angle and $x(t)$ is the horizontal distance of penetrated liquid in the capillary during the time t.

The Lucas-Washburn equation (11) applies only after equilibrium is reached between the wetting force and the viscous permeability drag. It suggests that the rate of liquid flow at a given time, t, in the capillary should be greater when the structure has larger effective radius. Practical studies, for example in the offset printing area (Rousu et $al.$ 2000), have shown, however, that smaller radius capillaries will initiate faster absorption and thus will initially fill faster than larger capillaries, which disagrees with the equation of Lucas-Washburn. There are differences between fine and large pores, and there are effects occurring on the short time-scale on the pore surfaces and within the pore network that Lucas-Washburn does not capture (Schoelkopf et $al.$ 2002, Ridgway et $al.$ 2002, Sorbie et $al.$ 1995). The flow entry effects into capillaries have been studied in respect to the energy loss equation of Szekely (Sorbie et $al.$ 1995). Bosanquet (Bosanquet 1923) considers the relative timescales of inertial wetting and viscous forces during the fluid entry into a cylindrical capillary from a reservoir or supersource of fluid,

$$\frac{\mathrm{d}}{\mathrm{d}t}\left(\pi r^2 \rho x \frac{\mathrm{d}x}{\mathrm{d}t}\right) + 8\pi \eta x \frac{\mathrm{d}x}{\mathrm{d}t} = p_\mathrm{e} \pi r^2 + 2\pi r \gamma_\mathrm{lv} \cos\theta \qquad (12)$$

where p_e is an external pressure, if applied, at the entrance of the capillary tube. The first term of the equation is the inertial drag, expressed as the rate of change of momentum, and the second is the frictional resistance derived from Poiseuille flow and dependent on the velocity of the meniscus front. Schoelkopf et $al.$ (Schoelkopf et $al.$ 2000) showed a solution of this equation for short timescale where the external pressure p_e is set to zero:

$$x = t\sqrt{\frac{2\gamma_\mathrm{lv} \cos\theta}{r\rho}} \qquad (13)$$

When inertia dominates before viscous flow is fully established, i.e. for absorption into pores close to $t = 0$, equation (13) shows that the finest pores absorb preferentially further and faster. Ridgway et $al.$ (Ridgway et $al.$ 2002) developed the Bosanquet result by taking account of the shape of meniscus and the recirculation regions behind the edges of the meniscus, applying the dynamic via an algorithm to a wetting front encountering the individual components of a pore network structure. If a network of such fine pores is considered, remembering that fine pores are typically equally as short as their diameter, i.e. too short to establish viscous drag, it can be visualised to show a preferred pathway effectively by-passing the larger pores, or at least limiting the access to them. This has been described by Ridgway et $al.$ (Ridgway et $al.$ 2001) where they have used the Pore-Cor[1] visualisation. In this pathway, the absorption rate is high and so the passage into the porous medium is defined by the combination of pore sizes within the inertial wetting

---

[1] Por-Core is a software network model developed by the Fluid and Environmental Modelling Group, University of Plymouth, PL4 8AA, UK.

regime (nanopores) and the connecting high volume structure consisting of larger pores which fill more slowly and develop the least permeation resistance. Thus, in relation to inkjet ink imbibition defined by pore structure, the short timescale phenomena in the nano-size capillaries are important in respect to rapid ink vehicle absorption.

2.2.3 Transport by diffusion

The diffusional phenomena, which may occur over the short timescale, are the main interest of this doctoral study. Probably, the most important forms of diffusion taking place during inkjet ink imbibition by the coating structure are (Figure 7) (Radhakrishnan *et al.* 2000, Shaw 1996, Liang *et al.* 1990):

– Bulk diffusion, which means general volumetric motion of the liquid or gas within the coating/deposited layer

– Surface diffusion, where the motion of atoms, molecules and clusters of atoms or molecules follows the surfaces of the solid material

– Knudsen diffusion, when the diffusivity is additionally determined by the size of capillaries instead of by the thermodynamic state of solvents or solutes alone (capillaries with small sizes or very low pressure)

– Osmosis, defined as the spontaneous net movement of water across a semi-permeable membrane from a region of low solute concentration to a region with a high solute concentration, down a water concentration gradient, or, as usually described, up a solute concentration gradient. It is a physical process in which a solvent moves, without input of energy.
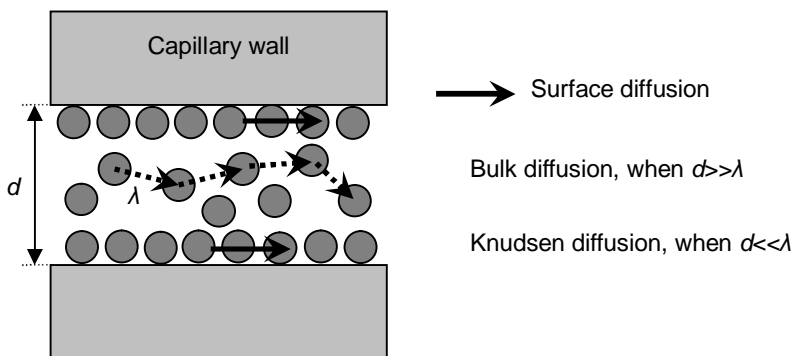
Figure 7. Diffusion types in inkjet ink transportation: d is pore diameter and λ distance between atoms, molecules, or atomic/molecular clusters. Based on Paper VI (Figure 1).

In this work, a linear relation between the absorbed liquid amount and the square root of time is detected with the results of the microbalance wicking measurement and the capacitance-based device (in Chapter 4). This indicates that the liquid after the first milliseconds proceeds either by equilibrated balance between wetting force and permeation resistance, i.e. a form of the Lucas-Washburn equation, and/or by diffusion, i.e. according to a Fick's Law diffusion response. Fick's first law describes the steady state of diffusion, where the concentration of diffusion volume does not change during time, equation (14). Fick's second law (equation (15) takes account of the concentration within the diffusion volume changing over time.

$$J = -D\frac{\partial c(x,t)}{\partial x} \tag{14}$$

$$\frac{\partial c(x,t)}{\partial t} = D\frac{\partial^2 c(x,t)}{\partial x^2} \tag{15}$$

where J is the diffusion flux, $c(x,t)$ is the concentration of liquid at position x and time t. D is the diffusion coefficient.

The formal solution to the diffusion equation (15) takes the form of the complementary error function,

$$c(x,t) = c(0,0)erfc\left(\frac{x(t)}{2\sqrt{Dt}}\right) \tag{16}$$

Usually, the first two terms of the corresponding Taylor series expansion are used.

$$c(x,t) = c(0,0)\left[1 - 2\left(\frac{x(t)}{2\sqrt{Dt\pi}}\right)\right] \tag{17}$$

A satisfactory working equation for practical purposes, and used in this work to describe mass transport, can be derived dimensionally. The denominator x^2 in equation (15) is proportional to the time t, and hence x is proportional to $\sqrt{t}$. The distance has a correlation to the volume of liquid being transported in the system and thus represents the mass of liquid uptake. Therefore the equation (12) can be written as

$$\frac{m(t)}{t} = D\frac{A \cdot c(x,t)}{x} \tag{18}$$

where $m(t)/t$ is mass flow rate during the time t and A area of cross-section where the liquid is taken up by diffusion.

The timescale of diffusion has been studied by several researchers (Desie and van Roost 2006, Alleborn and Raszillier 2007, von Bahr *et al.* 1999). Desie and van Roost (Desie and van Roost 2006), who studied inkjet ink imbibition phenom-

ena by using aqueous dye-based and pigment-based inks, showed that diffusion is the main liquid absorption driving phenomenon into polymeric blend materials in contrast to capillary absorption into microporous coating. The timescales of long range diffusion and evaporation are much closer together than the timescales of capillary wicking and subsequent evaporation of ink water. They concluded that the diffusion phenomenon for bulk transport appears seconds after the liquid arriving on the surface. Instead of concentration in equation (17), they considered volume $V(t)$ of liquid in a droplet in the form of a truncated sphere, radius R, sitting on the porous surface, and expressed the depletion of the droplet by bulk diffusion into the structure as

$$V(t) = V(0) - 2\pi R^2 \sqrt{\frac{Dt}{\pi}} \qquad (19)$$

where $V(0)$ is the volume of ink on the top of surface at the start of the inkjet ink imbibition process, R is the radius of the droplet in the form of a truncated sphere on top of the receiver, and D is the diffusion coefficient of the ink.

Von Bahr *et al.* (von Bahr *et al.* 1999) support the separate behaviour of capillary flow and bulk diffusion by dividing the liquid spreading onto a porous structure into a non-diffusive and a diffusive regime, but in their case they consider the diffusion of the surfactant present in solution rather than that of the solvent molecules. In the non-diffusive regime, the liquid spreading is described as very quick, and inertia, gravity and capillarity are the main controlling factors. In the second regime, the spreading is slower than in the first regime, and it is controlled by diffusion of surfactant molecules to the expanding liquid-vapour interface. However, von Bahr *et al.* (von Bahr *et al.* 2000, von Bahr *et al.* 2004) showed that when the front area of a surfactant containing liquid goes through the capillary network of sized paper, some of the surfactants transfer to the capillary walls. At the same time, more surfactants concentrate at the liquid surface and orientate by diffusion. They finally came to the conclusion that the surfactant diffusion has to work on a shorter timescale than seconds.

Alleborn and Raszillier (Alleborn and Raszillier 2004) connected the action of diffusion to a wetting front model with the concentration changes of the liquid front considered within the paper structure. As the solvent (water) moves forwards in the paper, the diffusion affects the behaviour of the paper fibres. The hygroscopic nature of a porous paper structure ensures that many mechanisms of moisture transport operate simultaneously (Massoquete *et al.* 2005, Radhakrishnan *et al.* 2000, Liang *et al.* 1990, Nguyen and Durso 1983). Moisture enters paper by vapour-phase diffusion through the interfibre void space, Knudsen diffusion in pores, surface diffusion over fibres, bulk-solid diffusion within fibres, and capillary transport (Liang *et al.* 1990). The first two mechanisms take place in the gas-phase and the other in the condensed state of the liquid. Liang *et al.* (Liang *et al.* 1990) saw that moisture transport is dominated by gas-phase transport through the interfibre voids or pores. The vapour-phase diffusion is reported to dominate in the paperboard at relative humidities below 60 %. At high moisture content, the

condensed phase or bound water movement appears to dominate. According to Ahlen (Ahlen 1970), the transport of water in the condensed or bound state was important even for relative humidity levels as low as 30–40 %. Similar diffusion behaviour was considered also to be relevant in the case of coating layers (Salminen 1988).

To consider more closely the diffusion rate over short distances through a spatially limiting polymer network, as is the case when considering water transport into, say, a swellable binder matrix, we need to consider the rate of movement of molecules as a function of the random thermodynamic energy and the resistance of movement in a viscous medium. The velocity of molecules thus depends on the temperature, the viscosity of fluid and the size of particle (molecule) according to the Stokes-Einstein relation (Reynolds and Goodwin 1984, Mehaffey and Cukier 1977), which for spherical particles passing through liquid at low Reynolds number is expressed as

$$D = \frac{k_B T}{6 \pi \eta r} \tag{20}$$

and for an electrically charged particle, such as the inkjet ink colorant molecule,

$$D = \frac{\mu_q k_B T}{q} \tag{21}$$

where D is the translational diffusion coefficient, k_B Boltzmann's constant, T absolute temperature, η viscosity and r radius of spherical particle, or equivalent hydrodynamic radius for non-spherical particles. The term μ_q is the electrical mobility of the charged particle and q the electrostatic charge.

Acceleration of flow by heating has been used in some high-speed inkjet printing nozzle applications. For example in the nozzles of Versamark® VX5000e the ink is heated to a temperature of 40 °C. The effect of the temperature on dye-based inkjet ink penetration into porous coatings was studied with the capacitance-based device in section 7.4 "Cationic additive applied directly onto the top of coating surface". The advantageous use of the electrical properties of inkjet inks, other than just the ionic interaction properties, has also been considered in some applications, such as the printing of electronics (Haverinen *et al.* 2009, Walther *et al.* 2009). Additionally, preheating the ink and/or substrate will increase the rate of diffusion of ink components.

It is very probable that the concentration of the components of ink varies during the ink setting process. This is a dynamic process occurring until the solvent has evaporated out of the printed surface and the other components of ink vehicle as well as ink colorant have become bound or settled into the structure. The concentration changes cause variation of osmotic pressure as a result of the distribution of concentration gradients within the structure, and especially when components become trapped within absorbing polymer networks, and this reflects in the resultant ink movement tendency. There can even appear transportation of components

in the reverse direction from the interim ink component location. The diffusion phenomenon appears even in the final stages of inkjet ink drying, where the concentration differences of ink components, caused by ink vehicle evaporation, generate the concentration gradient for diffusional movement. However, there are other dominant boundary condition phenomena to consider in the ink drying process coming from the process variable side, like the image size, desired print density, ink and paper type, sheet temperature and initial moisture content of paper (Agbezuge and Gooray 1991). In this work, the main interest is concentrated on the diffusional phenomena at the local position scale during inkjet ink imbibition, not during the final drying process.

2.2.4 Separation

In the inkjet ink setting process, it is desirable that the colorant part of ink fixes into the top layer of substrate and the ink vehicle part penetrates deeper into the structure. This takes the form of chromatographic separation in the case of dye-based inks (Donigian *et al.* 1998, Rousu *et al.* 2000). In pigment-based inkjet inks, the separation takes place between colorant pigments and vehicle, where the ink pigments form a filter cake or agglomerate on the top of the substrate (Donigian *et al.* 1998, Vikman and Vuorinen 2004b, Svanholm 2007). In the ink separation, the controlling ink properties are thought to be the viscosity and surface energy (von Bahr *et al.* 2000). The surface properties of the substrate also affect the ink vehicle-colorant separation and movement (Desie and van Roost 2006, von Bahr *et al.* 2000, Glittenberg *et al.* 2003).

In the area of offset printing, Rousu *et al.* (Rousu *et al.* 2000 and 2005) showed that the ink colorant pigment and diluent oil separated at the coating surface. Furthermore, it was shown that the oils, diluent (mineral oil) and solvent (vegetable oil) underwent chromatographic separation. The separation was controlled by specific surface area of pigment, degree of polarity and binder chemistry. The adsorption/desorption on the surfaces of pigments, therefore, leads to the chromatographic separation of ink diluent(s)/solvent(s) and colorant(s). The degree of separation depends on the surface area of pigments, if the comparison is made amongst chemically and morphologically similar pigments. However, it is the true surface chemistry of the pigments that is important, and this is defined more by the dispersant and/or surface adsorbed species and polymer(s) than the underlying pigment itself, unless the pigment is used in an undispersed or polymer-free environment. The morphology influences the hydrodynamic flow behaviour due to the changes in pore size, porosity and tortuosity. The addition of binder into the coating colour creates further surfaces, where the ink solvent as well as ink colorant can diffuse and/or adsorb, and in the case of swelling binder interpolymer matrix diffusion also takes place.

2.2.5 Adsorption

During inkjet imbibition, the ink colorant and some other molecules of the ink can adsorb on the surface of the solid phases depending on surface charge or polymer structure, forming a molecular or atomic layer, or in some cases a multilayer structure. In the adsorption to a true solid, the liquid or solute does not go into the adsorbent, but it diffuses or migrates along the surface, in this case the pore walls, until a sorption site is found. The ink vehicle, however, wets and film forms along the pore walls, but it does not adsorb directly, other than by surface dissolution, to the chemical groups of pore wall material in competition with ink colorant, though it may adsorb at other sites than the colorant. Adsorption is usually described through isotherms, which connect the adsorbate amount on the adsorbent with its partial pressure or concentration.

The chemical properties of coating structure affect the movement of liquid and water vapour on the surface. As the inkjet ink vehicle (mainly water) transfers in the porous structure, it influences the surface chemistry. As the water content increases in the paper structure, the polarity increases and this is reflected in the adhesion of polar components of ink, affecting such print properties as mottling and rub/abrasion resistance of the printed surfaces (Gane and Ridgway 2008).

2.2.6 Colorant fixing

The colorant adsorption can result in the forming of chemical bonds between the ink colorant and the different coating components. Lavery and Provost (Lavery and Provost 1997) named the possible bonds between the ink colorant and substrate in the order of decreasing strength of interaction: covalent bonding, Coulombic or ionic bonding, π-π interactions, hydrogen bonding, hydrophobic interactions, dipole-dipole interactions, and van der Waals forces. However, in this section they have been introduced in the order of the most probable binding force in the fixing action of aqueous-based dye inks.

Ionic interactions (ionic interactions, Coulombic bonds) exist, when the anionic ink contains water soluble groups, like SO_3^{2-}, COO^-, PO_3^{3-}, which can interact with cationic groups on the surface, for example Ti^{4+}, Al^{3+}, Ca^{2+}, and NR_4^+. The interaction is strong and it has an effect over a long range. The ionic bonds immobilize effectively the colorant molecules of dye giving good print quality (Lavery and Provost 1997). This interaction manifests itself via a force action at a distance via soluble ions, such that water/moisture or a polar solvent must be present. Adsorption on the surface by ionic bonds, however, provides a permanent fixation, and an improved water fastness of dye-based inks on the coated paper surface (Vikman 2003).

The dominating fixing interaction in the case of uncoated paper grades is the hydrogen bonding (hydrogen attached to an end group bonds via covalent bonding to an electronegative atom). Groups like −OH and −COOH can easily support hydrogen bonding. Hydrogen bonding is a quite weak interaction and greatly influenced by the geometrical orientation of the components. However, if the molecule

is large, there may be a large number of hydrogen bonding sites, and this increases the strength of the colorant bonding. There may moreover be interactions between the –OH groups of the cellulose and the π-cloud (electrons) of the aromatic groups of colorant.

Van der Waals interactions are amongst the stronger binding forces, but only occur when the interacting groups are very near each other. Van der Waals interactions act between all kinds of molecules. In the beginning of the ink setting process, there is a weak repulsion force between anionic dyes and the cellulosic substrate if uncoated. However, as the water of the ink absorbs, the colorant and paper interface becomes nearer and the opportunity for van der Waals attractive forces increases (Lavery and Provost 1997).

Dipole-dipole interactions are relatively weak and they are depending on the polarity of the interaction groups (Lavery and Provost 1997). Dipole-dipole interactions are forces that occur between two molecules with permanent dipoles. The molecules are two point dipoles which have opposite equal finite charges. The opposite charges of molecules attract each other forming dipole-dipole interaction.

π-π interactions are important when considering bonding between the colorant molecules themselves, and they can lead to dye aggregation or crystallization. Quite strong π-π interactions occur when the paper substrate contains aromatic groups. For example, the chromophores of phthalocyanines react like this (Lavery and Provost 1997).

In the case of reactive colorants, covalent bonding occurs (the strongest interaction), for example with cotton fibres. The electrophilic reactive group of ink reacts with a primary hydroxyl group. The reaction demands the action of temperature or pH. The final print has good fastness properties (Lavery and Provost 1997).

Hydrophobic interactions occur for solvent-based inks, which have hydrophobic groups such as alkyl chains. These interact with similarly hydrophobic groups on the paper. The hydrophobic interactions consist of a combination of hydrogen bonding and van der Waals interactions (Lavery and Provost 1997). The work by Wallqvist *et al.* (Wallqvist *et al.* 2006) has shown that the hydrophobic force develops itself between hydrophobic surfaces in water first only at short range as the surfaces approach each other, but then extends to long range as the surfaces are forced to retreat, suggesting that cavitation is the means by which the hydrophobic force can be expressed at long range. This force is expected to be highly sensitive to the location of chemical groups and the structure of the surface.

Surface wetting and the capillary imbibition driving force are intermolecular phenomena, and are mainly active via van der Waals, Coulombic and Lewis acid-base interactions (Gane *et al.* 1999). Van der Waals interactions form on the surface when there is unevenly distributed charge. Coulombic forces occur between charged surfaces and ions. When the surface has sites of specific electron donor-acceptor interactions between uncharged surfaces and molecules there occur Lewis acid-base interactions.

Hydrogen bonds and van der Waals forces can also support the fixing of colorant to coated papers and films. However, in the fixing process the electrostatic interactions (ionic or Coulombic forces) are dominant (Lavery and Provost 1997,

Pond 2000, Kallio *et al.* 2006, Vikman and Vuorinen 2004a) and the inks fix to the coating layer mainly through ionic forces (Lavery and Provost 1997, Pond 2000). The coating layer is more highly charged than the underlying fibrous, frequently surface sized, layer, resulting in attraction between the anionic colorant and the inorganic pigment, even in lightly coated papers. This interaction, of course, depends on the charge of the dispersing forces used to disperse the coating pigment in relation to the ionic charge of the dye. The inkjet coating structure has usually a cationic charge, which has been produced by applying a cationic additive. The cationic charge attracts the anionic dye, and this interaction increases the binding energies for the dyes. Vikman (Vikman 2003) showed that on anionic PVOH (fully hydrolysed, amount 5 and 10 pph) coatings the dye colorant is attached to the binder with hydrogen bonds, whereas on cationic PVOH coatings it attaches via ionic bonds. Donigian *et al.* (Donigian *et al.* 1998) hypothesized that the most important chemical groups of colorant from the binding point of view are carboxylic and sulphonic acid groups. By adjusting the pH of inkjet inks, the groups can become ionized (Donigian *et al.* 1998).

Besides the colorant ionic charge, the ink can contain other components that affect the final colorant fixing. There can be dispersant molecules, which have a portion that anchors them to the colorant surface, and a soluble polymer chain, which is not in contact with the colorant (Oka and Kimura 1995). It is via these chains that the colorant molecule fixes onto the coating layer. Such water-soluble polymers are, for example, polyethylene oxide, polyvinyl alcohol and polyvinyl pyrrolidone (Pond 2000). On the other hand, there is a possibility that the colorant remains physically at the paper structure (Morea-Swift and Jones 2000), for example within the roughness profile of the paper surface.

In the case of aqueous-based pigment inkjet inks, the colorant pigment forms a filter cake on the paper surface. The filter cake formation is also possible in the case of dyes. The dye can precipitate out of solution. One example of this being used is the designed evaporation of an amine to change the pH from basic to acidic when the ink reaches the paper surface (Pond 2000), and another for pigmented inks is the use of divalent cation, such as Ca^{2+} to act as a flocculant (Varnell 2001).

2.3 Effect of coating layer on inkjet ink imbibition

As described above, the coating layer materials as well as the forming structures play a very important role during the inkjet ink imbibition and in defining the final colorant bonding to the structure (Desie *et al.* 2004b, Agbezuge and Gooray 1991). The ionic charge of coating components affects the colorant molecules fixing in the case of water-based inks, and the ink sorption volume and rate is determined by the coating structure and wettability. The fixing and absorption properties influence further the final print quality formation. A proper colorant fixation produces high optical print density, bright colour tones, low print-through, high

sharpness, low bleeding and high rub resistance and water fastness (Vikman and Vuorinen 2004a, Morea-Swift and Jones 2000, Donigian *et al.* 1998).

The topography of the surface affects, in addition, the droplet impact (Heilmann and Lindqvist 2000). For example, it affects the apparent wetting delay. The material properties like contact angle, sizing, coating, capillary structure, temperature and relative moisture content are important in respect to local surface and pore interior topography during ink imbibition. The spreading and penetration are affected by the coated paper porosity, permeability, thickness, sizing, fibre type, moisture content, temperature and capillary structure (Agbezuge and Gooray 1991). The construction of the printer and/or the printing machine variables also affect the final droplet setting, and also play an interactive role with respect to surface properties. However, machine variables are a further field of study and remain beyond the scope of this literature survey.

2.3.1   Coating pigments

The sorption rate of liquids into the coating structure depends on the chemical properties of the surfaces encountered by the ink, and the pore network structure. Ridgway and Gane (Ridgway and Gane 2006) showed that the fine pores display a somewhat different effective surface chemistry to water than to non-polar alkanes. Fine pores are apparently more apolar than the large pores in that water suffers a delay in pore entry. They assumed that this is an effect caused by the swelling of polar, hydrophilic polyacrylates blocking the uptake of polar liquid into the finer pores, such that they appear apolar in respect to apparent wetting energy. By the choice of pigment particle size distribution and shape the coating layer structure can be manipulated. Gane and Ridgway (Gane and Ridgway 2008) showed that the broad particle size distribution of standard ground calcium carbonate produces slower initial adsorption of moisture than the more specialised narrow size distribution ground calcium carbonate pigments. The standard $CaCO_3$ provided a less permeable coating layer structure than the more specialised narrow size distribution $CaCO_3$. They concluded that the nodes or throats in the porous coating structure, defining connectivity, determine the equilibrium saturated sorption of water vapour. Schoelkopf *et al.* (Schoelkopf *et al.* 2000) showed the opposite results when considering the liquid bulk uptake by capillarity. This is one example of the complexity of the interactions between polar liquids and the coating layer components depending on the sorption mechanism taking place.

Traditionally, a good inkjet print quality is produced by silica pigment coatings, which have high porosity, consisting of both micropores in the pigment particles as well as inter-particle pores, and high surface area, providing rapid ink sorption and dye-based ink colorant fixation. In the case of pigment-based ink, the binder of the ink fixes the colorant pigment to the top of the coating layer and the ink vehicle penetrates into the coating structure. The colorant pigment effectively forms a filtercake on the top of the coating. This filtercake effect may be enhanced by flocculating the ink pigment. This practice is common-place on uncoated papers

(ColorLok® (Koenig *et al.* 2007)) and is increasingly being considered for the new generation of coated papers to enhance print density (Romano *et al.* 2011). However, the expensive silica pigments are being progressively replaced with other less expensive pigments, like surface modified calcium carbonate, surface modified clays, colloidal aggregated precipitated calcium carbonate, aluminosilicate and zeolite (Klass 2007, Malla and Devisetti 2005, Gane 2001, Vikman and Vuorinen 2004b). Nonetheless, the basic properties have remained similar – high porosity and high surface area – although their relative distributions throughout the coating structure can differ. The following discussion goes on to illustrate the progression of studies from the behaviour of traditional silica-based formulations to those resulting from the more recent introduction of speciality calcium carbonate.

Morea-Swift and Jones (Morea-Swift and Jones 2000) studied different particle size synthetic silicas. The silicas produced a coating layer that allows fast ink drying, i.e. fast droplet sorption into the coating structure. They noticed that larger particle size silica produces a coating layer with higher print density. The silica coating with small particle size produces the sharpest text edges, but the bleeding is problematic. They concluded that the silica with small particle size and high pore volume guarantees the best performance for text reproduction on coated papers. For photographic papers and advertising wide web media, the silicas with large particle size and high pore volume are to be considered optimal. The pigment-based inks form a pigment-rich layer, a filter cake, on the silica coating surface, whereas dye-based inks penetrate into the pores of silica pigment (Svanholm 2007). The larger particle size silica produces higher adhesion of pigment-based ink at a given certain pigment/binder ratio than smaller silica pigments (Adair 1998). At the same pigment/binder ratio of the coating colour, the smaller size pigments have more binder-free pigment-pigment contacts where the ink colorant pigment cannot bind.

Many studies (Shaw-Klein *et al.* 2007, Vikman and Vuorinen 2004a, Lee *et al.* 2002) have noticed that silica coatings can exhibit cracks. The cracks can be the results of shrinkage occurring from low solids content coating colours and the use of soluble binders that fail to resist shrinkage (Laudone *et al.* 2003). The smaller the particle size of silica, the greater is the surface tension force in the drying process and this can form cracks in the coating layer causing the gloss decrease of the surface (Lee *et al.* 2002).

Donigian *et al.* (Donigian *et al.* 1998) showed how dye-based ink fixes by different mechanisms to the silica and a comparative precipitated calcium carbonate (PCC) coating. In the case of silica coatings the high pore volume traps the whole ink, both ink colorant and vehicle. The silica provides a large specific surface area on which the ink colorant can bind as the evaporable part of the ink vehicle evaporates. The silica produces a higher affinity for the vehicle than PCC pigment. The PCC coating anchors the dye on the pigment surface while the vehicle penetrates deeper into the coating or base paper (Donigian *et al.* 1998, Glittenberg and Voigt 2001). PCC, however, has higher affinity for the dye components than silica. The colorant was shown in this case to bond mainly by hydrogen bonding to the chemical groups of the coating layer. One interesting result in their study is that the

yellow dye ink released more energy than would be predicted by the hydrogen bonds. This indicates that, in the case of this specific yellow colorant, some other or additional mechanism is involved in the bonding.

McFadden and Donigian (McFadden and Donigian 1999) showed that the brightness, and especially light scattering properties of the coating layer, has strong influence on the forming print density. They showed that inkjet coated papers often have lower opacity than the comparable offset or rotogravure coated papers, and this is actually beneficial for inkjet colour intensity. As the light scattering coefficient of the paper increased it is shown by these workers that the print density of the printed surfaces decreased (desktop printer using dye-based inks). High light scattering reduces print density contrast as the scattered white light raises the background spectral noise level.

Lee *et al.* (Lee *et al.* 2004) studied, in addition, the opportunity to reduce expensive and low solid content silica pigment by replacement with calcium carbonate pigments in higher gloss containing products. They studied the mixtures of fumed silica and precipitated calcium carbonate (PCC) or ultra fine ground calcium carbonate (UFGCC). The binder was partially hydrolysed polyvinyl alcohol. The coatings were applied as a single coat onto paper and subsequently calendered. Addition of carbonates increased the brightness of the coated papers. The addition of PCC increased gloss to the value of 60 % (TAPPI 75°) from 55 %, up to a PCC content of 30 % PCC. The packing of pigment particles explains the gloss improvement. In the case of UFGCC, gloss first decreased until a 30 % UFGCC pigment content, and after that it increased to the gloss level of 60 %. The use of $CaCO_3$ pigment, thus, has an effect on the gloss formation. The carbonate additions decreased somewhat the print densities of dye-based printed surfaces. The more permeable structure of $CaCO_3$ coatings, however, did not affect printed surface gloss.

Ridgway and Gane (Ridgway and Gane 2006) introduced a special modified calcium carbonate, which has small intra-particle pores. The pigment can absorb the diluent/solvent rapidly and it has high specific surface area. The final coating produced with this pigment has both nano- and micro-size pores. In their study, the pigment particle cakes produced from this pigment have ten times higher capability to take up fluid than normal offset quality ground calcium carbonate. The coating contains under 0.1 μm pores that control the fluid capillary action and, on the other hand, there are larger interconnected pores controlling permeability.

One way to affect the paper structure is to calender the paper. Calendering the pigment coating layer increases the gloss and smoothness of the surface. This was exemplified in the case of fumed alumina and fumed silica by Lee *et al.* (Lee *et al.* 2005) (25 pph polyvinyl alcohol was used as binder). The 3 soft-nip calendering with 60 °C temperature and 123 kNm^{-1} line load increased the gloss from 20 % up to 60 % (TAPPI 75° gloss). At the same time the Parker Print-Surf roughness decreased from 3 μm to 1.2 μm. A little higher relative gloss changes between unprinted and compact printed surfaces were detected with alumina than with silica coatings. For compact printed surfaces, the delta gloss changes were

the largest with alumina for both dye-based and pigment-based inks (Lee *et al.* 2002). The silica coatings maintained or even enhanced their coating gloss.

2.3.2 Binders

The most commonly used binder in inkjet coatings is polyvinyl alcohol (PVOH) because of its capability to produce sufficient surface strength of the coating layer even for fine high specific surface area pigment coatings. The binding strength of PVOH depends on the degree of polymerization (Kumaki and Nii 2010). The higher the degree of polymerization the higher is the binding strength. The peel strength of PVOH coating is further shown to be greater with the higher degree of polymerization (Hara 2006). Modified PVOH has also been used: carboxylic-, sulphonic-, acryl amide-, cationic- and silicone-modified PVOH. The use of other types of coating pigments in the inkjet area has brought some other binders into use, like polyvinyl pyrrolidone, polyacrylic acid, polyacrylamide, methylcellulose, cellulose derivatives, gelatin, polyvinyl acetate latex, vinyl acetate ethylene, cationic starch (Malla and Devisetti 2005, Yip *et al.* 2003, Morea-Swift and Jones 2000, Glittenberg and Voigt 2001, Khoultchaev and Graczyk 1999, Lavery and Provost 1997).

Oka and Kimura (Oka and Kimura 1995) introduced four different mechanisms to describe how an acid red dye (anionic) solution can set on a PVOH containing silica coating layer (Figure 8). Their first assumption was that the PVOH covers the silica pigment. The colorant part can attach onto the PVOH layer (A), dissolve in PVOH (B), complex with adsorbed cationic polymer (dye-fixing agent) in PVOH (C), adsorb on the silica pigment (D) and/or adsorb on silica with cationic polymer (E). They finally concluded that most of the used dyes form a complex with dye-fixing agent, and this disperses in the PVOH layer – the mechanism (C) is, thus, the dominant phenomenon. The rest of the dye remains as a colorant layer on the PVOH surface (A).
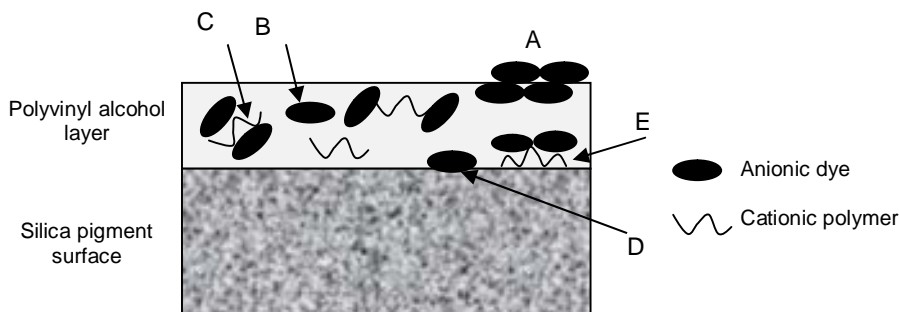
Figure 8. The colorant setting states of anionic dye-based inkjet inks in a silica/ PVOH coating (Oka and Kimura 1995).

The diffusion phenomenon that has been described above, and its connection to swelling binder polymer networks, could be expected to decrease the diameter of pore capillaries. The hydrophilic binders, such as polyvinyl alcohol, have higher swelling tendency than, for example, latices in water. Adding PVOH in the coating slows down the movement of water in the case of dye-based inks (Donigian *et al.* 1998).

Svanholm (Svanholm 2007) studied PVOH containing silica pigment coatings on fine paper surfaces. He showed that the silica pigments with large pigment particles and large inter-particle pores require more binder than pigments with smaller particles and smaller pores to get the dye colorant remaining at the top of the coating. The PVOH can form a film-like structure in the top part of the coating, and the colorant can thus be made to remain there. The best colour gamut and the sharpest line edges of dye-based inks were achieved using a partially hydrolyzed and higher molecular weight PVOH.

The light fastness of inkjet printed PCC and kaolin coatings were studied by Vikman and Vuorinen (Vikman and Vuorinen 2004b). They used PVOH and cationic starch with cationic styrene acrylate latex as binder. With dye-based inks, the significance of structural properties of the coating layer in the light fastness decreased when the strength of the chemical paper-ink interaction increased. The dye-based ink benefits from a dense coating structure, whereas a coarse structure of the coating appears to be advantageous for the pigment-based inks.

Hailmann and Lindqvist (Heilmann and Lindqvist 2000) studied water-based inks in the area of continuous inkjet printing. A sized uncoated paper, a silica coated paper and one, surface swelling, superabsorber-based glossy paper were studied. They applied a single ink droplet on the surface and measured the droplet penetration into the substrate from the top side and in the cross direction. After the first 50 ms, the droplets reached the final dot size on the silica coated paper, while on the surface sized paper it took as long as 500 ms. The swelling binder/absorber containing coating had a shorter ink levelling time than the non-swelling coating. In the case of non-swelling coating, the final dot size was reached in 100 ms. Furthermore, small scale changes in the surface topography were seen to affect the size and shape of the forming dot, if the droplet is small. However, in the case of larger droplets, the topography has only a minimal effect on the shape of the final forming dot.

Rousu *et al.* (Rousu *et al.* 2005) indicated in offset coatings that the latex properties affect the ink setting. Low glass transition temperature and gel content of latex, together with oil-matched solubility index through monomer composition, increase fast ink setting. However, the latex particle size can affect the packing of the coating layer, and, through that, modifies the setting speed. Moreover, Rousu *et al.* (Rousu *et al.* 2000, Rousu *et al.* 2005) showed that the latex influences the oil separation of offset inks. Even a small amount of latex affected the separation process. The reason behind this can be found from the non-polar nature of the latex polymer. Latices to date are not usually used in inkjet coatings.

2.3.3 Additives

Anionic inks are widely used in inkjet printing. From the point of view of colorant fixing, the coating layer should have opposite ionic charge to that of the ink colorant. The cationic charge is usually produced by adding a few percent of poly(diallyl dimethyl ammonium chloride) (poly-DADMAC) to the coating colour (Svanholm 2007, Malla and Devisetti 2005, Vikman and Vuorinen 2004b, Morea-Swift and Jones 2000).

Khoultchaev and Graczyk (Khoultchaev and Graczyk 1999) studied the effect of the charge density of ionic polymers in the coatings on the print quality of dye and pigment-based inkjet inks. They showed that a short dry time (time of ink set off onto an unprinted strip) does not always mean the best print quality. The quicker dry time surfaces can have cracks in the compact ink areas because the colour pigments separate too early out of the diluent/solvent and they flocculate with each other forming an uneven distribution of colorant on the coating surface. Moreover, they noticed that, on an anionic coated PET film, the pigment-based inks produced more cracks than on a cationic coated PET film. On the other hand, cationic coatings had lower print gloss than the anionic coatings. The increase of pH of coating slurry reduced the print gloss of both coatings.

One further opportunity to increase the bonding strength of ink colorant to the surface is to use cross-linkers or insolubilizers for coating formulations, like zirconium compounds (zirconium acetate, ammonium zirconium carbonate) (Hara 2006).
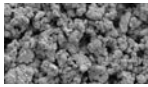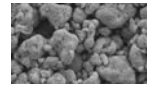
3. Experimental
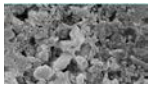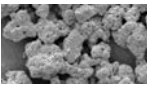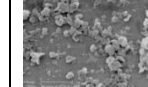
3.1 Materials

3.1.1 Calcium carbonate inkjet coating pigments

The most well-known pigment used traditionally in inkjet coatings is silica, which produces a print quality of high print density, low print-through, low bleeding and wide colour gamut. The capability of quick ink absorption combined with the high pore volume provides this high print quality. However, the price of silica pigments, their low solids content in suspension, as well as the demand of using more expensive high binding power additives makes silica today a less attractive coating pigment. Therefore, the emerging generation of more cost effective calcium carbonate ($CaCO_3$) pigments was chosen for this study, having been developed to generate coating layers that can provide a good inkjet print quality. These calcium carbonate-based pigments are introduced in Table 4. The $CaCO_3$ pigment selection was based on the diversity in the mean particle diameter and the specific surface area of the pigments. The idea was to illustrate the effects of particle size and internal pore structure, including raw material sources from ground calcium carbonate (GCC), subsequently modified to generate high surface area and internal pores (MCC), and precipitated calcium carbonate (PCC). It should be noted that all of the pigments exhibit a cationic slurry property, being designed to bind anionic ink dye. The coating pigments were provided in the form of slurry by the pigment suppliers. In *Papers V* and *VI*, the "MCC large" pigment was used as a dry pigment that was dispersed in two ways, the first with anionic sodium polyacrylate, and the second using cationic poly(diallyl dimethyl ammonium chloride).

Table 4. The calcium carbonate pigments, their naming in this work and their properties: in the last row it is indicated in which published paper(s) each pigment has been used. The pigment sizes have been provided by the pigment suppliers.

Properties	Ground calcium carbonate – GCC	Modified calcium carbonate – "MCC large"	Modified calcium carbonate – "MCC small"	Precipitated calcium carbonate – "PCC large"	Precipitated calcium carbonate – "PCC small"
Weight median pigment particle diameter, μm ($d_{50\%}$)	0.65 [a]	1.60 [a] 3.70 [b]	1.30 [a] 2.50 [b]	2.70 [c]	Fine fraction 0.02–0.03 Ave. 0.25 [d]
Specific surface area, m²g^{-1} (BET, ISO 9277)	10.7	46.2	27.0	63.7	73.9
Zeta-potential, mV (AcoustoSizer II [2])	-9	13	14	2	-1
Registered trade name	Hydrocarb 90 [3]	OMYAJET B6606 [3]	OMYAJET C3301 [3]	OMYAJET B5260 [3]	JetCoat 30 [4]
Structure of pigment	Rhombohedral	"Roses"	"Roses"	"Eggs"	Spherical
Illustrated structure of coating layer		Intra-particle pores	Intra-particle pores	Intra-particle pores	
Published paper(s) where the pigment has been used	*I, III, VI*	*I, V, VI*	*I*	*I, II, VII*	*I, III, VI*

a) Sedigraph 1500 [5,] b) MasterSizer 2000 [6], c) HELOS [7] d) NanoSight [8] (results had two peaks: fine at 20–30 nm and average at 0.25 μm).

3.1.2 Swelling and non-swelling coating binders

Polyvinyl alcohol (PVOH) is the most frequently used binder in the area of inkjet coating. It has high binding power and it has a hydrophilic nature. On contact with water, it swells. This swelling is caused by diffusion of water molecules into the polymer matrix. To compare the effects of a swelling versus a non-swelling binder, styrene acrylic synthetic emulsion polymerized latex (SA) was used in the study to complement the PVOH. The trade name of the SA latex was changed during the research due to a company takeover, but the material remained constant. The styrene acrylic latex type was selected because it is one of the least interactive latices when contacted by typical printing ink liquids, and can usually provide a more porous coating layer structure than styrene butadiene latex.

The PVOH binders had different degrees of hydrolysis. PVOH is produced by polymerization of vinyl acetate and the hydrolyzation is adjusted by saponification/hydrolysis of the hydrophobic acetate group ($OCOCH_3$) with a hydrophilic hydroxyl group (OH) (Miller and Cook 1990). The final product contains vinyl alcohol and vinyl acetate units (Figure 9). The resulting polymer has both crystalline and amorphous regions in the structure, and the higher the degree of hydrolysis the more the polymer contains crystal regions within the polymer matrix (Kumaki and Nii 2010). In the case of the K-Polymer KL-318[9] PVOH polymer, a carboxylic monomer (COO^-Na^+) has been added to the molecular chain. Table 5 shows the properties of the binders. The glass transition temperatures of the PVOH grades were not evaluated, but they usually lie between 40 °C and 80 °C (Mowiol 2003) depending on the origin, type and thermal history of polymer. PVOH does not have a defined particle size as it is applied as a soluble material, whereas latex has. The viscosity of SA latex was not measured.
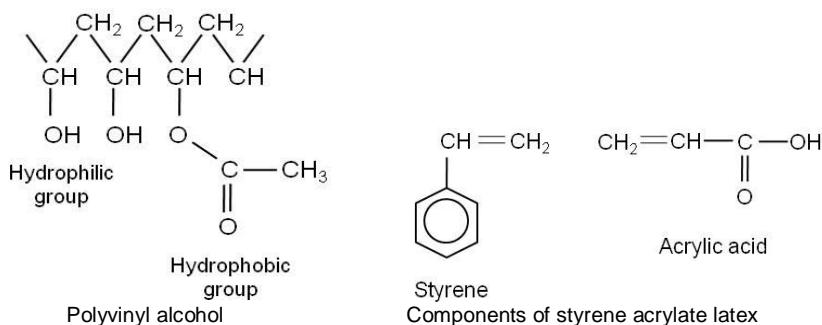
Figure 9. Chemical structure of polyvinyl alcohol and the components of styrene acrylate latex.

---

[9] Registered trademark of Kuraray Specialities Europe GmbH, Building D 581, D-65926, Frankfurt am Main, Germany.

Table 5. The properties of studied binder polymers.

Binder	Fully hydrolyzed PVOH (Mowiol 20-98[9])	Partially hydrolyzed PVOH (Mowiol 40-88[9])	Carboxylated PVOH (K-polymer KL-318[9])	Styrene acrylate latex (Latexia 212 = CSA 212[10])
Degree of hydrolysis, mol-%	98.4±0.4	87.7±1.0	87.5±2.5	
Density, gcm^{-3}	0.4–0.6 [*)	0.4–0.6 [*)	0.4–0.6 [*)	1.0
Glass transition temperature, °C	N/A	60–65 [**) 30–35 [***)	N/A	-20
Particle size, nm	-	-	-	180
Viscosity (4 % solution, 20 °C, DIN 53 015), mPas	20.0±1.5	40.0±2.0	25.0±5.0	N/A
Chemical nature	non-ionic	non-ionic	anionic	anionic

*) Measured according to DIN 53 468 by Clariant International AG from the granulates. **) bone dry, ***) ambient humidity.

3.1.3 Adjusting the ionic charge by additives

The ionic charge of the pigments and binders was adjusted by adding either anionic sodium polyacrylate (Polysalz S[10]), having a molecular weight of 4 000 gmol^{-1} or cationic poly(diallyl dimethyl ammonium chloride) (polyDADMAC, Cartafix VXU[11], a molecular weiht 75 000 gmol^{-1}). In the last *Paper* (*VII*), a cationic additive was applied to the surface of the top-coating of a double-coated fine paper surface in order to clarify the role of ionic charge concentrated on the top part of the coated paper. In this study, cationic poly(diallyl dimethyl ammonium chloride) (polyDADMAC, Cartafix VXU) was again used as the surface treatment additive.

3.1.4 Inkjet inks and printing devices

High-speed inkjet printing was carried out on a Versamark® VX5000e[12], which produces inkjet droplets by the continuous stream inkjet method. The printing

---

[10] Registered trademark of BASF AG, Paper Chemicals, 67056 Ludwigshafen, Germany.

[11] Registered trademark of Clariant International AG, Rothausstrasse 61, CH-4132 Muttenz 1, Switzerland.

[12] Registered trademark of Eastman Kodak Company, 343 State Street, Rochester, NY 14650 USA.

press applied dye-base inks, and the main diluent/solvent was water. The surface tensions of the inks were observed to fall within the small range of 53-55 mNm^{-1} (25 °C), depending on dye colour. At 40 °C, the surface tension was in the range of 48–52 mNm^{-1}. Figure 10 shows the surface tension of black and cyan dye inks. The viscosity of cyan dye at 23 °C was 1.05 mPas, and at 40 °C 0.80 mPas, reflecting the expected thinning of ink as a function of temperature rise. Viscosity was measured with a Bohlin Rheometer[13]. In this measurement 10–12 cm^3 of ink are inserted into the space between two concentrically rotating cylinders. The torsion, caused by transmission of the movement of one cylinder relative to the other, through the liquid is then converted via the shear rate applied into a viscosity value. At the same temperatures, black dye had a viscosity of 1.25 mPas and 0.95 mPas, respectively. During printing, Versamark$^®$ VX5000e ink was automatically heated to 40 °C in the printing nozzles – a feature of the press to ensure consistency of ink flow.
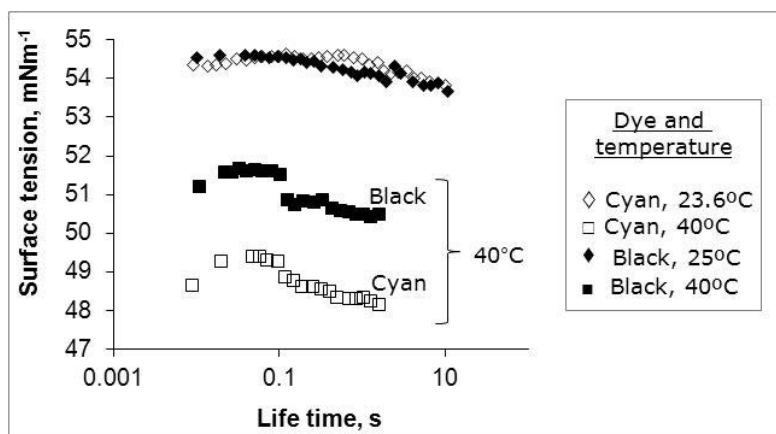
Figure 10. The dynamic surface tension of the cyan and black inks of Versamark$^®$ VX5000e, measured with a Bubble Pressure Analyser KSV BPA800[14], where the bubble life time is measured as a function of air flow. From this, the calculation of the dynamic surface tension is derived and indicates a possible dependence of the surface tension on the air flow speed.

In *Papers IV* and *VII*, laboratory formulated dye-based inks were used, in order to provide examples of inks containing either cationic or anionic cyan dye, respectively. The formula for the inks contained 4 (cationic) or 5 (anionic) wt-% colorant,

---

[13] Malvern Instruments Ltd, Enigma Business Park, Grovewood Road, Malvern, Worcestershire WR14 1XZ, United Kingdom.

[14] Registered trademark of KSV Instruments Ltd, Höyläämötie 11 B, FIN-00380 Helsinki, Finland.

5 wt-% polyethylene glycol (PEG 200), 5 wt-% diethene glycol, 0.3 wt-% Surfynol 465[15] and the remainder being water. The colorant was anionic (Basacid Blue 762[10], Cu phthalocyanine) or cationic (Basonyl® Blau 636[10], Victoria Blue FBO, Basic Blue 7, triarylmethane) (Figure 11). The colorant contained some impurities like sodium and sulphur. There was a slight difference between the surface tensions of the made-up inks: the anionic ink had a value of 49.5 mNm^{-1} and the cationic 55.9 mNm^{-1} (23 °C). This difference can have an effect on the colorant location due to the wetting characteristics in relation to the solid phase surface energy – binder in this particular case. By way of comparison, the surface tension of water at this temperature is 72 mNm^{-1}. The observably different blue tone of anionic and cationic cyan colorant comes from the intrinsic properties of the dyes.

In *Paper VII*, the samples were printed with a desk-top printer, HP Deskjet 3940[16]. The idea was to clarify how the cationic treatment of the coating layer affects the print quality of dye-based inks. All the inks, except the black, were water-based dyes, the black in this case being pigmented. The surface tension of the cyan and magenta ink was 25.0 mNm^{-1}, yellow 26.9 mNm^{-1} and black 50.5 mNm^{-1}.
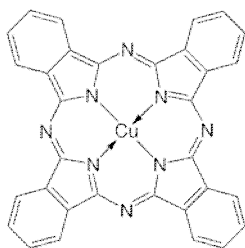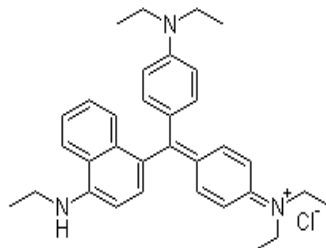
Basacid Blue 762, Cu phthalocyanine   Basic Blue 7, triarylmethane

Figure 11. The structure of Basacid Blue 762 and Basonyl® Blau 636 (Basic Blue 7) cyan colorant.

3.1.5 Substrate: pre-coated base paper

Two base papers (fine paper grade) were used to provide the necessary substrate support for the subsequent various coatings under study. One was used either without pre-coat or had a pre-coat applied in the course of this study, while the other was supplied already pre-coated. The idea of choosing a pre-coated sheet was to prevent the top-coating penetrating into the paper fibre structure.

---

[15] Registered trademark of Air Products PLC. Hersham Place Technology Park, Molesey Road, Hersham, Walton-on-Thames, Surrey KT12 4RZ, UK.

[16] Registered trademark of Hewlett-Packard Company, 3000 Hanover Street, Palo Alto, CA, 94304-1185, USA.

The papers were, respectively:

1. Commercial base sheet, as used for a coated fine paper, 67 gm^{-2}. The pre-coating applied was a typical GCC-based offset coating formulation. This base paper was used in *Papers I, II* and *VII* either with two coating layers of the test inkjet coating formulation or with the separately applied pre-coat and the test formulation as top-coat.

2. Somewhat heavier weight commercially pre-coated fine paper having a grammage of 78 gm^{-2} – this was industrially pre-coated (coarse GCC-based offset), and was used in the curtain coating trial (*Paper III*).

In cases where the application of the experimental coatings failed to deliver sufficient coat weight in a single pass, a double top-coating procedure was adopted. Thus, the coating layers reported in *Paper I* were double top-coated by applying the same coating colour twice with a blade coater in order to achieve the target coat weight of 10 gm^{-2}, which was not attainable with one pass. The first top-coating layer was allowed to dry and after that the second top-coating layer was applied.

In the trial reported in *Paper II*, the fine paper was first pre-coated with a coating layer of 7 gm^{-2} using a film coater (1 000 m·min^{-1}) on both sides of the base paper. The pre-coat had 100 pph of ground calcium carbonate (GCC) with a narrow particle size distribution, having 60 wt-% < 1 µm (Covercarb 60[3]), together with 12 pph styrene-butadiene latex (SB latex, DL966[17]) and 0.6 pph carboxymethylcellulose (CMC, Finnfix 10[18]). The work in *Paper VII* utilized these same papers as in *Paper II*. Table 6 introduces the studied base papers and their pre-treatments before the top-coating application.

---

[17] Registered trademark of Dow Chemicals Company, Dow Europe GmbH, Bachtobelstrasse 3, 8810 Horgen, Switzerland.

[18] Registered trademark of Noviant Oy, Kuhnamontie 2, M-realin tehdasalue, PL 500, 44101 Äänekoski, Finland.

Table 6. The base papers used.

	Base paper 1		Base paper 2
	Commercial fine base paper (67 gm^{-2}) [*]	**Commercial fine base paper (67 gm^{-2})** [*]	**Commercial pre-coated fine paper (78 gm^{-2})**
Pre-coating	No separate pre-coating (replaced by coating twice with same test colour)	100 pph GCC, 12 pph SB latex, 0.6 pph CMC	Industrially pre-coated (GCC-based offset coating)
Application device of pre-coating	-	Pilot film coater	N/A
Published paper(s) where the respective substrate has been used	*I*	*I, II, VII*	*III*

*) Same fine base papers.

3.2 Designed coating structures and binder films, and their production

The work in this thesis concentrates on the effects of coating structures and their components, especially "high diffusion-driving", "less diffusing-driving" and virtually "non diffusion-driving" binders, in respect to their swelling behaviour in water, i.e. during dye-based inkjet ink imbibition. The coating colour binder component effects were studied either separately in 100 % binder only films, or in combination with the coating pigments and other chosen additives in the form of both coating structure filtercakes and tablets, and, finally, as applied in top-coating formulations onto the pre-coated fine paper structures. Additionally, thin layer chromatography (TLC) was made to identify the separation mechanisms of ink colorant and vehicle within the various structures and films, using the same coating formulations as thin layers on glass slides.

The coating trials were performed both on the laboratory and pilot-scale. In the laboratory a film applicator was used (draw down coater, *Papers III, IV, V* and *VII*) and a semi-pilot coater (SAUKKO, *Paper I*) (Pajari *et al.* 2007), and on the pilot-scale a larger pilot coater using a short dwell application blade (*Papers II* and *VII*) and a curtain slide applicator (*Paper III*), respectively. *Paper IV* has details of the binder films, in which the cationic (polyDADMAC) or anionic (polyacrylate) additive was included. In *Papers V* and *VI* coated TLC plates and tablets were produced, and these contained differently charged (cationic/anionic) dispersed pigments. There were also coating layers which had only 1 pph of binder (PVOH or SA latex), each present to provide a physical stabilising effect without dominating the interaction, and to study the primary occupied site of the binder resulting from the formation and drying of the coating layer. The idea contained in *Papers V* and *VI* is to study basic phenomena during liquid (polar and non-polar) absorption. *Paper*

VII discusses results from coating cakes, which were re-ground/refined and the resulting powder exposed to the ink components analyzed by UV-VIS spectrometry.

Table 7 summarizes the coating colours and binder films that were studied. All of the carbonate pigments were sourced directly from pigment manufacturers, and most were in slurry form, and therefore the details of the dispersion agent and its amount are unknown. In the case of dry powder pigment(s), additional dispersant, when used, is described in the individual cases. The study samples of binder films, included films in which the cationic polyDADAMC (Cartafix VXU) or anionic sodium polyacrylate (Polysalz S) was added (1 or 4 pph) into the partially or fully hydrolyzed PVOH.

Table 7. The composition of studied coating colour structures, films and their ionic charge. Polyacrylate refers to anionic sodium polyacrylate. Each amount refers to the parts added per 100 parts of coating pigment.

Pigment			Binder		Dispersing agent (used for pigment makedown)		Additive	Ionic charge	Base paper
Type	Amount (pph)	Form	Type (degree of hydrolysis)	Amount (pph)	Type	Amount (pph)			
GCC	100	slurry	PVOH (partially)	7, 10, 15	N/A	N/A	-	Anionic	1
MCC large	100	slurry	PVOH (partially)	10	N/A	N/A	-	Cationic	1
MCC small	100	slurry	PVOH (partially)	10	N/A	N/A	-	Cationic	1
PCC large	100	slurry	PVOH (partially)	10	N/A	N/A	-	Cationic	1
PCC small	100	slurry	PVOH (partially)	7, 10, 15	N/A	N/A	-	Weakly anionic	1^+, 2^{++}
PCC large	100	slurry	PVOH (partially)	7, 12, 30	N/A	N/A	-	Cationic	1
PCC large	100	slurry	SA latex	7, 12, 30	N/A	N/A	-	Anionic	1
-	-	-	PVOH (partially)	100	-	-	-	Non-ionic	-
-	-	-	PVOH (partially)	100	-	-	Poly-DADAMC, 1 pph	Cationic	-
-	-	-	PVOH (partially)	100	-	-	Poly-DADMAC, 4 pph	Cationic	-
-	-	-	PVOH (partially)	100	-	-	Poly-acrylate, 1 pph	Anionic	-

-	-	-	PVOH (partially)	100	-	-	Poly-acrylate, 4 pph	Anionic	-
-	-	-	PVOH (fully)	100	-	-	-	Non-ionic	-
-	-	-	PVOH (fully)	100	-	-	Poly-DADAMC, 1 pph	Cationic	-
-	-	-	PVOH (fully)	100	-	-	Poly-DADMAC, 4 pph	Cationic	-
-	-	-	PVOH (fully)	100	-	-	Poly-acrylate, 1 pph	Anionic	-
-	-	-	PVOH (fully)	100	-	-	Poly-acrylate, 4 pph	Anionic	-
-	-	-	PVOH (carboxy-lated)	100	-	-	-	Anionic	-
-	-	-	SA latex	100	-	-	-	Anionic	-
MCC large	100	powder	-	-	Poly-acrylate	0.5	-	Anionic	-
MCC large	100	powder	-	-	Poly-DADMAC	0.5	-	Cationic	-
MCC large	100	powder	PVOH (partially)	1, 7	Poly-acrylate	0.5	-	Anionic	-
MCC large	100	powder	SA latex	1, 7	Poly-acrylate	0.5	-	Anionic	-
MCC large	100	powder	PVOH (partially)	1	Poly-DADMAC	0.5	-	Cationic	-
MCC large	100	powder	PVOH (partially)	1	Poly-acrylate	0.5	Poly-DADMAC, 3 pph	Cationic	-
GCC	100	powder	-	-	Poly-acrylate	0.5	-	Anionic	-
GCC	100	powder	PVOH (partially)	1	Poly-acrylate	0.5	-	Anionic	-
GCC	100	powder	SA latex	1	Poly-acrylate	0.5	-	Anionic	-
PCC small	100	slurry	-	-	N/A	N/A	-	Weakly anionic	-
PCC small	100	slurry	PVOH (partially)	1	N/A	N/A	-	Weakly anionic	-
PCC small	100	slurry	SA latex	1	N/A	N/A	-	Anionic	-

[+] in the case of 10 pph binder [++] in the case of 7 and 15 pph binder.

The short dwell applications (blade) in the pilot trials in *Paper II* were performed at a coating speed of 700 m·min^{-1}. The final top-coating layer consisted of 8 gm^{-2}. The recipes and the properties of the coating colours for the respective top-coats are summarized in Table 8. The final moisture content of each coated paper was 5 %.

Table 8. The top-coating colours in pilot trials.

Component	Coating colour labelled according to the binder level, pph					
	7 pph PVOH (partially)	12 pph PVOH (partially)	30 pph PVOH (partially)	7 pph SA	12 pph SA	30 pph SA
PCC large	100	100	100	100	100	100
PVOH	7	12	30			
SA				7	12	30
Polysalz S (sodium polyacrylate)				6	6	6
Measurement						
Solids content, %	25.1	24.3	22.2	28.1	31.0	30.9
Zeta-potential*, mV	2	2	3	-37	-33	-33
pH	8.4	8.5	8.4	8.5	8.2	7.9

*AcoustoSizer II

The role of coating layer thickness on the pre-coated fine paper surface, Base paper 2, was examined using coatings generated with a curtain slide applicator. The speciality small size "PCC small" pigment containing coatings were produced and used for this study. The coating colours had 7 pph or 15 pph of polyvinyl alcohol (Mowiol 40-88) based on 100 pph of pigment. All colours had an additional 0.2 pph of surfactant, Lumiten DF[10]. Lumiten DF is the sodium salt of an ester of sulphosuccinic acid and an isotridecanol ethoxylate. The inclusion of surfactant acted to stabilise the curtain formation. The coating speed was varied from 1 000 m·min^{-1} to 600 m·min^{-1} depending on the applied coating colour weight. The highest speed was used when the coat weight was the lowest and vice versa. The final moisture content of the coated web was 5.1–5.4 wt-%. This means that the drying temperature had to be increased when the coat weight was high.

The inkjet ink penetration through the coating layers was also studied by applying the coating colour on polyethylene plastic film (Imperial NMO[19]). The coatings contained 100 pph of "PCC small" or GCC pigment and the binder was partially

---

[19] Importer Kauppahuone Pesonen, Hermannin rantatie 12 A, PL 8, 00580 Helsinki, Finland.

hydrolyzed PVOH, which amount was 7 or 15 pph. An Erichsen[20] bench-top film coater (Model 288) was used, adopting wire wound spiral applicators (Spiral Film Applicator, Model 358[20]), and the coating layers were dried at 105 °C during 5 min. The produced coating layer thicknesses varied from 2 μm to 35 μm.

3.3 Analytical methods

Several different testing methods were used. The coating layers were mainly characterized with interest focused on their porosity and pore size distribution, as well as the ionic charge. The liquid absorption speed from an applied ink layer into the coating structures was studied with a method in which the gloss change caused by drying inkjet ink on the surface was detected, DIGAT device (Lamminmäki and Puukko 2007). However, the main interest of this work was focused on the mass transport of the ink into the structures and was analyzed with a microbalance, a capacitance-based (Clara) device (Lamminmäki *et al.* 2010) and by thin layer chromatography. The uptake of ink into the binder films was studied with a microbalance, and the colorant distribution by Time of Flight Secondary Ion Mass Spectrometry (ToF-SIMS) and optical microscopy imaging of *z*-direction coating cross-sections. Ultraviolet-visible (UV-VIS) spectroscopy was used in the study of the ab/adsorption by the different coating components. The coated paper samples were printed and the print quality was evaluated using the methods reported in Table 11. Each method is now discussed separately in more detail.

3.3.1 Porosity of coating structures

In *Papers I, III, V and VI*, the porosity of coating layer structures was characterized with several methods: a silicon oil absorption method, as well as water and hexadecane absorption in a microbalance measurement and mercury porosimetry determination. In silicon oil, water and hexadecane measurements the coating layer was immersed in each liquid and the weight change between the liquid saturated and air-filled sample prior to wetting was determined. Care was taken to allow escape of air from within the structure by maintaining a free surface not covered by liquid, relying on capillarity to fill the sample. In all cases, the studied material was a coating layer/structure without the paper, and they were produced with Teflon[®][21] moulds or with a tablet former (Ridgway and Gane 2005). In the mercury porosimetry, the cumulative pore volume and pore size distribution was detected from the intrusion curve as a function of intrusion pressure, applying the

---

[20] Registered trademark of Erichsen GmbH & Co., Am Iserbach 14, D-58675 Hemer, Germany.
[21] Polytetrafluoroethylene, Du Pont.

corrections contained in the software package Pore-Comp[22] to account for pene-
trometer expansion, mercury compression and compression of the sample skeletal
material according to Gane *et al.* (Gane *et al.* 1996). Both coated papers and
coating cakes/tablets were measured. There were some small differences be-
tween the results of the absorption-based measurements and those from mercury
porosimetry. The reasons behind this can be traced to one or more of the follow-
ing: the external pressure that has been used in the intrusion measurements, the
accuracy of pigment tablet size analyses in the case of determining the sample
volume for liquid absorption, the presence of excess external silicon oil and irre-
producibility when wiping off surface excess after the experiment, as well as the
differences in the actual coating layer production (pressure in the tablet former and
non-pressurized, shrinkage only, coating cake forming in the moulds).

3.3.2   Liquid penetration

The absorption mass transport into the coating cake was analysed by using the
microbalance (*Paper VI*) and the liquid movement through the pore networks of
the pigment packing structures with the thin layer chromatography method (TLC,
Paper I and *V*).

<u>Microbalance</u>

In the experimental recording of the uptake of liquid using the microbalance, the
studied pigments were "MCC large", GCC and "PCC small" and binders were
partially hydrolyzed PVOH and SA latex. The coating colours had 100 pph pig-
ment and binder amount was 1 and 7 pph. The dispersing was made with Polysalz
S or polyDADMAC (Cartafix VXU) to generate anionic and cationic coatings, re-
spectively. The coating tablets were produced from coating colours by a wet filtra-
tion system (Ridgway *et al.* 2005 Gane *et al.* 1999) under an external pressure of
20 bar. The tablets were dried at 60 °C overnight. The PVOH uniformity within the
tablets was studied with a Thermo Nicolet Nexus 870 FT-IR spectrometer[23] (IR
spectra from KBr-tablets). The results show that the wire filter side (lower surface)
of the tablet had a higher concentration of PVOH, explained as being a result of
the soluble nature of the PVOH (Figure 12). (For this differential binder distribution
determination, the PVOH content was 0.7 pph, whereas, in the microbalance
study, the binder amount used was slightly higher, 1 pph.) Therefore, the final
tablets fashioned for the microbalance absorption analysis were prepared so that
both sides of the tablet (top and bottom side) were tested, each having the same

---

[22] Pore-Cor and Pore-Comp are a software network model and sample compression correc-
tion software, respectively, developed by the Environmental and Fluid Modelling Group,
University of Plymouth, UK.

[23] Registered trademark of GMI, Inc. 6511 Bunker Lake Blvd., Ramsey, Minnesota, 55303 USA.

time in contact with the liquid, and an average formed. The filtrate that formed during the tablet making procedure was also analyzed with FT-IR spectrophotometry, and the result showed that it also contained traces of PVOH, confirming the soluble nature of the binder.
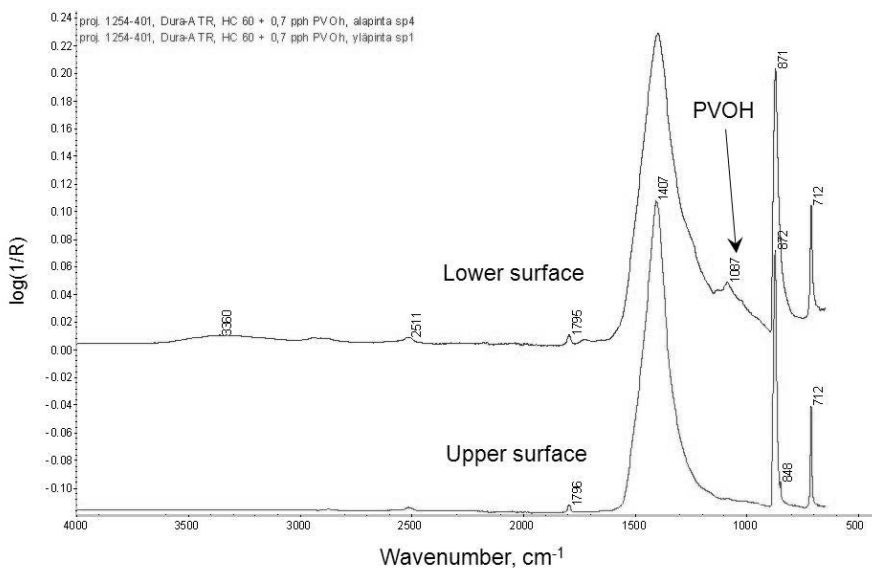
Figure 12. The IR spectra taken from the top and bottom surfaces of the tablet: GCC with 0.7 pph PVOH (partially hydrolysed). Notice the lower PVOH content of the colour in this measurement (= 0.7 pph) compared with the actual tablets made for the microbalance measurement (1 pph).) The lower surface was against the wire filter in the tablet former. The main peak of PVOH locates at the wavenumber 1 087 cm^{-1}. Based on Paper VI (Figure 2).

In the microbalance measurement, the polarity of the liquid, and its effect on imbibition into pigment tablets, was studied using distilled water (100 % polar) and hexadecane (100 % apolar), respectively. The edges of the formed samples were polished and covered with octamethyl trisiloxane/toluene[24] so that the pores of edge areas did not affect the liquid uptake by exterior planar wetting. In the microbalance experiment, the amount of absorbed liquid was measured as a function of time after contact between the sample and the liquid supersource. The uptake of the liquid was measured gravimetrically via an automated microbalance computer interface (Gane *et al.* 1999, Ridgway and Gane 2002). The temperature of the surrounding air was 23.0±1.5 °C. The weight loss due to the water evaporation

---

[24] Provided by Dow Corning GmbH, Postfach 13 03 32, 65201 Wiesbaden, Germany.

during the measurement was taken into account in the results. Hexadecane has a minimal evaporation over this time period.

Thin layer chromatography (TLC)

Both the eluent distance and the gray value change during time were detected in the TLC method. The coating pigment in question was "MCC large" and binders were partially hydrolyzed PVOH and SA latex. The coating layers had 100 pph of pigment and 1 pph binder. The dispersing of the pigment was made anionically by using sodium polyacrylate (Polysalz S) and cationically using polyDADMAC (Cartafix VXU). The coating colours were applied on glass plates with an Erichsen film applicator (Model 288). The applied coat weight was about 100 gm^{-2}. The coating layers were dried at room temperature overnight. De-ionized water was the eluent in the TLC analysis and the adsorbate (substance adsorbed) was provided by a range of concentrations of anionic cyan colorant (Basacid Blue 762). During the TLC development, the term "eluent" in our case refers to the water phase (ink vehicle equivalent) of a solution of dye applied as a supersource reservoir, i.e. not the classical eluent travelling past a previously dried colorant, but a carrier. The distance of the eluent (water phase) movement over time was measured. Simultaneously, the gray level of surface reflectance was detected with a digital camera (Dolphin F145C[25]). The illumination of the surface was made on the same side as that viewed by the camera (Figure 13). The measurements were made at a temperature of 20.0±1.5 °C. The image analysis software Image-Pro 6.2[26] was used to parameterise the image. The detection area started about 0.5 mm above the advancing eluent front and the total detection area was 100 mm^2. The gray level of the undeveloped plate was adjusted to a gray level of 150. The distance was expressed towards the base of the TLC plate passing from unsaturated to saturated sample.
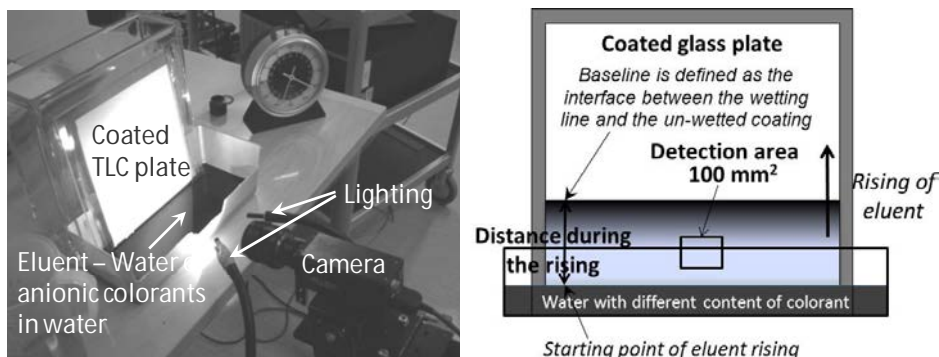
---

[25] Registered trademark of Allied Vision Technologies GmbH, Taschenweg 2a, D-07646 Stadtroda, Germany.

[26] Registered trademark of Media Cybernetics, Inc., 4340 East-West Hwy, Suite 400, Bethesda, MD, 20814-4411 USA.

Figure 13. The TLC development system and the location of gray value measurement and the distance of eluent front.

Capacitance-based measurement

The capacitance-based Clara device (Lamminmäki *et al.* 2010) Figure 14, *Papers II, III* and *VII*) was used both in the analysis of coated films as well as coated papers. The Clara measures the capacitance change during the liquid penetration through the sample. The maximum value of capacitance is about 190 pF, and this value depends on the capacitance of the plastic film backing the sample. When the capacitance reaches the maximum value, it is interpreted that the ink has penetrated through the whole paper structure. Figure 15 shows some examples of the resulting curves when different external pressure was used. We can assume that in the case of no external pressure the absorption is driven by the capillary wetting force in coating pores fine enough to exert a Laplace pressure drop (Oliver 1982) and by any inter-polymer liquid diffusion. In larger pores the movement is followed by thin layer wall wetting and surface and/or bulk vapour diffusion. When external pressure is small compared to the capillary pressure in the fine pores liquid starts to be forced into the larger pores under Poiseuille flow whilst capillary pressure filling continues as above. As the pressure is raised higher than the capillary force, or when all the pores up to and including the wetting front are filled, then the action is by permeation flow according to Darcy's law in saturated structures. The bimodal behaviour of each curve illustrates the competition between the initial capillary wetting and the permeable flow characteristic once capillaries/pores behind the wetting front are filled.
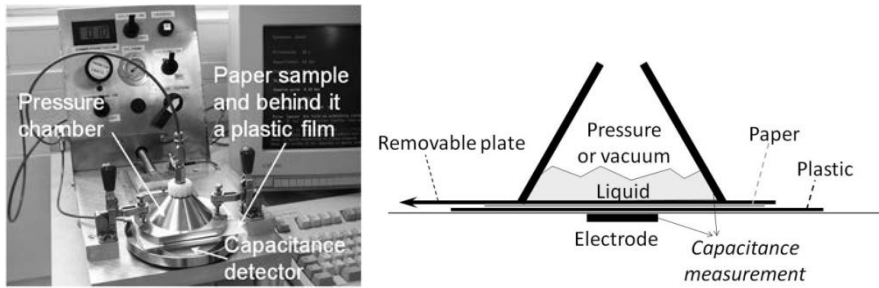
**Figure 14.** The structure of the Clara device.
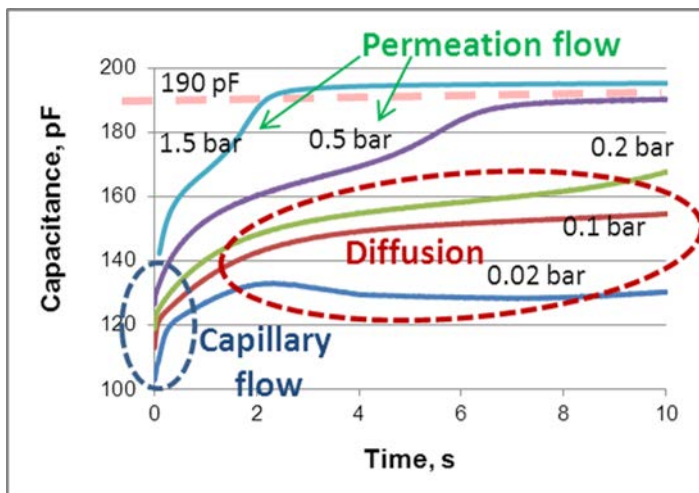
Figure 15. Result curves of Clara at five different external over-pressures: "PCC large" with 7 pph PVOH coated paper. The used liquid was cyan dye-based ink (used in Kodak Versamark® VX5000e). Based on Paper II (Figure 3).

The connection between the penetration depth and the capacitance value was evaluated by studying coating pigment cakes of GCC (lower porosity), "PCC small" (higher porosity) and "PCC small" with 7 pph SA latex (thickness 294–540 µm) into which different amounts of molten candle wax, containing a colorant for ease of observation, were allowed to absorb. The idea was that the wax fills partially the porosity of the coating structure and it simulates the liquid front at a certain depth within the sample. The capacitance of wax is on the same level as the relative highly porous inkjet PCC coatings, and clearly greater than air. The wax (partial insulator) in the coating structure does not interfere with skeletal connectivity, so the capacitance would be expected to rise. The capacitances (average from the results between 1 Hz and 1 000 Hz) and the wax imbibition distances (relative distance = wax distance divided with the sample thickness) were meas-

ured with another device than the Clara because the coating cakes were too small to be studied with the Clara. In this device, the detection area was 5 mm in diameter using a round detector. Figure 16 shows that, as the depth of wax increased, the higher were the capacitance values in the case of high porosity coating ("PCC small" and "PCC small" + 7 pph SA) layers. The reference value for the dielectric constant of plain candle wax was similar to, for example, polyethene and Teflon®, which have dielectric constants around 2.25 and 2.1, respectively. The action, therefore, is confirmed to be that of wax replacing air in the coating structure, and wax has a higher dielectric constant (~2) than air (~1).

The capacitance of air was lower ($5.55 \cdot 10^{-14}$ F) than that of wax ($1.04 \cdot 10^{-13}$ F). In the case where air plays very little role in the coating layer capacitance, as in the GCC coating case (Figure 16), it would be expected that as a low porosity structure with high skeletal connectivity starts to fill with wax the result trends toward wax, i.e. wax replaces the particle contact with a lower dielectric constant. On the other hand, if air plays a large role in the coatings, which have little skeletal connectivity (as for inkjet porous coatings, for example, where the particles hardly touch each other and are not rich in dispersant), then the opposite will happen – the air which isolated the particles gets filled with wax of higher dielectric constant. This means that the use of wax is a way of determining the connectivity between particles made by conductive charged dispersant. This model experiment confirms that capacitance-based measurement can be used in the evaluation of liquid penetration depth.
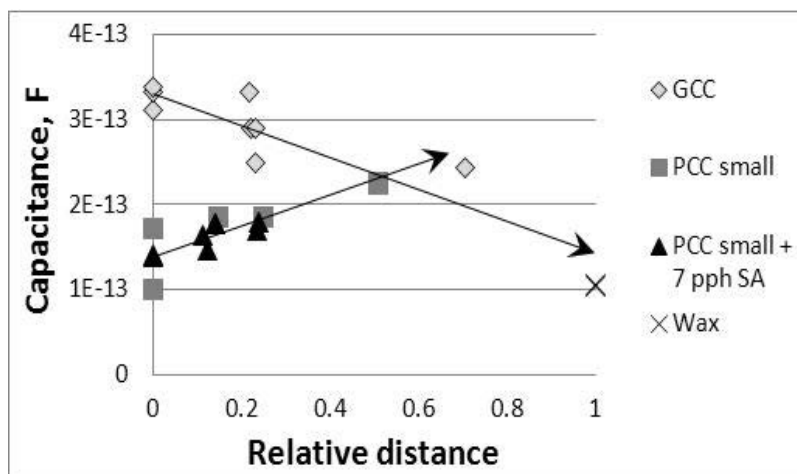
Figure 16. A connection between relative distance and capacitance determined using molten candle wax, containing a colorant for ease of observation, imbided into coating cake structures. Capacitance was measured with a Hewlett-Packard 4192A LF Impedance Analyzer with a 16451B Dielectric Test Fixture (Electrode-B). Based on Paper III (Figure 2).

If the finest pores are rendered inactive in respect to capillarity by the presence of swelling binder, the diffusion into the binder polymer network, represented in Figure 15, can be initiated at the shortest times once liquid contact is made, albeit that the volumes involved are at first small, corresponding to Hypothesis I.

From the capacitance result curves we can calculate the penetration depth and speed. Paper thickness, d_{paper}, in the *z*-direction can be divided into the dry, $d_{dry}(t)$, and wet, $d_{wet}(t)$, parts during the measurement. In the limiting case where dimensional changes on wetting are limited, d_{paper} remains constant.

$$d_{paper} = d_{dry}(t) + d_{wet}(t) \tag{22}$$

The total capacitance C_{tot} is the capacitive impedance series sum of the plastic capacitance, C_{pl}, coming from the plastic sheet under the sample, and the sample capacitance $C(t)$:

$$1/C_{tot} = 1/C(t) + 1/C_{pl} \tag{23}$$

The total wetted paper has practically no impedance (pure conductor), and thus the capacitance of paper depends on the thickness of the dry paper.

$$C(t) = A\varepsilon/d_{dry}(t) => d_{dry}(t) = A\varepsilon/C(t) \tag{24}$$

where A is the area and ε is the dielectric permittivity of the material.

The thickness of the wet part of the paper, which we estimate to be the penetration depth of the water front, can be calculated by combining equations 22, 23 and 24:

$$d_{wet}(t) = d_{paper} - A\varepsilon/C(t) = d_{paper} - A\varepsilon(1/C_{tot} - 1/C_{pl}) \tag{25}$$

The liquid penetration distance is thus

$$d_{wet}(t) = d_{paper} \left[1 - \frac{\dfrac{1}{C_{tot}(t)} - \dfrac{1}{C_{tot}(t=\infty)}}{\dfrac{1}{C_{tot}(t=0)} - \dfrac{1}{C_{tot}(t=\infty)}} \right] \tag{26}$$

In the capacitance-based measurement the over-pressure acts during the whole measuring time, which is a different situation than in the case of an inkjet ink droplet hitting the surface and then becoming imbibed. The other difference from reality is that the offered ink amount is greater than in the case of inkjet ink application.

3.3.3 Absorption of liquid into binder films

The absorption capability of binder films was studied in *Paper IV*. The SA latex films were produced with a draw down coater (drying in an oven at 105 °C for 5 min time) and PVOH films with Teflon® moulds. The absorption of liquid dye

solution was detected gravimetrically, and the samples for cross-section analysis were prepared by embedding the film in an LR White resin[27] and placing them in a refrigerator to reduce smearing of the dye. The cross-sections were then imaged in a light microscope. The colorant separation from the ink vehicle was studied with Time of Flight Secondary Ion Mass Spectrometry (ToF-SIMS) using a lithium tracer in the liquid water phase, and the water type, i.e. free or bound water in the binder film moisture content after absorption, determined with a differential scanning calorimeter (DSC) by observing the thermal energy of binding.

3.3.4 Absorption/adsorption of liquid colorant by coating components

The effect of coating components on the inkjet colorant absorption and/or adsorption was tested by using the measurement procedure that has been introduced in Figure 17. UV-VIS analysis has been used before in the inkjet ink adsorption study by Kallio *et al.* (Kallio *et al.* 2006), Shi *et al.* (Shi *et al.* 2004) and Hartus (Hartus 1998), but their sample preparation diverged from the method used here. Table 9 shows the coating colour formulations, and the layers of coatings produced from these formulations were formed in Teflon® moulds by letting the slurry dry at room temperature (23 °C). This meant that all components of the coating colours remained in the coating layer structure after drying. The dried coating layer was then ground with a homogenizer (three grinding balls with diameter 1 cm, at a rotation frequency of 30 s^{-1}) for 2 min. By grinding the pigment coating structure systems, the extended pore network structure effect present in coating cakes or layers could be avoided, thus enabling the structure surface-related phenomena to be isolated. The grinding effect was assumed to be similar for each coating layer, and that the sample treatment was assumed to provide a sufficiently homogeneous distribution of structural components despite the potential for some soluble species migration during drying. During the grinding, some newly exposed surfaces of the pigment could appear that would otherwise be covered with binder. Additionally, new binder surfaces could also be exposed as the binder film breaks. However, these effects were assumed to be minimal as the energy delivered during grinding was relatively low. The ground powder was screened through a 300 µm slit screen, to ensure that the powders did not contain inhomogeneous lumps and that the particles of the resulting coating "mini-structures" were as monosize as possible.

---

[27] Registered trademark of Electron Microscopy Sciences, 1560 Industry Road, Hatfiled, PA 19440, USA.

Table 9. The studied "MCC large" coating structure systems. Zeta-potential was measured with an AcoustoSizer II.

Coating structure system	Dispersing agent, amount added to define the charge of the surface	Binder, amount	Zeta-potential, mV
MCC large powder in water	-	-	21
Anionic MCC large	Sodium polyacrylate, 0.5 pph	-	-37
Anionic MCC large + 7 pph PVOH	Sodium polyacrylate, 0.5 pph	PVOH, 7 pph	-12
Anionic MCC large + 7 pph SA	Sodium polyacrylate, 0.5 pph	SA latex, 7 pph	-37
Cationic MCC large	polyDADMAC, 0.5 pph	-	24
Cationic MCC large + 7 pph PVOH	polyDADMAC, 0.5 pph	PVOH, 7 pph	11

In the UV-VIS analysis of the adsorption phenomenon anionic ink was used, which was formulated in the laboratory to be sure that it contained only one colorant. The ink contained 5 wt-% anionic colorant (Basacid Blue 762), 5 wt-% polyethylene glycol (PEG 200), 5 wt-% diethene glycol, 0.3 wt-% Surfynol 465 (surface active agent) and the rest being water. The surface tension of the ink was 49.5 mNm^{-1} (measured at 23 °C using a Bubble Pressure Analyser KSV BPA800 tensiometer). The ink was diluted with water (7 cm^3 ink per dm^3 water, recalling that the original ink contained 5 wt-% dye colorant). 10 cm^3 diluted ink was mixed with 5 g of the produced coating structure system powder to form a suspension of the powder particles in the diluted ink. Mixing was continued for a series of selected times (5 min, 30 min, 2 h and 18 h). Then each mixture was centrifuged, and the remaining dye concentration in the filtrate was analyzed in the UV-VIS spectrophotometer. The experiments were carried out at room temperature (23±2 ºC). The UV-VIS spectroscopy quantified the relation of the intensity of incident, I_0, and transmitted, I, radiation as a function of wavelength in the ultraviolet-visible spectral region. The absorbance result was detected at a wavelength of 610 nm, where the absorption maximum of cyan dye was located. The maximum absorbance ($A = -\log(I/I_0)$) value of colorant at 610 nm was about 3.7. Repetitive trials showed that the values varied between ±0.2 from the average value.
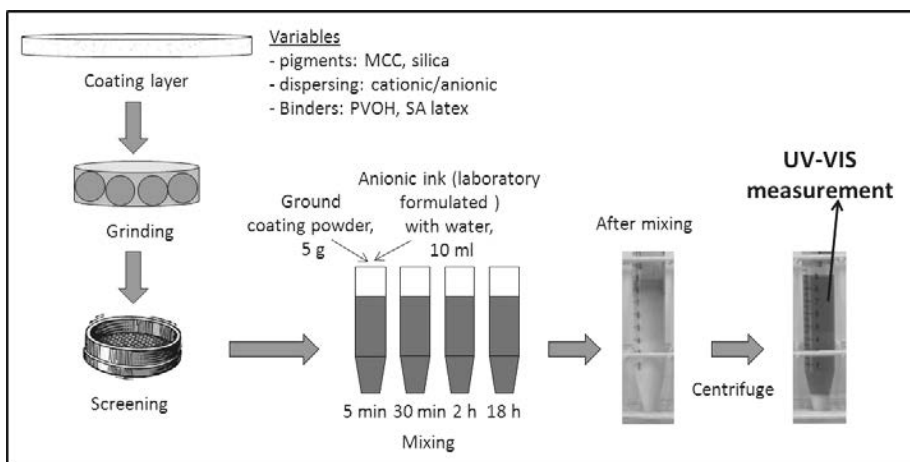
Figure 17. The treatment of coating structure before UV-VIS analysis in the ad/absorption study.

3.3.5 Use of more conventional paper testing methods

More conventional paper testing methods (Table 10) of the coated papers were also applied: coat weight, thickness, air permeance, surface energy (contact angle of liquid) and scanning electronic microscopy (SEM). The liquid absorption speed into the surface was studied with a DIGAT device (Lamminmäki and Puukko 2007), which detects the time from the arrival of a sprayed liquid to the moment when the gloss of the liquid has disappeared. This is determined by measuring the voltage change in a glossmeter. The light source of DIGAT is a red laser (wavelength 633 nm) with light incidence and detection angle 20° from the horizontal plane. The used ink in the DIGAT measurement was cyan dye-based ink from Versa-mark® VX5000e, and the applied ink amount was 8 gm^{-2}.

Table 10. Methods used in the basic property characterization of coating layers.

Property	Measurement	Description of method	Principle
Electrical charge of coating colour	Zeta-potential	Applying a high frequency electric field across the coating colour and measuring an ultra-sound signal generated by the motion of the charged particles in the alternating field.	Electro-acoustic technique
Pore volume	Si-oil porosity	Silicon oil absorption amount after one hour immersion time vs. the weight of sample before adsorption.	Gravimetric
Cumulative pore volume	Mercury porosimetry	The intrusion of mercury into the structure under the influence of low ($0 < \Delta P < 140$ Pa) and high ($140 < \Delta P < 440$ Pa) pressure (adopting the Pore-Comp correction)	Mercury intrusion
Pore size distribution	Mercury porosimetry	The differential mercury intrusion into the structure under the influence of low ($0 < \Delta P < 140$ Pa) and high ($140 < \Delta P < 440$ Pa) pressure (adopting the Pore-Comp correction)	Mercury intrusion
Permeance	Air permeance, ISO2471:2008	Parker Print-Surf air permeance measurement using 20 kPa measuring pressure (permeation resistance of a material of undefined thick-ness)	Air leak

3.3.6 Print quality

Printing was performed primarily with a high-speed inkjet printing press (Versa-mark® VX5000e), which adopted aqueous-based dyes. The printing speed was 50 m·min^{-1} (*Paper III*) and 100 m·min^{-1} (*Papers I, II, III*), and the drying drum and hot air dryer were set to a temperature of 70 °C (*Paper III*), 80 °C (*Paper I, II*) and 100 °C (*Paper I*). The ink amount was adjusted to match with the ink demand of a commercial coated fine paper which the printing press manufacturer recommend-ed. After adjustment, each paper was printed with these commercial paper values so that the ink amount on the surface was maintained constant. Alternatively, in *Paper VII*, the printing was run on an HP Deskjet 3940 desk-top printer because the abovementioned inkjet printing press was no longer available. This printer used the drop-on-demand inkjet technique (piezo crystal). It also applied water-

based cyan, magenta and yellow dye colorants. There were slight differences between the surface tensions of the inks of this latter printer. The print quality was analyzed by means of print density, print-through, bleeding (line width, raggedness, edge width), mottling and water fastness tests, as Table 11 summarizes.

In the water fastness test, the colour change was measured with a spectrophotometer (GretagMacbeth SpectroEye[28]) by using the basic formula given in the standard SCAN-P 49:83:

$$\Delta E = \sqrt{\Delta L^{*2} + \Delta a^{*2} + \Delta b^{*2}} \tag{27}$$

where

$$\Delta L^* = L_{after}^* - L_{before}^* \tag{28}$$

$$\Delta a^* = a_{after}^* - a_{before}^* \tag{29}$$

$$\Delta b^* = b_{after}^* - b_{before}^* \tag{30}$$

The term L^* is a function of Y-value (luminous reflectance value), and a^* and b^* are calculated using the tristimulus values X, Y and Z. The subscript term "before" refers to the measured value before water treatment and "after" the result after a 5 min de-ionized water immersion treatment.

The print-through and show-through were measured by using a flatbed scanner (Epson Perfection V700 Photo[29], resolution 300 dpi). The printed surface was observed from the reverse side of the printed paper (print-through) or through a further sheet of un-printed paper (same paper as the printed material, show-through). The detection area was 30 x 30 mm^2. The image was analyzed with the MATLAB[30] based PTA[31] program. The colour difference on the printed surface was reported as Delta E94 (ΔE94), which followed the CIE 1994 colour difference equation. Mäkinen et al. (Mäkinen et al. 2007) showed that CIE 1994 takes better account of the different colours of the printed surface than conventional CIELab* described colour in terms of lightness, red-green and blue-yellow axes. In CIE 1994, the colour difference, ΔE94, is defined using the changes in lightness (ΔL^*), chroma (ΔC^*) and hue (ΔH^*):

---

[28] Registered trademark of Gretag-Macbeth AG, Althardstrasse 70, CH-8105 Regensdorf, Switzerland.

[29] Registered trademark of Espon Corporate, 3840 Kilroy Airport Way, Long Beach, CA 90806, USA.

[30] Registered trademark of The MathWorks, Inc. 3 Apple Hill Drive, Natick, MA 01760-2098, USA.

[31] Name of the computer program that has been written at the University of Joensuu, Tulliportinkatu 1, 80100 Joensuu, Finland.

$$\Delta E_{94} = \left[\Delta L^{*2} + \left(\frac{\Delta C^*}{1 + 0.045\overline{C}^*} \right)^2 + \left(\frac{\Delta H^*}{1 + 0.051\overline{C}^*} \right)^2 \right]^{0.5} \tag{31}$$

Where

$$\overline{C}^* = \sqrt{C_1^* C_2^*} \tag{32}$$

$$\Delta C^* = C_2^* - C_1^* \tag{33}$$

$$C^* = \sqrt{a^{*2} + b^{*2}} \tag{34}$$

$$\Delta H^* = \sqrt{\Delta a^{*2} + \Delta b^{*2} - \Delta C^{*2}} \tag{35}$$

and where subscript number 1 refers to an unprinted area and number 2 to the printed area.

The strike-through describes the ink penetration and show-through the opacity of the sheet. Together they define print-through (Larsson and Trollsås 1972). Thus, the print-through can be expressed as

$$\text{Print-through = Show-through + Strike-through} \tag{36}$$

In inkjet prints, the ink vehicle and colorant penetrates into the paper structure and the print becomes more visible from the reverse side as the penetrated colorant amount and depth increases. In the final printed product the role of ink vehicle in the print-through is probably lower than in offset printed products, because most of the ink vehicle will evaporate out of the structure whereas in offset the oil leads to persistent translucency.

The printed surface bleeding was evaluated in terms of edge width (Figure 18), line width and raggedness. In this evaluation, the printed line was scanned with the Epson Perfection V700 Photo scanner (resolution of 2 400 dpi). From the scanned image, the gray level profile of the printed line was measured with an image analysis program. Two definition points, A and B, were defined from the gray values. Point A was 15 % brighter than the darkest region and B 15 % darker than a background (in some cases the definition of A and B set to 10 % was also adopted). The zero value was defined as the black surface, and the white given a value of 254. Each unprinted paper was adjusted to the gray value 170. The line width is defined as a mean normal separation between the printed line and the background un-printed area outline, i.e. as an average distance between the 90 % reflectance and 10 % reflectance boundaries of the image. The raggedness of the line was defined by ISO-13660. This value is the standard deviation of the residuals

from a line fitted to the 60 % reflectance threshold of the line. The raggedness describes the geometric distortion of the edge from its ideal position.

Edge of two different colours
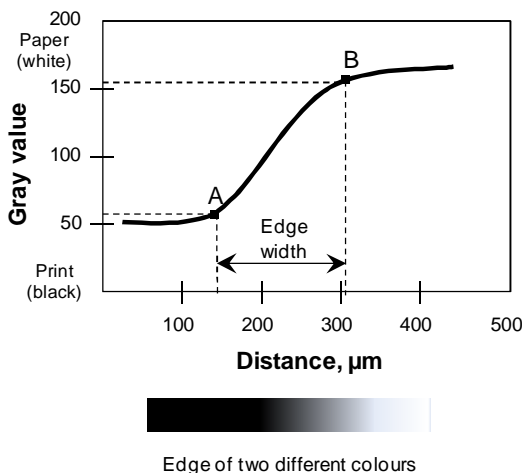
Figure 18. The evaluation of edge width in the bleeding measurement.

The mixing of black and cyan ink at the high-speed inkjet press was also detected on-line with a camera system (*Paper III*), which was located 54.2 cm distance from the yellow nozzles (Figure 19). The target of this camera detection during the trial was to clarify the rate of bleeding. The on-line figures were detected with a digital camera (Dolphin F145C, i.e. the same camera that was used in the TLC detection).
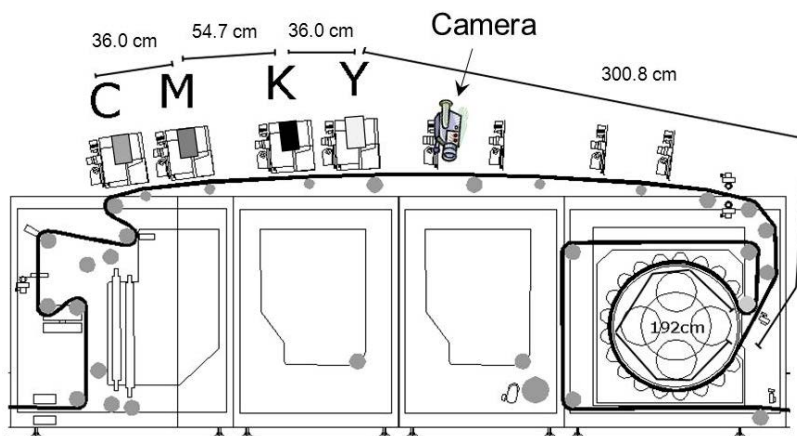
Figure 19. The location of inkjet ink nozzles and the video camera at the Versa-mark VX5000e press trial. The meaning of the abbreviation letters above the inkjet print heads: C – cyan, M – magenta, K – black and Y – yellow. The distance from the yellow print head to the camera was 54.2 cm.

Table 11. Measurements in the print quality evaluation.

Property	Description of method
Print density	GretagMacbeth D196 spectrophotometer.
Print-through	The reverse side of printed area was scanned and analyzed with image analysis (MATLAB based PTA program). Result was Delta E94.
Show-through	The printed area was scanned through a contacting un-printed sheet of the same material and analyzed with image analysis (MATLAB based PTA program). Result was ΔE_{94}.
Mottling	Printed area was scanned (Epson Expression 1680 Pro, 300 dpi) and the scanned figure was manipulated mathematically with a wavelet transform (PapEye program[32]) to evaluate the unevenness of printed (at least 20 mm^2) area. The resolution-dependent values of the mottling curve are used to determine the mottling index that corresponds to the visual impression of the human eye.
Bleeding (line width, edge width, raggedness)	Imaging the line and calculating from the gray value changes the edge width, the line distance of edge area and the total line width.
Water fastness	Putting the printed sample into de-ionized water for 5 min immersion, and measuring the print density and CIELab* values with a spectrophotometer (SpectroEye, enhanced polarization filter according to ISO/DIS 13655) before and after water treatment.
On-line ink mixing measurement	Detecting with video camera a black line printed on a prior applied cyan surface during the high-speed inkjet printing trial – without inter colour drying.

3.3.7 Summary

The main interest for the study of the coating layers was directed toward the absorption and adsorption properties in relation to inkjet ink vehicle and colorant. The thesis Hypotheses were individually challenged by considering the effects of pore structure on capillarity and permeability to decouple these from interpolymer liquid diffusion (binder swelling) and surface charge properties, affecting the ab- and adsorptive diffusion dynamic, respectively. Each physical property was studied using a variety of coating pigments with either anionic or cationic charge introduced on their surface, together with combinations of PVOH types or SA latex, identifying swelling properties and permeability constraints of the binders. Additionally, ink colorants with different charge were investigated to complement the coating charge experiments. Finally, coated papers were used to visualise the impact on print quality of the parameters investigated, and a specially prepared cationic surface treatment was evaluated as a fixing agent for anionic dye to cap-

---

[32] Registered trademark of Tapio Technologies, Nuijalantie 13, FI-02630 Espoo, Finland.

ture the dye effectively at the coating surface. Table 12 summarizes the used sorption methods and in which paper each method has been used.

Table 12. Summary of methods used in the coating layer liquid sorption measurements and the colorant final location study.

Property	Measurement	Description of method	Principle	Paper(s)
Absorption rate and amount into the coating	Microbalance	Liquid transport into the porous structure on both the short and long timescales.	Gravimetric	*VI*
Absorption rate and adsorption of colorant in the coating	Thin layer chromatography (TLC)	TLC liquid rising distance and gray level change – videoing during water or inkjet colorant rising in coating layer – as a function of time.	Eluent distance, gray level	*V*
Absorption rate and permeation through the coating	Clara	Liquid movement through the sample, measuring capacitance change over time.	Capacitance change	*II, III, VII*
Liquid thin film absorption speed	DIGAT	Liquid penetration into the surface structure from given ink volume arriving at and disappearing into the structure.	Gloss change recorded as glossmeter voltage	*I, II, III*
Liquid uptake rate of binder films	Microbalance	Liquid/moisture uptake of binder films over time.	Gravimetric	*IV*
Water phase distribution	Time of Flight Secondary Ion Mass Spectrometry (ToF-SIMS)	The distribution of chemical compounds in the cross-sectioned sample as a function of depth (lithium as a tracer for the vehicle imbibition path).	Detecting ions/electrons released from the surface	*IV*
Colorant location/ distribution	Cross-section optical microscopy imaging and image analysis	Printed sample, LR White resin embedding and placing into refrigerator, cutting with microtome, imaging in a light microscope.	Optical microscopy and imaging	*I, II, III, IV*
Water types	Differential scanning calorimeter (DSC)	The binder film analyzed in DSC at two moisture contents. Detection of difference in the amount of heat required to increase the temperature of a binder sample.	Calorimeteric	*IV*
Colorant ab/adsorption into/onto the coating components	Ultraviolet-visible (UV-VIS) spectroscopy	Powder-form pigment system mixed with ink, centrifuged, filtrate (liquid phase) analysis by UV-VIS spectrometry.	Colorant absorbance of the liquid phase	*VII*

# 4. The structural effect of the coating layer on inkjet ink imbibition

The porosity and pore size distribution of the coating structure determine how much, in which direction and at what speed the coating layer absorbs the inkjet ink. By selecting correctly amongst the various speciality coating pigments one can control to a large extent the inkjet ink imbibition into the structure. On the other hand, the binder of the coating layer, which is often a high binding power capacity polymer, like polyvinyl alcohol (PVOH), influences the ink movement by changing both the coating structure and its pore network characteristics, and in the case of it being water soluble can interact dynamically during the penetration. The role of binder in combination with various pigments will be the main discussion point in this chapter, and a more detailed discussion of binder properties alone affecting liquid colorant interaction will be the topic of the next chapter.

4.1 Impact of coating pigment type and binder selection on the structure formation of the coating layer

The pigment selection is probably the most important parameter in the formation of the porosity and the pore network structure, including pore size distribution in the coating layer. There exist many types of structural pigments consisting of calcium carbonate as the main or starting material. The studied pigments of this thesis were introduced more closely in the section "3.1.1 Calcium carbonate inkjet coating pigments". The first one was standard ground calcium carbonate (GCC). Two further pigments were GCC subsequently modified to generate high surface area and internal pores (MCC), differing in respect to particle size ("MCC large" and "MCC small") and the last two precipitated calcium carbonate (PCC), differing similarly in respect to particle size. "MCC large", "MCC small" and "PCC large" pigments had both intra- and inter-particle pores which produced a coating layer with a discrete bimodal pore size distribution – described further below. The "PCC small" pigment had mainly nano-size particles with occasional agglomerates only.

**Coating tablets and cakes (coatings without the base paper)**

The results of mercury porosimetry from three out of the five studied $CaCO_3$ pigments have been introduced more closely in *Paper VI*. Figure 20 shows the pore volumes and pore size distributions of "MCC large", GCC and "PCC small" pigment tablets, which were produced with the tablet former (Ridgway and Gane 2005). All pigment slurries were made by using an anionic dispersing agent. The ground calcium carbonate produced the lowest specific pore volume, reflecting the high packing factor for the broad size distribution GCC. The finest pore diameters were reached with the "PCC small" pigment, which had the smallest particle size (20–30 nm), but nonetheless produced a higher pore volume than the GCC. The "MCC large" pigment, with its discrete bimodal pore size distribution, developed the greatest pore volume and displays a dual pore size distribution reflecting the structure of the coating layer having both 20–60 nm pores and larger pores in the region of 200–800 nm. The finer diameter peak of the "MCC large" coating structure describes the intra-particle pores, and the larger diameter peak the inter-particle pores.

A   B
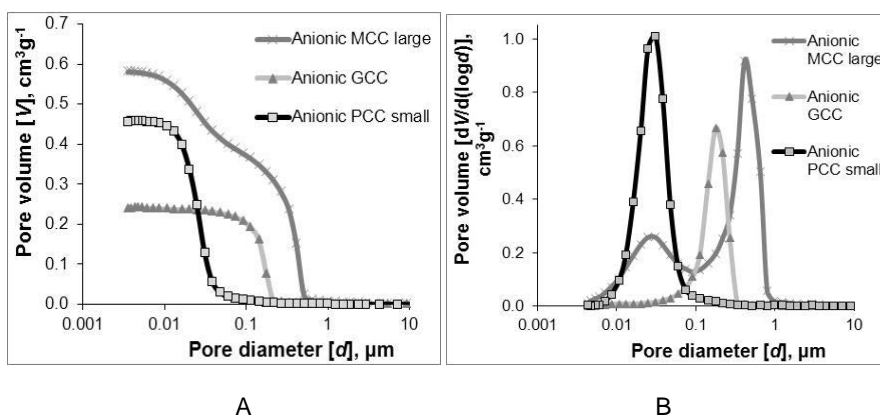
Figure 20. The specific pore volumes (A) and the pore size distributions (B) of "MCC large" GCC and "PCC small" coatings, measured from pigment tablets. Figure B is based on Paper VI (Figure 4).

The fractional pore volumes (%) of these same coating pigments and the pigments with PVOH or SA latex binder have been introduced in Figure 21. "MCC large" and "PCC small" pigments produced very similar pore volume within the coating tablets, whereas the ground calcium carbonate had clearly lower pore volume, as the prior mercury porosimetry results already showed. The addition of 7 pph PVOH binder into the "MCC large" pigment structure decreased the pore volume, whereas the addition of SA latex had very minimal effect comparing the pore volume of the pigment system alone without binder. The PVOH can transfer into the pigment intra-particle pores, as the results later will show, and therefore the pore volume is

diminished. The SA latex does not fit into the intra-particle pores (20–60 nm) because of the relatively large latex particle size of 180 nm, and therefore the porosity of the latex containing coating diverges from the porosity of the PVOH containing coating. In the case of GCC and "PCC small" pigment coatings, where the structure had a mainly monomodal pore size distribution, the addition of SA latex decreased the pore volume more than the addition of PVOH. In this case, the SA latex has filled the structure, whereas the PVOH has probably become transported more out of the tablet during the tablet forming process than during the forming of the "MCC large" pigment tablet.
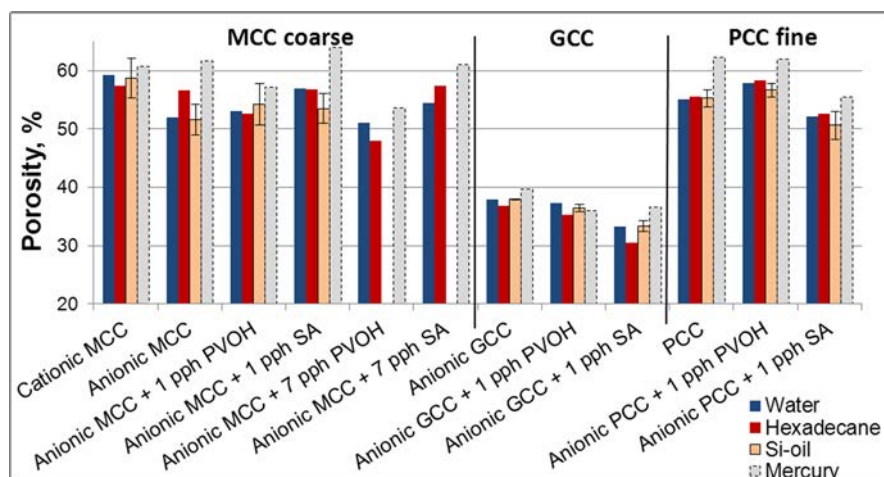
Figure 21. The porosities of "MCC large", GCC and "PCC small" pigment structures with and without the selected binders. Measurements were made by using the absorption of silicon oil, water and hexadecane and the penetration of mercury under different applied pressures. Before the abbreviation of pigment type there is added the dispersing agent nature: "anionic" means that the pigment has been dispersed with anionic dispersing agent (sodium polyacrylate). Based on Paper VI (Figure 3).

The pore size distribution of coating tablets containing the chosen binders was also measured by mercury porosimetry. Figures 22A, 22B and 22C show the effect of 1 pph binder addition on the pore size distribution for each pigment. As the previous results of the coating pigments showed, the "MCC large" pigment produced a coating layer with a dual pore size distribution, and this structure characteristic could also be seen at a binder content of 1 pph. The addition of PVOH into the coating colour decreased the inter-particle pore diameter from 410 nm to 330 nm and the SA latex addition increased it to 790 nm. The result indicates that the PVOH fills some of the porous structure, whereas the latex produces some larger pores probably due to the repulsion of latex (anionic) and pigments (anionic, -37 mV) at the depletion flocculation stage (Ridgway *et al.* 2011). SA latex does

not fit into the intra-particle pores, and therefore the porosity of the coating layer diverges from the porosity of the PVOH containing coating. Thus, as the binder type is changed from PVOH to styrene acrylate latex (SA), the formed coating layer structure changes also.

The addition of 1 pph PVOH to the "MCC large" coating did not influence the size of intra-particle pores, but at 7 pph PVOH content there is already a decrease in the amount of the smallest pores, as will be illustrated later in Figure 27. 1 pph PVOH or 1 pph SA had a very minimal influence on the pore size distribution of ground calcium carbonate (Figure 22B). The 1 pph addition is such a low amount that it does not significantly show in respect to pore filling. The same could be seen in the structural results of adding small amounts of binder to the "PCC small" pigment (Figure 22C).

A – "MCC large" pigment   B – GCC pigment

C – "PCC small" pigment
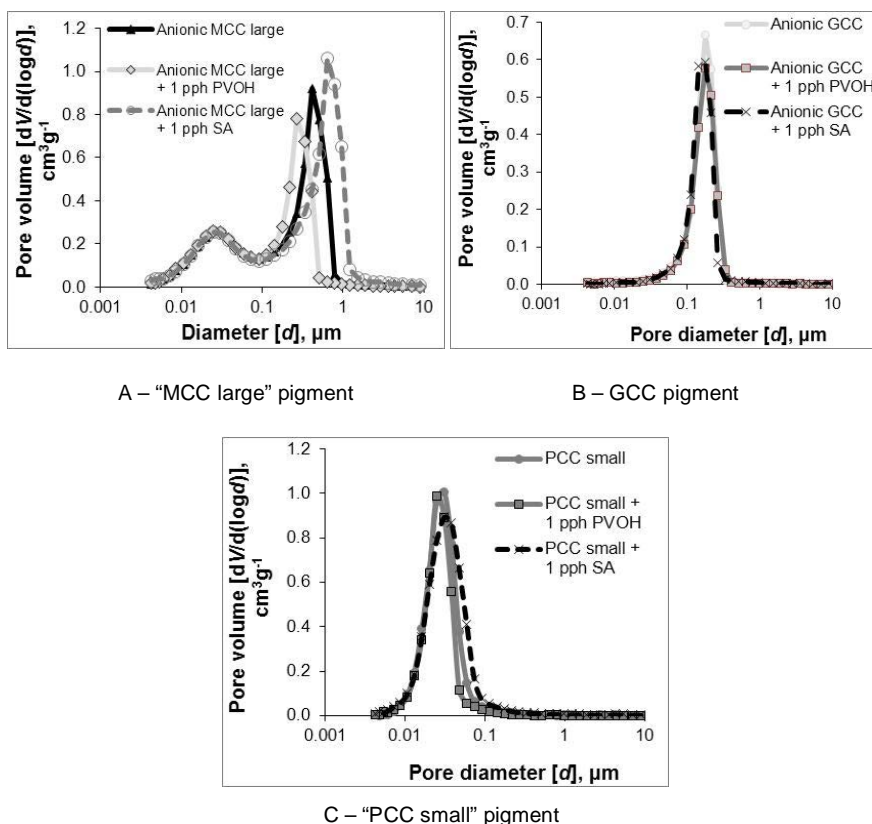
Figure 22. The pore size distributions of "MCC large", GCC and "PCC small" coatings. A – "MCC large" with different binders and binder amount (tablets), B – GCC with and without PVOH and SA latex (tablets) and C – "PCC small" with and without PVOH and SA latex (tablets). Based on Paper VI (Figure 4).

At this stage, the pigment selection was broadened so that there would be several pigments that have dual pore size coating structures. All five of the calcium carbonate pigments were studied with 10 pph PVOH binder, and "MCC large", "MCC small" and "PCC large" pigments produced both intra- and inter-particle pores in the coating layer. The coating cakes and their detailed analysis are introduced in *Paper I*. Figure 23 shows that the porosities of the studied calcium carbonate pigment coatings containing 10 pph of PVOH maintained the same ranking as in the case of non-binder containing coatings. The largest diameter pigments, "MCC large" and "PPC large", produced the highest porosities because there remains more open space between the large particles. However, the third dual-porosity pigment "MCC small" had a medium porosity (30 %) amongst these studied coating layers. The smaller diameter of the "MCC small" pigment provided a more densely packed coating structure. The lowest porosity was produced once again also in this series by the GCC pigment, having both smaller pigment size and broader particle size distribution than the larger sized speciality pigments. The finest pigment "PCC small" developed a medium porosity. However, all the porosity values are lower than in the case of 1 pph of PVOH in the previous series, indicating that a higher PVOH binder amount fills the porous coating structure.
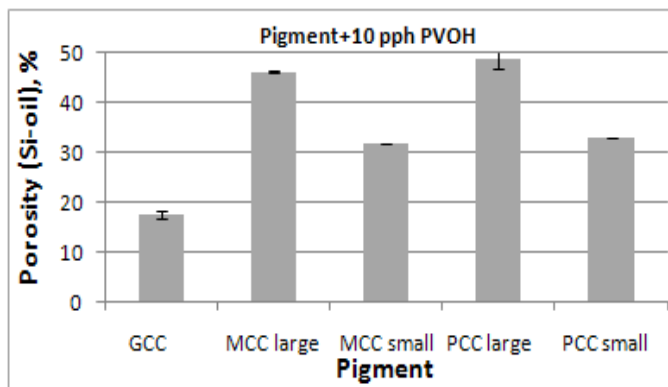

Figure 23. The porosity of different calcium carbonate containing coatings with 10 pph of PVOH (partially hydrolyzed). The measurement was made from coating cakes by using a silicon oil absorption method. Based on Paper I (Figure 2).

The location of PVOH in the coating structure was studied more closely by detection in two different coating cake structures, derived from pigments having the same porosity without binder, namely "MCC small" and "PCC small". To enable this more detailed analysis, coating cakes of "MCC small" and "PCC small" with and without PVOH were produced, and portions used for mercury porosimetry. Figure 24 shows that the pigments without binder addition produced very similar specific pore volumes. It was noticed that 10 pph PVOH (partially hydrolyzed) added with the pigment decreased the pore volume in both cases, but that "MCC

small" pigment showed a greater decrease than "PCC small". The "PCC small" coating structure had only nano-size pores in the 20–60 nm range (Figure 24B), whereas the "MCC small" coatings had both large and small size pores, indicating that the "MCC small" structures had both intra- and inter-particle pores. The PVOH addition decreased to some extent the volume associated with large size pores, but the peak of intra-particle pores in the "MCC small" pigment decreased most markedly, clearly indicating that PVOH had filled the intra-particle pores.

A   B
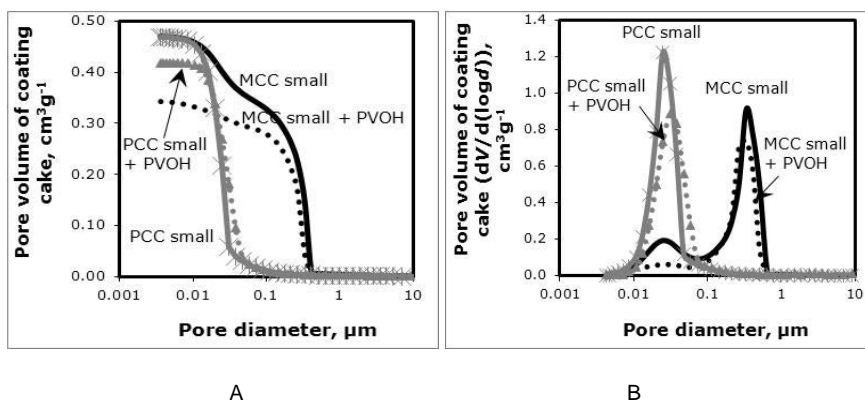
Figure 24. The effect of the addition of PVOH (10 pph, partially hydrolyzed PVOH) into the structure of "PCC small" and "MCC small" coatings. A – cumulative pore volume, B – the first derivative of the mercury intrusion curve indicating the pore size distribution. Based on Paper I (Figure 5).

CaCO$_3$ coatings on fine paper surface

The same model coatings with 10 pph PVOH, as studied above, were applied on the commercial fine base paper surface, which did not have any pre-coating layer. All coating colours were applied twice so that the target of coating amount, 10 gm^{-2}, could be achieved. Between each application time, the coating layer was dried. The coated paper production has been described in chapter 3 section 3.2 "Designed coating structures and binder films, and their production". *Paper I* contains the complete results from the testing of these coated papers. The cumulative pore volumes of the coated papers, determined by mercury porosimetry, are illustrated in Figure 25A. The results show that most of the coating colours had some partial penetration into the base paper structure, which can be seen as a higher level of the specific pore volume of the base paper than those of coated papers. The porosities of the coating layers were calculated from the coated paper results by taking into account the base paper effect and the amount of coating layer, following the method of Ridgway and Gane (Ridgway and Gane 2003). Figure 25B shows the cumulative pore volumes of the coating layers. The "PCC large" coating produced again the greatest pore volume, and it had more large size pores. The

lowest porosities were seen for GCC and "MCC small" coatings. The porosity results of the "MCC small" coating diverged somewhat between the mercury porosimetry and the silicon oil based measurement. In the case of silicon oil, the results of the porosity of "MCC small" and "PCC small" coating cakes were close to each other, whereas, in the case of coated paper, they were clearly on different levels. One reason for this can be in the PVOH location. In the coating cake production, the whole coating colour is in the cake, i.e. it is a closed system, whereas in the case of coated paper some of the PVOH can also transfer into the base paper. Otherwise, it seems that the porosity results comparing coating cake and coated paper agree with each other very nicely.

A   B
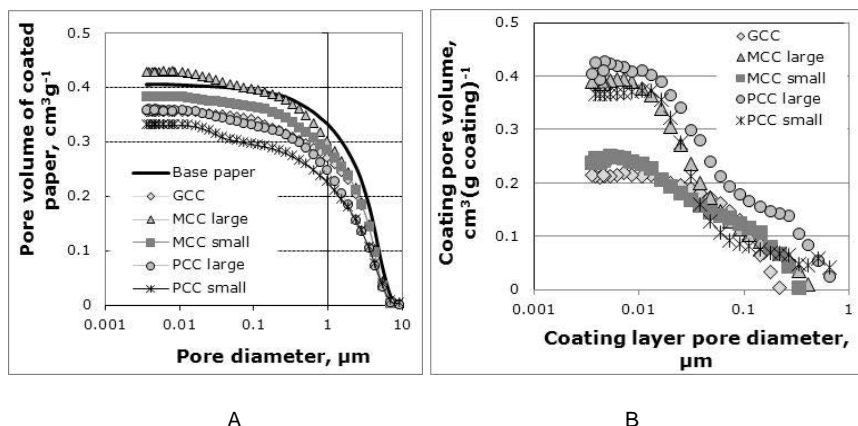
Figure 25. The cumulative pore volume distribution as a function of pore size of the different calcium carbonate containing coatings containing 10 pph partially hydrolyzed PVOH, measured with mercury porosimetry. A – the results from double-coated papers, i.e. 2x experimental coating formulation, B – the results as the base paper values have been subtracted from the results using the method of Ridgway and Gane (Ridgway and Gane 2003). Based on Paper I (A – Figure 11 and B – Figure 3).

The pore size distributions of the studied $CaCO_3$ pigment coatings, containing the 10 pph PVOH, as derived from the cumulative intrusion curves in Figure 25, are illustrated in Figure 26. The standard ground calcium carbonate (GCC) had mainly pores in the diameter range of 100–300 nm, with a decreasing amount of nanopores. The very small particle size inkjet coating pigment, "PCC small", produced also a coating structure that had mainly monosize pores and they located predominantly in the nano-size area, 20–60 nm. The "MCC large" and "PCC large" pigment coatings had dual-pore size distributions, meaning that there were nanoscale pores in the diameter region of 20–60 nm as well as large pores in the greater than 700 nm region. This bimodality once again describes the discrete pore structures, namely the intra-particle pore volume, representing those inside the particles themselves, and the inter-particle pore volume, representing those

between the particles. The "MCC small" pigment had some small size pores but the main pore volume is associated with pores located in the area of 200–600 nm.


A   B
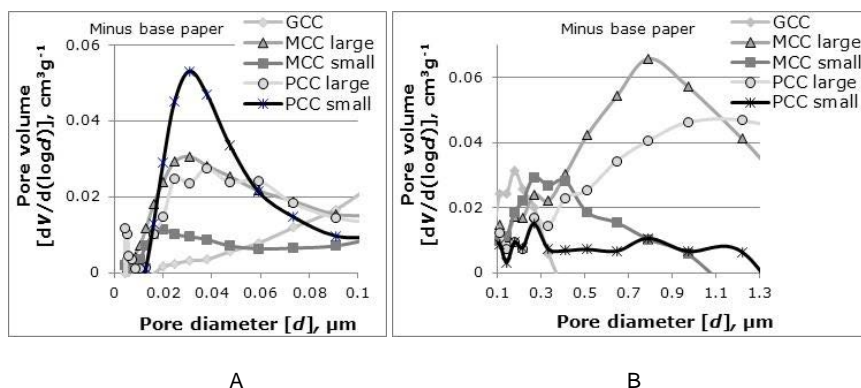
Figure 26. The pore size distribution curves from the mercury porosimetry of the studied $CaCO_3$ coated papers containing 10 pph PVOH (partially hydrolyzed). The base paper values have been subtracted from the results by using the same method as proposed by Ridgway and Gane (Ridgway and Gane 2003). A – nano-size pores, B – large size pores. Based on Paper I (Figure 12).

The effect of binder amount was studied further in *Paper II*, and the hydrophilic, soluble PVOH was compared to the styrene acrylate latex in the "PCC large" pigment model coatings. In the case of the latex, the polymer itself is hydrophobic, but the surface is partially carboxylated, and together with the stabilising surfactant used in emulsion polymerisation the surface is hydrophilic. Figure 27 shows the pore size distribution of the coatings. The top-coatings were applied on the GCC pre-coating that contained 12 pph SB latex and 0.6 pph CMC. The measurement was made with another mercury porosimetry device than the previous measurements. In these results, the *y*-axis has been shown as per cent and not specific volume. PVOH coatings displayed more of the smaller diameter pores than the SA latex containing coatings. This can also be seen in the cross-section micrographs (Figure 28) of coated paper structure where the SA latex containing coating has a more porous and thicker structure than the PVOH containing structure at the same coat weight. The particle size of SA latex was quite large compared to the pore size, 180 nm, which can keep the pigment particles apart from each other during the consolidation, whereas the soluble PVOH can fill the capillaries immediately under the influence of capillary forces. The increase of PVOH binder content thus decreased the pore diameters and the volumetric amount of small size pores because of the filling effect of binder polymer. At the binder content of 30 pph, the PVOH coating had fewer pores within the 35–85 nm diameter region than for the case of the SA containing coating. The PVOH has continued to fill the smallest pores. On the other hand, from the pore size intrusion results, the basic pigment dual-pore size distribution can still be seen to some extent.
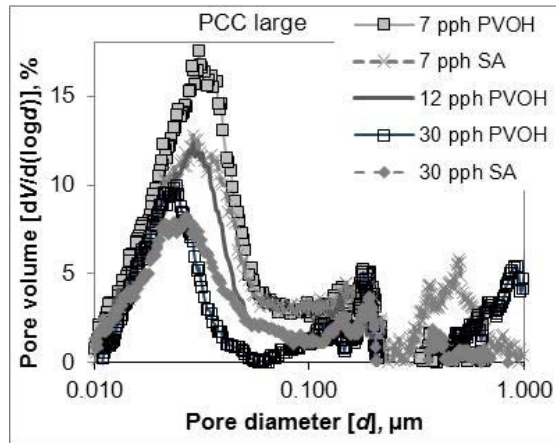
Figure 27. The pore size distributions of "PCC large" coatings with 7, 12 and 30 pph PVOH and 7 and 30 pph SA latex measured from the application of the experimental coating on pre-coated paper (SB latex containing GCC coating). Based on Paper 1 (Figure 8) and Paper II (Figure 5).

   "PCC large" + 7 pph PVOH   "PCC large" + 7 pph SA   50 μm
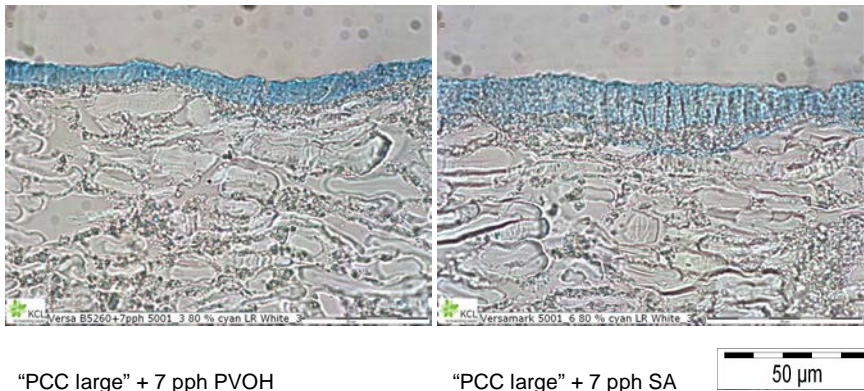
Figure 28. Cross-section micrographs of coatings comparing the cases with 7 pph of PVOH and SA binder, respectively. The paper had a pre-coating of offset type coating colour (SB latex containing GCC coating). Printed with cyan dye from Versamark® VX5000e. Based on Paper II (Figure 15).

By using PVOH and styrene acrylate latex as contrasting binders, representing soluble versus particulate, different kinds of coating structures as well as potentially different interactions with water can be produced. These changes in the coating structures will affect the absorption properties of the layers, which were subsequently studied more closely by observing the inkjet ink absorption as a function of gloss change (DIGAT), gravimetric determination (microbalance) and electrical capacitance (Clara), as well as the colorant chromatographic separation (thin layer

chromatography, TLC). By using these methods, the absorption rate and the pore volume uptake differences can be detected, and furthermore the role of inter-polymer diffusion during inkjet ink imbibition into the coating structures can be evaluated (Hypothesis I) along with surface adsorption behaviour.

4.2 The effect of coating structure and binder selection on liquid imbibition rate

4.2.1 Inkjet ink absorption into the top layer of coating

The coating layer structure as analyzed above affects the ink absorption rate into the coated paper structures, and this has been studied in *Papers I* and *II*. The wet ink causes an increase of gloss on the paper surface, and the gloss decreases during the time it takes the ink to penetrate into the structure. The gloss change as a function of time was detected with the DIGAT device, which has been described in section 3.3.5 "Use of more conventional paper testing methods". The GCC coating had the longest absorption time (Figure 29A) because of it both having the lowest porosity and a monomodal pore size distribution limiting the permeability (*Paper I*). The more highly porous and permeable surfaces made from the special-ity pigments absorbed the ink quicker. As the binder amount in the coating layer increased from 7 pph to 12 pph (*Paper* II) the absorption time became longer (Figure 29B). The high binder polymer amount decreases the porosity of the struc-ture, and the PVOH can move into the intra-particle pores, as we have seen in the previous pore analysis studies. However, interestingly, the further increase of binder amount (30 pph) did not change the absorption time any more. In the case of PVOH containing coating, the inkjet ink diffusion into the binder polymer causes the swelling of polymer and this diffusion compensates for the structural impact on penetration rate, keeping the rate on the same level (600 ms) as it was in the 12 pph PVOH containing coating.

When the inkjet ink droplet arrives onto the coated paper surface, the ink should first penetrate quickly enough into the structure so that the mixing of the droplets is controlled. At this point, an optimal balance between spreading and absorption is obtained. The droplets always spread to some extent, but the mixing of different colour inks should not be so large that intercolour bleeding becomes a problem. As the results of Figure 29 show, the large or medium porosity coating structures generated here a quick absorption of inkjet ink into the coating layer just after the ink has arrived onto the coating surfaces. On the other hand, it is known that large porosity is not a sufficient criterion for fast absorption. These structures should additionally have more nano-size pores. It seems that when the inertia dominates, after the surface wetting, the finest pores will absorb liquid further into the structure and faster, if there is sufficient permeability to allow access to these pores. This is essential for quick inkjet absorption. The work of Bosanquet (Bosanquet 1923) and the further studies of Schoelkopf *et al.* (Schoelkopf *et al.* 2000) and Ridgway *et al.* (Ridgway *et al.* 2001) show that when the inertia domi-

nates on the short timescale, when imbibing liquid encounters a sudden change in geometry or pore size within the network structure, the nano-size pores play a very important role in the liquid imbibition during the local short time absorption. The penetration distance of liquid by absorption into the small nano-size pores has proportionality to time, t (Bosanquet equation (12)), rather than the equilibrium flow associated with viscous drag, which is proportional to $\sqrt{t}$ (Lucas-Washburn equation 11).

A

B

C
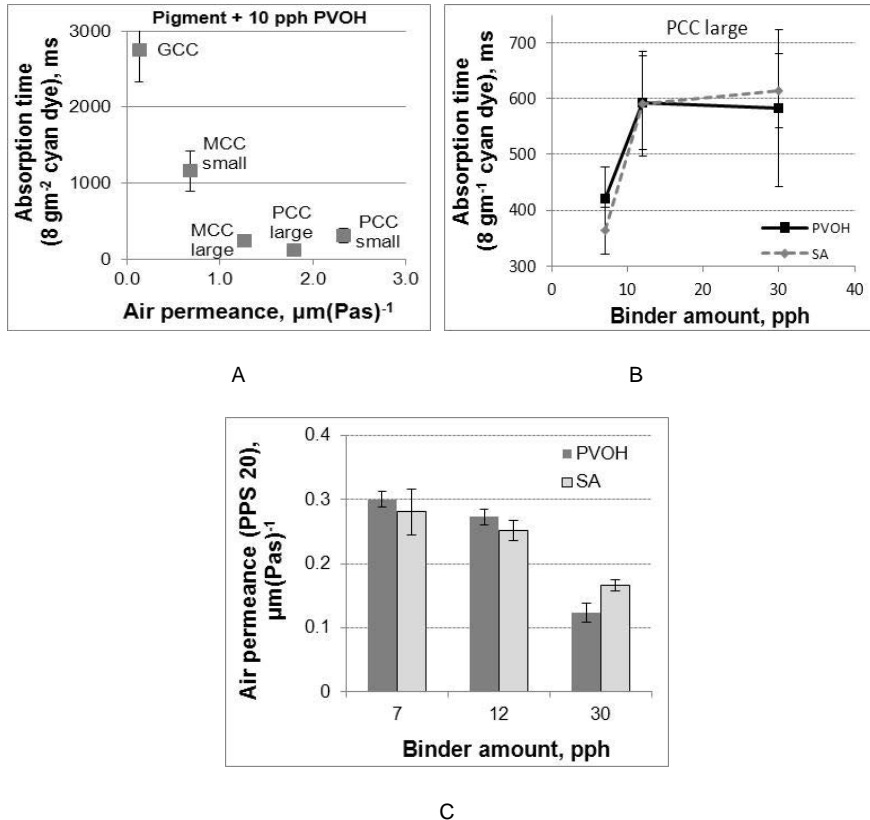
Figure 29. The absorption time of applied ink on the 10 pph PVOH (partially hydrolyzed) containing $CaCO_3$ pigments (A, Paper I, Figure 13) and "PCC large" coatings with different amounts of PVOH and SA latex (B, Paper II, Figure 6): measured with the DIGAT device using 8 gm^{-2} Versamark® cyan dye-based ink. (C) – the air permeance of "PCC large" pigment with the different binder content of PVOH or SA latex (Paper II, Figure 4).

4.2.2 Gravimetric determination of liquid absorption into the coating structure

In the hypotheses of this thesis it was presented that the inter-molecular diffusion of the vehicle of inkjet ink into the polymer binder matrix acts on a sufficiently fast timescale and in sufficient volume to compete with the permeation of ink through coating structures. The first approach to study the role of diffusion was to measure the polar (water) and non-polar (hexadecane) absorption rate into the coating tablets with a microbalance measurement (*Paper VI*), which was described in section 3.3.2. The studied "MCC large", GCC and "PCC small" structures con-tained (a) different dispersing agent (cationic or anionic) and (b) different binder type (PVOH or SA latex) and binder amount. Figure 30 illustrates one example of the result curves. At first, all result curves had a higher absorption rate and after about 2 s the rate decreased. The resultant curves of all the studied coating tab-lets are shown in Figure 31. Both parts of the curves, expressed as volume uptake per unit area, had a linear relation to the square root of time, $\sqrt{t}$, and therefore the absorption rate study was divided into short and long timescale absorption. The slope of the curves describes the effective absorption rate. Figure 32 shows the absorption rate results of the short and long timescale of studied coating tablets, and the discussion below has been divided into two parts: short and long time-scale absorption.


A   B
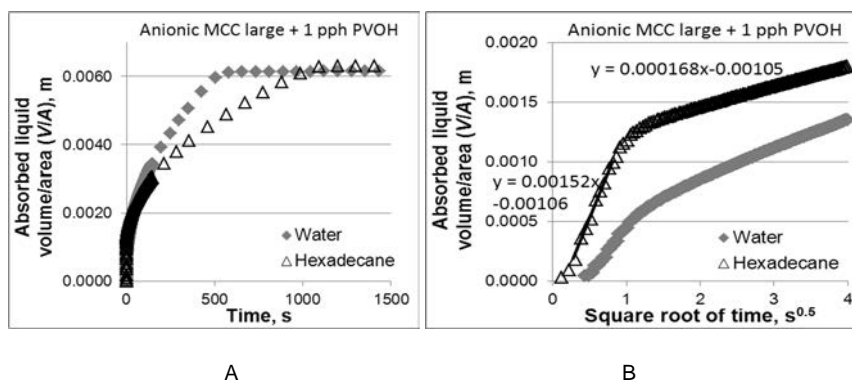
Figure 30. The gravimetric result curves of water and hexadecane imbibing into the anionic "MCC large" coating structure with 1 pph PVOH: A – the results of the measuring time up to 1 500 s. B – the results of the first 4 $s^{0.5}$. Based on Paper VI (Figure 5).
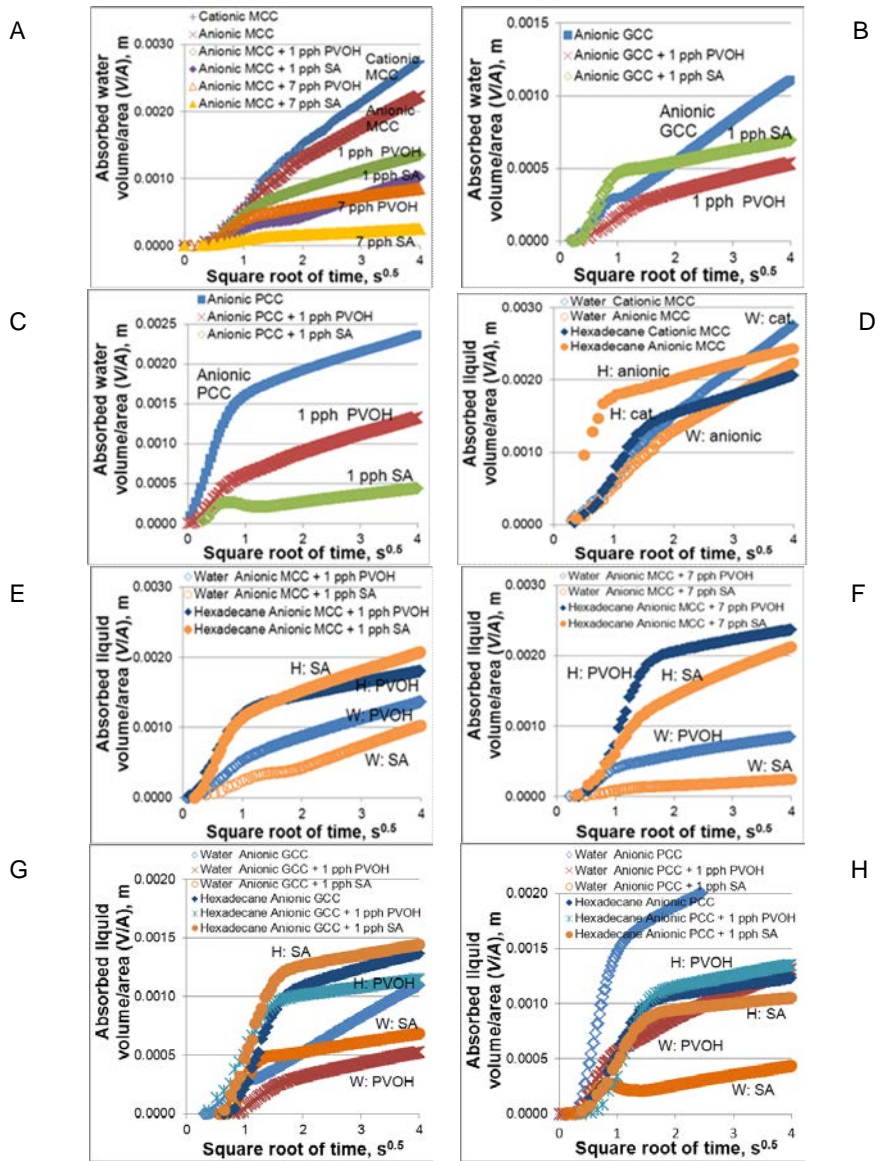
Figure 31. Absorbed liquid volume/unit contact area of water (polar) and hexade-cane (non-polar) into the studied coating structures. A, B, C – the absorption amount of water into the "MCC large" (in figure marked MCC), GCC and "PCC small" (marked PCC) coatings, respectively. D, E, F – the differences between water and hexadecane absorption into the MCC coatings. G – the absorption of water and hexadecane into the GCC coatings. H – the absorption of water and hexadecane into the "PCC small" (marked PCC) coatings. In figures water has marked with ab-breviation W and hexadecane with H. Based on Paper VI (Figure 6).
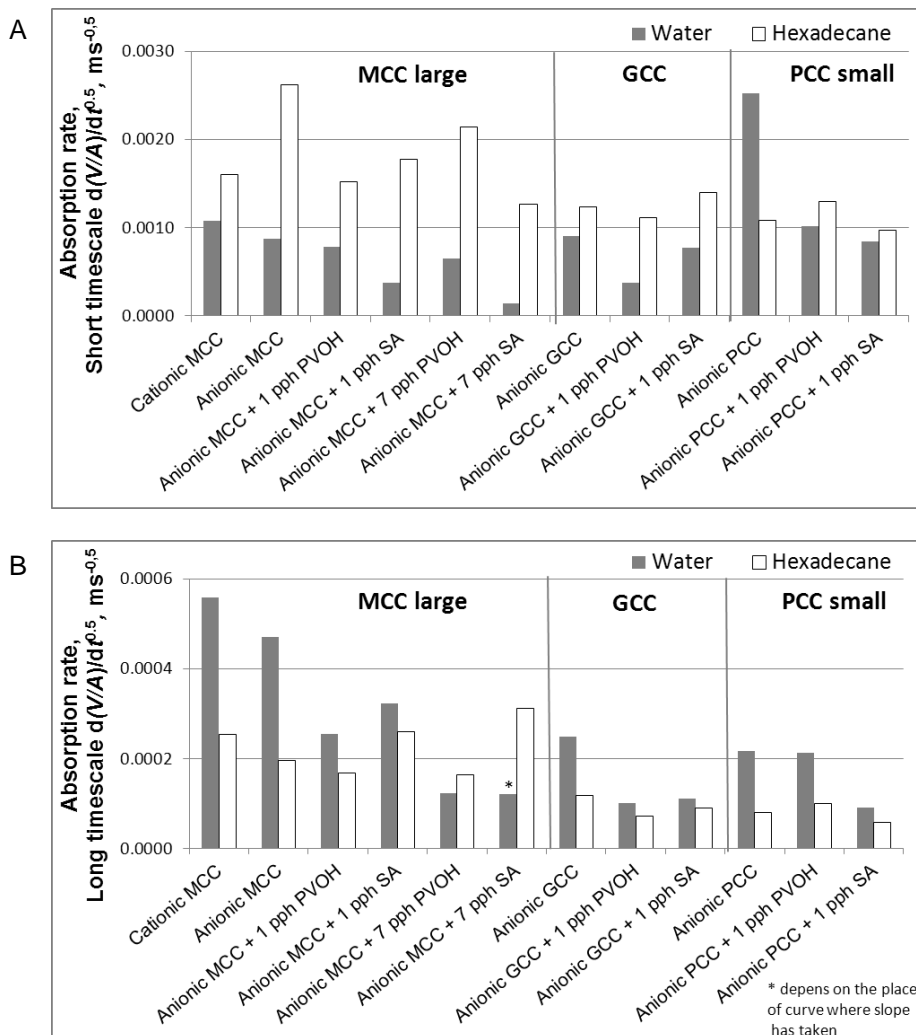
Figure 32. Absorption rate of modified, ground and precipitated calcium carbonate pigment coatings. The short (A) and long (B) timescale $d(V(t)/A)/dt^{0.5}$ data are derived from the gradients of the absorption curves. Based on Paper VI (Figure 7).

Short timescale absorption

The short timescale absorption rate in Figure 32A (*Paper VI*), the first few seconds time from liquid arriving onto the coating layer, shows that non-polar liquid (hexadecane) absorbs more quickly into the coating layers than the polar liquid (water). The liquid is driven primarily by the capillary flow of the porous coating structure, and one competing phenomenon, amongst others, is diffusion (Ridgway *et al.* 2011).

The dispersing agent is a hydrophilic polymer that allows water molecules to diffuse into the inter-polymer space, causing swelling of the polymer at the entry to the finest pores, and this at first slows down the liquid water uptake. However, hexadecane does not diffuse into the polymer and therefore the capillary flow dominates in this non-polar liquid transfer. In addition, the results show that the coating structure with both intra- and inter-particle pores ("MCC large") transports the hexadecane most effectively. Similar pore size structure coatings were found by Ridgway and Gane (Ridgway and Gane 2005) to be favourable for inkjet inks. Firstly, the small capillaries transfer liquid quickly into the structure and from there and behind the wetting front it moves further into the larger pores. This has a connection to Hypothesis III, where it is presumed that the bimodal pore size distributions provides an optimal pathway for quick absorption of inkjet inks.

If the water absorption rate into the dispersed pigments (without binder) is studied, the "MCC large" and GCC pigment coatings had very similar rate, whereas "PCC small" coating absorbs the polar liquid fastest. One possible explanation for this higher absorption rate can be in respect to the surface agents of the pigment dispersion. The GCC and the "MCC large" pigments were dispersed by using an anionic polyacrylate dispersant, which remains on the pigment surface. The water diffuses into this polyacrylate polymer network, swells it and renders it fully hydrophilic, and this needs time. In the case of "PCC small", it requires additional polyacrylate to render it more strongly anionic in dispersion. This indicates that the "PCC small" has a higher polyacrylate demand to render it more strongly anionic in dispersion. Thus, the "PCC small", effectively underdispersed in respect to a given polyacrylate dose, reverses the absorption preference from hexadecane to water at the shortest timescales.

The addition of 1 pph of PVOH or SA latex binder in the pigment tablets provided still faster hexadecane absorption rates at the short timescale for "MCC large" pigment coatings than for GCC and "PCC small" coatings. The importance of both intra- and inter-particle pores in the non-polar liquid transfer is again reflected here. Both binders absorb only a minimal amount of non-polar liquids (Figure 46 in chapter 5 section 5.1 "Liquid absorption by binder films"). This means that swelling of the polymer in the presence of hexadecane is minimal, and therefore the smallest pores in the coating remain open during the hexadecane absorption and the diameters of pores are unchanged. Thus, during the non-polar liquid imbibition, the capillary flow dominates.

If the water absorption into the PVOH and SA latex containing "MCC large" and "PCC small" pigment coatings are studied, it is seen that the SA containing coating had lower absorption rate results than in the PVOH containing coatings. The PVOH containing "MCC large" coating had more small-diameter pores than the SA coating, as Figure 22A shows, and the swelling of hydrophilic PVOH binder changes the amount of small pores dynamically during the water absorption. The PVOH absorbs polar liquid, like inkjet ink (Figure 46 in chapter 5 section 5.1 "Liquid absorption by binder films"). This polymer diffusion causes the PVOH to swell and therefore some of the nano-size pores will close and/or there will also be a diminishing volume/number of these pores already at the short timescale, supporting

the Hypothesis I. In the case of SA latex containing coatings, the latex polymer does not swell in the presence of water (as the chapter 5 "Mechanisms influencing liquid absorption in coating binders" later shows) and thus the capillary flow controls the water imbibition. The reason for slower absorption rates can be in the hydrophobic nature of SA latex polymer that prevents the penetration of polar water and thus a loss of effective absorptive volume. However, wetting will still occur, and this is probably related to the surfactant and/or carboxylation used to stabilize the latex. A similar binder behaviour difference between PVOH and SA containing coatings in respect to water uptake was noticed with the "PCC small" coatings.

Long timescale absorption

In long time absorption (Figure 32B, *Paper VI*), the diffusion is still progressing, and, in parallel, the porosity of the structure (permeation flow) permits continued liquid imbibition by pore surface wetting and subsequent meniscus flow. The absorption rates of polar and non-polar liquids at the long timescale were slower than in the short timescale region. During the progressive absorption over time, the viscous drag increases in proportion to the length over which the liquid flows within the structure, as the Poiseuille equation indicates (equation (7)), and this slows down the absorption. The results show further that the water absorbs quicker than hexadecane. The polymer structures on the pigment surfaces have had time to reorient due to the water vapour front diffusion and this promotes polar liquid movement.

The "MCC large" coatings had again higher absorption rate values than either the GCC or the "PCC small" coatings. The coating with the dual-porosity structure is confirmed to be the most advantageous in respect of liquid absorption rate because it produces a coating structure with high permeability (Figure 20A) and it contains nano-size pores (Figure 20B) that drive the liquid front forward.

In the long absorption timescale, the SA latex containing "MCC large" coatings absorbed water faster than PVOH containing. In the short timescale absorption, the results were vice versa. In the over 2 s time absorption regime, the small diameter pores at the wetting front retain their action of providing the driving force, but the rate is determined by the permeation flow in the large pores, defining resistance to that driving force. The PVOH containing coating had smaller pore diameters (intra-particle pores) than the SA latex containing, as Figure 22A shows. These findings support the conclusions of Ridgway and Gane (Ridgway and Gane 2005).

4.2.3 Liquid and colorant movement – impact of charge on chromatographic separation in the coating layer

The second approach was to study how the liquid transfers through the different coating structures in thin layer chromatography (TLC, *Paper V*). The variables of coating colours were the ionic charge of dispersing agent (anionic/cationic), the

inter-polymer hydrophilicity of binder type (hydrophilic/hydrophobic) and the cationic additive application. "MCC large" pigment was selected because of its capability to produce a coating layer with the dual pore size structure and so producing a guaranteed fast absorption of inkjet ink, as the previous results in Figure 29A showed. The hydrophilic partially hydrolyzed PVOH and inter-polymer hydrophobic styrene acrylate latex were again selected for comparison, and the binder amount chosen to be sufficiently low that the chromatographic separation can be detected. The effect of the ionic charge of the coating layers was observed by using anionic (anionic sodium polyacrylate) or cationic (polyDADMAC) dispersing agent in the production of coating slurry. The pore volumes were measured from the coating tablets, and the results were very near each other, as Figure 33 shows. The SA latex containing coating had a little bit higher porosity than the other anionic coatings.
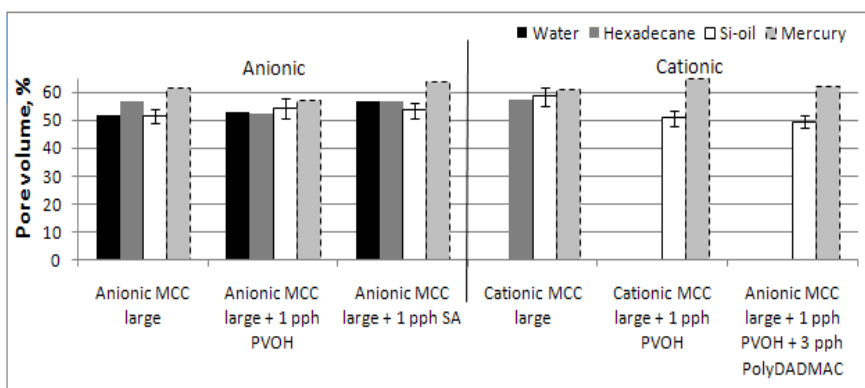
Figure 33. The pore volume of "MCC large" coatings (tablets) that were used in the thin layer chromatography research. Based on Paper V (Figure 4).

On contact with supersource soluble anionic colorant, the results show that there always exists a wetting front rising within the anionic coating structure in advance of the anionic colorant front (Figure 34) and behind this comes a colorant-rich ink layer and after that a less colorant containing ink eluent area. There is no obvious retardational adsorption mechanism on the basis of charge alone. The wetting water front height in this anionic case was about one millimetre ahead of the colorant front. The retarded colorant fronts were darker than the following (trailing) colours (Figure 35, anionic coatings). As the finest pores of the coating structure drive the wetting front forward, they seem to exclude the dye colorant. It seems that the surface area associated with the finest pores of these structures is either not available for adsorption of the dye molecules or a further rate determining step is involved. These results suggest that the anionic repulsion is the primary exclusion mechanism. This can be one force in the coating layer that might act against the diffusion.
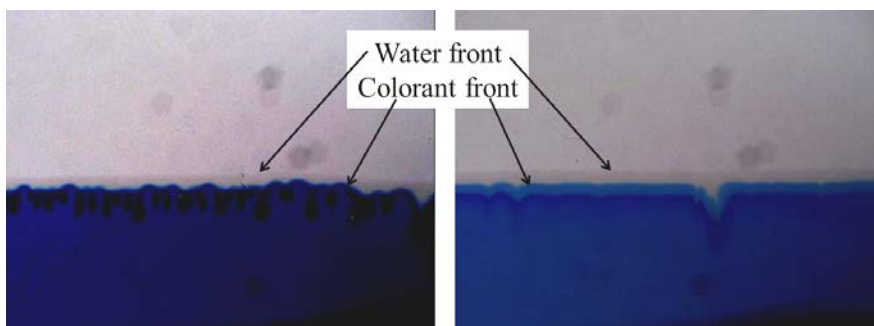
Figure 34. The water front is seen to be ahead of the anionic colorant front in the anionic "MCC large" coating layers after 4 min: left 5.00 wt-% and right 0.54 wt-% anionic colorant in water. Based on Paper V (Figure 11).

The highest water rising distance and the highest penetration rate was observed for the binder-free coating structures (again considering the "MCC large" pigment structures). The coating with SA latex had a plateau height value roughly half that of the binder-free coating, and the lowest values were for PVOH containing coatings (Figures 35 and 36). Only 1 pph binder addition already caused such a significant difference to the liquid movement and final rise position. The SA latex containing coating had somewhat larger pore volume than the coating without binder and this can be one reason for a lower eluent rise. There were also less small capillaries that drive the eluent front forward, and the hydrophobic nature of SA latex can further reject the polar eluent, as will be described further below. The SA latex network does not support the diffusion of polar liquid into the polymer network whereas the polyvinyl alcohol binder can. In the case of PVOH containing coating, the polar eluent diffuses into the binder structure and the binder polymer matrix swells causing the closing of the smallest pores and the diminishing of remaining pore size. At the same time, the pore volume of the coating layer decreases and this slows down the eluent movement. Thus, the diffusion into the PVOH affects the permeability of the coating structure and so slows the permeation flow in the layer. The eluent colorant content did not change the behaviour, in that all the studied ink colorant amounts proceed to similar distance values upon each given coating TLC plate.

In the cationic coatings, the anionic colorant initially stayed at the bottom edge of the coating. After a development time of ten minutes, the fixed dye edge appeared to fill with colorant and part of the colorant volume started to rise little by little. Especially, this could be seen when there was the higher concentration (5.0 wt-%) of colorant in the water. The surface area associated with the cationised pores takes part in adsorption, and only when the surface area of pigment is saturated with colorant can the colorant move forward into the structure. The degrees of freedom of the normally random walk mechanism of diffusion is therefore limited by the local adsorption mechanism, which requires charge potential equilibration, and hence local concentration of anionic dye by

diffusion of the colorant to the surface. Only then is random diffusion re-established until the next surface charge accumulation is encountered.

The importance of very small pores in inkjet ink imbibition can also be detected in the study of thin layer chromatography (*Paper V*). The surface coating structure first wets and the capillary flow drives the ink into the nano-size pores. The small size of a water molecule, 0.27–1.00 nm (depending on the amount of molecules in one cluster) (Topgaard and Söderman 2001), enables the capillary flow in the nano-size pores to occur, i.e. in the intra-particle pores of "MCC large" pigment (20–70 nm). The colorant-free wetting front connected with the higher colorant concentration just after the colorant front, as noted previously, suggests that the mechanism here is an anionic repulsion from the finest pores, allowing the water to imbibe into these pores, but not the dye. It can be concluded, therefore, that charge exclusion limits the passage, i.e. excludes the response to capillarity of the dye in the eluent into the pores. This sets up a diffusion gradient of colorant within the eluent when the charge of the surface is of the same sign as that of the colorant. As the amount of ink increases, the permeation flow in larger pores increases so that there are no more open pores in the coating. The size of a colorant molecule is about 1.3 nm (taking account of the length of different bonds in the Cu phthalocyanine colorant molecule and assuming the molecule is planar), which means that the colorant fits well into the 20–70 nm intra-particle pores. In the case of the cationic coating layer, the water front rises very similarly as in the anionic coating layers, and behind the capillary flow comes the filling of large pores (permeation flow), but now the anionic dye becomes fixed to the cationic surface in the bottom of the TLC plate.
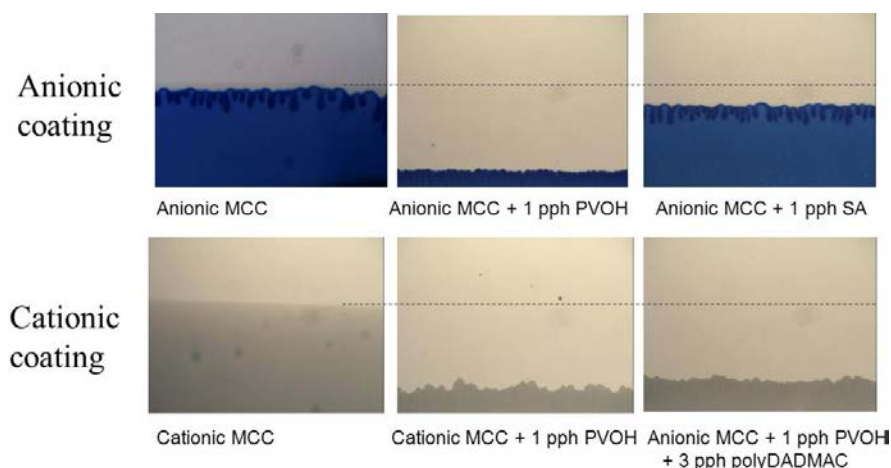
Figure 35. The 5.0 wt-% anionic cyan colorant rising within different "MCC large" coating layers. Measured after 4 min time delay. Based on Paper V (Figure 6).

The structure of the coating layer and the selection of binder type affects how far the ink moves through (along in the case of TLC) the coating layer and how quickly. At first, the slope of the distance curves seems to be at its greatest, and it decreases as the development time increases. The TLC eluent moves further and with a faster rate in the anionic dispersed pigment layer than in 1 pph binder containing layers (Figure 36). After a distance of 30 mm there was no further change in the distance travelled in the anionic pigment layer, whereas in the PVOH containing coating the front of the eluent stopped after 7 mm, and in the SA coating after 17 mm. The balance between the wetting force (Young-Laplace equation) and the viscous drag determines the rate of progress. As the viscous drag increases in proportion to the length over which the liquid flows within the structure, and to the inverse fourth power of the typical equivalent capillary size (Poiseuille effect), there comes a point when the drag equals the wetting force. The SA coating had a higher pore volume indicating that it could both accommodate more liquid and, if permeable, transport it further than could the lower pore volume PVOH structure. The SA latex swells only a few percent under the influence of water (Lamminmäki *et al.* 2010). Thus, the capillary flow controls the water imbibition in SA latex containing coatings. The difference between the SA latex containing coating and dispersed pigment alone is additionally suggested to be caused by the possible difference in the hydrophilic/hydrophobic natures. The SA latex has a more hydrophobic nature indicating that the contact angle of polar liquid may effectively increase in contact with the polymer, or the timescale for the surfactants present to reorient, and so permit wetting, may delay the passage of water, and thus the effective capillary pressure decreases. The equilibrium point comes much sooner with binder containing coatings, both due to reduced pore connectivity and surface chemistry effects, and these are reflected in the distance the liquid front finally travels. The measurement in the TLC analysis lasts up to 40 min, and the evaporation of eluent (water) has therefore an influence on the results. However, the evaporation study of water in *Paper V* indicated that evaporation has only a minor effect on the eluent movement in respect to the influence on the wetting force and viscous drag force. Only towards the very end of the experiment can we expect evaporation to be a further equilibrating factor additional to the wetting force-retardation balance.
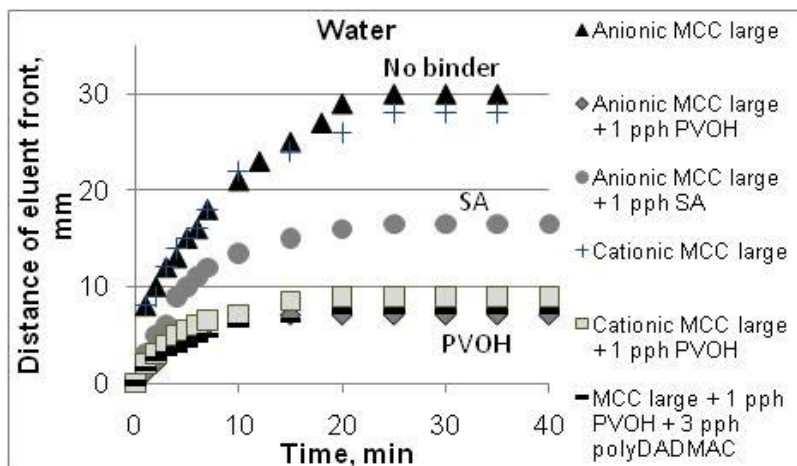
Figure 36. The distance of eluent (water) front during the time in the chromatographic development. The coating pigment was "MCC large" and the eluent, water (deionized). Based on Paper V (Figure 8).

### 4.2.4 Inkjet ink penetration in coated papers monitored by electrical capacitance

In conventional contact printing methods, the external pressure has an important role to play in the penetration of low viscosity liquids, such as fountain solution in the offset process, or ink vehicle in low ink solids flexography. The exception is for the case of paste offset inks, where the penetration in the nip is minimal (Oittinen 1976). However, in inkjet printing, the only external pressure is occurring when the droplets hit the paper surface, and subsequently from the curvature of the ink droplet in relation to its surface tension. If a 15 pl dye-based inkjet ink droplet (density 1 000 kgm^{-3}) arrives onto the paper surface with speed 15 ms^{-1}, as in the Versamark® VX5000e technology, for example, the pressure of the droplet hitting the paper surface is a little under 0.10 bar. This pressure is soon dissipated in practice, and in the following experiments it is applied primarily to initiate stable wetting. A value of 0.10 bar is expected to be less that the capillary pressure in the fine pores. If the capillary pressure, p_c, of a liquid is calculated by the Young-Laplace equation (equation (10), considering a 100 nm diameter pore (nano-size pores), a contact angle of 50° (contact angle of water on the 7 pph PVOH containing "PCC large" coating, Figure 72) and a surface tension of 54 mNm^{-1} (the cyan Versamark® VX5000e ink at 24 °C, Figure 10) we obtain for the Laplace capillary pressure, 13.9 bar, which is a lot higher than the used 0.10 bar. This means that the capillarity in the finest pores will act to cause the wetting. However, a capillary diameter of 1 μm develops a pressure which is ten times less, i.e. 1.39 bar, and 10 μm, 0.14 bar etc. So, the pressure of 0.10 bar forces ink by intrusion into pores which have a diameter of at least 13 μm. The studied coating layers have only a

few or none of this size pores, and therefore the coating structure will allow some very small amount of externally-driven permeation only. However, the 1.5 bar pressure forces liquid into over 1 μm pores. This means that, at this pressure, the long term intrusion becomes dominated by permeation for many inkjet coatings. If the wetting force of 100 nm diameter pores is calculated, the equation $\pi r^2 p_c$ gives 11 nN, which is a very low force despite the high pressures involved.

To illustrate the effect of pressure over a wider range, the study of inkjet ink penetration below has been divided into three different external over-pressures: 1.50 bar, 0.10 bar (inkjet droplets hitting pressure) and 0.02 bar (effectively no external pressure). By using different over-pressures, the separation between the effects of capillarity, permeability and diffusion can be detected. The work at high pressure permits to characterise the permeability, the medium pressure mostly capillary and diffusion, and the zero pressure capillary competing with diffusion of liquid and vapour. The results are based on *Paper II*.

<u>Absorption properties at 1.50 bar over-pressure</u>

Figure 37 shows how the capacitance results at 1.50 bar external over-pressure changed when the amount of binder in the "PCC large" coating layer increased. The studied surface had two coating layers on the fine base paper. The pre-coating contained offset quality GCC and top-coating "PCC large" inkjet pigment. A series of top-coatings were thus tested having different amounts of partially hydrolyzed PVOH or styrene acrylate latex. In section 3.1.5 "Substrate: pre-coated base paper" has introduced the studied materials and in Table 8 the recipes of the coating colours are described. The coating which contained more binder had a slower capacitance change. The bimodal nature of the capacitance curve indicated the relative change from capillarity to permeability. Clearly, the highest binder level of PVOH dampened the capillary effect as the resulting graph becomes monotonic. It took from 2.4 s to 11.0 s for the inkjet ink to penetrate through the structure with PVOH containing coatings, whereas with SA containing coatings only from 0.9 s to 2.7 s. The fastest ink penetration speed through the pores was reached with lowest binder content and ink penetrated more quickly through the SA coating papers than through the PVOH papers.

A   B
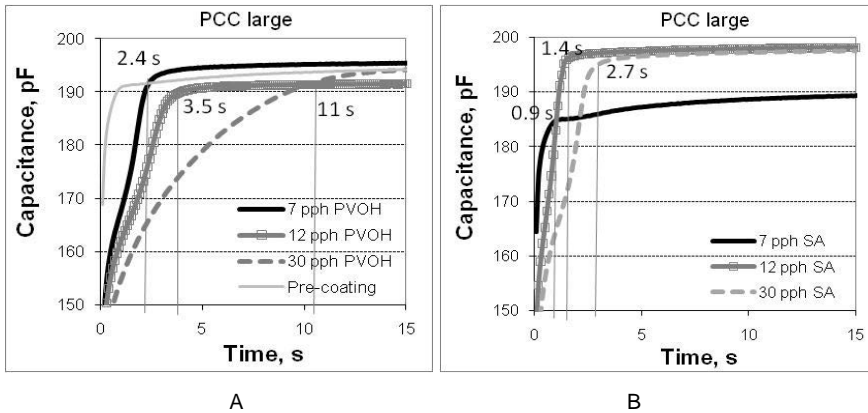
Figure 37. Cyan dye-based ink (from Versamark® VX5000e) penetration through the "PCC large" coated papers at the external over-pressure of 1.50 bar, as measured with the Clara device: A – refers to the different content of PVOH and B – refers to the different content of SA latex, respectively. Based on Paper II (Figure 7).

We can calculate the penetration speed and depth from the capacitance results by assuming that the ink has gone through the whole paper structure as the highest capacitance values have been reached, as the method section indicated (Section 3.3.2 "Liquid penetration"). Figure 38 illustrates how the inkjet ink penetrated through these papers coated with "PCC large". The thicknesses of the coating layers together (both top- and pre-coating) were about 20 µm, but part of the pre-coating colour had probably penetrated during the consolidation into the top layer of the base paper, as we noticed earlier in Figure 25 with the 10 pph PVOH containing coatings. Therefore, we can assume that the effect of the coating layer can influence even as deep as 30 µm. The ink penetrated with higher speed through the SA latex containing coatings than through PVOH containing, and the penetration through the coating layer was lower as the binder content increased. The air permeance values of each comparable paper at a given binder amount were very similar, indicating that the PVOH blocked the capillarity-acting fine pores, whilst overall permeability comparing the binder systems appeared similar.

There appears a turning point in the curve of the inkjet ink penetration speed, which refers to a point located deep within the base paper. This supports the assumption that either the components of pre-coating or the polyvinyl alcohol of top-coating have penetrated deeply rendering the diffusion effect active throughout the sheet or the predicted over-pressure effect has created a significant difference in position between the wetting front relative to the coating saturation front, created by the permeation lead through the larger more connected pores, and that it requires further wetting front penetration before the saturation front has reached the base paper. In the coating layer consolidation, the PVOH can follow the liquid phase of the coating colour deeper into the paper structure and so affect the forming porosity. The pre-coating penetration into the base paper, as mentioned previously,

can also be an explanation. During the water-based ink imbition, the penetrated PVOH swells under the influence of water, and this affects the absorption into the smallest pores by closing and/or diminishing them and this is reflected in the Clara results. The PVOH can also dissolve partially into the inkjet ink during the penetration process, as we shall later see in chapter 5 section 5.2.1 "Diffusion coefficient", and so affects for example the process viscosity and surface tension of penetrated liquid.


A   B
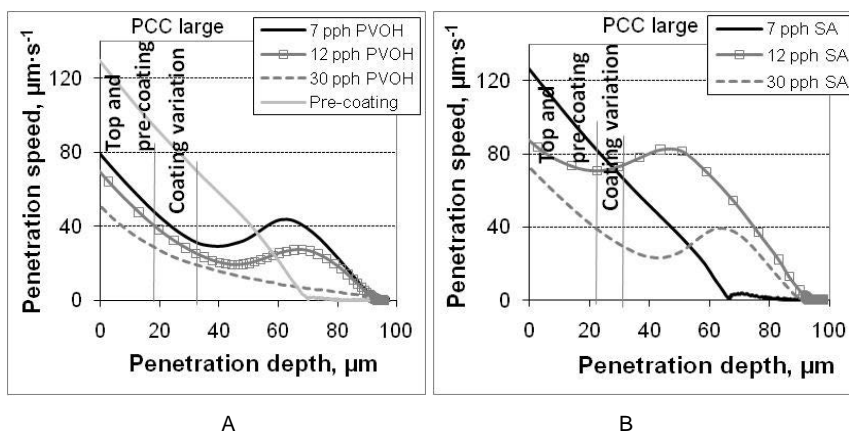
Figure 38. Cyan dye-based ink (from Versamark[®]VX5000e) penetration speed, as recorded by capacitance change, through the paper structures having PVOH and SA containing "PCC large" coatings at external over-pressure 1.50 bar. The coating variation refers here to the thickness differences of the coating layer: A – refers to PVOH and B – refers to SA latex, respectively. Based on Paper II (Figure 8).

Absorption properties at the inkjet droplet hitting pressure

Figure 39 shows the capacitance results of the range of $CaCO_3$ pigment structures, as formed on the coated papers (same papers that were used before in the study at the 1.50 bar over-pressure), during imbition of inkjet ink at 0.10 bar over-pressure. At the lowest binder amount (7 pph), the used cyan ink penetrated more rapidly in the SA latex containing "PCC large" coating than in the PVOH containing. The capacitance values of SA containing coating were still higher than the values of PVOH containing. When the binder amount increased, the curves of PVOH and SA coatings came closer to each other. We see that the bimodal nature of the curves is far less at the lower over-pressure than at the 1.50 bar, supporting the dominance in this case of capillary pressure over that of permeation-driven flow. At the 0.10 bar over-pressure, only in the coating with 7 pph of latex could any indication of bimodality be seen, and this supports the likelihood of there being greater permeability in this structural case, such that even at low pressure some external pressure-driven Poiseuille flow can be established. In the case of "PCC small" coatings (Figure 39D), the capacitance curves were very near each

other during the time of the first few seconds. The slope of PVOH containing coating was slightly higher in the beginning of the measurement indicating higher initial absorption rate of the coating layer. This indicates that the pre-diffusion of vehicle into the binder accelerates the penetration.
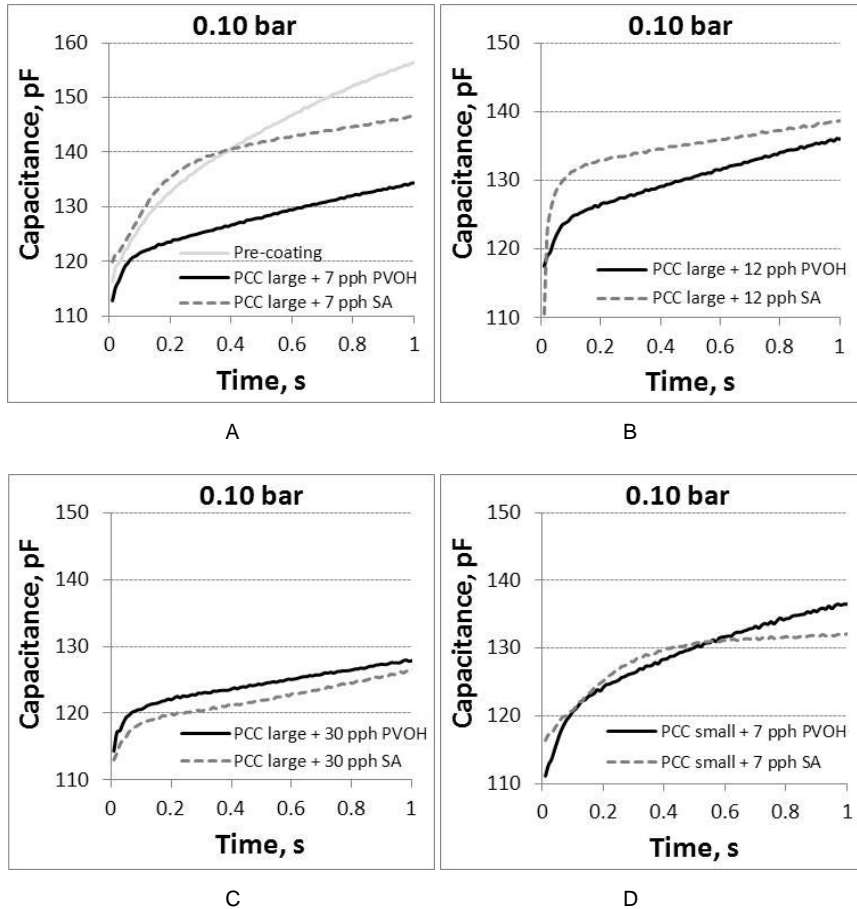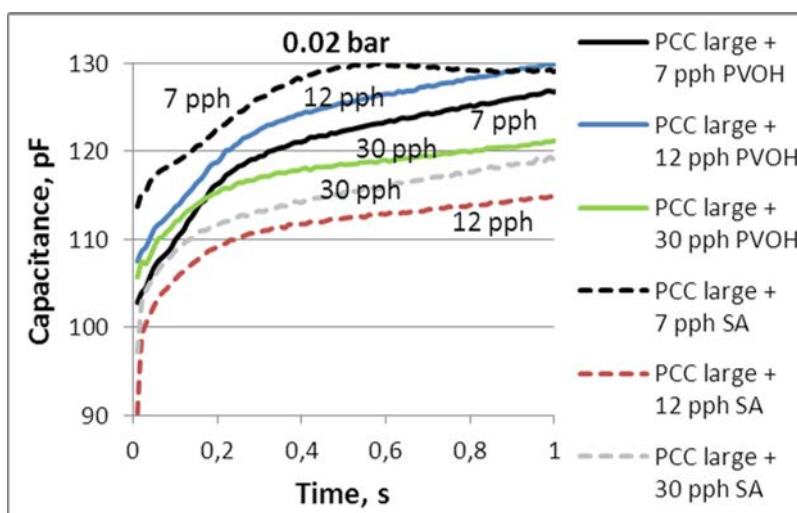

Figure 39. The effect of binder type and binder amount in the "PCC large" and "PCC small" coatings on the results of Clara. Measured with Versamark® cyan ink using 0.10 bar over-pressure: A, B, and C refer to 7, 12 and 30 pph binder levels in "PCC large" coatings, respectively, and D – refers to 7 pph PVOH and SA "PCC small" coatings. Based on Paper II (Figure 9).

Absorption in the non-pressurized regime

Figure 40 shows the capacitance results of the same coating layers at the external over-pressure of 0.02 bar (effectively no additional pressure). The 7 pph SA latex

"PCC large" coating produced again the higher capacitance results than PVOH containing, but the slope of the curves in the beginning of the measurements were already very similar. The capacitance results of 12 pph and 30 pph PVOH/"PCC large" coatings were seen to be at a higher level than the results of comparable SA latex containing (12 pph binder: PVOH 107-125 pF and SA 90-110 pF; 30 pph binder: PVOH 105-115 pF and SA 100-112 pF). It seems that the importance of inkjet ink diffusion into the binder and at the same time the swelling of the binder network increases as the coating colour has more binder and/or the external over-pressure decreases. This argument supports the conclusion that diffusion must compete against permeation-driven flow, which, under external pressure, can exceed the rate of diffusion into the water-swellable binder. The hydrophilic PVOH can absorb inkjet ink whereas the hydrophobic SA polymer latex matrix cannot. The bimodality can still be seen in the 7 pph SA coatings.

Figure 40. The effect of binder type and binder amount in "PCC large"coatings on the results of Clara at the external over-pressure 0.02 bar. Measured with Versa-mark[®] cyan ink.

Short-time and transition penetration in the coating structure

In the beginning of capacitance-based measurements, at 0.02 bar over-pressure, similar polar liquid inkjet ink penetration rate into the 7 pph SA containing coating and the 7 pph PVOH coating could be detected. When the binder amount in-creased to 12 pph or 30 pph, the PVOH containing "PCC large" coating produced a higher capacitance value than the comparable SA containing coatings. However, the situation changes when the external over-pressure is increased to the 0.10 bar, corresponding to the inkjet ink droplet hitting to the paper surface, or even higher, 1.50 bar. The pressure increase speeds up the penetration of the liquid

into the structures, and the penetration speed of SA latex containing coating increases more during the pressure increase than the PVOH coatings. The SA containing coatings had less binder interaction with the fine pores whilst permeability is maintained. At lower pressure, the ink penetration is controlled strongly by the nano-capillary absorption and diffusion into the PVOH. The pressure increase raises the speed of ink permeation more in large pores than in the small diameter pores because the capillary pressure of small pores is higher than the pressure in the large pores. At the higher external over-pressure, the permeation flow has the greater role to play in the liquid transfer than at the lower pressure.

We recall that the short timescale results of binder containing "MCC large" tablets in the microbalance measurement showed that PVOH containing coatings absorbed water quicker than SA latex coatings. However, this kind of difference could not be detected with the Clara measurements from "PCC large" coated papers at 0.10 bar external over-pressure, where inkjet ink penetrated quicker through the 7 and 12 pph SA containing coating layers than through the PVOH containing. There is also some variation in the results of Clara (*Paper III*) as well as in the microbalance, but by variation alone the differences in the results cannot be explained. Both pigments had very similar intra-particle pores and therefore the short timescale penetration speeds were expected to be similar while the chemistry of the structure remained similar. At the lowest 0.02 bar over-pressure, this kind of indication of slower penetration speed with the SA containing coatings than with the PVOH coatings could again be detected, especially at 12 and 30 pph binder content. The significance of diffusion increases, but primarily the permeability dominates whenever pressure is applied. Furthermore, the likely wetting delay caused by surfactant reorientation in the latex case is overcome once a small external pressure is applied, launching the system into absorption. The Clara results indicate, therefore, that the low pressure, which the inkjet droplets cause on initial contact at the paper surface, is high enough that at the beginning of the ink imbibition it significantly affects the inkjet ink movement in the top layer of the coating structure, i.e. it induces forced wetting.

The capacitance-based measurement at over-pressure 0.10 bar shows that there are turning points in the slope of capacitance results. The turning points located at a time of 0.02-0.20 s (Figure 39), and, on the basis of both 0.10 bar and 1.50 bar results, this is the moment when the capillary force-filled pores are starting to become saturated and the remaining larger pores fill under the external pressure. This changes the mechanism from capillary flow to permeation. This continues through the wetting of the base paper as the rate of base paper penetration is controlled by the permeability of the coating layer. If we now consider the absorption time of 0.36 s for the 7 pph SA-containing coating, as measured by DIGAT (Figure 29), we can conclude that the ink has already penetrated through the coating layers at the moment when the gloss of the 8 gm^{-2} ink layer disappears.

At a binder amount of 12 pph and at the 0.10 bar external over-pressure, the SA latex containing "PCC large" coating absorbs the ink still more rapidly than PVOH. The effect of diffusion becomes more and more important when the external pressure decreases, and this acts to differentiate between the binders. At the

0.02 bar over-pressure, only the lower level of 7 pph SA binder containing "PCC large" coating remains at higher capacitance, from 115 pF to 130 pF, than the PVOH containing, from 105 pF to 115 pF (Figure 40).

<u>Long-time penetration</u>

The long timescale penetration means the time after the turning point in the capacitance results curve. In this regime, either the external pressure has forced the transition to permeation flow or the equilibrium has been reached at low external pressure between the capillary wetting force and the viscous retardation. The SA containing "PCC large" coatings had similar or even faster penetration speed of the inkjet ink than the PVOH containing coatings, depending on the external pressure. This result is very similar to that of the microbalance with "MCC large" coatings, and indicates that the permeability of the SA containing coatings is greater than that of the PVOH containing, once the external pressure dominates.

At the 0.10 bar over-pressure, the results varied depending on binder content, and at 1.50 bar the ink penetrated through the SA containing "PCC large" coatings quicker than through the PVOH containing coatings. One explanation for the slope variation at the over-pressure of 0.10 bar, consistent with the discussion above, can be that the structures combined with this inkjet ink might exhibit a critical pressure response in this region, where the normally dominating diffusion, combined with capillarity, becomes less important as the permeation starts to dominate.
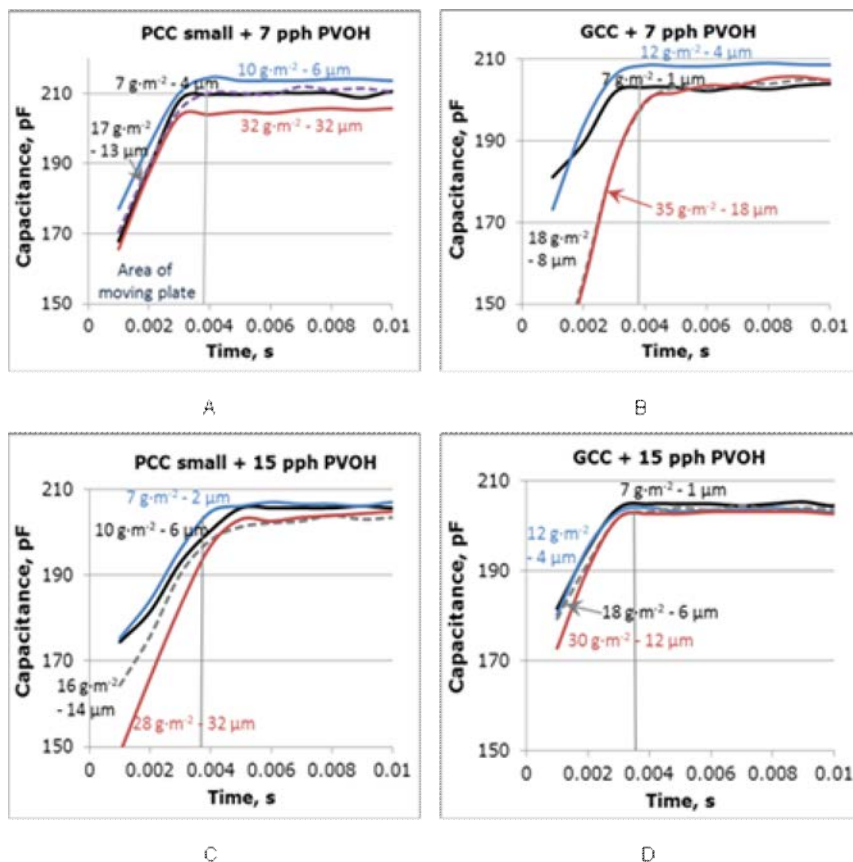
4.3 The role of coating layer thickness in inkjet ink penetration

One way to affect the volume capacity where the inkjet ink can absorb is to increase the thickness of the coating layer. The research into this coating thickness effect was made by using "PCC small" or GCC pigment, and partially hydrolyzed PVOH as the binder. The binder amount was 7 or 15 pph. The coating colours were applied on plastic film using different coat weights to generate the different coating thicknesses. In section 3.2 "Designed coating structures and binder films, and their production", the production of these samples has been described more closely. Figure 41 shows first of all that the inkjet speciality "PCC small" pigment provided thicker coating layers on the plastic film surface than the offset standard GCC at equivalent coat weight (*Paper III*). The GCC pigment produces a more tightly packed coating layer structure, as the Si-oil porosity results indicated (Figure 20). Most of the Clara absorption result curves reached the maximum value of capacitance at the short time of 0.004 s (Figure 41). Inkjet ink has more or less penetrated through the coating layers which were applied on the plastic film surface, even though the thickness is up to 35 μm, during 0.004 s time. The pigment type or binder amount did not change the situation, as *Paper III* shows. The transit of the removable plate out of the measuring area lasted the first 0.0038 s, and so the relevant data are on the limit of stable detection.

The results show that, at longer time delays than 0.004 s, permeation flow dominates in the coating structures. The results agree very well with the results of Ridgway *et al.* (Ridgway *et al.* 2001, Ridgway *et al.* 2002). They calculated with a Pore-Core computer model of void structure how quickly alcohols and water move in the coating layer structure. Their results showed that smaller radius capillaries fill initially faster than larger ones. The fine capillaries filled faster until 0.00026 s to 0.00056 s, depending on the equation used in the calculation (Bosanquet inertia versus Szekely pore entrance energy loss), and only after this time do the larger pores start to fill at a faster rate.

The coating layer penetration results of the Clara device indicate, therefore, that the initial nano-capillary flow is too fast for the device. Using the Bosanquet absorption equation (Bosanquet 1923), which takes into account the inertial flow of liquid, the time of absorption into a 0.1 µm length pore is below 10 ns (Ridgway *et al.* 2002). However, the Clara starts the detection of penetration from 1 ms. From this it can be concluded that the liquid in the coating has already passed via the first preferred pathway wetting front point in an idealised free access structure (non-permeability limited) to about the scale of a centimetre. The maximum coating thickness in this study was 35 µm, which, since it is a complex network, probably does not exhibit direct *z*-directional centimetre scale pathways for ink, but is highly likely to have been traversed by the leading liquid front via a tortuous path through the complete sample thickness during this relatively long timescale in absorption terms.

Figure 41. The effect of coating layer thickness on the capacitance results. The inkjet speciality "PCC small" (A and C) and offset standard GCC (B and D) coatings are on a plastic film. The thickness of each coating layer has been added after the coat weight value. The ink was cyan dye-based ink from Versamark® VX5000e and the external over-pressure at the chamber 0.10 bar. The final capacitance level of Clara results depends on the variation of the plastic film (204–212 pF). Based on Paper III (Figure 7).

At the beginning of the measurement, it seems that the higher the coat weight the lower starts the values of the capacitance curves. This suggests that the thicker coating layer, in this case a higher coat weight on the plastic film, has more pore volume during the first few milliseconds of absorption than the thinner one. On the other hand, this can be an indication of the different kind of coating layer structures of the low and high coat weights. The thicker coating structure is less ink absorbing in the beginning stage of absorption. Laudone *et al.* (Laudone *et al.* 2006) found out that a high coat weight coating had lower porosity than a low coat weight coating because high coat weights tend to consolidate more. However, we

must remember that during the first 0.0038 s time the plate on the Clara device is still moving, and therefore the detected capacitance measurement area progressively increases. Additionally, the Clara is based on making an average dielectric permittivity assumption, and the thicker coating will have a higher permittivity weighting and so appear to accelerate the liquid passage in that region. Nonetheless, this provides more likely evidence for the preferred pathway wetting phenomenon as a greater proportion of pores are initially by-passed as the length of the sample increases.

The effect of coat weight on the paper surface was studied by applying the 7 and 15 pph PVOH (partially hydrolyzed) containing "PCC small" coating with a curtain coater on the commercially pre-coated fine paper surface (*Paper III*). Section 3.2 "Designed coating structures and binder films, and their production" introduces the coating procedure. The penetration distance results, which were calculated from the capacitance results, show (Figure 42) that in the beginning of the absorption into curtain-coated "PCC small" coatings, the distances have quite a linear relation to the square root of time, indicating either equilibrated Poisueille laminar flow according to the long timescale applicable Lucas-Washburn equation, and/or a Fick's Law diffusion response. There are two linear regions with respect to the square root of time during the first second timescale, with the turning point between them located at time 0.2 s (Figure 42), similarly as in the microbalance results though the turning point located at a different time moment. Ström *et al.* (Ström *et al.* 2008) had similar results in their study of PVOH containing coatings. In the first linear region of capacitance-based results, the properties of the coating structure predominantly affect the absorption, and in the second region the porous structure of the base paper dominates. This turning point seems to locate at a distance of 15 μm to 35 μm from the top of coating layer, depending on the coating layer thickness. The thicknesses of the applied curtain-coating layers were in the region of 2.5 μm and 8.5 μm. The thickness of the pre-coating layer was not measured, but it seems that the turning point locates neither in the pre-coating layer nor just under it. The turning point locates deeper within the base paper. The reason for this may again be in the PVOH polymer moving into the base structure and/or diluting or more likely the difference in preferred pathway wetting front and the line of saturation.

A   B
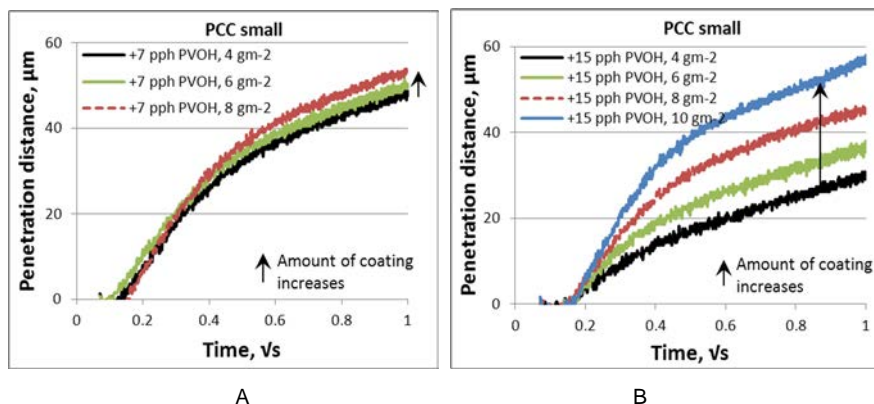
Figure 42. The penetration distance of dye-based ink (Versamark® VX5000e cyan) in the inkjet speciality "PCC small" coatings during square root of time clearly showing the two regimes of absorption. The external over-pressure at the chamber 0.10 bar. A – "PCC small" with 7 pph PVOH, B – "PCC small" with 15 pph PVOH. Based on Paper III (Figure 11).

The turning point becomes more and more visible as the coat weight and binder amount increases, indicating a greater effect of the top-coating layer in the complete sheet construction on the apparent inkjet ink imbibition. This could, however, be an artefact of the measurement since the permittivity of the coating layer distance is different to that of the base paper, and in the Clara calculation it assumes an average permittivity throughout (section 3.3.2 "Liquid penetration"). The penetration rate apparently increased as the coating layer thickness increased (Figure 42). The higher pore volume combined with more nano-size pores (Figure 43) promotes the ink penetration into the coating layer structure, but the increased permeation resistance of the thicker coating should act eventually to slow progress. This evidence highlights the weakness of the Clara device in that it probably misinterprets the coating thickness effects on imbibition speed due to the ratios in permittivity of the different layers. The higher coat weight structure, nonetheless, has larger pore volume and therefore more nano-size pores, which will keep the high capillarity action active for longer.

A   B
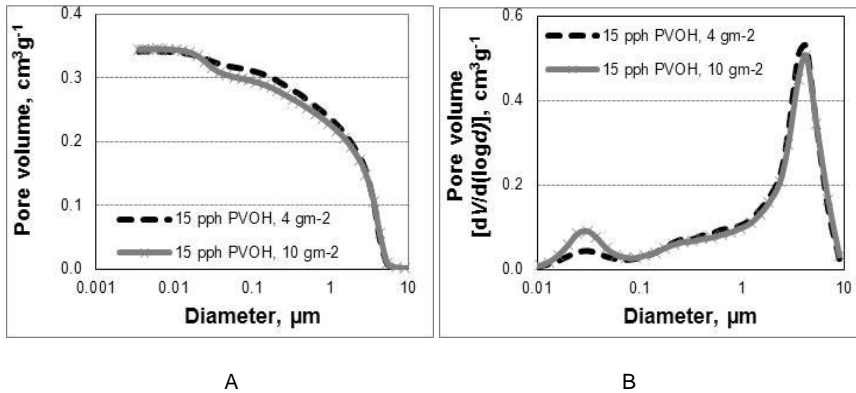
Figure 43. The pore volume (A) and pore size distribution (B) of different coat weight "PCC small" coatings. Measured with mercury porosimetry. Based on Paper III (Figure 4).

The findings suggest that in the lower coat weight coating, the ink stays longer in the top-coating layer because the ink first penetrates quickly in the small nano-size pores of the structure caused by high capillarity and the Bosanquet inertial wetting regime, and the wetting front pins for a while in the interface between the small pore size fraction of the top-coating and the underlying pre-coating before it continues the penetration. The longer the ink front remains pinned in the top-coating means that inks have higher probability to mix with each other.

4.4   Summary of the coating structure effect on ink imbibition

All the results of absorption measurements, namely microbalance, thin layer chromatography and capacitance-based Clara measurement, indicate that the rate of liquid transport in the coating layer structures varies depending on the moment of detection. Each research method has a turning point of sorption, and before and after this point the penetration rate has a linear relationship to the square root of time. The moment of turning point depends on the sample preparation, tablet versus coating on film versus hand coating on pre-coated paper versus curtain coating, measuring principle, liquid being transferred upwards or downwards, from a supersource or a layer, including lateral spread or not, and the external pressure. The capacitance-based results show further that the over-pressure, caused by the inkjet ink droplet coming onto the paper surface, is in fact large enough to initiate wetting, but that we can consider it negligible in relation to capillarity but effective in promoting initial permeation. Therefore, in the ideal experimental situation the pressure should be removed after the start of the experiment, as of course happens in the real printing situation. Additionally, weaknesses in the capacity measurement theory, when based on the average assumption of constant permittivity throughout a coated paper, have been highlighted.

At the first instant of the liquid arriving onto the coating structure, the liquid penetrates more quickly into the very top-coating structure than later in the imbibition process. This is suspected to be an effective surface wetting phenomenon including the surface nanopores. After the liquid has wetted the coating surfaces, the major driving parameters for ink absorption into porous coating structures are capillarity and permeability in relation to the fine pores and the larger interconnected pores, respectively. The capillary force is active in the fine pores, and once the capillaries become saturated then permeability is the controlling factor for further imbibition to enable access to further unsaturated nanopores, indicating either equilibrated Poiseuille laminar flow according to the long timescale applicable Lucas-Washburn equation, and/or a Fick's Law diffusion response. In the case of inkjet ink imbibition, the polar ink vehicle firstly moves into the nano-size capillaries of the coating layer and forms the wetting front, where the colorant part of ink, if of the same charge as the pore walls is repelled or if of opposite charge is held by that charge, cannot transfer or does so only slowly by concentration-driven diffusion. Thus, anionic repulsion hinders the anionic colorant penetration into nanopores, and cationic attraction pins the colorant initially at the first contact point until concentration of colorant increases.

The permeation flow in coating layers becomes dominant as the resistive component after the first 0.004 s time. Depending on external pressure, the existence of fine nano-size pores either speeds up the sorption rate of the polar liquid ahead of the pore saturation front in the case of zero or low external pressure, or permeation dominates and the finest pores fill behind those of the larger connecting pores when sufficient external pressure is applied. In practice, external pressure only occurs at initial contact of the printing ink droplet. The results show that the coating with the dual-porosity structure provides an optimal balance of these two effects, i.e. it promotes the fast liquid absorption because it produces a coating structure with high permeability and it contains nano-scale pores that drive the liquid front forward, whilst the charge distribution defines the pinning and fixing characteristics of the colorant, thus supporting Hypothesis III.

> **Hypothesis III** – the verity of Hypotheses I and II can be used to design porous coating structures, based on discretely bimodal pore size distributions, using binder and surface charge distribution characteristics to provide rapid fixing of ink colorant optimally close to the coating surface.

The pigment selection affects strongly the forming of the coating layer structure, but the binder type and its amount has also a major role in determining connectivity, permeability and interaction with liquid.

The DIGAT results from the gloss decay of a wet ink layer showed that the inkjet ink can initially stay on the top of the PVOH and SA latex containing coatings for a quite similar delay before it penetrates into the coated papers, but the ink penetration speed in the coating layer is higher in the SA bound coatings, especially under a high external pressure, indicating a permeability controlled difference between the structures using different binders – the particulate SA binder leading to a coating structure that is generally more permeable. The local-

ised hydrophobicity of SA containing coating slows firstly the inkjet ink penetration into the structure, related to the likely action of the wetting delay by surfactant. In the coating structure, the PVOH can locate in the intra-particle pores as well as on the surface of large pores, whereas SA latex remains in the large pores associated with the inter-particle interstices. Even a small binder addition, 1 pph, has a remarkable effect on the liquid movement in the coating structure as the TLC and microbalance measurements showed.

The PVOH polymer matrix can be diffused into by the polar liquid, as in the case of water-based inkjet ink, and the swelling of PVOH closes the nano-size pores in the coating structure and decreases the total porosity. Therefore, the ink can transfer in the PVOH containing coating structure but with lower speed than in the non-swelling SA containing coating. However, in the non-pressurized condition, and at the short timescale, the PVOH containing coating with nano-size pore structures absorbed polar liquid quicker than the SA containing structure. This indicates that the ink diffusion in the PVOH binder happens at the same timescale as the ink capillary flow in the SA coating. In parallel, the longer timescale absorption becomes permeability limited, and so the mechanism collapses back into equilibrium viscosity controlled flow. The quicker ink penetration speed (as measured by the capacitive method, Clara) and the same ionic charge of ink and binder in the SA latex containing coating structure causes colorant transport through to the top part of the base paper, and therefore print-through problems can occur, as we shall see in the print quality section.

The results showed that the nano-size pores are important in the polar liquid imbibition, but the pre-diffusion into binder is an additional short timescale phenomenon due to the location of the swellable binder in both those same nanopores and on the pore walls. The capillary flow controls the polar liquid imbibition in the short timescale, but the diffusion of water into binder polymer is taking an active part in this process. Water molecules diffuse into and within the hydrophilic PVOH polymer causing binder swelling, which closes some of the small pores and decreases the diameter of remaining pores, thus slowing the capillary flow as a function of time. The SA latex does not absorb the ink vehicle to the same extent as the PVOH, and therefore the dominating phenomenon in the coating structure is then capillary absorption and permeation. These findings support Hypothesis I.

Hypothesis I – inter molecular diffusion of the liquid phase of inkjet ink into polymers acts on a sufficiently fast timescale and in sufficient volume to compete with the permeation of ink through coating structures.

One way to increase the inkjet ink penetration speed is to apply a higher coat weight of an optimally designed absorbent coating structure on the paper surface. The higher coat weight produces more pore volume and a greater proportion of that optimally designed coating pore network structure, and so there is more space where a high inkjet ink amount can transfer. In this research, the coating pigment had intra-particle pores and therefore the higher coat weight means also more nano-size pores, which promote quicker ink penetration.

# 5. Mechanisms influencing liquid absorption in coating binders

5.1 Liquid absorption by binder films

The diffusion of liquid into polyvinyl alcohol and on styrene acrylate latex binders, without the effect of coating pigments, was studied by using films formed using the binder polymers alone. The SA latex films were produced with a draw down coater and the PVOH films in the moulds. The study is based on *Paper IV*. In this research, the same styrene acrylate latex that was used in the coating studies and three polyvinyl alcohols – partially and fully hydrolyzed, and carboxylated – were used. Table 5 in chapter 3 shows the basic properties of the polymers. Besides the study of these polymer films, the effect of the addition of cationic or anionic additive in the soluble binders was clarified. To achieve this, the cationic poly-DADMAC or anionic sodium polyacrylate was added in an amount of 1 and 4 pph in the partially or fully hydrolyzed PVOH. The absorption of liquid into the films was mainly studied by using self formulated anionic and cationic ink, as well as commercial cyan ink (Versamark® VX5000e), but the behaviour of pure liquid was also considered in some measurements by using de-ionized water or hexane to provide contrast between a purely polar and purely dispersive (non-polar) liquid. The measuring method has been described in section 3.3.3 "Absorption of liquid into binder films". This section concentrates on the second hypothesis of this thesis work: *Hypothesis II* – the colorant follows ink vehicle into the binder polymer matrix, the vehicle acts as a colorant carrier, and this phenomenon competes with the surface adsorption of colorant.

Polyvinyl alcohol is a hydrophilic binder (Hara 2006, Pinto and Nicholas 1997), and absorbent. This is shown by the absorption results of the PVOH binder films (200–250 µm) in the case of exposure to anionic and cationic aqueous dye-based inkjet ink, Figure 44. The ink absorption amount depends on the binder type and the degree of the polymerization of PVOH. The fraction of absorption (absorption capacity) of the fully hydrolyzed PVOH is seen to be in the region of 20–30 wt-%, and that of the partially hydrolyzed PVOH 30–40 wt-%. The carboxylated PVOH had the highest absorption capacity. The carboxylated PVOH also has the lowest degree of hydrolysis meaning that this polymer has more amorphous regions that

can hydrogen bond the ink. The amount of amorphous and crystalline regions in the polymer structure defines the content of absorbed liquid (Ricciardi *et al.* 2004, Hasimi *et al.* 2008). At certain relative moisture content, a polymer with a low crystallinity absorbs more moisture than one with high crystallinity (Hasimi *et al.* 2008, Salmén and Back 1980). The results of this study in Figures 44 and 45 illustrate that the more crystalline structures containing fully hydrolyzed PVOH (Kumaki and Nii 2010, Hasimi *et al.* 2008) absorbed less of the inkjet inks (or moisture) than the partially hydrolyzed. This confirms that the amorphous regions of the PVOH polymer can absorb water molecules and likely hydrogen bond readily, whereas the crystalline part cannot. The diffusion and fixing of water molecules to the amorphous region of the PVOH matrix causes the swelling of the polymer, whereas in the crystalline part either the water is excluded or the molecules penetrate through the PVOH structures without binding there. Iordanskii *et al.* (Iordanskii *et al.* 1996) introduced a third mechanism that can affect the water movement at the supermolecular level: collapse of domains or transformation in the interface layer of polymer. Water molecules form clusters in the range of 0.27–1.00 nm, depending on the amount of molecules in one cluster, (Topgaard and Söderman 2001), and these are small enough to fit into the polymer network without disrupting it. The order of the studied films remained the same regardless of absorption time, indicating no chemical change occurred. The standard deviation of the absorption results was at a maximum of 2.0 wt-%, but in most cases it was lower than 1.0 wt-%.

The least absorption of polar ink amongst the studied binders was shown in the case of the styrene acrylate latex film. The SA latex polymer has a hydrophobic nature, and it is the surfactants on the polymer surface that permit its dispersion in water and allow wetting of the polymer surface.
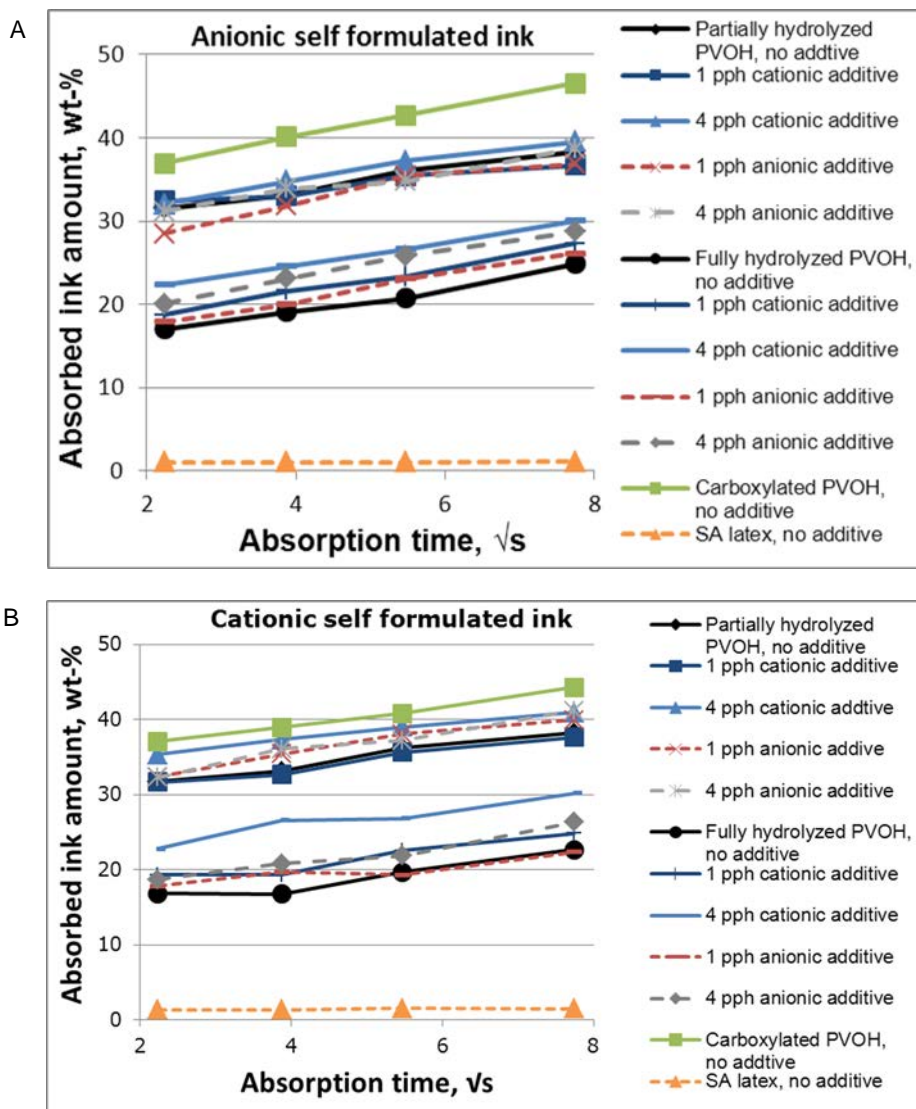
Figure 44. The absorption of anionic and cationic self formulated inks into the PVOH and SA latex films, expressed as the weight fraction of film weight. The standard deviation of absorbed ink amount was at maximum 2 wt-%, but in most cases it was under 1 wt-%. Cationic additive was polyDADMAC, and anionic additive sodium polyacrylate – the charge additives being dosed into the binder before film forming. Based on Paper IV (Figure 2).

The addition of cationic or anionic additive into the PVOH binder caused no significant differences in the absorption by the partially hydrolyzed PVOH, but in the case of fully hydrolyzed PVOH there were some differences, especially when the absorption results of films with 4 pph additive and binder films without additive were compared. This indicated that the additives either have very similar absorption properties for inks as those of partially hydrolyzed PVOH or the amount of additives were so low that they did not affect the results significantly indicating that the amorphous nature of the binder is the overriding factor. However, since they did affect the fully hydrolyzed PVOH, we can probably conclude that if there was an effect going to happen for the partially hydrolyzed it would have been seen. In common formulations of inkjet coatings, the amount of additives is usually within this same range. Thus, the charge additives probably disrupt the ordered hydrolyzed film structure forming, and therefore it is probable that they do not affect the diffusion into binder polymers if the binder itself is poorly absorbing unless this disruption takes place.

Since very similar absorption results were reached when the same binder films were immersed in either the anionic or the cationic dye-based ink (Figures 44A and 44B), we can conclude that the ionic charge of ink affects only the ink colorant fixing but not the absorption of ink vehicle. The same chemical groups of the polymer are involved in both cases, and the water-based ink vehicle hydrogen bonds to the groups of the binder.

As the absorption time increases, so the amount of ink absorbed into the films increases. The binder films will reach a stage of saturation if the absorption time is long enough, as Figure 46 shows with the partially hydrolyzed PVOH and SA latex films.

Figure 44 shows further that the amount of absorbed ink had a linear relation to the square root of time indicating that the polymer diffusion follows Fick's second law (chapter 2), where the liquid position is proportional to the square root of time and the position is related to the volume of ink and thus represents the mass of liquid uptake. All lines of absorption data in the PVOH films are parallel, indicating equal absorption rates. However, they locate at different heights in relation to the y axis. This is accounted for by differences in the moisture content of the binder films under ambient room conditions (23 °C and 50 %RH (relative humidity), Figure 45), but the greatest increase in the absorption results appears between the time moments 0 s and 5 s. These results indicate that another phenomenon has occurred prior to the first measurement time. It can only be speculated what this might be, but one may suspect a polymer swelling effect once exposed to moisture, which might be a selective molecular weight dependent phenomenon, i.e. low molecular weight species.
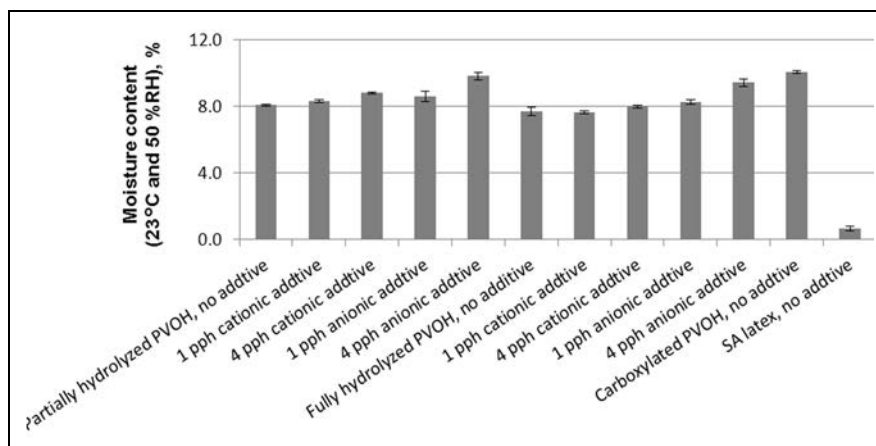
Figure 45. Moisture content of PVOH and SA binder films at 23 °C and 50 %RH. Cationic addtive was polyDADMAC and the anionic sodium polyacrylate.

Besides water, inkjet inks contain other components, like glycols (Svanholm 2007), which affect the absorption properties of the binders, too. Figure 46 illustrates the absorption differences between water (polar), hexane (non-polar, i.e. purely dispersive or apolar) and commercial inkjet ink (cyan ink from Versamark® VX5000e) into the partially hydrolyzed PVOH film. The PVOH film absorbed 30.2 wt-% water at the 5 s absorption time and 4.3 wt-% non-polar hexane. The same PVOH film exhibited a 29.2 wt-% absorption when exposed to the commercial cyan dye-based ink for 5 s, and this value will be used in the theoretical calculations of section 5.5 "Binder swelling – impact on nano-size capillaries", where the effect of PVOH swelling on the coating pore diameters is studied more closely. The role of other components in the ink is usually to make the ink more controllable at the nozzle and to form a droplet quickly enough after the nozzle before contacting the media surface. The replacement of some small part of ink with less hydrophilic components causes this more desirable small drop size. The styrene acrylate latex film absorbed only 1.4 wt-% of cyan inkjet ink. The hydrophobicity of the underlying latex prevents absorption of the polar ink.
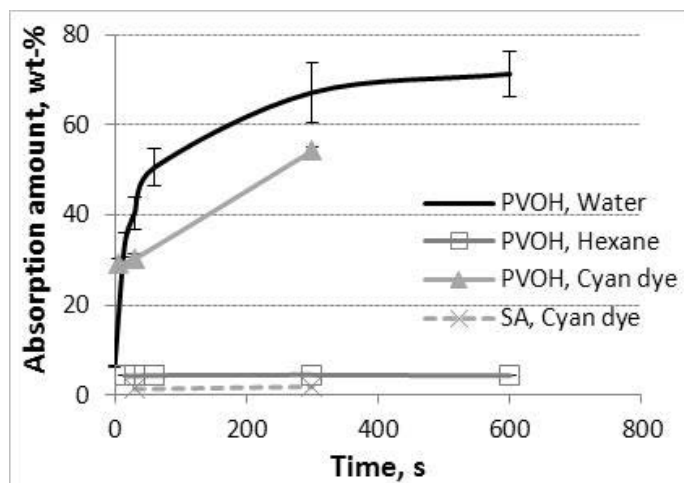
Figure 46. The absorption amount of polar and non-polar liquids into PVOH (partially hydrolyzed) and SA latex films. Assumed is a specific gravity for water of 1 and hexane 0.657, and the swelling fraction is given by (mass of liquid absorbed/mass of binder)* 100. Water and Cyan dye commercial ink were polar liquids, and hexane non-polar. Based on Paper I (Figure 15).

5.2 Diffusion of liquid into coating binders

5.2.1 Diffusion coefficient

The diffusion coefficient of liquid into binder films was studied by detecting the absorption data for water moisture into binder films using the techniques of Dynamic Vapour Sorption, DVS-1[33], which is a gravimetric moisture sorption measurement. This has also been shown in *Paper VI*. The analyses were made with partially hydrolyzed PVOH and SA latex films using different moisture contents of surrounding air (Figure 47). The shape of the moisture absorption result curves are an inverse exponential, and therefore there has been applied the so-called Case II or Linear Driving Force Mass Transfer Model in the calculation of diffusion coefficient (Carslaw 1997). Carslaw considers an axially symmetrical system for heat transfer from the exterior to the centre of a material cylinder.

---

[33] Surface Measurement Systems, 5Wharfside, Rosemont Road, Alperton, Middlesex, HA0 4PE, United Kingdom.
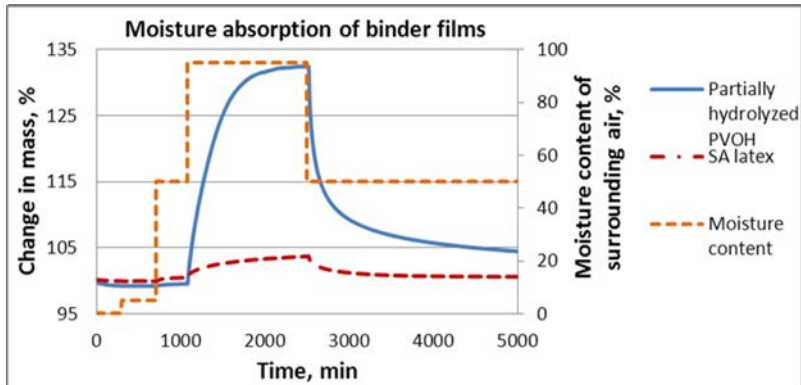
Figure 47. Absorption curves for water vapour diffusion for partially hydrolyzed PVOH and SA latex films. The broken line describes how the moisture content of surrounding air was changed. Based on Paper VI (Figure 8).
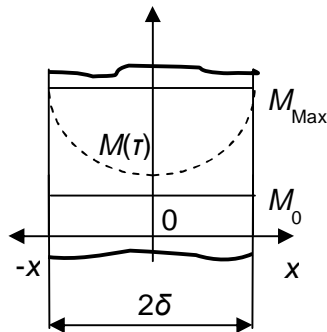
Figure 48. A schematic view of an isolated film cross section, i.e. symmetrical exposure to moisture from both sides. This corresponds in geometry to the cross-section of a cylinder through its central plane. M_0 is the initial moisture content in the film, M_{Max} the maximum moisture content achievable when exposed to the moisture. Based on Paper VI (Figure 9).

Considering Figure 48, it can be seen that exposure of a single film to liquid on both sides adopts the same geometry as a single cross-section of a cylinder of absorbing material through its central axis. It is assumed that there exists an analogous substitution between heat transfer and moisture mass transfer (thermal diffusivity "a", normally found in the Carslaw/Mass Transfer Model equation, is replaced with moisture diffusion coefficient "D"), such that for cylindrical geometry

$$\frac{M(\tau)}{M_{Max}} = 1 - \frac{4}{\pi} \sum_{n=0}^{\infty} \frac{(-1)^n}{(2n+1)} \cos\left(\frac{2n+1}{2}\pi\frac{x}{\delta}\right) \exp\left[-\left(\frac{2n+1}{2}\right)^2 \pi^2 \frac{D\tau}{\delta^2}\right] \quad (37)$$

where τ is time, D the molecular diffusion coefficient and n the consecutive layers describing the build-up of the material around an axial symmetry. This is acceptable since both follow the diffusion equation. Thurn (Thurn 2008) used a similar equation in his study of the diffusion of water in silica coatings. The other variables are described in Figure 48. The equation (37) can be simplified for mass change of moisture in the middle of the plate-like film, i.e. at $x = 0$ and for $n = 0$.

$$\frac{M(\tau)}{M_{Max}} = 1 - \frac{4}{\pi} \exp\left[-\frac{\pi^2}{4} \frac{D\tau}{\delta^2} \right]$$

(38)

In equation (37) the factor $4/\pi$ describes an axially symmetric system consisting of an infinite number of concentric layers, responding to pulse heating in the Carslaw case. Here, however, the geometry is planar, and so the factor is removed according to the boundary condition of zero absorption at zero time, i.e. at the initial time $\tau = 0$ the right side of the equation would become negative, but it should be 0. So, the following equation is used for diffusion coefficient estimation in the planar case considered here. The results are introduced in Table 13.

$$\frac{M(\tau)}{M_{Max}} = 1 - \exp\left[-\frac{\pi^2}{4} \frac{D\tau}{\delta^2} \right]$$

(39)

Table 13. The thickness of binder films and the diffusion coefficient calculated with equation (39).

Binder film	Thickness, m	Diffusion coefficient, m^2s^{-1}
PVOH (partially hydrolysed)	2.25E-04	3.0E-13
SA latex	2.84E-04	3.5E-13

Ideally, a calibration should be used to define the multiplicative factor in the exponential term, but since it is not possible to define the central position of the film thickness, i.e. impossible to define the absorbed mass at the centre experimentally, the term $\pi^2/4$ is retained as an approximation.
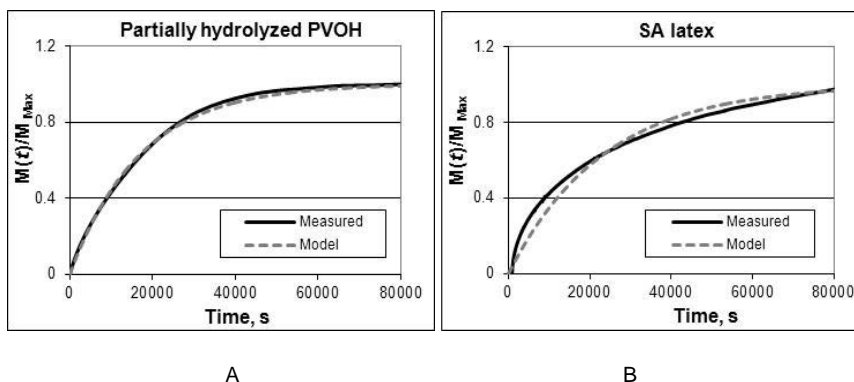
Figure 49. The matching of model and measured data. A, B – the measured absorption amounts divided by the maximum absorption of PVOH or SA latex films and the values of the model (equation (39)), respectively. Based on Paper VI (Figure 10).

In this calculation, it was assumed that the diffusion happens into the plate-like film structure. This is actually valid for the PVOH binder, where water molecules diffuse into the polymer network, but not for the latex. In the case of latex, only a few water molecules can transfer onto the film (Figures 45–47), meaning that the diffusion is more a surface diffusion. If the thickness factor of the plate-like structure is decreased to near zero, the surface diffusion should be derivable. However, at the near-zero stage, the mass transfer becomes zero in equation (39), which cannot be true in the real liquid transfer, and so the problem changes to one of adsorption. Nonetheless, equation (39) fits the experimental diffusion data quite well, and it delivers a reasonable diffusion coefficient for latex, although the model is insufficient for the latex case.

The results of diffusion coefficients for water vapour in films made from the PVOH and SA latex binders are both close to $3.0 \cdot 10^{-13}$ m^2s^{-1}, whereas in the coating structures, such as the "MCC large" pigment with 1 pph of PVOH or SA, they are each about $2.5 \cdot 10^{-11}$ m^2s^{-1}. Hill *et al.* (Hill *et al.* 2011) show that by crosslinking the binder polymer (PVOH and polyvinyl pyrrolidone) the diffusion coefficient for binders can be increased to the range of $1.7\text{-}4.4 \cdot 10^{-11}$ m^2s^{-1}. Thurn (Thurn 2008) showed that a thermally-grown silica coating had a minimal swelling whereas the corresponding evaporated and physical vapour deposited (sputtered) coatings swell significantly. The diffusion coefficient for the sputtered silica coating in the Thurn case was $1 \cdot 10^{-15}$ m^2s^{-1}, a factor of hundred times smaller than in the case of the polymers here, and Riegel *et al.* (Riegel *et al.* 1997) showed that the diffusion constant of water into a silica aerogel was $3 \cdot 10^{-10}$ m^2s^{-1}. Is seems that the polymer film allows water diffusion at the same rate as silica. In comparison, for cellulose fibres the water vapour diffusion coefficient is also about 10^{-11} m^2s^{-1} (Topgaard and Söderman 2001), and for paper, with porosity of 20 %, 10^{8} m^2s^{-1} (Hellén *et al.* 2002). The porous structure of a fibre mat structure enables the higher diffusion because

there are more surfaces accessible by permeation by the vapour where the diffusion into the fibre body can happen. Therefore, it can be concluded that the permeability of the coating structure enhances the diffusion rate beyond that of a single binder film alone.

On the other hand, the water phase type, i.e. separate molecules, clusters or films, seems to differ between the cases of the PVOH and SA latex films. The results of differential scanning calorimetry (DSC) made on water absorbed binder films, Figure 50, show that the SA latex film had proportionally more free water than the PVOH film at both 1.0 % and 4.0 % moisture content. In the DSC measurement, the difference in the amount of heat required to increase the temperature of a sample by a defined amount is detected. In the measurement, the freezing of unbound water was analyzed by the latent heat effect at -0.5 °C. The bound water was then identified as the total moisture content of the film found during drying by heating minus the amount of unbound water. The water molecules diffuse in the polyvinyl alcohol polymer network and they can hydrogen bond to the hydrophilic groups of the amorphous region of PVOH (Kumaki and Nii 2010, Lavery and Provost 1997, Hodge *et al.* 1996). Latex does not have chemical groups that can fix the water molecules to the same extent as the PVOH. This kind of difference in the fixing capability between the binders must also exist during practical inkjet ink imbibition.
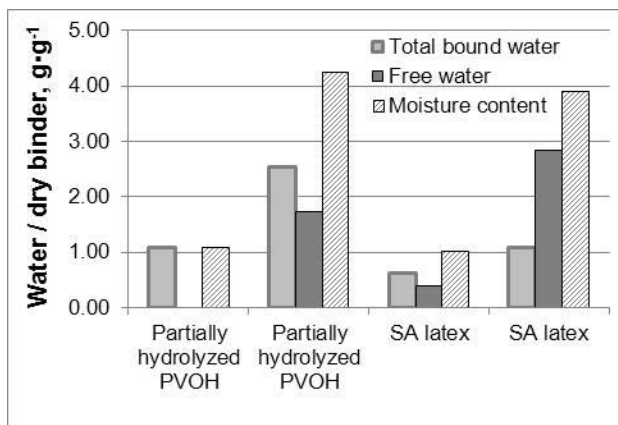
Figure 50. The water type (bound versus unbound) in PVOH (partially hydrolyzed) and SA latex films, as measured with DSC for 1 % and 4 % moisture containing films. The dissolving of PVOH has likely some effects on the results. Based on Paper IV (Figure 3).

The water-solubility of PVOH polymer means that during the contact of inkjet ink some of the PVOH can also dissolve out of or within the film. Figure 51 shows that from the studied partially hydrolyzed PVOH film several wt-% of polymer can disappear during the liquid absorption test, whereas the SA latex film lost far less

polymer than the PVOH. In the latex case it can be assumed that surfactant and/or residual monomer may have dissolved. The polymerised SA latex does not dissolve into the polar liquid, unlike PVOH.
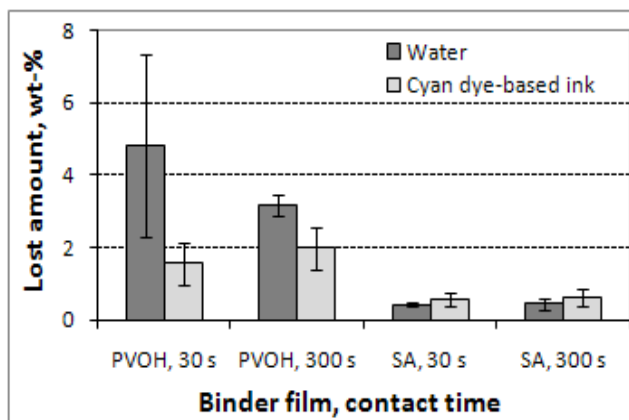
Figure 51. The disappeared (dissolved) binder amount during the liquid absorption test. The PVOH (partially hydrolyzed) and SA latex films have been immersed in water or cyan dye-based ink (Versamark[®] VX5000e) for 30 s or 300 s.

5.2.2 Colorant penetration

The colorant location in the binder films after the absorption test was studied by producing cross-section images from all three polyvinyl alcohols (partially hydrolyzed, fully hydrolyzed and carboxylated) (*Paper IV*). The same binders and binders with cationic or anionic additive were studied, as above in the absorption amount study, and the ink was again the self formulated anionic or cationic ink. Figure 52 shows the location of cyan colorant in the PVOH binder films after the 5 s absorption time. The ink colorant has penetrated into the binder film, regardless of colorant ionic charge, but not completely through the film, and the narrowest colorant layer in both ink cases located on the top part of the fully hydrolyzed PVOH film which had also the lowest absorption amount of the respective inks, Figure 44. The results demonstrate that the colorant has moved into the PVOH matrix with the ink vehicle (mainly water). The vehicle diffuses into the binder film and bonds to the amorphous regions of PVOH and therefore the polymer structure opens so that the colorant fits into the interpolymer structure. The result is in good agreement with the observations of Oka and Kimura (Oka and Kimura 1995) and Svanholm and Ström (Svanholm and Ström 2004). The z-direction figures indicate further that there is more colorant at the top part of the film than deeper in the colorant containing layer. During the absorption test, the top part of the film is first in contact with the ink and as the absorption time increases the deeper the ink vehicle, as well as ink colorant, penetrates, producing a concentration gradient of colorant.
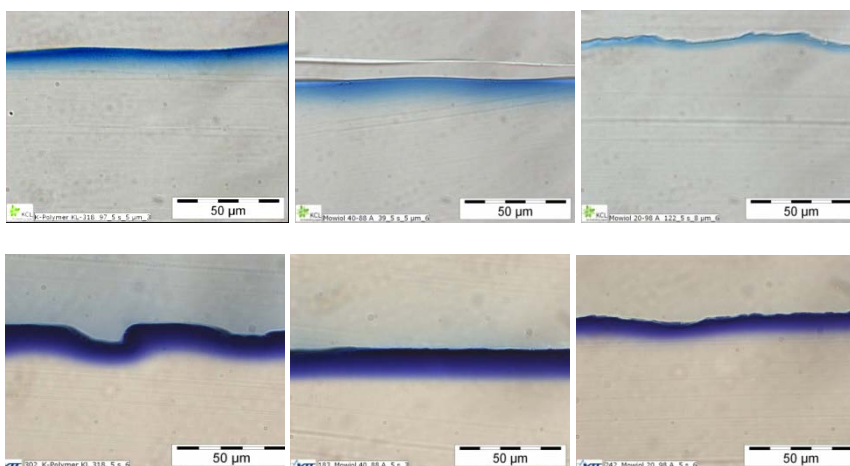
Carboxylated PVOH   Partially hydrolyzed PVOH   Fully hydrolyzed PVOH

Figure 52. Anionic (upper image series) and cationic (lower image series) dye colorant location in the z-direction of PVOH binder films (cross-section figures). Based on Paper IV (Figure 8).

The colorant location in the partially hydrolyzed PVOH was also studied with Time of Flight Secondary Ion Mass Spectrometry (ToF-SIMS), using commercial ink (Versamark® VX5000e cyan water-based dye) as the colorant provider. The similar PVOH film as was used in the previous absorption study was immersed in cyan dye or cyan dye with an addition of 1 gdm^{-3} lithium for 5 min exposure time. It was assumed that the lithium, with its very low molecular weight (small atomic radius), followed the water molecules, and so could be used as a tracer for the vehicle imbibition path decoupled from that of the larger radius dye molecules. The ink colorant contained copper and sodium, and with these elements it was additionally tried to provide a trace for the colorant. The colour immersed sample was dried at 50 %RH and 23 °C overnight. The sample was embedded, cross-sectioned, covered with platinum and finally polished before the ToF-SIMS analysis, as has been descibed in *Paper IV*. Figure 53 shows the distributions of sodium, copper and lithium atoms, and the figure on the extreme right shows the total ion map of the analyzed sample. The amount of copper and sodium, however, was so low that it was very difficult to detect the colorant with certainty. On the other hand, Figures 53 and 54 indicate that the tracer lithium can be found deeper in the binder film structure than copper. There was also a concentration gradient of colorant as well as lithium, indicating water movement within the film and the highest copper concentration located on the top of the film. Thus, there is a chromatographic separation of colorant, and hence penetration differential of colorant into the polymer network. The results converge well with the results of cross-section figures shown before. These results confirm that the ink vehicle

absorbs into the binder polymer network and it behaves as a colorant carrier during the liquid absorption, as Hypothesis II argues.

PVOH film with cyan ink


Na   Cu   Li   Total ion

PVOH film with cyan ink + 1 g dm^{-3} Li

Na   Cu   Li   Total ion   100 μm
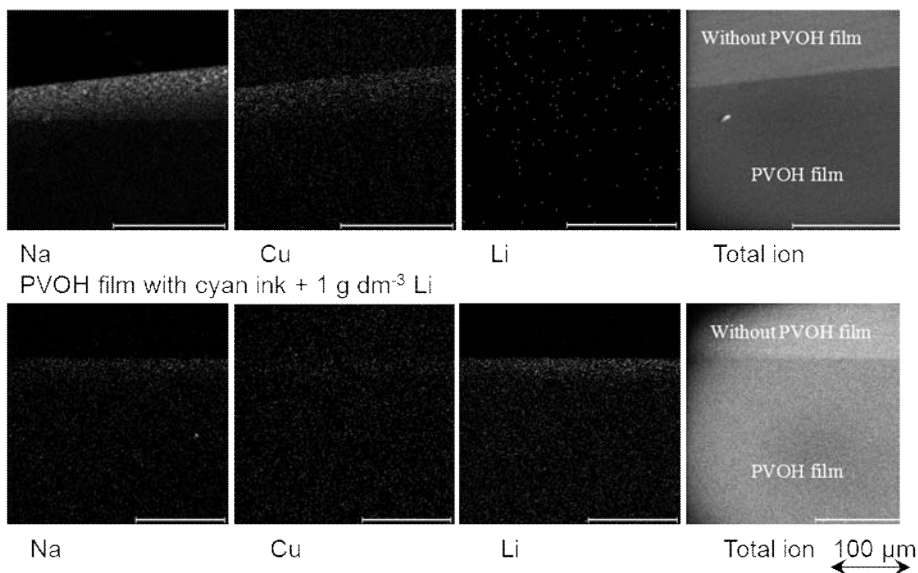
Figure 53. The location of sodium, copper and lithium in the PVOH film analyzed with Time of Flight Secondary Ion Mass Spectrometry (ToF-SIMS). Ink was Versamark VX5000e cyan ink, which contained sodium and copper. Lithium was used as a tracer in the water (made from $Li_2SO_4 \cdot H_2O$). Based on Paper IV (Figure 4).

Interestingly, in Figure 54B, the picture is not so clear regarding the sodium trace. If the results of sodium curves in Figures 54A and 54B are compared, the sodium distribution appears to penetrate deeper into the layer than into the non lithium containing layer. This suggests that sodium in the ink is released from a complex in partial exchange equilibrium with the lithium.

A   B
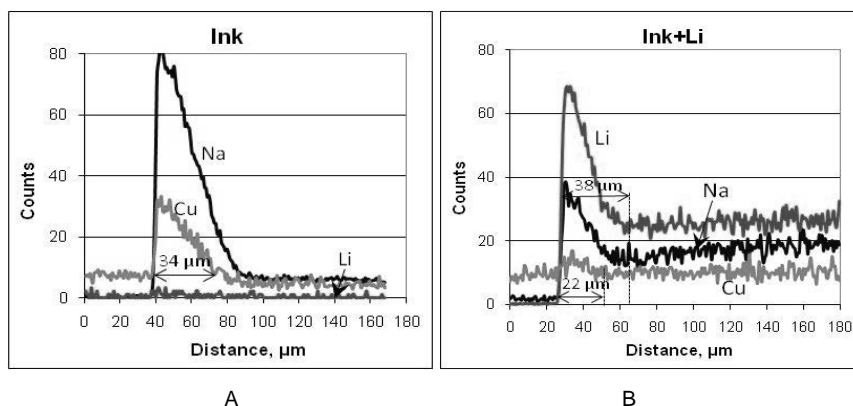
Figure 54. The location of ink (Cu and Na) and water (Li) in the PVOH film layer. Ink was cyan dye from Versamark® VX5000e. Measured with ToF-SIMS. Base on Paper IV (Figure 5).

Figure 55 shows a ranking by cyan colouring. The carboxylated PVOH produced the darkest cyan colour after the 5 s ink absorption time, then came the partially hydrolyzed PVOH and the SA latex film did not have cyan colour at all. The result demonstrates that the higher the ink absorption amount the higher was the colorant content in the binder polymer, and the higher amount of cyan colorant means further that the structure contains more of the colour producing components. Again, the capability to absorb the polar liquid, as inkjet ink, enhances the opening of the polymer matrix where the colorant moves more readily and the greatest absorption produced the darkest cyan colour. The high absorption amount means as well there have been more possibilities for the ink colorant to transfer into the polymer matrix. The SA latex did not have blue colour at all indicating that polymer does not have chemical groups that can bind the colorant at the timescale of 5 s in the inkjet ink immersion. The latex did not absorb water molecules and so the binder polymer structure remained closed to colorant uptake. These contrasting effects of binder could be expected to influence print density distribution properties in inkjet coatings.

Carboxylated   Partially hydrolyzed   Fully hydrolyzed   SA latex
PVOH   PVOH   PVOH
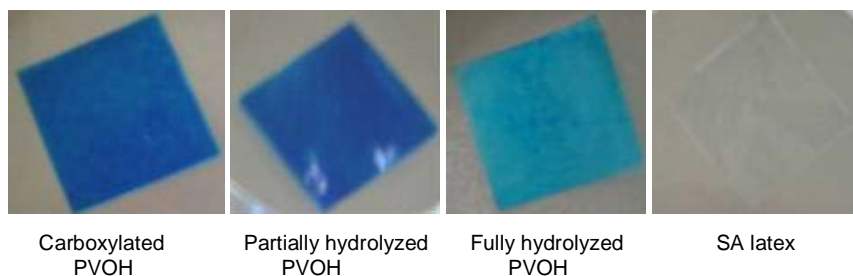
Figure 55. The cyan colour darkness of PVOH and SA latex films after 5 s absorption time. Ink was anionic cyan aqueous-based dye.

Figure 56 shows the SA latex films after 5 s and 60 s of cationic and anionic self formulated ink absorption. The films were produced with the film coater and dried in an oven (105 °C, 5 min). *Paper IV* describes the details of this study. Figure 56 shows that the cationic ink colorant has fixed to the anionic film after 5 s absorption and the film becomes darker blue as the absorption time increases. The opposite ionic charge of binder film and colorant enables the ionic attraction. More colorant molecules have fixed to the binder polymer film structure, when adsorption exposure time was longer, 60 s, and therefore the film had a darker blue colour. The situation is different when the ink colorant has the same ionic charge as the latex binder film. After 5 s adsorption, the SA film did not have any colorant, and after 60 s some small amount only, but not as much as in the case of cationic ink. The light cyan colour of SA latex film at the 60 s exposure time might have a connection to the latex dispersion stabilising surfactant. Altogether, the ionic interactions are the main forces acting in respect to the colorant fixing onto the SA latex.

Cationic ink

Anionic ink
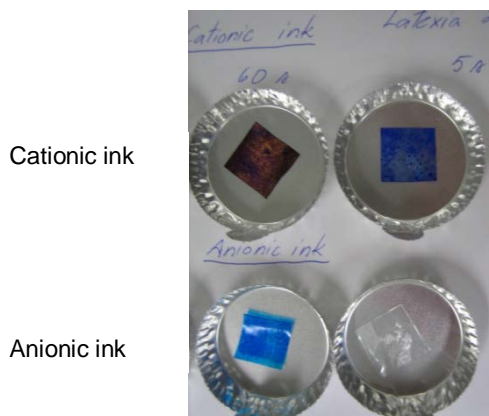
Figure 56. The colour of SA latex films after the immersion of 5 s or 60 s time in the anionic and cationic self formulated inks. Based on Paper IV (Figure 6).

The addition of cationic additive (polyDADMAC) in the PVOH polymer fixed the anionic colorant effectively into the top part of the film, whereas in the case of non-additive or anionic additive containing films the colorant penetrates deeper into the films and there forms a chromatographic colorant separation (Figure 57). The Coulombic forces bind the opposite charges of the chemical groups effectively to each other.
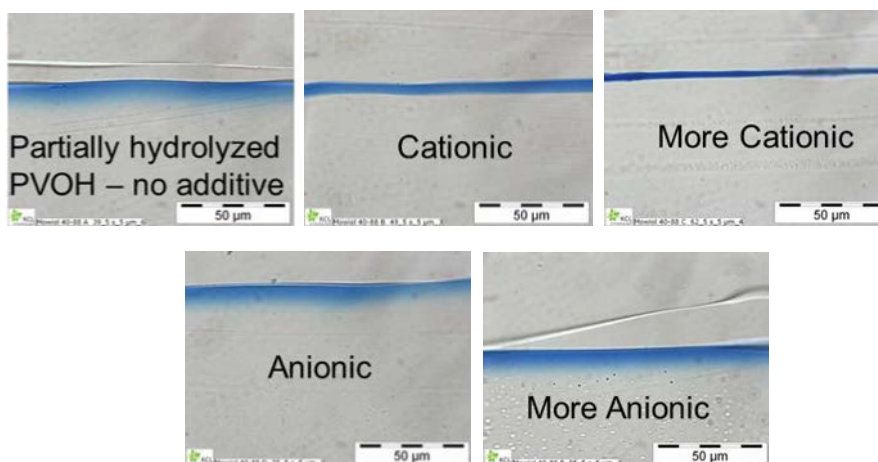
Figure 57. The anionic colorant location in the partially hydrolyzed PVOH films where have been added 1 pph or 4 pph (more) cationic or anionic additive. Cationic additive is polyDADMAC and anionic additive anionic sodium polyacrylate.

5.3 Water and colorant in the binder film structure

In the polyvinyl alcohol binder, the water molecules diffuse into the polymer matrix and form hydrogen bonds with the hydrophilic groups of the amorphous region of polymer whilst some of them remain as free water in the network as DSC results show. The water molecular diffusion causes the swelling of the polymer matrix and the further opening of the PVOH network microstructure so that the colorant molecules subsequently fit into the binder structure. The transfer of ink vehicle promotes the movement of colorant molecules into the PVOH matrix. The SA latex polymer microstructure has less chemical groups that can fix the water molecules and therefore during the absorption test there is more free water at a given liquid content than bound water on the surface network of SA binder – assumed to be related to surfactant or surface carboxylation. Figure 55 shows that, after 5 s absorption time of dye-based ink, the SA latex film did not have any ink colorant at all, whereas all PVOH films had a blue colour. On the other hand, the results of the absorption by binder films showed that PVOH films took up anionic aqueous dye-based ink more than SA latex film. The high binding capacity of PVOH means that the polymer attracts (absorbs) the water molecules and the concentration of water in the PVOH is therefore higher than in the latex, although the diffusion rate of water vapour in relation to the polymer itself remains similar, albeit bulk diffusion in the case of PVOH and surface diffusion in the case of SA latex. This means that in the case of PVOH the diffusion happens in the polymer network structure, whereas in the latex the diffusion occurs mainly on the surface of the polymer network (Figure 58). It might also be so that the surface active polymers of latex

that have been used in the polymer production extend for a small but significant distance from the actual surface into the outer bulk.

We may conclude that at the beginning of ink imbibition into PVOH containing coatings, the dominating diffusion will be surface diffusion and osmosis, followed by Knudsen diffusion when the polymer swelling has decreased the effective coating structural pore diameters. In the SA latex containing coatings, the role of Knudsen diffusion must be insignificant and the diffusion is mainly surface diffusion. The next section will now illustrate the validity of this conclusion.
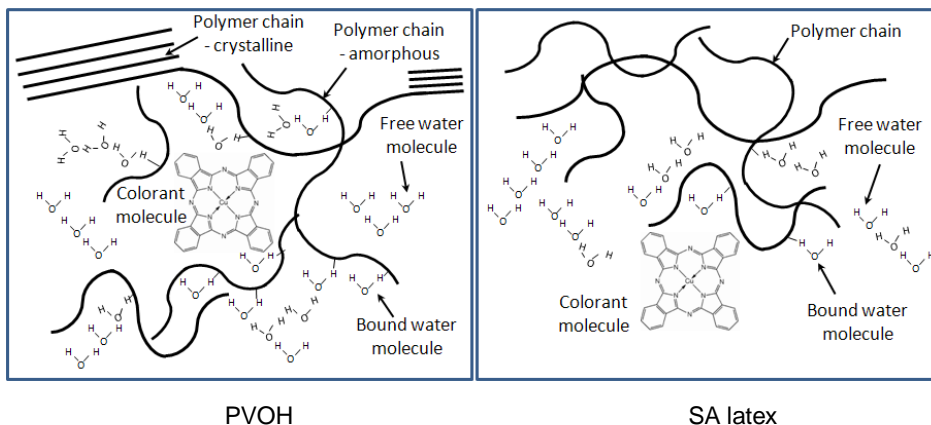
PVOH   SA latex

Figure 58. The water molecules and ink colorant in the PVOH and SA latex polymer network. Based on Paper IV (Figure 9).

5.4   Diffusion in the coating layer during inkjet ink absorption

During the coating layer consolidation, the PVOH molecules can form a binding layer on the coating pigment surfaces as well as binding "bridges" between the pigments, but they can fit also in the intra-particle pores of a porous pigment, such as the $CaCO_3$ inkjet coating pigments, as Figure 24 in chapter 4 shows. The SA latex binder instead remains sited in the inter-particle pores, because the particle size of latex is usually over 100 nm (in this research SA latex had 180 nm) and the intra-particle pores are in the region of 20–60 nm. If the same "MCC small", "MCC large" and "PCC small" pigment coatings with 10 pph PVOH are studied, as in section 4.1 "Impact of coating pigment type and binder selection on the structure formation of the coating layer" on the pilot pre-coated paper (*Paper I*), it can be noticed that the commercial cyan dye from Versamark[®] VX5000e has distributed quite uniformly through the "MCC large" and "PCC small" coating layers (Figure 59). This could indicate that PVOH has covered the pigments and colorant is predominantly in the PVOH. The zeta-potential of these coating layers was 13.1 mV and 1.6 mV, respectively. These findings suggest that either the ink does not encounter the cationic nature of the pigment or the coating is too permeable to provide

surface contact for all the colorant as it flows through the structure. However, in the GCC coating, which had anionic charge -9.0 mV, the anionic cyan colorant seems to locate more on the top part of the coating layer. The anionicity has prevented colorant location in the coating structure other than on the coating layer top. The low pore volume and anionic nature, combined with the thicker PVOH binder layer on the pigment surface, have prevented the colorant penetration deeper into the structure. These results show that the diffusion potential for ink vehicle into the coating binder does not alone guarantee the optimal colorant location. If the coating is highly permeable, then either the flow through the coating is too fast for bulk diffusion to occur and/or the anionic surface of the pigment provides a long range Coulombic repulsion. If, however, the permeability is low, the same ionic repulsion, and volume loss by binder swelling, confines the colorant to the top part of the coating layer, but of course absorption of vehicle is too slow for satisfactory ink drying. The porosity and permeability of the coating structure are very important in determining the final colorant location.

GCC   MCC small

MCC large   PCC small

50 µm
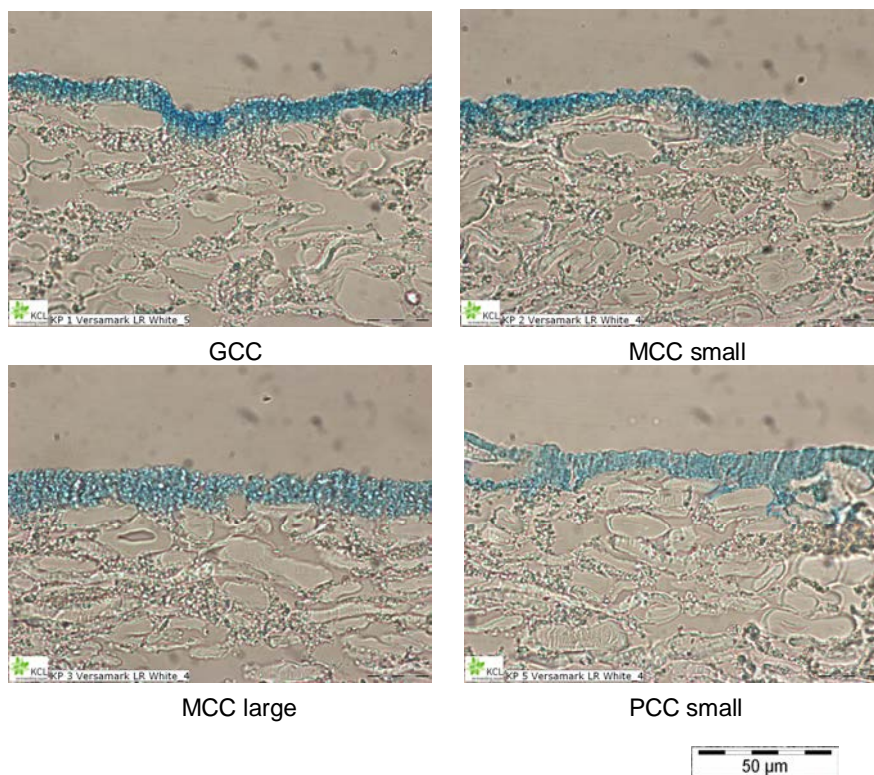
Figure 59. The cross-section images from GCC, "MCC small", "MCC large" and "PCC small" containing coatings that had 10 pph of PVOH (partially hydrolyzed). Papers had been printed with Versamark[®] VX5000e. Based on Paper I (Figure 19).

The results of TLC (*Paper V*), Clara device (*Paper II*) and microbalance (*Paper VI*), shown previously in section 4.2, "The effect of coating structure and binder selection on liquid imbibition rate", demonstrate that the binder can nonetheless have an effect, even with a small amount, on the inkjet ink imbibition speed. The use of 1 pph PVOH in the "MCC large" pigment containing coating decreased the rate of absorption front rise of a water/colorant mixture on the coated TLC plate clearly from 0.050 mm·s^{-1} in dispersed "MCC large" pigment to 0.017 mm·s^{-1} in dispersed "MCC large" with PVOH. The capacitance-based results corroborate this lower rising rate in such a way that the PVOH containing coatings had longer penetration time through the coated papers than in the case of the SA latex containing, and as the binder amount increased so the penetration rate decreased. In the microbalance research, a similar lower absorption rate of water was detected at the long timescale absorption, again indicating a permeability controlled mechanism. Although the volume of the liquid uptake of PVOH containing coating structure, related to PVOH swelling, can be smaller than the structure of SA latex containing coating, it acts to dominate the comparative inkjet ink imbibition.

The similar diffusion coefficient for PVOH and SA latex means that the flux of water vapour in these coatings is dominated by the pore structure of the coating, and thus also the local liquid concentration difference across the wetting front during the imbibition time. This supports the findings of Gane and Ridgway (Gane and Ridgway 2008), who presented moisture pickup results from pigment tablets of dispersed GCC of various particle size distributions. They concluded that the initial moisture absorption rate of pigments depends on the permeability of the structure. Once access of vapour to the pore structure has occurred, contact with absorbent binder provides the transition to bulk diffusion within the polymer network.

At the short timescale absorption of the inkjet ink, in the form of polar liquid, the role of diffusion is also significant in the capillaries of the coating layer when containing hydrophilic, water-swellable binders. Figure 60A illustrates the predominant forces in the case of such a hydrophilic absorbing surface. The absorption study with the microbalance shows that up to 2 s timescale the PVOH containing "MCC large" and "PCC small" coatings absorbed water at a quicker rate than the SA containing coating (Figure 31). This illustrates the absorption of ink into the polymer as well as surface diffusion on the interface of the pore wall of the PVOH containing coatings. The appearance of swelling means that the absorption-describing mechanism, in our discussion here being exemplified by the Bosanquet equation (12), would require two additional components that describe the diffusion of polar inkjet ink into the binder component and modification of the structure by swelling, respectively. This can already be partially taken into account in the external pressure part and the inertial drag, if the dynamic radius change of capillaries, $r(t)$, is considered (Figure 60A). Above all, this becomes important in the nanoscale capillaries, which have been shown to be very advantageous for fast penetration of the inkjet ink vehicle into the coatings.

Thus, in the case of hydrophilic swelling binder, the Bosanquet equation becomes a convolution of the situation in a static structure with the structural change, i.e.

$$\left[\frac{\mathrm{d}}{\mathrm{d}t}\left(\pi r^2 \rho x \frac{\mathrm{d}x}{\mathrm{d}t}\right) + 8\pi\eta x \frac{\mathrm{d}x}{\mathrm{d}t}\right] \otimes swelling = \left[p_e \pi r^2 + 2\pi r \gamma_{lv} \cos\theta\right] \otimes diffusion \quad (40)$$

and, if the diffusion is expressed as in equation (39) and the dynamic changes of capillaries are assumed to be in cylindrical form, the model can be formed as two simultaneous equations,

$$\left.\begin{array}{l} \dfrac{\mathrm{d}}{\mathrm{d}t}\left(\pi r^2(t)\rho x \dfrac{\mathrm{d}x}{\mathrm{d}t}\right) + 8\pi\eta x \dfrac{\mathrm{d}x}{\mathrm{d}t} = p_e \pi r^2(t) + 2\pi r(t)\gamma_{lv}\cos\theta \\[4mm] r(t) = r_0 - \dfrac{r_0^2 - r^2(t)}{2r(t)} \end{array}\right\} \quad (41)$$

where the volume of water diffused across unit capillary surface in time t is given by the second term in the second of the simultaneous equations above

$$\frac{\Delta V(t)}{A_{\text{capillary surface}}} = \frac{\pi(r_0^2 - r^2(t))x}{2\pi r(t)x} \quad (42)$$

and is related to the diffusion coefficient by a rearrangement of equation (39), including a reduction of the diffusion coefficient by an approximate factor ½ since the access to the binder film is one sided only,

$$\Delta V(t) = V_{\text{tot}}\left\{1 - \exp\left[-\frac{\pi^2}{4}\frac{\frac{1}{2}Dt}{r^2(t)}\right]\right\} \quad (43)$$

where V_{tot}, the total absorbed volume per unit capillary surface area, can be determined experimentally. For example, the swelling of PVOH was shown to reach ~30 %.

In the above description, the term $r(t)$ describes the radius during the time t, ρ density of fluid, x distance where the fluid progresses in the capillary, η liquid viscosity, p_e external pressure, γ_{lv} surface tension at the liquid-vapour interface, θ dynamic contact angle and D diffusion coefficient. Although this algorithm is not applied in this work, it forms the basis of the analysis in the next section where the nanopores are reduced in radius and volume due to the swelling of the PVOH, and the absorption affected as a result.

In the case of internally hydrophobic binders, at the beginning of inkjet imbibition, the hydrophobicity prevents the polar ink penetration (Tiberg *et al.* 2000) as the results of the microbalance measurement indicated (Figure 32A). After a while, the penetration starts as surfactants permit surface wetting, and it is faster than in the hydrophilic swelling binder containing coatings due to greater permeability of the non-swelling binder case, as the results of the microbalance and the capacitance-based measurements showed (Figures 32B and 37). The diffusion on the hydrophobic coating binder surface is more or less a surface diffusion related to

surfactant/carboxylation and this affects the surface wetting force, $\gamma_{lv}\cos\theta$, and thus the effective frictional resistance by producing a concentration gradient of ink vehicle molecules (Figure 60B). This has probably a connection to the Marangoni effect, where the molecular motion occurs in the edge areas between liquid and solid material, connected by the surfactant(s) associated with the latex. The counter force for the diffusion in this case is the hydrophobic resistance of the non-swelling binder/capillary wall. However, these forces caused by the diffusion must be small in the SA containing coatings compared with the other forces during the inkjet ink imbibition, and so the local changes in surface energy are impossible to capture in such a spatially averaged model.
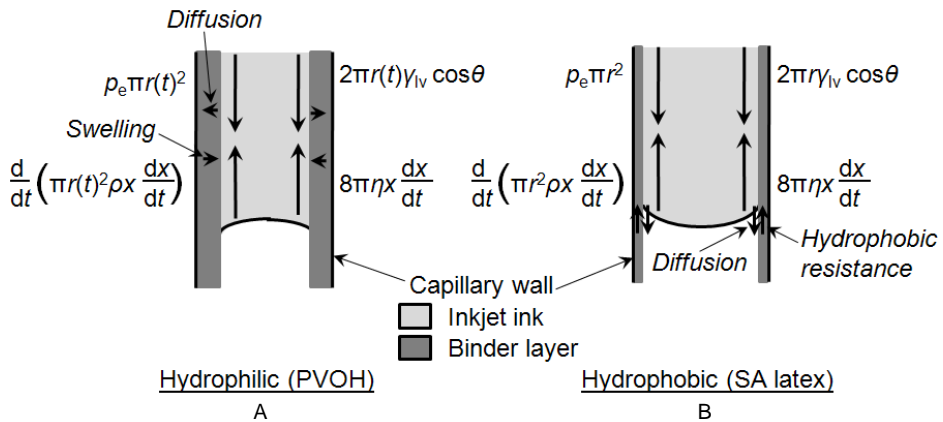
Figure 60. The effect of the diffusion of inkjet ink (polar) into/on the capillary wall that contains hydrophilic (PVOH, A) or internally hydrophobic (SA latex, B) binder at the beginning of inkjet ink imbibition.

5.5 Binder swelling – impact on nano-size capillaries

The significance of swelling on the conditions of the high-speed inkjet printing press was clarified with a theoretical calculation. In *Paper I* a description was introduced to describe how the swelling affects the closing of nano-size pores. The mercury porosimetry results show that the PVOH binder can go into the intra-particle (Figure 24) as well as the connecting pores, and covers the surface of the larger inter-particle pores as Boisvert and Guyard (Boisvert and Guyard 2003) and Wedin *et al.* (Wedin *et al.* 2006) assumed in their studies. At sufficiently high levels, the interactions between the binder and the liquid phase of the ink become important, not only in the structural modification of pore volume but in the diffusion of liquid into the polymer network. In the case of PVOH and inkjet ink this relates to binder swelling.

In this theoretical calculation, the binder layer thickness is considered to be present on the pigment surface as a homogeneously distributed layer, and its thickness will depend on the specific surface area of pigment (thicker binder film on a lower specific surface area pigment). The geometry of the pore is assumed to

be simple: the binder forms a uniform layer on the interior surface of the circular equivalent capillary (Figure 61, left side), thus controlling the capillary diameter. In this way, it can be calculated how the round pore entrance area changes during the binder swelling process. The pore volume and amount of binder represents that to be found in 1 g of coating structure, and the coating formulation proportion was taken into account. The right side of Figure 61 shows how the delay in pore area growth as a function of original pore diameter increases with binder addition. The first line on the left (Figure 61, right side) is the pore area when the structure has been formed from pigments alone. The addition of 10 pph binder into the coating colour decreases the pore diameters, they being reduced by the absorbed layer of PVOH binder on the pigment surface by a diameter amount of 13 nm when the PVOH is dry. The inkjet ink caused a 29.2 % swelling of PVOH, as Figure 46 shows. This swelling closes further the pore diameter by 5 nm. The point at which the pore diameter is closed increases at the same time from 19 nm to 24 nm, i.e. the swelling renders the pores finer than this original diameter value as they become progressively closed. This leads to complete blocking of the finest pores, reduction in pore size in general and loss of connectivity in the structure when the binder is concentrated at pore nodes. A higher amount of binder produces a thicker binder layer on the pore wall, and thus the effect of swelling also increases. The calculations show that the swelling affects the intra-particle pores region in the pore size distribution. If higher specific surface area pigments are used, the thickness of binder layer on the pigment surface decreases, and therefore the pore area growth curves move toward the direction of lower pore diameters. For example, at a specific surface area of 70 m^2g^{-1}, and a 30 pph PVOH binder content, the swelling closes up the under 10 nm diameter pores.
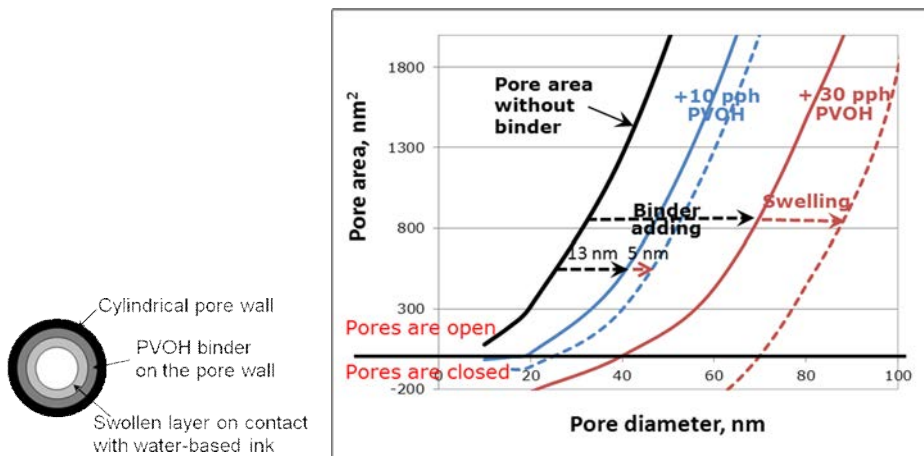
Figure 61. The theoretical calculation of PVOH swelling effects. The coating amount was 1 g and density of PVOH 1.26 $g \cdot cm^{-3}$. The swelling of PVOH film was 29.2 % after 5 s (cyan dye). Specific surface area of pigment 10 m^2g^{-1}. Based on Paper I (Figure 16).

The calculations show that the binder swelling can affect the absorption of inkjet inks through the closing up of small pores in the timescale of 5 s. Table 14 shows the time delays in the inkjet printing machine Versamark$^®$ VX5000e. At 100 m·min^{-1} speed, the delay between the first inkjet nozzles and the beginning of drying is 2.6 s, and to the end of drying 3.8 s. The 5 s time considered in the calculations is within this same timescale. At the printing speed 15 m·min^{-1}, the swelling of binder polymer has clearly a strong influence on the closing of capillaries. The effect of swelling diminishes when liquid has less time to affect the binder, and therefore we can assume that swelling has a smaller role to play at higher printing speeds, but it will not totally disappear. Thus, diffusion into polymer networks is a relevant phenomenon within the timescale of current inkjet printing, even in the high-speed printing domain.

Table 14. Time delays in the Versamark$^®$ VX5000e printing press.

Position on the inkjet press	Speed 15 m·min^{-1}	Speed 100 m·min^{-1}
Cyan print head to yellow print head (CMKY)	5 s	0.8 s
Yellow print head to beginning of drying	12 s	1.8 s
From beginning to the end of drying	8 s	1.2 s
SUMMARY	25 s	3.8 s

5.6 Summary of diffusion mechanisms in coating binders

Inkjet ink penetration into the coating layer structure depends on the type of binder used in the coating colour. The hydrophilic PVOH binder allows the diffusion of the inkjet ink vehicle into the polymer matrix and this causes the swelling of the polymer. This acts to close and/or diminish the number of active nano-size pores and therefore slows down the capillary flow of ink in the coating structure. At the same time, the pore volume decreases as the binder swells. On the other hand, the calculations of the water moisture diffusion coefficient show that the hydrophilic partially hydrolyzed PVOH film has a very similar diffusion coefficient as that of the surface diffusion on the internally hydrophobic SA latex film. This result together with the different water phase-structure types shows that the water molecules diffuse into the PVOH polymer matrix whereas they stay on the SA latex network surface, meaning that the mechanism of water diffusion is different in the PVOH and SA latex binders. The SA latex does not absorb the ink vehicle, and therefore the dominating phenomenon in the SA containing coating structure is then structural only and impacts the static structural capillary absorption, with only a minor effect arising from the latex dispersion stabilising surfactant acting to delay wetting. In the case of PVOH, the diffusion can start via surface diffusion and osmosis, followed by Knudsen bulk diffusion, and these diffusion regimes compete at the beginning of inkjet ink imbibition with the capillary flow and later with the capillary and permeation flow, respectively.

The speed of sorption is determined by the porosity and permeability of the coating layer structure, but in the case of hydrophilic coating binder, the swelling of polymer will affect this rate strongly. The short timescale results, less than 2 s, of the microbalance indicate that the diffusion of water into PVOH binder can speed up the sorption. The coating structures that contained nano-size pores absorbed polar liquid initially quicker when the coating contained PVOH than when it contained SA latex. Thus, during inkjet ink sorption into the hydrophilic binder containing coating structure, the diffusion is acting as a short timescale rate determining phenomenon, and so could be represented in a description of the absorption dynamic, such as that offered by the Bosanquet equation.

> *Hypothesis I* – inter molecular diffusion of the liquid phase of inkjet ink into polymers acts on a sufficiently fast timescale and in sufficient volume to compete with the permeation of ink through coating structures.

The opening of the PVOH polymer matrix during the swelling allows furthermore that the colorant molecules can fit into the binder polymer matrix. The ink vehicle acts as a carrier of the colorant as is hypothesised in Hypothesis II. There develops a concentration gradient of colorant in the binder layer and the largest amount of colorant remains on the top of the PVOH binder film.

> *Hypothesis II* – inter molecular diffusion of the liquid phase of inkjet ink into polymers, acting as a colorant carrier, is a competing mechanism to the surface adsorption of ink dye.

The research, where the anionic or cationic additive was mixed with the binder polymer, shows that the produced cationic charge of the film surface fixes the anionic colorant effectively to the top layer of the film, promoting partially the Hypothesis III. The opposite ionic charge of film binds the colorant to the surface via the Coulombic forces. However, the additional few parts of additives have very minimal effect on the inkjet ink absorption amount.

> *Hypothesis III* – the verity of Hypotheses I and II can be used to design porous coating structures, based on discretely bimodal pore size distributions, using binder and surface charge distribution characteristics to provide rapid fixing of ink colorant optimally close to the coating surface.

6. Inkjet ink colorant fixing and transfer into the coating layer

6.1 Colorant fixing to the anionic or cationic coating layer

The predominating driving force for the adsorption of azo dyes is found to be electrostatic (Coulombic forces) and/or hydrophobic interaction (Kallio *et al.* 2006, Lavery and Provost 1997). The coating layer is usually highly charged, and this promotes the attraction between the anionic colorant and the inorganic pigmented layer. These interactions of course depend on the charges of the coating components used in relation to the ionic charge of the dye. Donigian et al. (Donigian et al. 1998) hypothesized that the most important chemical groups of a colorant for the fixing of the dyes are carboxylic and sulphonic acid groups. Vikman and Vuorinen (Vikman and Vuorinen 2004a) showed further that the most important chemical groups supporting the ink colorant fixing mechanism to the coating layer components are hydrogen and ionic bonds. In this research work, the fixing of the colorant is studied in the context of thin layer chromatography, adopting UV-VIS analysis and ToF-SIMS.

6.1.1 Thin layer chromatography

The target of the thin layer chromatography study, TLC (*Paper V*), was to detect how the ionic charge of the model coating structure affects the colorant and eluent movement and colorant fixing, respectively, in an inkjet coating. In this study, "MCC large" pigment coatings were applied on a glass plate. The coating colours were defined either as pigment alone or with binder additives. In the case of pigment alone, the "MCC large" pigment was dispersed either with 0.5 pph anionic sodium polyacrylate or 0.5 pph cationic poly(diallyl dimethyl ammonium chloride) (polyDADMAC). The differently dispersed coatings were also formed with either 1 pph polyvinyl alcohol (partially hydrolyzed PVOH) or 1 pph SA latex. All TLC coating layers had about 100 gm^{-2} coating colour. The eluent was de-ionized water, into which were added different amounts of anionic dye-based colorant.

Table 15 shows the zeta-potential of the studied coating colours. The highest negative charge was seen for the coating colour formulations having anionically

dispersed "MCC large" alone or anionic "MCC large" pigment with SA latex. The anionicity of latex showed to be on the same level as the dispersing agent provided on the pigment. The addition of PVOH decreased the anionic charge, although the PVOH has a non-ionic nature. Probably the PVOH polymer has covered the anionic pigment surface so that ionic charge remains ineffectively under the non-ionic polymer or the addition of an uncharged soluble species simply reduces the average zeta-potential leaving the particles themselves charged as before. This suggests that if interacting according to the first option, the PVOH is associating with the charged groups of the dispersed pigment. The "MCC large" pigment with cationic dispersing produced the highest cationic zeta-potential, 24 mV, and the addition of PVOH to the cationic dispersed pigment decreased the zeta-potential value to 11 mV. This promotes the idea that the PVOH polymer may be capable of covering the pigment surface, and so it decreases the externally effective ionic charges on the surface of the pigments, most likely in the final coated layer.

Table 15. Zeta-potential of "MCC large" pigment colours. Measured with AcoustoSizer II.

Pigment system	Zeta-potential, mV
MCC large powder in water	21
Anionic MCC large	-37
Anionic MCC large + 7 pph PVOH	-12
Anionic MCC large + 7 pph SA	-37
Cationic MCC large	24
Cationic MCC large + 7 pph PVOH	11

The section 4.2.3 "Liquid and colorant movement – impact of charge on chromatographic separation in the coating layer" illustrates how the liquids become transported through different distances, and how the ink colorant fixed differently to the anionic and cationic coatings. The thin layer chromatography results (Figure 35) show that, as expected, there was no ink colorant binding to the coating layer when the colorant and the coating layer had the same sign of ionic charge. The colorant follows the eluent wetting front up the coated plate because there are no attractive ionic forces between the coating components and colorant molecules. On the other hand, opposite ionic charge fixes the colorant to the coating layer, related to the attractive force and diffusion of colorant, and the anionic colorant stayed at the bottom edge of the cationic TLC coating layer. This observation agrees with many other equivalent results, such as those in (Lavery and Provost 1997, Donigian *et al.* 1998, Pond 2000, Vikman and Vuorinen 2004 a and b, Kallio *et al.* 2006). However, the results show further that the anionic colorant started to rise up the cationic TLC coating after ten minutes exposure to the supersource of colorant solution had elapsed (Figure 62). The fixed bottom edge appeared to fill

with colorant molecules. Clearly, the surface area of the pigment associated with the cationised pores takes part in adsorption, and only when the surface area is saturated can the colorant move forward into the structure. This sorption control is effectively a titration measure of specific charge density per unit TLC length.

| Coating layer | Coating layer | | | Ink colorant |

Coating layer   Rising of water   Fixed colorant: layer first fills and then starts to rise

Time: 0 min   1 min   6 min   25 min   50 min
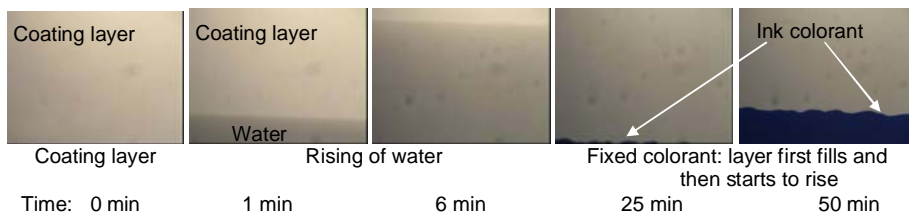
Figure 62. Anionic colorant (5 wt-%) movement on the cationic "MCC large" TLC plate. Based on Paper V (Figure 7).

As the eluent rose up through the TLC coatings, the gray level changes were detected. The gray value of the coating layer without any eluent was set to 150. Figure 63 shows how at first the gray value decreased because the eluent first arrived at the detection area and then occupied it progressively little by little. The eluent changed the coated plate by reducing the light scatter as pores filled, making the appearance darker and therefore the gray value decreased. For the cationically dispersed "MCC large" structure it took 2 min to cover the whole detection area, whereas for PVOH containing coatings it took 4 and 5 min, respectively. The swelling of PVOH causes a decrease of pore volume, and importantly connectivity, in the coating layers, and therefore it takes more time for liquid to transfer through the whole detection area, as the distance results indicated before in chapter 4.

A

B

C
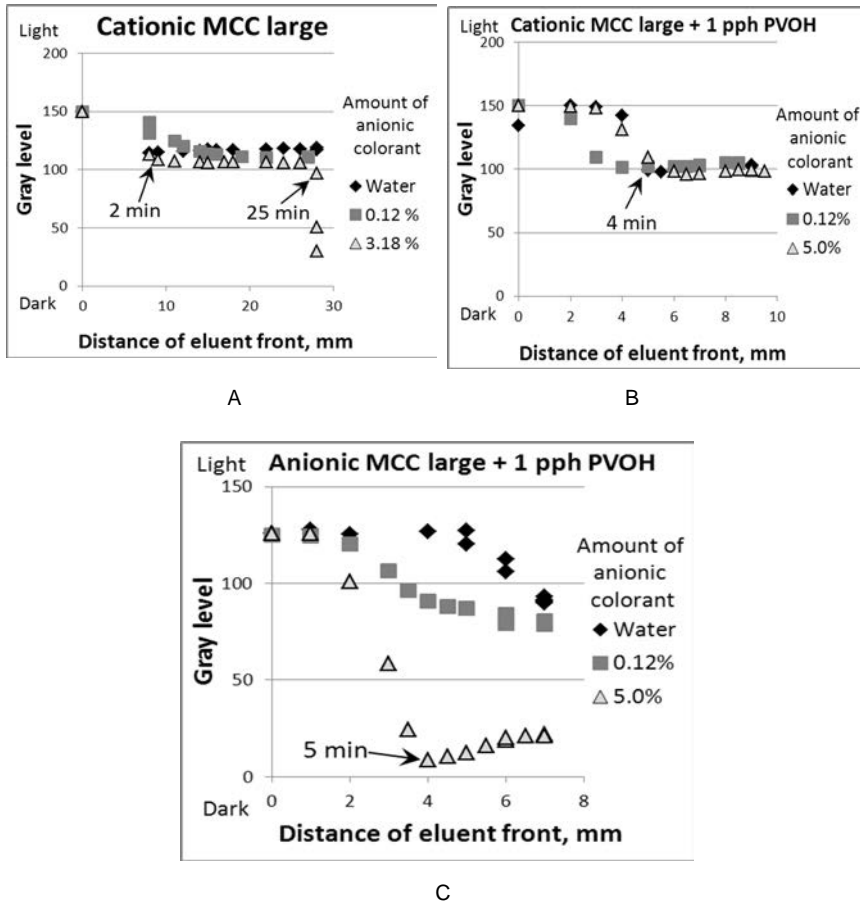
Figure 63. The effect of anionic cyan dye at the levels of 0, 0.12 and 5 % on the gray values in the TLC development. A – cationically dispersed "MCC large" pigment, B – the cationically dispersed "MCC large" pigment with 1 pph PVOH, C – the anionically dispersed "MCC large" pigment with 1 pph PVOH. The time 2, 4 and 5 min describe the moments when the eluent front has occupied the detection area totally. Based on Paper V (Figure 9).

Figure 63 shows that the gray level values of cationic surfaces remained on a higher level than those of anionic layers. The cationic coatings fix the anionic colorant to the bottom of the TLC plate and the changes of gray value are caused at first expressly by the eluent water, whereas, in the case of anionic coating, the colorant follows water immediately just after the wetting front, contributing to the darkening effect. The filling of the colorant at the bottom edge can be seen on the cationically dispersed "MCC large" coating as the gray value which starts to decrease at the 25 min development time (Figure 63A). The addition of 1 pph PVOH did not change the gray level, indicating that the cationic charge combined with the

very small amount of PVOH fixed the colorant effectively to the bottom of the coating plate until colorant ad- and absorption saturation were reached.

In the case of the anionic coating, the ionic repulsion dominates, and the colorant diffusion into the small amount of PVOH binder is insufficient to capture a high colorant saturation level. If the binder amount had been higher, then the anionic repulsion of the pigment charge would have been at least partly compensated. The transfer of colorant molecules into the binder film by following the ink vehicle competes with the anionic repulsion.

6.1.2 Absorption and/or adsorption of coating components

The colorant absorption into and/or adsorption onto the coating components were studied more closely with the UV-VIS spectroscopic method (*Paper VII*). The pigment coating structure systems used in this part contained the same "MCC large" pigment as above. The dispersions were made by using either the anionic or cationic dispersing agent (0.5 pph) as previously described. Besides the dispersed coating pigment system, the anionic pigment was used in coating colours with either 7 pph partially hydrolyzed PVOH or 7 pph SA latex. The cationic pigment was similarly studied together with 7 pph PVOH (partially hydrolyzed). All these coating colours were dried and ground as described in section 3.3.4 "Absorption/adsorption of liquid colorant by coating components". The concept of grinding is largely to avoid the extended pore network structure or chromatographic separation effect present in coating cakes or TLC layers, thus enabling the structure surface-related phenomena to be isolated from the permeability characteristics. However, the grinding of the coating layer may act undesirably to expose more surfaces by breaking the binder polymer bridges or by pealing/debonding the binder polymer away from the pigment surface. By adopting a relatively low energy of grinding, this effect is expected to be minimal. The ground powder was screened and 5 g of powder was mixed with 10 cm^3 anionic dye-based self formulated ink at different time delays (5 min, 30 min, 2 h and 18 h). After that the mixture was centrifuged and the filtrate was analyzed by ultraviolet-visible (UV-VIS) spectroscopy. The idea was that the inkjet ink colorant absorbs and/or adsorbs in/onto the coating structure system during their mixing, and this can be detected as a change of colorant absorbance in the liquid phase remaining after centrifugation with the UV-VIS. Thus, the absorbance result arising from the colorant in the supernatant liquid solution phase has an inverse relation to the absorbed/adsorbed colorant amount depending on the prior contacted surrounding surface chemistry: the higher the optical absorbance, the less dye colorant has been absorbed/adsorbed onto the pigment system. The term "absorb" is used in the case for the interaction with PVOH, relating to the molecular motion of ink vehicle into the binder polymer network (diffusion), affecting the uptake of colorant.

Figure 65 shows that the "MCC large" pigment ground powder alone adsorbed some of the colorant molecules because that UV-VIS absorbance results from the supernatant were clearly on a lower level (2.3–2.9) than the maximum value 3.7

(ink value without the pigment system adsorption, Figure 64). This indicates that the dry powder has some cationic sites on the pigment surface already before extra dispersing agent addition.
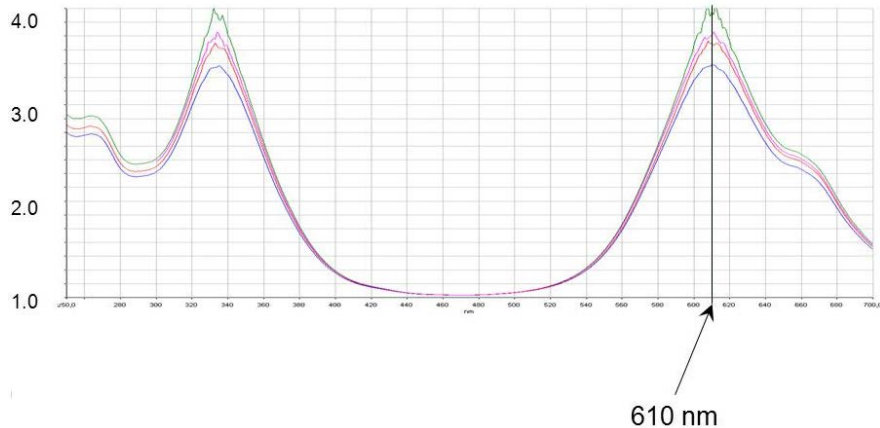

Figure 64. An example of UV-VIS result curves from different concentrations of colorant dye.

The "MCC large" pigment dispersed with extra cationic dispersing agent produced the lowest absorbance value in the supernatant indicating that the colorant sorption was clearly greater with this cationic system than in any anionic system, and even in the original cationic pigment case without the extra charged polymer addition. This refers again to the action of Coulombic attraction. The addition of PVOH to the cationically dispersed "MCC large" had only a minimal effect on the absorbance results, and importantly in the ground materials, the added PVOH does not prevent the colorant sorption. It seems that the cationic charge of the pigment system binds the anionic colorant effectively. The lower zeta-potential (11 mV), when the non-ionic PVOH polymer was added, suggesting that it is either on the pigment surface, and/or within the intra-particle pores and/or distributed throughout the structure, did not change the situation. This shows that the adsorption dominates over absorption, in that the action of Coulombic attraction over a distance onto a high surface area exceeds the amount undergoing diffusion into the binder polymer matrix. However, the diffusion of the water molecules into the hydrophilic PVOH network persists, and the colorant will transfer into the polymer network by absorption, especially if in excess of the pigment surface adsorption capacity.

The addition of an anionic dispersing agent in the coating pigment system increased the absorbance results from the supernatant to the level 3.1. The anionic components have fixed to the cationic parts of the pigment surface and there are clearly less available cationic groups which can bind colorant molecules. The addition of anionic SA latex did not change the absorbance, but as the polyvinyl alcohol was added to the anionic coating colour the absorbance of colorant de-

creased, illustrating the diffusion absorption of colorant into PVOH. This finding promotes the Hypothesis II of this work. It is possible that the colorant is trapped in the PVOH polymer network. Thus, the results show that in the anionic, PVOH containing, coatings the dye colorant is associated with the binder, whereas in the cationic, PVOH containing, coatings the dye undergoes both ionic attachment to the pigment surface and association with the PVOH polymer matrix when adsorption capacity is reached.
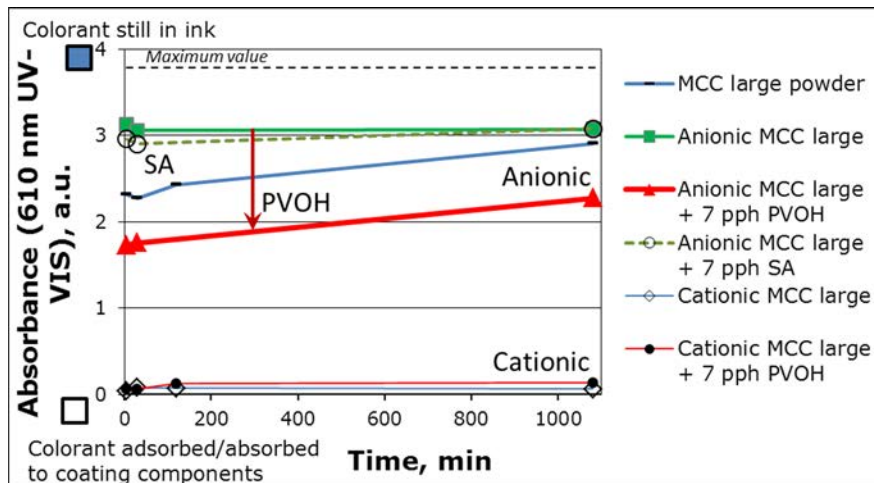
Figure 65. The UV-VIS light absorbance of supernatant liquid containing anionic cyan dye after the mixing procedure of different "MCC large" pigment systems. Self formulated anionic dye-based ink. Extra charged polymer is used to define either anionic or cationic coatings. Based on Paper VII (Figure 3).

The results in Figure 65 show further that the long mixing time did not significantly release the colorant from the cationic "MCC large" pigmented coating colour systems. However, with regard to the anionic dispersion, the dispersed pigment powder and the pigment with PVOH showed an increase in the supernatant absorbance value over time. This might be an indication that a dissolution or release of polymer species from the coating colour mix may occur. The results in Figure 51 showed already that some of the PVOH film disappeared during the measurement of liquid absorption. To confirm this, the centrifuged material was re-suspended in de-ionized water, filtered, diluted and repeatedly washed. After each washing, the dissolved fraction in the filtrate was measured by drying and weighing.

Figure 66 illustrates how strongly the dispersing agent polyDADMAC has adsorbed and become fixed to the "MCC large" pigment by studying the polymer content in the filtrate after progressive washing of the dispersed pigment powder system. Some of the cationic polyDADMAC was seen to be released from the mix, and from the data it was possible to calculate that 15.7 % of the originally added

24.9 mg·g^{-1} was recovered during washing. Thus, some of the cationic polymer is released, but probably not from the charged pigment surface, but rather because it is in excess of the surface adsorption capacity of the anionically charged sites on the pigment. However, the UV-VIS measurements showed that despite this cationic polymer loss the fixed colorant remains with the cationized surface, passing into the deposit after the centrifugation such that the filtrate remains clear. This further supports the suggestion that the lost polyDADMAC was in excess of the surface adsorption site capacity.
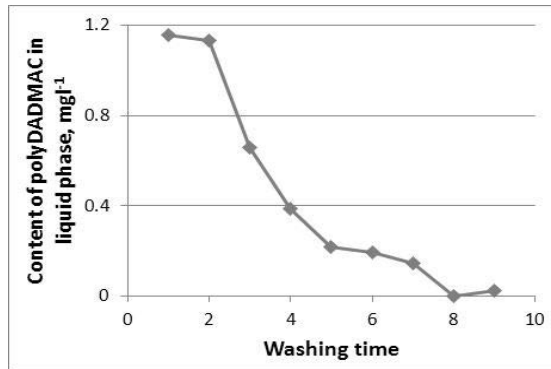
Figure 66. The content of polyDADMAC in the filtrate after washing. At first, 5 g of pigment (dispersed with 0.5 pph of polyDADMAC) was mixed with de-ionized water (20 cm^3) for 1 min, followed by transferring to a Büchner funnel and filtering. The filtrate was dried and the dry weight content was measured. After that a further 20 cm3 of water was added to the filtercake and the filtrate therefrom again analyzed. The procedure of water addition was repeated eight times with analysis made after each dilution (called here "washing"). It was assumed that the pigment remained on the filter paper (the filtrate after each washing was transparent). Based on Paper VII (Figure 4).

The anionic ink location was also detected within the printed coated papers. By imaging the printed anionic colorant location in the cationic "MCC large" pigment, with 10 pph PVOH (13.1 mV) double coated on the non pre-coated fine paper surface, Figure 67, the anionic colorant was seen not to have fixed totally into the top layer of cationic coating, contrary to what might have been expected on the basis of different ionic charges between the coating layer and the ink colorant. The cationicity did not prevent the colorant penetration into the bottom part of the coating layer. Thus, either speed of transit of the ink vehicle flow into the pore structure was too high for the capture to occur and/or the colorant was in excess of the local adsorption charge capacity of the surface of the coating structure. Similar effects were noticed by Svanholm and Ström (Svanholm and Ström 2004) in their study. However, the UV-VIS results indicated that the 7 pph PVOH containing "MCC large" coating structure system (11 mV) had very similar absorbance results to that of the cationically dispersed "MCC large" coating. This supports the case that

the reason for the colorant passage deep into the coating layer itself, is that the competing electrical attraction is not high enough to attract all the colorant molecules in the timescale available. The coating is so permeable that the permeation flow dominates too much during the ink penetration, and it cannot provide enough time for the colorant to bind onto the coating surfaces. Thus, there must be some kind of optimum between the ink flow rate and the ionic attraction where the inkjet ink colorant fixes optimally to the top layer of coating components.

MCC large + 10 pph PVOH   50 µm
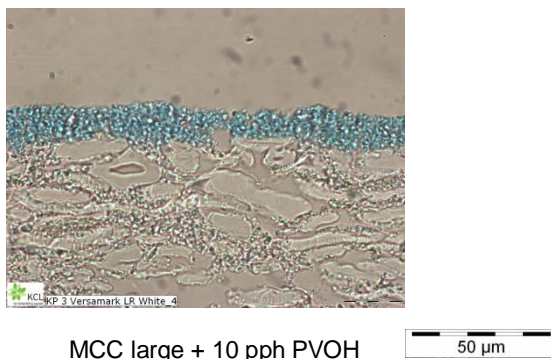
Figure 67. The cross-section of high-speed inkjet printed (Versamark® VX5000e) 10 pph PVOH containing "MCC large" coating. Anionic cyan colour located very uniformly in the cationic coating layer, indicating a rate limited adsorption or colorant amount exceeding the adsorption capacity of the pigment surface. Based on Paper I (Figure 19).

6.2   Colorant transfer into the binder

The ToF-SIMS studies with partially hydrolyzed PVOH films and commercial cyan dye-based ink, and with the same ink with lithium addition (chapter 5, *Paper IV*), showed that the dye-based colorant separates from the water vehicle of ink during the ink absorption/adsorption into and within the PVOH film. Figure 54 (chapter 5) shows the ToF-SIMS results expressing the colorant location in the PVOH film, and this proves that the low molecular weight lithium follows the water molecules, and the colorant follows the ink vehicle (water) into the film. This finding agrees well with the results of Oka and Kimura (Oka and Kimura 1995). The water molecules open the polymer matrix, and, after that, the colorant, about 1.3 nm in diameter (calculated by taking account of the length of different bonds in the Cu phthalocyanine colorant molecule and assuming the molecule is planar), fits into the binder network. Figures 52 and 54 (chapter 5) each shows further that most of the colorant content is located at the surface of the PVOH film, which has been the longest in contact with the inkjet ink. There is, therefore, a chromatographic separation of colorant molecules from the ink vehicle. Moreover, the added cationic

additive in the binder films fixed the anionic dye more in the top layer. The results of ToF-SIMS and cross-section images, therefore, promote Hypothesis II.

6.3 Summary of colorant fixing and movement

Hypothesis II assumed that the diffusion of inkjet ink vehicle carries the ink colorant into the polymer matrix component(s) in the coating layer. The results of the PVOH film verified that the water molecules diffuse into the binder polymer and the colorant follows them, and there happens a chromatographic separation. The colorant becomes trapped in the PVOH binder matrix structure after the evaporation of water.

> ***Hypothesis II*** – inter molecular diffusion of the liquid phase of inkjet ink into polymers, acting as a colorant carrier, is a competing mechanism to the surface adsorption of ink dye.

The ionic charge of dye colorant and the surface charge capacity of the coating colour combined with diffusion into the binder determine the adsorption potential for dye colorant. The porosity and permeability in turn define the bulk absorption rate and compete in speed with the adsorption and diffusion mechanisms in relation to the end position of colorant during the print drying process. The opposite charge of the coating components and colorant molecules binds the colorant effectively to the coating layer, as Hypothesis III argues. However, the colorant binding requires that the opposite charge is available in the coating structure. The effect of Coulombic attraction can be partially overcome by rapid passage of the ink due to a too large permeation flow of the inkjet ink through the pore network. The addition of polymeric soluble binder, such as PVOH, acts to reduce the permeability and provides additional diffusion absorption and interpolymer matrix fixing of the colorant. Thus, there is an optimum imbibition rate for the ink such that the colorant has sufficient time to bind to the available oppositely charged surface chemical groups and to be drawn into the soluble binder polymer network by vehicle diffusion. To aid the control of imbibition rate, the design of pore structure based on discretely bimodal pore structures, i.e. porous particles packed together, has been proposed and demonstrated by way of particle size combinations (Ridgway *et al.* 2011). Thus, we can support Hypothesis III:

> ***Hypothesis III*** – the verity of Hypotheses I and II can be used to design porous coating structures, based on discretely bimodal pore size distributions, using binder and surface charge distribution characteristics to provide rapid fixing of ink colorant optimally close to the coating surface.

7. Factors influencing the print quality of dye-based ink prints

The target of the printing trials was to verify how the produced structural as well as ionic charge and hydrophilic changes of the coating layers influence the performance in a high-speed inkjet printing environment and in the final print quality. A Versamark[®] VX5000e high-speed inkjet press was used in *Papers I, II* and *III*. The selected printing conditions of these studies have been described in section 3.3.6 "Print quality". The printing nozzles of the press work by the continuous jetting principle. Aqueous dye-based inks were used, which were heated in the nozzle to a temperature of 40 °C. A further inkjet printer was used for testing, namely a desk-top printer (HP DeskJet 3940), which was applied in the last paper (*Paper VII*), because the previous print press was not available at this stage of the work.

7.1 Coating layer structure

Different coating layer structures were constructed for study using five different calcium carbonate pigments, in each case adopting 10 pph partially hydrolyzed PVOH as binder. The coating pigments had different diameters, ranging from nano-size (20–30 nm in the fine fraction of "PCC small") to the largest (2.7 µm ("MCC large")), and displayed different morphological structures, namely with and without internal (intra-particle) pores. The porosities of the coating layers ranged from 17 % to 48 %. The coatings were applied with a semi-pilot scale coater, and the details of the coating procedure have been described in section 3.1.5 "Substrate: pre-coated base paper". Each coating colour was applied as two separate application layers on the fine paper surface as the target coat weight of 10 gm^{-2} was not achievable with a single coating application on the semi-pilot coater. The details of the coating layers and their analyses are described in *Paper I*. The printing conditions, as stated above, are described in 3.3.6 "Print quality".

Figure 68 shows the print densities of dye-based inks (Versamark[®] VX5000e) on the different $CaCO_3$ coated papers. The "PCC small" pigment provided the highest print density and "MCC large" the lowest. The "PCC small" is virtually an optically inert pigment (Figure 69A), whereas the other pigments affect the print density formation more due to their intrinsic light scattering. According to the theory

of Kubelka-Munk (Kubelka and Munk 1931) those particles which have a diameter of the order of the wavelength of light (0.1–1.0 µm) affect strongly the light scattering of the structure. The opacity and light scattering coefficient of the studied "PCC small" pigment coating (Figure 69B) remains on a lower level than those of the other pigments because the size of the pigment is so small, 20–30 nm. Figure 69 illustrates further that the other pigments produced quite similar opacities on glass plates as well as on the fine paper surface. On the basis of these results, it can be expected that coating containing "PCC small" would provide a higher print density (McFadden and Donigian 1999). The cross-section figures (Figure 70) show that despite the different coating layer structures the ink colorant remains in the coating layers and does not penetrate into the base paper. In the case of the "PCC small" pigment, the colorant remaining in the coating layer complements the optical weakness of the coating pigment, providing sufficient print density due to the lack of coating light scattering – reduced background white noise and improved image signal to noise ratio. Therefore, there is still enough colorant present so that it can participate in the print density formation. It can also be expected that the coatings with high pore volume produce more light reflecting surfaces and so have an effect on print density formation. The correlation between the pore volume of the whole paper and print densities was in the range -0.904−-0.949, whereas correlation between the pore volume of the coating layer alone and print density was as low as -0.050−-0.217. This shows that the whole paper structure, therefore, takes a part in the print density formation, not only the coating layer. This of course depends on the nature of the base paper.

The lowest inter-colour bleeding results, indicating sufficient absorption balanced against surface spreading, were seen for the "PCC large" coating, and then somewhat higher values for the "MCC large" and "PCC small" pigment coatings. The "MCC small" and standard GCC showed the most bleeding tendency. "MCC large" and "PCC large" coatings provided the coating layers with the highest porosity, and they had the largest inter-particle pores but also nano-size pores associated with the particle structure. The bleeding distance (Figure 68B) depends on the rate of absorption, available pore volume and surface wetting of the coating layer. The high pore volume provides more volume where the applied ink can transfer from the surface to the internal structure. Although the "PCC small" coating contained the most nano-size pores, and thus the highest capillarity on the short timescale, the porosity was only on a medium level, thus limiting both permeability (assuming a connective structure) and total absorption capacity. The observation that the bleeding was also on a medium level promotes the importance of nano-size pores in quick inkjet ink sorption into the coating layer structure so that the ink colorant mixing can be prevented. The quickest absorption (DIGAT) of an inkjet ink application was also reached with coating structures containing these nano-size pores (Figure 29).

A   B
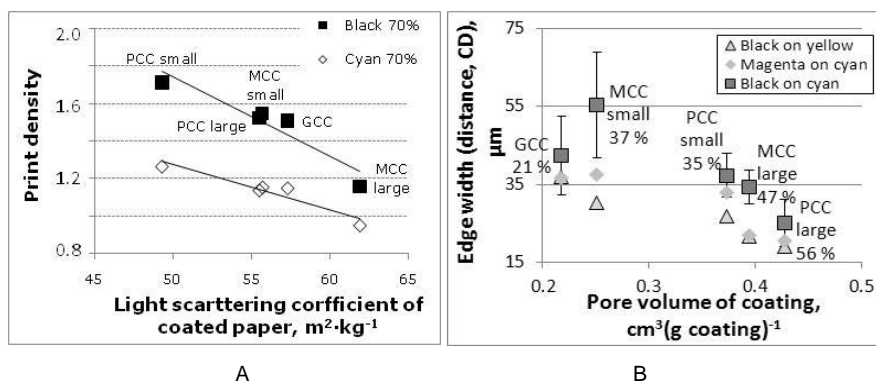
Figure 68. The print density (A) and inter-colour bleeding (B) of $CaCO_3$ pigment coated fine papers. Printed with Versamark[®] VX5000e with printing speed 100 m·min^{-1}, and drying drum plus hot air dryer at 80 $^{\circ}$C. Ink amount was constant. The coatings had 10 pph PVOH (partially hydrolyzed) and they were double-coated having in total 10 gm[-2] coating. The print density was measured from 70 % half tone dot area by using GretagMacbeth D196 spectrophotometer. The bleed-ing was measured from compact (100 % half tone dot) printed area. The porosity of each coating structure has been added under the name of each pigment in (B). The bleeding is defined as a line width between 10 % of the maximum and 10 % of the minimum of grey value. Based on Paper I (Figure 18 and 21).

A   B
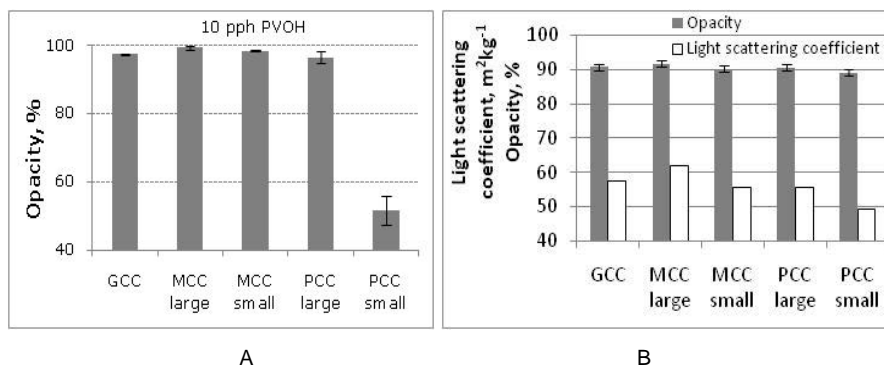
Figure 69. The opacity of $CaCO_3$ coatings which contained 10 pph PVOH (partial-ly hydrolyzed) on a glass plate (A) and on a fine paper (B). Coat weight on glass plate was 100 gm[-2]. During the measurement of $R_∞$, a white board was placed behind the coated glass plate, having an opacity of 94.8 % and ISO-brightness 91.3 %. Based on Paper I (Figure 17).
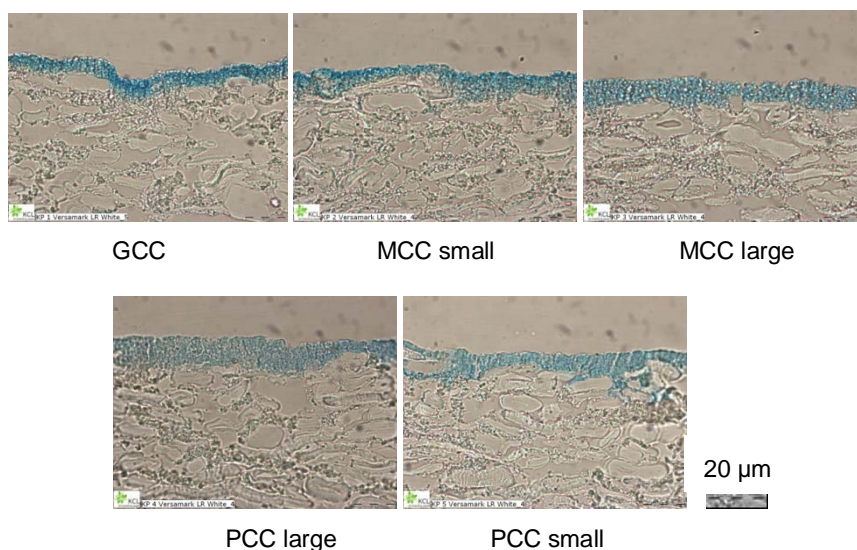
Figure 70. The cross-section images of dye-based ink (cyan) printed on the various $CaCO_3$ coated fine papers. Printed with Versamark[®] VX5000e using constant ink amount. Based on Paper I (Figure 19).

7.2 Binder amount and type

The effect of binder diffusion on the print quality formation was studied in *Papers I* and *II* by changing the amount of binder and using alternately a diffusion inert and diffusion promoting coating binder. The coating colours studied were based on the "PCC large" pigment including 7, 12 or 30 pph of either partially hydrolyzed PVOH or SA latex and were applied on the pilot pre-coated fine base paper surface. The printing was performed with the Versamark[®] VX5000e using a constant ink amount for all the tests. Figure 71A shows that the coating binder amount had a minimal influence on the print densities of the cyan dye-based ink, at least for this ink amount per printed area. The only exception was the 7 pph SA coating that produced a higher print density than the other coatings, although the strike-through (describing the penetration of the colorant through the coated paper structure) was clearly higher with the SA containing coatings than with the PVOH containing. These results emphasize once again the importance of the optical properties of the complete coated paper in respect to the resultant print density formation. The coating with 7 pph SA latex had the highest ISO-brightness and opacity, as Figure 72A shows.

The bleeding in this case was illustrated by the line edge-area distance (width) and the results show that the 12 and 30 pph SA latex containing coatings produced greater bleeding than the other printed surfaces (Figure 71B). All the SA latex containing coating layers were clearly surface wetting resistant, i.e. pseudo

hydrophobic in respect to contact angle (Figure 72B), but clearly not actually hydrophobic in respect to pore chemistry as absorption proceeded without hindrance (Figures 29B and 37). Figure 73 shows the printed lines on the half tone dot area 65 %. The black line on the 30 pph SA containing coating has clearly wicked more than on the 7 pph SA containing coating. Since the apparent contact angle was greater than 90°, the image bleed must have been via sub-surface wicking/capillarity. The 12 pph and 30 pph binder containing coatings had similar absorption time (DIGAT) for dye-based ink (8 gm^{-2} ink amount, Figure 29B), indicating that the dye absorbs into the coating layer structures with the same speed. The porosity values alone cannot explain this result, because the 30 pph SA latex containing coating had even higher air permeance than the coating containing the same amount of PVOH (Figure 29C). The capacitance-based results (Figures 37 and 38) show that the inkjet ink is imbibed at a faster rate in the SA containing coating layer paper than in the PVOH containing. Therefore, these results indicate that the higher bleeding results have a connection to the surface wetting resistance of SA containing coatings, and likely to the surfactants on the latex polymer surface that have been used in latex production. The surfactants could aid lateral transport of colorants within the top part of the coating, although the penetration speed of the ink is in principle quick enough normally to have prevented the appearance of colour bleeding.

A   B
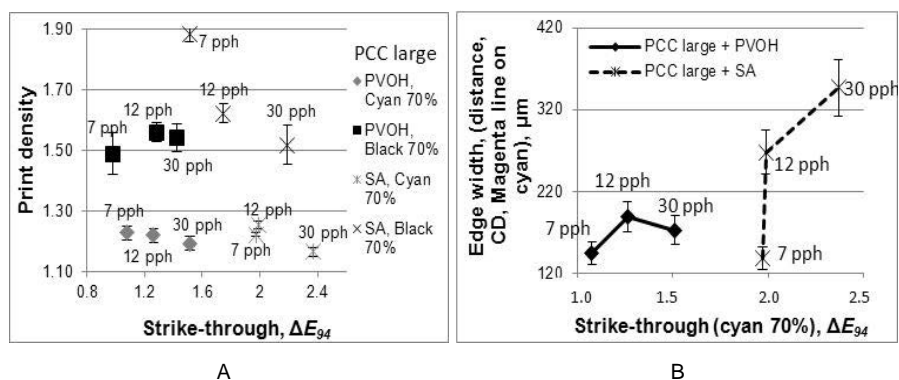
Figure 71. Print density (A) and bleeding (B) against strike-through of dye-based ink printed "PCC large" coating surfaces containing different amounts of PVOH or SA latex. Coat weight was 8 gm^{-2}. Printed with Versamark® VX5000e (speed 100 m·min^{-1}, drying at 80 °C), constant ink amount. The print density was measured with GretagMacbeth D196 spectrophotometer. Bleeding definition: 15 % of minimum and maximum grey value. Based on Paper II (Figure 10 and 11).

A   B
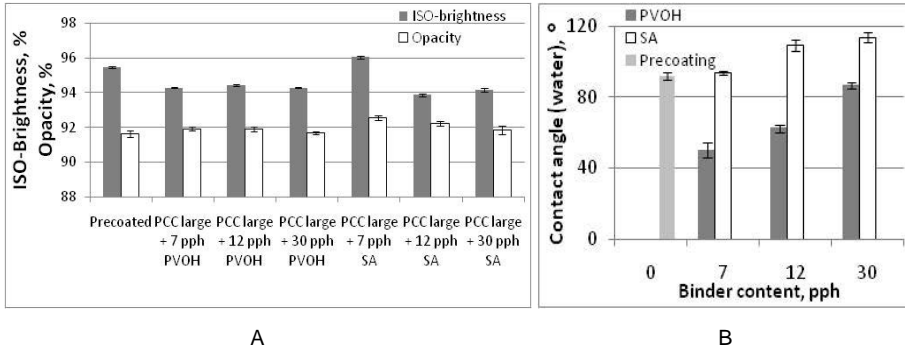
Figure 72. The ISO-brightness, opacity (A) and contact angle of water (B) as function of increasing amount of PVOH (partially hydrolyzed) and SA latex containing "PCC large" coatings, respectively. Coat weight was 8 gm^{-2}.

7 pph SA latex   30 pph SA latex
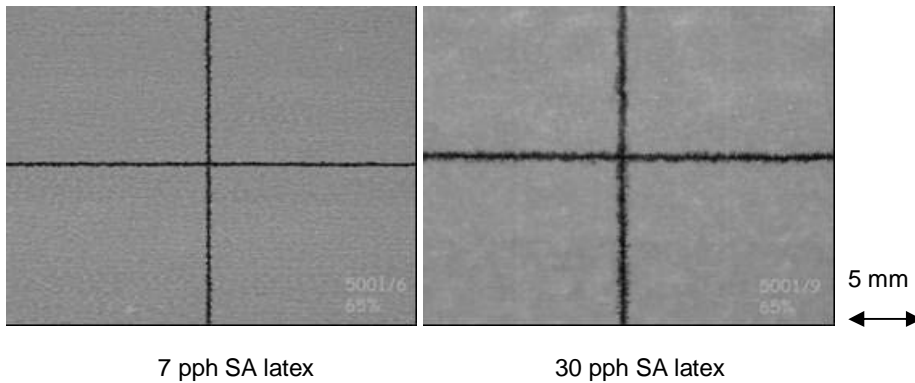
Figure 73. Printed black lines on cyan 65 % half tone dot area on the 7 pph SA and 30 pph SA containing coating layers. Printed with Versamark® VX5000e (speed 100 m·min^{-1}, drying 80 °C).

All of the dye colorant was found to locate in the coating layer (Figure 74, 7 pph binder figures were also shown previously in Figure 28), and takes part in defining the print density formation. Nonetheless, the distribution of colorant within the coating is very different in the case of the 7 pph PVOH containing "PCC large" pigment coating compared with the case of the higher binder level 30 pph PVOH containing. In theory, if the lateral cyan colorant distribution in the 30 pph coating had been more uniform, it would probably have produced higher print density as it was seen to be located more on the top of the coating layer, and the opacity of the 30 pph binder coatings was somewhat lower than that of the 7 pph binder containing coatings. The structural non-uniformity was reflected further in the mottling results. The 30 pph PVOH coating image (Figure 74) shows a place in the coating layer where the ink colorant has penetrated as far as the base paper. This could

be a position in the coating layer where the PVOH, having formed initially a film-like structure, has subsequently developed a hole in the drying film as it shrank (Figure 75).

In the case of SA latex containing coatings, the cyan colorant can be seen to have penetrated as far as into the top of the base paper. The greater permeability as well as the anionic nature of the SA containing coatings allows the anionic colorant to penetrate freely through the structure together with the ink vehicle. There are no colorant-fixing cationic groups and the high permeability provides pathways for ink to transfer deep into the structure. This explains why the SA latex containing coatings had higher strike-though results than the PVOH containing (Figure 71). However, despite the colorant location in the bottom part of the coating layers, no decrease in print density was observed. The cross-section images of the SA coating structures show that the colorant also locates partly within the coating layers. The explanation for satisfactory print density can, therefore, be related to the ink amount. Probably sufficient ink has been applied that there still remains enough colorant within the coating layer to produce a similar print density as in the case of PVOH containing coating.

7 pph PVOH   30 pph PVOH

7 pph SA   30 pph SA   50 µm

Cyan colorant
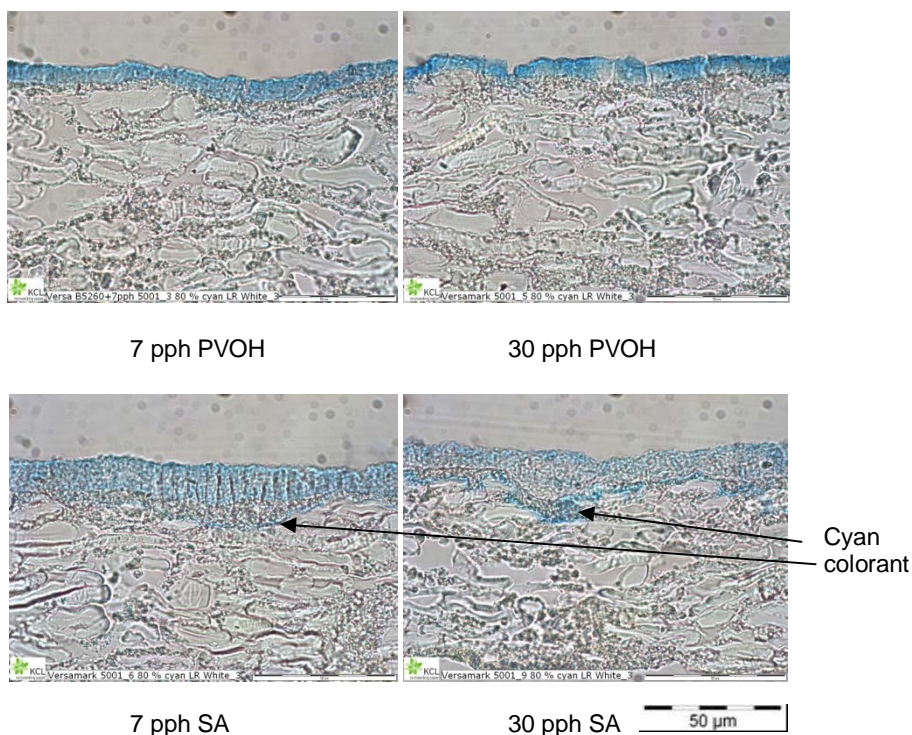
Figure 74. Cross-section images of 7 and 30 pph PVOH or SA containing "PCC large" coatings that have been printed with cyan dye (Versamark[®] VX5000e using speed 100 m·min^{-1} and drying temperature 80 °C), constant ink amount. Coat weight was 8 gm[-2]. Based on Paper 1 (Figure 23).
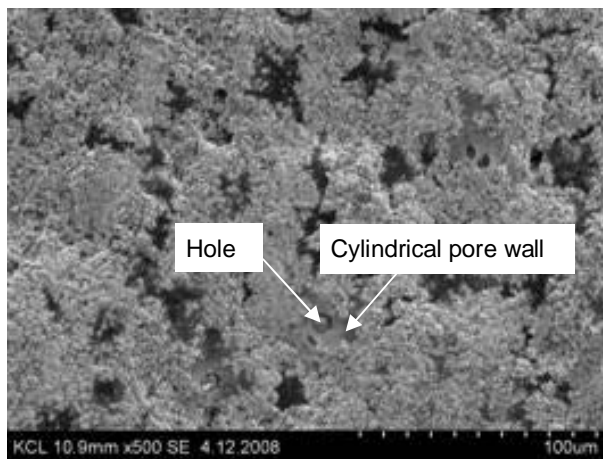
Figure 75. Topographic image (SEM) of 30 pph PVOH "PCC large" pigment coating. Based on Paper I (Figure 27).

Figure 76A shows how the uniformity of the printed PVOH containing surfaces varied the most in the resolution area of 0.34 mm and 0.67 mm. This is the area where the pigment size and state of flocculation affect the result the most. As the binder amount of "PCC large" coatings increased, so grew the mottling values at this resolution. The non-uniform coating layer structure and the holes in the 30 pph binder containing coating produce the highest mottling values as the ink penetrates very unevenly into the coating layer. The use of "PCC small" pigment, in contrast, produced the lowest mottling values. The "PCC small" pigment provides a coating layer structure with nano-size pores and the colorant transfers into this kind of structure more uniformly. In the case of SA containing coatings, a similar mottling increase was detected as the binder amount increased (Figure 76B). However, the maximum values located in the coarser resolution area (0.67–1.34 mm), indicating large size variation on the cyan printed surface.
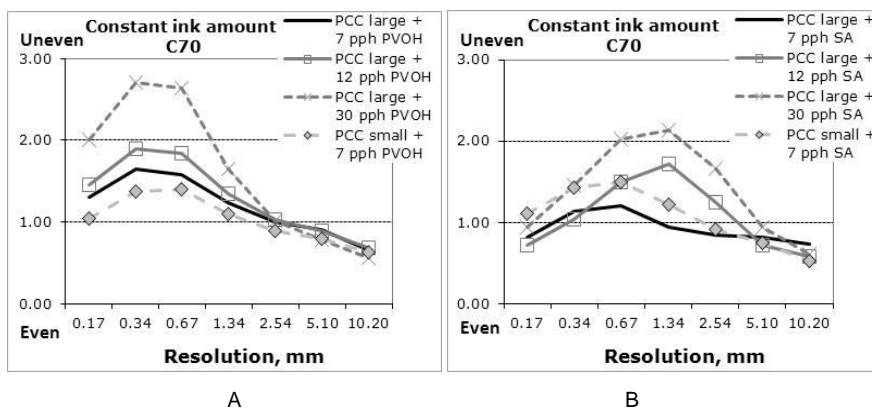
Figure 76. The mottling (mottling index) of cyan ink (C70 – 70 % halftone dot area) printed "PCC large" and "PCC small" coating surfaces. The PVOH (A) or SA latex (B) content varied between 7 and 30 pph. Coat weight was 8 gm^{-2}. Printed with Versamark$^®$ VX5000e by using printing speed of 100 m·min^{-1} and drying temperature 80 °C. Based on Paper I (A: Figure 24).

Important print quality properties, from the point of view of the printed inkjet paper user, are water fastness and rub resistance. The print should be resistant to exposure to water and the ink colorant should stay in/on the prints without transferring to the user's fingers or spreading on the printed surface when touched. Figure 77 shows the water fastness of 70 % half tone dot cyan dye-based ink prints (CIELab*) on the different PVOH and SA latex content "PCC large" coatings after they had been treated by immersing for 5 min in water. The PVOH containing coatings produced clearly lower density change values after the exposure to water than the SA latex containing, indicating that the water treatment changed less the colour of the prints on PVOH containing coatings. PVOH contains chemical groups which can bind colorant molecules, and/or the polymer structure can permit diffusion by the ink, so that it is subsequently more difficult to get colorant molecules out of the coating structure during the water fastness test. All PVOH containing coatings had slightly cationic charge (zeta-potential about 2 mV) that promotes ionic adsorption of the dye, and the hydrophilicity of PVOH binder means that hydrogen bonds can also take a part in the colorant fixing. The colorant thus becomes trapped within the binder polymer structure after ink vehicle evaporation. In the SA latex containing coatings, the same sign of ionic charge of coating layer and colorant molecules causes an anionic repulsion between the binder and colorant. There is no diffusive motion into the binder polymer (the diffusion is surface diffusion only) that could otherwise assist colorant movement into the binder structure.
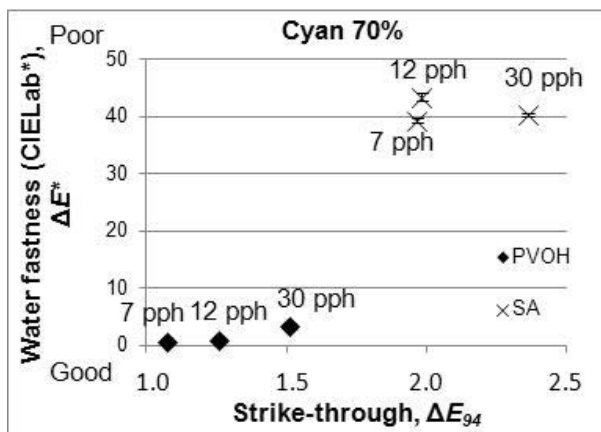
Figure 77. The water fastness of cyan dye-based ink printed on "PCC large" surfaces with different content of PVOH (partially hydrolyzed) or SA latex as a binder. Coat weight was 8 gm^{-2}. Printed with Versamark® VX5000e (speed 100 m·min^{-1} and drying temperature 80 °C), constant ink amount. Based on Paper II (Figure 12).

7.3 Coat weight

The effect of coat weight was studied in *Paper III* by using the coatings that contained the inkjet pigment, "PCC small", and 15 pph of PVOH (partially hydrolyzed). The coatings were applied with a pilot-scale curtain coater on the top of pre-coated fine paper. The printing was carried out on the Versamark® VX5000e using the same ink feed during the whole printing series. The printing speeds were 50 and 100 m·min^{-1}. The on-line camera images in Figure 78 show how much the inkjet inks have mixed together on the different coat weight "PCC small" coatings during printing. All images show wicking paths where the black ink has moved into the area of the cyan colour. The highest coat weight coatings produced the narrowest and the most uniform printed black line next to the cyan ink. There is enough pore volume in these coatings where the ink can penetrate quickly and sufficiently, in regard of ink mixing. Figure 43 illustrates that the higher coating weight paper has more pore volume and it contains more nano-size pores. If the coating layer has a constant pore structure (pore size distribution) and the only variable is the thickness of coating layer, a thicker layer would have more pore volume where the ink can penetrate quickly than the thinner layer. In the low coat weight coating, the ink arrives at the interface between the coatings and base paper earlier, and it pins there for a while. This means that at a certain moment there is more colorant that can spread in the lateral direction, whereas in the thicker coating case the ink still continues to move in the *z*-direction. The printing speed increase expected in high-speed inkjet presses means that the time delays between the nozzles become shorter, and the sorption rate of ink into the coating layers becomes even more important.
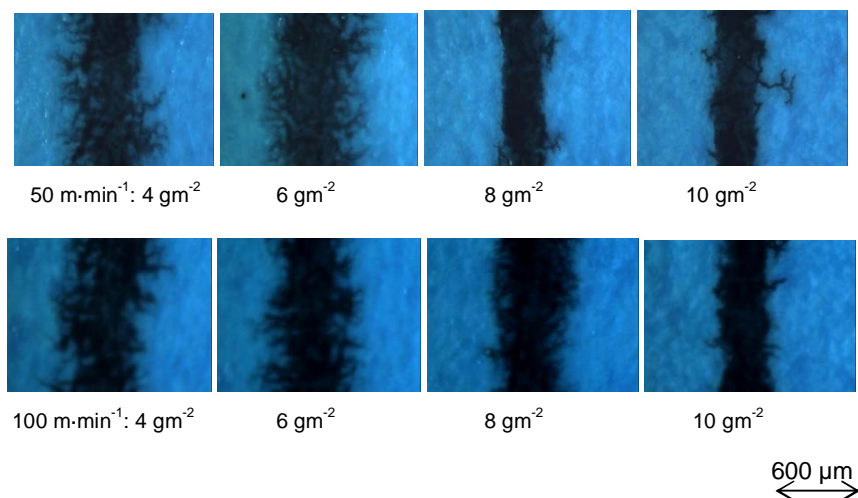
Figure 78. On-line images of intercolour bleeding from "PCC small" coatings that contained 15 pph PVOH (partially hydrolyzed) using printing speeds of 50 and 100 m·min^{-1}. The time delay between cyan application and the on-line camera system was 2.2 s (50 m·min^{-1}) and 1.1 s (100 m·min^{-1}), respectively. The time delay between cyan and black nozzles was 1.1 s and 0.54 s depending on printing speed, respectively. Based on Paper III (Figure 13).

The results of paper analyses show that the highest coat weight (10 gm^{-2}) of curtain-coated "PCC small" with 15 pph PVOH surface produced the highest total paper porosity, and, hence, greatest pore volume, with the 20–60 nm diameter pores providing for the quickest inkjet ink absorption rate. All these findings relate to the simple relationship between the top-coating proportion and the total sheet weight. On-line images collected on the press show further how inkjet inks mixed together less if the coating layer has high coat weight. However, on the 70 % halftone dot area the 4 gm^{-2} coat weight produced higher print density than the 10 gm^{-2} coat weight (Figure 79). Nilsson and Fogden (Nilsson and Fogden 2008) noticed also the print density decrease on PVOH containing spherical polystyrene plastic pigment coatings, which had nominal particle diameter of 0.14 µm, when the coat weight increased from 5 gm^{-2} to 20 gm^{-2}. The colorant remains in the coating layer and therefore the lower coat weight structure has relatively more colorant molecules in the coating volume than the higher coat weight structure. In the high coat weight case, the colorant has moved deeper into the coating layer structure, and therefore there are less colorant molecules that can take part in print density formation. From the print density point of view, when the coating colour has an anionic charge like that of the dye, the coat weight should be low. To minimise the colorant spreading in the *x,y*-direction it is, however, necessary to have sufficient pore volume in the coating, which requires the adoption of high coat weight.

Coat weight: 4 gm^{-2} 8 gm^{-2} 10 gm^{-2}
Print density (C70 %): 1.26   1.26   1.14
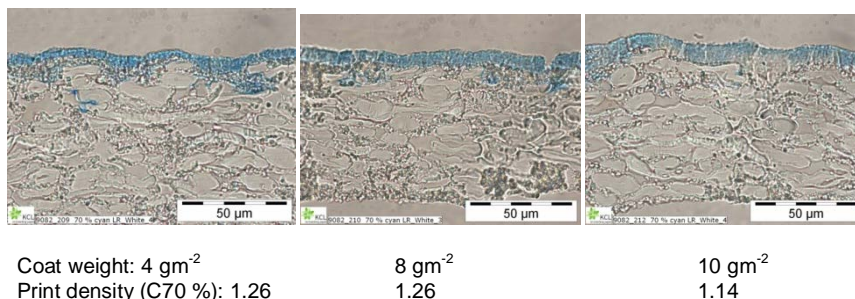
Figure 79. Cross-section images of printed 15 pph PVOH (partially hydrolyzed) containing speciality coatings (70 % half tone dot area). Printed with Versamark® VX5000e, 100 m·min^{-1}, drying 70 °C, constant ink amount. Coat weights 4, 8 and 10 gm^{-2}. Based on Paper III (Figure 14).

7.4   Cationic additive applied directly onto the top of coating surface

One way to design coatings for controlled dye-based ink colorant penetration and fixing is to use a multi-layer structure where each coating layer has a specific purpose. From the colorant fixing point of view, the top applied layer should have an opposite ionic charge than the colorant such that the desired high print density and good colour gamut is usually achieved by ensuring that the colorant will stay in the top part of the layer structure. This kind of layer structure was studied in *Paper VII*. In this research, a cationic polyDADMAC was applied as a post treatment conversion with a draw down coater on the "PCC large" top-coating layer that contained either 7 pph of SA latex (anionic) or 7 pph of PVOH (partially hydrolyzed) – the base paper was pilot pre-coated fine paper. The penetration properties of the surfaces for ink were measured with the capacitance-based device (Clara) using water and cyan dye ink (Versamark® VX5000e), the water being at the temperature of 23 ºC and the dye ink at 23 ºC and 40 ºC. The 2.0–3.2 gm^{-2} application of cationic polymer on the surface slowed down the speed of water and dye-based ink absorption into the structure (Figure 80), as expected. The polymer reduced the permeability of the surface so that it took more time for liquid to penetrate into the surface. The lowest capacitance results, i.e. slowest imbibition, were shown by water, then the anionic dye-based ink at the temperature of 23 °C, and the quickest was seen with the same ink at the higher temperature. The surface tension of water at 23 ºC is 72 mNm^{-1}, and cyan dye at 24 ºC is 54 mNm^{-1} and at 40 ºC, 49 mNm^{-1}, which promotes the faster penetration rate. Additionally, the temperature affects viscosity. The viscosity of the cyan dye ink decreases from 1.05 mPas (23 ºC) to 0.80 mPas (40 ºC) which also promotes a faster absorption. Figure 81 shows two examples of the various Clara results, and they confirm that the differences in the results are reproducible and cannot be explained by random variations.
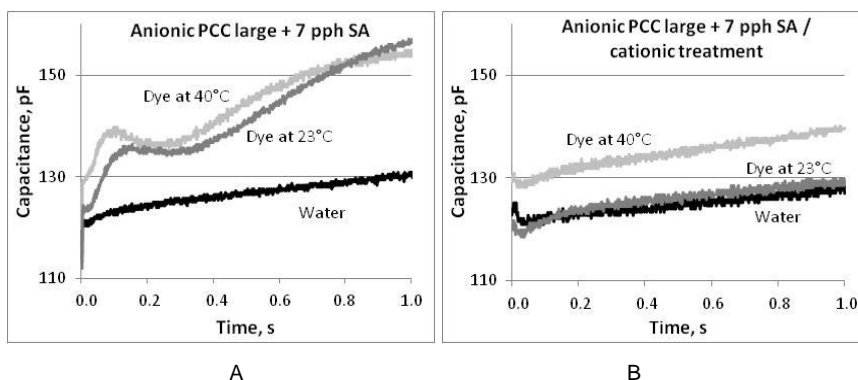
Figure 80. The capacitance changes of papers, having a top-coat of anionic "PCC large" + 7 pph SA latex, and same surface where polyDADMAC (cationic) has been post-applied plotted against time. The penetration of water (23 °C) and dye-based inks (23 °C and 40 °C) into the anionic "PCC large" coating at the timescale of 1 s (A) and polyDADMAC treated surface at 1 s (B). The external over-pressure was 0.10 bar. Based on Paper VII (Figure 6).
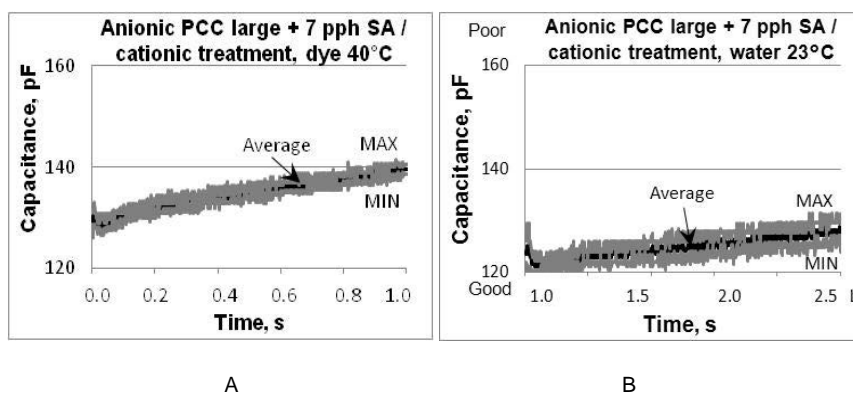

Figure 81. The progression of the capacitance values of anionic "PCC large" + 7 pph SA latex with the polyDADMAC (cationic) treated surface in the Clara device. External over-pressure was 0.10 bar and the liquid was anionic dye at 40 °C (A) and water at 23 °C (B). Based on Paper VII (Figure 7).

The higher temperature (40 ºC) affects the diffusion velocity of ink component molecules, such that the macromolecular motion depends on temperature, viscosity of the surrounding fluid and size of particle/macromolecule, according to the equation of Stokes-Einstein (Mehaffey and Cukier 1977). The diffusional motion of macromolecules is greater at 40 ºC than at 23 ºC, and therefore the ink imbibition is accelerated by use of a warmer ink, as viscosity also falls exponentially with temperature (Figure 10 in section 3.1.4 "Inkjet inks and printing devices"). Another

advantage of using higher temperature ink is the possibility to speed up the final drying of the ink. In the real printing process, the use of warmer ink is limited by the printing nozzles. The ink must not be allowed to start to dry in the nozzles or accumulate on the nozzle exit edge area. The surface tension of the ink, in addition, depends on temperature, especially if this is defined by surfactant action, which itself is diffusion dependent.

The surfaces with and without polyDADMAC treatment were also printed using an HP DeskJet 3940 printer, and the print quality was analyzed. The bleeding was measured from the magenta line (Figure 82), which was either printed as the first colour laid on the paper surface (line spreading on the coating surface) or onto a pre-printed yellow surface (ink mixing). The application of cationic polyDADMAC on the surface decreased the line width, both for the single colour and the magenta on yellow cases. The cationic additive application did not decrease the raggedness of the magenta/yellow line, but the magenta line on the coated paper alone had less raggedness on the polyDADMAC treated surface than on the 7 pph SA-containing coating without treatment. The cationic components of polyDADMAC prevented the anionic colorant spreading, although the added polymer partially closed the structure. The opposite charge of surfaces (electrostatic forces) binds the anionic colorant effectively on the surface so that the colorant cannot spread on the *xy*-plane of the surface. Svanholm (Svanholm 2007) showed that the addition of cationic additive into the coating colour did not always diminish bleeding tendency of dye-based inkjet ink printed coatings. The cationic additive in the coating layer does not necessarily locate on the top part of the coating layer, because, during the consolidation process, the additive can transfer deeper into the coating layer, or even to the base paper, and so it cannot effectively take part in the binding of the colorant. On the other hand, the porosity of the coating layer affects the ink spreading, and in the cationic additive containing coating layer the capillary and permeation flow competes more strongly with the ionic interactions than in the polyDADMAC polymer coated layer, as we saw in section 6.1.2 "Absorption and/or adsorption of coating components". Thus, the additive must locate on or very near the top of the coating layer to fix the colorant quickly enough to the surface so that bleeding problems cannot appear. The only exception could be detected with the magenta ink on the yellow surface, where the raggedness was higher with the cationically treated surface than with the SA containing coating. This indicates that once the ink is isolated from the cationic layer by a previously applied colour, and, as the absorption of ink vehicle is slowed by the presence of the polymer reducing the permeability, the dye can migrate more freely.
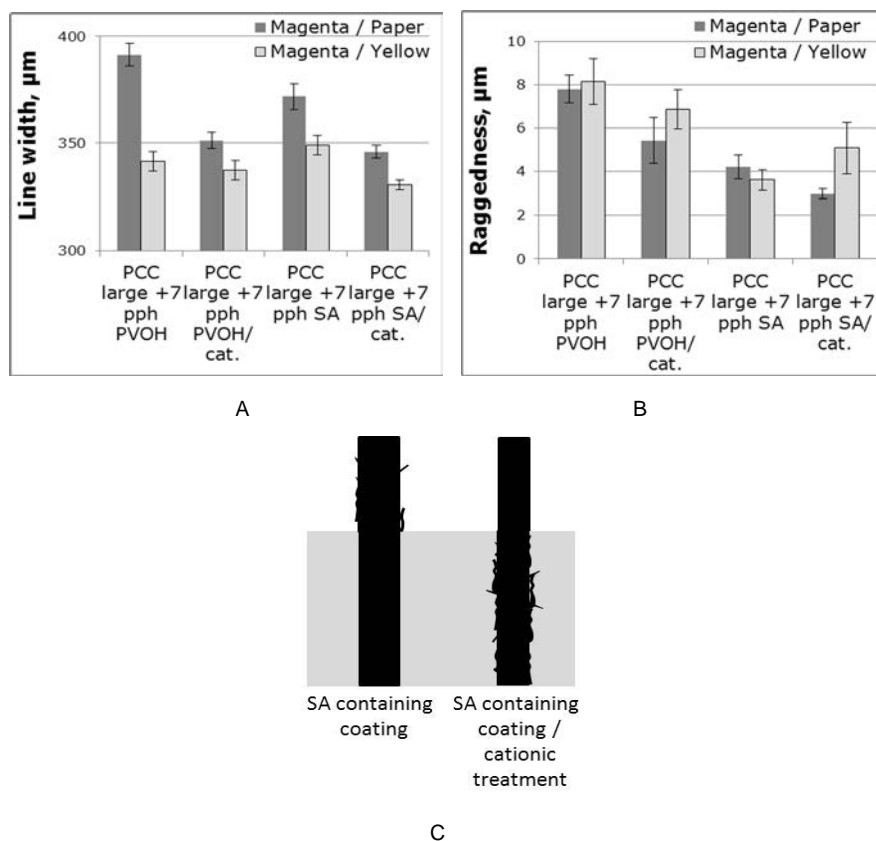
Figure 82. The line width (A) and raggedness (B) of a magenta line printed on the "PCC large" coated paper surface with and without cationic post-treatment (cat.), and on the same surface with a pre-printed yellow compact area. C – a schematic illustration of printed magenta line on the pre-printed yellow and on the non pre-printed paper surface. Printed with HP Deskjet 3940, which had dye-based inks. Based on Paper VII (Figure 9).

The water fastness was measured for this coating series, as before, by detecting the print density changes and ΔE^* of cyan 100 % printed surface after immersion for 5 min in water (23 °C). The results are shown in Figure 83. The print density differences between before and after water treatment were greater on the SA containing coatings than on the PVOH containing surfaces. The water treatment of printed SA coating releases the colorant out of the printed surface because the colorant has no effective binding to the latex, whereas in the PVOH containing coating there forms hydrogen bonding and/or colorant trapping, and the slightly cationic charge of the coating, about 2 mV, provides for ionic interactions. If the SA latex containing coatings with different binder content are compared, somewhat larger changes in ΔE^* were seen with the 30 pph SA containing structure

than with the 7 pph SA containing. The 30 pph SA containing coating has fewer surfaces where the colorant can bind and therefore more colorant can release out of the coating. On the 7 pph PVOH containing coatings, the cationic additive application had quite minimal influence on the change in print density results, indicating an adequate colorant fixing to the PVOH polymer. No large differences were observed between the different PVOH content coatings. A similar value was recorded for the ΔE^* values.

On the SA coatings, the polyDADMAC treated surface produced the lowest ΔE^* value, and the results were very similar to those of PVOH containing coatings. The cationic additive treated SA containing coating fixes the anionic colorant more permanently to the coating layer than the anionic SA latex containing coating alone. The ionic interactions (Coulombic attraction) fix the colorant effectively to the treated surface. The difference between the slightly cationic PVOH containing coating and the cationic polyDADMAC treated PVOH coating surface is small. This indicates that polyDADMAC and the PVOH containing surface behaved very similarly in the water fastness test. The cationicity of the surface does not promote stronger colorant binding more than the diffusion of colorant into the PVOH polymer. The slightly cationic nature combined with the suitable inter-polymer matrix diffusion capability of the coating binder seems to be sufficient for an adequate colorant fixing, so that the colorant does not release out of the surface during the water fastness test as used here.

A   B
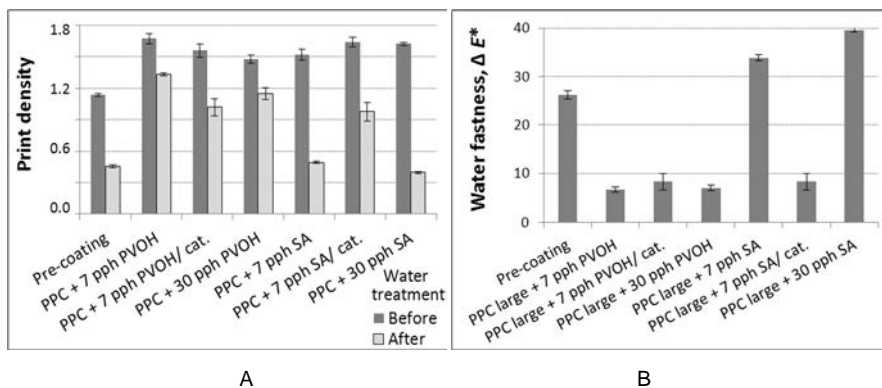
Figure 83. The water fastness of surfaces: print density (100 % cyan) before and after water treatment (A) and the corresponding ΔE* (B, 100 % cyan surface). High fastness implies small ΔE*. Printed with HP Deskjet 3940 which had dye-based inks – the coating had "PCC large" pigment with 7 or 30 pph PVOH (partially hydrolyzed) or SA latex with and without cationic post-treatment (cat.). Measurements were made with SpectroEye spectrophotometer. Based on Paper VII (Figure 10).

7.5   Summary of print quality formation

Beside the selection of printing press variables, inkjet print quality depends on the selection of coating components as well as the amount of each component in the formulation. The main coating layer properties that affect the bleeding formation are the pore volume and the pore size distribution in respect to connectivity and permeability, and thereby the penetration rate of inkjet ink.

   If the coating layer contains latex, in this case study styrene acrylic (SA), the surfactants of the latex assist the sub-surface colorant lateral motion but the penetration speed of ink is high enough to prevent colour bleeding. The SA latex containing coatings have no chemical groups that can fix the colorant quickly to the coating layer. However, in the combination studied here, the optical properties of the speciality coating layer alone play only a minor role in the print density formation of the high-speed inkjet printed surface. The optical properties of the whole fine paper structure dominate in the print density formation.

   In the case of PVOH containing coatings, the ink vehicle diffuses into the hydrophilic polymer network, causing polymer matrix swelling, and this acts to close the nano-size pores thus reducing the ink penetration rate, as was seen previously for the model coating structures. The diffusion transfer seems to be high enough to prevent bleeding problems in the studied coating layers indicating that the diffusion of the liquid phase of inkjet ink into the absorbing polymers acts on a sufficiently fast timescale (Hypothesis I).

> *Hypothesis I* – inter molecular diffusion of the liquid phase of inkjet ink into polymers acts on a sufficiently fast timescale and in sufficient volume to compete with the permeation of ink through coating structures.

The ink colorant locates within the PVOH containing coating layer, thus supporting the idea that colorant transfers into the polyvinyl alcohol matrix by following the ink vehicle (Hypothesis II). Although generally positive, a too high PVOH binder content in the coating colour when applied to paper can produce film-like structures in the coating layer and shrinkage of the wet film during drying can lead to surface defects/holes. During printing, the inkjet ink can penetrate through these holes as far as the base paper, and, as a result, the print uniformity suffers. The PVOH containing coatings on paper had good water fastness results, despite the slightly cationic charge of the coating bulk, as was also seen for the model coatings, indicating that the diffusion of ink colorant into the binder polymer matrix and hydrogen bonding to the polymer matrix is sufficient that the water treatment cannot release the colorant from the structure.

> *Hypothesis II* – inter molecular diffusion of the liquid phase of inkjet ink into polymers, acting as a colorant carrier, is a competing mechanism to the surface adsorption of ink dye.

In the case of anionic SA latex containing coatings, the surface has no chemical groups that can bind the anionic colorant and/or allow the colorant molecules to

diffuse into the binder matrix, and therefore water can release colorant from the printed surface during the water fastness test. This lack of adsorption can also be seen as the anionic colorant partially penetrates through the SA bound coating structure to the top of the base paper, and therefore print-through problems occur. The hydrophobicity of the latex polymer, as well as the action of surfactants on the SA latex surface, affects the molecular motion on the coating surface.

The use of higher coat weight is illustrated by the 15 pph PVOH containing "PCC small" pigment coatings. Higher coat weight in this case speeds up the ink penetration into the coating layer because of the greater pore volume of the absorbent top coating layer. The high pore volume means that ink transfers continuously in the z-direction of the coating layer for longer, and therefore there appears less lateral colorant motion. Despite this positive effect on bleeding, at the same time, the print density decreases because the colorant can transfer deeper into the coating layer.

By application of a small amount of cationic polymer onto an already formed anionic coating layer surface, the bleeding tendency of the ink can be decreased, although the absorption rate of the ink also decreases due to the presence of the polymer. The opposite ionic charge of cationic additive and that of the ink colorant fixes (Coulombic attraction) the colorant molecules within the top part of the coating structure. However, there was no clear connection between the cationic nature of the surface and the print density. Furthermore, once a print colour has been applied, it acts to mask the applied cationic charge, such that subsequent ink colorant application has greater freedom to bleed. The improvement in single colorant fixing is reflected additionally in respect to the water fastness properties in the case of latex containing coatings. The cationic additive application on the PVOH containing coating layer, on the other hand, had quite minimal influence on the water fastness results, indicating the adequate fixing effect of PVOH alone.

The use of higher temperature ink allows quicker diffusion of the ink molecules into the polymer structure of PVOH, and therefore the ink sorption rate can be increased.

8. Conclusions

8.1 The effect of coating structure, binder properties and surface adsorption on inkjet ink imbibition and colorant distribution

8.1.1 The interplay of capillarity and diffusion

The porosity and pore size distribution, in respect to the connected wettable pore network structure of an inkjet paper coating, dominates the imbibition properties for ink vehicle during high-speed inkjet printing. The wetting force of capillaries drives the ink into the coating layer structure, whilst the viscous drag as the net-work fills resists it. At first, there forms a wetting front of ink vehicle where the capillary flow drives the ink forward through a selective pathway depending on the ratio of pore diameter, with the finest pores acting on the shorter timescale. As the viscous drag increases in proportion to the length over which the liquid flows within the structure, and to the inverse of the fourth power of typical equivalent capillary size (Poiseuille effect), there comes a point when the drag equals the wetting force. However, this equilibrium point is never reached within the dimensions of paper coatings and permeation can continue, even through the coating into the basepaper. In the case where hydrophilic soluble binder is used in the coating formulation, the polar ink vehicle (water) diffuses into the binder polymer matrix. As a result, the polymer swells, and this has an effect on the capillary flow by decreasing the pore diameters leading to closure of the smallest pores. As a result, even during the short timescale absorption, the capillary flow becomes reduced and progressively substituted locally by the diffusion into the swelling-generated inter-polymer space. When the smallest capillaries have been filled by a combination of free liquid and liquid bound between the binder polymer chains, the inkjet ink continues to transfer along the large pore structure according to permeation flow. In the case of dye-based inks, the dye follows the vehicle, and, if encountering surface adsorption sites, becomes chromatographically separated from the bulk flow. Dye transport occurs also within the binder polymer network if diffusion is additionally driving absorption into the binder, such that dye becomes bound or trapped within the polymer matrix. In the case of vehicle-repellent binder polymers,

both vehicle and colorant are excluded from the binder, and interaction with ink is limited to the action of surface carboxylation and/or surfactants used to stabilise the otherwise hydrophobic binder particle.

8.1.2 Detailed role of binder

During the ink transfer process, the hydrophilicity/hydrophobicity of binder has a strong effect on the diffusional movement of vehicle and dye. The work here illustrated the impact of binder type in more detail by focusing on two examples, partially hydrolyzed PVOH and styrene acrylic latex. In all cases, the presence of binder slows the absorption rate compared to pure coating pigment. However, at short timescale, the diffusion mechanism in hydrophilic PVOH speeds up the polar liquid absorption relative to the "diffusion-inert" SA latex, which acts to slow the polar liquid movement primarily due to its modification of the surface chemistry by means of associated surfactant used in the emulsion polymerisation process producing the latex. The structural effect of latex is to reduce permeability less than in the case of soluble binder. As a hydrophilic polymer, such as PVOH, absorbs the inkjet ink, the polar ink vehicle (mainly water) diffuses in the polymer network structure and opens it by the action of swelling. The vehicle changes the amorphous region of the polymer. The ink colorant follows the vehicle that acts as a colorant carrier into the polymer matrix. The colorant forms either hydrogen bonding with the chemical groups of PVOH and/or becomes trapped into the structure after ink water evaporation. There is a chromatographic separation, and the dye colorant fixes to the polymer and the vehicle of the ink transfers deeper into the polymer structure proceeding with a depletion of the colorant. The highest content of colorant can be seen on the binder surface that has been longest in contact with the ink. The swelling occurs at a few seconds timescale, which is of similar timescale to the delay that can occur in high-speed inkjet presses between the nozzles and dryers. In the case of effectively non-swelling SA latex, the water and colorant remain excluded from the polymer matrix, and the colorant cannot fix other than by external charge interaction if present. The hydrophobic nature of latex prevents the diffusion of the polar liquid into the polymer structure, but wetting still occurs, once again probably related to the surfactant and/or carboxylation used to stabilize the latex when in suspension. However, the diffusion coefficient in contact with PVOH and SA latex films seems to be similar, although the mechanisms of bulk diffusion and surface diffusion are different. The main polar liquid driving phenomena in the SA latex containing coatings are related to the capillary flow, and the diffusion acts as a molecular motion on the interface of capillary wall and liquid phase, i.e. surface diffusion.

On the longer timescale the diffusion still continues, but the dominating inkjet ink (polar) transport happens in the large pores, and the resulting permeation flow is the most dominant mechanism defining the resistance/competition to capillarity and molecular translation toward diffusion absorbing and charge adsorbing surfaces. One thing that should not be forgotten during inkjet ink imbibition into PVOH

containing coatings, i.e. in the general case of soluble binders, is the dissolution of PVOH itself into the inkjet ink, and this has an effect on the viscosity and surface tension of the ink and further ink and binder transport.

8.1.3 Adsorption and dye fixation

The results of thin layer chromatorgraphy (TLC) show that a surprisingly small amount of binder (1 pph) affects the liquid transfer through (along) the coating layers. The capillary flow is again shown to be the main inkjet ink driving phenomenon in the coating structure. However, the swelling of the PVOH polymer acts on the short timescale liquid absorption, due to the short nano-scale distances involved in the finest pores, despite it being a diffusion-controlled process. The permeation flow offers the resistance to the capillary and diffusion-controlled driving forces in the continuing liquid mass transfer, and swollen binder acts to impede that flow. The latex containing coating carries the water further along a TLC plate than in the PVOH containing. The slightly larger pores of the SA containing coating structure and the non-swelling nature of latex allows a quicker liquid permeation, rather than the smaller pores and reduced connectivity of the PVOH containing coatings.

The studies with the anionic dye and anionic coating layer on the TLC plates show that there is a colorant-free wetting front and behind that a concentrated ink colorant containing layer followed by a lighter colorant area. The surface area associated with the finest pores in these structures is either not available for adsorption of the dye or the charge similarity leads to an exclusion of colorant at the pore entry points. The concentrated colorant layer existing behind the wetting front suggests that charge exclusion is the more likely mechanism. In the case of a cationic coating layer, the anionic colorant fixes immediately into the first contact layer of coating on the TLC plate and remains there until the coating layer specific adsorptive surface area is saturated totally by the colorant, after which the colorant begins to migrate further into the coating.

The penetration of dye-based inks was also studied by means of recording the capacitance change induced by the liquid filling the porous structure. This technique allows the application of an external pressure range, namely 0.02, 0.1 and 1.5 bar in this study. The results measured from the coatings of both standard offset-quality ground calcium carbonate and an inkjet purpose designed precipitated calcium carbonate, combined with different PVOH contents and applied on a plastic film, showed that after as short a time as 0.004 s the permeation flow becomes established in the coating layer when external pressure is applied. The capillary flow, however, acts continuously as the internal driving force throughout. The pigment type, the binder amount or the coating layer thickness (up to 35 gm^{-2}) did not influence this mechanistic result even though their interaction with ink vehicle controls the permeation rate. Similar sorption rate differences were also noticed between the PVOH and SA latex containing coatings as in the TLC, and direct microbalance measurements also confirmed this finding. However, the turning

points between short and long timescale absorption were located at different times depending on the measurement system used. The differences in the non-pressurised microbalance and the slight overpressure applied in the capacitance technique were related directly to the pressure difference, in that the overpressure forced the imbibition into an early permeation mode. The external overpressure caused by an inkjet ink droplet hitting the paper surface is quite low, being approximately equivalent to the capacitance study using 0.10 bar, but it is large enough to have a meaningful effect on the initial sorption results causing an initial wetting by forced surface permeation.

The use of higher temperature ink in the capacitance-based measurement allows a quicker diffusion of the ink molecules into the polymer structure. Additionally, higher temperature lowers the surface tension and viscosity of the ink, and therefore the ink wets and flows more readily.

8.2 Print quality – factors relating to the identified interaction mechanisms

The coating layer structural properties have an effect on the print quality via the ink absorption speed and the pore volume capacity. Too low ink absorption speed into the coating structure means that the colorant of the inks has more time to mix together and bleeding problems are more visible. The optical properties of the *whole coated paper* dominate the print density formation. The reason behind this is that inkjet coating pigments are generally designed to have low scattering potential, and so the base paper, if optically active, has a strong effect in respect to show-through in the coating layer.

The coat weight study shows that absorption speed is not the only criterion for preventing intercolour bleeding during inkjet ink drying, but the combination of the continuity of absorption over time coupled with sufficient total pore volume within the rapidly absorbing layer is the key factor. The only way to decrease the coat weight of speciality inkjet coating layers and still have satisfactory print quality, therefore, is to use pigments that produce a structure with a high proportion of nano-pores and high permeability. The presence of diffusion controlling binder is seen as a limiting factor to achieving optimal inkjet coatings at low coat weights in the case where pore structure derived from the pigment alone is properly designed. The PVOH binder swelling, however, was shown to have a quite minimal influence on the bleeding results. The SA latex on the other hand with its associated surfactant(s) on the latex polymer surface, stabilising the latex in suspension, increased the bleeding results strongly despite the SA containing coating having higher penetration rate than the PVOH containing coating.

Furthermore, the binder type strongly affects the water fastness properties of the inkjet printed surface. The PVOH binds and/or traps the anionic dye colorant molecules so that it is difficult to get them out of the coating structure during exposure to water in the water fastness measurement. The results show that the SA latex can neither bind ink colorant nor prevent bleeding upon wetting. The post-

application of cationic polyDADMAC polymer on the surface of SA latex containing anionic coating decreases the bleeding and produces improved water fastness results, indicating better colorant fixing to the surface despite the slower absorption rate through the surface. The opposite ionic charge of the surface binds the ink colorant molecules in the top part of the structure by Coulombic forces, and the lack of colorant penetration seems not to prevent this rapid fixing of the dye colorant.

The adsorption of colorant in the fixing process can be detrimentally limited if too great a permeation flow of inkjet ink occurs during the imbibition. Especially the fixing of colorant by PVOH containing coatings showed that the dynamics of colorant hydrogen bonding following diffusion into the binder polymer network and/or Coulombic forces acting at pore surfaces can be slower than the bulk flow transport of the colorant past the relevant adsorption sites. These results suggest that, for good colorant fixing, there is an optimum in the ink sorption flow rate into the coating structure, such that the colorant has sufficient time to bind to the available opposite charge and/or binder chemical groups.

9. Suggestions for future work

The results of this study show that the diffusion-driven and ionic charge interactions between the components of the coating layer and the ink colorant are complex, and that they are strongly dependent on the coating formulation and how the coating layer structure is produced, i.e. in terms of drying, porosity, or use of multilayer structures. At the same time, the results suggest that there would be an optimum absorption permeation rate for inkjet inks in terms of colorant fixing. Further studies to generate a better understanding of ionic charge location and polymer distribution in/on the coating layer structure is therefore identified as a potential means for helping inkjet substrate designers in their search for inkjet coating colour formulations for the rapidly emerging market in high-speed inkjet printing.

There are identifiable trends in the inter-colour bleeding results that suggest the outermost surface and immediate sub-surface energy of the coating layer(s) can influence the inkjet ink mixing tendency. This discovery certainly needs more comprehensive research to define the effects more thoroughly, and probably would lead to further correlations with the ionic properties of the coating layer. This is a research area where some work has already been made, but the connections between surface energies and print quality aspects have not been shown in sufficient detail. This research could include the role of surfactant action associated with latex.

One aspect that has not been studied in this thesis is the drying of inkjet prints: how the coating layer with absorbing binder combined to the structural variation affect the drying rate, and, if the water is held by the diffusive mechanism in the coating, how does it effect to the final drying of printed surface. Thermal properties of the various formulations in respect to efficient heat transfer could be connected to this.

The research work in this thesis concentrated on dye-based aqueous inkjet inks. There are now many developing applications that use pigment-based aqueous inks, and the interest in pigment inks is increasing all the time. The currently reducing cost of pigment-based inks is pushing their development further, but still the ink does not work reliably enough in the nozzles and produces at best only similar print quality to the dye-based inks, in respect to colour gamut, in high-speed inkjet printing. Nevertheless, the growth in pigment-based inks will continue, partly due to the improved holdout properties and reduced demand for extremely

high absorbency in the coating, and so the understanding of their setting interactions on coating layers and the surface sized structures is important for application at high printing speeds. The other area, in respect of the inks likely to be used for high-speed inkjet printing, is the behaviour of UV-curing inks on coated surfaces and especially how the coating components affect the UV-curing.

In the case of the use of a swelling binder, changes to the absorption dynamic are identified, e.g. modification of the Bosanquet equation as applied to pore networks, but a detailed development was not undertaken in this thesis. To capture such an effect in an algorithm would be a subject for later work, and could, for example, be applied to a time-evolving network model. In effect, the absorption driver of diffusion, although positively active, is, however, giving a negative feedback and so reducing the capillary-driven absorption.

Perhaps one of the most important aspects to consider now and in the future is the recycling potential of inkjet printed papers. A control of the interaction of ink and substrate will be a key feature for developing optimally recyclable substrates. It is hoped that such future work will benefit from the findings presented in this thesis.

References

Adair, P. C.: Ink jet coatings for pigmented inks, IS&T NIP14: International Conference on Digital Printing Technologies, October 18–23, 1998, Toronto, Canada, IS&T: The Society for Imaging Science and Technology, Springfield, USA, 1998, 146–149.

Agbezuge, L., Gooray, A.: Drying of ink jet images on plain papers – falling rate period, IS&T's NIP7: International Conference on Digital Printing Technologies, 1991, Portland, USA, IS&T: The Society for Imaging Science and Technology, Springfield, USA, 1991, 173–184.

Ahlen, A.T.: Diffusion of Sorbed Water Vapor Through Paper and Cellulose Film, Tappi Journal 53(1970)7, 1320–1326.

Alleborn, N., Raszillier, H.: Spreading and sorption of a droplet on a porous substrate, Chemical Engineering Science 59(2004)2, 2071–2088.

Alleborn, N., Raszillier, H.: Dynamics of films and droplets spreading on porous substrates, Tappi Journal 6(2007)3, 16–23.

von Bahr, M., Tiberg, F., Zhmud, B.: Spreading Dynamics of Surfactant Solutions, Langmuir 15(1999)20, 7069–7075.

von Bahr, M., Kizling, J., Zhmud, B., Tiberg, F.: Spreading and Penetration of Aqueous Solutions and Water-borne Inks in Contact with Paper and Model Substrates, Advances in Printing Science and Technology –Advances in Paper and Board Performance, 27th Research Conference of the International Association of the Research Institutes for the Printing, Information and Communication Industries (Iarigai), 2000, Graz, Austria, 87–102.

von Bahr, M., Tiberg, F., Zhmud, B.: Oscillations of sessile drops of surfactant solutions on solid substrates with differing hydrophobicity, Langmuir 19(2003)24, 10109–10115.

von Bahr, M., Seppänen, R., Tiberg, F., Zhmud, B.: Dynamic wetting of AKD-sized papers, Journal of Pulp and Paper Science 30(2004)3, 74–81.

Batz-Sohn, C., Lembach, A., Nelli, L., Müller, A., Roisman, I., Tropea, C.: Speed of ink absorption on modified paper surfaces, IS&T's NIP26 International Conference on Digital Printing Technologies, 2010, Austin, USA, IS&T: The Society for Imaging Science and Technology, Springfield, USA, 2010, 503–506.

Bauer, W., Baumgart, D., Macholdt, H.-T., Zoeller, W.: Lightfast colorants for ink jet applications, Ink World 4(1998)10, 52–58.

Bermel, A. D., Bugner, D. E.: Particle size effects in pigmented ink jet inks, Journal of Imaging Science and Technology 43(1999)4, 320–324.

Biry, S., Dietliker, K. [online]: UV ink jet printing: Market and technology, http://www.ciba.com/pf/docMDMS.asp?targetlibrary=CHBS_ce_MADS&docnumber=3272, 2006, 14 p. [Cited: 12.02.2008].

Boisvert, J.-P., Guyard, A.: Influence of structural properties of nanoporous silica-polymer materials on ink absorption, Nordic Pulp and Paper Research Journal 18(2003)2, 210–216.

Bosanquet, C. H.: On the flow of liquids into capillary tubes, Philosophical Magazine, Serie 6, 45(1923)267, 525–531.

Carslaw, H. S.: Conduction of heat in solids, Clarendon Press, Oxford, UK, 1997, p. 100.

Cawthorne, J. E., Joyce, M., Fleming, D.: Use of a Chemically Modified Clay as a Replacement for Silica in Matte Coated Ink-Jet Papers, Journal of Coatings Technology 75(2003)937, 75–81.

Chapman, D. M.: Coating structure effects on ink-jet print quality, Tappi Coating Conference, 1997, Philadelphia, USA, Tappi Press, Atlanta, USA, 73–93.

Colour Index: [online] Colour Index Numbers (CIN). Available online at: http://www.artiscreation.com/Colour_Index_International_ci.htm, [cited: 7.12.2011]

Darcy, H.: Les fontaines publiques de la ville de Dijon, V. Dalmont (ed.), Paris, 1856, 647.

Desie, G., Deroover, G., De Voeght, F., Soucemarianadin, A. (a): Printing of dye and pigment-based aqueous inks onto porous substrates, Journal of Imaging Science and Technology 48(2004)5, 389–397.

Desie, G., Deroover, G., De Voeght, F., Claes, R. (b): Fundamental mechanisms in ink media interactions for aqueous, UV-curing and solvent based inks, IS&T's NIP20: International Conference on Digital Printing Technologies, 2004, Salt Lake City, USA, IS&T: The Society for Imaging Science and Technology, Springfield, USA, 2004, 774–779.

Desie, G., Van Roost, C.: Validation of ink media interaction mechanisms for dye and pigment-based aqueous and solvent inks, Journal of Imaging Science and Technology 50(2006)3, 294–303.

Donigian, D. W., Wernett, P. C., McFadden, M. G., McKay, J. J.: Ink jet dye fixation and coating pigments, Tappi Coating/Papermakers Conference, 1998, New Orleans, USA, Tappi Press, Atlanta, USA, 393–412.

Gane, P. A. C., Kettle, J. P., Matthews, G. P., Ridgway, C. J.: Void Space Structure of Compressible Polymer Spheres and Consolidated Calcium Carbonate Paper-Coating Formulations, Industrial and Engineering Chemistry Research 35(1996)5, 1753–1764.

Gane, P. A. C., Matthews, G. P., Schoelkopf, J., Ridgway, C. J., Spielmann, D. C.: Observing fluid transport into porous coating structures: Some novel findings, TAPPI Advanced Coating Fundamentals Symposium, 1999, Toronto, Canada, Tappi Press, Atlanta, USA, 1999, 213–236.

Gane, P. A. C.: Mineral Pigments for Paper: Structure, Function and Development Potential (Part II), Wochenblatt für Papierfabrikation 129(2001)4, 176–179.

Gane, P. A. C., Ridgway, C. J.: moisture pickup in calcium carbonate coating structures: role of surface and pore structure geometry, TAPPI 10th Advanced Coating Fundamentals Symposium, 2008, Montreal, Canada, Tappi Press, Atlanta, USA, 24 p.

Girard, F., Attané, P., Morin, V.: A new analytical model for impact and spreading of one drop: application to inkjet printing, Tappi Journal 5(2006)12, 24–32.

Glittenberg, D., Voigt, A.: Economic formulations for improved quality ink-jet papers, Paper Technology 42(2001)9, 24–29.

Glittenberg, D., Voigt, A., Donigian, D.: novel pigment-starch combination for the online and offline coating of high-quality inkjet papers, Paper Technology 44(2003)7, 36–42.

Hara, K.: Specialty PVOH in ink jet coating formulations, Paper Technology 47(2006)3, 27–30.

Hamada, H., Bousfield, D. W.: The effect of cationic additives on ink penetration, Journal of Pulp and Paper Science 35(2009)3–4, 118–122.

Hartus, T.: Adsorption and Desorption Behaviour of Ink Jet Dye on Paper, Graphic Arts in Finland 27(1998)3, 3–9.

Hasimi, A., Stavropoulou, A., Papadokostaki, K. G., Sanopoulou, M.: Transport of water in polyvinyl alcohol films: Effect of thermal treatment and chemical crosslinking. European Polymer Journal 44(2008)12, 4098–4107.

Haverinen, H. M., Myllylä, R. A., Jabbour, G. E.: Inkjet printing of light emitting quantum dots, Applied Physics Letters 94(2009)7, 073108, 3 p.

Hayes, R. A., Ralston, J.: The molecular-kinetic theory of wetting, Langmuir 10(1994)1, 340–342.

Heilmann, J., Lindqvist, U.: Effect of drop size on the print quality in continuous ink jet printing, Journal of Imaging Science and Technology 44(2000)6, 491–494.

Hellén, E. K. O., Ketoja, J. A., Niskanen, K. J., Alava, M. J.: Diffusion through fiber networks, Journal of Pulp and Paper Science 28(2002)2, 55–62.

Hill, D. J. T., Whittaker, A. K., Zainuddin: Water diffusion into radiation cross-linked PVA-PVP network hydrogels, Radiation Physics and Chemistry 80(2011)2, 213–218.

Hladnik, A.: Use of Specialty Pigments in High-End Ink-Jet Paper Coatings, Journal of Dispersion Science and Technology 25(2004)4, 481–489.

Hodge, R. M., Edward, G. H., Simon, G. P.: Water absorption and states of water in semicrystalline poly(vinyl alcohol) films, Polymer 37(1996)8, 1371–1376.

Iordanskii, A. L., Razumovskii, L. P., Krivandin, A. V., Lebedeva, T. L.: Diffusion and sorption of water in moderately hydrophilic polymers: From segmented polyetherurethanes to poly-3-hydroxybutyrate, Desalination 104(1996)1–2, 27–35.s

Josserand, C., Zaleski, S.: Droplet splashing on a thin liquid film, Physics of Fluids, 15(2003)6, 1650–1657.

Kallio, T., Kekkonen, J., Stenius, P.: Acid/base properties and adsorption of an azo dye on coating pigments, Journal of Dispersion Science and Technology, 27(2006)6, 825–834.

Kang, H. R.: Water-based ink-jet ink. 1. Formulation, Journal of Imaging Science 35(1991)3, 179–188.

Kettle, J., Lamminmäki, T., Gane, P.: A review of modified surfaces for high speed inkjet coating, Surface and Coatings Technology 204(2010)12–13, 2103–2109.

Khoultchaev, K., Graczyk, T.: Polymer-polymer and polymer-pigment interactions – implications on ink jet universal media, Tappi Coating Conference, 1999, Toronto, Canada, 155–168.

Klang, J. A., Balcerski, J. S.: UV Inkjet Technology: Issues for Inkjet Formulations, Ink Maker online, September 2002, 7 p.

Klass, C.P.: New modified natural zeolite, Paper360°, August 2007, 24–26.

Koenig, M. F., Yang, S., Hartman, R. R., Schultz, S., Stoffel, J., Tran, H., Askeland, R., Sperry, W. R., Gibson, L.: Recording sheet with improved image dry time, International Paper Company, USA. U. S. Pat. 2007/0087138, Available online at: http://www.patents.com/us-20070087138.html [cited: 9.12.2011]

Kubelka, P., Munk, F.: Ein Beitrag zur Optik der Farbanstriche, Zeitschrift für technische Physik 12(1931)11a, 593–601.

Kumaki, K., Nii, S.: Polyvinyl alcohol in ink jet coatings, Tappi PaperCon, 2010, Atlanta, USA, Tappi Press, Atlanta, USA, 27 p.

Van Laethem, J.: New security printing possibilities with industrial digital presses, International Conference on Digital Production Printing and Industrial Applications, 2003, Barcelona, Spain, 124–126.

Lamminmäki, T., Puukko, P.: New ink absorption method to predict inkjet print quality, Advances in Printing and Media Technology, 34th International Research Conference of Iarigai, 2007, Grenoble, France, 231–239.

Lamminmäki, T., Lampinen, H., Hyvärinen, S., Kataja, K.: Measuring the Penetration Properties of Starch-Treated Wood-Free Paper, Nordic Pulp and Paper Research Journal 25(2010)3, 372–379.

Larsson, L. O., Trollsås, P. O.: Genomtrycket och dess komponenter, Svensk Papperstidning 75(1972)8, 317–321.

Laudone, G. M., Matthews, G. P., Gane, P. A. C.: Coating shrinkage during evaporation: observation, measurement and modelling within a network structure, Tappi 8th Advanced Coating Fundamentals Symposium, Chicago, USA, 2003, Tappi Press, Atlanta, USA, 116–129.

Laudone, G. M., Matthews, G. P., Gane, P. A. C.: Effect of Latex Volumetric Concentration on Void Structure, Particle Packing, and Effective Particle Size Distribution in a Pigmented Paper Coating Layer, Industrial and Engineering Chemistry Research 45(2006)6, 1918–1923.

Lavery, A., Provost, J.: Color-media interactions in ink jet printing, IS&T's NIP13: International Conference on Digital Printing Technologies, 1997, Seattle, USA, IS&T: The Society for Imaging Science and Technology, Springfield, USA, 1997, 437–442.

Lee, H.-K., Joyce, M. K., Fleming, P. D., Cameron, J. H.: Production of a Single Coated Glossy Inkjet Paper Using Conventional Coating and Calendering Methods, Tappi Coating and Graphic Arts Conference and Trade Fair, 2002, Orlando, USA, 24 p.

Lee, H.-K., Joyce, M. K., Fleming, P. D.: Influence of Pigment Particles on Gloss and Printability for Inkjet Paper Coatings, IS&T's NIP20: International Conference on Digital Printing Technologies, 2004, Salt Lake City, USA, IS&T: The Society for Imaging Science and Technology, Springfield, USA, 2004, 934–939.

Lee, H.-K., Joyce, M. K., Fleming, P. D., Cawthorne, J. E.: Influence of silica and alumina oxide on coating structure and print quality of ink-jet papers, Tappi Journal 4(2005)2, 11–16.

Liang, B., Fields, R. J., King, C. J.: The mechanisms of transport of water and n-propanol through pulp and paper, Drying technology 8(1990)4, 641–665.

Lundberg, A., Örtegren, J., Alfthan, E., Ström, G., Microscale droplet absorption into paper for inkjet printing, Nordic Pulp and Paper Research Journal 26(2011)1, 142–150.

Malla, P. B., Devisetti, S.: Novel Kaolin Pigment for High Solids Ink Jet Coating, Paper Technology 46(2005)8, 17–27.

Marmur, A.: Kinetics of penetration into uniform porous media: Testing the equivalent-capillary concept, Langmuir 19(2003)14, 5956–5959.

Massoquete, A., Lavrykov, S., Ramarao. B. V.: Non-fickian behaviour of moisture diffusion in paper, Journal of Pulp and Paper Science 31(2005)3, 121–127.

McFadden, M. G., Donigian, D. W.: Effects of coating structure and optics on inkjet printability, Tappi Coating Conference, 1999, Toronto, Canada, Tappi Press, Atlanta, USA, 169–177.

Mehaffey, J. R., Cukier, R. I.: Kinetic-Theory Derivation of the Stokes-Einstein Law, Physical Review Letters 38(1977)19, 1039–1042.

Miller, G. D., Cook, G. R.: Polyvinyl alcohol – a specialty polymer for specialty papers, Tappi Short Course, Boston, USA, Tappi Press, Atlanta, USA, 1990, 43–70.

Morea-Swift, G., Jones, H.: The use of synthetic silicas in coated media for ink-jet printing, Tappi Coating Conference and Trade Fair, 2000, Washington, USA, Tappi Press, Atlanta, USA, 317–328.

Mowiol: Mowiol Polyvinyl Alcohol, procure of the chemical, Clariant, Available online at: http://www.kuraray-am.com/pvoh-pvb/downloads/Mowiol_brochure_en_KSE.pdf, 2003, [cited: 1.11.2012]

Mäkinen, M. O. A., Happonen, J., Sahivirta, J., Hartus, T., Paltakari, J., Jääskeläinen, T., Parkkinen, J.: Color difference model for estimating real perceived print-through, Journal of Pulp and Paper Science 33(2007)1, 35–43.

Nguyen, H. V., Durso, D. F.: Absorption of water by fiber webs: an illustration of diffusion transport, Tappi Journal 66(1983)12, 76–79.

Nilsson, H., Fogden, A.: Inkjet print quality on model paper coatings, Appita 61(2008)2, 120–127.

Oittinen, P.: Fundamental rheological properties and tack of printing inks and their influence on ink behaviour in a printing nip, Dissertation, 1976, Helsinki University of Technology, Helsinki, Finland.

Oka, H., Kimura, A.: the physicochemical environment of acid red 249 insolubilized in an ink-jet paper, Journal of Imaging Science and Technology 39(1995)3, 239–243.

Oliver, J.F.: Wetting and penetration of paper surfaces, in Colloids and Surfaces in Reprographic Technology, M. Hair, M. D. Croucher, 1982, American Chemical Society, Washington, USA, 435–453.

Pajari, H., Juvonen, K., Jokio, M., Koskela, H., Sneck, A.: Dynamic measurement of coating colour consolidation with a new laboratory coater, 23rd PTS Coating Symposium, 2007, Baden-Baden, Germany, Paper 28, 13 p.

Pan, Y.-L., Yang, S.: Wetting and liquid absorption characteristics of ink jet paper, IS&T's NIP 12: International Conference on Digital Printing Technologies, 1996, San Antonio, USA, 399–402.

Pinto, J., Nicholas, M.: SIMS studies of ink jet media, IS&T's NIP 13: International Conference on Digital Printing Technologies, 1997, Seattle, USA, IS&T: The Society for Imaging Science and Technology, Springfield, USA, 1997, 420–426.

Pond, S.: Inkjet technology and product development strategies, USA 2000, 406 p.

Radhakrishnan, H., Chatterjee, S. G., Ramarao, B. V.: Steady-state moisture transport in a bleached kraft paperboard stack, Journal of Pulp and Paper Science 26(2000)4, 140–144.

von Raven, A., Strittmatter, G., Weigl, J.: Cationic coating colors – a new coating system, Tappi Journal 71(1988)12, 141–148.

Reynolds, P. A., Goodwin, J. W.: Direct measurement of the translational diffusion coefficients of aggregated polystyrene latex particles, Colloids and Surfaces 11(1984)1-2, 145-154.

Ricciardi, R., Auriemma, F., Gaillet, C., De Rosa, C., Laupretre, F.: Investigation of the Crystallinity of Freeze/Thaw Poly(vinyl alcohol) Hydrogels by Different Techniques. Macromolecules 37(2004)25, 9510–9516.

Ridgway, C., Schoelkopf, J., Matthews, G. P., Gane, P. A. C., James, P. W.: The Effects of Void Geometry and Contact Angle on the Absorption of Liquids into Porous Calcium Carbonate Structures, Journal of Colloid and Interface Science 239(2001)2, 417–431.

Ridgway, C. J., Gane, P. A. C.: Controlling the absorption dynamic of water-based ink into porous pigmented coating structures to enhance print performance, Nordic Pulp and Paper Research Journal 17(2002)2, 119–129.

Ridgway, C. J., Gane, P. A. C., Schoelkopf, J.: Effect of Capillary Element Aspect Ratio on the Dynamic Imbibition within Porous Networks, Journal of Colloid and Interface Science 252(2002)2, 373–382.

Ridgway, C. J., Gane, P. A. C.: Bulk density measurement and coating porosity calculation for coated paper samples, Nordic Pulp and Paper Research Journal 18(2003)1, 24–31.

Ridgway, C. J., Gane, P. A. C.: The Impact of Pore Network Structure on the Absorption of Pigmented Inkjet Inks, Tappi Coating Conference, 2005, Toronto, Canada, Session 6, Tappi Press, Atlanta, USA, 15 p.

Ridgway, C. J., Gane, P. A. C.: Correlating pore size and surface chemistry during absorption into a dispersed calcium carbonate network structure, Nordic Pulp and Paper Research Journal 21(2006)5, 563–568.

Ridgway, C. J., Schoelkopf, J., Gane, P. A. C.: Competitive absorption of polar and non-polar liquids into latex bound porous structures of fine ground calcium carbonate, Transport in Porous Media 86(2011)3, 945–964.

Riegel, B., Hartmann, I., Kiefer, W., Gross, J., Fricke, J.: Raman spectroscopy on silica aerogels, Journal of Non-Crystalline Solids 211 (1997)3, 294–298.

Romano, C. E. JR., Schlicsman, L. J. JR., Niemiec, J. P.: Inkjet recording medium, Newpage Corporation, USA, U. S. 2011, Pat. 2011/0037818. 5 p.

Rousu, S., Gane, P., Spielmann, D., Eklund, D.: Separation of off-set ink components during absorption into pigment coating structures, Nordic Pulp and Paper Research Journal 15(2000)5, 527–535.

Rousu, S., Gane, P., Eklund, D.: Print quality and the distribution of offset ink constituents in paper coatings, Tappi Journal 4(2005)7, 9–15.

Salminen, P.: Studies of water transport in paper during short contact times, Dissertation, 1988, Department of Chemical Engineering, Åbo Akademi, 94 p.

Salmén, N. L., Back, E. L.: Moisture-dependent thermal softening of paper, evaluated by its elastic modulus, Tappi J. 63(1980)6, 117–120.

Schoelkopf, J., Ridgway, C. J., Gane, P. A. C., Matthews, G. P., Spielmann, D. C.: Measurement and Network Modeling of Liquid Permeation into Compacted Mineral Blocks, Journal of Colloid and Interface Science 227(2000)1, 119–131.

Schoelkopf, J., Gane, P. A. C., Ridgway, C. J., Matthews, G. P.: Practical observation of deviation from Lucas–Washburn scaling in porous media, Colloids and Surfaces A: Physicochemical and Engineering Aspects, 206(2002)1–3, 445–452.

Shaw, D. J.: Introduction to colloid & surface chemistry, 4th edition, Reed Educational and Professional Publishing Ltd, 1996, 306 p. ISBN 0 7506 1182 0

Shaw-Klein, L., Wexler, A., Giacherio, D., Demejo, L.: Materials for high-quality inkjet papers, PTS 23rd Coating Symposium, 2007, Baden-Baden, Germany, 8 p.

Shi, J., Schuman, T. P., Stoffer, J. O.: Ink-jet printing paper with improved waterfastness, Journal of Coating Technology Research 1(2004)3, 225–234.

Shore, J.: [online] Colorants and auxiliaries, Organic Chemistry and Application Properties, Volume 1 – Colorants. Available online at: http://www.scribd.com/doc/50173889/3/COLOUR-INDEX-CLASSIFICATION, [cited: 7.12.2011]

Smyth, S.: The Future of Inkjet Printing to 2015, Global Market Forecasts, Pira International Ltd, 2010, 208 p.

Sorbie, K. S., Wu, Y. Z., McDougall, S. R.: The Extended Washburn Equation and Its Application to the Oil/Water Pore Doublet Problem, Journal of Colloid and Interface Science 174(1995) 2, 289–301.

Sundquist, J.: Tekstiiliväriaineet, Kemia – Kemi, 11(1985)11, 937–944.

Svanholm, E., Ström, G.: Influence of polyvinyl alcohol on inkjet printability, International Printing and Graphic Arts Conference, Vancouver, BC, Canada, 2004, PAPTAC, 187–207.

Svanholm, E.: Printability and Ink-Coating Interactions in Inkjet Printing, Doctoral thesis, Karlstad University, Faculty of Technology and Science, Chemical Engineering, 2007:2, Karlstad 2007, 48 p.

Thurn, J.: Water diffusion coefficient measurements in deposited silica coatings by the substrate curvature method, Journal of Non-Crystalline Solids 354(2008)52–54, 5459–5465.

Tiberg, F., Zhmud, B., Hallestensson, K., von Bahr, M.: Capillary rise of surfactant solutions, Physical Chemistry Chemial Physics 2(2000)22, 5189–5196.

Topgaard, D., Söderman, O.: Diffusion of Water Absorbed in Cellulose Fibers Studied with H-NMR, Langmuir 17(2001)9, 2694–2702.

Varnell, D. F.: Composition and method for improved ink jet printing performance, US6207258 B1, 2001, 12 p.

Vikman, K.: Fastness Properties of Ink Jet Prints on Coated Papers – Part 2: Effect of Coating Polymer System on Water Fastness, Journal of Imaging Science and Technology 47(2003)1, 38–43.

Vikman, K., Vuorinen, T. (a): Water Fastness of Ink Jet Prints on Modified Conventional Coatings, Journal of Imaging Science and Technology 48(2004)2, 138–147.

Vikman, K., Vuorinen, T. (b): Light Fastness of Ink Jet Prints on Modified Conventional Coatings, Nordic Pulp and Paper Research Journal 19(2004)4, 481–488.

Wallqvist, V., Claesson, P. M., Swerin, A., Schoelkopf, J., Gane, P. A. C.: Interaction forces between talc and hydrophobic particles probed by AFM, Colloids and Surfaces, A: Physicochemical and Engineering Aspects 277 (2006)1–3, 183–190.

Walther, M., Ortner, A., Meier, H., Löffelmann, U., Smith, P. J., Korvink, J. G.: Terahertz metamaterials fabricated by inkjet printing, Applied Physics Letters 95(2009)25, 251107, 3 p.

Ward, N.: A primer on inkjet presses, Printing Impressions 53(2010)3, 32, 34–35.

Washburn, E. W.: The Dynamics of Capillary Flow, Physical Review 17(1921)3, 273–283.

Wedin, P., Svanholm, E., Alberius, P. C. A., Fogden, A.: Surfactant-Templated Mesoporous Silica as a Pigment in Inkjet Paper Coatings, Journal of Pulp and Paper Science 32(2006)1, 32–37.

Yip, K. L., Lubinsky, A. R., Perchak, D. R, Ng, K. C.: Measurement and Modeling of Drop Absorption Time for Various Ink-receiver Systems, Journal of Imaging Science and Technology 47(2003)5, 388–393.

Young, T.: An Essay on the Cohesion of Fluids, Philosophical transactions of the Royal Society of London, 1805.

PAPER I

Inkjet print quality: the role of polyvinyl alcohol in speciality CaCO$_3$ coatings

Inkjet Print Quality: The Role of Polyvinyl Alcohol in Speciality CaCO$_3$ Coatings

T. LAMMINMÄKI, J.P. KETTLE, P. PUUKKO, P.A.C. GANE and C. RIDGWAY

The aim of this work is to clarify the controlling role of polyvinyl alcohol (PVOH) as a binder in the formation of coating and pore structure and how it affects the high-speed inkjet image quality formation. The results show that the pigment type and the binder amount have a large interactive effect on pore structure formation. The studied PVOH can transfer into the intra-particle pores of pigments, and the swelling of PVOH closes up the pores which have diameters of ~30 nm, but this depends on the amount of binder used. The optical properties of the whole paper, not just the coating, are the most important regarding print density, but the properties of the coating layer itself have a dominant effect when considering the ink bleeding.

L'objectif de cet ouvrage est de clarifier le rôle de régulateur que joue l'alcool polyvinylique (PVOH) comme liant dans la formation du couchage et la structure des pores, et de démontrer comment elle affecte la qualité de la formation de l'image à jet d'encre à haute vitesse. Les résultats démontrent que la sorte de pigment et la quantité de liant ont un impact interactif important sur la formation de la structure des pores. L'alcool polyvinylique étudié peut se transférer à l'intérieur des pores de pigments intra-particulaires, et son gonflement resserre les pores ayant un diamètre de ~30 nm. Cependant, ceci dépend toujours de la quantité de liant utilisée. Les propriétés optiques du papier entier, et non seulement le couchage, sont les facteurs les plus importants en ce qui a trait à la densité d'impression, mais les propriétés de la couche de couchage ont un impact dominant relativement aux bavures de l'encre.

INTRODUCTION

There is an increasing trend for the use of aqueous-based inkjet inks in high-speed commercial printing, and this challenges the hydrophilic and absorptive properties of the surface of paper [1]. There is an urgent need to develop the coating layer properties based on the mechanisms which control these properties

T. Lamminmäki, J. Kettle and
P. Puukko
    VTT Tech. Res. Centre Finland
    P.O. Box 1000
    FIN-02044 VTT, Finland
    (taina.lamminmaki@vtt.fi)
P.A.C. Gane
    TKK, Vuorimiehentie 2,
    FIN-01250 Espoo, FINLAND,
    and OMYA Development AG
    CH-4665 Oftringen
    Switzerland
C. Ridgway
    OMYA Development AG
    CH-4665 Oftringen
    Switzerland

in inkjet printing, and the interaction of pigment and typical inkjet paper coating formulation binders, in determining coating pore structure, is an area that has received insufficient attention in this respect.

The absorption speed and volume of the ink diluent/solvent challenge the capacity of the paper surface to generate acceptable inkjet print quality. The water-solvent should absorb very rapidly into the paper. The applied ink droplets should not mix together on the surface or intermingle in the structure of the sheet. Ink droplet setting is a phenomenon that happens on a millisecond scale, but the final ink drying can take hours [2]. The amount of applied solvent can be very high, so the paper needs a high porosity to get all of the water-solvent into the paper structure. Even in emerging systems where the volume of diluent is strictly controlled, the rate of absorption still plays a decisive role.

The absorption volume and speed is commonly explained adopting the Lucas-Washburn equation. According to Lucas-Washburn's equilibrium equation, the volume of liquid in a capillary should be greater, the larger the radius, at a given time. On the other hand, the practical studies have shown that smaller radius capillaries initially fill faster than larger capillaries. Ink sets faster on a fine pore structure coating layer than on a highly porous, large pore containing coated paper. This disagrees with the model of Lucas-Washburn. Clearly, there is a distinction between fine and large pores and furthermore, there are effects occurring on the short timescale on the surface and in the pore network as well as in a single and several interconnected capillaries that Lucas-Washburn does not capture [3-5].

Ridgway et al. [3] further studied the Lucas-Washburn equation. They showed that there are a number of more detailed descriptions of flow entry effects into capillaries, such as the energy loss equation of Szekely [5]. Bosanquet [6] added the inertial wetting term associated with an accelerating fluid. A solution of the equation of Bosanquet for short times is proposed by Schoelkopf et al. [7],

which showed that liquid penetration distance by absorption into the finest capillaries over short timescales has a direct proportionality to the time elapsed. When inertia dominates, the finest pores will absorb further and faster. Furthermore, if we consider a network of such fine pores, remembering that a fine pore in coatings is typically equally as short as its diameter is wide, then in combination with enough reservoir volume between them, we can visualize a preferred pathway effectively by-passing the larger pores or at least limiting the access to them. This has been constructed by Ridgway et al. [8] using the Pore-Cor visualization (Pore-Cor and Pore-Comp are a software network model and a sample compression model, respectively, developed at the University of Plymouth, Plymouth, UK). In this pathway, the velocity of absorption is high, and so the passage into the porous medium is defined by the combination of pore sizes within the inertial wetting regime (nanopores) and the connecting reservoir structure consisting of larger pores which fill more slowly. Therefore, we can assume that small pores are needed for quick inkjet ink penetration at the moment of droplet setting and large pores are needed for the storage of all the solvents into the structure. The connectivity relation between these is crucial if the maximum absorption rate for large volumes is to be maintained.

In coating colours, we have, besides the pigments with their particle packing characteristics and internal pore structure, if present, the binder. By changing binder amount or binder type we can influence the inkjet ink penetration. Primarily, the binder amount should be sufficient enough to ensure that the coating colour has adequate adhesion to the paper surface and cohesion so that dusting problems are minimal. The surface strength is not needed at such high levels as in traditional offset printing, but nonetheless dust generation is critical, as it could lead to blockage or damage of the inkjet nozzles, and so diminish the print quality and reduce the lifetime of expensive print engine components. In coating colours for inkjet papers, polyvinyl alcohol (PVOH) is a very commonly used binder, and it has a high capability to bind pigments. It is also a very hydrophilic binder, and exhibits swelling on contact with water [9-11]. Pinto et al. [11] showed in their study that ink diffusion is unrestrained by PVOH, and the colorant concentration profile is uniform in a PVOH layer as shown by time-of-flight secondary ion mass spectrometry (TOF-SIMS) analysis. Lately, the binder type has been shown to have an effect on the inkjet ink print density and bleeding development, Nilsson [12] and Svanholm [13]. However, the binder swelling tendency in the inkjet print quality formation of Versamark VX5000e has not been studied so widely.

The aim of this work is to clarify:

– the role of PVOH as a swelling binder in the porous $CaCO_3$ coating layer structure,

– the role of porosity and pore diameters in the inkjet ink setting process, and

– how the PVOH coatings work in the print quality formation of dye-based inks in high-speed inkjet printing.

MATERIALS AND METHODS
Coating Compositions and Coating Trials

A range of calcium carbonate-based pigments provided by Omya AG, Oftringen, Switzerland and one $CaCO_3$ pigment from Minerals Technology Europe, Zaventem, Netherlands were used. The main idea behind this pigment selection was to vary the mean particle diameter and specific surface area of the pigments (Table 1). The binder in the coating colours was polyvinyl alcohol (PVOH, Mowiol 40-88 provided by Clariant International AG, Muttenz, Switzerland). The selected PVOH had a degree of hydrolysis 87.7 ± 1.0% and a molecular weight of 204 000 g·mol^{-1} [14].

The study was started by looking at the properties of pure pigments. Pigment cakes and 100 g·m^{-2} coating layers on glass plates were produced from a range of formulations. The cakes were made with Teflon moulds, drying them at 23°C. The glass plates were coated with an Erichsen film applicator (Model 288, Hemer, Germany) using blades with a fixed gap height between 100 and 500 µm. All the pigments had been dispersed by the pigment manufacturers themselves.

The pigment properties are shown in Table 1. The choice of pigments was made to illustrate the effects of particle size and internal pore structure, including raw material sources from ground calcium carbonate (GCC), subsequently modified to generate high surface area and internal pores (MCC), and precipitated calcium carbonate (PCC). The pigment diameters were determined by sedimentation (Sedigraph 1500, Micromeritics, Norcross, GA, USA) or by laser light scattering (NanoSight, Amesbury, UK) and the values given are quoted from the specifications of the manufacturers. The pH and zeta-potential (AcoustoSizer II, Colloidal Dynamics/Agilent Technologies, Espoo, Finland) were determined in the coating colour, which in this case contained 10 pph PVOH (based on 100 pph by weight pigment). We note that all but one of the pigments exhibit a cationic slurry property, being designed to adsorb anionic ink dye so as to prevent strike through and to maximize print density by concentrating the colorant near the coating surface. Coulombic interaction also acts to maintain water fastness of the ink.

The liquid uptake capacity of the porous structures was measured with Si-oil absorption. During the oil absorption, the pigment cake was left for one hour in Si-oil, and the weight of cake before and after Si-oil saturation was measured. The available porosity for oil absorption is determined at normal air pressure and is defined as absorbed Si-oil volume in the coating cake, divided by the sum of the coating layer volume without oil, plus the absorbed Si-oil volume.

The pore volume and pore size distribution was measured with mercury porosimetry (Micrometrics AutoPore IV), adopting the Pore-Comp correction to account for penetrometer expansion, mercury compression and compression of the sample skeletal

	TABLE I				
	PIGMENT PROPERTIES				
Properties	Ground calcium carbonate - GCC	Modified calcium carbonate - "MCC large"	Modified calcium carbonate - "MCC small"	Precipitated calcium carbonate - "PCC large"	Precipitated calcium carbonate - "PCC small"
Weight median pigment particle diameter, µm ($d_{50\%}$,)	0.65	2.70	1.30	2.70	Small 0.02-0.03 Av. 0.25 *)
Specific surface area, m²g^{-1} (BET, ISO 9277)	10.7	46.2	27.0	63.7	73.9
Zeta-potential, mV (AcoustoSizer II)	-9	13.1	13.6	1.6	-0.6
Registered trade name	HYDROCARB 90	OMYAJET B6606	OMYAJET C3301	OMYAJET B5260	JetCoat 30
*) NanoSight (results had two peaks: small at 20-30 nm and average at 0.25 µm)					

I/2

Pigment/Binder	Colour 1	Colour 2	Colour 3	Colour 4
TABLE II **THE TOP COATING COLOURS**				
"PCC large"	100	100	100	
"PCC small"				100
PVOH	7	12	30	7
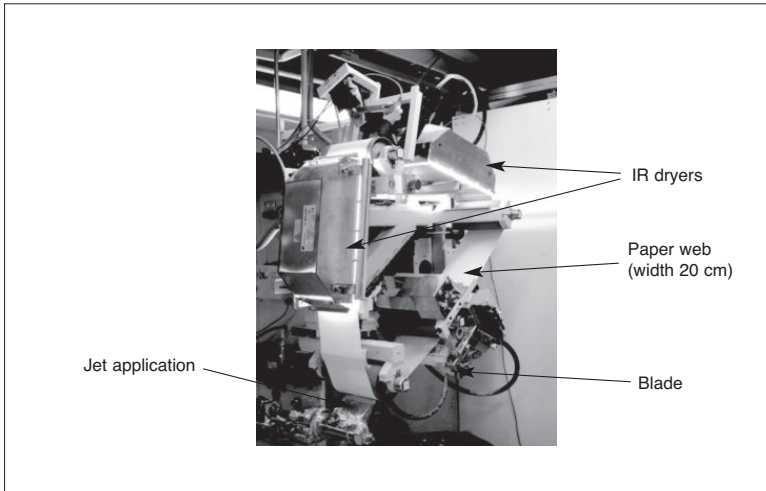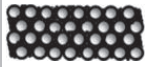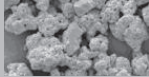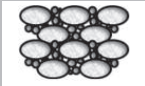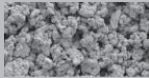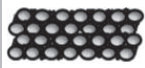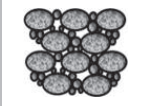
Fig. 1. Image of KCL SAUKKO [16].

TABLE III
THE STRUCTURAL ILLUSTRATION OF COATING LAYERS AFTER THE SAUKKO COATING.
ALL COATINGS HAD 10 PPH PVOH

Pigment	Air permeance, $\mu m.(Pa.s)^{-1}$	Porosity (coating cakes),%	Structure of pigment	Illustrated coating layer structure
GCC	0.1	17.7	Rhombohedral	
"MCC large"	1.3	46.2	"Roses"	
"MCC small"	0.7	31.9	"Roses"	
"PCC large"	1.8	48.9	"Eggs"	
"PCC small"	2.3	32.9	Spherical	

material, expressed as the elastic bulk modulus, according to Gane et al. [15]. The coatings, with their different binder amounts were analyzed up to 140 Pa (low pressure port) and 440 Pa (high pressure port), respectively. The coated glass plates were analyzed by the thin layer chromatography method (TLC), putting the plate into the eluent (equivalent to either the ink diluent alone or the whole ink, depending on volume or chromatographic separation analysis). The distance of eluent movement during time was measured. The optical properties of the coating layer were studied as a function of eluent uptake and distance, e.g., opacity according to ISO 2471:2008. Behind the coated glass plate a stock of blotting boards (fully bleached) was used as backing.

The KCL pilot coater was used to apply coatings on a larger scale to traditional base paper, which was chosen to be a commercial base sheet for a coated fine paper, 53 g·m⁻². The base paper was first pre-coated so that the top coating of main interest was prevented from penetrating into the base paper. The pre-coating of 7 g·m⁻² was applied with a film coater on both sides of the paper, and the actual studied coating layer of 8 g·m⁻² with short dwell application (blade). The pre-coating had 100 pph of GCC (Hydrocarb 60), 12 pph styrene-butadiene latex and 0.6 pph carboxymethylcellulose. The recipes of the top coating are introduced in Table 2. The coating speed was 1800 m·min⁻¹ and the final moisture content of the coated web was 5 wt%.

The role of pigment properties alone in the inkjet ink setting process was also studied, so as to subsequently identify the interactive roles of pigment and binder combined. In this case the coating was applied with a semi-pilot coater, KCL SAUKKO (Fig. 1), using jet application and blade. The coating was dried with two infra red dryers. The speed of the web was 900 m·min⁻¹. The same base paper was used as in the pilot coating. Based on the pilot-trials the binder amount was selected to be 10 pph of PVOH (Mowiol 40-88) to represent commercially acceptable strength and anti-dusting properties. The structural illustrations of produced coatings are given in Table 3. The target coating layer amount of 10 g·m⁻² was not achieved in one single coating layer. The low solids content and the low viscosity of the coating colours limited the applied coating layer thickness, and therefore we had to apply the same coating colour twice.

The air permeance of coated papers was measured with Parker-Print Surf measurement using 20 kPa pressure. The opacity was measured according to the standard ISO2471:2008 and light scattering coefficient ISO 9416. The surface strength of coated papers was studied with an IGT device using ISO 3783 with medium viscosity oil. The absorption time of dye was measured with DIGAT that has been introduced and described in detail in the literature [17]. The ink was anionic dye-based

I/3

ink (from a Versamark VX5000e) and the applied ink amount was 8 g·m^{-2}. The surface structure of the coating layer was imaged with the scanning electronic microscope (SEM).

Inkjet Printed Surfaces

Inkjet printing was carried out on a Versamark VX5000e, which produces inkjet droplets by the continuous stream inkjet method. The inks were dye-base and the main diluent/solvent was water. The surface tensions of the inks were observed to fall in the small range of 51-55 mN·m^{-1} (25°C), depending on dye colour, and the viscosity was 1-2 mPa·s. Printing speed was 100 m·min^{-1} and the drying drum and hot air dryer were set to a temperature of 80°C (when studying pigment type to emphasise absorption criteria) and 100°C (when studying the range of binder amount to provide runnability at the highest binder level).

The print density of the printed surface was measured with GretagMacbeth D196. Both a camera and scanner systems were utilized to analyze the bleeding, in terms of distance from the formal colour boundary. The parallel reporting from the two systems was also a part of the development of the scanner method. In the camera system, a picture was taken with an imaging camera from a solid printed line used to define the bleeding boundary, and a grey level profile across the line was constructed. The normal edge width for the given print was measured as the distance between two points A and B. Point A was defined as the point at which the surface across the line image was 10% brighter than the darkest region in the line and B, 10% darker than a given background. The black surface had grey value zero and white 254. Each unprinted paper was adjusted to the value 170. The normal edge width described the bleeding distance of inks. The smaller the number, the sharper is the printed line. In the scanner system, an Epson Perfection V700 Photo was used, with a resolution of 2400 dpi. The grey level profile of the line was again measured with an image analysis program using a similar definition of the points A and B, but now A was 15% brighter than the darkest region and B, 15 % darker than a background. The grey levels were adjusted as in the previous camera system. The differences in the optics caused some differences in the results between these methods. Mottling was analyzed with a scanner system. The printed surface was scanned with an Epson Expression 1680 Pro scanner using a resolution of 300 dpi. The scanned figure was handled with a wavelet transform (PapEye program). The ink colorant penetration was studied by embedding the printed surface in LRWhite resin (Electron Microscopy Sciences, Hatfield, PA, USA). The embedded sample was placed in a refrigerator to reduce smearing of the dye. The cross-sections were then imaged in a light microscope (Zeiss Axioskope 2 plus).

RESULTS

PVOH and Porosity Formation of the Coating Layer

The intrinsic structure of the coating layer, without the influence of the base paper, was studied using the coating cake material. At this point, we have to remember that the structure of the coating cake, formed by drying a relatively large volume of coating colour, could be expected to be somewhat different to that of the structure of a thinly applied coating layer on a paper surface, where the coating process variables affect the forming structure, including differences in shrinkage behaviour. This issue has been resolved to some extent by the development of a pigment tablet formation device at Omya AG [7], however this was not used in this work as the PVOH binder is soluble, and filtration might have led to an unwanted depletion of binder. In this current work, however, we saw that the differences were in fact minimal between the measurements on the
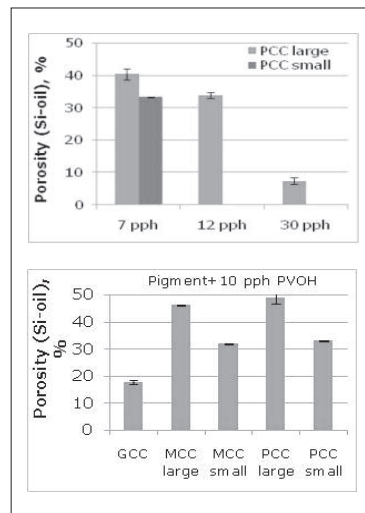
Fig. 2. Absorption capacity of pigment cakes as a function of PVOH binder level, measured by the Si-oil absorption method.

Fig. 3. The cumulative pore volume distributed as a function of pore size, as measured using mercury porosmietry.

coated papers and the coating cakes.

The absorption capacity of the coating cakes was analyzed with Si-oil absorption (Fig. 2). As expected, increasing the binder amount reduced the level of porosity as measured by this technique. At the binder level 10 pph, the porosities of fine particulate "MCC small" and "PCC small" pigments were found to be on the same level. The highest porosities were produced by the large particle size coatings. This illustrates the likely particle packing characteristics.

The porosities of the coating layers were also calculated from mercury porosimetry results, when the base paper effect and the amount of coating layer are taken into account, following the method of Ridgway et al. [18]. The cumulative intruded pore volumes of the coating layers are illustrated in Fig. 3. The "PCC large" coating produced again the greatest pore volume, and it had more large size pores. The lowest porosities were seen for GCC and "MCC small".

The results of Si-oil porosity and mercury porosimeter measurements correlate very well (Fig. 4). The slight differences can be analyzed in respect to the high pressures used in the mercury measurement. At the final stages of mercury intrusion, the pressures are sufficiently high to compress any elastic components present as part of the skeletal structure of the porous material. Polymers, in particular

Fig. 4. Correlation between the results of Si-oil porosity and mercury porosimeter.

I/4

binder, undergo such compressive effects. The result is an absence of hysteresis between the intrusion and extrusion curves as a function of pressure increase and decrease, respectively. The gradient of this elastic region can be determined and related to a bulk modulus expressing the volume compressibility of the material, Gane et al. [15]. The bulk modulus of the paper coating, based on "PCC large" with 10 pph PVOH, was 30.6×10^3 MPa and based on "PCC small", also with 10 pph PVOH, was 22.0×10^3 MPa. This means that the "PCC large" paper can resist pressure on the skeletal components more so than "PCC small" paper. This reflects the distribution of polymer in respect to the pigment particle packing and the pore sizes present. The finer pigment, with its higher surface area, will necessarily present more polymer species and amount, including dispersant, to the coating colour.

The pigment cakes made from "MCC small" and "PCC small" with binder had very similar Si-oil absorption volume capacities, as seen in Fig. 4, but exhibited very different porosity values when analyzed with the mercury porosimeter. This lets us deduce, that binder tends to blank off the entry to, or connectivity between, pores. Thus, the oil cannot access all the pore volume, whereas the intruding mercury can break through the pore-blanking binder films. This effect is confirmed by the equivalence between the two methods for the pigment cakes without PVOH, in which both techniques access the same pore volumes (Fig. 5).

Traditionally, taking the first derivative of the cumulative mercury intrusion curves provides a pore size distribution. This description, although limited to an equivalent bundle of capillaries, and thus ignoring pore shielding effects, is nonetheless useful for comparison purposes between topologically different structures, Gane et al. [19]. We see that the PCC coating structure has only ultrafine pores in the 20-60 nm range (Fig. 5). In contrast, the MCC coatings have both large- and small-size pores, indicating that the MCC structures have both intra- and inter-particle pores. The addition of 10 pph PVOH decreases the pore volume of the MCC coating structure more than that of PCC. The peak of intra-particle pores of the MCC pigment decreases most markedly, clearly indicating that PVOH has filled intra-particle pores.
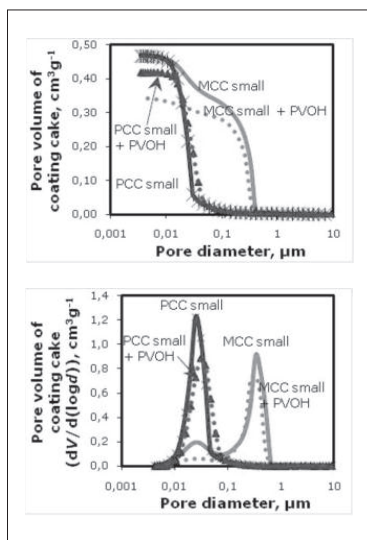
Effect of Pigment Properties on Internal Liquid Transport

The thin layer chromatography method was used to analyze the eluent movement through the pore networks of the pure pigment packing structures. Long-time passage of liquid through a porous network is defined by the surface wetting force resisted inversely by the permeability of the structure. The greater the permeability and the more the occurrence of fine pore structure surrounding that permeable pathway, the greater will be the transport length in a given time. The longest water/ethanol eluent transport distance through the structure was achieved with the most porous pigments (Fig. 6). The "MCC large" and "PCC large" pigments have very similar size and amount of intra-pigment pores, but MCC has smaller inter-particle pores and so less large pores to contribute to permeability, as Fig. 12 later shows. The GCC and "MCC small" coatings have quite similar capability to transport eluent. The distances are short because of the lack of permeability. The "PCC small" pigment unexpectedly transfers the liquid further in the structure than the other pigments. This would not be expected when looking purely at the fine pore structure, but the sample structures made from the "PCC

small" pigment had a multitude of cracks, which contribute to the permeable transfer of eluent effectively in the pigment layer. This effect is not one of intrinsic particle packing, but the response to shrinkage as the layer forms. These cracks are seen as essential if this pigment is to work in transporting liquid. The results indicate that pigments with higher pore volume transfer liquid more effectively than the lower pore volume structures depending on permeability.

Coating Layer Structure on Paper Surface
Role of Binder

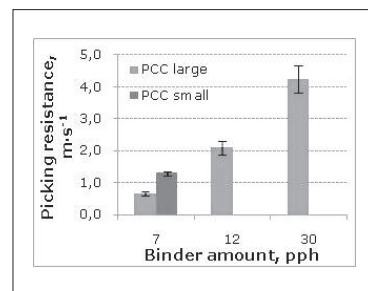The higher binder amount increased the surface strength of the coated papers (Fig. 7).

Fig. 7. Surface strength of coated papers measured with the IGT pick test method.

At a binder amount of 7 pph, the "PCC small" had a slightly higher surface strength then "PCC large". Once again, this is due to the difference in interior structure permeability determining the level of binder depletion likely to occur when applied to an absorbent substrate. The surface strength of 2 m·s⁻¹, defined as the speed at which the tack oil begins to induce pick from the coated paper in the test nip, is considered high enough to ensure attachment of the coating to the paper substrate and to prevent dusting during the inkjet printing.
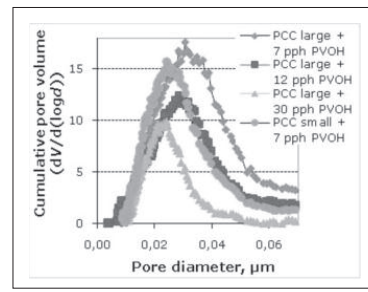
Fig. 5. Cumulative pore volume and pore size distribution curves of "MCC small" and "PCC small".

Fig. 6. Water/ethanol eluent (50%/50%) transfer over time in the thin layer pigment chromatography layers formed on glass plates without binder.

Fig. 8. The first derivative of the cumulative mercury intrusion curves (Pascal porosimeter) illustrating the effect of the binder level.
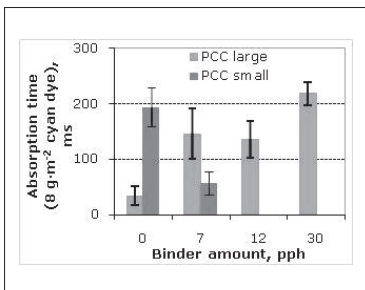
Fig. 9. Effect of binder amount on absorption time (DIGAT) for PCC coatings on glass plate.

Figure 8 shows how the binder amount increase decreases most of all the volume associated with the 30-50 nm size pores within the pore diameter area 0-0.1 μm, primarily responsible for the capillary driven absorption.

The absorption speed into the thin layer coatings on glass using the DIGAT apparatus became slower as the binder amount increased (Fig. 9). It was based on surface strength versus ink absorption speed results, that the PVOH amount of 10 pph was selected for our studies of different CaCO$_3$ pigments.

The binder amount had very minimal effect on print density in the case of the "PCC large" structures (Fig. 10). However, the pigment change from "PCC large" to "PCC small" at a binder amount of 7 pph clearly increased the print density. Therefore, at these binder levels and at these short absorption times, the binder swelling is unlikely to close the larger pores. The "PCC large" structure determines the colorant transport on this case.
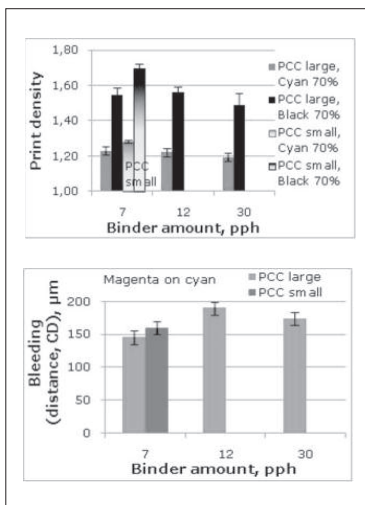
Fig. 10. Print density (measured from 70% halftone dot field) and bleeding distance of dye-based ink printed on PCC surfaces as a function of PVOH content.

A higher amount of binder generated a significant increase in the amount of bleeding. The coatings with 12 pph and 30 pph of PVOH produced the widest bleeding distance (Fig. 10). Interestingly, the bleeding did not increase indefinitely as the binder amount increased, but rather plateaued, showing the loss of pore volume is likely to be countered by the swelling nature of the PVOH in its ability to absorb and hold liquid once sufficient PVOH is present. The other explanation can be in the ink amount. The ink amount could be so low in
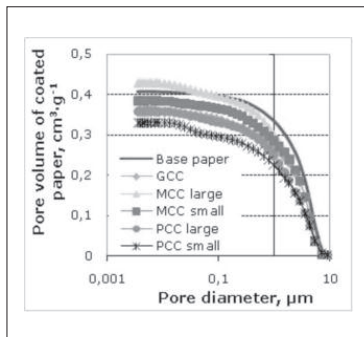
Fig. 11. The cumulative mercury intruded pore volume of coated papers. All coatings had 10 pph of PVOH.
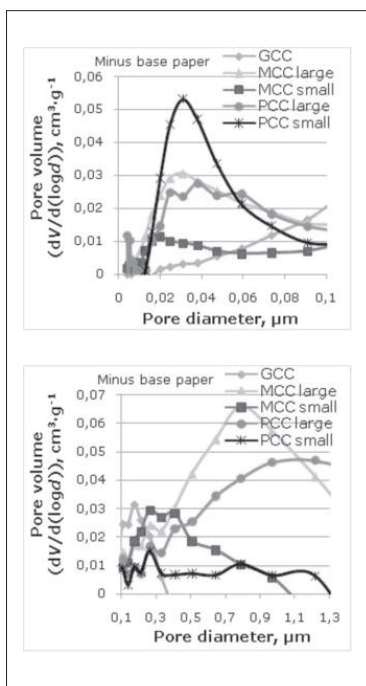
Fig. 12. The pore size distribution curves from mercury porosimetry of studied coated papers. The base paper values have been subtracted from the results. The coatings have 10 pph PVOH.

the printing that the absorption time of 220 ms can still be short enough to prevent the onset of bleeding. The effect of time delays will be discussed later.

Effect of Pigment Variables

Figure 11 shows the cumulative pore volume intrusion by mercury of the coated papers which had been produced with five different pigments. The coating layers have partly penetrated into the base paper structure. All of the coated papers have lower pore volume results in the area of 1-10 μm than the base paper before coating.

The pore size distributions of the studied coatings are illustrated in Fig. 12. Generally, the pore size distributions of the coatings on paper reflected the main features of those of the cakes and of the thin layer chromatographic slides. "MCC large", "PCC large" and "PCC small" coatings have small pores, 20-40 nm in diameter, whereas GCC and "MCC small" had clearly less of such small pores. The coatings with the two large 2.7 μm diameter pigments ("MCC large" and "PCC large") had the same amount of small-scale pores. The GCC coating
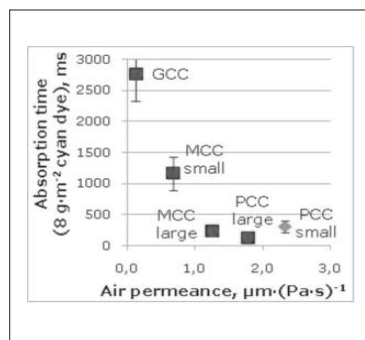
Fig. 13. Effect of air permeance on absorption speed (DIGAT).

had mainly 0.1-0.3 μm diameter pores and "PCC large" had the largest diameter pores, 1.0-1.3 μm. "MCC large" and "PCC large" had both small and large-scale pores. "PCC small" coating had mainly only small-scale pores.

The absorption speed into the coated papers was quickest with "PCC large", with the three pigments "MCC large", "PCC large" and "PCC small" all absorbing within the high speed range. The slowest absorption was, as to be expected, with GCC (Fig. 13). The relative requirements of capillarity and permeability are well reflected in these data. The capillarity is provided by the ultrafine pores and the liquid transfer by the permeability of the coating layer, Ridgway and Gane [20].

The highest print density (Fig. 14) was achieved with the coating structure on paper derived from "PCC small", and the lowest
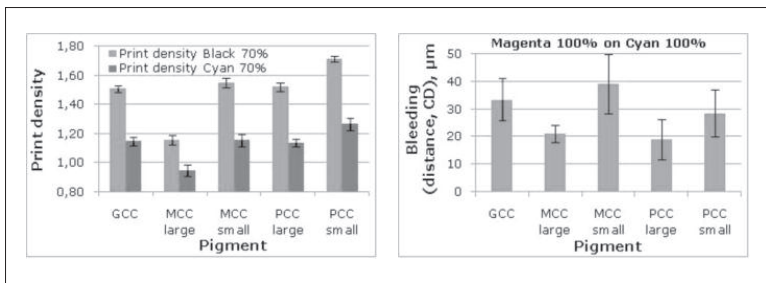
Fig. 14. Effect of coating pigment type on print density and bleeding (distance, measured with camera system) of dyes.

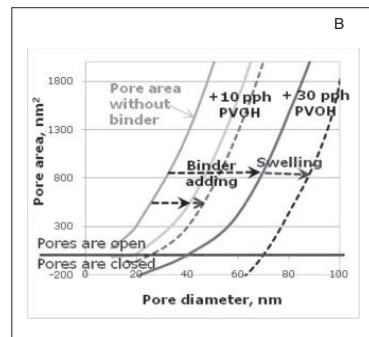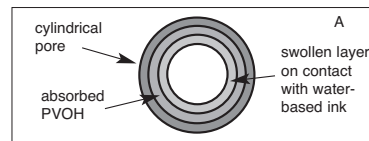**Fig. 16. The theoretical calculation of PVOH swelling effects. The coating amount was 1 g and density of PVOH 1.26 g·cm⁻³. The swelling of PVOH film was 29.2 % after 5 s (cyan dye). Specific surface area of pigment 10 m²·g⁻¹.**

from "MCC large". At the same time, "MCC large" and "PCC large" coatings produced the lowest bleeding values.

DISCUSSION

Role of PVOH Swelling

We can assume, on the basis of mercury porosimetry results, that PVOH binder can go into or cap (film over the entry) intra- as well as the connecting pores, and exists around the larger inter-particle pores as Boisvert et al. [21] and Wedin et al. [22] assumed in their studies. At sufficiently high levels, any interaction of the binder with the liquid phase of the ink becomes important, not only in the structural modification of pore volume but in the diffusion of liquid through the polymer network, effecting swelling in the case of PVOH.

We made a theoretical calculation about the binder swelling effect within the pores. Firstly, we assumed that the binder forms a uniform layer on the pore wall (Fig. 16A) and the thickness of this layer depends on the specific surface area of the pigment (thicker binder film at lower specific surface). The geometry of the pore is also assumed to be simple, as that the binder forms a uniform
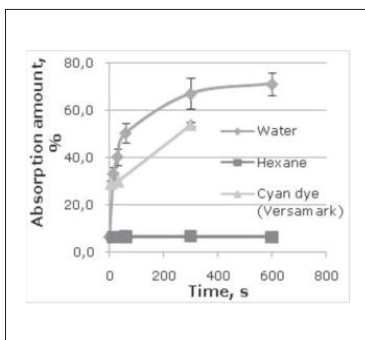
Fig 15. Absorption amount of PVOH films as a function of time. Assuming that the specific gravity of water = 1 and PVOH = 1.26. The swelling factor is given by absorption amount. Absorption amount = 100 * (mass of liquid absorbed into the film/mass of dry binder).

layer on the interior surface of a circular equivalent capillary. In this way, we can calculate how the pore entrance area changes during the binder swelling process.

PVOH is a hydrophilic binder [10,11]. Figure 15 illustrates how a PVOH film (200-250 μm) absorbs water but not non-polar hexane as a function of time. The PVOH film exhibited a 29.2% swelling when exposed to cyan dye-based ink (Versamark VX5000e) after 5 s, and this value has been used in our calculations.

The results of the calculation are illustrated in Fig. 16. The pore volume and amount of binder represent what is to be found in 1 g of coating structure, as taken from mercury porosimetry and the coating formulation, respectively. The first line on the left is the pore area when the structure has been formed from pigments alone. The addition of 10 pph binder into the coating results in pore diameters being reduced by the absorbed layer of PVOH by an amount of 13 nm when the PVOH is dry - this being twice the absorbed thickness to describe diameter loss in a cylindrical pore. The closing point of pore diameter increases to 24 nm when the binder swelling found to be 29.2 % occurs on contact with inkjet ink. This can lead to complete blocking of the finest pores, reduction in pore size in general and loss of connectivity in the structure when the binder is concentrated at pore nodes. The higher the amount of binder the thicker the binder film is, and thus the effect of swelling also increases. It seems that the swelling affects most or nearly all of the intra-particle pores. This means that these pores are effectively acting purely via a binder-swelling liquid uptake mechanism.

So in theory, the binder swelling can affect the absorption speed of inkjet inks through the closing up of small pores. Table 4 shows the extent of the time delays that exist in the inkjet printing machine. At 100 m·min⁻¹, the delay between the first inkjet nozzles to the beginning of drying is 2.6 s, and to the end of drying, 3.8 s. The 5 s time considered in binder swelling is within this same timescale. The effect of swelling diminishes when liquid has less time to affect the binder and therefore we can assume that swelling has a smaller role at higher printing speeds, but it will not totally disappear. Thus, diffusion into polymer networks can occur within the timescale of inkjet printing, even at high speeds.

How Does PVOH Work with Different Types of Calcium Carbonates?

From the optical point of view, "PCC small" pigment particles are so fine that they cannot scatter light effectively and in that sense, the pigment is optically inactive (Fig. 17). According to the theory of Kubelka-Munk [23], those particles which have a diameter of

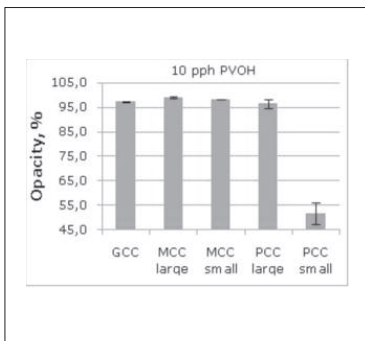| TABLE IV		
TIME DELAYS IN THE VERSAMARK VX5000E PRINTING PRESS		
	Speed 15 m·min⁻¹	Speed 100 m·min⁻¹
Cyan to yellow (CMKY)	5 s	0.8 s
Yellow to drying beginning	12 s	1.8 s
Drying beginning to end	8 s	1.2 s
SUMMARY	25 s	3.8 s

Fig. 17. Opacity of coating layers on the glass plate (100 g·m⁻²).

the order of the wavelength of light (0.1-1 µm) affect strongly the light scattering. The opacity and light scattering coefficient of the "PCC small" coating layer remains lower because the pigment size is so small, 20-30 nm. The results agree with other previous results [24,25]. The other pigments had quite similar opacities on glass plates.

The optical properties of the whole coated paper dominate the print density formation. The "PCC small" is virtually optically inert (Fig. 18), whereas the other pigments strongly affect the light scattering and therefore the level of print density. The correlation between the pore volume of the whole paper and print density was in the range of -0.904 – -0.949, whereas correlation between the pore volume of the coating layer alone and print density was as low as -0.050 – -0.217. Therefore, the whole paper structure plays a role in generating the print density, not only the coating layer. This of course depends on the nature of the base paper, but if optically interactive it will contribute to the background light white noise and so reduce print density, especially of penetrated dye-based inks.

If we consider the case of pigment-based inks found in many new high-speed inkjet devices, the finer intra-particle pores will selectively exclude the ink pigments, in a
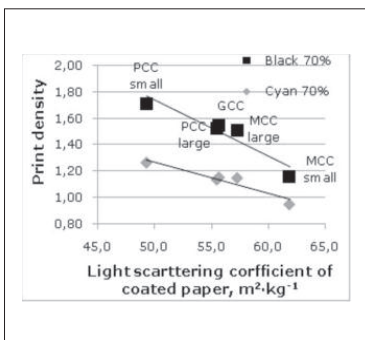
Fig. 18. Effect of light scattering coefficient on print density. Correlation: black -0.943 and cyan -0.950.

GCC

MCC large

MCC small

PCC small   20 µm
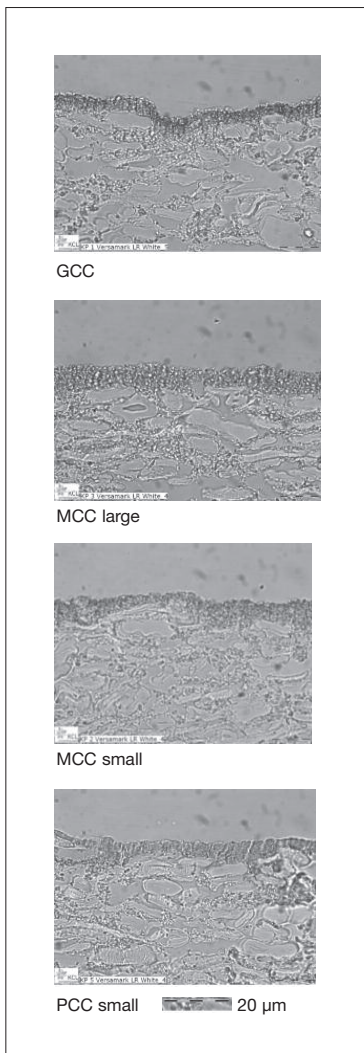
Fig. 19. Cross-section dye-base ink printed surfaces.

such a way that the colorant will be more concentrated in the remaining permeable structure between the particles, i.e., in the inter-particle pores. Therefore, depending on the amount of PVOH present, and whether it fills just the intra-particle pores or also the inter-particle pores, we can expect either a greater transfer of ink pigment into the underlying base paper or a better ink pigment holdout, respectively, i.e., to achieve good ink pigment holdout, the permeability has to be reduced. The ink pigments form a filter cake in the more closed case and this leads to reduced permeability. Therefore, the properties of the whole paper structure will have either a major or minor role in determining print density depending on the level of permeability.

In these experiments, where speciality

coating was applied to a pre-coated paper, the colorants stay in the coating layers and do not penetrate into the base paper (Fig. 19). However, it seems that the colorant is quite uniformly distributed in the coating layer including "MCC large". Even the cationic nature of the "MCC large" pigment did not fix the colorants in a manner that was visibly differently from the anionic pre-coat GCC. This suggests that either (i) the surface area is insufficient to trap all the colorant, (ii) the ink does not encounter the cationic nature of the pigment, or (iii) the coating is too permeable to provide surface contact for all the colorant as it flows through the structure. There is some slight detectable concentration gradient for the finer pigments, and this reflects the reduced internal pore network permeability.

The cross-section in Fig. 20 is of a PVOH film absorbed with cyan ink. It shows that ink colorants have penetrated significantly into the binder film after 30 s absorption time, but not completely. Therefore, the colorants can be expected to diffuse into the PVOH layer together with the water. The result is in good agreement with the observations of Oka et al. [26] and Svanholm et al. [27]. In a coating structure, colorants are distributed quite uniformly through the coating layer. This could be an indication that PVOH has covered the pigments and colorants are predominantly
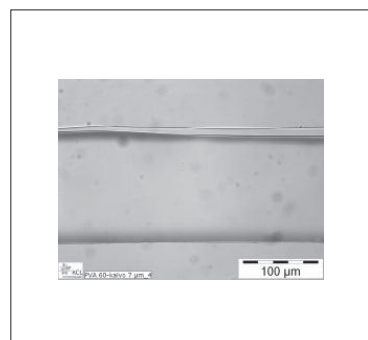

Fig. 20. Cross-section figure of cyan dye-based ink into PVOH film. About 200 µm thick film had sunk into the cyan ink during 30 s time.

in the PVOH. Therefore, the pigment type or charge has very minimal effect on colorant location when PVOH is used as binder.

The bleeding distance (Fig. 21), however, seems to be dependent on the pore volume of the coating layer, but not the pore volume of the whole paper. This confirms the lack of transfer of ink to the base paper for these coating layer configurations. Table 5 shows all the porosity related aspects of coating layer correlate well with bleeding. In addition, the increase of surface energy decreases the bleeding distance. If we consider comparing the results of bleeding measured with dye-
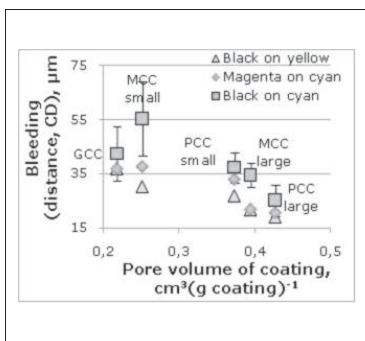
Fig. 21. Bleeding of the studied coated surfaces. Bleeding measured with high-resolution camera.

based inks versus pigment-based inks, the bleeding distances for pigment-based ink can often be considered to be less, because the filter cake formation effect of ink pigments prevents sub-surface lateral spread. However, we must recall that this depends strongly on the permeability characteristics of the coating and, hence, interaction with the base paper.

The large porosity "MCC large" and "PCC large" coatings had fine pores of similar amounts and sizes, but in the large-size area of the bimodal distribution (inter-particle pores), the "PCC large" has ~1.2 μm diameter pores whereas the "MCC large" has smaller inter-particle pores at 0.8 μm. The larger pores of PCC allow ink to penetrate more quickly into the coating structure and therefore the bleeding formed is less. In addition, the binder swelling influences more strongly in the MCC pigment coating than in the PCC. The thickness of binder layer is higher on the MCC coating because the specific surface area of pigment is lower.

The PVOH swelling phenomenon should have a strong effect on GCC and "MCC small" coatings, which have less of the ultrafine 20-60 nm diameter pores than the other pigments. As the "MCC small" does have some more of the smaller pores than GCC, so the swelling should affect mostly these pores, rendering them ineffective. The bleeding values are indeed quite similar.

Comparing the "MCC small" and "PCC small" coatings, the porosities are quite similar, but "PCC small" has more of the finest pores. The "MCC small" coating absorbs ink clearly slower than "PCC small". The binder swelling closes up pores during the ink absorption process. It seems that in our medium porosity area, the coating with smaller pores give less bleeding. This illustrates that the bleeding effect is surface absorption rapidity defined.

One aspect that we have not yet discussed is the web drying on the high-speed inkjet press. This accelerates the inkjet ink drying process and so affects the degree of ink penetration. However, we propose that a more important aspect of current dryers is in the web behaviour in and after the dryer when the rolled printed paper becomes unwound and exposed to the new environment. The print quality of the paper should remain high after the opening of its printed reel. Furthermore, if the ink has been insufficiently dried before the rewinding state, the ink can transfer onto the back side of the paper and the set-off problem can be expected to become more obvious.

Effect of Binder Amount

"PCC large" and "PCC small" pigments were studied more closely by using different PVOH amounts. All the print density results are very near each other (Fig. 22). The cross-section images from printed papers (Fig. 23)

indicate that the colorants of ink distribute within the coating layer at 7 pph PVOH and at these coat weights do not penetrate into the base paper. At 30 pph PVOH in the coating, colorants are concentrated more in the top layer of the coating. However, there are places where the colorants have moved into the base paper due to the cracks in the coating, and this
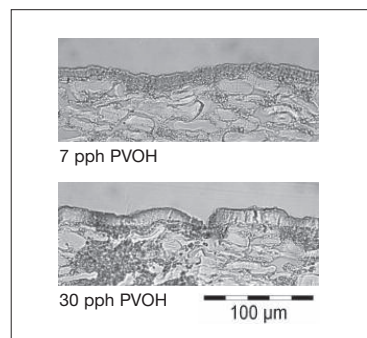

7 pph PVOH

30 pph PVOH

100 μm

Fig. 23. Cross-section images of coatings containing different amounts of PVOH, that have been printed with cyan dyes.

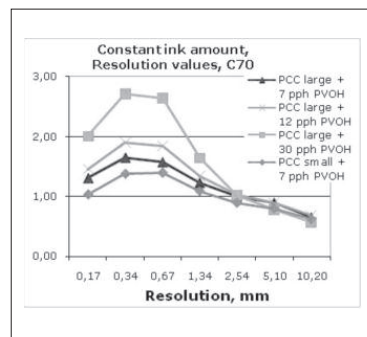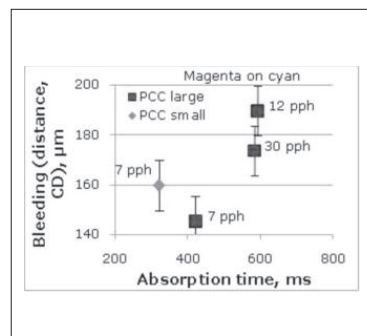**Fig. 24. Mottling of cyan ink (70% halftone dot area) printed surfaces.**

Fig. 22. Connections between print density and air permeance as a function of PVOH amount.

Fig. 25. Bleeding distance against absorption time. Measurement by scanner system and absorption time with DIGAT (8 g·m⁻² cyan dye).

TABLE V CORRELATIONS BETWEEN BLEEDING DISTANCES AND PORE STRUCTURE PROPERTIES			
Paper property	Bleeding distance		
	Magenta on cyan	Black on cyan	Black on yellow
Pore volume of coating layer	-0.898	-0.951	-0.943
Ink absorption speed (cyan)	0.653	0.745	0.994
Air permeance	-0.575	-0.786	-0.883
Surface energy of coated paper*	-0.653	-0.724	-0.978
Pore volume of whole paper	-0.210	0.063	-0.104
*Surface energy as defined by the sessile drop model, albeit a gross approximation for absorbent surfaces.			

decreases the print density as well as increases the small scale mottling values (Fig 24). The results of light scattering (S-coefficient 52.9-54.1 m^2kg^{-1}) from all the papers are very near each other. Therefore, knowing that the pigments have very different light scattering, the whole paper properties are dominant in this respect.

Again, the bleeding distance depends on the fine pore coating properties. Therefore, not unsurprisingly, the least bleeding distance is reached with the lowest binder content coating (Fig. 25). The higher binder amount increases the bleeding.

Figure 26 shows that absorption time gets longer when binder amount increases from 7 pph to 12 pph. However, the 30 pph of binder is on the same level as 12 pph. These results are similar to those of Nilsson et al. [12]. When the binder amount is lower the ink moves into the coating layer mainly by
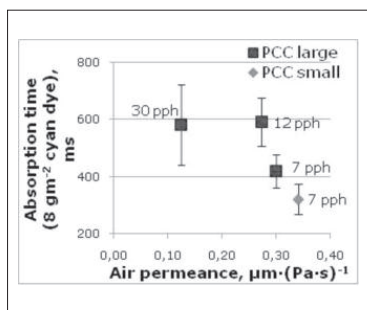
Fig. 26. Effect of PVOH amount in relation to air permeance and absorption time of cyan dye.

capillary flow. At 30 pph binder amount, smaller capillaries are already closed and the dominating liquid transfer mechanism is diffusion in the binder layer, as Gane et al. [28] indicate for their case of swelling polyacrylate dispersant covering the pigment surface. However, once a PVOH threshold amount is reached, specific for each pigment, this diffusion dominates and so provides a constant absorption speed from that binder level
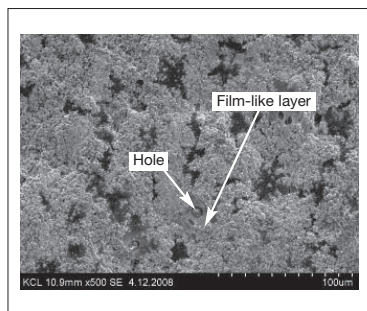
Fig. 27. Topographic image (SEM) of 30 pph PVOH "PCC large" pigment coating.

upwards (Fig. 26). The threshold point for the influence of binder swelling within these coatings should be expected at a binder amount of 12 pph.

Another significant problem with the 30 pph coating is the coating layer distribution. The SEM image (Fig. 27) shows that the 30 pph PVOH coating layer is not very uniform and there are places where the binder has formed film-like layers which exhibit significant clumping. As a result, holes distributed across the film-like layer can also be seen.

Although, the increase of PVOH amount closes up the coating structure, at higher amounts of PVOH the shrinkage associated with the soluble binder formulation causes an uneven coating layer structure and this is reflected in a deterioration of print quality.

CONCLUSIONS

The major controlling parameters for liquid ink absorption into porous inkjet coating structures are confirmed to be capillarity and permeability in relation to the fine pores and the larger interconnected pores, respectively. A quick absorption of ink can be reached even with medium porosity coating structures, provided the coating has a lot of nano-size pores. In the case of porous pigment particles, such as modified or structured calcium carbonate, the fine pores are associated with intra-particle pores and the larger pores are defined by the particle packing.

The role of PVOH binder is shown to be complex both in relation to pore structure modification and its affect on liquid uptake by diffusion. PVOH swells during the diffusion process. Although the volume of liquid imbibition related to PVOH swelling can be small at low binder levels, it acts to dominate the ink interaction with the pigment surface and the fine pore structure as binder levels increase, even at those levels required to prevent dusting. It seems that the colorants of dye-based inks locate more uniformly in the coating structure because PVOH covers the pigment surfaces and masks any surface cationicity of the pigment. The dye follows the aqueous liquid as it diffuses into the surface layer of PVOH. The impact of diffusion processes is even seen at high printing speeds, though the shorter the time to reach dryers, if present, the less is the volume of liquid involved. The swelling affects especially the accessibility to the intra-pigment pores of porous pigments.

The coating layer properties have a connection to print quality via the ink absorption speed and volume capacity. An ink absorption that is too slow at the coating surface means that the colorants have more time to mix together and bleeding problems are more visible. The surface energy of the coating layer also affects the colorant movement.

The optical properties of the whole coated paper dominate the achievable print density. This is because inkjet coating

pigments are generally designed to have low scattering potential and so the base paper, if optically active, has a strong show through effect through the coating layer.

REFERENCES

1. SMYTH, S., "The Future of Inkjet Printing to 2013", Proc. PIRA Intl., 182 (2008).

2. SWERIN, A., KÖNIG, A., ANDERSSON, K. and LINDGREN, E., "The Use of Silica Pigments in Coated Media for Inkjet Printing: Effects of Absorption and Porosity on Printing Performance", Proc. 23rd PTS Coating Symp., Baden-Baden, Germany (2007).

3. RIDGWAY, C.J., GANE, P.A.C. and SCHOELKOPF, J., "Effect of Capillary Element Aspect Ratio on the Dynamic Imbibition within Porous Networks", *J. Colloid Interface Sci.* 252:373-382 (2002).

4. SCHOELKOPF, J., GANE, P.A.C., RIDGWAY, C.J. and MATTHEWS, G.P., "Practical Observation of Deviation from Lucas–Washburn Scaling in Porous Media", *Colloids Surfaces A - Physicochemical Engin. Aspects* 206(1-3):445-454 (2002).

5. SORBIE, K.S., WU, Y.Z. and McDOUGALL, S.R., "The Extended Washburn Equation and Its Application to the Oil/Water Pore Doublet Problem", *J. Colloid Interface Sci.* 174(2):289-301 (1995).

6. BOSANQUET, C. M., "On the Flow of Liquids into Capillary Tubes", *Philosophical Magazine,* Series 6, 45(267):525-531 (1923).

7. SCHOELKOPF, J., RIDGWAY, C.J., GANE, P.A.C., MATTHEWS, G.P. and SPIELMANN, D.C., "Measurement and Network Modelling of Liquid Permeation into Compacted Mineral Blocks", *J. Colloid Interface Sci.* 227(1):119-131 (2000).

8. RIDGWAY, C.J., SCHOELKOPF, J., MATTHEWS, G.P., GANE, P.A.C. and JAMES, P.W., "The Effects of Void Geometry and Contact Angle on the Absorption of Liquids into Porous Calcium Carbonate Structures", *J. Colloid Interface Sci.* 239:417-431 (2001).

9. CHAPMAN, D.M., "Coating Structure Effects on Ink-Jet Print Quality", Proc. Coating Conference, TAPPI, 73-93 (1997).

10. HARA, K., "Speciality PVOH in Ink Jet Coating Formulations", *Paper Technol.* 47(3):27-30 (2006).

11. PINTO, J. and NICHOLASM M., "SIMS Studies of Ink Jet Media", Proc. IS&T's NIP 13: Intl. Conf. Digital Printing Technol., Seattle, WA, USA, 420-426 (1997).

12. NILSSON, H. and FOGDEN, A., "Inkjet Print Quality on Model Paper Coatings", *Appita J.* 61(2):120-127 (2008).

13. SVANHOLM, E., WEDIN, P., STRÖM, G. and FOGDEN, A., "Colorant Migration in Mesoporous Inkjet Receptive Coatings", Proc. 9th Advanced Coating Fund. Symp., TAPPI, 221-228 (2006).

14. Mowiol Polyvinyl Alcohol, procure of the chemical: https://69.28.233.249/exchweb/bin/redir.asp?URL=http://www.kuraray-am.com/pvohpvb/downloads/Mowiol_brochure_en_KSE.pdf, Clariant (1999)

15. GANE, P.A., KETTLE, J.P., MATTHEWS, G.P. and RIDGWAY, C.J., "Void Space Structure of Compressible Polymer Spheres and Consolidated Calcium Carbonate Paper-Coating Formulations, *Ind. Engin..Chem. Res.* 35(5):1753-1764 (1996).

16. PAJARI, H., JUVONEN, K., JOKIO, M., KOSKELA and H., SNECK, A., "Dynamic Measurement of Coating Colour Consolidation with a New Laboratory Coater", Proc. 23rd PTS Coating Symposium, Baden-Baden, Germany (2007).

17. LAMMINMÄKI, T. and PUUKKO, P., "New Ink Absorption Method to Predict Inkjet Print Quality", Proc. 34th Intl. Res. Conf. of Iarigai, Grenoble, France, 231-239 (2007).

18. RIDGWAY, C. and GANE, P.A.C., "Bulk Density Measurement and Coating porosity Calculation for Coated Paper Samples", *Nordic Pulp Paper Res. J.* 18(1):24-31 (2003).

19. GANE P.A.C., SALO M., KETTLE J.P. and RIDGWAY C.J., "Comparison of Young-Laplace Pore Size and Microscopic Void Area Distributions in Topologically Similar Structures: A New Method for Characterising Connectivity in Pigmented Coatings", *J. Mater. Sci.* 44(2):422–432 (2009).

20. RIDGWAY C.J. and GANE P.A.C., "Modified Calcium Carbonate Coatings with Rapid Absorption and Extensive Liquid Uptake Capacity", *Colloids Surfaces A - Physicochemical Engin. Aspects* 236(1-3):91-102 (2004).

21. BOISVERT, J.-P. and GUYARD, A., "Influence of Structural Properties of Nanoporous Silica-Polymer Materials on Ink Absorption.", *Nordic Pulp Paper Res. J.* 18(2):210-216 (2003).

22. WEDIN, P., SVANHOLM, E., ALBERIUS, P.C.A. and FOGDEN, A., Surfactant-Templated Mesoporous Silica as a Pigment in Inkjet Paper Coatings, *J. Pulp Paper Sci.* 32(1), 32-37 (2006).

23. KUBELKA, P. and MUNK, F., "Ein Beitrag zur Optik der Farbanstriche", Z. Techn. Physik 12(11a):593-601 (1931).

24. DONIGIAN, D.W., "Ink Jet Dye Fixation and Coating Pigments", Proc. Coating Conf., TAPPI, 393-412 (1998).

25. McFADDEN, M.G. and DONIGIAN, D.W., "Effect of Coating Structure and Optics on Inkjet Printability", Proc. Coating Conf., TAPPI, 169-177 (1999).

26. OKA, H. and KIMURA, A., "The Physicochemical Environment of Acid Red 249 Insolubilized in an Ink-Jet Paper", *J. Imaging Sci. Technol.* 39(3):239-243 (1995).

27. SVANHOLM, E. and STRÖM, G., "Influence of Polyvinyl Alcohol on Inkjet Printability", Preprints Intl. Printing Graphic Arts Conf., PAPTAC, 187-207 (2004).

28. GANE, P.A.C. and RIDGWAY, C.J., "Moisture Pickup in Calcium Carbonate Coating Structures: Role of Surface and Pore Structure Geometry", Proc. 10th Advanced Coating Fund. Symp., TAPPI, 24 (2008).

REMINDER TO SUBSCRIBERS

Have you renewed your subscription to JPPS for 2010?

You can renew your subscription on-line at www.paptac.ca

or by contacting the Publications Coordinator at

PAPTAC:

Tel.: 514-392-6956 / Fax: 514-392-0369

jlemieux@paptac.ca

The role of binder type in determining inkjet print quality

The role of binder type in determining inkjet print quality

Taina Lamminmäki, John Kettle, Pasi Puukko, Jukka Ketoja, and **Patrick Gane**

SUMMARY: There is an increasing trend for the use of aqueous-based inkjet inks in high-speed commercial printing and this challenges the hydrophilic and absorptive properties of the paper surface. The aim of this work is to clarify the role of polyvinyl alcohol (soluble polymer) and styrene acrylate latex (suspension polymer) as binder in the formation of the coating structure for the purpose of inkjet printing. The coating layer properties were studied in combination with a chosen speciality calcium carbonate pigment. The inkjet image quality was assessed on coated papers. The role of diffusion of colorant as well as vehicle absorption was studied using dye-based inks. Among the other traditional paper surface characterization methods, the surfaces were analyzed with the Clara device, which shows how the external pressure affects the inkjet ink penetration into the coated paper structure by measurement of capacitance changes during ink penetration through the paper. The method indicates that inkjet ink penetration depth and speed depends on binder type. The chemical nature of binders affects the ink movement. The polyvinyl alcohol concentrates within the fine pores of the structure and absorbs water in its polymer matrix, and is seen simultaneously to adsorb ink dye, whereas the styrene acrylate acts effectively as a hard sphere, affecting the packing structure of the coating forming a more permeable coating layer. Therefore, structural as well as chemical differences of coating layers determine the final inkjet print quality.

ADDRESSES OF THE AUTHORS: Taina Lamminmäki (taina.lamminmaki@vtt.fi), **John Kettle** (john.kettle@vtt.fi), **Pasi Puukko** (pasi.puukko@vtt.fi), **Jukka Ketoja** (jukka.ketoja@vtt.fi): VTT Technical Research Centre of Finland, Biologinkuja 7, FIN-02150 Espoo, Finland and **Patrick A. C. Gane** (patrick.gane@tkk.fi): Aalto University, School of Science and Technology, Faculty of Chemistry and Materials Sciences, Department of Forest Products Technology, P.O. Box 16300, FIN-00076 Aalto, Finland

There is often reported a high expectation for growth in the field of inkjet printing. Growth is predicted across the range of print formats, including both traditional offset markets as well as for small print runs and for variable information printing. The use of aqueous-based inkjet inks challenges many aspects of a paper coating surface, including its structure and absorptivity. The water of

the ink should absorb rapidly into the porous structure. At the same time, the spread of the ink on the surface should be controlled so that the absorption front moves mainly in the thickness direction of the paper whilst providing sufficient spread for continuity of the image without the onset of colour bleeding. There is an urgent need to develop the coating layer properties further based on the mechanisms which control these properties in inkjet prints.

Traditionally, the best inkjet print quality is achieved with coated papers which contain silica pigments. The most common binder is polyvinyl alcohol (PVOH). This choice is dictated because it is one of the few binders that produce sufficient surface strength of the coating layer for fine high specific surface area pigments (Miller et al. 1996). Modified PVOH has also been used: carboxylic-, acryl amide-, sulfonic-, cationic- and silicone-modified PVOH. The use of other types of pigments in the inkjet area has been accompanied by the introduction of some other binders such as polyvinyl pyrrolidone, polyacrylic acid, polyacrylamide, methylcellulose, cellulose derivatives, gelatin, polyvinyl acetate latex, vinyl acetate ethylene and cationic starch (Lavery, Provost 1997, Khoultchaev, Grazyk 1999, Morea-Swift, Jones 2000, Glittenberg, Voigt 2001, Yip et al. 2003, Malla, Devisetti 2005). The attributes of PVOH include its non-ionic, hydrophilic nature, its ability to cross-link whilst being plasticizable. It is both shear and temperature stable and provides strong binding strength (Miller et al. 1996, Pinto, Nicholasm 1997). The binding strength of PVOH depends on the degree of polymerization; high peel strength being achieved with a high degree of polymerization (Hara 2005).

Svanholm et al. (2006) and Svanholm (2007) studied silica pigments with PVOH binder coated on fine papers. It was shown that the silica pigments with large internal pore diameters require more binder than pigments with smaller pores to get the dye colorants to remain on top of the coating. It was reported that PVOH can form a film at the upper surface of the coating and assist colorant fixing. A partially hydrolyzed and higher molecular weight PVOH gave the best colour gamut and the sharpest line edges, and also sufficient binding strength. Cawthorne et al. (2003) found that the partially hydrolyzed PVOH produced a lower roughness of the coating layer than did a fully hydrolyzed PVOH. There are fewer hydrogen bond interactions between

FOR FULL COLOUR SEE ARTICLE AT: www.npprj.se

II/1

silica pigment and the partially hydrolyzed PVOH. At the coating drying stage, there exists, therefore, less shrinkage, which is often responsible for increased coating surface roughness. More recently, the binder type has been shown to have an effect on the inkjet ink print density and bleeding development, (Nilsson, Fogden 2008). However, the behaviour of inkjet inks in relation to binders under the influence of external pressure, representing the surface tension of the inkjet droplets, has not been studied so widely.

Vikman and Vuorinen (2004a) studied light fastness of an inkjet printed surface containing PCC, kaolin, and their blends. The binders were PVOH and cationic starch together with cationic styrene acrylate latex. With dye-based inks, the significance of structural properties of the coating layer regarding the light fastness decreased when the strength of the chemical paper-ink interaction increased. The dyes benefit from a dense coating structure, whereas a coarse structure of the coating appears to be advantageous for the pigment-based inks. However, this kind of coating structural connection to water fastness was not detected as the single controlling factor, rather the surface adsorption via Coulombic interaction was key for water fastness in the case of dye-based ink (Vikman 2004b).

Heilmann and Lindqvist (2000) studied water-based inks in the area of continuous inkjet. The studied surfaces consisted of sized uncoated paper, a coated paper, and one, surface swelling, superabsorber-based glossy paper. They applied a single droplet of ink on each of the surfaces and measured the droplet penetration from the top side and in the cross direction. The droplets reached the final dot size on the silica coated paper in the first 50 ms, whilst on the surface sized paper it took as long as 500 ms. Coating with swelling binder/absorber displayed a little faster ink levelling time than the non-swelling coating. The non-swelling coating reached the final dot size within the first 100 ms.

The role of latices in inkjet coatings has not been studied in much detail. In offset coatings, Rousu et al. (2005), amongst others, showed that the properties of latex affect the ink setting. Low glass transition temperature and gel content of latex, together with oil-matched solubility index through monomer composition, increase ink setting rate. However, the latex particle size can affect the packing of the coating layer, and, through that, modifies the setting speed. Moreover, Rousu et al. (2000 and 2005) showed that the latex type influences the degree of chromatographic separation of the oils from the offset ink within the coating structure. Even a small amount of latex affected the

separation process. The reason behind this can be found from the polar/non-polar nature of the latex polymer. The diffusion phenomenon and associated binder swelling, acts to preferentially absorb certain oils and further decreases the diameter of pore capillaries. Hydrophilic binders, for example polyvinyl alcohol, have higher swelling tendency than latices in water. Donigian et al. (1998) noticed similar behaviour in their study. Adding PVOH in the coating generally slows down the movement of water in the case of dye-based inks.

The aim of this work is
- to clarify the role of styrene acrylate latex versus polyvinyl alcohol binder in the formation of the coating structure in terms of inkjet printing, and
- to find out how the dye-based inkjet ink movement within the coated paper structure during absorption depends on the binder properties.

Materials and Methods

Coating compositions and coating trials

An inkjet speciality precipitated calcium carbonate coating pigment (OMYAJET B5260, provided by Omya AG[1]) was used as the sole pigment. The pigment diameter (weight median, d_{50} with Sedigraph 5100) was 2.70 μm, specific surface area 63.7 m^2g^{-1} (BET, ISO 9277) and zeta-potential of the slurry 1.6 mV. The binders were polyvinyl alcohol (PVOH, provided by Clariant International Ltd.[2]) and styrene acrylate latex (SA, provided by Ciba Specialty Chemicals[3]). PVOH had a degree of hydrolysis of 87.7±1.0%, molecular weight of 204 000 $g·mol^{-1}$ and density 1.26 $g·cm^{-3}$ ($20^{\circ}C$). SA latex had a particle size of 180 nm, glass transition temperature of -20°C and density of the dispersion 1.03 $g·cm^{-3}$. In SA-containing coating colours, the virtually non-ionic nature of the PCC slurry was first changed to anionic by adding sodium polyacrylate (Polysalz S[4]), having a molecular weight of 4 000 $g·mol^{-1}$. The chemical structures of PVOH and the compounds which form the SA latex are introduced in *Fig 1*.

The coated papers were produced on the KCL pilot coater[5]. The base paper, 53 $g·m^{-2}$, was a commercial fine paper designed for a coated fine paper grade. The base paper was first pre-coated so that the top coating could not penetrate into the base paper, and so it is ideal for isolating the coating effects.
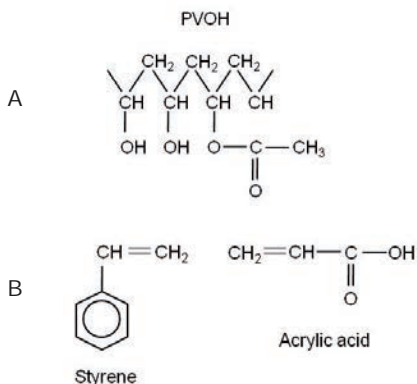
Fig 1. The chemical structure of polyvinyl alcohol and the components of styrene acrylate latex.

A pre-coating of 7 g·m^{-2} was applied with a film coater (1 000 m·min^{-1}) on both sides of the base paper, and the final top coating layer of 8 g·m^{-2} was applied with a short dwell application (blade) using a coating speed of 700 m·min^{-1}. The pre-coat had 100 pph of ground calcium carbonate with a narrow particle size distribution of 60 wt-% < 1 µm (Covercarb 60[1]), 12 pph styrene-butadiene latex (DL966[6]) and 0.6 pph carboxymethylcellulose (Finnfix 10[7]). The recipes of the top coats are summarized in *Table 1*. The final moisture content of the web for each coating point was 5%.

The degree to which inkjet ink penetrated into the coated paper structure was studied with the Clara device (*Fig 2*) (Salerma 1998, Lamminmäki 2009b). The measuring principle of Clara is based on the fact that the resistivity of a dry surface is very high whereas a moistened surface conducts electricity more readily.

Analysis of the coated papers
The coated papers were analyzed using the methods outlined in *Table 2*.

Table 1. The top coating colours in pilot trials. *AcoustoSizer II

Component	Coating colour					
/ pph	7 pph PVOH	12 pph PVOH	30 pph PVOH	7 pph SA	12 pph SA	30 pph SA
Inkjet PCC	100	100	100	100	100	100
PVOH	7	12	30			
SA				7	12	30
Polysalz S				6	6	6
Measurement						
Solids content, %	25.1	24.3	22.2	28.1	31.0	30.9
Zeta-potential*, mV	2.4	2.1	2.6	-37	-33	-33
pH	8.4	8.5	8.4	8.5	8.2	7.9

Table 2. Used measuring methods.

| Property	Method	Notice
Thickness and apparent bulk density	ISO 12625-3:05	
Coat weight with ash content	ISO 1762:01	
Permeability	Air permeance	Parker Print Surf using 20 kPa measuring pressure
Contact angle of water	Droplet	Fibro 1100 DAT with 2 µl drop, apparent contact angle after 0.5 s
Ink absorption time	VTT internal	DIGAT (Lamminmäki et al. 2007), cyan dye-based ink (used in Versamark® VX5000e, applied ink amount 8 gm^{-2})
Cumulative porosity of coating	Mercury intrusion porosimetry (Åbo Akademi[8])	Pascal porosimeter[9] using 140 Pa (low pressure port) and 440 Pa (high pressure port)
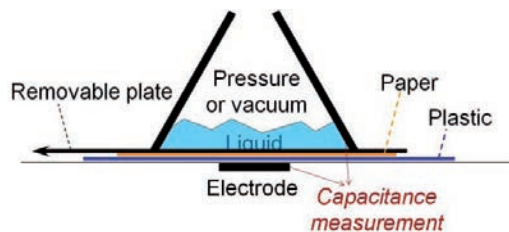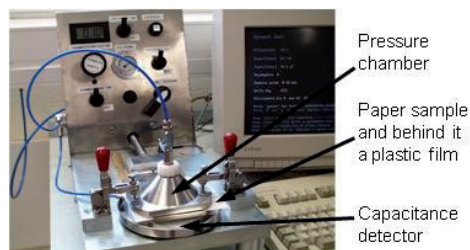
Fig 2. The structure of Clara.

The liquid forms a conducting material whose movement affects the capacitance between the liquid chamber and the electrode under the studied sample. The chamber can be pressurized from an under pressure of -0.5 bar to an over pressure of +5 bar. The measuring area is 6.8 cm^2. In the measurement, cyan ink, as used in Versamark® VX5000e[10], was applied at an amount of 5 ml. The measurements were made after equilibration under a relative humidity of 50% RH and 23°C temperature. The result is expressed as a curve of capacitance change during time as the liquid penetrates through

---

[6] DL966: styrene butadiene latex supplied by Dow Suomi Oy, Urho Kekkosenkatu 7 B, PL 117, 00101 Helsinki, Finland

[7] Finnfix is a tradename of Noviant Oy, Malminkatu 34, 00100 Heslinki, Finland

[8] Åbo Akademi, Porthaninkatu 3-5, FI-20500 Turku, Finland

[9] Ing. Prager Elektronik HandelsGmbH, Traunstrasse 21, A - 2120 Wolkersdorf, Austria

[10] Easman Kodak Company, 343 State Street, Rochester, NY 14650, USA

the sample in the *z*-direction. The resulting curve is an average of five parallel measurements.

The maximum value of capacitance is about 190 pF, and this value depends on the capacitance of the plastic film backing the sample. When the capacitance reaches this maximum value, it is interpreted that the ink has penetrated through the whole paper structure.

Fig 3 shows some examples of the resulting curves. We can assume that the contact of liquid with a porous hydrophilic substrate goes in the following order (Oliver 1982):

1. When there is no external pressure:

All the absorption is by capillary wetting force in coating pores fine enough to exert a Laplace pressure drop. In pores larger than those exerting significant wetting force, the movement is followed by thin layer wall wetting and diffusion.

2. When pressure is applied:
a.   If the pressure is small compared to the capillary pressure in the fine pores, then liquid starts to be forced into the larger pores under Poiseuille flow whilst capillary pressure filling continues as above.
b.   If the pressure is higher than the capillary force, or all the pores are filled, then the action is by permeation flow according to Darcy's law in saturated structures.
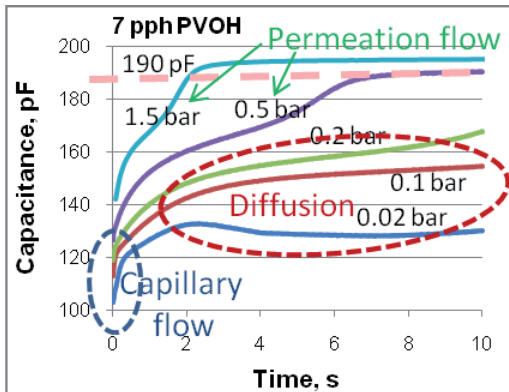
Fig 3. Result curves of Clara at five different external pressures. The used liquid was cyan dye-based ink (used in Kodak Versamark® VX5000e).

The bimodal behaviour of each curve illustrates the competition between the initial capillary wetting and the permeable flow characteristic once capillaries/pores are filled.

Paper thickness, d_{paper}, in the *z*-direction can be divided into the dry, $d_{dry}(t)$, and wet, $d_{wet}(t)$, parts during the measurement.

$$d_{paper} = d_{dry}(t) + d_{wet}(t) \qquad [1]$$

The total capacitance C_{tot} is the capacitive impedance series sum of the plastic capacitance C_{pl}, coming from the plastic sheet under the sample, and the sample capacitance $C(t)$:

$$1/C_{tot} = 1/C(t) + 1/C_{pl} \qquad [2]$$

The total wetted paper has practically no impedance (pure conductor), and thus the capacitance dependence on paper depends on the thickness of the dry paper.

$$C(t) = A\varepsilon/d_{dry}(t) \quad => \quad d_{dry}(t) = A\varepsilon/C(t) \quad [3]$$

where A is the area and ε is the dielectric permittivity of the material.

The thickness of the wet part of the paper, which we estimate to be the penetration depth of the water front, can be calculated by combining equations 1, 2 and 3:

$$d_{wet}(t) = d_{paper} - A\varepsilon/C(t) = d_{paper} - A\varepsilon(1/C_{tot} - 1/C_{pl}) \quad [4]$$

The pressure exerted by inkjet ink droplets in a high speed inkjet press are clearly less than 1.5 bar. If we assume that the droplet size is 15 pl, as quoted by Kodak for the Versamark[10] technology, the speed of impingement of the droplet onto the paper surface is 15 m·s^{-1} and ink density 1 000 kg·m^{-3}, the pressure that we estimate, by utilizing the common pressure, density and speed formula, of the droplet hitting the paper surface is a little under 0.1 bar. The measured capacitance values of Clara remain in this pressure area under the maximum value of 190 pF after 10 s measuring time at 0.1 bar pressure (*Fig 3*). This indicates that the studied ink did not penetrate through the whole paper, and so the ink front is still within the paper structure. If we assume that the maximum capacitance value is achieved in the thickness d_{paper}, then the penetration depth and speed turn out to be too high compared with the calculated pressure penetration. This finding fits well with the work of Schoelkopf, Gane et al. (2000), which showed that absorption proceeds by a preferred pathway network of pores depending on pore entry criteria, including inertia retarding the filling of larger pores. Such a preferred pathway network results in the wetting front being non-uniform and liquid can reach deep into the structure leaving a proportion of unfilled pores.

Printing trials

The coated papers were printed with the Kodak Versamark® VX5000e[5] inkjet printing unit, which works with a continuous stream inkjet principle. The inks are dye-based inks and the main diluent/solvent is water. The surface tensions of the inks were measured as 51-55 mN·m^{-1} (25°C), depending on dye colour, and the viscosity 1-2 mPa·s. The printing speed was 100 m·min^{-1} and the drying drum and hot air dryer had a temperature of 80°C.

The inkjet colorant penetration depth was characterised in respect to print density and print-through. The print density was measured with GretagMacbeth D196[11]. In the analysis of print-through, a scanner system with image analysis (MATLAB based PTA program) was utilised. The scanner system adopted an Epson Perfection V700 Photo scanner with resolution of 300 dpi. In the print-through evaluation, the studied area was taken from the reverse side of a printed area, with the reference area in all cases being unprinted. The show-through was measured from the printed area upon which was placed an unprinted sample of the same coated paper. The strike-through was then calculated by subtracting the show-through from the print-through. The colour difference was reported as Delta E94, which followed the CIE 1994 colour difference equation. This takes better account of the different colours of the printed surface than conventional ΔE^* (Mäkinen et al. 2005 and 2007).

In the study of bleeding (mixing of the inks at their interface), a scanner system was used. The scanning was made again with the Epson Perfection V700 Photo scanner, with a chosen resolution of 2 400 dpi. The grey level profile of the printed line was measured with an image analysis program using a definition of the points A and B. Point A was 15% brighter than the darkest region and B 15% darker than a background. The black surface had grey value set to zero, and white a value of 254. Each unprinted paper was adjusted to the value 170. The normal edge width described the bleeding distance of inks.

Table 3. Properties of coated papers.

Coating	Coat weight / g·m⁻²	Bulk thickness / μm	Apparent bulk density / kg·m⁻³	Cumulative pore volume / cm³g⁻¹	Contact angle (water) / ° (STDEV / %)
Base paper	-	85.8±0.6	777±5	0.620	N/A
Pre-coating	7.4±0.6	90.3±0.6	906±6	0.439	91.8 (2.0)
7 pph PVOH	8.2±0.2	97.3±0.5	928±4	0.507	50.2 (4.0)
12 pph PVOH	8.3±0.1	95.6±0.3	937±3	0.441	62.4 (2.0)
30 pph PVOH	8.8±0.3	97.2±0.4	922±4	0.500	86.7 (2.0)
7 pph SA	8.5±0.5	97.6±0.5	929±5	0.483	93.6 (1.0)
12 pph SA	9.7±0.5	97.9±0.8	937±7	N/A	109.0 (3.0)
30 pph SA	6.6±0.3	94.2±0.7	937±7	0.464	114.0 (3.0)

The ink colorant penetration depth was illustrated by embedding the printed surface in LR white resin[12] (with refrigerator) and taking a cross-section image with a light microscope (Zeiss Axioskope 2 plus).

The colorant fixing properties were studied by testing the water fastness. The printed single-colour 70% half-tone dot areas were immersed into de-ionised (23°C) water for 5 min. After that the samples were left hanging to dry in dark conditions at 23°C temperature and 50% RH moisture content overnight (at least 17 h). Similar methods have been used in other studies (Ryu 1999, Khoultchaev 2001, Vikman 2004a). The colour change ΔE^* was measured with a GretagMacbeth SpectroEye[7] spectrophotometer. The spectrophotometer used a configuration of 2° measuring angle, D65 illuminant, UV-filter on and the coated unprinted paper defined as a white area. CIELab^* values were measured before and after the water-treatment. ΔE^* was calculated following the standard equation of SCAN-P 89:03.

Results

Coated paper properties

Table 3 shows the results of coat weight, bulk, thickness, density, cumulative pore volume of coated papers and contact angle of water. *Fig 4* illustrates how binder amount increase decreased the air permeance results of the whole paper.
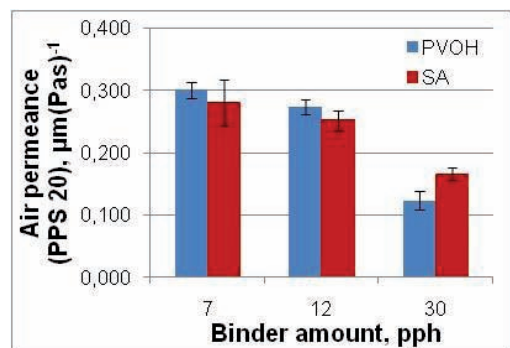

Fig 4. The air permeance of studied layer structures.

Fig 5 shows that the pores of the pre-coating layer are located in the area of 100-550 nm. The first derivative curves (Laplace equivalent pore size distribution, ignoring pore shielding) of PVOH and SA coatings, where the derivative results of pre-coated paper have been subtracted, are illustrated in *Fig 5* (right side). PVOH coatings displayed more of the smaller diameter pores than in the case of the SA latex coatings. At the binder amount of 30 pph,

---

[11] Gretag-Macbeth AG, Althardstrasse 70, CH-8105 Regensdorf, Switzerland

[12] Electron Microscopy Sciences, P.O. Box 550, 1560 Industry Road, Hatfield, PA-19440, USA

II/5

the PVOH coating had less pores within the 35-85 µm diameter region than the SA coating. These results indicate a pore filling behaviour of the PVOH.
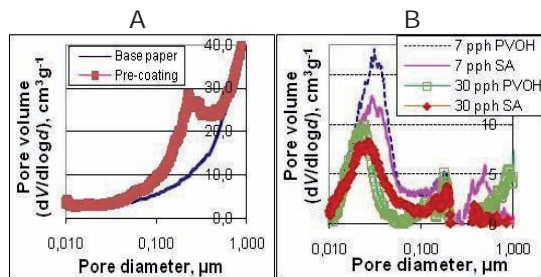

Fig 5. The first derivative of cumulative mercury intrusion curves of base paper and pre-coated paper (left side) and PVOH and SA coated papers (right side). A refers to substrate and B the pore size distributions of the coatings with the substrate and pre-coat subtracted.

Ink absorption time

The ink absorption time into the top coating layer was measured with the DIGAT (Lamminmäki et al. 2007), which records the glossmeter voltage change as a result of the applied inkjet ink layer during time. The absorption time is the time between 10% of maximum voltage and 10% of saturation voltage value. It was seen (*Fig 6*) that the 7 pph binder coatings had the quickest absorption, and that there was very little difference between the values for the 12 pph and 30 pph binder containing top coatings. There was only a slight difference between the ink absorption values for the two types of binder used.
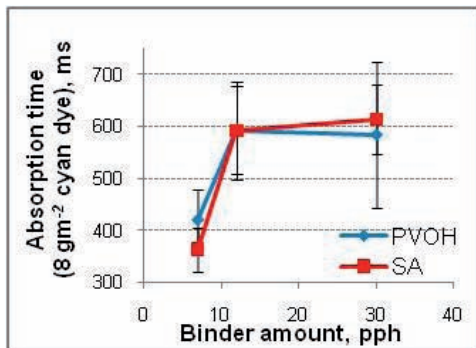
Fig 6. Absorption time of inkjet ink into coatings with different amount of binder. Absorption time was measured with DIGAT device using 8 g·m⁻² cyan dye-based ink (used in Versamark® VX5000e press).

Absorption properties of whole paper structure at 1.5 bar

The capacitance results at 1.5 bar (*Fig 7*) show that ink movement through the paper is dependent on the amount of binder present, i.e. the coating which had more binder had a slower capacitance change. Measurement at this pressure represents most strongly the permeability of the coating. The relative change from capillarity to permeability can

be distinguished by the bimodal nature of the curve. Clearly, the highest binder levels dampened the capillary effect as the curve becomes monotonic. For the ink to penetrate through the structure with PVOH coatings took from 2.5 s to 11 s, and with SA coatings from 0.9 s to 3 s. The fastest ink penetration speed was reached with 7 pph binder and ink penetrated more quickly through the SA coating papers than through the PVOH papers.

Fig 8 illustrates how penetration speed of cyan dye developed through the studied papers at the external pressure of 1.5 bar. In the discussion part, we shall come back to these figures and their interpretation.
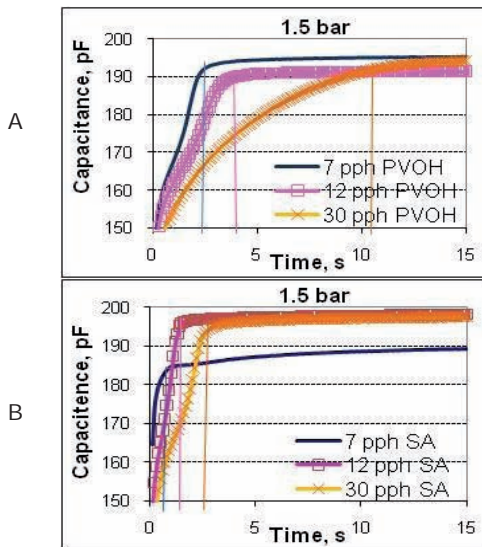

Fig 7. Cyan dye-based ink penetration through the coated papers at the external pressure of 1.5 bar, as measured with the Clara device: A – refers to PVOH and B – to SA latex, respectively.

Absorption properties of coated paper at 0.1 bar

Fig 9 shows how the studied dye penetrates through PVOH and SA-containing coatings at 0.1 bar external pressure, i.e. within a pressure regime caused by inkjet droplets and their impingement. At the lowest binder amount, 7 pph, the used cyan ink penetrates more rapidly in the SA latex coating than in the PVOH coating. The slope of the curve in the beginning of the measurement is larger with the SA coating than with PVOH. When the binder amount is increased, the curves of PVOH and SA coatings come closer to each other.

We see that the bimodal nature of the curves is far less at the lower pressure, supporting the dominance in this case of capillary pressure. Only in the case of the low level of latex do we see an indication of bimodality, and this supports the likelihood of there being greater permeability in this case, such that even at low pressure some external pressure driven Poiseuille flow can be established.
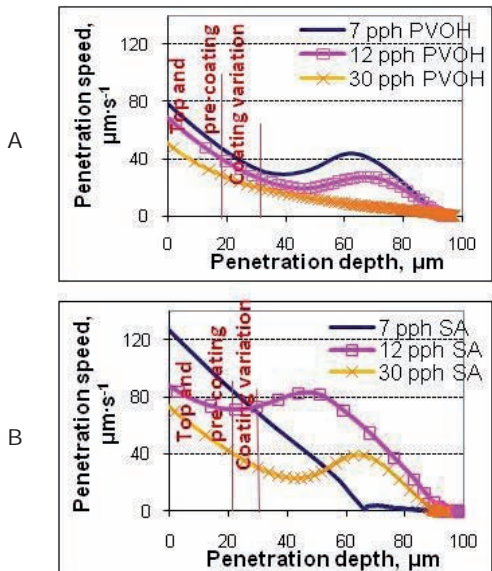
II/6

Fig 8. Cyan dye-based ink penetration speed through the paper structures having PVOH and SA coatings at external pressure 1.5 bar. The coating variation refers here to the thickness differences of the coating layer : A – refers to PVOH and B – to SA latex, respectively.

Print quality

The black ink produced higher print densities than cyan ink (*Fig 10*). There were observed to be a couple of black print density results on the SA latex coatings that were on a somewhat higher level than the other results, but otherwise print densities were very close to each other. The strike-through was lower with PVOH coatings than with SA, again supporting the greater permeability of the latex-containing coatings.

The highest bleeding tendency was exhibited by the SA coatings with binder amounts of 12 pph and 30 pph, respectively (*Fig 11*). The finding that applying a high level of binder does not prevent strike-through illustrates the role of base paper as coating pore volume becomes limited. Although the increased binder level leads to a semi-sealing of the coating layer to permeation, the excess liquid volume must proceed into the body of the paper. It is then the transmission of liquid through the base paper, by fibre wall wicking, for example, that leads to the appearance of ink on the reverse side of the sheet.
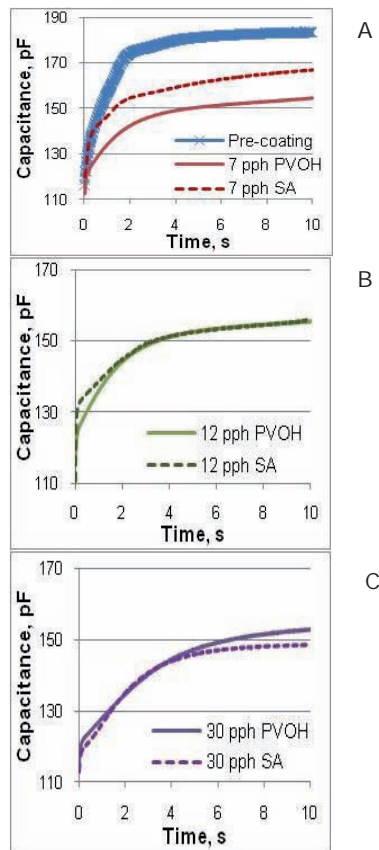
Fig 9. The effect of binder type and binder amount on the results of Clara. Measured with Versamark® cyan ink using 0.10 bar external pressure: A, B, and C refer to 7, 12 and 30 pph binder levels, respectively.
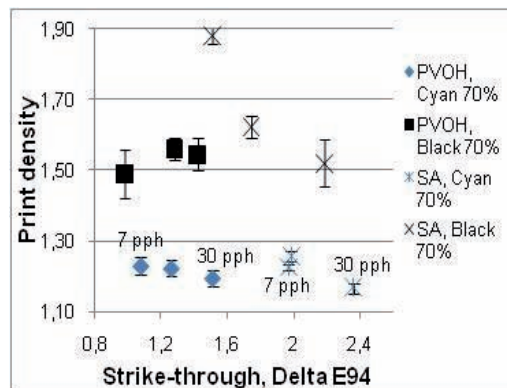

Fig 10. Print density against strike-through of dye-based ink printed surfaces. Printed with Versamark® VX5000e.
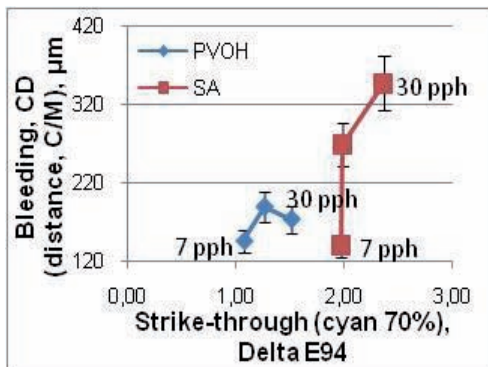
II/7

Fig 11. The bleeding (distance, CD - against printing direction, C/M – magenta line on cyan preprinted surface) against strike-through of studied coated papers.

In the water fastness properties, *Fig 12*, the PVOH and SA-containing coatings showed a totally different nature. The colorant had become fixed in the case of the PVOH coatings faster (lower ΔE^*) than in the SA coatings. The colour changes in black surfaces were minimal. However, cyan, magenta and yellow ink had clearly poorer fixing to the SA coatings than to the PVOH coatings.
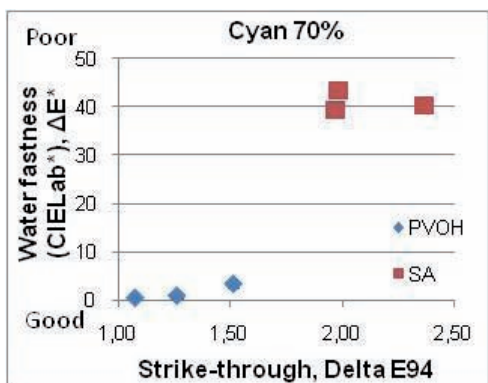
Fig 12. The water fastness of cyan dye-based ink printed surfaces. Printed with Versamark® VX5000e.

Discussion

Ink penetration through the coated paper, at 1.5 bar

The Clara results of coated papers at 1.5 bar external pressure (*Fig 8*) show that the form of penetration speed curves in coating layers is very similar for the PVOH-containing coatings, and this continues until a depth of 32 μm. The thickness of top-coating is about 10 μm and pre-coating about 7 μm. This means that ink penetration has continued very similarly within the coating layers dominated by the external pressure. The rate at the higher pressure level is determined more strongly by permeability, and thus the rate is determined by the layer of least permeability, i.e. the top-coating.

In our earlier study it was noticed (Lamminmäki et al. 2009) that the used PVOH can go into the intra-particle pores (pore diameter of 20-60 nm) of speciality porous coating pigments. The pore intrusion derivative curve (*Fig 5*) shows that most of the pore diameters of pre-coating are between 100 nm and 550 nm. Therefore, it is possible that the PVOH contained in the top-coating colour has also penetrated into the pre-coating layer. Secondly, the PVOH can dissolve in the inkjet ink water vehicle and be transported in part from the coating, as *Fig 13* shows, and so it can affect ink properties during the penetration process. Thus, there can be several aspects which can affect the inkjet ink movement in the coating layer. However, the lack of permeation change tells us that the top coat dominates the permeation property, since larger pores below it simply act to maintain the flow rate under pressure rather than speeding it up. Therefore, even though PVOH can in effect be somewhat mobile, the effect is not strong enough to be observed here.
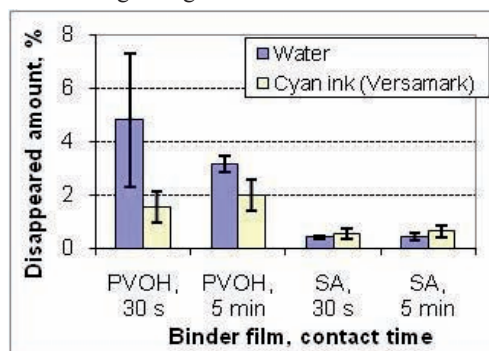

Fig 13. The dissolving of binder films in de-ionized water and cyan dye-based ink - film thickness 200-250 μm. In the binder film absorption measurement, the PVOH film was put in the test liquid for duration of either 30 s or 5 min. After that the liquid was weighted and put into the oven to evaporation. The result is the relative change of liquid (before and after drying).

Moreover, the hydroxyl groups of PVOH can bind ink solvent (water) within the porous coating layer, and this process causes swelling and closing of the smallest coating pores (Lamminmäki et al. 2009). It has been shown previously that a PVOH film (200-250 μm) absorbed Versamark® VX5000e cyan ink up to 29.2% of its volume after 5 s (Lamminmäki et al. 2009). At the same time, SA latex film (200-250 μm) absorbed only 1.0% of its own volume of the same cyan ink. Therefore, we can assume that the swelling of SA latex affects less in the SA coatings.

The Clara results indicate that ink penetrates under pressure quicker in SA coatings than in the PVOH coatings. PVOH-containing coating has the lower permeability when compared with the SA latex bound coating (*Fig 14*). In addition, the PVOH binder swells under diffusion by ink vehicle,

II/8

whereas SA binder cannot. Therefore ink becomes held longer in the PVOH-containing coating before it continues travelling further under capillary action, or is retarded by reduced pore connectivity as a result of the swelling under permeation. Thus, there must also be a concentration difference of ink at a certain moment between PVOH and SA bound coatings. We may also assume that the latex part of the top-coating cannot transfer into the pre-coating structure to the same extent as PVOH might during the coating process, because the mean diameter of latex particles (180 nm) is partially too large to flow into the pores of the pre-coating (100-500 nm). Furthermore, once the topcoat is immobilized this flow cannot happen within the topcoat either. Therefore, the top- and pre-coating layers of latex coatings are probably more separately defined than those in the case of PVOH bound coatings. The role of diffusion in these binders will be studied more closely in our forthcoming work.
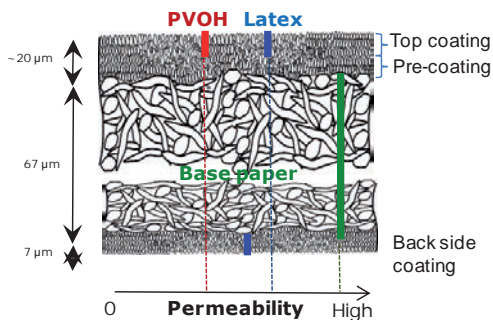
Fig 14. Binder type effect on permeability under external pressure (1.5 bar) through the studied coatings with PVOH and SA latex. Red line describes the permeability level in PVOH coated papers and blue line is the permeability in SA latex coatings. Green is the permeability of base paper.

Ink transportation at small external pressure, 0.1 bar

At lower pressure, 0.1 bar, corresponding to that of an inkjet ink droplet impingement at the paper surface, the ink moves slower into the coating structure than at 1.5 bar. The ink penetration is controlled more strongly by capillary absorption, and again more slowly in the PVOH coating than in the SA coating, supporting the supposition that PVOH absorbs ink water, swells and causes the closing of the small pores. Moreover, this means that at a certain moment the ink concentration in the pre-coating is lower because the ink stays longer in the top-coating. This can influence the ink spreading behaviour in and on the top-coating.

In the SA coating, the ink moves faster in the coating layer, similarly as seen before at the higher pressure. Some action of permeability can now be expected even at low pressure. This is effectively a drainage effect superposed on the capillary effect. At the pressure 0.1 bar, it is possible to notice

changing points of the capacitance slope as measured in the 7 pph SA-containing coated papers. The first changing point of the capacitance curve located at a time of 0.3 s (*Fig 9*), on the basis of both 0.1 bar and 1.5 bar results, is when the capillary force filled pores are starting to become saturated and the remaining larger pores fill under the low but present external pressure. This changes the mechanism from capillary wetting to permeation. This continues through the wetting of the base paper as the rate of base paper penetration is controlled by the permeability of the coating layer. If we now consider the absorption time of 0.36 s for the 7 pph SA-containing coating, as measured by DIGAT, we can conclude that the ink has already penetrated through the coating layers at the moment when the gloss of the ink layer disappears. The PVOH bound coating does not display this kind of clear changing point of penetration speed at any of the studied binder amounts. The reason behind this considered to be the same as at 1.5 bar external pressure, i.e. the absorption by a swelling of the PVOH.

The addition of binder amount, up to 12 pph and 30 pph, decreases the porosity and permeability of the coating layers. At a binder amount of 12 pph, the SA-containing coating absorbs the ink still more rapidly than PVOH. However, deeper in the paper the ink moves very similarly regardless of binder type. The ink goes through the SA coating quicker than through the PVOH coating, but stays longer in the interface of base paper and pre-coating, where the pore size increases. At the binder amount of 30 pph, the capacitance values are pretty much same. Initial wetting of the base paper at low external pressure is therefore assumed to be the rate controlling factor and is predominantly diffusion limited.

Ink movement effect on print quality

On the basis of the Clara capacitance results we can expect that the SA bound coatings with higher ink penetration speed produce lower print density and higher print-through because the colorants can move deeper into the coated paper structure. As *Fig 10* shows, the strike-through is higher with SA papers than with PVOH papers. The cross-section figures (*Fig 15*) show how the cyan colorants have been transported eventually to the base paper from the SA bound coated surface, whereas the colorants are held within the coating layer containing PVOH.

On the other hand, SA bound coatings will display both hydrophilicity, due to the latex stabilising surfactants and carboxylation, and a certain hydrophobic nature associated with the underlying polymer matrix. Previous workers predicted less ink droplet spreading (Bahr 2000) due to

hydrophobicity. The results here indicate that neither the latex nor the quick ink movement in the paper structure prevent the colorants from spreading on the SA coatings. One explanation for this can be the surfactants that have been used in latex production. They could aid lateral transport of colorants on the top part of the coating, although the penetration speed of the ink is quick enough to prevent the existence of inter-colour bleeding. A further consideration is that the larger pored latex bound coatings evidence less "capture" of the wetting front compared to the internal diffusion responding PVOH. We see that this could be related either to the reduced permeability of PVOH coatings and/or the slight cationicity of the PVOH itself since the coating pigment is itself had z-potential of 1.6 mV. If the SA latex bound coating would contain additional chemical components that could fix the colorants of the ink, and arrest lateral spread, then SA or any other latex type might have a better possibility to work functionally in inkjet coatings.

PCC large+ 7 pph PVOH

PCC large+ 7 pph SA

50 μm
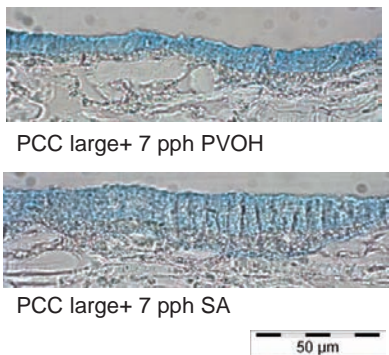
Fig 15. Cross-section micrographs of coatings comparing the cases with 7 pph of PVOH and SA, respectively. Printed with Versamark® VX5000e.

The water fastness results (*Fig 12*) show that the colorants, other than black, have reduced capability to withstand the water treatment and remain less within the printed SA bound coatings than within the PVOH coatings. *Fig 16* shows how cyan ink that was applied directly to a film of the binder alone has attached to the PVOH film but not to a corresponding SA latex film. We see therefore, that the PVOH has a positive action by direct adsorption of dye.

PVOH   SA

Fig 16. Colorant fixing to PVOH and lack of fixing to SA latex films after 30 s absorption time.

In the case of PVOH coatings, the longer ink residence time in the coating layer, has not become reflected as a larger bleeding tendency (*Fig 11*). It seems that the ink vehicle diffusion in the PVOH layer has happened so quickly that the colorants have no time to transfer in the *xy*-direction on the top of the coating. The colorants stay adsorbed to the PVOH binder and no print-through problems occur.

Conclusions

The inkjet ink penetration speed depends on the used binder type in the coating layer and the level of external pressure, if applied. The PVOH binder can allow diffusion of the inkjet liquid phase, and swells under the influence of the ink. This acts to close the nano-size pores and therefore slows down the ink penetration speed in the coating structure. Moreover, PVOH dissolves and this may have an effect on the ink properties and binder transport during the penetration process.

It is also possible that PVOH binder can move into a pre-coating or base paper structure during the coating process and close up some of the smallest pores there too. The results show, that ink penetration speed depends on both capillarity and permeability. The capillary wetting force is most active in the finer pores, and once these become saturated then permeability is the controlling factor for further imbibition, this latter being even more dominant when external pressure is applied. The structure of SA latex bound coatings allow the ink penetration into the paper structure to occur faster than in PVOH bound coatings, since the SA-containing coatings are effectively more permeable.

The ink seems to stay initially on the top of the studied coatings displaying a quite similar delay before it penetrates into the coated papers, but the ink penetration speed in the coating layer is higher in SA bound coatings, especially under external pressure. This indicates that the ink diffusion in the PVOH binder happens as quickly as the ink flow in the SA-containing coating. The quicker ink penetration speed (as measured by the capacitive method, Clara) in the SA bound coating structure causes colorant transportation to the top part of base paper, and therefore print-through problems occur. The SA latex can neither bind ink colorant nor prevent bleeding compared with the inter-diffusion action of the ink liquid phase in the PVOH. The structural as well as chemical differences of coating layers determine the final inkjet print quality formation.

Literature

von Bahr, M., Kizling, J., Zhmud, B., Tiberg, F. (2000): Spreading and Penetration of Aqueous Solutions and Waterborne Inks in Contact with Paper and Model Substrates, Advances in Printing Science and Technology – Advances in Paper and Board Performance, 27th Research Conference of the International Association of the Research Institutes for the Printing, Information and Communication Industries, Sep.10-13, Graz, Austria, 88-102.

Cawthorne, J.E., Joyce, M., Fleming, D. (2003): Use of a Chemically Modified Clay as a Replacement for Silica in Matt Coated Ink-Jet Papers, J. Coat. Tech., 75(937), 75-81.

Donigian, D.W., Wernett, P.C., McFadden, M.G., McKay, J.J. (1998): Ink jet Dye Fixation and Coating Pigments, Tappi Coating/Papermakers Conference, May 4-6, 1998, New Orleans, LA, USA, TAPPI Press, Atlanta, GA 1998, 393-412.

Glittenberg, D., Voigt, A. (2001): Economic Formulations for Improved Quality Ink-Jet Papers, Paper Tech., 42(9), 25-29.

Hara, K. (2005): Speciality PVOH in Ink Jet Coating Formulations, Paper Tech., 47(3), 27-30.

Heilmann, J., Lindqvist, U. (2000): Effect of Drop Size on the Print Quality in Continuous Ink Jet Printing, J. Imaging Sci. Tech., 44(6), 491-494.

Khoultchaev, K., Graczyk, T. (1999): Polymer-polymer and Polymer-pigment Interactions – Implications on Ink jet Universal Media, Tappi Coating Conference, May 2-5, 1999, Toronto, Canada, TAPPI Press, Atlanta, GA 1999, 155-168.

Khoultchaev, K., Graczyk, T. (2001): Influence of polymer-polymer interaction on properties of ink jet coatings, J. Imaging Sci. Tech., 45(1), 16-23.

Lamminmäki, T., Puukko, P. (2007): New ink absorption method to predict inkjet print quality, Advances in Printing and Media Technology, 34th International Research Conference of iarigai, Grenoble, France, Sep. 2007, Acta Graphical Publishers, 231-239.

Lamminmäki, T., Kettle, J., Puukko, P., Gane, P.A.C., Ridgway, C. (2009a): Inkjet print quality: the role of polyvinyl alcohol upon structural formation of $CaCO_3$ coatings, International Paper and Coating Chemistry Symposium, 10-12 June 2009, Hamilton, Canada, 13 p.

Lamminmäki, T., Kettle, J. Puukko, P., Gane, P. (2009b): The role of binder type in defining inkjet print quality, 24th PTS Coating Symposium, Sept. 22-24, 2009, Baden-Baden, Germany, 15-1 – 15-2.

Lavery, A., Provost, J. (1997): Color-Media Interactions in Ink Jet Printing, in Proc. IS&T's NIP13 Conference, IS&T, Nov. 2-7, 1997, Seattle, Washington, USA, 437-442.

Malla, P.B., Devisetti, S. (2005): Novel Kaolin Pigment for High Solids Ink Jet Coatings, Paper Tech., 46(8), 17-27.

Miller, G., Jones, R., Boylan, J. (1996): Polyvinyl Alcohol – a Specialty Polymer for Paper and Paperboard, 1996 TAPPI Coating Binders Short Course, Baton Rouge, LA, USA, 9-10 Jan. 1996, TAPPI Press, Atlanta, GA 1996, 43pp.

Morea-Swift, G., Jones, H. (2000): The Use of Synthetic Silicas in Coated Media for Ink-jet Printing, Tappi Coating Conference and Trade Fair, May 1-4, 2000, Washington, DC, USA, TAPPI Press, Atlanta, GA 2000, 317-328.

Mäkinen, M.O.A., Parkkinen, J., Jääskeläinen, T. (2005): Generized Opacity based on CIELAB Color Coordinates and CIE94 Color Difference Formula, J. Pulp Paper Sci., 31(3), 61-67.

Mäkinen, M.O.A., Happonen, J., Sahivirta, J., Hartus, T., Paltakari, J., Jääskeläinen, T., Parkkinen, J. (2007): Color Difference Model for Estimating Print-through, J. Pulp Paper Sci., 33(1), 35-43.

Nilsson, H., Fogden, A. (2008): Inkjet print quality on model paper coatings, Appita, 61(2), 120-127.

Oliver, J.F. (1982): Wetting and Penetration of paper Surfaces, in Colloids and Surfaces in Reprogrphic Technology, M. Hair, M.D. Croucher, 435-453.

Pinto, J., Nicholasm M. (1997): SIMS Studies of Ink Jet Media, in Proc. IS&T's NIP 13 Conference, IS&T, 2-7 Nov. 1997, Seattle, Washington, 420-426.

Rousu, S., Gane, P., Eklund, D. (2005): Print quality and the distribution of offset ink constituents in paper coatings, Tappi J., 4(7), 9-15.

Rousu, S., Gane, P., Spielmann, D. (2000): Separation of off-set ink components during absorption into pigment coating structures, Nordic Pulp Paper Res. J., 15(5), 527-535.

Ryu, R.Y., Gilbert, R.D., Khan, S.A. (1999): Influence of cationic additives on the rheological, optical and printing properties of ink jet coatings, Tappi J., 82(11), 128-134.

Salerma, M. (1998): Menetelmä ja laitteisto nesteen imeytymisen mittaamiseksi väliaineeseen, Patent FI 102571 B (Issued Dec. 31).

Schoelkopf, J., Ridgway, C.J., Gane, P.A.C., Matthews, G.P., Spielmann, D.C. (2000): Measurement and Network Modeling of Liquid Permeation into Compacted Mineral Blocks, J. Coll. Int. Sci., 227(1), 119-131.

Svanholm, E., Wedin, P., Ström, G., Fogden, A. (2006): Colorant Migration in Mesoporous Inkjet Receptive Coatings, 9th TAPPI Advanced Coating Fundamentals Symposium, Feb. 8-10, 2006, Turku, Finland, TAPPI press, Atlanta, GA 2006, 221-228.

Svanholm, E. (2007): Printability and Ink-Coating Interactions in Inkjet Printing, Doctoral thesis, Karlstad University, Faculty of Technology and Science, Chemical Engineering, 2007:2, Karldstad 2007, 48 p.

Vikman, K., Vuorinen, T. (2004a): Light fastness of ink jet prints on modified conventional coatings, Nordic Pulp Paper Res. J., 19(4), 481-488.

Vikman, K., Vuorinen, T. (2004b): Water Fastness if Ink Jet Prints on Modified Conventional Coatings, J. Imaging Sci. Tech., 48(2), 138-147.

Yip, K.L., Lubinsky, A.R., Perchak, D.R, Ng, K.C. (2003): Measurement and Modeling of Drop Absorption Time for Various Ink-receiver Systems, J. Imaging Sci. Technol., 47(5), 388-393.

II/11

PAPER III

Limitations of current formulations when decreasing the coating layer thickness of papers for inkjet printing

Limitations of Current Formulations when Decreasing the Coating Layer Thickness of Papers for Inkjet Printing

Taina Lamminmäki,*,† John Kettle,† Hille Rautkoski,† Annaleena Kokko,† and Patrick Gane‡,§

†VTT Technical Research Centre of Finland, Bioliginkuja 7, FI-02150 Espoo, Finland

‡Department of Forest Products Technology, School of Chemical Technology, Aalto University, P.O. Box 16300, FI-00076 Aalto, Finland

§Omya Development AG, CH-4665 Oftringen, Switzerland.

ABSTRACT: The porous network structure of a coating layer has a major effect on how quickly inkjet ink penetrates into the coated paper, and how large the pore volume is determines the capacity for ink volume uptake within the coating layer. If the penetration rate and/or pore volume are insufficient, the ink colors stay too long on the surface, resulting in undesirable mixing (intercolor bleeding) and trans-surface wicking (feathering). The aim of this work was to clarify whether it is possible to decrease the coating layer thickness of the specialty inkjet layer and still produce an inkjet printed surface using dye-based inks with low bleeding and, thereby, to define the reasons for limitations with respect to coat weight reduction. The online study of printed figures following printing nozzles on a high-speed inkjet printing press, by means of optical image capture, showed that the tendency for intercolor bleeding depends strongly on the coating layer thickness. As the printing speed increases, the pore network structure of the coating layer becomes increasingly important. The results show that, under the external pressure, aused by the surface tension and impact of the ink droplets themselves, the permeability of the coating layer dominates after at least 4 ms from the time of ink application. The coating pigment selection and the amount of poly(vinyl alcohol) binder did not influence this permeability onset time. Permeability allows the required ink volumes eventually to be absorbed, even if the total porosity of the coating is insufficient at low coat weight.

1. BACKGROUND

A good-quality dye-based inkjet ink-printable paper currently means that the base paper is coated with special pigments and special binders.[1-3] A great deal of interest is focused on developing cheaper inkjet coatings with similar inkjet printability properties shown by the specialty coated papers available today. One way to reduce the costs of paper is to decrease the coat weight.

The pore size distribution and network structure of the coating layer, together with the type of binder present, determine how quickly ink penetrates into the available pore volume. It is the pore volume of the uppermost coating layer that provides the region where the inkjet ink can be held during the ink setting process.[4-6] The use of smaller-diameter pigment pores in the coating structure provides a coating layer that directs penetration of the inkjet ink droplets mainly in the z direction of the structure, rather than allowing them to spread along the structure[7] surface, and the inclusion of fine pores increases capillarity and, therefore, the sorption rate. This is one way to diminish the tendency for bleeding on coated paper. The speed of liquid absorption into the coating pore structure and the total amount of liquid penetrated have been studied in detail.[2,4,8-11] Several studies have also been reported in the literature on the potential for inkjet ink droplet penetration into coating layer structures that contain different coating pigments, binders, and additives as detected by means of the contact angle of a sessile or dynamic drop[2,7,12-14] or its volume change with time. In these studies, the ink penetration rate inside the coated paper structure was not clarified. More recently, the role of the surface morphology (roughness) of the underlying polymer layers present in the

highest-quality inkjet printing products has been studied in other applications, such as the printing of electronics.[15,16] The more basic phenomenon of low-viscosity liquid sorption in a capillary tube has also been studied,[17,18] but the diameters of capillaries in these studies were in the range of micrometers rather than nanometers.

Ridgway et al.[4] summarized the existing theoretical knowledge surrounding the sorption phenomena of coating layer structures by applying the Lucas–Washburn, Bosanquet, Szekely, and Sorbie equations and showing their relative merits and shortcomings when considering the short time scales involved during initial pore filling. The liquid front velocity upon first contact depends inversely on the radius of the capillaries. Later in the absorption process, the connectivity and pore size ratio dominate. The important controlling component in the liquid movement in an empty pore is the capillary element aspect ratio, that is, the length of the capillary divided by its radius, l/r. There seems to be an optimal aspect ratio for fastest filling, and it falls in the range $0.1 < l/r < 10$ for pores with $l < 100\ \mu m$. The limited aspect ratio range is due to the viscosity-independent initial stage of wetting predicted by Bosanquet and Szekely, occurring over ~10 ns, which favors entry into nanopores that are of similar dimensions in both radius and length. This knowledge related to the throatlike structures of capillaries provides a better

opportunity to simulate the liquid penetration process at the shortest time scales.

The penetration speed at different depths of the substrate structure, including the ability to transmit liquid into the underlying precoat or base paper, has not been studied as widely. In the area of offset coatings, the role of coat weight has been studied more. Xiang and Bousfield[19] showed, for example, that different drying conditions produced different pore structures in the coating layer. A low coat weight of clay/ground calcium carbonate blends (80/20 pph) produces more porous structures than a high coat weight. In a Micro-Tack tester analyzer, a low-coat-weight coating displayed a more rapid offset ink tack rise and earlier ink tack decay than the corresponding high-coat-weight coating. These effects are related to coating consolidation and shrinkage.

In contrast to the shortest-time-scale nonequilibrium capillary-induced absorption discussed above, equilibrium liquid uptake under external pressure and viscous laminar flow can be derived from the Navier—Stokes equation as the Poiseuille equation (eq 1), showing the connection between the penetration rate per unit cross-sectional area $[dV(t)/dt]$ and the equivalent permeation radius, r_{perm}, representing the unit area in question

$$\frac{dV_\alpha(t)}{dt} = \pi \frac{(r_{perm\alpha})^4 \Delta P}{8 \eta \Delta L} \qquad (1)$$

where $V_\alpha(t)$ is the volume of flow across a unit area of the sample (m³), t is the time (s), $r_{perm\alpha}$ is the permeation radius for a unit area of the sample (m), ΔP is the pressure drop (N m⁻²), ΔL is the sample depth (m), and η is the fluid viscosity (N s m⁻²).

Darcy's law (eq 2) is also a special solution of the Navier—Stokes equation and follows the condition of Poiseuille flow through the sample, such that there is a flux of liquid $[dV(t)/dt]$ forced through a saturated porous medium under the action of a pressure gradient[8]

$$\frac{dV(t)}{dt} = -\frac{K \Delta P}{\eta \Delta L} A \qquad (2)$$

The term K is the permeability of the porous medium. In the case of inkjet ink setting, K describes the flow when the wetting front lies deep within the coating structure or when the inertia of the impacting droplet causes initial penetration into the top layer of the coating. Darcy's law assumes that the pores fill completely with the liquid, that is, that permeation operates under conditions of saturation.

Alternative expressions have been established for penetration rate,[17] but the initial absorption into the fine pores was not taken into account in that study. More recently, Ridgway et al.[4] based comparisons on either inertial retardation or energy terms related to pore entry loss and adopted the interpretation of plug flow occurring in nanopores prior to the establishment of the viscous drag of liquid, together with inertial retardation prior to entry into large pores, following the Bosanquet expression.

The role of coating layer thickness on the inkjet-printed surface bleeding was studied by Nilsson and Fogden[3] and Glittenberg et al.[20] Their results showed that the coating pigment size has an effect on the inkjet-printed color range and print density. Larger pigment particles provided a lower print density, and with the larger pigment size, a higher coat weight gave a lower color range. Styrene—butadiene latex-containing coatings

Table 1. Coating Colors on the Plastic Film

component	color 1	color 2	color 3	color 4
PCC (specialty inkjet pigment)	100	100		
GCC (offset coating pigment)			100	100
PVOH	7	15	7	15

were shown to behave differently than coatings containing poly-(vinyl alcohol) or carboxymethyl cellulose.

The aim of this work was to clarify how inkjet ink penetrates through the different thicknesses of a coating layer and, thus, to the underlying precoat or base paper. The focus here is on the role of diffusion in soluble binders, which adds time-scale and pore-structure information to the original findings. Topcoatings were applied to wood-free fine paper using a curtain coater. The impact of coat weight on the inkjet ink imbibition was studied as a function of soluble poly(vinyl alcohol) (PVOH) binder. In addition to the commonly used measurements of paper properties, a capacitance-based liquid absorption device, Clara,[21] was used to determine ink permeation, and online imaging was used to monitor the bleeding tendency of two inkjet inks applied with a Versamark VX5000e high-speed inkjet press.

2. MATERIALS

2.1. Coating Colors on Plastic Film. Inkjet ink penetration into coating layers alone, having different thickness, was first studied by applying the coating color to impermeable plastic film. Table 1 introduces the studied coating color formulations. The high-porosity inkjet coatings contained a specialty precipitated calcium carbonate (PCC, JetCoat 30) from Minerals Technology Europe. The weight-median pigment particle diameter (NanoSight) was 20—30 nm, with a size distribution showing some larger particles in the range of 250 nm. The specific surface area [Brunauer—Emmett—Teller (BET), ISO 9277] was 73.9 m² g⁻¹, and the pigment had a primarily calcitic rhombohedral structure. The low-porosity coating constituted a typical offset-coating pigment consisting of ground calcium carbonate (GCC, Hydrocarb 90) provided by Omya AG. The weight-median pigment particle size was 0.65 µm, and the specific surface area was 10.7 m² g⁻¹. The binder was poly(vinyl alcohol) (PVOH, Mowiol 40-88 provided by Clariant International AG), which had a degree of hydrolysis of (87.7 ± 1.0)%. The colors were applied with an Erichsen draw-down coater using a speed of 1.4 m min⁻¹ and spiral applicators (Spiral Film Applicator, model 358). The coatings were dried for 5 min inside an oven at 105 °C.

2.2. Coating Composition in Curtain-Coating Trials. The role of coating layer thickness on the fine paper surface was studied with coatings containing the specialty PCC pigment (JetCoat 30). The coating colors had 7 or 15 pph of poly(vinyl alcohol) (Mowiol 40-88) based on 100 pph of pigment. All colors had 0.2 pph surfactant, Lumiten DF provided by BASF. Lumiten DF is the sodium salt of an ester of sulfosuccinic acid and an isotridecanol ethoxylate. The inclusion of surfactant acted to stabilize the curtain formation.

The coatings were applied to a precoated fine paper provided by Stora Enso having a grammage of 78 gm⁻². By using the precoated paper, we wanted to prevent the topcoating penetration into the base paper structure. The findings, therefore, are not directly transferable to rough nonprecoated substrates, in which the fiber-mat base paper frequently provides the absorption sink
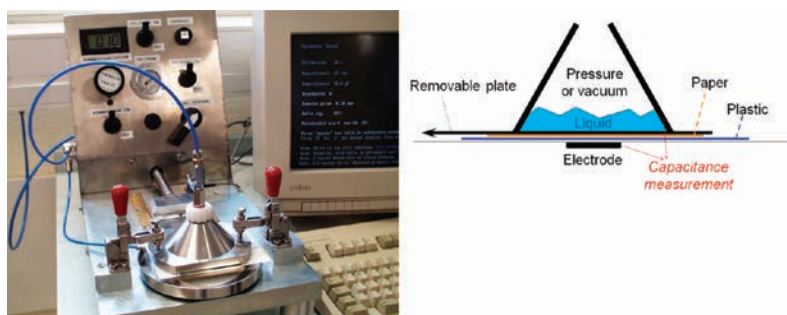
Figure 1. Clara device and its working principle.

in the case of lighter-weight inkjet coatings. However, the use of a typical low-cost precoat might be more effective with respect to cost/performance tradeoffs than the loss of specialty coating into the surface voids. Furthermore, the precoating layer can act as an absorption sink, preventing the wetting, and thus cockling, of the fiber base paper.

The coating trial was performed on a Metso pilot coater using a curtain slide applicator. The coating speed was varied from 1000 to 600 m min^{-1} depending on the weight of the applied coating. The highest speed was used when the coat weight was the lowest and vice versa. The final moisture content of the coated web was 5.1−5.4 wt %. This means that the drying temperature had to be increased when the coat weight was high. It was not possible to achieve a coat weight of 10 gm^{-2} with the 7 pph PVOH-containing coating because of the low solids content of the color. The coated papers were printed with a Versamark VX5000e high-speed inkjet press, which had aqueous-based dye inks.

3. TESTING METHODS

The thickness of samples was measured according to standard ISO 12625-3:05. The air permeance of coated papers was measured using a Parker-Print Surf testing machine (20 kPa) following the ISO 5636/1 standard. The porosity of coating layers was measured independently by silicon-oil absorption at 1 bar pressure and by mercury porosimetry. In the Si-oil measurement, the porosity was calculated from the weights of dry and Si-oil-immersed samples. The results reported are the averages of three measurements each. A Micrometrics AutoPore IV mercury porosimeter was used, including the Pore-Comp correction to account for penetrometer expansion, mercury compression, and compression of the sample skeletal material, expressed in terms of cumulative pore volume, according to the method Gane et al.[22] The contact angles of water on the surfaces were measured with Fibro 1100 DAT instrument with a 2 μL drop, as the apparent contact angle after 0.1 s.

The absorption time of ink was measured with a DIGAT device (Dynamic Ink Gloss and Absorption Tester).[11] It measures the absorption time by detecting changes in the gloss level as the surface liquid retreats into the pore structure and the remaining ink components dry. The measurement started from the moment the ink arrives at the surface and lasted until the gloss of the ink reached an equilibrium value. Ink was applied on the surface with a glass capillary tube, using the ejector principle, and the ink formed an even layer on the paper surface. The light

source was a laser (wavelength = 633 nm). The detector part in the DIGAT apparatus measures the voltage from the glossmeter as a function of time. The laser beam and the detector were both fixed at an angle of 20° to the horizontal surface. The results are given in terms of absorption time corresponding to the time between 90% of the maximum gloss value and 10% of the equilibrium liquid saturation gloss value. In this measurement, the ink was an anionic aqueous dye-based ink from a Versamark VX5000e high-speed inkjet press. The applied ink amount in the device was 8 gm^{-2}.

The inkjet ink penetration in the coating layers and base paper was studied with a capacitance-based device, as shown in Figure 1. The measuring principle is based on the fact that the resistivity of a dry surface is very high, whereas a moistened paper and inkjet ink conduct electricity. The liquid, therefore, forms a conducting material whose movement affects the capacitance between the liquid chamber above and an electrode beneath the studied sample. Figure 1 (right side) shows a schematic illustration of how the Clara device works. The chamber can be pressurized from −0.5 to +5 bar, which allows a pressure to be generated for the ink-transfer region that is similar to what might occur due to the impact of the ink droplet in actual inkjet printing. Although this pressure refers to impact only, it is probably one factor that initiates wetting. Its continued presence has an effect on the penetration. The measuring area was 6.8 cm^2. The area over which the applied liquid covered the sample surface was clearly larger than the detection area, and therefore, the wetted area next to the detection area limited sideways liquid motion. The level of capacitance to be measured was preadjusted to be on the correct expected level, derived from experience, in order to maximize sensitivity.

To evaluate the relation between the penetration depth and the capacitance value, a further experiment was made using coating filtercakes of PCC and PCC with 7 pph SA latex (thickness 294−540 μm) into which different amounts of molten candle wax, containing a colorant for ease of observation, had been allowed to absorb. The wax partially filled the porosity of the coating structure and, therefore, simulated the liquid front at a certain depth within the sample. Wax has a capacitance similar to that of the relative highly porous inkjet PCC coating, and importantly, it has a capacitance greater than air. Thus, as air is replaced by wax in the coating structure, provided that the wax does not interfere with skeletal connectivity, the capacitance would be expected to rise. The capacitances (averages of results between 1 and 1000 Hz) and the wax imbibition distances (relative distance = wax distance divided with the sample
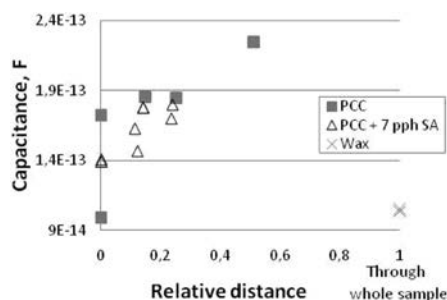
Figure 2. Connection between relative distance and capacitance determined using molten candle wax, containing a colorant for ease of observation, imbibed into coating filtercake structures. The samples were PCC and PCC with 7 pph SA latex cakes.

thickness) were measured. As the depth of wax increased, higher capacitances were observed (Figure 2). (Note that, in this case, we could not use the original Clara capacitance-based device because the samples were too small for the detector. Therefore, we used a device that had a round electrode with a 5-mm diameter.) The device produced a reference value for the dielectric constant of plain candle wax, similar to, for example, those of polyethene and Teflon, which have dielectric constants of about 2.25 and 2.1, respectively. The action, therefore, was confirmed to be that of wax replacing air in the coating structure, as wax has a higher dielectric constant ($\sim$2) than air ($\sim$1).

It can be imagined that a deviation from this increase in capacitance could occur if the skeletal connectivity of the porous structure were disrupted by the uptake of the dielectric material and that the connectivity itself would contribute to the dielectric properties. However, a polar liquid (i.e., water in inkjet ink) increases the conductivity of the sample markedly more than such a change could manifest itself, so that the capacitance method can be considered valid for the uptake of conductive liquids.

Before the actual sample measurement, the capacitance of a plastic film, used as a fixed-point backing, was evaluated and recorded; it was found to be approximately 190 pF. The sample testing was then started. First, the liquid was applied to the chamber and pressurized. The capacitance measurement started when the removable plate was taken away and the liquid started to penetrate the substrate. The plate had to move for 3.8 ms before it had moved away from the detection area. The capacitance was measured at 1-ms intervals. The liquid amount applied was clearly higher than that used in actual inkjet printing, and the pressure had an effect throughout the measurement time. The final result was a curve of capacitance change over time, and each sample was measured five times in parallel. In practice, an external pressure of 0.1 bar was used as representative of the internal pressure caused by the impact of the inkjet droplets. This corresponds to an inkjet ink droplet with a size of 15 pL (used in Versamark VX5000e high-speed inkjet press) flying with a velocity of 15 m s^{-1} causing about 0.1 bar of pressure on the surface. The dye-based cyan ink, from the Versamark VX5000e set, expressed a surface tension of 52.8 mN m^{-1} at 25 °C and a viscosity of 1.1 mPas. In the inkjet printing, the pressure that the droplet impact causes to the paper surface is only initially present. In the Clara experiment, the external pressure affected the entire measuring time, even after the initial wetting. However, the

pressure was relatively small compared to the pressure of capillaries. The amount of ink applied was 5 cm^3 to provide an initial supersource. Some disturbances could appear in the results during the first few milliseconds in time because of the plate movement, and the area over which the ink made contact with the coating layer increased during the plate movement as well. To ensure similarity between the curtain-coated surfaces on precoated base paper and the pure coating structure on plastic film, a corresponding plastic film layer was placed behind the paper samples. The Clara device was also operated during a second measurement regime under a negative pressure (-0.1 bar). The aim of this experiment was to reduce the impact of externally driven permeability, such that capillarity acted initially to fill pores and, subsequently, the air permeation due to the negative pressure led to an equilibration of the wetting front.

If the thickness of the coated paper is known, one can calculate the penetration speed, assuming that the liquid has penetrated through the entire available structure behind the wetting front. This approximation is equivalent to the so-called Darcy approximation of length penetrated as a function of volume and filled porosity. That it is not the case was predicted by the work of Ridgway et al.[4] and the experimental work of Gane and Koivunen.[23] Nonetheless, it is a representative average approximation. The paper thickness, d_{paper}, in the z direction, can be divided into two parts: the thickness of the wet sample, $d_{wet}(t)$, and that of the dry sample, $d_{dry}(t)$.

$$d_{paper} = d_{dry}(t) + d_{wet}(t) \qquad (3)$$

The wet part contains ink, and this increases the capacitance values. The total capacitance, C_{tot}, is the capacitive impedance series sum of the plastic capacitance, C_{pl}, coming from the plastic sheet under the sample and the sample capacitance, $C(t)$

$$\frac{1}{C_{tot}} = \frac{1}{C(t)} + \frac{1}{C_{pl}} \qquad (4)$$

The total wetted paper has practically no impedance (pure conductor), and thus, the capacitance depends on the thickness of the dry paper

$$C(t) = \frac{A\varepsilon(\omega)}{d_{dry}(t)} \Rightarrow d_{dry}(t) = \frac{A\varepsilon(\omega)}{C(t)} \qquad (5)$$

where A is the area and $\varepsilon(\omega)$ is the dielectric permittivity of the dry material at frequency ω. The permeability can be further expressed as the product $\varepsilon(\omega) = \varepsilon_0 \varepsilon_r$ of the vacuum permittivity ε_0 and the relative permittivity of the material ε_r. At the end of the measurement, when the whole paper has been wetted, the paper has no impedance (= 1/capacitance). Thus, the plastic capacitance can be estimated to be the total capacitance at the end of the measurement [$C_{pl} = C(t=\infty)$].

The thickness of the wet part of the paper, which we estimate to be the penetration depth of the water front, can be calculated by combining eqs 3–5

$$d_{wet}(t) = d_{paper} - \frac{A\varepsilon(\omega)}{C(t)} = d_{paper} - A\varepsilon(\omega)\left(\frac{1}{C_{tot}} - \frac{1}{C_{pl}}\right) \qquad (6)$$

III/4

Table 2. Porosity of Speciality PCC and Standard GCC Coating Cakes Measured with Silicon Oil Absorption

| sample	Si oil porosity (%)
PCC 7 pph PVOH	48.3 ± 0.1
PCC 15 pph PVOH	37.0 ± 0.3
GCC 7 pph PVOH	39.1 ± 0.2
GCC 15 pph PVOH	21.5 ± 5.4
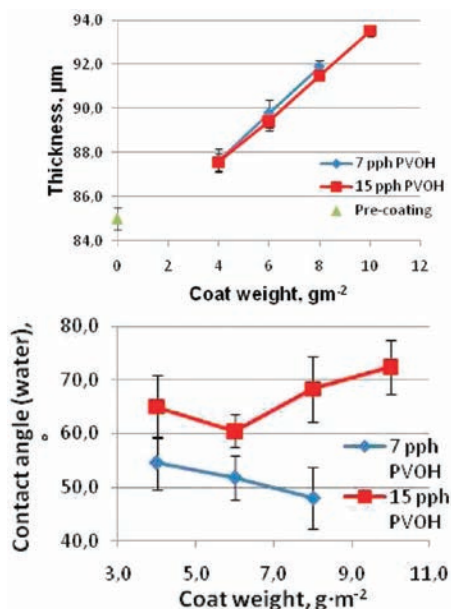
Figure 3. Thickness (top) and contact angle (water at 0.1 s, bottom) of PCC-coated papers.

The final $d_{wet}(t)$ equation used is

$$d_{wet}(t) = d_{paper} \left[1 - \frac{\dfrac{1}{C_{tot}(t)} - \dfrac{1}{C_{tot}(t = \infty)}}{\dfrac{1}{C_{tot}(t = 0)} - \dfrac{1}{C_{tot}(t = \infty)}} \right]$$

(7)

4. RESULTS

4.1. Intrinsic Properties of Coating Layers Measured on Plastic Film. Table 2 lists the results of Si-oil porosity measurements for the inkjet specialty PCC and offset standard GCC coating layers. The inkjet specialty PCC coatings, as expected, had higher porosities than the offset standard GCC coatings at comparable PVOH binder doses. Our previous study,[24] in which we used the same pigments with 10 pph of the same PVOH binder, also showed that the specialty PCC coating not only produces a coating layer with a higher pore volume but also displays a significantly greater pore volume associated with the smaller-diameter pores (20−70 nm) than the standard GCC
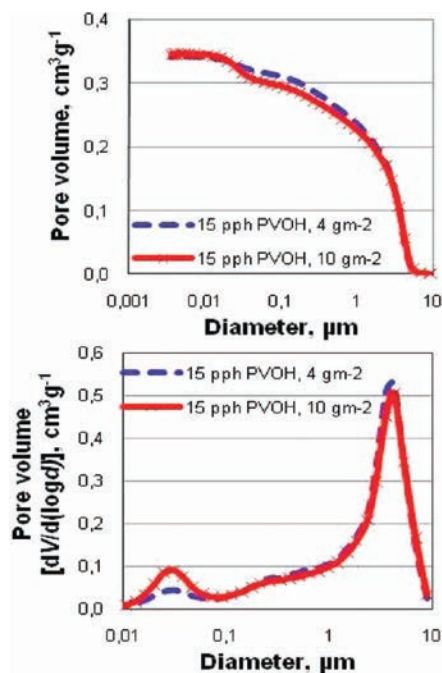
Figure 4. Cumulative pore volume (top) and first derivative of the pore size distribution (bottom) of inkjet PCC with 15 pph PVOH coatings with 4 and 10 gm^{-2} coat weight on standard precoated paper, measured by mercury porosimetry.

coating. The GCC coating, in contrast, has more specific pore volume in the range of 0.1−0.3 μm.

4.2. Basic Properties of Curtain-Coated Papers with Specialty Inkjet PCC. The thicknesses of curtain-coated papers are illustrated in Figure 3. At a defined coat weight, the 7 and 15 pph PVOH specialty PCC-coated papers had very similar thicknesses, and a link exists between the pore volume and coating thickness for these coatings. Figure 4 shows how the 10 gm^{-2} coating provided a higher specific pore volume to the coated paper than the 4 gm^{-2} coating. In addition, the 10 gm^{-2} coating structure had slightly less pore volume associated with pore diameters of >1 μm, whereas it had more 20−60-nm-diameter pores. Importantly, there appears to be no difference in the characteristics of the pore size distributions; that is, no additional peaks occurred to differentiate between the coat weights to suggest any major changes in coating structure. This effect on specific pore volume size distribution, therefore, closely represents the proportion of specialty coating in relation to the total paper.

The contact angle of water (at 0.1 s) in equilibrium is seen in Figure 3. Both the 7 and 15 pph PVOH coatings were hydrophilic, and the 7 pph PVOH-containing coatings provided lower contact angles than the 15 pph PVOH coatings. It seems that the 15 pph PVOH-containing coatings were, therefore, less hydrophilic than the 7 pph PVOH-containing coatings, although binder swelling might act as a pinning mechanism. Furthermore, the roughness of the 7 pph PVOH coatings was on the level of 90 mL min^{-1} (Bendtsen), whereas that of the 15 pph PVOH
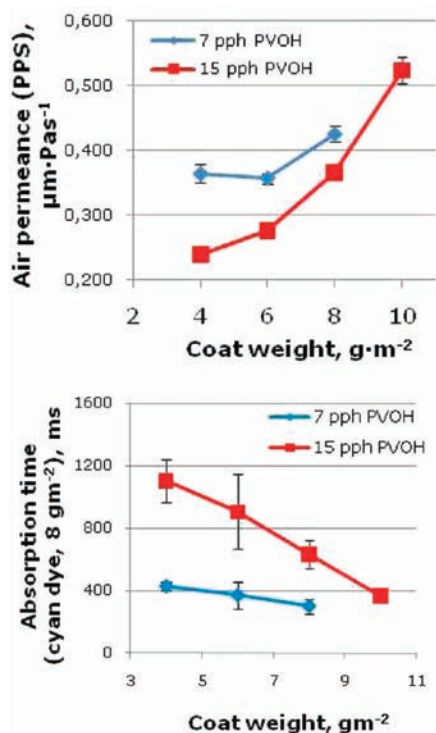
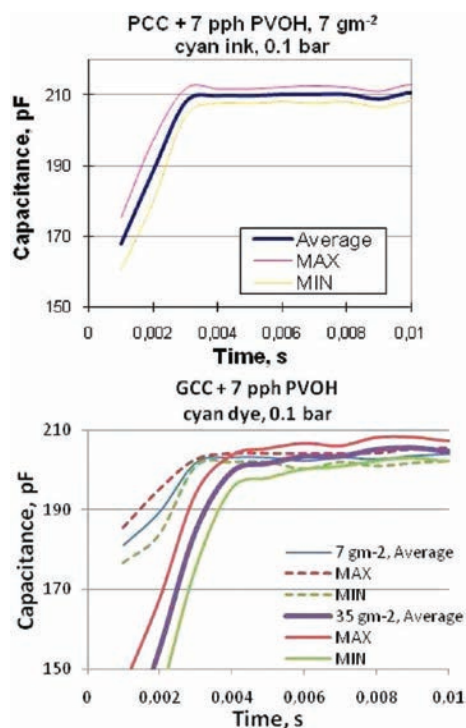**Figure 5.** Apparent air permeance (top) and ink absorption speed (bottom, DIGAT device, dye-base ink amount 8 g·m^{-2}) of specialty inkjet PCC-coated papers.

Figure 6. Two examples of the average and confidence interval of results from coatings during Clara measurements. The examples are from the inkjet specialty PCC coating containing 7 pph PVOH and the standard offset GCC with 7 pph PVOH on the plastic film surface. The ink was dye-based cyan ink, and the measuring pressure was 0.1 bar.

coatings was 120 mL min^{-1}, and this might be an additional reason for the contact angle difference.

The air permeance results for the specialty inkjet coatings are shown in Figure 5 (top). The higher the coat weight, the greater the apparent air permeance. This result is different from the results of Xiang and Bousfield,[14] who studied offset coatings. The difference is directly due to the measurement technique and its relation to the paper structure. Air permeance is measured by applying an external pressure to force air through the paper sheet. It is, however, not a suitable method for determining the permeability of layered structures where, for example, a significant coat weight of a more permeable layer is applied on top of a less permeable layer. In this case, the precoat forms a less permeable layer than that generated by the specialty inkjet coating. Instead of passing through the complete sheet, the air is directed by preferential permeability laterally through the more permeable top layer, escaping proportionally to the sides of sample. Thus, as coat weight increases, so do the effective permeation radius and escape path length (eq 1), and one can see, in Figure 5 (top), that the effect is therefore exponential as a function of coat weight.

The absorption speeds of 7 pph PVOH coatings were very near each other (Figure 5, bottom), being only slightly dependent on coat weight. The 15 pph PVOH coatings, however, although exhibiting slower absorbance than the lower-binder-level coatings at low coat weights, gradually absorbed more

rapidly as the coat weight increased, approaching the speeds of the lower-binder-level coating at the highest coat weights. This behavior reflects the relative total porosities of the coating layers, which are the sums of the available pore volumes per unit area of liquid contact. This pore volume available for absorption is controlled by binder level (more binder reduces it) and coat weight (higher coat weight increases it). That the two coating structure types have absorption rates that approach each other asymptotically at higher weights shows that the final absorption rate is determined by permeability once sufficient pore volume is present. All of these results show that the structures of the coating layers differ from each other mainly as a function of binder level. The function of coat weight relates primarily to the total available pore volume for a given binder dose. Thus, at this stage, it is possible to state that the differences are due mainly to the structural changes in the total sheet as the coat weight of the specialty layer changes (i.e., they are related primarily to the topcoat/precoat ratio). The presence of a higher dose of PVOH clearly plays the major role in reducing the absorption efficiency by limiting the available pore volume per unit absorption time, and because PVOH itself absorbs water by interpolymer network diffusion, this dependence most likely is manifested as one of diffusion rate.

7256

dx.doi.org/10.1021/ie102114s |Ind. Eng. Chem. Res. 2011, 50, 7251–7263
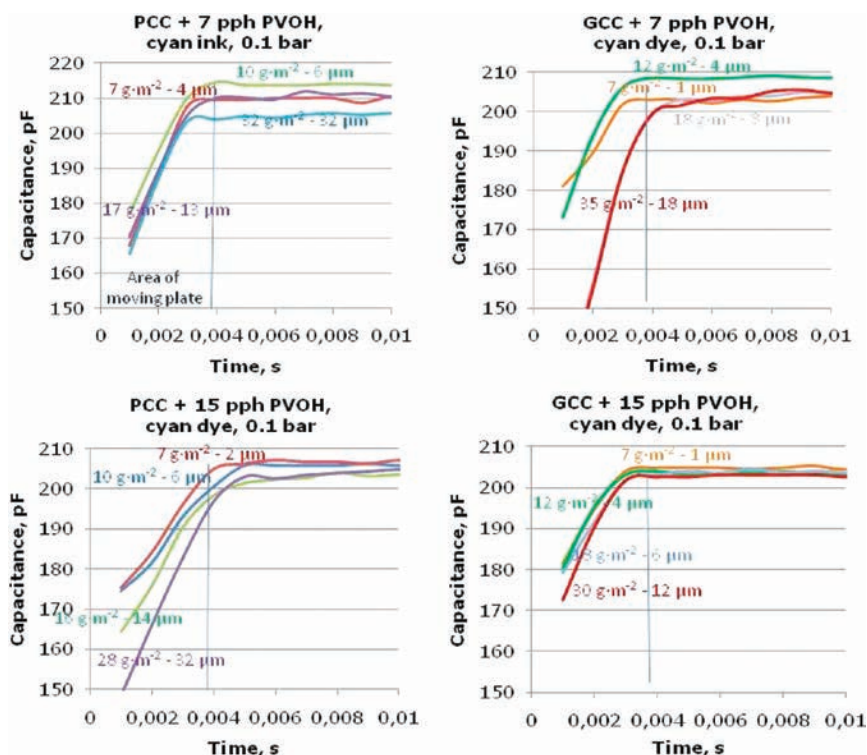
Figure 7. Effect of coating layer thickness on capacitance (Clara). The inkjet specialty PCC and offset standard GCC coatings in this case were on plastic film. The thickness of each coating layer was added after the coat weight value. The ink was cyan dye-based ink from a Versamark VX5000e inkjet press. The final capacitance level of Clara results was found to depend on the variation of the used plastic film (204—212 pF).

4.3. Clara Liquid Permeation Measurements. *Coating Layers on Impermeable Film.* The reproducibility of the results from the Clara capacitance device can be seen in the examples shown in Figure 6. One can, with confidence, differentiate the results of different coating thicknesses in the case of the GCC coatings, as they lie well outside the limits of variation. From this finding, one can assume that, if the results for different coatings appear similar to each other, despite differences in coat weight, then the liquid transport properties are the same, as in the case of specialty PCC coating containing 7 pph PVOH (Figure 7).

Figure 7 shows, first, that the inkjet specialty PCC coating provided thicker coating layers than the offset standard GCC coating at an equivalent coat weight. The GCC pigment forms a more tightly packed coating layer structure, as indicated by the Si-oil porosity results.

We expect that the ink would penetrate through the thinner coating layer in a shorter time than it would penetrate through the thicker one, and this is evident in the results of the Clara device. Figure 7 shows how the cyan dye-based ink penetrated very quickly through the whole of the applied coating layers at 0.1 bar of external pressure. Most of the result curves reached the maximum value of capacitance during a time of 0.004 s. The removable plate transferred out of the measuring area during the first 0.0038 s, and therefore, the results of the first millisecond of time are highly affected by the plate removal, as well as the fact that the detection area was not yet completely covered with ink.

Thus, one must remember that the results are reliable when using the Clara device only after 0.0038 s. If the results of the first milliseconds in time are studied more closely, it seems that higher coat weights on the film were associated with lower locations of the starting point of the capacitance curve. The lower starting point difference relates to the absorption occurring nonuniformly during the removal of the covering plate. The correspondence to the inverse relation of capacitance with sample thickness is taken into account in the measurement, and, therefore, the relative capacitances reflect structural/compositional differences with respect to the dielectric constant of the medium created. Once again, this relates to the increasing portion of the specialty layer as a function of coat weight.
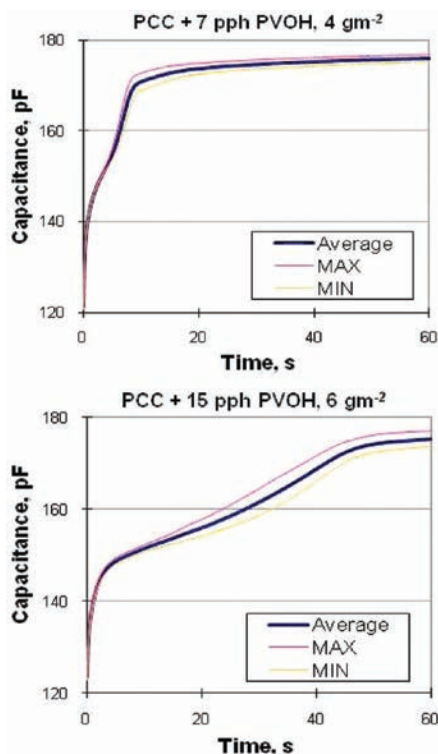
The capacitance results of specialty PCC coating layers exposed to liquid ink on the plastic film under the influence of negative pressure (−0.1 bar vacuum) are illustrated in Figure 8. The capacitance was highest in the beginning of the measurement, and it decreased over time, indicating the removal of liquid from the permeation-controlling pore structure.

Curtain-Coated Papers. The reproducibility of coated paper results is illustrated in Figure 9. There was no significant variation in the results from repeated measurements on fresh samples from a single example coated paper, indicating that the paper had a uniform structure and that the measurement was reproducible.

The inkjet coatings applied to the precoated paper were studied first with an external pressure of 0.1 bar to measure
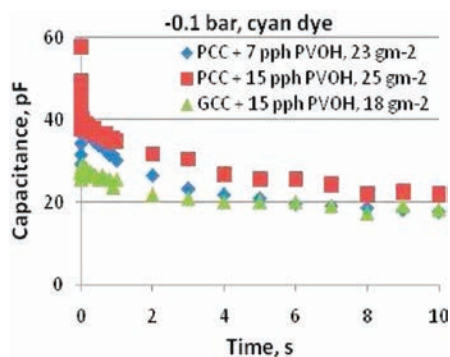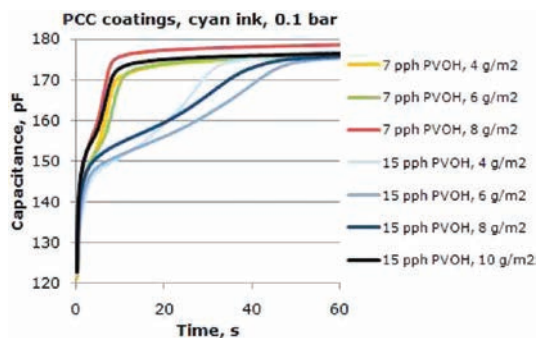
Figure 8. Capacitance results of cyan ink under the influence of −0.1 bar vacuum. The inkjet specialty PCC and offset standard GCC coatings in this case were on the plastic film. The ink was cyan dye-based ink from a Versamark VX5000e inkjet press. The final capacitance level of Clara results depends on the variation of used plastic film (18−22 pF).

Figure 10. Effect of coat weight on the penetration of cyan inkjet ink in the inkjet specialty PCC coatings that contained 7 and 15 pph of PVOH. The external pressure of the Clara measurement was 0.1 bar.

Figure 9. Two examples of the average and confidence interval of inkjet specialty PCC-coated papers measured with the Clara device. The average, minimum, and maximum values were calculated from the results of five parallel measurements of each sample.

liquid permeation. The bimodal behavior of each curve (Figure 10) illustrates the competition between the initial capillary wetting and the permeable flow characteristic once

the capillaries/pores are filled. At equivalent coat weights, the 15 pph PVOH coatings exhibited longer liquid penetration times through the sample than the 7 pph PVOH coatings. The ink penetration through the structure of the 7 pph PVOH coatings took from 7.5 to 11 s, and that through the 15 pph PVOH coatings took from 8 to 50 s. Thus, a higher amount of PVOH decreased the coating layer porosity and permeability. Therefore, it took more time for ink to penetrate through the coating layer, and because the permeability was reduced, it took longer to force liquid through the top layer into the substrate. Additionally, a higher PVOH amount likely leads to more migration of the PVOH into the underlying structure.

From the air permeance point of view, the 7 pph PVOH coatings with 4 and 6 gm^{-2} and the 15 pph PVOH coating with 8 gm^{-2} were very similar. The capacitance-based results were partly in harmony with these results, especially during the first second. However, the data points after 1 s diverged and the ink went through the 15 pph PVOH coating surfaces slower than through the 7 pph PVOH coatings. The results of DIGAT device showed a similar difference. On the other hand, the capacitance and DIGAT results were very similar in the case of the 8 gm^{-2} 7 pph PVOH coating and the 10 gm^{-2} 15 pph PVOH coating, but the air permeance of the 15 pph coating was higher because of the greater lateral cross section associated with its increased coat weight.

5. DISCUSSION

5.1. Ink Penetration in Coating Layers on Film. The results in Figure 7 show that inkjet ink from the applied supersource volume more or less penetrates through the coating layer, even though it is up to 35 μm thick, during 0.004 s of time at an external pressure 0.1 bar, and all resulting curves look very similar regardless of the coating pigment type, the binder amount, or the thickness of the coating layer. It seems that capillary absorption in the coatings occurs on a time scale equal to or shorter than 0.004 s. In contrast, for time delays longer than 0.004 s, permeation flow dominates in the coating structures. These results agree very well with the results of Ridgway et al.[4,25] With a Pore−Core computer model of void structure, they calculated how quickly alcohols and water move in the coating layer structure. They concluded that smaller-radius capillaries initially fill faster than larger ones. The fine capillaries were found to fill faster until 0.00026 to 0.00056 s,
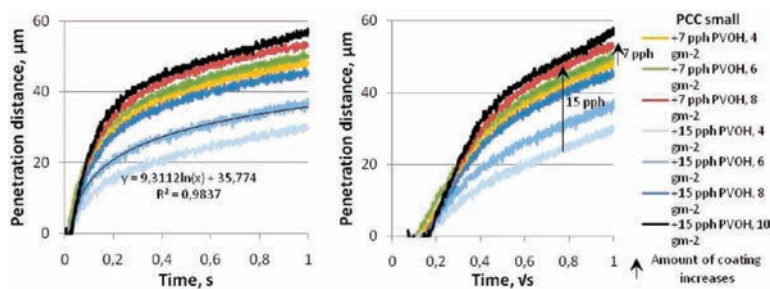
Figure 11. Penetration distance of dye-based ink in the inkjet specialty PCC coatings as a function of time and square root of time, respectively, clearly showing the two regimes of absorption, measured with the Clara device at a pressure of 0.1 bar using cyan dye-based ink.

depending on the equation used, and after this time, the larger capillaries started to fill at a higher rate.

The results indicate that the capillary flow of the coating layer is too fast for the Clara device. Using the Bosanquet absorption equation,[26] which takes into account the inertial flow of liquid, the speed of absorption into a 0.1-μm-length pore is below 10 ns.[4] However, the Clara device starts the detection at 1 ms. This means that the coating passed by the first preferred-pathway wetting front in an idealized free-access structure (nonpermeability limited) is about the scale of 1 cm. The maximum coating thickness used was 32 μm, which, because the network is complex, probably does not exhibit centimeter-scale pathways for ink, but is highly likely to have been traversed completely by the ink meniscus front in this relatively long time scale in absorption terms.

The starting points of capacitance curves (Figure 7) seemed to be located at lower levels when the coat weight was increased. This means that thicker coating layers had more open pore volume during the first few milliseconds of absorption than thinner ones. However, one must remember that, during the first 0.0038 s of time, the detected area was still increasing because of the plate movement during removal. The area increased during this time, and the ink transferred deeper into the coating layer of the starting edge than near the plate edge. Nonetheless, this provides more likely evidence for the preferred-pathway wetting phenomenon, described by Ridgway et al.,[4,25] as a greater proportion of pores are initially bypassed as the length of the sample increases.

The capacitance results under a vacuum indicate that, at first, the ink penetrates some way into the coating structure, and therefore, the highest capacitances occur during the first 0.007 s. Then, the absorbed liquid retracts and saturates to the level of 18–22 pF. This suggests that a migration of liquid occurs after the first capillary absorption as the pore structure fills ever closer to the wetting front, forming a nonpermeable liquid layer that then gets drawn under the negative pressure to the top surface. The PVOH-containing coatings have a hydrophilic and hygroscopic nature, and therefore, the capillary rise depends on the bulk concentration of surfactants in the ink and the surface tension of the liquid/vapor interface that has already developed at the contact with the capillary.[12] Additionally, the water diffuses rapidly into the PVOH polymer network. It seems that these PVOH swelling forces lead to a closure of air permeability, so that the ink is effectively forming a mobile but impermeable barrier within the coating that is forced back to the surface layer of coating by the negative pressure of the vacuum. A strong positive

capillary pressure is therefore required before the liquid starts to equilibrate again in the capillaries.

5.2. Ink Penetration in Curtain-Topcoated Papers. Figure 11 shows how the penetration distance of dye-based ink develops differently depending on coating layer structure and, thus, especially in 15 pph PVOH-containing coatings. In general, the ink penetrates deeper in a given time when the paper has a higher ink absorption speed. The 7 pph PVOH-containing coatings were quite similar, and the curves of ink penetration were located very near each other. At equivalent coat weights, the ink has penetrated less into the coating structure containing 15 pph PVOH than into that containing 7 pph PVOH. Figure 11 illustrates that, in the beginning of the absorption into the specialty inkjet coated paper, the penetration distance results have quite a linear relation to the square root of time, indicating either equilibrated Poisueille laminar flow according to the long-time-scale-applicable Lucas–Washburn equation and/or a Fick's law diffusion response. However, there seem to be two linear regions with respect to the square root of time during the first second: the first from the beginning to a time of 0.2 s and the second from 0.2 s onward (Figure 11). This result agrees with the results of the study of PVOH-containing coatings reported by Ström et al.[2] In the first linear region, the properties of the coating layer structure predominantly affect how the ink will move there, and in the second region, the porous structure of the base paper influences how the ink moves. This turning point seems to be located at a distance of 15–35 μm into the coating, depending on the coating layer thickness. The thicknesses of the applied curtain-coating layers were between 2.5 and 8.5 μm (Figure 3). It was impossible to measure the thickness of the precoating layer directly, but it seems that the turning point was located neither in the precoating layer nor just under it. The turning point was located deeper within the base paper. This suggests either that the fiber base paper is effectively a zero-resistance layer in comparison to the coating structures or that the poly(vinyl alcohol) has also penetrated deeply, rendering the diffusion effect active throughout the sheet. If the external pressure had been lower, then the role of diffusion would have been even higher. In the coating layer immobilization process, PVOH can penetrate into the deeper areas of the paper structure, thereby affecting the porosity of the top layer of base paper, effectively making it a continuation of the coating itself. On the other hand, PVOH swells under the influence of water-based ink, which will act to close the smallest pores and diminish the pore diameters during the ink penetration. PVOH can also dissolve partially into the inkjet ink during the penetration process,

thereby affecting the liquid properties. The precoating penetration into the base paper could be a further reason. This result suggests that, in the structure of swelling PVOH, the movement of ink after the first capillary-driven absorption follows a diffusion rate according to the PVOH liquid uptake. In parallel, the longer-time-scale absorption becomes permeability-limited, and so, as the relevant short-time-scale equations of Bosanquet and Szekely predict, the mechanism collapses back into equilibrium-viscosity-controlled flow.

If the results on coated plastic film and those for the same coating color on the paper surface are compared, one can notice that, on the paper surface, at 0.05 s, the ink has penetrated a distance of 8.5 μm, whereas on the plastic film coating, it took only 0.004 s to penetrate a 32-μm-thick coating. In the case of the coating layer on the plastic film, there is more or less a single well-defined pore size distribution and porosity, which provides a system wherein the ink moves more or less uniformly at the same rate through the coating layer. Furthermore, on plastic, all applied coating components are located in the coating layer. On paper, the coating layer is less uniform, and there are permeable regions where the liquid can be forced under pressure through the coating into the substrate pore structure, delaying the effective penetration into the neighboring intact coating structure. With respect to imbibition mechanisms, the capillary flow is first active in the finest pores, and once these surface capillaries become saturated, the permeability becomes the controlling factor for further imbibition. When coated on plastic, the ink, once having penetrated through the coating layer, can spread only in the coating layer edge structure areas because of the nonpermeable nature of the film. In the case of coated papers, the structure contains different layers, namely, the topcoat, the precoat, and ultimately the base paper, with very different pore-size distributions and porosities. The PVOH applied in the topcoat layer can be partially located in the precoating and/or the base paper, and therefore, the ink does not proceed at the same rate through the whole structure. The coating layer has more fine pores than the base paper, and therefore, the ink transfer is faster with respect to pore-filling rate. In the case of polar inkjet ink, the diffusion into the hydrophilic matrix of both the coating layer and the base paper affects the ink movement dynamic by changing the effective small capillary diameters, where the swelling polymer is located and, hence, the uptake amounts in these structures during measurements. We can conclude that capillary flow dominates in the coating layer on plastic, but in the case of coated paper, which has only a 10 gm^{-2} coating, it is hard to see the capillary effect with the Clara measurement while permeation dominates. Permeation flow and diffusion, therefore, dominate with respect to volume imbibition when lightweight coatings are applied to paper.

Figure 12 shows how the penetration speed into the specialty coated paper decreased in the coated paper structures when the ink moved deeper into the layer. The penetration front curves of 7 pph PVOH-containing coatings are very near each other, and the coat weight differences in the coatings had very minimal effect on the penetration speed, suggesting that the coatings have very similar structures and are not permeation-limited, such that the coating layer thickness has a very small impact on the speed of ink penetration in the 7 pph PVOH-containing coating layers. On the other hand, in the 15 pph PVOH-containing coatings, there was clearly a greater difference in the apparent air permeance, related to the increased lateral cross-sectional area for air escape balanced by the increased binder dose, and in the
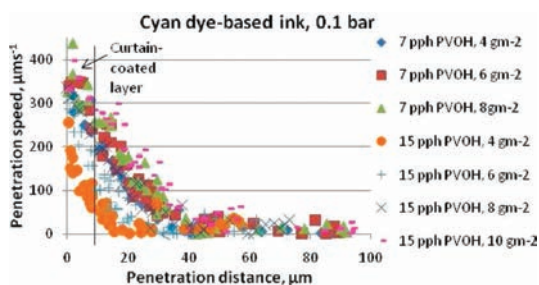

Figure 12. Penetration speed of commercial cyan ink at the different layer depths in specialty inkjet pigment topcoated paper, having a standard offset precoat and woodfree base paper, measured with the Clara device using cyan dye-based ink at an external pressure of 0.1 bar.

absorption speed. This could be readily detected in the Clara capacitance results. The ink penetrated with higher speed in the thicker coating layer, showing that it was pore-capacity-limited because of the extra binder. No unambiguous connection was found between the results for the contact angle of water and penetration speed in the coating layer. The reason might be in the contact angle measurement itself, where the coated surfaces had different roughness levels, but also in terms of the dominance of structural effects. The results at coat weights of 4 and 6 gm^{-2}, however, did indicate that a lower contact angle results in faster inkjet ink absorption, as might be expected.

Ridgway et al.[4] indicated that the coating structure has an optimal aspect ratio for the fastest filling of liquid into individual pores, and the optimum seems to be located in the range 0.1 < l/r < 10, where l is the length and r is the radius of the pores. For pores of 30-nm diameter, this means that the length of the pores in the optimal range is between 3 and 300 nm. One might expect to have this type of pores in the lowest-coat weight structure, too (i.e., at a coat weight where the connectivity is not yet fully established, so that the longer-term flow is not permeability-limited in the specialty layer). The mercury porosimeter results indicated that the specialty coating with 15 pph PVOH at a coat weight of 4 gm^{-2} had a smaller volume of 30 nm size pores than did the 15 pph PVOH coating at the higher weight of 10 gm^{-2}. In the case of 500-nm-diameter pores, the specific pore volume values spanning from 50 nm to 5 μm indicate that the low-coat-weight coatings with 2.5 μm thickness can hardly work in the fastest filling area. To achieve the fastest filling area by means of large-pore-diameter coatings, the thickness of the coating layer should be greater. By planning the coating layer so that there are small enough pores, one can also decrease the coating layer thickness and still reach the fastest ink penetration into the structure. The limitation then comes with respect to the underlying layers and the role of binder.

5.3. Effect of Ink Permeation on Intercolor Bleeding and the Final Print Quality. The structural properties of the coating reflect the ink tendency for intercolor bleeding during the ink setting process. Figure 13 shows online images of figures from Versamark VX5000e printing just after the print heads. The images illustrate how the coat weight and the printing speed affect the black ink intermixing with the cyan on the surface. All of the images show wicking paths where the black ink has moved into the area of the cyan color. The narrowest, most uniform black line was reached with the highest coat weight of specialty
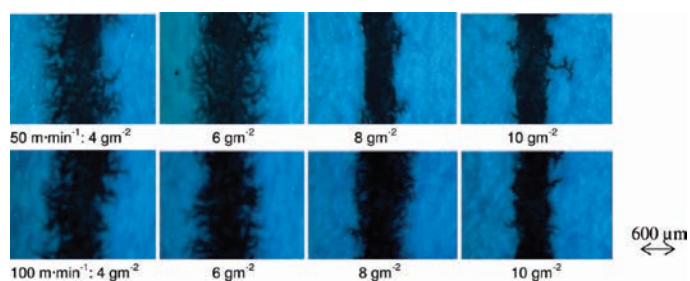
Figure 13. Online images of intercolor bleeding from specialty coatings that contained 15 pph PVOH using different printing speeds. The time delays between cyan and the online camera system were 2.2 s (50 m min^{-1}) and 1.1 s (100 m min^{-1}). The time delays between cyan and black were 1.1 and 0.54 s depending on printing speed.
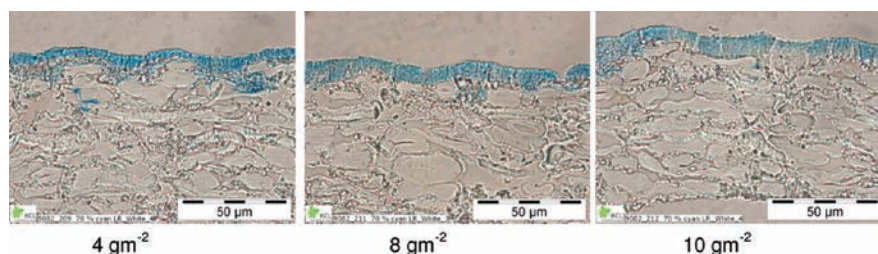
Figure 14. Cross-sectional images of printed 15 pph PVOH containing specialty coatings (70% half tone dot area). Coat weights of 4, 8, and 10 gm^{-2}.

inkjet surfaces. There was enough volume in these cases that the ink could penetrate quickly and sufficiently, that is, under conditions of the highest porosity with the highest penetration coefficient and the highest ink penetration speed.

The droplet speed of the Vesamark VX5000e inkjet press was 15 m s^{-1}, and the volume was 15 pL. The online images were detected on the 100% area at a resolution of 300×300 dpi. Using these values, we obtain an ink amount of 2.09 $\text{cm}^3 \text{ m}^{-2}$ on the surface. Assuming that all coating layers had a total pore volume of 0.35 $\text{cm}^3 \text{g}^{-1}$, which was almost the case of 15 pph PVOH-containing coatings, the 10 gm^{-2} coating would have a pore volume of 3.5 $\text{cm}^3 \text{ m}^{-2}$; the 8 gm^{-2} coating, 2.8 $\text{cm}^3 \text{ m}^{-2}$; the 6 gm^{-2} coating, 2.1 $\text{cm}^3 \text{ m}^{-2}$; and the 4 gm^{-2} coating, 1.4 $\text{cm}^3 \text{ m}^{-2}$. Thus, the applied ink can fill the coating structure completely when the coat weight is 6 gm^{-2} or below. In the Clara device, this total filled pore volume corresponds to a thickness of 4.5 μm at a time of 0.035 s.

An increase in the printing speed from 50 to 100 m min^{-1} (Figure 13) seemed to have a quite minimal effect on the intercolor mixing on the 15 pph PVOH inkjet coatings when the coat weight was low (i.e., 4 and 6 gm^{-2}). The black ink mixed with cyan already during the detection time delay 1.1 s (100 m min^{-1}). However, the 8 gm^{-2} papers produced a narrower, more uniform black line when a lower printing speed was used. The delays between the cyan and black nozzles decreased from 1.1 s (at 50 m min^{-1}) to 0.54 s (at 100 m min^{-1}), and it seems that the lower printing speed gave the cyan ink enough time to penetrate into the structure so that the black ink could not mix with it. The Clara and DIGAT results show also that the penetration speed of the ink increased as coat weight increased. From the color-mixing point of view, the penetration speed of the first color seems to have a very important role in the dye-based ink inkjet press. One

way to affect the intercolor mixing is to plan the location of the drying part carefully.

The online images of 7 pph PVOH-containing coatings (Figure 15 at a printing speed 50 m min^{-1}) look very similar to the images of 15 pph PVOH-containing coatings at 4 and 6 gm^{-2}. There were less noticeable differences between the coat weights or printing speeds (not shown herein).

Figure 14 shows the cyan colorant location in the coating layer after printing. It seems that the colorant is located more on the top part of the coating layer when the coat weight increases. It is probably the poly(vinyl alcohol) of the coating color that takes the colorant with the water into the polymer matrix. At the lowest coat weight, some of the colorant could also be detected in the base paper structure. It can also be seen that the coatings had cracks, probably related to the shrinkage of polymer in flocculated/immobilized structures during drying.

If the pore structure (pore volume and pore size distribution) of the coating layer were constant and the only variable were the thickness of the coating, a thicker coating layer would have more total pore volume into which the ink could penetrate. This means that, on a lower-coat-weight coating, the ink stays longer on the top of the coating layer because the ink first penetrates quickly into the small-pore-size fraction of the coating structure and the wetting front is pinned for a while at the interface between the absorption regimes of the small- and large-pore-size fractions, inertially delayed, before progressing into the underlying pre-coating. This result agrees well with the results of Svanholm.[13] The longer the ink front remains pinned in the topcoating, the higher the probability that the inks will mix with each other. The 7 pph PVOH coatings at 4 and 6 gm^{-2} and 15 pph PVOH coating at 8 gm^{-2} had similar air permenace results. Figure 15 shows the inks mixing after 2.2 s (50 m min^{-1}) after the cyan ink printing.
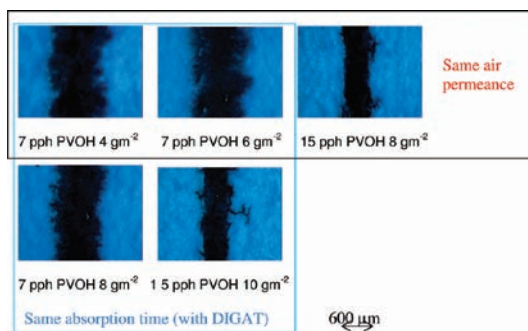
Figure 15. Inks mixing in coatings having the same air permeance and same absorption time but different coat weights. Online images at a printing speed of 50 m min^{-1}.

The highest coat weight produced the narrowest black line on the cyan surface, and there was less ink mixing. If the same absorption time is achieved in coatings with different thicknesses (Figure 15, 7 pph PVOH-containing coatings versus 15 pph PVOH-containing coatings with 10 gm^{-2}), one can notice again that the thicker coating layer provides a narrower black line and less ink mixing than the coating with the lower coating layer thickness. A higher coat weight coating has a higher volume into which the ink can penetrate.

These results collectively indicate that absorption speed is not the only criterion for preventing intercolor bleeding during inkjet ink drying. Rather, the combination of continuity of absorption over time coupled with sufficient total pore volume within the rapidly absorbing layer is key. The presence of diffusion-controlling binder is seen as a limiting factor to achieving optimal inkjet coatings at low coat weights in cases where the pore structure derived from the pigment alone is properly designed.

6. CONCLUSIONS

The penetration of dye-based inks in specialty inkjet coatings at the external pressure caused by the impact of inkjet ink droplets was studied with the capacitance-based Clara permeation device. The results measured from specialty coating layers on plastic film showed that permeation flow dominates in the coating layer only after at least 0.004 s after the application of the ink. Capillary flow, therefore, acts earlier in time than permeation. The pigment type, the binder amount, and the coating layer thickness were found to have no influence on these relative results.

The highest coat weight (10 gm^{-2}) of curtain-coated specialty inkjet surfaces produced the highest total paper porosity, the highest apparent air permeance, and hence the greatest pore volume. The thicker the coating layer, the higher the penetration speed. The highest coat weight also had the most 20−60 nm diameter pores relative to the total paper structure. All of these findings relate to the simple relationship between the topcoating proportion and the total sheet weight. Online images collected on the press show how inkjet inks mix together less when the coating layer has high air flow and high absorption speed. When surfaces with same air permeance or absorption speed are compared, the thicker coating layer produces less ink wicking and reduced intercolor bleeding. The printing speed affects the mixing of inks, as the speed influences the delays between the

different color nozzles, and higher coat weight provides greater pore volume.

In summary, the results indicate that absorption speed is not the only criterion for preventing intercolor bleeding during inkjet ink drying. Rather, the combination of continuity of absorption over time coupled with sufficient total pore volume within the rapidly absorbing layer is key. The only way to decrease the coat weight of specialty inkjet coating layers, therefore, is to use pigments that produce a structure with a high proportion of nanopores and a high permeability. The presence of a diffusion-controlling binder is seen as a limiting factor to achieving optimal inkjet coatings at low coat weights in the case where the pore structure derived from the pigment alone is properly designed.

■ AUTHOR INFORMATION

Corresponding Author
*E-mail: taina.lamminmaki@vtt.fi.

■ REFERENCES

(1) Donigian, D. W.; Wernett, P. C.; McFadden, M. G.; McKay, J. J. Ink jet Dye Fixation and Coating Pigments. Presented at the *TAPPI Coating/Papermakers Conference*, New Orleans, LA, May 4−6, 1998; Paper 12-3.

(2) Ström, G. R.; Borg, J.; Svanholm, E. Short-Time Water Absorption by Model Coatings. Presented at the TAPPI 10th Advanced Coating Fundamentals Symposium, Montreal, Canada, Jun 11−13, 2008; Paper 19.

(3) Nilsson, H.; Fogden, A. Inkjet Print Quality on Model Paper Coatings. *Appita J.* **2008**, *61*, 120.

(4) Ridgway, C.; Gane, P. A. C.; Schoelkopf, J. Effect of Capillary Element Aspect Ration on the Dynamic Imbibition within Porous Networks. *J. Colloid Interface Sci.* **2002**, *252*, 373.

(5) Ridgway, C.; Gane, P. A. C. Controlling the Absorption Dynamic of Water-Based Ink into Porous Pigmented Coating Structures to Enhance Print Performance. *Nord. Pulp Pap. Res. J.* **2002**, *17*, 119.

(6) Olsson, R.; van Stam, J.; Lestelius, M. Effects on Ink Setting in Flexographic Printing: Coating Polarity and Dot Gain. *Nord. Pulp Pap. Res. J.* **2006**, *21*, 569.

(7) Ivutin, D.; Enomae, T.; Isogai, A. Ink Dot Formation in Coating Layer of Inkjet Paper with Modified Calcium Carbonate. Presented at the NIP 21 International Conference on Digital Technology, Baltimore, MD, Sep 18−23, 2005; Paper 119.

(8) Ridgway, C.; Gane, P. A. C. Correlating Pore Size and Surface Chemistry during Absorption into a Dispersed Calcium Carbonate Network Structure. *Nord. Pulp Pap. Res. J.* **2006**, *21*, 563.

(9) Schoelkopf, J.; Gane, P. A. C.; Ridgway, C. J.; Matthews, G. P. Practical Observation of Derivation from Lucas−Washburn Scaling in Porous Media. *Colloids Surf. A: Physicochem. Eng. Aspects* **2002**, *206*, 445.

(10) Gane, P. A. C.; Ridgway, C. J. Rate of Absorption Studies of Fexographic Ink into Porous Structures: Relation to Dynamic Polymer Entrapment during Preferred Pathway Imbibitions. Presented at the *27th IARIGAI Research Conference: Advances in Paper and Board Performance*, Graz, Austria, Sep 10−13, 2000; Paper 2.1.

(11) Lamminmäki, T.; Puukko, P. New Ink Absorption Method to Predict Inkjet Print Quality. Presented at the *34th IARIGAI International Research Conference: Advances in Printing and Media Technology*, Grenoble, France, Sep 9−12, 2007; Paper 25.

(12) von Bahr, M.; Kizling, J.; Zhmud, B.; Tiberg, F. Spreading and Penetration of Aqueous Solutions and Water-Borne Inks in Contact with Paper and Model Substrates. Presented at the *27th IARIGAI Research Conference: Advances in Paper and Board Performance*, Graz, Austria, Sep 10−13, 2000; Paper 2.2.

(13) Svanholm, E. Printability and Ink-Coating Interactions in Inkjet Printing. Ph.D. Dissertation, Karlstad University, Karlstad, Sweden, 2007.

(14) Desie, G.; Van Roost, C. Validation of Ink Media Interaction Mechanisms for Dye and Pigment-based Aqueous and Solvent Inks. *J. Imag. Sci. Technol.* **2006**, *50*, 294.

(15) Walther, M.; Ortner, A.; Meier, H.; Löffelmann, U.; Smith, P. J.; Korvink, J. G. Terahertz Metamaterials Fabricated by Inkjet Printing. *Appl. Phys. Lett.* **2009**, *95*, 251107.

(16) Haverinen, H. M.; Myllylä, R. A.; Jabbour, G. E. Inkjet Printing of Light Emitting Dots. *Appl. Phys. Lett.* **2009**, *94*, 073108.

(17) Quéré, D. Inertial Capillarity. *Europhys. Lett.* **1997**, *39*, 533.

(18) Zhumd, B.; Tiberg, F.; Hallstensson, K. Dynamics of Capillary Rise. *J. Colloid Interface Sci.* **2000**, *228*, 263.

(19) Xiang, Y.; Bousfield, D. W. Effect of Coat Weight and Drying Condition Structure and Ink Setting. Presented at the TAPPI Advanced Coating Fundamentals Symposium, San Diego, CA, May 4—5, 2001; Paper 1-3.

(20) Glittenberg, D.; Voigt, A.; Donigian, D. Novel Pigment—Starch Combination for Online and Offline Coating of High-Quality Inkjet Papers. *Pap. Technol.* **2003**, *44*, 36.

(21) Lamminmäki, T.; Kettle, J.; Puukko, P.; Ketoja, J.; Gane, P. The Role of Binder Type in Defining Inkjet Print Quality. Presented at the *PTS Coating Symposium*, Baden-Baden, Germany, Sep 22—25, 2009; Paper 15.

(22) Gane, P. A. C.; Kettle, J. P.; Matthews, G. P.; Ridgway, C. J. Void Space Structure of Compressible Polymer Spheres and Consolidated Calcium Carbonate Paper-Coating Formulations. *Ind. Eng. Chem. Res.* **1996**, *35*, 1753.

(23) Gane, P. A. C.; Koivunen, K. Relating Liquid Location as a Function of Contact Time Within a Polous Coating Structure to Optical Reflectance. *Transport Porous Media* **2010**, *84*, 587.

(24) Lamminmäki, T.; Kettle, J.; Puukko, P.; Gane, P. A. C.; Ridgway, C. Inkjet Print Quality: The Role of Polyvinyl Alcohol in Specialty CaCO$_3$ Coatings. Presented at the *7th International Paper and Coating Chemistry Symposium*, Hamilton, Ontario, Canada, Jun 10—12, 2009; Paper 49.

(25) Ridgway, C.; Schoelkopf, J.; Matthews, G. P.; Gane, P. A. C.; James, P. W. The Effect of Void Geometry and Contact Angle on the Absorption of Liquids into Porous Carbonate Structure. *J. Colloid Interface Sci.* **2001**, *239*, 417.

(26) Bosanquet, C. M. On the Flow of Liquids into Capillary Tubes. *Philos. Mag., Ser. 6* **1923**, *45*, 525.

III/13

Absorption capability and inkjet ink colorant penetration into binders commonly used in pigmented paper coatings

Absorption Capability and Inkjet Ink Colorant Penetration into Binders Commonly Used in Pigmented Paper Coatings

T. T. Lamminmäki,*,[†] J. P. Kettle,[†] P. J. T. Puukko,[†] and P. A. C. Gane[‡,§]

[†]VTT Technical Research Centre of Finland, P.O. Box 1000, 02044 VTT, Finland

[‡]Aalto University, School of Science and Technology, Faculty of Chemistry and Materials Sciences, Department of Forest Products Technology, P.O. Box 16300, FIN-00076 Aalto, Finland

[§]Omya Development AG, CH-4665 Oftringen, Switzerland

ABSTRACT: The absorption of coating binders used in inkjet coatings plays an important role apart from that of the porosity and pore structure of the pigment coating layer. The aim of this work is to clarify how different binder films absorb water-based dye-containing inks and how changes in the ionic nature of both ink dye and binder films affect the ink absorption capability and the final colorant location in the binder film. The studied commercial binders were one carboxylated, and a range of partially hydrolyzed and fully hydrolyzed polyvinyl alcohol (PVOH), and these were compared to an anionic styrene acrylic latex. The hydrolysis modifies the effective crystallinity and hence the swelling tendency. The results show that as the hydrophobicity of the PVOH binder increases, the less the binder absorbs the water-based ink vehicle and the colorant of the ink locates/fixes more on the top part of the coating structure. Both ink vehicle and dye colorant diffuse into the binder film. It was observed that the carboxylated PVOH film produces the most intense coloration (darkest blue color of cyan ink) as the greater ink vehicle absorption promotes the high colorant amount in the film. The combination of opposite charges of the binder film and dye-based ink colorant fixes the colorant most effectively to the top part of the film by the action of chromatographic separation and adsorption.

■ INTRODUCTION

The high specific surface area of inkjet coating pigments requires binders that have a high binding capacity. The most common binder used in inkjet coatings is polyvinyl alcohol (PVOH). The binding strength of PVOH depends on the degree of hydrolyzation.[1] The peel strength of PVOH is higher when the degree of polymerization is also high.[2] Modified PVOH has also been used: carboxylic-, sulfonic-, acryl amide-, cationic-, and silicone-modified PVOH. The use of other types of pigments in the inkjet area has brought some binders: polyvinyl pyrrolidone, poly(acrylic acid), polyacrylamide, methylcellulose, cellulose derivatives, gelatin, polyvinyl acetate latex, vinyl acetate ethylene, and cationic starch.[3−8]

The role of binder has mainly been studied in the coating layers. Svanholm[9] studied silica pigments with PVOH binder in coated fine papers. He noticed that the silica pigments with large internal pore diameters require more binder than pigments with smaller pores in order to get the dye colorants to remain on or near the top of the coating. The PVOH can form a film in the top part of the coating, where the colorant of inkjet ink can become fixed. A partially hydrolyzed and higher molecular weight PVOH gave the best color gamut and the sharpest line edges, and also sufficient binding strength. The effect of binder type was studied by Ström et al.[10] They showed that binder type affects the water imbibition on the silica surfaces and the PVOH and starch containing coatings have a linear relationship between absorption amount and the square root of time, indicating that they followed the Poiseuille equilibrium flow inherent in the Lucas—Washburn equation. The latex bound coatings, in contrast, had a linear absorption response with time. Additionally, it must be

remembered that diffusion also follows a square root of time dynamic, and this is often overlooked in such studies, and could have alternatively been a potentially key difference between these coatings based on binder type. Vikman and Vuorinen[11] studied light fastness of the inkjet printed surface using PCC and kaolin, and their blends. The binders were PVOH and cationic starch with cationic styrene acrylate latex. With dye-based inks, the significance of structural properties of the coating layer in the light fastness decreased when the strength of the chemical paper-ink interaction increased. The dyes benefit from a dense coating structure, whereas a coarse structure of the coating appears to be advantageous for pigment-based inks.

Pinto et al.[12] studied inkjet ink colorant location in the binder film layers by using Time of Flight Secondary Ion Mass Spectrometry (ToF-SIMS). They mainly studied polyvinylpyrrolidone (PVP) and its copolymers, but there are also some results with PVOH-containing films. They concluded that both PVP and PVOH engage in intermolecular hydrogen bonding interactions. The cross-sectional images of samples containing PVP restricted the ink colorant to the media surface.

Oka and Kimura[13] introduced four different mechanisms to describe how an acid red dye (anionic) can set on a silica pigment that has been covered with PVOH. First the colorant can attach onto the PVOH layer. In the second mechanism, the colorant can dissolve in PVOH, and in the third, colorant forms a complex

with adsorbed cationic polymer (dye-fixing agent) and stays in the PVOH. In the last two mechanisms, the PVOH does not have an effect on the final colorant location. The colorant attaches on the silica pigment and adsorbs on silica with cationic polymer present. They concluded that most of the used dyes form a complex with dye-fixing agent, and this disperses in the PVOH layer and, thus, this is the dominant phenomenon. The rest of the dye remains as a colorant layer on the PVOH surface. We supported in our hypothesis the ideas of Oka and Kimura, but we assume that the colorant can follow the diffused water molecules into the binder network.

Different kinds of additives have been widely used in inkjet coatings as cationic components[4,5,7,12,14,15] and cross-linkers.[2,16] The reason for using the additives has been to adjust the colorant fixing or the adsorption properties of the coating layers and/or the rheology of coating colors. Ryu et al.[14] showed that the cationic additives increase the viscosity of typical coating colors. The inkjet print density remained more or less the same and, among the studied cationic additives, polyDADMAC improved the water fastness of the printed surface the most. The poly-DADMAC-containing coating also had less color bleeding than the coating without additive. However, there are only a few studies in which the colorant of inkjet inks fixes in the binder layers. The occurrence of the separation of ink vehicle and colorant has not been studied.

The aim of this work is to clarify how anionic and cationic dye-based inks absorb into the different polyvinyl alcohols tested, compared with anionic styrene acrylate latex. The observations were made using binder films, and the role of ionic change in the films is linked to colorant location. The dye separation phenomenon was additionally studied using Time of Flight Secondary Ion Mass Spectrometry.

■ MATERIALS AND METHODS

The binders in this work were chosen from different types of polyvinyl alcohols (PVOH), one being carboxylated and the others ranging in degree of hydrolysis, provided by Kuraray (Kuraray Specialties Europe GmbH, Building D 581 D-65926, Frankfurt am Main, Germany) and one anionic styrene acrylate latex from BASF (BASF Aktiengesellschaft, Paper Chemicals, 67056 Ludwigshafen, Germany). PVOH contains vinyl alcohol and vinyl acetate units (Figure 1). The resulting polymer has crystal and amorphous parts in the structure, and the greater the degree of hydrolysis the more there form crystal regions within
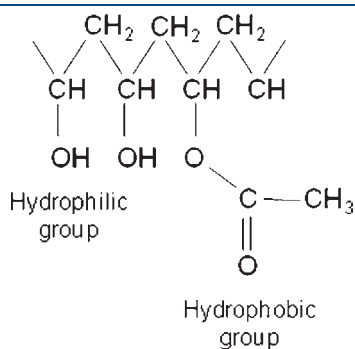
Figure 1. Chemical structure of polyvinyl alcohol.

the polymer matrix.[17] In the K-Polymer KL-318 (PVOH) polymer, a carboxylic monomer (COO^-Na^+) has been added. Table 1 shows the properties of the binders. The charge of the binders was adjusted by adding either anionic sodium polyacrylate [Polysalz S (BASF AG, Paper Chemicals, 67056 Ludwigshafen, Germany)], having a molecular weight of 4000 $g \cdot mol^{-1}$, or cationic poly(diallyl dimethyl ammonium chloride) (polyDADMAC, Cartafix VXU (Clariant International AG, Rothausstrasse 61, CH-4132 Muttenz 1, Switzerland). The content of additives was set at two values, 1 and 4 pph.

The PVOH binder films were produced by cooking the respective polymer and drying it in Teflon (Polytetrafluoroethylene, Du Pont) molds at 23 ± 2 °C. The latex film was subsequently made with an Erichsen (Erichsen GmbH & Co., Am Iserbach 14, D-58675 Hemer, Germany) film applicator (Model 288) followed by drying them in an oven at 105 °C for 5 min. The thickness of the films was 205−260 μm.

The inks were self-made and they contained 4 (cationic) or 5 (anionic) wt-% colorant, 5 wt % polyethylene glycol (PEG 200), 5 wt % diethene glycol, 0.3 wt % Surfynol 465 (surface active agent from Air Products (Air Products PLC, Hersham Place Technology Park, Molesey Road, Hersham, Walton-on-Thames, Surrey KT12 4RZ, U. K.) and the remainder was water. The colorants were anionic (Basacid Blue 762, Cu phthalocyanine) and cationic (Basonyl Blau 636, Victoria Blue FBO, Basic Blue 7, triarylmethane) dyes provided by BASF. There was a slight difference between the surface tensions of the inks: the anionic ink had 49.5 $mN \cdot m^{-1}$ and the cationic 55.9 $mN \cdot m^{-1}$ (23 °C). This can have an effect on the colorant location due to the wetting characteristics in relation to the binder surface energy. The observably different tone of blue of anionic and cationic cyan colorants came from the basic properties of the dyes.

In the absorption measurement, a binder film, sized 2.0 × 2.0 cm, was immersed into the self-made cationic or anionic dye-based inkjet ink. After each defined measuring time, the sample was removed from the ink and dried lightly between two blotting boards. The weight of film was measured before and after the immersions. The absorption amount is defined as the difference between the absorbed and the dry weights, with initial adjustment made for the moisture content of original binder film. This was then divided by the weight of the film to give a specific uptake, i.e., per unit weight of film. The measurement was made under standard conditions of relative moisture content 50% RH and temperature 23 °C. The result is composed of three parallel measurements.

The colorant and water separation was studied using Time of Flight Secondary Ion Mass Spectrometry (ToF-SIMS). In the measurement, the partially hydrolyzed PVOH binder (Mowiol 40−88) film was immersed in a commercial anionic ink (Versamark VX5000e cyan ink) or this same anionic ink with an addition of 1 $g \cdot dm^{-3}$ lithium for 5 min time and subsequently dried at 23 ± 1 °C and 50% RH overnight. We assumed that the lithium, with its very low molecular weight (small atomic radius) followed the water molecules, and so could be used as a tracer for the vehicle imbibition path. The ink absorbed binder films were embedded in a LR White resin (Electron Microscopy Sciences, P.O. Box 550, 1560 Industry Road,Hatfield, PA-19440, U.S.). The samples were then cross-sectioned and covered with platinum and polished. In the ToF-SIMS measurement 10 ns pulse, ions/electrons are released from the surface. ToF-SIMS analyzes the chemical compounds of the cross-sectioned sample as a function of depth, z. By measuring the gray scale values of the

IV/2

Table 1. Properties of the Studied Polymers

binder	fully hydrolyzed PVOH (Mowiol 20—98)	partially hydrolyzed PVOH (Mowiol 40—88)	carboxylated PVOH (K-polymer KL-318)	styrene acrylate latex (Latexia 212)
degree of hydrolysis, mol-%	98.4 ± 0.4	87.7 ± 1.0	87.5 ± 2.5	
density, g·cm^{-3}	0.4—0.6 ^{a}	0.4—0.6 ^{a}	0.4—0.6 ^{a}	1.03
glass transition temperature, °C				−20
viscosity (4% solution, 20 °C, DIN 53 015), mPas	20.0 ± 1.5	40.0 ± 2.0	25.0 ± 5.0	
ash content maximum (calculated as Na$_2$O), %	0.5	0.5	N/A	N/A
chemical nature	nonionic	nonionic	anionic	anionic

^{a} Measured according DIN 53 468 by Clariant International AG from the granulates.

location of different components in the *z*-direction of the sample, we generated information about the distribution of each constituent chemical compound.

The water type, i.e., free or bound water in the binder film moisture content after absorption, was measured with a differential scanning calorimeter [DSC, Mettler DSC 30 (Mettler-Toledo, Inc., 1900 Polaris Parkway, Columbus, OH 43240, U.S.)], which measures the difference in the amount of heat required to increase the temperature of a sample by a defined amount. In the measurement, the freezing of unbound water was analyzed by the latent heat effect at −0.5 °C. The bound water was then identified as the total moisture content of the film found under drying by heating minus the amount of unbound water. We recall here that the binder films under test were polyvinyl alcohol (Mowiol 40—88) and styrene acrylate latex (Latexia 212). In DSC and absorption measurements, we have to remember that part of the PVOH films may dissolve and this can have some effects on the results. In our earlier study,[18] we showed that after a 30 s absorption time, the dissolving part of polymer can be about 5% of the initial weight of PVOH, whereas the SA latex dissolves only about 1%, and this latter amount is related primarily to surfactants, residual monomers, oligomers, and so forth, rather than the binder itself.

■ RESULTS AND DISCUSSION

Absorption Amount into Binder Films. The amount of ink absorption into the binder films was studied for the self-made anionic and cationic dye-based inks. The highest absorption amount was reached with carboxylated PVOH film (Figure 2). Then came partially hydrolyzed and fully hydrolyzed, with the SA latex film had the lowest absorption. As the absorption time increased, a higher amount of ink was absorbed into the films. The order of the films remained the same regardless of absorption time, indicating no chemical change occurred. The amount of absorbed ink had a linear relation to the square root of time, as shown in Figure 2. The addition of cationic or anionic additive in the binder film has only a very minimal effect on the absorption properties. The more important aspect seems to be the hydrophilic nature of the binder polymer itself. This can indicate that the additives do not fix to the PVOH hydroxyl groups and so do not prevent the water molecules and/or colorant fixing to the binder molecules.

We see in Figure 2 that the lines are parallel in the cases where absorption takes place, indicating equal absorption rates. However, they have different heights in relation to the *y* axis. These differing heights indicate that another phenomenon has occurred
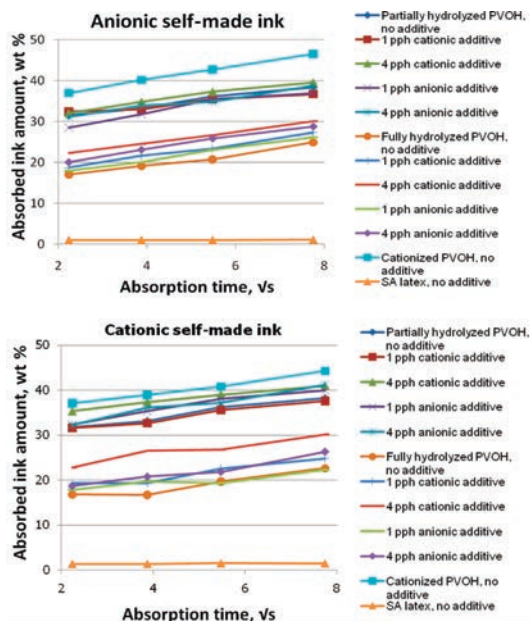

Figure 2. Absorption of anionic and cationic self-made inks into the PVOH and SA latex films, expressed as the weight fraction of film weight. The standard deviation of absorbed ink amount was at maximum 2 wt %, but in most cases, it was about under 1wt %.

prior to the first measurement time. This phenomenon is therefore occurring at different rates within the different binder films. We can only speculate what this might be, but suspect a polymer swelling effect once exposed to moisture. Interestingly, one combination stands out as being differently sensitive to this shorter time scale effect—that of cationic ink as a function of highly cationically treated fully hydrolyzed PVOH. Similarly, we see that cationic ink also lifts the line for partially hydrolyzed PVOH when no added cationic agent is present, though the effect is less marked. It could be that the network strength of the PVOH is being affected. To study this further, the binding strength could be evaluated.

The amount of amorphous and crystalline regions in the polymer affects the content of absorbed moisture.[19,20] At any given relative moisture content, a polymer with a low crystallinity absorbs more moisture than one with high crystallinity.[20,21] This
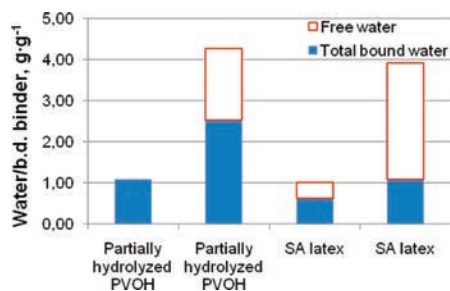
IV/3

Figure 3. The water type (bound versus unbound) in PVOH and SA latex films, as measured with DSC. The dissolving of PVOH likely has some effect on the results.

confirms that the amorphous region of the polymer can bind water molecules readily, whereas the crystalline part cannot. Our results in Figure 2 illustrated that the fully hydrolyzed PVOH, with more crystalline structures,[17,20] absorbed less of the inkjet inks than the partially hydrolyzed: the water diffuses and fixes to the amorphous region of PVOH causing swelling of the polymer, whereas in the crystalline part, the small size water molecules penetrate through the adjacent PVOH structures without binding there. Water molecules are small enough to fit into the polymer network without disrupting it.

If the movement of water molecules in the binder film is studied in terms of bound and unbound water, then we notice that the water molecules diffuse in the polyvinyl alcohol polymer network and they can hydrogen bond to the hydrophilic groups of PVOH.[8] This can happen only in the noncrystal regions of the polymer.[17] At certain water content, the PVOH film has both free
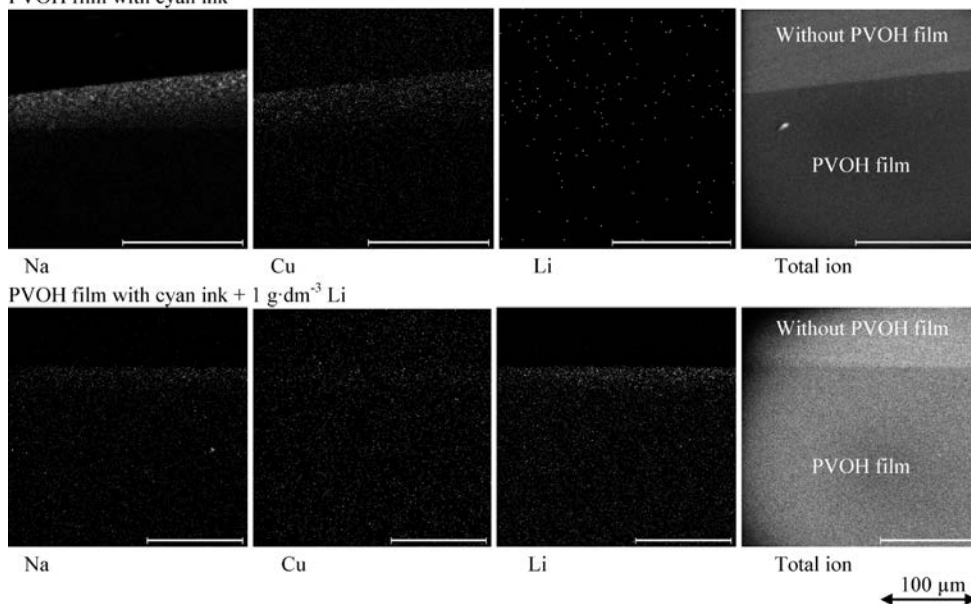
Figure 4. The location of sodium, lithium, and copper in the PVOH film analyzed with Time of Flight Secondary Ion Mass Spectrometry (ToF-SIMS). The ink was Versamark VX5000e cyan ink, which contained copper and sodium. Lithium was used as a tracer in the water (made from $Li_2SO_4 \cdot H_2O$).
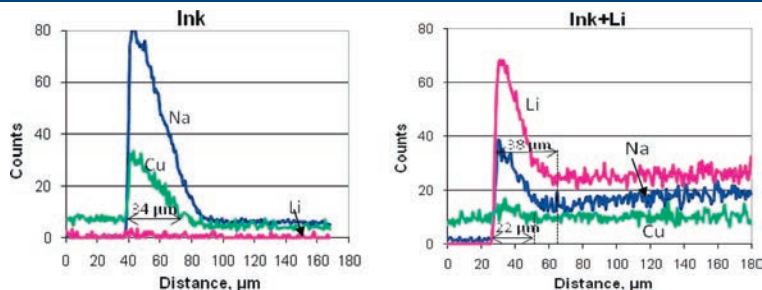
Figure 5. The location of ink (Cu and Na) and water (Li) in the PVOH film layer. Measured with ToF-SIMS.

3290

dx.doi.org/10.1021/ie102178x |*Ind. Eng. Chem. Res.* 2011, 50, 3287–3294

IV/4

water and bound water. The results of differential scanning calorimetry, in Figure 3, show that the PVOH film has, at the moisture content of 1%, only bound water, whereas the latex film has some bound and some unbound. At the 4% moisture content, the PVOH film still shows proportionally more bound water than the SA latex film. Latex does not have chemical groups that can fix the water molecules to the same extent as the PVOH. This kind of difference in the fixing capability between the binders must also exist in the practical inkjet ink setting stage.

Separation of Colorant and Water. The ToF-SIMS analysis of the sample having absorbed commercial ink indicates the location of water and colorant in the PVOH film. The amount of colorant was so low, however, that it was very difficult to locate

Figure 6. The self-made cationic and anionic dye-based ink absorption into the anionic latex film after 60 and 5 s absorption times, respectively.

the colorant with certainty. The colorant molecule contained copper and sodium. However, Figures 4 and 5 indicate that the tracer lithium can be found deeper in the binder film structure than copper. Thus, there is a falling concentration gradient of colorant within the film in relation to the ink vehicle front. We can conclude, therefore, that there is a chromatographic separation, and hence adsorption of colorant to the polymer network.

Interestingly, in Figure 5, the case where lithium salt is added, the picture is not so clear regarding the sodium trace. Compared with the situation where no lithium ion was added, the sodium distribution appears to penetrate deeper into the layer. This suggests that sodium is being released from a complex in partial exchange equilibrium with the lithium.

Colorant Fixing to the Binder Films. Figure 6 shows how the anionic nature of SA latex prevented the anionic colorant from fixing to the film after the short ink exposure time of 5 s. The anionic SA film had no colorant at all, whereas cationic ink adhered to the anionic latex film. After the 60 s absorption time, both anionic and cationic ink showed blue coloration of the SA latex film, though a much darker blue color was achieved with the longer 60 s absorption time for the cationic dye. The PVOH films, however, always displayed a blue color independent of the ionic nature of the colorant (Figure 7). When the various PVOH films were immersed, each with one dye, it was noticeable that the coloration of the films was very similar. The cationic or anionic additive did not change the observed color intensity.

Figure 8 shows how the anionic dye-based colorant located within the top part of the PVOH films. It did not penetrate in any case through the whole film. The anionic colorant located even more on the top part of the binder film when the cationic additive had been added to the binder (Figure 8 in the middle). The higher the additive amount, the narrower the area of colorant
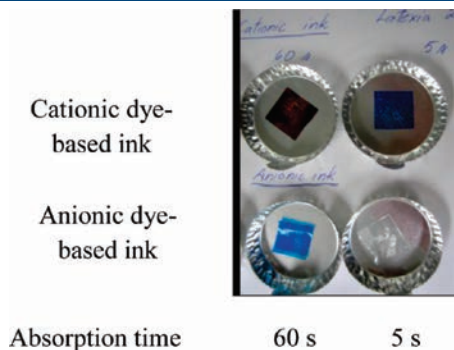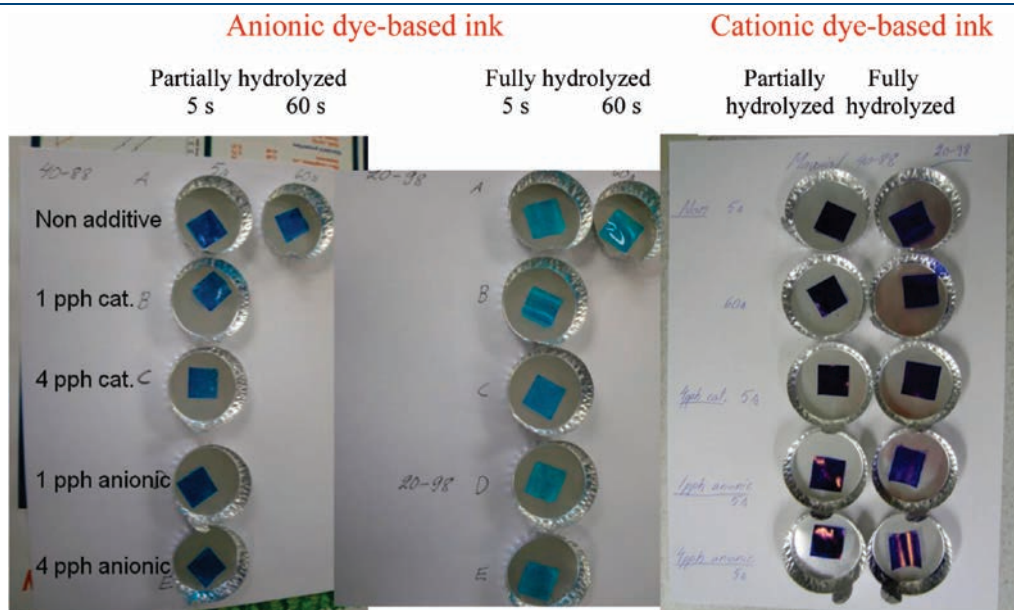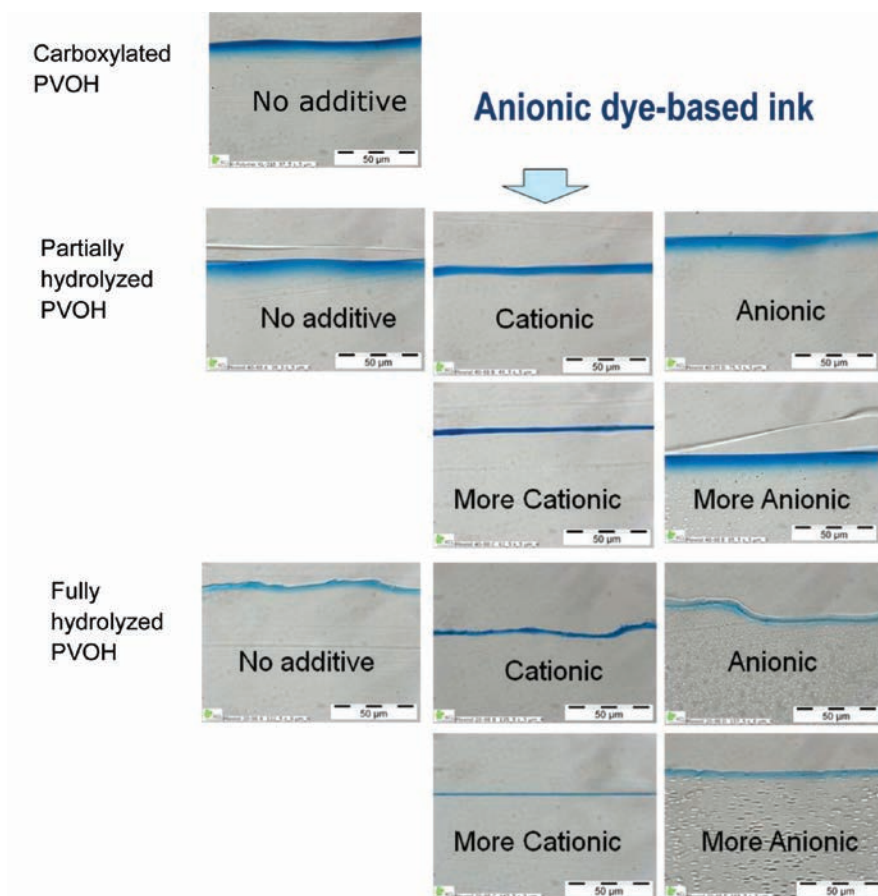

Figure 7. The color of partially and fully hydrolyzed PVOH binder films after the self-made anionic and cationic ink absorption measurement. Absorption times were 5 and 60 s, respectively.

IV/5

Figure 8. The cross-section optical microscopy images of polyvinyl alcohol films after 5 s self-made anionic ink absorption. The additive amount was 1 pph (cationic or anionic) or 4 pph (more cationic or more anionic).

thickness on the top of the film became. The lowest blue color of the binder film was achieved with fully hydrolyzed PVOH film, indicating a holdout of colorant. The optical direct observation was so definitive that it was not necessary to resort to instrumentation for color determination. Similar colorant location in the top part of the binder film could be seen when the ink had cationic nature and the binder contained anionic additive (not shown here).

The cross-section images in Figure 8 show that colorant locates in the top part of the binder film even in the case when the colorant and binder film have same anionic nature. This suggests that in the coating layers, we could get an acceptable uptake of ink with any type of PVOH binder. The opposite ionic nature of PVOH and colorant is not essential to bring the colorant into the coating layer, i.e., it is carried in the water. However, the opposite ionic nature promotes the colorant fixation more in the top part of the structure. In addition, the cross-section figures illustrate that the darkest blue color locates on the top of the film by a concentration gradient decreasing (fading) into the z-direction of the film. In the absorption, the colorant accumulates more within the first encountered surface,

which necessarily has had a longer contact time to the ink. The colorant follows the ink vehicle into the film and there occurs a chromatographic separation of colorant molecules from ink vehicle. This result agrees well with the results of Oka and Kimura.[13] The results of ToF-SIMS also indicate that the greatest colorant content located at the top of the film and the separation of dye and water can take place during the absorption.

The other interesting result is that the anionic carboxylated PVOH produced the darkest blue color with both anionic and cationic ink. This suggests, especially in the anionic ink case, that the colorant follows the water into the structure, and the higher absorption capability of this binder film promotes ink colorant diffusion into the film. The absorption results show that the carboxylated PVOH absorbs more of both inks than the other studied polyvinyl alcohols. This is likely to relate to the "super absorbant" nature of sodium polyacrylate, acting to draw larger volumes of water, and hence nonadsorbed dye, through its own polymer network.

The low inkjet ink absorption amount into fully hydrolyzed PVOH (see Figure 9), which contained more crystalline regions,
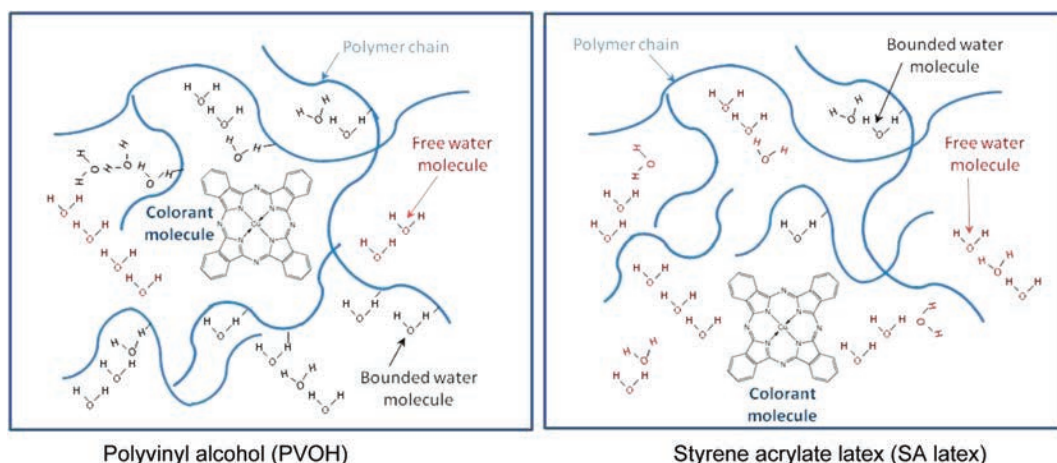
IV/6

Figure 9. A schematic representation of inkjet ink absorption into the PVOH and latex polymer network before the evaporation of water molecules.

would mean that water probably stays more in/on the top part of the film, and the polymer swelling which happens there causes further restriction acting against the colorant migrating between the polymer chains. This restriction acts to hold the colorant also near the top but will reduce the amount of colorant uptake overall, and therefore cyan color darkness will be low despite the colorant being apparently fixed near the top. This could result also in poor water fastness because the colorant locates too near the top part of polymer surface.

The results show that the cationic or anionic nature also affects the inkjet ink colorant location in binder films. When the colorant has an opposite ionic charge from that of the produced binder structure, then the colorant locates more in the top part of the film. The higher amount of counter charge additive in the film, the more the colorant locates within the uppermost top part, i.e., there exist more chemically charged groups that can fix with ionic interactions to the opposite charge groups of colorant molecules. The colorant locating more within the top surface in the coating layer means that we do not need so much ink to produce a certain print density or color gamut. The other advantage of using additives can be in the improvement of colorant fixing strength: the ionic interactions together with the hydrogen bonds produce improved water fastness.[14,15]

The Role of Binder Absorption in the Dye Colorant Location/Fixing. The results show that the water molecules absorb and fix in the binder polymer network differently depending on the hydrophilic nature of binder polymer. It seems that the water molecules diffuse in the PVOH polymer structure and open the network (Figure 9) so that the colorant molecules fit also into the swollen matrix. The size of a water molecule is $0.27-1.00$ nm (depending on the amount of molecules in one cluster)[22] and the colorant molecule about 1.3 nm (taking account of the length of different bonds in the Cu phthalocyanine colorant molecule and assuming the molecule to be planar). Finally, the colorant fixes to the hydroxyl groups (hydrogen bonding) or to the opposite ionic nature groups (ionic interactions) with PVOH or just become trapped in the structure after the water evaporation.

The latex clearly has fewer chemical groups that can fix water molecules, and therefore the network of polymer does not swell (Figure 9). The colorant does not fit in the structure of the latex network and the only place where colorant can fix locates on the outside of the polymer network. We can assume that in the case of

latex, the main mechanism of colorant fixing is the ionic interactions (electrostatic interactions, Coulombic attraction) on the binder film.

■ CONCLUSIONS

The hydrophilicity and absorptivity of the coating binder very strongly affects where the colorant locates after the ink setting process. When a swelling polymer, such as PVOH, absorbs the inkjet ink, the water in the ink diffuses in the polymer network structure and opens it up by an action of swelling, depending on the level of crystallinity. The ink colorant follows the water and the colorant forms hydrogen bonds or ionic interactions with the chemical groups of PVOH and/or becomes trapped in the structure after water evaporation. In the case of nonswelling SA latex, the water and colorant remain outside the polymer matrix, and the colorant cannot fix other than by external charge interaction if present.

We can affect the final ink colorant location by adding either cationic or anionic additive into the binders. The opposite ionic charge of additive and the ink colorant fixes the colorant more within the top part of the binder film. The increase of additive content from 1 to 4 pph seems to fix the colorant more toward the uppermost part of binder film provided the ink dye has an opposite charge. If the charge is similarly anionic, then the colorant passes deeper into the binder film, due to the super absorbing nature of the anionic additive (sodium polyacrylate).

It seems that during the aqueous-based inkjet ink absorption into the binder film, the binder cannot bind all of the offered water molecules, and there will be both bound and unbound water molecules in the polymer network structure. One explanation for unbound molecules is the level of crystallinity of the PVOH related to the degree of hydolysis: the crystalline areas of polymer cannot bind the water molecules. The fully hydrolyzed PVOH has more crystalline areas than the partially hydrolyzed PVOH, and therefore it is less hydrophilic and swells less during the uptake of water or inkjet ink.

■ AUTHOR INFORMATION

Corresponding Author
*E-mail: taina.lamminmaki@vtt.fi

■ REFERENCES

(1) Miller, G. D.; Cook, G. R. *Polyvinyl Alcohol—A Specialty Polymer for Specialty Papers*. Tappi Short Course, May 17−18, 1990, Boston, MA, USA, 43-70.

(2) Hara, K. Specialty PVOH in Ink Jet Coating Formulations. *Paper Tech.* **2005**, *47* (3), 27–30.

(3) Yip, K. L.; Lubinsky, A. R.; Perchak, D. R.; Ng, K. C. Measurement and Modeling of Drop Absorption Time for Various Ink-Receiver Systems. *J. Imaging Sci. Technol.* **2003**, *47* (5), 388–393.

(4) Malla, P. B.; Devisetti, S. Novel Kaolin Pigment for High Solids Ink Jet Coatings. *Paper Tech.* **2005**, *46* (8), 17–27.

(5) Morea-Swift, G.; Jones, H. *The Use of Synthetic Silicas in Coated Media for Ink-jet Printing*. Tappi Coating Conference and Trade Fair, May 1−4, 2000, Washington, DC, USA, 317-328.

(6) Glittenberg, D.; Voigt, A.; Donigian, D. Neuartige Pigment-Stärke-Kombination zum Online- und Offline-Streichen höherwertiger Inkjet-Papier. *Wochenblatt Papierfabrik.* **2002**, *130* (19), 1279–1285.

(7) Khoultchaev, K.; Graczyk, T. *Polymer−Polymer and Polymer−Pigment Interactions—Implications on Ink jet Universal Media*. Tappi Coating Conference, May 2−5, 1999, Toronto, Canada, 155−168.

(8) Lavery, A.; Provost, J. *Color-Media Interactions in Ink Jet Printing*. IS&T's NIP13: International Conference on Digital Printing Technologies, November 2−7, 1997, Seattle, Washington, USA, 437−442.

(9) Svanholm, E.; Wedin, P.; Ström, G.; Fogden, A. *Colorant Migration in Mesoporous Inkjet Receptive Coatings*. 9th TAPPI Advanced Coating Fundamentals Symposium, February 8−10, 2006, Turku, Finland, 221−228.

(10) Ström, G. R.; Borg, J.; Svanholm, E. *Short-Time Water Absorption by Model Coatings*; TAPPI 10th Advanced Coating Fundamentals Symposium, June 11−13, 2008, Montreal, Canada; Tappi Press: Atlanta, GA, 204−216.

(11) Vikman, K.; Vuorinen, T. Light fastness of ink jet prints on modified conventional coatings. *Nordic Pulp Paper Res. J.* **2004**, *19* (4), 481–488.

(12) Pinto, J.; Nicholasm M. *SIMS Studies of Ink Jet Media*. in Proc. IS&T's NIP 13 Conference, IS&T, 2−7 Nov. 1997, Seattle, Washington, 420-426.

(13) Oka, H.; Kimura, A. The Physicochemical Environment of Acid red 249 Insolubilized in an Ink-Jet Paper. *J. Imaging Sci. Technol.* **1995**, *39* (3), 239–243.

(14) Ryu, R. Y.; Gilbert, R. D.; Khan, S. A. Influence of Coating additives on the Rheological, Optical, and Printing Properties of Ink-jet Coatings. *Tappi J.* **1999**, *82* (11), 128–134.

(15) Vikman, K.; Vuorinen, T. Water Fastness if Ink Jet Prints on Modified Conventional Coatings. *J. Imaging Sci. Technol.* **2004**, *48* (2), 138–147.

(16) Rich, Y. R.; Richard, D. G.; Saad, A. K. Influence of cationic additives on the rheological, optical, and printing properties of ink-jet coatings. *Tappi J.* **1999**, *82* (11), 128–134.

(17) Kumaki, K.; Nii, S. *Polyvinyl Alcohol in Ink Jet Coatings*, Tappi PaperCon 2010, 2−5 May 2010, Atlanta, GA, USA, 27 p.

(18) Lamminmäki, T.; Kettle, J.; Puukko, P.; Ketoja, J.; Gane, P. The role of binder type in determining inkjet print quality. *Nordic Pulp Paper Res. J.* **2010**, *25* (3), 380–390.

(19) Ricciardi, R.; Auriemma, F.; Gaillet, C.; De Rosa, C.; Laupretre, F. Investigation of the Crystallinity of Freeze/Thaw Poly(vinyl alcohol) Hydrogels by Different Techniques. *Macromolecules* **2004**, *37* (25), 9510–9516.

(20) Hasimi, A.; Stavropoulou, A.; Papadokostaki, K.; Sanopoulou, M. Transport of Water in Polyvinyl Alcohol Films: Effect of Thermal Treatment and Chemical Crosslinking. *Eur. Polym. J.* **2008**, *44*, 4098–4107.

(21) Salmén, N. L.; Back, E. L. Moisture-Dependent Thermal Softening of Paper, Evaluated by Its Elastic Modulus. *Tappi J.* **1980**, *63* (6), 117–120.

(22) Topgaard, D.; Söderman, O. Diffusion of Water Absorbed in Cellulose Fibers Studied with H-NMR. *Langmuir* **2001**, *17* (9), 2694–2702.

IV/8

The chromatographic separation of anionic dye in inkjet coating structures

The chromatographic separation of anionic dye in inkjet coating structures

T.T. Lamminmäki [a,*], J.P. Kettle [a], P.J.T. Puukko [a], P.A.C. Gane [b,c]

[a] VTT Technical Research Centre of Finland, P.O. Box 1000, 02044 VTT, Finland
[b] Aalto University, School of Science and Technology, Faculty of Chemistry and Materials Sciences, Department of Forest Products Technology, P.O. Box 16300, FIN-00076 Aalto, Finland
[c] Omya Development AG, CH-4665 Oftringen, Switzerland

ABSTRACT

During the ink setting process on coated inkjet paper, the porosity and pore size distribution of the coating structure determines how much, in which direction and at what speed the surface can absorb the ink. The capillary and permeation flow drives the liquid into the structure and controls the volume flow, respectively. The coating binder, quite often polyvinyl alcohol, has an effect on the inkjet ink imbibition by occupying a proportion of the available pore volume and absorbing via swelling of the polymer matrix. The aim of this work is to clarify the role of the porous structure and the coexistent swelling of binder during the liquid imbibition, with special attention paid to the fixation of dye and its distribution during the chromatographic separation process. The results confirm that water molecules diffuse into and within hydrophilic polyvinyl alcohol binder causing the binder swelling. The swelling affects the number of active small pores remaining available for capillary, by reducing the diameter and volume of the remaining free pores, thus slowing the capillary flow, such that the permeation flow rapidly becomes the rate determining step rather than the desired fine capillary-driven liquid imbibition. On the other hand, water molecules diffusing into the binder structure open the polymer network so that the colorant molecules can also fit into it. This mechanism is reflected in the observation that, in the case of dye-based inks, there is always a clear (non-coloured) wetting front advancing before the colour front. The swelling binder, therefore, though reducing absorption dynamic, does act to provide sorbtion volume and surface for colorant, aiding an otherwise coating surface area limited function in respect to dye capture and fixation.

© 2011 Elsevier B.V. All rights reserved.

1. Introduction

The penetration of inkjet ink and soluble dye colorant fixing into the structure of coated paper during imbibition is complex and cannot adequately be described by a single phenomenon, such as capillarity or direct surface adsorption alone. Fig. 1 shows one demonstration of the interaction phenomena during the inkjet ink setting process [1]. Initially, the ink droplet arrives onto the paper surface and the wetting of the paper begins. At this stage, the inertia of the droplet affects the ink movement [2,3]. The capillary force in the z-direction of paper competes with the spreading in the x,y-direction [4]. The capillary force becomes a dominating phenomenon and it forces the ink vehicle and mobile components into the pore structure. Microcapillary penetration starts typically after about 0.1 ms from the droplet arriving [5]. Nanopores in the structure (<0.1 μm), on the other hand, generate absorption with

a timescale of single pore filling of approximately 10 ns [5]. After a few milliseconds, the separation of the ink components starts and the capillary penetration continues strongly [6,7]. After about one second from the droplet arriving, the significance of liquid adsorption onto the coating structure surface increases [8]. The diffusional movement takes place already at the capillary imbibition between liquid and surface interface, but it is traditionally assumed to be a quite small effect at this stage [8]. The significance of diffusion of ink components was assumed to increase only over time as the ink has penetrated deeper into the structure [7,9]. The role of diffusion at the beginning of the inkjet ink imbibition process has not been studied in detail until very recently. Lamminmäki et al. [10], have shown that the presence of soluble and swelling binder, such as polyvinyl alcohol, reacts under water diffusion rapidly over the very short distances associated with the nanopore structure of discretely bimodally distributed pores in modern precipitated and modified calcium carbonate-based inkjet coatings [11]. At the final stages of ink setting, although inkjet inks touch dry rapidly, polymerization of pigment adhesives, if present, is nonetheless a relatively slow process, which can take the order of several hundreds of seconds, and a final drying time of the ink is in the order of hours [2].

* Corresponding author.
E-mail addresses: taina.lamminmaki@vtt.fi (T.T. Lamminmäki), john.kettle@vtt.fi (J.P. Kettle), pasi.puukko@vtt.fi (P.J.T. Puukko), patrick.gane@aalto.fi (P.A.C. Gane).
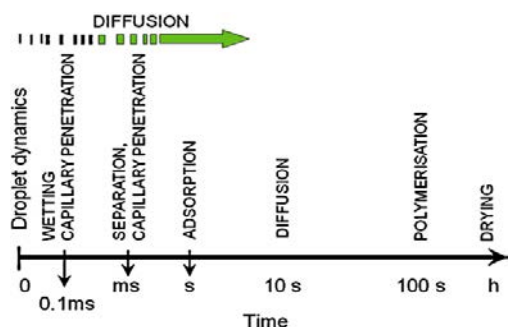
Fig. 1. The presumed interaction phenomena of the inkjet ink setting process and their relevant onset timescales [1]. Superposed, above the time spectrum, is the relatively new observation that absorbent binder, distributed within high surface nanopores, as part of discretely bimodal pore structures, acts to absorb at the short timescale also by diffusion.

Thin layer chromatography (TLC) has been utilized before in a study of inkjet ink fixing by Donigian et al. [12,13] and Glittenberg et al. [14]. In all these researches, TLC was used in the study of dye colorant fixing to the coating layer in a conventional way. A droplet of dye-based ink was spotted onto the precipitated calcium carbonate and silica coatings and allowed to dry there. In the TLC development process, the ink vehicle was used then as the eluent. The colorant and eluent front location after the development process was detected and from them was calculated the R_f value (the ratio of the distance that the substance travels to the distance that the solvent travels up the plate). They varied the content of polyvinyl alcohol and cationic additive in their study. However, the coatings did not at that time display the marked discretely bimodal pore distribution, characteristic of the fastest carbonate absorbing structures today.

The objective of this work is to establish the relationship between colorant dye charge and concentration of dye upon penetration into an inkjet coating of the colorant and vehicle, respectively. With thin layer chromatography, model calcium carbonate coatings, displaying the discretely bimodal pore structure property, are studied to illustrate a comparison of a diffusive and non-diffusive coating structure. Polyvinyl alcohol (PVOH) is used as a "diffusion driving" binder and compared with a styrene acrylate latex as a "less-diffusing", or virtually non-diffusing, binder, where both categories of diffusion behaviour refer to the case of exposure to water.
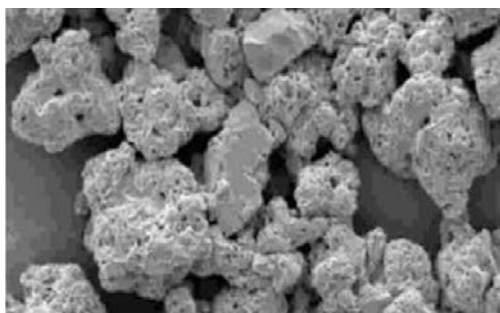
Fig. 2. The SEM picture of MCC pigment.

2. Materials and methods

2.1. Raw materials

The chosen pigment was a modified calcium carbonate (MCC), Omyajet B6606.[1] The weight median diameter of the MCC pigment particles ($d_{50\%}$) was 2.7 μm and the specific surface area, 46.2 m^2 g^{-1} (BET, ISO 9277). The pigment particle provides capillary absorption capacity and high surface adsorption area via its intra-particle pores (Fig. 2). The packing of such internally porous particles develops the characteristic bimodal pore size distribution when used in the inkjet coating layer, Fig. 5. The pigment was provided by the manufacturer as a dry powder, which had some cationic dispersing agent on the surface of the pigment particles designed to be applied for coatings accepting anionic dye-based inkjet inks. Two contrasting binders were used: a non-ionic polyvinyl alcohol (PVOH, Mowiol 40-88[2]) and an anionically stabilized styrene acrylate latex (SA, Latexia 212[3]). The PVOH had a degree of hydrolysis of 87.7 ± 1.0%. The latex had a particle size of 180 nm and glass transition temperature of −20 °C. An anionic sodium polyacrylate (Polysalz S[3], molecular weight 4000 g mol^{-1}) and a cationic poly(diallyl dimethyl ammonium chloride) (poly-DADMAC, Cartafix VXU[4]) were used as dispersing and charge modifying agents, respectively.

The respective charge modifying agent (anionic dispersant and/or polyDADMAC) amount was 0.5 pph. In the case of making down anionic coating colours, the anionic dispersing agent was added into the initial water, as normal, before the cationic pigment addition, in order to "flip" the charge from cationic to anionic. The mixing of pigment and anionic dispersing agent took 30 min. Into those coating colours that were to contain binder, the PVOH or SA latex was applied next and the mixing lasted again 30 min. The coating layers had only 1 pph of binder because the chromatographic eluent movement was desired to be as free flowing as possible. In the complementary case of making down cationic colours, the addition of polyDADMAC was made after PVOH binder addition. Due to the anionic nature of the SA latex, no corresponding cationic colour using this binder was prepared.

2.2. Testing methods

In our study, the target was to detect how the dye-based colorant in water moves during the ink imbibition. Therefore, we used the thin layer chromatography (TLC) technique differently than Donigian et al. [12,13]. Coated glass plates were used as the basis for the coatings in TLC. Deionized water was the eluent in the TLC analysis and the adsorbate (substance adsorbed) was provided by a range of concentrations of anionic cyan colorant (Basacid Blue 762[3], Cu phthalocyanine). The model coatings were applied to the glass plate surface using an Erichsen[5] film applicator (Model 288). The applied coat weight was about 100 g m^{-2}. The coating layers were dried at room temperature over night. During the TLC development in our case, the term "eluent" now refers to the water phase (ink vehicle equivalent) of a solution of dye applied as a supersource reservoir, i.e. not the classical eluent travelling past a previously dried colorant, but a carrier. The distance of the eluent (water phase) movement over time was measured. Simultaneously, the gray level of surface reflectance was detected with a digital camera
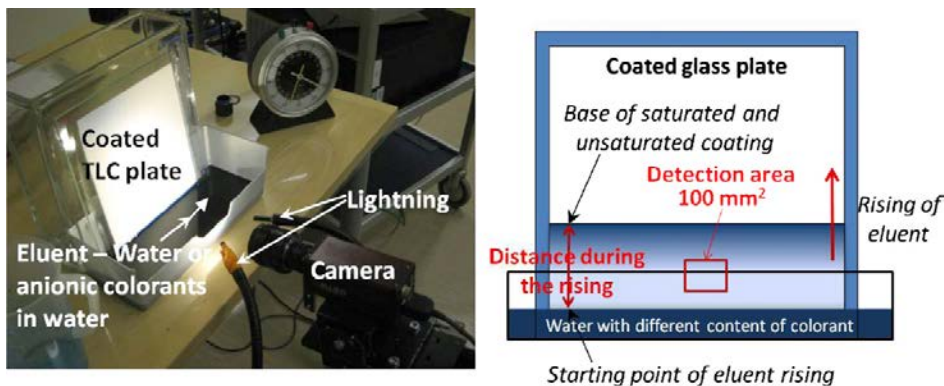
Fig. 3. The TLC development system and the location of gray value measurement and the distance of eluent front.

(Dolphin F145C[6]). The illumination of the surface was made on the same side as that viewed by the camera (Fig. 3). The measurements were made at a temperature of $20.0 \pm 1.5\,°C$. The image analysis software Image-Pro 6.2[7] was used and the detection area started about 0.5 mm above the advancing eluent front and the total detection area was $100\,mm^2$. The gray level of the undeveloped plate was adjusted to a gray level of 150. The distance was expressed toward the base of the TLC plate passing from unsaturated to saturated sample.

The porosities of the coating layers were analyzed by a silicon oil (Si-oil) absorption saturation method and mercury porosimetry. In the Si-oil measurement, the pigment cake was left for one hour in the oil, and the weight of cake before and after oil saturation was measured. The absorbed liquid volume was measured as the weight change between the "dry" and the saturated sample divided by the density of the silicon oil ($0.934\,g\,cm^{-3}$). The density of each pigment system was also measured and this can be one reason for variation in the results. The porosity was thus defined as the volume of absorbed liquid at saturation divided by total volume of sample, all determined at room temperature and atmospheric pressure. In the mercury porosimetry (Micrometrics AutoPore IV[8]) measurement, the coating layer was impregnated with mercury using both low and high pressure. The pore volume and pore size distribution were analyzed adopting the Pore-Comp[9] correction, which takes account for penetrometer expansion, mercury compression and compression of the sample skeletal material, expressed as the elastic bulk modulus, according to Gane et al. [15].

3. Results

3.1. Coating layer properties

Fig. 4 shows the porosity results of coating layers measured with the silicon oil absorption and mercury porosimetry. The relative accessibility for oil under imbibition and mercury under external pressure to penetrate into the coating structure resulted in some divergence in the results for porosities. It is possible that some of the coating structure was not saturated with liquid oil, especially

due to it being a non-pressurized measurement, as the presence of binder may have limited pore connectivity. The highest Si-oil porosity result was for the cationically dispersed pigment. Otherwise the results were on the same level. The porosity results of mercury porosimetry were altogether on a higher level than the results of Si-oil measurement, but they also indicated very similar porosity to those of studied coatings.

Fig. 5A shows the cumulative pore volume and Fig. 5B the pore size distribution of the coatings determined by mercury porosimetry. The first derivative of the cumulative mercury intrusion curves, although limited to a model of an equivalent bundle of capillaries, and thus ignoring pore shielding effects, is nonetheless useful for comparison purposes between topologically similar structures [16]. The MCC pigment coatings had both intra and inter-particle pores and thus results in curves of pore size distribution having two peaks (Fig. 5B). The addition of 1 pph of binder had a very minimal influence on intra-particle pores (below 70 nm). In the inter-particle pore area (over $0.1\,\mu m$), the anionic pigment with PVOH had more $0.27\,\mu m$ diameter pores than the others. The largest pores were produced by the anionic coating with 1 pph SA latex ($0.65\,\mu m$).

3.2. Anionic colorant movement in the swelling and non-swelling binder-containing coating

The results show that there always exists a wetting front rising within the coating structure in advance of the colorant front, and this was seen to be true for both the combinations of charge, i.e. anionic dye–cationic coating, and anionic dye–anionic coating.

At first sight, the formation of a colorant-free wetting front was unexpected for the combination of anionic colorant and anionic coating layer, as there is no obvious retardation adsorption mechanism on the basis of charge alone. The wetting water front height in this anionic case was about one millimetre ahead of the colorant front. It was also noted that the retarded colorant fronts were darker than the following (trailing) colours (Fig. 6, anionic coatings). It is concluded that as the finest pores of the coating structure drive the wetting front forward, they can be assumed to exclude the dye. This provides an important corollary, in that the surface area associated with the finest pores in these structures is either not available for adsorption of the dye, or a further rate determining step is involved. Experience suggests that the *anionic repulsion* is the primary exclusion mechanism.

In the cationic coating, the anionic colorant initially stayed at the bottom edge of the cationic coating layer in contact with the liquid reservoir. After ten minutes the fixed bottom edge appeared to fill with colorant and part of the colorant volume then started to
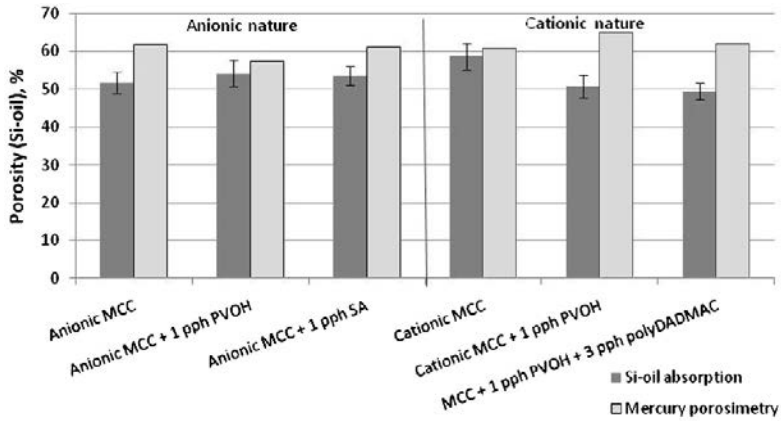
Fig. 4. Porosity of coatings measured with silicon oil absorption and mercury porosimetry.
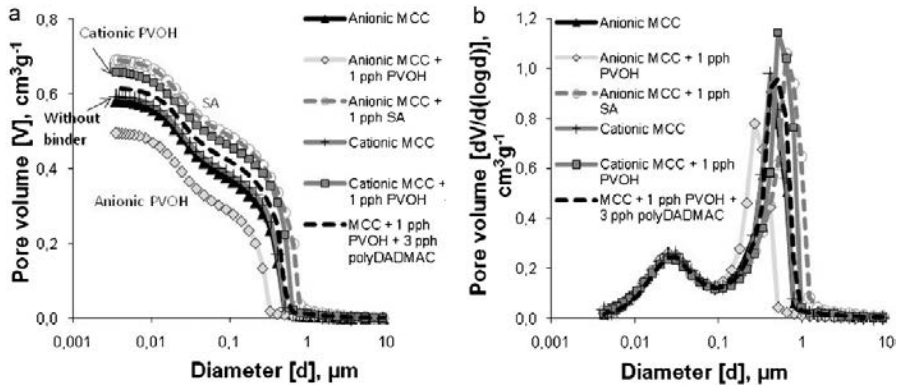

Fig. 5. The cumulative pore volume (A) and pore size distribution (B) of coatings. Measured with mercury porosimetry – an example of the discretely bimodal pore size distribution of MCC in a coating structure, generated by the nanopores within the particles and the micropores between them.
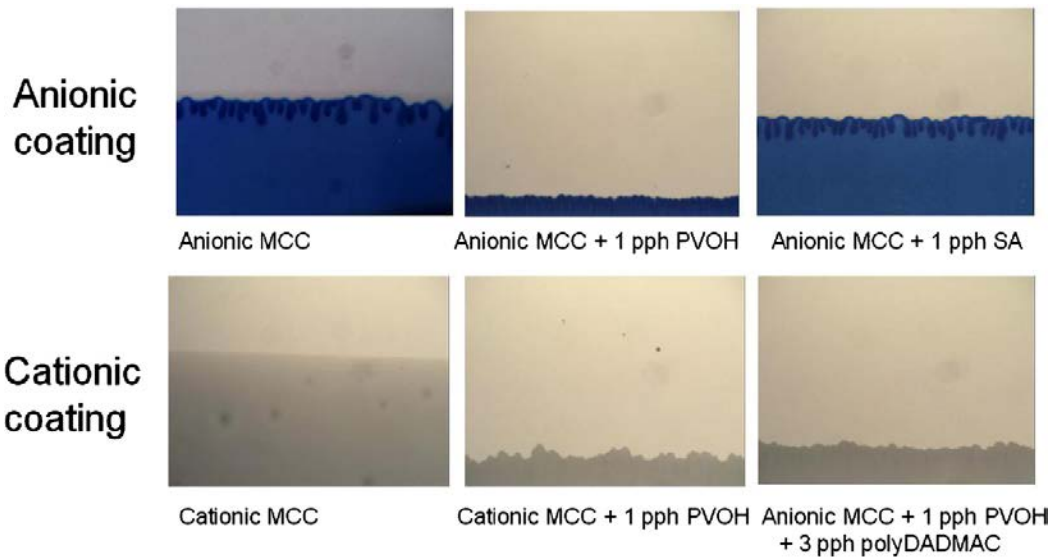

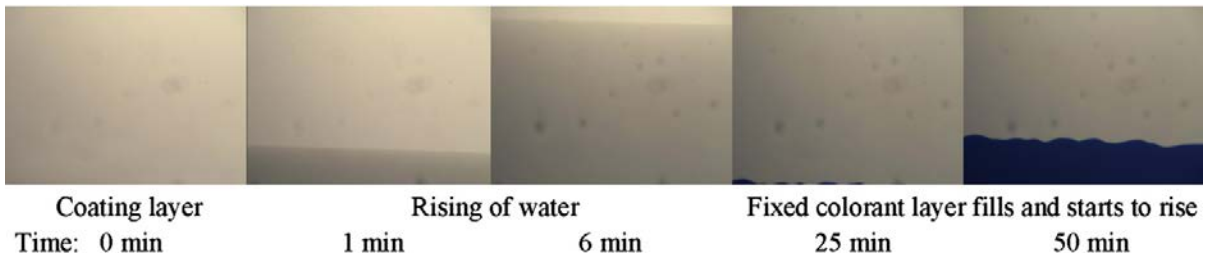**Fig. 6.** The 5.0 wt% anionic cyan colorant rising within different coating layers. Measured after 4 min time delay.

Fig. 7. Anionic colorant (5 wt%) movement on the cationic MCC TLC plate.

rise little by little: especially, this could be seen when there was a higher concentration of 5.0 wt% colorant in water (Fig. 7). Clearly, the surface area associated with the cationised pores took part in adsorption, and only when the surface area was saturated could the colorant move forward into the structure.

Fig. 8 shows the water front distance as the eluent rose through the coating structure. The highest water rising was observed in the binder-free systems. The coating with SA latex had a plateau height value roughly half that of the binder-free coating, and the lowest values were for PVOH containing coatings.

Fig. 9 shows the gray level values of MCC coatings. The eluent was pure water or water with different amounts of anionic cyan colorant. In the anionic coatings, the gray level value change was caused by the movement of water and colorant, whereas in the cationic surfaces it was caused by water movement only until adsorption saturation at a given height was reached. The change of gray value measured above the coloured region was caused by the coating layer progressively filling with water advancing ahead of the colorant: when the value is high, it means that the change toward a darker appearance on the plate was small, and when the value is low it indicates a greater darkening effect was observed. The water, and water with different colorant contents, penetrated very similar distances, as Fig. 8 indicated, in the respective coating structures, regardless of cyan colorant amount in water.

4. Discussion

The TLC development lasted quite long time, even as long as 40 min, and the evaporation of water might have some effect on the liquid movement during this time. Therefore, we detected the evaporation of water by measuring the weight change over time at

Fig. 8. The distance of eluent (water) front during the time during the chromatographic process.

the same temperature as the TLC measurement proceeded. From this weight we calculated the effect of evaporation on the eluent distance through the TLC coating by taking account of the water density and the coating layer dimensions on the glass plate. Fig. 10 shows the evaporation rate of water, from which could be calculated the effect of evaporation on the rate of liquid. The evaporation causes at the maximum about 0.005 mm min^{-1} retardation on the TLC plate, whereas in the coating layer the water moves at 3.0 mm min^{-1} at its fastest rate, and then slows down from that. On the other hand, the accuracy of the TLC method used did not reach under 0.5 mm liquid distance change, and therefore we could not notice very slow liquid movement to sufficient accuracy. We can conclude, therefore, that at the beginning of the TLC development the water evaporation seems to have a very minimal influence on the eluent rising. During the time the influence was seen to decrease to 0.002 mm min^{-1}, and it is probable that after 40 min development time the evaporation still has only a minor effect on the liquid movement when comparing the influence of wetting force and viscous drag force. Only toward the very end of the experiment can we expect evaporation to be a further equilibrating factor additional to the wetting force-retardation balance.

The balance between the wetting force and the viscous drag determines the rate of progress. As the viscous drag increases in proportion to the length over which the liquid flows within the structure, and decreases to the fourth power of the typical equivalent capillary diameter (Poiseuille effect), there comes a point when the drag equals the wetting force. The Young–Laplace equation (Eq. (1)) [2,7,17,18] describes the wetting force, $\pi r^2 p_c$, of a liquid contacting the walls of a capillary,

$$p_c = \frac{-2\gamma_{lv} \cos \theta_{eq}}{r} \tag{1}$$

where p_c is the Laplace capillary pressure, r the internal capillary radius, γ_{lv} the interfacial tension at the liquid–vapour interface, and θ_{eq} is equilibrium contact angle. During liquid motion, the Young–Laplace pressure drives the liquid against the viscous Poiseuille drag force, given by

$$\frac{dV}{dt} = \frac{\pi r^4}{8\eta l} \Delta P \tag{2}$$

where dV/dt describes the volume flow rate of a liquid of viscosity η through the effective capillary pipe of radius r and length l under the driving pressure difference ΔP.

4.1. Anionic dye–anionic coating

The upper three pictures in Fig. 9 show how water and the anionic dye colorant with water rose through the anionic TLC coating plates during the chromatographic experiment. The gray level becomes darker and darker until, at a certain moment, the liquid has filled the pores of the coating layer that are located within the chosen analyzed area. The turning point in gray value
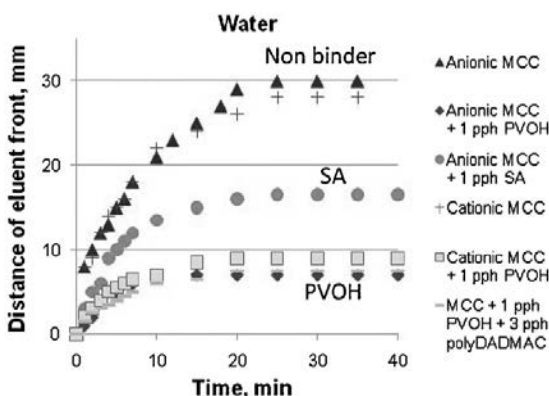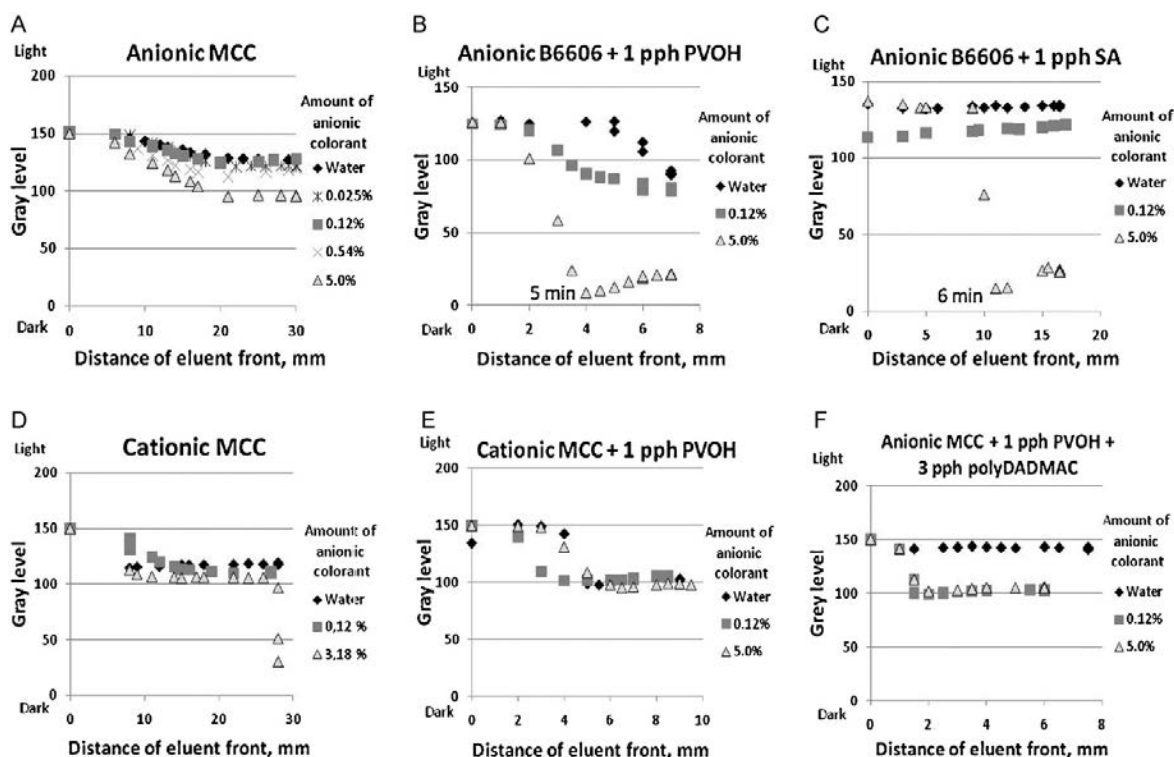
Fig. 9. The gray level values of coatings during the chromatographic sorption process. The content of anionic colorant was adjusted by applying colorant into the water (weight-percent). The measurement of anionic MCC coating had a lower light intensity than the others. A – anionically dispersed MCC, B – anionic MCC with 1 pph PVOH, C – anionic MCC with 1 pph SA latex, D – cationically dispersed MCC, E – cationic MCC with 1 pph PVOH, F – anionic MCC with 1 pph PVOH and 3 pph polyDADMAC.

traversing the analyzed distance takes between 4 min and 6 min with these 100 g m^{-2} coatings. The small size of a water molecule, 0.27–1.00 nm (depending on the amount of molecules in one cluster) [19], enables the capillary flow in the intra-particle pores. The surface of the coating structure first wets and the capillary flow drives the ink vehicle into the small pores. As the amount of ink increases, the permeation flow in larger pores increases so that there are no more air-containing pores which could reflect the light. The size of a colorant molecule is about 1.3 nm (taking account of the length of different bonds in the Cu phthalocyanine colorant molecule and assuming the molecule is planar), which means that the colorant fits well into the 20–70 nm diameter intra-particle pores, provided these pores are accessible. It seems that the col-orant follows the pigment surfaces and the bridges between the pigment particles almost everywhere.

After the gray value turning points (Fig. 9), where the curves reach the minimum value, the gray level of the plates increases slightly. The anionic dye washes out from the anionic coating layer as the eluent proceeds because there are no chemical groups that can fix the colorant. At high colorant amounts there were more visible changes in gray level values. Real inkjet inks contain about 3–8 wt% of colorant [20], so the use of a 5 wt% solution is within the range of commercial practice. In TLC analysis the amount of liquid is clearly higher than in the real inkjet printing and therefore this washing effect is likely to be less important in practical inkjet ink setting.
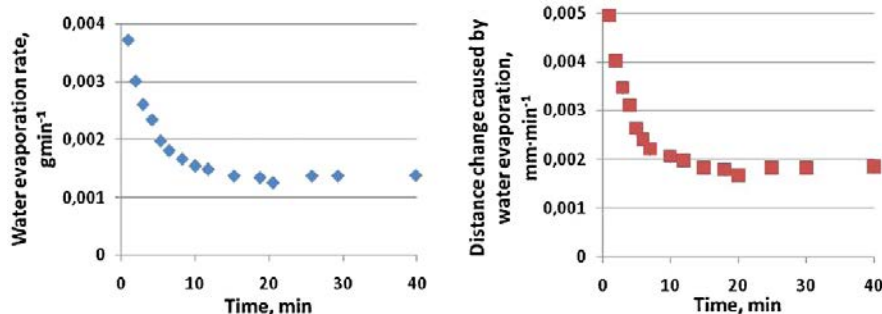

Fig. 10. The evaporation rate of water during the time and from that calculated the effect of water evaporation on the eluent rate through the TLC plate. In the distance evaluation, the coating layer width was 150 mm and thickness 100 μm and the porosity of coating layer was taken to be 50%.
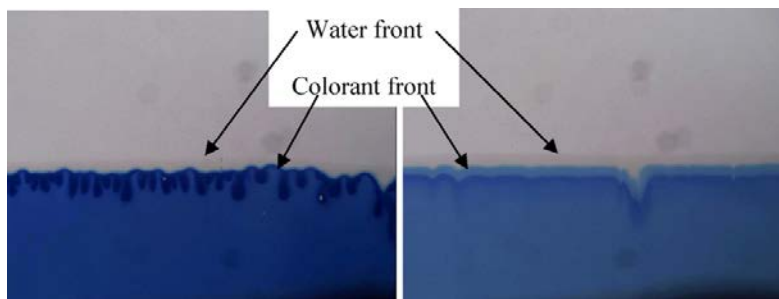
Fig. 11. The water front is seen to be ahead of the colorant front in the anionic coating layers after 4 min: left 5.00 wt% and right 0.54 wt% anionic colorant.

It is also observed that the eluent moves further in the anionic dispersed pigment layer than in 1 pph binder-containing layer. After a distance of 30 mm, there was no further change in the distance travelled in the anionic pigment layer, whereas in the PVOH coating the eluent front stopped after 7 mm, and in the SA coating after 17 mm (Figs. 8 and 9). On the basis alone of the larger pore volume of SA-containing coating, due to structural spacing, we might expect that eluent would rise further than through the non-binder containing coatings. However, the determining factors are a combination of fine pores (driving the capillarity at the wetting front) and the larger pore-throat constructions (defining the minimal flow resistance pathway) in the network structure. Furthermore, the hydrophobicity of latex polymer can act to prevent partially the polar liquid penetration, unlike in the case of hydrophilically dispersed pigment. Furthermore, the PVOH-containing coating had smaller pore diameters than the SA coating, which would promote greater capillary forces acting on the eluent. The smaller pore volume of PVOH coating can have an influence here also, but more likely the hydrophilic interpolymer diffusive nature of PVOH, causing the polymer to swell, closes the nano-size pores so that eluent cannot rise through further through the structure.

The 1 pph binder addition slightly decreases the porosity and the average pore diameter of PVOH coating (Figs. 4 and 5). On the other hand, PVOH is a hydrophilic binder, and the swelling of PVOH (absorption by such a binder film is shown to be 30.2% [21]) changes the accessible amount/size/volume of small pores during the water absorption process [21]. A rough estimation of swelling effects indicates that the uniform layer of 1 pph PVOH (density 1.26 g cm^{-3}) produces a 0.17 nm thick binder layer on the surface of the pigment (46.2 m^2 g^{-1} specific surface area) and the swelling increases the thickness to 0.26 nm. Thus, PVOH can decrease and even block the nano-size pores of coating layer, and so reduce the capillary driving force, although this will be replaced by the diffusion potential as water diffuses between the polymer chains.

However, the results of mercury porosimetry indicate that the SA containing coating had a little higher porosity and larger pores than the pigment structure without binder. The higher pore volume would suggest that SA coating could transport liquid further than the lower pore volume structure. The SA latex swells only a few percent under the influence of water [21]. Thus, the capillary flow controls the water imbibitions in SA containing coatings. The difference between the dispersed pigment coating and the SA latex containing coating is suggested to be caused by the difference in the hydrophilic nature. The SA latex has hydrophobic nature, which means that the contact angle of polar liquid increases and thus the capillary pressure of pores decreases. The hydrophobicity is mediated probably by the surfactant and/or carboxylation used to stabilize the latex, whereas the dispersing agent in the case of the pigment has produced a hydrophilic structure [22]. Altogether, the equilibrium point, at which the capillary and permeability forces

balance, comes much sooner with binder containing coatings, both due to physical connectivity and due to surface chemistry effects, and these are reflected in the distance the liquid front finally travels.

Fig. 11 shows that, in the case of an anionic coating, the water molecules form a wetting front and the anionic colorant front follows behind it. If the speed of eluent in the plate is taken into account, we see that the wetting front is from 30 s to a few minutes ahead of the ink colorant front, depending on the coating layer pore structure and interaction with binder. In the case of coated paper, we assumed that the liquid is moving in the z-direction of the coating structure in a quite similar way as in the TLC coating layers studied, i.e. the ink is moving with constant speed in the coating layer, the thickness of the coating layer is between 10 and 20 μm, and the absorption time of the layer is about 300 ms (as measured by DIGAT) [21]. This would mean that the wetting front is somewhere between ~0.1 μm and ~10 μm ahead of the colour front, depending on coating thickness.

Fig. 11 shows also that the colorant concentration is increased at the colorant front. The mechanism is, therefore, assumed to be one of anionic repulsion from the finest pores, allowing the water to imbibe into these pores, but not the dye. This also explains why the water fastness of anionic coatings for anionic dyes is so poor [23], because the dye cannot be protected from the external water flow as it is concentrated in the inter-particle voids that constitute the permeable pathway during washing. The anionic dye cannot adsorb onto the anionic surface because of charge repulsion.

4.2. Anionic dye–cationic coating

In the cationic coating layer, the anionic dye becomes fixed to the cationic surface, being drawn by the electrostatic interactions (ionic concentration and Coulombic force). This results in a concentration of dye right at the start position in the TLC experiment, and this observation agrees with many other equivalent results, such as those in [12,20,23–26]. The gray level decreases in Fig. 9 from 150 to 100, because the detected area fills with water. When the surface, available for colorant adsorption, is saturated, the colorant migrates further with the eluent liquid (Fig. 7). This could also be noticed in Fig. 9, where the gray value results dropped from the 100 gray level to the level of 30 with the highest colorant amount in the cationic MCC coating. The gray values of cationic MCC decreases in the distance of 28 mm because the anionic colorant started to rise to the detection area.

5. Conclusions

The results show that even a surprisingly small amount of binder affects the liquid transfer along the MCC pigment coating layers. The capillary flow drives the liquid into the coating structure. On

the other hand, the polar liquid (water) diffuses into hydrophilic binder polymers and acts as a swelling agent, causing closure of some pores and a reduction generally of pore diameters. This acts on the short timescale liquid absorption, due to the short nano distances involved in the finest pores despite being a diffusion process, but reduces the available volume. The balance between the wetting force and the viscous drag determines the rate of progress. The permeation flow is the main resistance determining factor to the capillary and diffusion controlled driving force in the continuing liquid mass transfer.

The results of SA latex containing coatings show that the hydrophobic nature of latex prevents the diffusion of the polar liquid into the structure of the binder layer matrix, but wetting still occurs probably related to the surfactant and/or carboxylation used to stabilize the latex. Also, the SA latex coating carries water further along a TLC plate than in the PVOH containing. The slightly larger pores of the SA containing coating structure allow for quicker liquid penetration, rather than the smaller pores and reduced connectivity of the PVOH containing coatings.

References

[1] J. Kettle, T. Lamminmäki, P. Gane, A review of modified surfaces for high speed inkjet coating, Surface and Coating Technology 204 (12) (2010) 2103–2109.

[2] L. Agbezuge, Drying of ink jet images on plain papers – falling rate period, in: IS&T's NIP7: International Conference on Digital Printing Technologies, Portland, USA, 1991, pp. 173–184.

[3] M. von Bahr, F. Tiberg, B. Zhmud, Oscillations of sessile drops of surfactant solutions on solid substrates with differing hydrophobicity, Langmuir 19 (24) (2003) 10109–10115.

[4] F. Girard, P. Attané, V. Morin, A new analytical model for impact and spreading of one drop: application to inkjet printing, Tappi Journal 5 (12) (2006) 24–32.

[5] C.J. Ridgway, P.A.C. Gane, Controlling the absorption dynamic of water-based ink into porous pigmented coating structures to enhance print performance, Nordic Pulp and Paper Research Journal 17 (2) (2002) 119–129.

[6] M. von Bahr, J. Kizling, B. Zhmud, F. Tiberg, Spreading and penetration of aqueous solutions and water-borne inks in contact with paper and model substrates, in: Advances in Printing Science and Technology – Advances in Paper and Board Performance, 27th Research Conference of the International Association of the Research Institutes for the Printing, Information and Communication Industries, Graz, Austria, September 10–13, 2000, pp. 88–102.

[7] G. Desie, G. Deroover, F. De Voeght, A. Soucemarianadin, Printing of dye and pigment-based aqueous inks onto porous substrates, Journal of Imaging Science and Technology 48 (5) (2004) 389–397.

[8] M. von Bahr, F. Tiberg, B. Zhmud, Spreading dynamics of surfactant solutions, Langmuir 15 (15) (1999) 7069–7075.

[9] K.L. Yip, A.R. Lubinsky, D.R. Perchak, K.C. Ng, Measurement and modelling of drop absorption time for various ink-receiver systems, Journal of Imaging Science and Technology 47 (5) (2003) 388–393.

[10] T.T. Lamminmäki, J.P. Kettle, P.J.T. Puukko, C.J. Ridgway, P.A.C. Gane, The role of ink component diffusion during absorption into inkjet coatings, in: 11th Advanced Coating Fundamentals Symposium, Munich, Germany, October 11–13, 2010, pp. 195–214.

[11] C.J. Ridgway, P.A.C. Gane, The impact of pore network structure on the absorption of pigmented inkjet inks, in: Tappi Coating Conference, Toronto, Ontario, Canada, Session 6, April 17–20, 2005, 15 pp.

[12] D.W. Donigian, P.C. Wernett, M.G. McFadden, J.J. McKay, Ink jet dye fixation and coating pigments, in: TAPPI Coating Conference 1998, New Orleans, USA, Tappi Press, Atlanta, USA, May 4–6, 1998, pp. 393–412.

[13] D.W. Donigian, P.C. Wernett, M.G. McFadden, J.J. McKay, Ink-jet dye fixation and coating pigments, Tappi Journal 82 (8) (1999) 175–182.

[14] D. Glittenberg, A. Voigt, D. Donigian, Novel pigment-starch combination for the online and offline coating of high-quality inkjet papers, Paper Technology 44 (7) (2003) 36–42.

[15] P.A. Gane, G.P. Matthews, C.J. Ridgway, Void space structure of compressible polymer spheres and consolidated calcium carbonate paper-coating formulations, Industrial and Engineering Chemistry Research 35 (5) (1996) 1753–1764.

[16] P.A.C. Gane, M. Salo, J.P. Kettle, C.J. Ridgway, Comparison of Young–Laplace pore size and microscopic void area distributions in topologically similar structures: a new method for characterising connectivity in pigmented coatings, Journal of Materials Science 44 (2) (2009) 422–432, doi:10.1007/s10853-008-3134-8.

[17] J. Schoelkopf, C.J. Ridgway, P.A.C. Gane, G.P. Matthews, D.C. Spielmann, Measurement and network modeling of liquid permeation into compacted mineral blocks, Journal of Colloid and Interface Science 227 (1) (2000) 119–131.

[18] C.J. Ridgway, P.A.C. Gane, J. Schoelkopf, Effect of capillary element aspect ration on the dynamic imbibition within porous networks, Journal of Colloid and Interface Science 252 (2002) 373–382.

[19] D. Topgaard, O. Söderman, Diffusion of water absorbed in cellulose fibers studied with H-NMR, Langmuir 17 (9) (2001) 2694–2702.

[20] S. Pond, Inkjet Technology and Product Development Strategies, USA, 2000, 406 pp.

[21] T. Lamminmäki, J. Kettle, P. Puukko, P.A.C. Gane, C. Ridgway, Inkjet print quality: the role of polyvinyl alcohol upon structural formation of CaCO$_3$ coatings, in: International Paper and Coating Chemistry Symposium, Hamilton, Canada, June 10–12, 2009, 13 pp.

[22] P.A.C. Gane, C.J. Ridgway, Moisture pickup in calcium carbonate coating structures: role of surface and pore structure geometry, in: TAPPI 10th Advanced Coating Fundamentals Symposium, Montreal, Canada, Tappi Press, Atlanta, USA, June 10–13, 2008, 22 pp.

[23] K. Vikman, T. Vuorinen, Water fastness of ink jet prints on modified conventional coatings, Journal of Imaging Science and Technology 48 (2) (2004) 138–147.

[24] A. Lavery, J. Provost, Color-media interactions in ink jet printing, in: IS&T's NIP13: International Conference on Digital Printing Technologies, Seattle, Washington, USA, November 2–7, 1997, pp. 437–442.

[25] K. Vikman, T. Vuorinen, Light fastness of ink jet prints on modified conventional coatings', Nordic Pulp and Paper Research Journal 19 (4) (2004) 481–488.

[26] T. Kallio, J. Kekkonen, P. Stenius, Acid/base properties and adsorption of an Azo dye on coating pigments, Journal of Dispersion Science and Technology 27 (September) (2006) 825–834.

Short timescale inkjet ink component diffusion

An active part of the absorption mechanism into inkjet coatings

Short timescale inkjet ink component diffusion: An active part of the absorption mechanism into inkjet coatings

T.T. Lamminmäki [a,*], J.P. Kettle [a,1], P.J.T. Puukko [a,1], C.J. Ridgway [c], P.A.C. Gane [b,c]

[a] VTT Technical Research Centre of Finland, P.O. Box 1000, 02044 VTT, Finland
[b] Aalto University, School of Science and Technology, Faculty of Chemistry and Materials Sciences, Department of Forest Products Technology, P.O. Box 16300, FIN-00076 Aalto, Finland
[c] Omya Development AG, CH-4665 Oftringen, Switzerland

ARTICLE INFO

ABSTRACT

The structures of inkjet coatings commonly contain a high concentration of fine diameter pores together with a large pore volume capacity. To clarify the interactive role of the porous structure and the coincidentally occurring swelling of binder during inkjet ink vehicle imbibition, coating structures were studied in respect to their absorption behaviour for polar and non-polar liquid. The absorption measurement was performed using compressed pigment tablets, based on a range of pigment types and surface charge polarity, containing either polyvinyl alcohol (PVOH) or styrene acrylic latex (SA) as the binder, by recording the liquid uptake with a microbalance. The results indicate that, at the beginning of liquid uptake, at times less than 2 s, the small pores play the dominant role with respect to the inkjet ink vehicle imbibition. Simultaneously, water molecules diffuse into and within the hydrophilic PVOH binder causing binder swelling, which diminishes the number of active small pores and reduces the diameter of remaining pores, thus slowing the capillary flow as a function of time. The SA latex does not absorb the vehicle, and therefore the dominating phenomenon is then capillary absorption. However, the diffusion coefficient of the water vapour across separately prepared PVOH and SA latex films seems to be quite similar. In the PVOH, the polar liquid diffuses into the polymer network, whereas in the SA latex the hydrophobic nature prevents the diffusion into the polymer matrix and there exists surface diffusion. At longer timescale, permeation flow into the porous coating dominates as the resistive term controlling the capillary driven liquid imbibition rate.

© 2011 Elsevier Inc. All rights reserved.

1. Introduction

In inkjet printing, the ink transfer, meaning the delivery, spreading and penetration of an ink droplet on and into the substrate surface is the most important property that is reflected in the final print quality. During the inkjet printing process, there is no physical contact between the ink nozzles and paper surface, contrary to the case of conventional printing nips, and therefore the importance of the dynamics of free ink transfer onto the surface is emphasized in inkjet printing. Currently there are two main types of drop delivery systems: drop-on-demand (DOD) and continuous jetting (CJ). In DOD, only those droplets are produced, which are intended to arrive on the printing surface, whilst in CJ, there is a stream of droplets produced at high frequency, from which most of the droplets are deflected away and only a few of them reach the substrate

surface. In the CJ inkjet, a piezo crystal causes a pressure change in the nozzle and the ejection of ink out of the nozzle. In the DOD method, there are several different droplet formation techniques used, but the most common are piezoelectric and thermal.

As the droplet has formed during the flight between nozzle and printing surface it arrives finally at the substrate surface with a given impact related to the inertia of the droplet mass arriving at the defined velocity, which delivers a lower force than those associated with traditional printing press nips. There are many studies concerned with droplet impact and settling onto substrate surfaces [1–9]. Two theoretical approaches are considered to dominate when describing fluid spreading on a porous surface during droplet impact – the hydrodynamic model [3,6,10–12] and a molecular kinetic model [13,14]. These models have been frequently combined [15,16]. The droplet formation and flight dynamics have been studied, for example, by the working groups of Eggers and Villermaux [8] and Basaran [4,5] and the effect of the impact of the droplet onto the surfaces by Lembach et al. [9] and Reznik et al. [3]. The mass-related forces are related to the motion of the inkjet ink droplet, for example when it undergoes acceleration (usually in the form of deceleration). The Bond

* Corresponding author. Fax: +358 20 722 7026.
E-mail addresses: taina.lamminmaki@vtt.fi (T.T. Lamminmäki), john.kettle@vtt.fi (J.P. Kettle), pasi.puukko@vtt.fi (P.J.T. Puukko), cathy.ridgway@omya.com (C.J. Ridgway), patrick.gane@tkk.fi, patrick.gane@omya.com (P.A.C. Gane).
[1] Fax: +358 20 722 7026.

number describes the relationship between the droplet response to acceleration and surface tension. A low Bond number indicates that surface tension dominates over the impact process. As the droplet strikes the substrate, the connection between the kinetic energy flow and surface tension of liquid is described by the Weber number. If the Weber number is high, it indicates that the kinetic energy dominates at the droplet striking and liquid thin film flowing. In the practical case, for example in a Versamark® VX5000e inkjet printing press, where the droplet strikes the surface with a fairly high kinetic energy, the droplet can arrive onto the paper surface with the speed of 15 m s^{-2}. Under these conditions, the ink spreading is dominated by inertia.

The commonly used aqueous-based dyes or pigment inks should lose their liquid diluent at an adequate speed into the substrate surface structure so that the various ink colours cannot mix together and exhibit intercolour bleeding. On the other hand, the ink amount is usually greater than in the case of traditional offset or gravure printing, and therefore the substrate surface should contain adequate pore volume to accommodate the entire applied ink vehicle (meaning the solvent water and the soluble chemical compounds in the inkjet ink) into the structure.

The fluid movement in a saturated structure is commonly stated to comply with the Navier–Stokes equation, from which, in the case of low viscosity inkjet ink, once again it can be derived that the most important properties of the ink are represented by surface tension, viscosity and specific gravity of the fluid [3,7,12]. The theory of fluid movement in the pores is thus based on the balance between viscous drag and the wetting force, commonly expressed in the form of the Lucas–Washburn equation [17]. Most work in the previous literature relates to the loss of liquid from saturated pore structures, usually during the drying process, for example the modelling description of Brethour and Scriven [18] who also consider convection as a potential mechanism during drying. The absorption phenomenon into nanostructures of a few molecular dimensions in thickness has been studied by Gerung et al. [19,20]. Conversely, studies of liquid absorption are generally observational, and provide either interpretation of equilibrium absorption [13] or qualitative deviation from Lucas–Washburn [21]. Without resorting to molecular dynamics, short timescale phenomena occurring during the initial absorption phase need to be considered outside the equilibrium phenomena described typically in the Lucas–Washburn force balance. These can be captured by considering the role of droplet impact inertia in initiating the top surface void filling and subsurface structure by liquid, followed by the action of nanopores in defining the liquid uptake as bulk inertial drag retards uptake into the deeper-lying larger pores. This has been described and modelled by Schoelkopf et al. [15] and Ridgway and Gane [22], who apply the Bosanquet equation [23] to highlight the role of pore size differentiation prior to the onset of viscous drag equilibrium. It is shown that the finest pores drive the initial capillary filling at the wetting front [22].

Besides the requirements of absorption during the very fast short timescale phenomena of initial ink uptake, the ink colourant should bind to the top part of the substrate to develop a high print density and good rub-off resistance and water fastness. As the inkjet ink penetrates into the porous substrate, and particularly in the case of coated media, i.e. the coating layer structure, a variety of interaction phenomena influence where the ink vehicle and colourant molecules penetrate and finally become distributed. At first, the arrived ink should wet the surfaces of pigment and binders forming the surface void structures leading to capillary flow by internal pore wetting into the bulk of the coating pore network structure, during which there is a separation of the ink components, via mechanisms including adsorption, diffusional movement, polymerisation (if there exist polymerisable components) and during drying of the ink and coating [24].

The main interest in the work reported here is concentrated on the diffusional movement which happens already at the capillary flow boundary between the liquid and surface interface, but in the prior literature is generally assumed to be a quite small effect in volume terms [2], even though the vapour diffusion at the interface is frequently implicated in defining the advancing contact angle [25]. The significance of diffusion of ink components into such structures as polymer layers is usually assumed to increase during time, when the ink has penetrated deeper into the structure. These assumptions were derived from studies of generally homogeneously distributed pores. Modern inkjet coatings, however, consist of a collection of individual porous particles, for example modified calcium carbonate, which, when packed together in the coating, generate a discretely bimodal pore size distribution [26–28]. The bimodality is related to the combination of high capillarity internal pores and the permeability-controlling inter-particle pores. The role of diffusion into soluble binders, which can fill or partially fill the accessible intra-particle pores, and thus occurring at the beginning of the inkjet ink setting process, has not been studied so widely.

During the diffusion of inkjet ink molecules, ink vehicle as well as the colourant molecules migrate from a region of high concentration to a region of lower concentration by Brownian motion [29]. The driving force is maintained in this phenomenon by the gradient of concentration. There exists many different types of diffusional movement, but probably the most important, with respect to inkjet inks, are described by [29–31] as:

– Bulk diffusion, which means general motion of the inter-skeletal (region between the solid particles of the porous matrix) bulk molecules of the liquid or gas within the coating/deposited layer.
– Surface diffusion, where the motion of atoms, molecules and atomic clusters follows the surfaces of material.
– Knudsen diffusion, when the diffusivity is determined by the size of capillaries instead of the solvents or solutes alone (Fig. 1).
– Osmosis, defined as the spontaneous net movement of water across a semi-permeable membrane from a region of low solute concentration to a region with a high solute concentration, down a water concentration gradient, or, as more usually described, up a solute concentration gradient. It is a physical process in which a solvent moves, without input of external energy.

The external pressure, temperature, moisture content and uniformity of the materials define which diffusion mechanism dominates in the absorption and/or adsorption of water molecules [29,32]. There are only a few studies which support the idea of diffusional movement at short timescale of inkjet ink during imbibition [27,33,34]. Resulting surface and just-subsurface flow during the inertially-driven drop impact affects the establishment of wetting, i.e. overcomes any likelihood of top surface wetting delay.
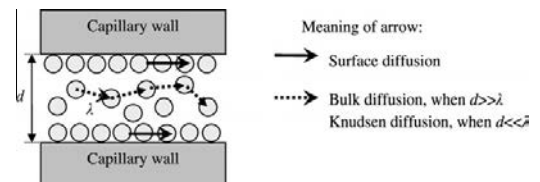

Fig. 1. Diffusion types in the inkjet ink transfer. d is pore diameter and λ distance between atoms, molecules, or atomic clusters (mean free path).

This is followed by absorption into the nanopores, which is expected to account for the filling of the finest internal structure elements [26] acting with a linear proportionality to time. The establishment of longer time viscous limited capillary flow is manifest by a square root of time proportionality.

The objective of this work is to clarify the role of liquid polarity (ink vehicle polarity) upon the sorption and diffusion of vehicle into different coating pigment containing structures combined with either a hydrophilic, swelling polyvinyl alcohol (PVOH), or an internally hydrophobic, non-swelling styrene acrylic latex (SA). Throughout, the imbibition of ink is progressively limited by the prerequisite of diffusion-controlled wetting, either of the polymer filled nanopores (PVOH) or of the polymer surface film on the pigments (PVOH or SA latex). Model coatings are studied based on comparing a standard anionically dispersed ground calcium carbonate (GCC) and two calcium carbonate-based inkjet coating pigment technologies, one based on modified calcium carbonate (MCC, displaying a discretely bimodal pore size distribution) and the other based on precipitated calcium carbonate (PCC). PVOH is used as the example of a "diffusion driving" (water diffusive) binder and is compared with an SA latex considered as a binder being internally non-diffusive to water.

A comparison of water moisture diffusion into and on films made from the two binder types allows a comparison to be drawn in respect to their diffusion capacity rates. The concentration gradient of liquid water rather than vapour is shown to enhance the volume diffusion uptake even further.

2. Materials and methods

2.1. Raw materials

The idea was to use coating pigments which provide different coating layer structures: one with large pores versus one with small pores and the third structure having both small and large pores distributed with discrete bimodality. The pigments were modified calcium carbonate (MCC, Omyajet B6606[2]), ground calcium carbonate (GCC, Hydrocarb 90[2]) and precipitated calcium carbonate (PCC, JetCoat 30[3]). The properties of the pigments are introduced in Table 1. MCC and GCC were provided as dry powders. The GCC was derived from Turkish marble, in dispersant-free form. The moisture and water equilibrium in suspension provides the cationic starting point in respect to zeta potential, i.e. adsorbed $CaOH^+$ ion (cationic) in equilibrium with the dissolution of Ca^{2+} and OH^-. This is then very quickly translated by the adsorption of polyacrylate via the calcium neutralisation and coagulation effect to the anionic form, as Eriksson et al. [35] have shown. The PCC, on the other hand, was supplied in pre-dispersed slurry form. Using image analysis particle tracking during Brownian motion (NanoSight[4]) it could be shown that the PCC pigment contained two distinct particle sizes. The smaller diameter (20–30 nm) particles were the primary particles, whereas the larger particles, located in the area of 260–300 nm, consisted of agglomerates of the finer primary ones. The two distributions together gave an average particle size of 250 nm.

Two contrasting binders were used: a non-ionic polyvinyl alcohol (PVOH, Mowiol 40–88[5]) and an anionically stabilized styrene acrylate latex (SA, CSA 212[6]). The PVOH had a degree of hydrolysis of 87.7 ± 1.0%. The latex had a particle size of 180 nm and a glass

transition temperature of −20 °C. An anionic sodium polyacrylate (Polysalz S[6], molecular weight 4000 $gmol^{-1}$) and a cationic poly(diallyl dimethyl ammonium chloride) (polyDADMAC, Cartafix VXU[7]) were used as dispersing and charge modifying agents, respectively. In the pigment particle dispersing, the dispersing agent amount was 0.5 pph (parts by weight of binder per 100 parts of pigment). In Table 2, the pigments, in their final water suspended form, are described in formulations both prior to and after the addition of binder. The binder content was 1 or 7 pph (Table 2). Though not all the coating colours were measured in respect to zeta potential, the colours were anionic except the originally cationically dispersed MCC, and the coatings with SA latex provided a higher anionicity than the PVOH containing coating colours.

2.2. Testing methods

The coating tablets were produced from coating colours by a wet filtration system [26,36] under the external pressure 20 bar. The tables were dried at 60 °C over night. The PVOH uniformity within the tablets was studied with a Thermo Nicolet Nexus 870 FT-IR spectrometer[8] (IR spectra from KBr-tablets, Fig. 2). The actual amount of PVOH was not calculated from the results of the IR spectra, only the IR spectra difference between the sides of the tablet was detected. The results show that the wire filter side (lower surface) of the tablet had a higher concentration of PVOH. (For this difference measurement, the PVOH content was 0.7 pph, whereas, in our microbalance study, the binder amount used was slightly higher, 1 pph.) Therefore, the final tablets fashioned for the microbalance absorption analysis were prepared so that both sides of the tablet (top and bottom side) were tested and an average formed, each having the same time in contact with the liquid. The filtrate that formed during the tablet making procedure was also analyzed with FT-IR spectrophotometry, and the result showed that it also contained PVOH, confirming the soluble nature of the binder.

The polarity of the liquid, and its effect on imbibition into pigment tablets, was studied using distilled water (100% polar) and hexadecane (100% apolar), respectively (Table 3). The edges of the formed samples were polished and covered with octamethyl trisiloxane/toluene[9] so that the pores of edge areas did not affect the liquid uptake by exterior planar wetting. The uptake of the liquid was measured gravimetrically with an automated microbalance [36–38]. The temperature of surrounding air was 23.0 ± 1.5 °C. The weight loss due to the water evaporation during the measurement was taken into account in the results. Hexadecane has a minimal evaporation over this time period.

The porosities of the coating layers were determined by a silicon oil absorption saturation method as well as the microbalance analysis by water and hexadecane at equilibrium saturation. In the silicon oil measurement, the pigmented tablet was left for 1 h in the oil, and the weight of tablet before and after oil saturation was measured. For all liquids, the absorbed liquid volume was measured as the weight change between the "dry" and saturated sample divided by the density of the respective liquid. The porosity of the sample for each liquid was thus defined as the volume of absorbed liquid at saturation divided by total volume of sample. All determinations were made at room temperature (23 ± 2 °C) and normal atmospheric pressure.

The pore size distribution was analyzed by mercury porosimetry (Micrometrics AutoPore IV[10]). The coating structure was impregnated with mercury using both low and high pressures. The

Table 1
The properties of coating pigment.

Pigment property	Ground calcium carbonate (GCC) [35]	Modified calcium carbonate (MCC)	Precipitated calcium carbonate (PCC)
Weight median diameter of particle ($d_{50w/w\%}$) (µm)	1.10	2.70	Small fraction 0.02–0.03 Ave. 0.25[*]
Specific surface area (BET, ISO 9277) ($m^2 g^{-1}$)	8.5	46.2	73.9
Product form	41.7 (without added dispersant) and −40.2 mV (added sodium polyacrylate)	Powder (cationically predispersed)	Anionic slurry
SEM picture			

[*] NanoSight (results had two peaks: small fraction at 0.02–0.03 µm and average at 0.25 µm).

porosity and pore size distribution were calculated adopting the Pore-Comp[11] correction, which takes account of penetrometer expansion, mercury compression and compression of the sample skeletal material, expressed as the elastic bulk modulus, according to Gane et al. [41].

Binder films were produced in order to establish the moisture uptake associated with the binder alone. PVOH was formed into a film using a Teflon®[12] mould and dried at 23 ± 2 °C. The thickness of the partially hydrolysed PVOH film was 225 µm. A latex film formed from the SA binder was made to a thickness of 284 µm using an Erichsen[13] film applicator (Model 288) followed by drying in an oven at 105 °C for 5 min. The diffusion coefficient for water into the binder films, was calculated also from the results of the microbalance showing weight change as a function of the moisture content of the surrounding air in the balance chamber. The moisture content was adjusted step by step starting from 0.1% RH and progressing to 5%, 50%, 93% RH and finally to 50% RH. The temperature of the measuring chamber was controlled to be at 23.5 ± 0.3 °C.

3. Results

3.1. The coating layer structures

The porosities of the coating layers are shown in Fig. 3: the coating made from the normal offset standard GCC had the lowest porosity, and the coating of the dual-pore size MCC and inkjet speciality PCC the highest. In the case of MCC, the addition of SA latex produced a coating layer structure that had slightly higher pore volume than when using the same amount of polyvinyl alcohol. The cationic dispersing of the MCC pigment seems to produce a slightly higher porosity than the subsequent anionic re-dispersing (no binder), suggesting either a slight flocculation remains in the cationic state or that the additional polymer itself reduces pore volume. With GCC and PCC pigments, SA latex addition gave a lower pore volume than when adding PVOH. The results from different measurements had some differences, especially when the results of non-pressurized measurements (saturation by imbibition) are compared to the results of mercury porosimetry (pressurized).

The pore size distributions of the coatings diverged a lot (Fig. 4A–C), thus enabling the effect of pore structure to be studied in detail. The PCC pigment coating produced the smallest pore diameters, which were in the area of 15–60 nm. The pores of the GCC pigment structure located in the area of 90–330 nm, and

MCC had a dual-pore size distribution, where the pore diameters located in the area of 20–60 nm (intra-particle) and 300–700 nm (inter-particle). The addition of PVOH binder decreased the inter-particle pores of MCC coatings to 200–400 nm and SA latex addition increased it to 500–1000 nm. In the case of GCC, all pore size distributions were very similar since the amount of binder added was confined to 1 pph.

3.2. The transport of polar and non-polar liquid

Fig. 5A illustrates, as an example, the absorbed water or hexadecane volume per initial tablet–liquid contact area against time for the coating tablet structures during the microbalance measurements. In the beginning of the absorption, the liquids absorbed very quickly into the coating layer. Then there was a region of slower increase and finally the uptake stopped due to the saturation. A closer study of the absorption results (Fig. 5B) shows that there exist two increasing regions in the absorption curve in the case of MCC with just 1 pph of PVOH, both of which have a linear correlation with square root of time. All the coatings had a linear proportionality to $\sqrt{t}$ over a ∼2 s timescale. The domination of different sorption phenomena in the coating structure varies during time. Therefore, it can be assumed that before ∼2 s the capillary wetting and surface diffusion dominate, and after that it turns toward a domination of permeation resistance acting to equilibrate against the capillary wetting and bulk diffusion forces. In a high-speed inkjet printing press, such as the Versamark® VX5000e, the delay between the first printing nozzle and the beginning of the dryer is 17 s at a web speed of 15 m min⁻¹ and at 100 m min⁻¹, 2.6 s. Therefore, it can be concluded that the times considered here, and the transition of phenomena between them, are highly relevant when considering inkjet printing. The MCC coating with 7 pph SA had only a slight change in the slope of curve with $\sqrt{t}$ (Fig. 5D), reflecting the reduced permeability of this coating as shown by the lower specific pore volume associated with the larger pore size in the discrete bimodal distribution (Fig. 4). Furthermore, if we look at the data over the longer time scale (Fig. 5C), this sample containing the higher level of latex shows a further time-dependent variation of the water absorption rate. This accelerated response over time probably relates further to the action of latex-associated surfactant.

The absorption rate of short and long timescale during the liquid uptake can be expressed [15,42] as

$$\frac{d(V(t)/A)}{d\sqrt{t}} = \frac{d((m(t)/\rho)/A)}{d\sqrt{t}} \quad (1)$$

where $V(t)$ is the volume of uptaken liquid at the time t, A the cross-section area of tablet, $m(t)$ is the mass uptake of the liquid and ρ the

---

[11] Pore-Comp are a software network model and sample compression correction software, respectively, developed by the Environmental and Fluid Modelling Group, University of Plymouth, PL4 8AA, UK.
[12] Polytetrafluoroethylene, Du Pont.
[13] Erichsen GmbH & Co., Am Iserbach 14, D-58675 Hemer, Germany.

Table 2
The formulation of the coating colours.

Coating (pph)	Cationic MCC	Anionic MCC	Anionic MCC + 1 pph PVOH	Anionic MCC + 1 pph SA	Anionic MCC + 7 pph PVOH	Anionic MCC + 7 pph SA	Anionic GCC	Anionic GCC + 1 pph PVOH	Anionic GCC + 1 pph SA	PCC[a]	Anionic PCC + 1 pph PVOH	Anionic PCC + 1 pph SA
Pigment												
MCC	100	100	100	100	100	100						
GCC							100	100	100			
PCC										100	100	100
Dispersing agent												
Anionic sodium polyacrylate		0.5	0.5	0.5	0.5	0.5	0.5	0.5	0.5	0.5	0.5	0.5
Cationic polyDADMAC	0.5											
Binder												
PVOH (partially hydrolysed)		No	1		7		No	1		No	1	
SA latex				1		7			1			1
Zeta-potential (AcoustoSizer II[b]), mV	23.6	−36.7	N/A	N/A	−11.9	−37.0	−9.0	N/A	N/A	−3.1	N/A	N/A

[a] PCC pigment was provided by the manufacturer as a slurry-form: exact type and amount of dispersing agent are not known.
[b] AcoustoSizer II is a product name of Colloidal Dynamics/Agilent, Technologies (Finland Oy), Linnoitustie 2B, FI-02600, Espoo, Finland.

density of liquid. The absorption rate is recorded as a linear trend line from the gradient of the volume per contact area of sample against the square root of time. We separated the short timescale (under 2 s) and the long timescale absorption for all the pigment and binder combinations (Figs. 6 and 7).

When the liquid arrives in the contact with coating layer surface, the liquid front undergoes the wetting process of the constituent surfaces and the following bulk liquid fills first of all the smallest capillaries and finally proceeds into the large pores. This process is commonly explained by a purely hydrodynamic model [6,10,11], which assumes that the loss of energy during the liquid imbibition in the porous structure is based on the viscous drag within the spreading liquid. However, Schoelkopf et al. [38] draw attention to the role of pore size differentiating inertial effects, as summarised in the Bosanquet equation [23]. This differentiation means that the nanopores, if short, as they are in such coating structures, will constitute the first imbibing structure component by plug flow. Only later will the hydrodynamic viscous flow become active as a significant distance in the pore structure is filled and the larger reservoir pores also fill. At this latter stage, the balance between the wetting force of capillaries and the viscous drag determines the rate of progress. As the viscous drag increases in proportion to the length over which the liquid flows within the structure, and to the inverse of the fourth power of the typical equivalent capillary size (Poiseuille effect), there comes a point when the viscous drag equals the wetting force. If an external pressure is raised above the difference between the capillary force and the viscous drag, or when all the pores behind the wetting front are filled, then the action is by permeation flow according to Darcy's law in saturated structures. The bimodal behaviour of each curve illustrates the competition between the initial capillary wetting and the permeable flow characteristic once capillaries/pores behind the wetting front are filled.

It is interesting to note in Figs. 6A and C and 7B that the transition from the shorter time absorption to the longer time absorption for water in the presence of the 1 pph SA binder in MCC and PCC coatings shows a delay at the point of transition before the longer time behaviour is fully manifest. This suggests that there is a time controlling step required after the preferred pathway pores are filled, before the remaing structure can begin to fill. Such effects are either related to a change in structure or a diffusional effect, usually of surfactant origin [12,43]. Since the SA latex polymer matrix is known to be relatively inert to both oil and water, it is unlikely that structural changes are the cause for the delay. Rather, the surfactant associated with the latex may act as a wetting agent to allow passage of water via latex adjacent connecting throats in the pore network. The reorientation of the surfactant in relation to the wetting front may, therefore, control the access to the remaining pore network. Similar effects were seen by Ridgway et al. [42] in their study of the competitive absorption of hexadecane and water using dispersed GCC and similar SA latex as binder. Addition of further latex is likely to reduce permeability to such a level that the turning point of the slopes may disappear, as was seen by Ström et al. [43] with their 11 pph latex offset coatings.

Fig. 8 shows the results of short (upper figure) and long (lower figure) timescale absorption rates. At the short timescale, hexadecane absorbed quickest into the MCC coatings and the ground and precipitated calcium carbonate had very similar absorption rate values. However, the results for water were mostly on the same level in all tablets, only exception was the PCC based structure. The comparison between the short time results of binder containing MCC tablets shows that PVOH containing coatings absorbed water quicker than SA latex coatings. Fig. 7 shows that the results of long timescale absorption rates were smaller in ranking to those at short timescale. Both water and hexadecane absorbed quicker into the coating structures during the first 2 s time than after that. At
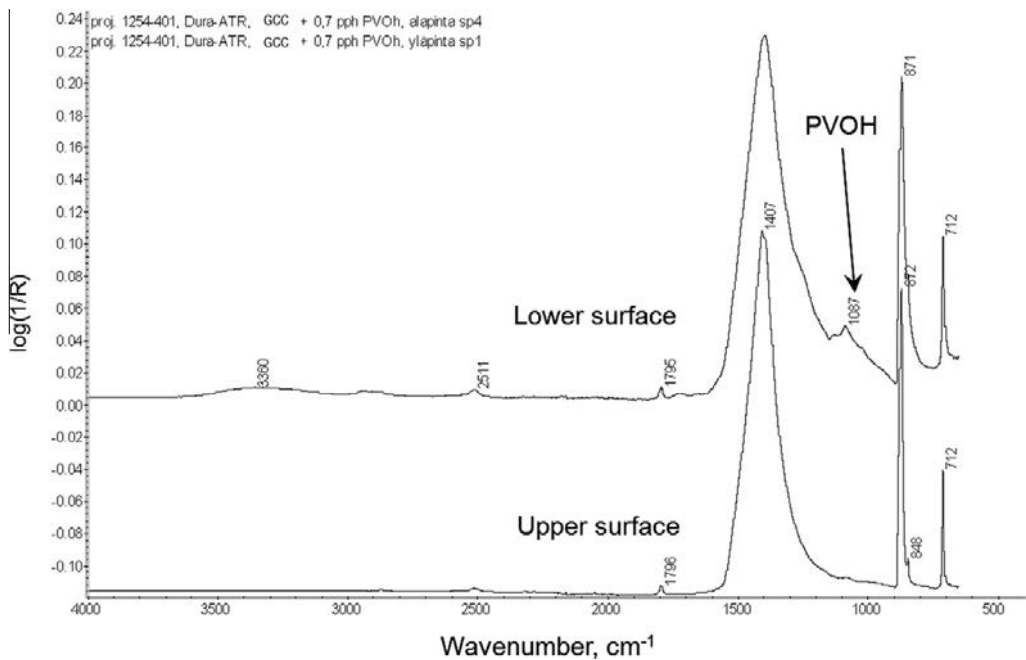
Fig. 2. The IR spectra of the tablet GCC with 0.7 pph PVOH (partially hydrolysed), measured with the FT-IR spectrometer. (Notice the lower PVOH content of colour in this measurement (=0.7 pph) compared with the actual tablets made for the microbalance measurement (1 pph)). The lower surface was against the wire filter in the tablet former. The main peak of PVOH locates at the wavenumbers of 1087 cm^{-1}.

Table 3
Properties of water and hexadecane.

Liquid	Density (20 °C) (g cm^{-3})	Dielectric constant	Polarity index	Surface tension (mN m^{-1})	Viscosity (20 °C) (mPa s)
Water, H$_2$O	0.988	80.2	9.0[a], 10.2[b]	72.8	1.002
Hexadecane, CH$_3$(CH$_2$)$_{14}$CH$_3$	0.773	2.0	0.0	27.5	3.340

[a] Snyder [39].
[b] Snyder [40].

Table 4
The thickness of binder films and the diffusion coefficient calculated with Eq. (4).

Binder film	Thickness (m)	Diffusion coefficient (m^2 s^{-1})
PVOH (partially hydrolysed)	2.25E−04	3.0E−13
SA latex	2.84E−04	3.5E−13

long timescale, water provided higher absorption rates than hexadecane and the SA containing MCC coatings had now either the same or even higher absorption rate with water than the PVOH containing coatings.

3.3. Diffusion in binder films

The diffusion coefficient evaluation was made by studying the water vapour absorption into the binder films. The target of this small study was to find out the differences in the diffusion rate between the PVOH and SA latex films. In the real case of inkjet ink sorption, the aqueous-based ink diffuses quicker into the binder film than the vapour-form water because of the higher amount of water molecules, i.e. greater surface concentration of water. Fig. 9 shows how the studied PVOH film absorbs water to an amount of 37% of the film's original weight at 30 s, whereas in

the vapour-form the same film took up water to only 0.01 % under saturated humidity in addition to the amount already in the binder film under room temperature and humidity conditions. At the same time, the SA latex film absorbs a clearly lower amount of water or inkjet ink. Therefore, it can be assumed that during the inkjet ink setting process, the provided liquid water from the inkjet ink diffuses faster (concentration gradient dependent) into the binder film than the water moisture used in this part of the study. Additionally, the thickness of the polymer layer existing within nanopores will only constitute some few polymer molecules and so the path length for diffusion is also extremely short within such structure as the wetting front encounters the polymer.

There were two reasons why moisture rather than liquid water was selected to determine diffusion coefficient in this study. The first reason was that the absorption amount of SA binder film was low (Fig. 9) and the diffusion comparison between binder films needed to be made. The second reason was the accuracy of the crude immersion gravimetric method, where binder film was submerged into the water. Some of the polymer can transfer to the blotting boards, and in the case of hydrophilic PVOH film the polymer partially dissolves into the water during the measurement. Therefore, whilst the diffusion coefficient remains the same for moisture and for liquid water, the concentration difference is much
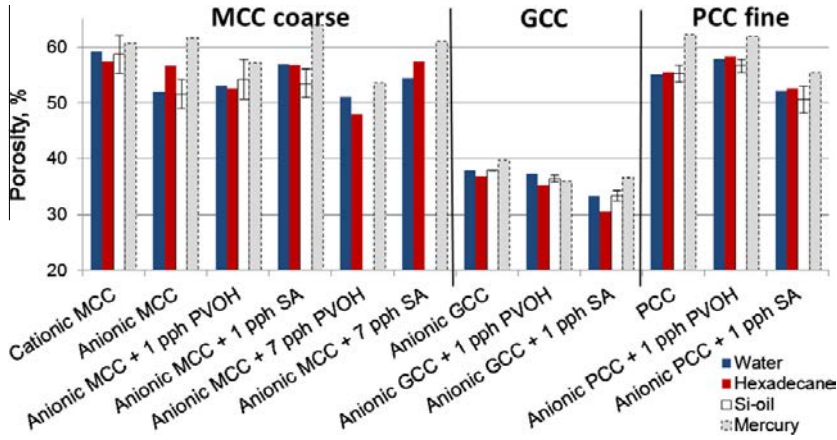
Fig. 3. The pore volume of coatings. Measured with Si-oil, water and hexadecane absorption and the mercury porosimetry.

A – MCC, GCC and PCC pigments

B – MCC coatings (+ binder)
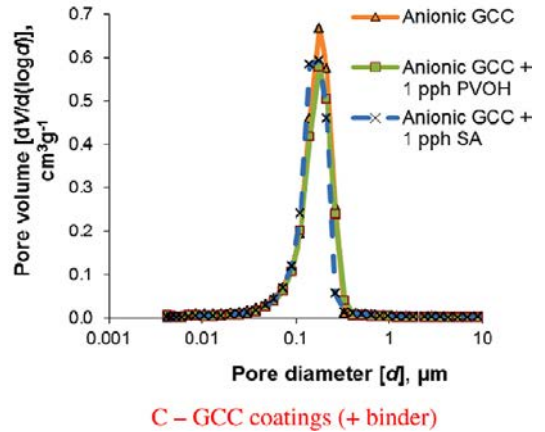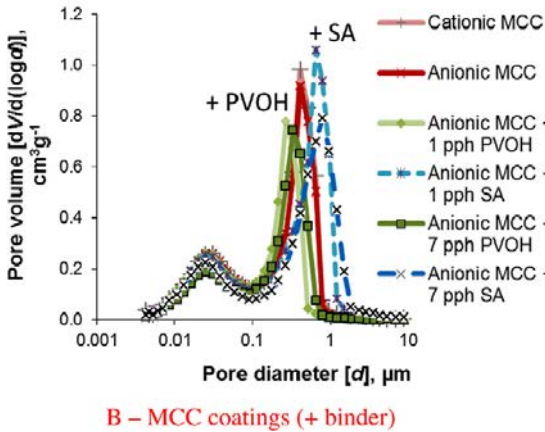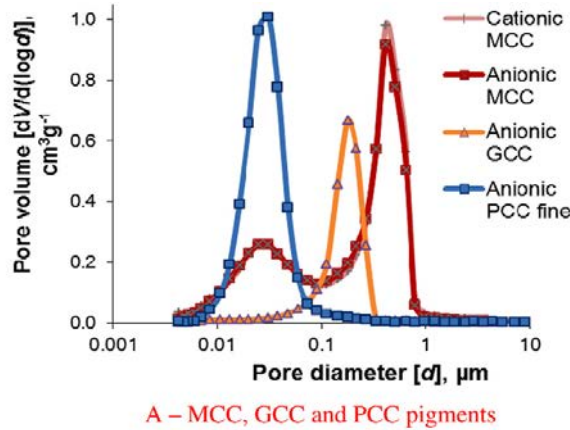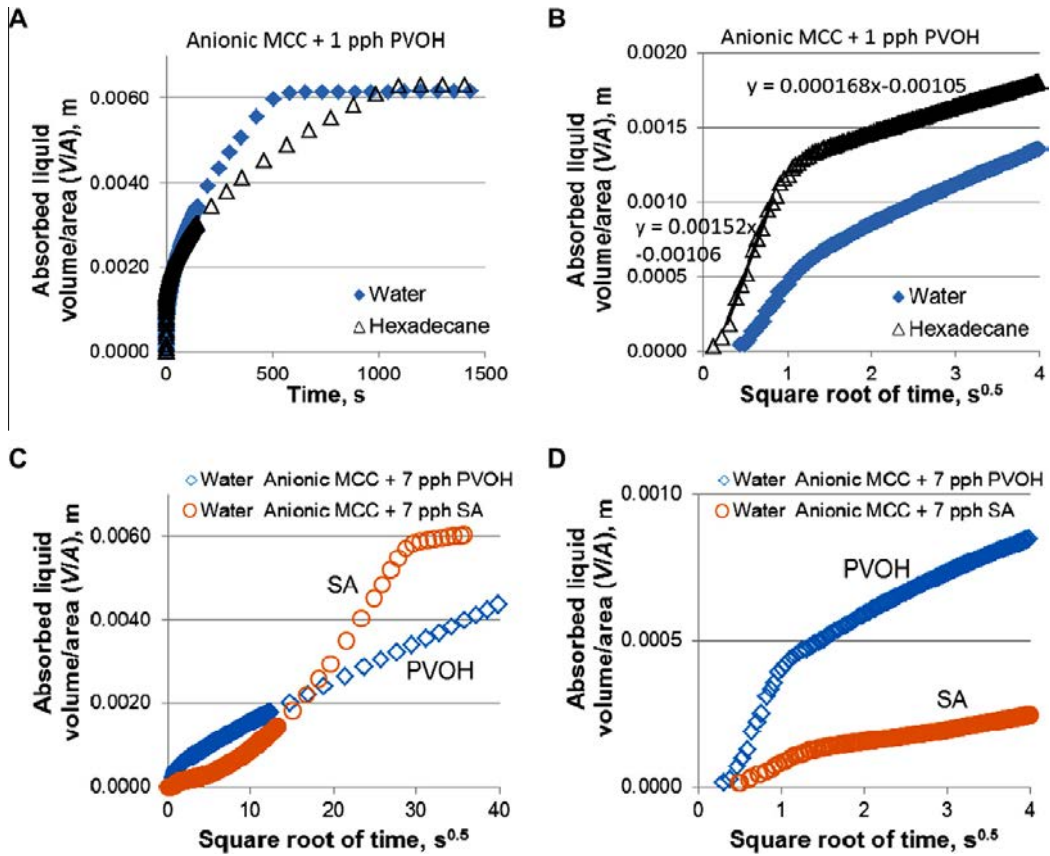
C – GCC coatings (+ binder)

Fig. 4. The pore size distributions of the coating structures. (A) Differences between MCC, GCC and PCC pigment coatings (no binder addition). (B) The modified calcium carbonate (MCC) after adding the relevant binder amounts. (C) Ground calcium carbonate (GCC) as a function of a small amount of binder addition.

Fig. 5. The result curves of water and hexadecane imbibing into the anionic MCC coating structure with 1 pph PVOH (A and B). (A) Results of the measuring time up to 1500 s. (B) results of the first 4 $s^{0.5}$. (C) The result curves of water into the 7 pph PVOH and 7 pph SA latex containing coatings up to 40 $s^{0.5}$. (D) The same results as in C but the time scale is shorter, up to 4 $s^{0.5}$.

higher for liquid water at the polymer surface, and so the absolute uptake is greatly increased in the case of absorbing liquid.

Absorption data for water into binder films were analyzed using the techniques of Dynamic Vapour Sorption, DVS-1,[14] which is a gravimetric moisture sorption measurement. The analyses were made with partially hydrolysed PVOH and SA latex films using different moisture contents of surrounding air. The results are shown in Fig. 10. The shape is that of an inverse exponential, and therefore we have applied the so-called Case II or Linear Driving Force Mass Transfer Model in the calculation of diffusion coefficient [44].

There was assumed to be an analogous substitution for heat transfer with mass transfer (thermal diffusivity "a" is replaced with moisture diffusion coefficient "D"), such that

$$\frac{M(\tau)}{M_{\text{Max}}} = 1 - \frac{4}{\pi} \sum_{n=0}^{\infty} \frac{(-1)^n}{(2n+1)} \times \cos\left(\frac{2n+1}{2}\pi\frac{x}{\delta}\right) \exp\left[-\left(\frac{2n+1}{2}\right)^2 \pi^2 \frac{D\tau}{\delta^2}\right] \quad (2)$$

where τ is time, D the molecular diffusion coefficient and n the consecutive layers. The other variables are described in Fig. 11. The Eq. (2) can be simplified for mass change of moisture in the middle of the plate, i.e. at $x = 0$ and for $n = 0$.

$$\frac{M(\tau)}{M_{\text{Max}}} = 1 - \frac{4}{\pi} \exp\left[-\frac{\pi^2}{4}\frac{D\tau}{\delta^2}\right] \quad (3)$$

In the Eq. (3) $4/\pi$ was taken away because at the initial time $\tau = 0$ the right side of the equation is negative, but it should be 0. So, following equation was used for diffusion coefficient estimation

$$\frac{M(\tau)}{M_{\text{Max}}} = 1 - \exp\left[-\frac{\pi^2}{4}\frac{D\tau}{\delta^2}\right] \quad (4)$$

The measured absorption amounts and the values from the diffusion Eq. (4) match very well (Fig. 12).

In this calculation, the diffusion was assumed to happen into the plate-like structure. This is actually valid for the PVOH and not for the latex. In the latex case, only a few water molecules can transfer into the film, meaning that the diffusion is more a surface diffusion. If we then decrease the thickness factor of the plate-like structure near zero, we shall get the surface diffusion. The mass transfer in the near-zero stage becomes zero in the Eq. (4), which cannot be true in the real liquid transfer. Nonetheless, the Eq. (4) fits the experimental diffusion data quite well. It delivers
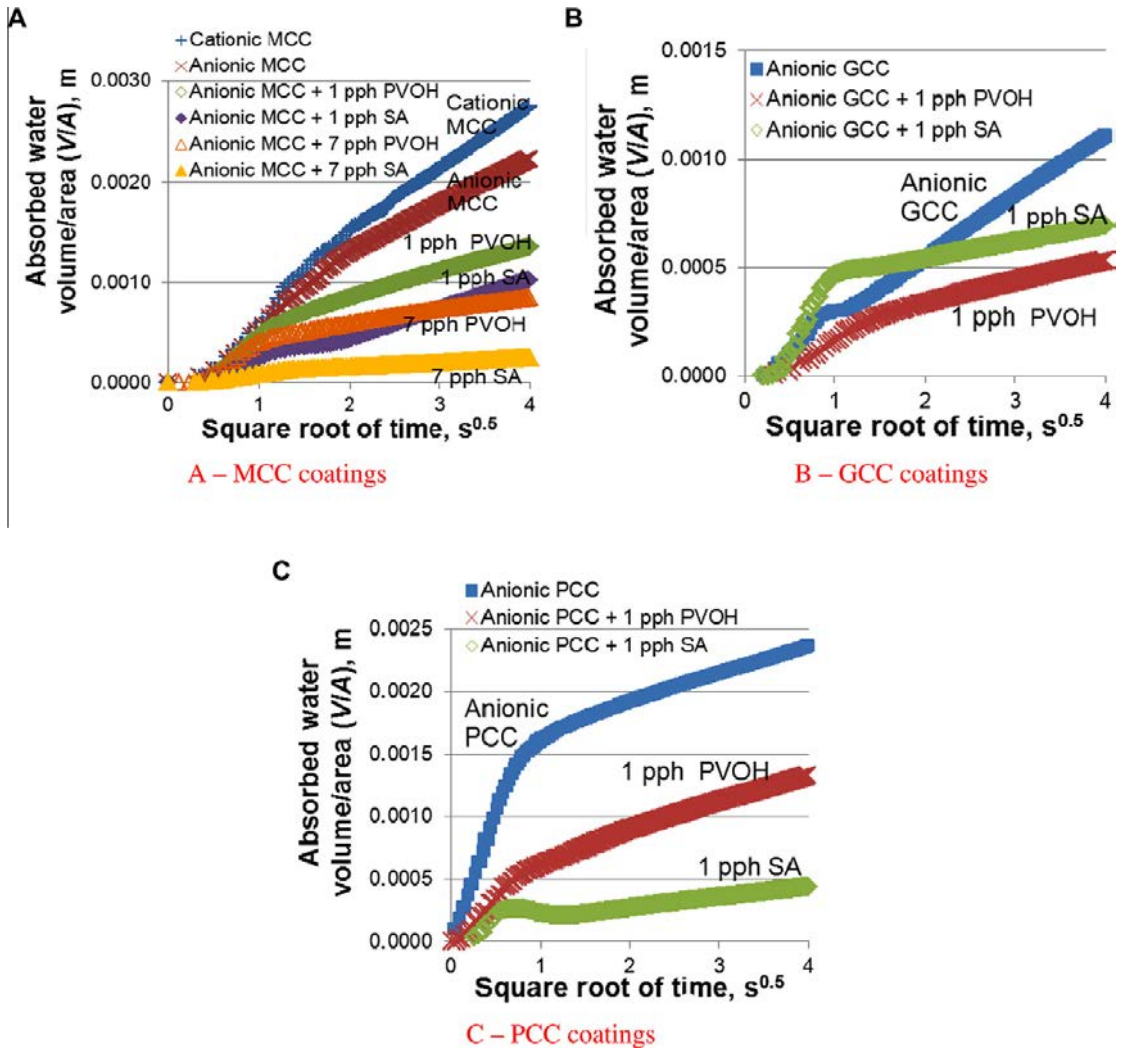
Fig. 6. Absorbed liquid volume/contact area of water (polar) and hexadecane (non-polar) into the studied coating structures. (A–C) The absorption amount of water into the MCC, GCC and PCC coatings, respectively.

a reasonable diffusion coefficient for latex, though it is insufficient for the latex case.

4. Discussion

Figs. 5–7 show that the results of absorbed liquid amount have two quite linear relations to the square root of time. This indicates either equilibrated Poisueille laminar flow, only applicable to the long timescale [15,23] according a Lucas-Washburn-type equation, and/or a Fick's Law diffusion response, which could apply to both the short as well as the long timescales. Fick's first law describes the steady state of diffusion, where the concentration of diffusion volume is unchangeable during time. Fick's second law describes the situation when the concentration within the diffusion volume changes during the time,

$$\frac{\partial c(x,t)}{\partial t} = D\frac{\partial^2 c(x,t)}{\partial x^2} \tag{5}$$

where $c(x, t)$ is the concentration of liquid at position x and time t. D is the diffusion constant. Thus, by dimensions, the denominator x^2 is proportional to the time t, and hence x is proportional to $\sqrt{t}$. Deriving from this, the diffusion length is often shown as $2\sqrt{(Dt)}$. The distance has a connection to the volume of liquid in the three-dimensional system and thus represents the mass of liquid uptake. Therefore, we can write the Eq. (5) as

$$\frac{m(t)}{t} = D\frac{A \cdot c(x,t)}{x} \tag{6}$$

where $m(t)/t$ is mass flow rate during the time t and area A of cross-section where the liquid is taken up.

4.1. Short timescale absorption

The short timescale absorption rate in Fig. 8 (upper side) shows that *non-polar* liquid (hexadecane) absorbs quicker in the anionic coating layer than polar liquid (water). The PCC coating without
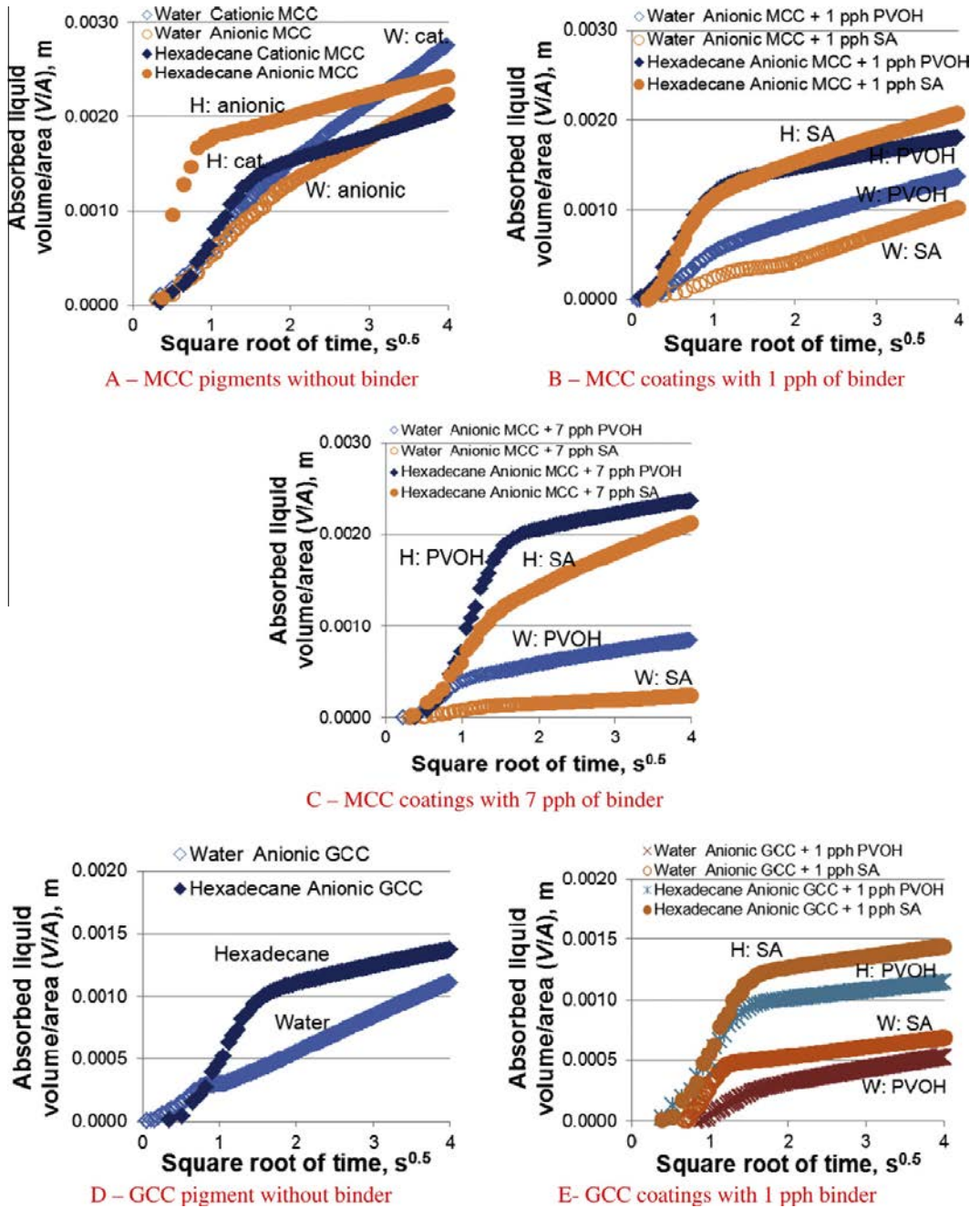
Fig. 7. (A–C) The differences between water and hexadecane absorption into the MCC coatings. (D and E) The absorption of water and hexadecane into the GCC pigment coatings. (H and J) The absorption of water and hexadecane into the PCC pigment coatings. In figures water has marked with abbreviation W and hexadecane with H.

binder forms the only exception, where water seems to absorb quicker than hexadecane in the structure. This was also shown by Ridgway and Gane [27]. One possible explanation also advanced by Ridgway et al. is that the chemical compounds used in the pigment dispersion may cause this difference. Both the GCC and the MCC contain anionic polyacrylate dispersant, which itself requires a diffusion time for water to infiltrate the polymer network, swelling it and rendering it fully hydrophilic, whereas the PCC requires additional polyacrylate to render it more strongly anionic in dispersion. Thus, the PCC forms the notable exception in this series,
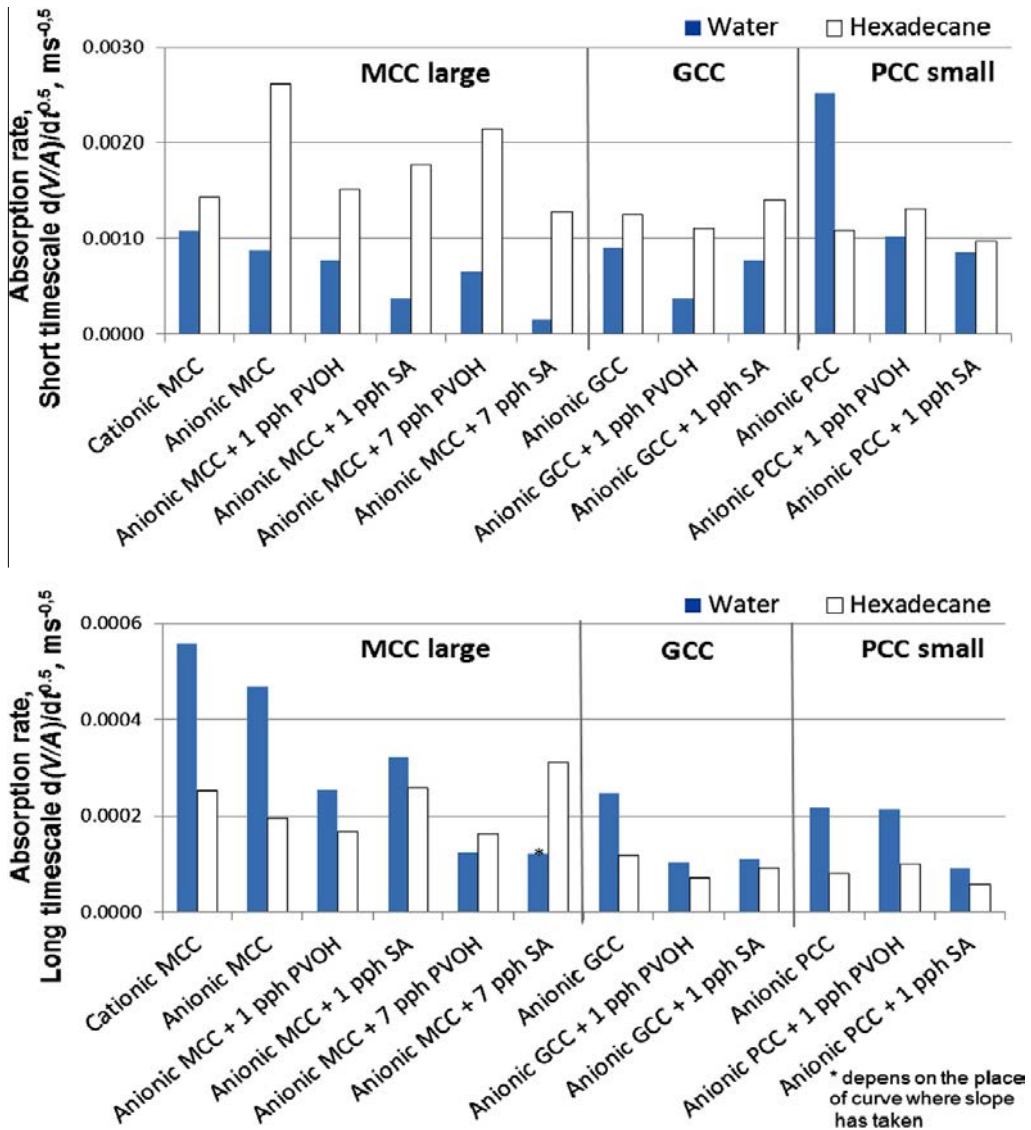
Fig. 8. Absorption rate of modified, ground and precipitated calcium carbonate pigment coatings. The short (upper figure) and long (lower figure) timescale $d(V(t)/A)/dt^{0.5}$ data are derived from the gradients of the curves, exemplified in Fig. 6, where the x-axis follows $\sqrt{t}$.

reversing the absorption preference from hexadecane to water at the shortest timescales.

The situation changes again when binder is present. The PVOH cannot absorb non-polar liquids meaning that swelling of the polymer in the presence of hexadecane is minimal. The smallest pores in the coating remain open during the hexadecane absorption and the diameters of inter-particle pores are unchanged [27]. Thus, during the non-polar liquid imbibition, the capillary flow dominates. In addition, the results show that the coating structure with both intra- and inter-particle pores (MCC) transports the hexadecane most effectively. Similar pore size structure coatings were found to be favourable for inkjet inks by Ridgway and Gane [27].

At short timescales, initially surprisingly, the slowest rate of absorption values with *water* were shown by the MCC/SA coatings, which had a slightly higher overall porosity and larger pores than the MCC/PVOH coating structures. The PVOH containing coating has more small pores than the SA coating. Thus, the apparent anomaly can be explained by the swelling of hydrophilic PVOH [28] changing the volume amount of small pores during the initial water absorption. The SA latex has a non-swelling nature [28,43] in the presence of water and thus the capillary flow controls the water imbibition in this case. The reason for slower absorption rate can be in the hydrophobic nature of SA latex that prevents the polar water penetration, probably related to the spatial orientation of surfactant and/or the carboxylation, used to stabilize the latex in
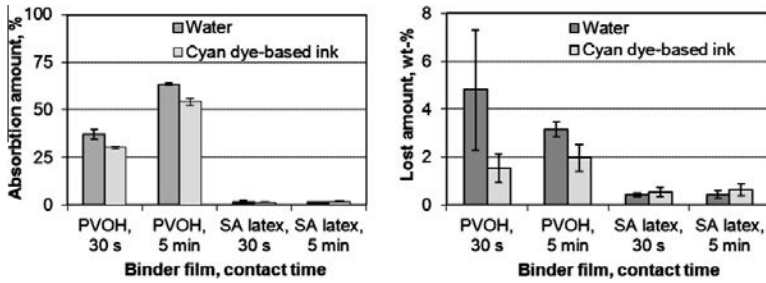
Fig. 9. Absorption of liquid water (A) into the PVOH and SA latex films (thickness about 200 μm) after 0.5 min and 5 min absorption time, and the loss of mass from the polymer film (B) into the water during the same measurement. The binder films were submerged into the water and removed after a certain time, dried gently between blotting boards and weighed.
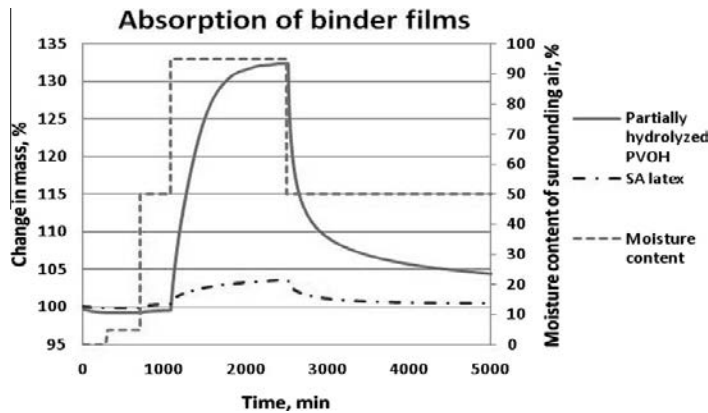

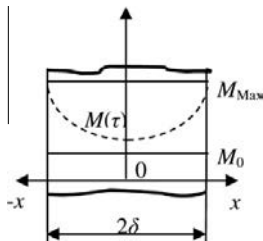**Fig. 10.** Absorption curves for water vapour diffusion for different films.

Fig. 11. A schematic view of the plate (film) body. M_0 is the initial moisture content in the plate; M_{Max} the maximum moisture content achievable in the plate.

dispersion, being both lower than in the case of anionically dispersed pigment and less polar than cationically dispersed systems. Similar binder behaviour in respect to water uptake was noticed with the PCC pigment coatings, too. It seems that the smallest pores are important in the polar liquid imbibition, but the necessary pre-diffusion into binder that inhabits these pores is an additional short timescale phenomenon. The capillary action controls the polar liquid imbibition in the short timescale, but the diffusion of water into binder polymer is also taking an active part in this process.

4.2. Long timescale absorption

In long time absorption (Fig. 8, lower side), the diffusion is still progressing but the porosity of the structure (permeation flow) permits the continued liquid imbibition by pore surface wetting and subsequent meniscus flow. In the long time area, the absorption rates are slower than in the short timescale area. In addition, the water absorbs quicker than hexadecane. The MCC coatings had again higher absorption rate values than either the GCC or the PCC containing coatings. The coating with the dual-porosity structure seems again to be the most advantageous.

When the MCC pigment with PVOH and SA containing coatings are compared on the long timescale, we can notice that the absorption rate of SA containing coating is the same or higher than that of the PVOH containing coating. In the over 2 s time absorption regime, the small diameter pores at the wetting front retain their action of providing the driving force, but the rate is determined by the permeation flow resistance to that driving force. These findings further support the conclusions of Ridgway and Gane [27].

4.3. Diffusion during inkjet ink absorption

The diffusion coefficients for water vapour in films made from the PVOH and SA latex binders are both close to $3 \cdot 10^{-13}$ m^2 s^{-1} (Table 4), whereas in the coating structures, such as the MCC pigment with 1 pph of PVOH or SA, they are each about $2.5 \cdot 10^{-11}$ m^2 s^{-1}. In comparison, for cellulose fibres the water va-
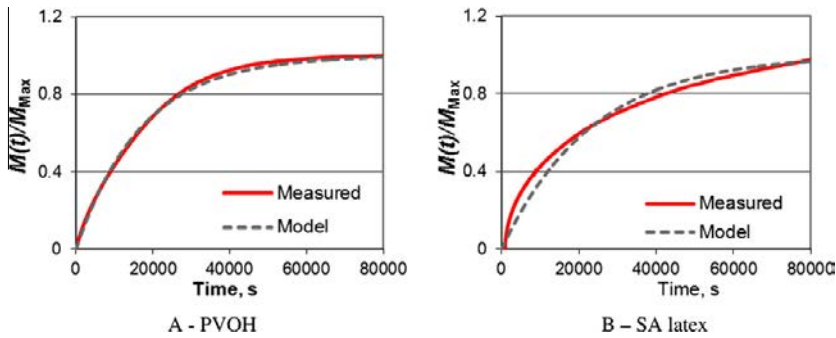
Fig. 12. The matching of model and measured data. (A and B) The measured absorption amounts divided by the maximum absorption of PVOH or SA latex films and the values of model (Eq. (4)), respectively.
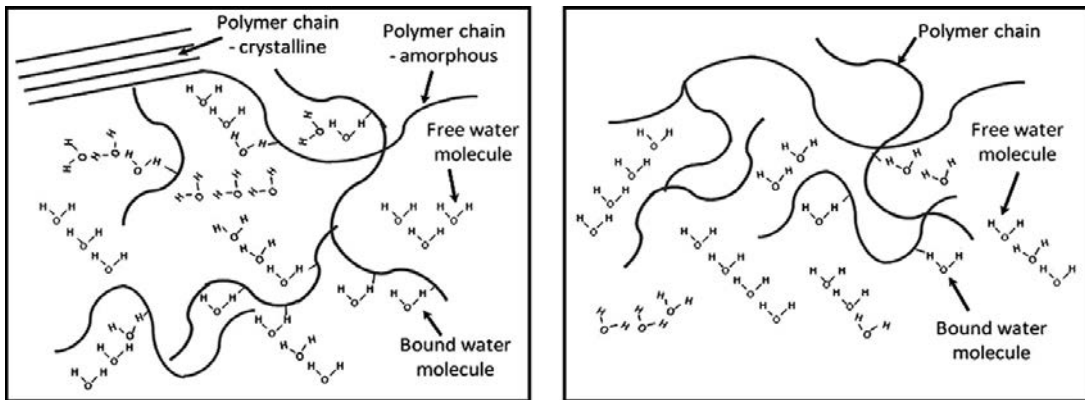

Fig. 13. The water molecules in the PVOH and SA latex polymer network.

pour diffusion coefficient is also about 10^{-11} m^2 s^{-1} [45], and for paper, with porosity of 20%, 10^{-8} m^2 s^{-1} [46]. Therefore, we can conclude that the permeability of the coating structure enhances the diffusion rate of that of binder alone. There are, then, no significant differences between the diffusion coefficient for PVOH and SA binder films or the coatings containing these binders. The same diffusion coefficient means that the flux of water vapour in these coatings is dominated by the pore structure of the coating, and thus also the local liquid concentration difference across the wetting front during the imbibition time. This supports the findings of Gane and Ridgway [34], who presented moisture pickup results from pigment tablets of dispersed GCC of various particle size distributions.

We suggest that, in the PVOH binder, the water molecules diffuse into the polymer chain network and form hydrogen bonds with the hydrophilic groups of the amorphous region of polymer whilst some of them remain as free water in the network. The water molecules cause the swelling of the binder and the further opening of the PVOH network microstructure so that the colourant molecules may subsequently fit into the binder structure (Fig. 13). In the SA latex case, the polymer microstructure has less chemical groups that could fix the water molecules and therefore there exists more free water than bound water in the network of SA binder during the water imbibition. The effective binding capacity of PVOH means that the polymer attracts (absorbs) the water molecules and the concentration of water in the PVOH is therefore higher than in the latex, although the diffusion rate of water vapour in relation

to the polymer itself remains similar. It seems that in the case of PVOH we identify possible "interpolymer" diffusion meaning that the diffusion is happening in the polymer network structure, whereas in the latex case the diffusion happens mainly on a surface of polymer network. It might be so that the surface properties of the latex extend for a significant distance from the actual surface, and we may suspect a swollen stabilizing layer. In the case of PVOH containing coating, the dominating diffusion can start from surface diffusion and osmosis, followed by Knudsen diffusion when the swelling has decreased the effective pore diameters. In the SA coatings, the role of Knudsen diffusion is assumed to be insignificant.

5. Conclusions

The results of the liquid uptake studies show that, in the beginning of the inkjet ink vehicle absorption, the small diameter (nano) pores play a dominant role and they provide the continuing driving force throughout imbibition. The capillary force drives the liquid into the coating structure. The polar liquid (water) diffuses into the polymer network of hydrophilic binder polymer (PVOH) and partially fixes there acting as a swelling agent, causing closure of some pores and a general diminishing of the binder-free portion and hence a reduction in pore diameters. This limits the available volume but assists the liquid faster absorption. The water molecule diffusion opens the PVOH polymer network. At the long timescale, the polymer swelling continues, but the permeation flow is the main

resistance determining factor to the capillary and surface diffusion controlled driving force in the continuing liquid mass transfer.

The absorption results of SA latex containing coatings show that the water uptake of initially hydrophobic coating proceeds more slowly at the short timescales, probably due to spatial orientation of latex stabilizing surfactant, whereas at the longer timescale the liquid transports quicker in the SA containing coatings than in the PVOH containing. It seems that the hydrophobic nature of latex prevents the diffusion of the polar liquid into the polymer network of the binder and there exists only a surface diffusion, probably related to the surfactant and/or carboxylation used to stabilize the latex.

References

[1] H.R. Kang, J. Imaging Sci. 35 (3) (1991) 195–201.
[2] M. von Bahr, F. Tiberg, B. Zhmud, Langmuir 15 (15) (1999) 7069–7075.
[3] S.N. Reznik, A.L. Yarin, Int. J. Multiphase Flow 28 (9) (2002) 1437–1457.
[4] A.U. Chen, O.A. Basaran, Phys. Fluids 14 (1) (2002) L1–L4.
[5] O.A. Basaran, AIChE J. 48 (9) (2002) 1842–1848.
[6] G. Desier, F. Deroover, F. De Voeght, A. Soucemarinadin, J. Imaging Sci. Technol. 48 (5) (2004) 389–397.
[7] F. Girard, P. Attané, V. Morin, Tappi J. 5 (12) (2006) 24–32.
[8] J. Eggers, E. Villermaux, Rep. Prog. Phys. 71 (036601) (2008) 79.
[9] A.N. Lembach, H.-B. Tan, I.V. Roisman, T. Gambaryan-Roisman, Y. Zhang, C. Tropea, L. Yarin, Langmuir 26 (12) (2010) 9516–9523.
[10] N. Alleborn, H. Raszillier, Chem. Eng. Sci. 59 (10) (2004) 2071–2088.
[11] C. Josserand, S. Zaleski, Phys. Fluids 15 (6) (2003) 1650–1657.
[12] M. von Bahr, F. Tiberg, V. Yaminsky, Coll. Surf. A: Phys. Chem. Eng. Aspects 193 (1–3) (2001) 85–96.
[13] J. Marmur, Langmuir 19 (14) (2003) 5956–5959.
[14] R.A. Hayes, J. Ralston, Langmuir 10 (1) (1994) 340–342.
[15] J. Schoelkopf, P.A.C. Gane, C.J. Ridgway, G.P. Matthews, Colloid Surf. A 206 (1–3) (2002) 445–454.
[16] K.S. Sorbie, Y.Z. Wu, S.R. McDougall, J. Colloid Interface Sci. 174 (2) (1995) 289–301.
[17] E.W. Washburn, Phys. Rev. 17 (3) (1921) 273–283.
[18] J.M. Brethour, L.E. Scriven, in: 10th Int. Coating Sci. Tech. Symp., Scottsdale, USA, Int. Soc. Coating Sci. Tech., 2000, pp. 97–100.
[19] H. Gerung, Z. Yanrui, W. Li, R.K. Jain, T.J. Boyle, C.J. Brinker, S.M. Han, Appl. Phys. Lett. 89 (11) (2006) 111107 (p. 3).
[20] H. Gerung, T.J. Boyle, L.J. Triby, S.D. Bunge, C.J. Brinker, S.M. Tan, J. Am. Chem. Soc. 128 (15) (2006) 5244–5250.
[21] J.S. Preston, N.J. Elton, A. Legrix, C. Nutbeem, J.C. Husband, Tappi J. 1 (3) (2002) 3–5.
[22] C.J. Ridgway, P.A.C. Gane, J. Colloid Interface Sci. 252 (2) (2002) 373–382.
[23] C.M. Bonsanquet, Philos. Mag. Ser. 6(45) (1923) 267, 525–531.
[24] J. Kettle, T. Lamminmäki, P. Gane, Surf. Coat. Technol. 204 (12–13) (2010) 2103–2109.
[25] R.J. Good, K.L. Mittal (Eds.), Koninklijke Wöhrmann BV, Zutphen, The Niederlands, 1993, pp. 3–36.
[26] C.J. Ridgway, P.A.C. Gane, J. Schoelkopf, Colloids Surf. A 236 (1–3) (2004) J91–J102.
[27] C.J. Ridgway, P.A.C. Gane, in: TAPPI Coat. Conf., Toronto, Canada, Tappi Press, Atlanta, USA, 2005, 15pp.
[28] T. Lamminmäki, J. Kettle, P. Puukko, P.A.C. Gane, C. Ridgway, in: Int. Paper Coating Chem. Symp., Hamilton, Canada, 2009, 13p.
[29] D.J. Shaw, Introduction to Colloid & Surface Chemistry, Reed Educational and Professional Publishing Ltd., 1996, 306p.
[30] B. Liang, R.J. Fields, J.C. King, Drying Technol. 8 (4) (1990) 641–665.
[31] H. Radhakrishnan, S.G. Chatterjee, B.V. Ramarao, J. Pulp Pap. Sci. 26 (4) (2000) 140–144.
[32] A.T. Ahlen, Tappi J. 53 (7) (1970) 1320–1326.
[33] G. Desie, G. Deroover, F. De Voeght, A. Soucemarianadin, J. Imaging Sci. Technol. 48 (5) (2004) 389–397.
[34] P.A.C. Gane, C.J. Ridgway, in: TAPPI 10th Adv. Coating Fund. Symp., Montreal, Canada, Tappi Press, Atlanta, USA, 2008, 24p.
[35] R. Eriksson, J. Merta, J.B. Rosenholm, J. Colloid Interface Sci. 326 (2) (2008) 396–402.
[36] P.A.C. Gane, G.P. Matthews, J. Schoelkopf, C.J. Ridgway, D.G. Spielmann, in: TAPPI Adv. Coating Fund. Symp., Toronto, Canada, Tappi Press, Atlanta, USA, 1999, pp. 213–236.
[37] C.J. Ridgway, P.A.C. Gane, Nordic Pulp Pap. Res. J. 17 (2) (2002) 119–129.
[38] J. Schoelkopf, P.A.C. Gane, C.J. Ridgway, J. Spielmann, G.P. Matthews, Tappi J. 2 (6) (2003) 9–13.
[39] L.R. Snyder, J. Chromatogr. A 92 (2) (1974) 223–230.
[40] L.R. Snyder, J.L. Glajch, J.J. Kirkland, Practical HPLC Method Development, second ed., Willey, New York, NY, USA, 1988, pp. 722–723.
[41] P.A. Gane, J.P. Kettle, G.P. Matthews, C.J. Ridgway, Ind. Eng. Chem. Res. 35 (5) (1996) 1753–1764.
[42] C.J. Ridgway, J. Schoelkopf, P.A.C. Gane, in: Tappi Adv. Coating Fund. Symp., Munich, Germany, Tappi Press, Atlanta, GA, USA, 2010, 19p.
[43] G.R. Ström, J. Borg, E. Svanholm, in: TAPPI 10th Adv. Coating Fund. Symp., Montreal, Canada, Tappi Press, Atlanta, USA, 2008, pp. 204–216.
[44] H.S. Carslaw, Conduction of Heat in Solids, Clarendon Press, Oxford, UK, 1997, p. 100.
[45] D. Topgaard, O. Söderman, Langmuir 17 (9) (2001) 2694–2702.
[46] E.K.O. Hellen, J.A. Ketoja, K.J. Niskanen, M.J. Alava, J. Pulp Pap. Sci. 28 (2) (2002) 55–62.

Absorption and adsorption of dye-based inkjet inks by coating layer components and the implications for print quality

Absorption and adsorption of dye-based inkjet inks by coating layer components and the implications for print quality

T.T. Lamminmäki [a,*], J.P. Kettle [a,1], P.A.C. Gane [b,c,2]

[a] VTT Technical Research Centre of Finland, P.O. Box 1000, 02044 VTT, Finland
[b] Aalto University, School of Science and Technology, Faculty of Chemistry and Materials Sciences, Department of Forest Products Technology, P.O. Box 16300, FIN-00076 Aalto, Finland
[c] Omya Development AG, CH-4665 Oftringen, Switzerland

ARTICLE INFO

ABSTRACT

Inkjet printed surfaces should have good ink fastness properties so that the printed paper can be finished and remain durable during post-treatment and use. To achieve this, the ink colorant requires adequate fixing to the paper surface. In the case of coated inkjet papers, the coating layer surface is engineered to generate good printability using parameters of pore network structure, surface area and surface chemistry of coating pigment(s), and polymer additive properties. The aim of this work was to clarify how the ionic charge, and particularly its distribution in the coating layer, combines with binder to impact on the dye fixation properties of dye-based inkjet inks. The studied pigments were a specially chosen ionically surface-inert organo silica and a modified calcium carbonate (MCC) and binders were non-ionic polyvinyl alcohol (PVOH) and anionic styrene acrylate (SA) latex. Additionally, surface treatment, by applying a cationic polymer (polyDADMAC), was used to study the effect of surface charge on the ink penetration and the resulting print quality. The absorption/adsorption of ink colorant was studied with UV–VIS spectroscopy to evaluate the absorbance resulting from ink dye mixed with model coating structure suspensions, which were prepared by grinding, sieving and suspending in aqueous dispersion. The results showed that addition of PVOH into a coating formulation based on anionically dispersed coating pigment increased the colorant absorption/adsorption. The PVOH supports interpolymer diffusion of the polar ink vehicle, which opens the polymer matrix so that the colorant can transfer into the binder network and remain there. Additionally, providing an opposite charge between the coating and inkjet ink is well known to act to bind the colorant most effectively. When applied to paper, the use of a cationic additive application specifically to the coating layer surface slowed down the ink penetration into the paper structure, by reducing coating permeability, and bound the anionic colorant at the top layer by charge interaction, so that reduced bleeding and improved water fastness could be achieved.

© 2011 Elsevier B.V. All rights reserved.

1. Introduction

There are many different kinds of inkjet inks used in the field across the range of inkjet presses, including both aqueous and solvent-based vehicles, adopting dye and/or pigment colorant. In home and office printers, as well as the first generations of high-speed presses, anionic aqueous-based dyes are commonly used. This means that, to enable the effective fixing of colorant into the top part of a coating layer, it requires a coating which has an opposite ionic charge than that of the ink colorant. In the case of anionic ink, a cationic charge is needed, and it is usually provided by adding a cationic poly(diallyl dimethyl ammonium chloride) (polyDAD-MAC) into the coating color [1–5]. Other cationic additives have also been used [6,7], and the role of cationic binder, for example cationic starch, has also been considered [8,9]. The cationic additive application to the top of the coating layer has been studied by Nguyen et al. [10]. The opposite ionic charges mean that the colorant can fix to the coating structure by ionic interactions, by means of long range electrostatic forces (Coulombic attraction).

Kallio et al. [11] studied the adsorption of disazo (Food Black 2) dye onto coating pigments, which did not have dispersant, from polar liquids, such as water (distilled), ethanol, acetone and ethylene glycol, and non-polar cyclohexane. They noticed that the electrostatic interactions are the predominating driving force for the colorant adsorption to kaolin, precipitated calcium carbonate, amorphous SiO_2, TiO_2 and Al_2O_3. In the case of hydrophobic talc, the driving force is hydrophobic interaction. The studied pigments had both acidic and basic surface groups. However, the presence of polar liquid reduced the influence of Lewis acid–base

* Corresponding author. Tel.: +358 40 578 1479; fax: +358 20 722 7604.
E-mail addresses: taina.lamminmaki@vtt.fi (T.T. Lamminmäki), john.kettle@vtt.fi (J.P. Kettle), patrick.gane@aalto.fi, patrick.gane@omya.com (P.A.C. Gane).
[1] Tel.: +358 40 593 6013; fax: +358 20 722 7026.
[2] Tel.: +41 62 789 2422; fax: +41 62 789 2410.

interactions. It seems that the adsorption was prevented by the competitive adsorption of polar liquid molecules. Hartus [12] studied the adsorption phenomena with paper fibres and pigments and noticed that the fibres (eucalyptus, deinked pulp (newsprint), softwood sulphate pulp, birch sulphate pulp and TMP) adsorbed diazo type dyes (Food Black and Fast Black) less than the pigments (precipitated calcium carbonate, Kaolin and Talc). The cationic starch had the highest absorption capability.

The surface chemistry of the coating layer affects the liquid and vapour water movement on the surface, for example, how the moisture hydrogen bonds to the surface. In the particular case of dispersed pigments the hygroscopy of the dispersant polymer layer needs to be considered as a dominant factor. As water moves in the porous structure, it itself influences the surface chemistry. The polarity increases with water content increase and this reflects the adhesion of polar components of ink, mottling and rub/abrasion resistance [13].

Donigian et al. [14] showed, furthermore, using thin layer chromatography that silica and precipitated calcium carbonate (PCC) coatings fix inkjet dyes by different mechanisms and the binding strength depends on the pigment type. Their study included coating colors having different amounts of fully hydrolyzed PVOH. The results showed further that the fluid holding capacity is different with these studied silica and PCC pigments. Silica pigments provide a high pore volume for ink and a large specific surface area on which the dye can fix during the ink imbibition. The silica absorbs both diluent/solvent and dye, whereas PCC anchors the dye on the pigment surface while the diluent/solvent penetrates deeper into the coating or base paper [8,14,15]. The binder addition in the coating color can play a role in dye adsorption. The addition of cationic additive in the pigment slurry was shown to retard dye migration in the resulting coating structure.

The objective of this work was to clarify how the ionic charge of the pigment coating structure system combined with either non-ionic polyvinyl alcohol or anionic styrene acrylate latex coating binder influences anionic dye-based inkjet ink absorption and adsorption. The absorption and/or adsorption of the ink colorant by each coating component was studied using UV–VIS spectrometry, by monitoring the change in absorbance when ink is mixed with an aqueous suspension of previously ground dried coating. The study also considered how a cationic additive on the coating layer surface, when applied to paper, affects the dye and vehicle distribution. The connection to the final print quality was explored by printing with a desktop printer (dye-based inks).

2. Materials and methods

In the first part of our study, we determined the sorption of ink dye into fine particulate "mini-structures" of coating. The pigments used to form the coating layers in this case were either modified calcium carbonate (MCC, OMYAJET B6606[3]) or epoxy silane colloidal silica (silica, Bindzil CC 40[4]). The silica was not designed for application in inkjet, but we wanted to have a coating pigment that would not adsorb charged ink dye itself and so could permit a study directly of the action of PVOH addition. The MCC was in the form of a dry pigment powder, and the hydrophobicsed silica pigment was dispersed as slurry by the pigment supplier using an ionic wetting agent/surfactant having an anionic charge (Table 1). This silica was used to provide an inert surface to dye, but that the surfactant present to provide dispersion in water, being anionic, may display some residual attraction for cationic dye. The MCC had a weight median particle diameter of 2.70 μm ($d_{50\%}$) and silica 12 nm. The

specific surface area (BET, ISO 9277) of MCC was 46 m^2 g^{-1} whereas with silica it was 220 m^2 g^{-1}. Polysalz S[5], sodium polyacrylate, was used as an anionic dispersing agent. Cationicity, when required, was provided by the cationising agent poly(diallyl dimethyl ammonium chloride) (polyDADMAC, Cartafix VXU[6]). The amount of agent used for providing the chosen charge was 0.5 pph. The binder was either non-ionic polyvinyl alcohol (PVOH, Mowiol 40-88[7]) or anionically stabilised styrene acrylate latex (SA, CHP 212[5]). In this work, each pigment with a given dispersing agent or pigment with dispersing agent and a chosen binder is referred to as the respective "coating structure system". In the case of MCC pigment, the coating color contained 7 pph of binder, and in the silica case it was 15 pph to provide sufficient binding power due to the higher surface area.

The ink was formulated by ourselves, to be sure that it contained only one colorant. The ink contained 5 wt% anionic colorant (Basacid Blue 762, Cu phthalocyanine), 5 wt% polyethylene glycol (PEG 200), 5 wt% diethene glycol, 0.3 wt% Surfynol 465[8] (surface active agent) and the rest being water. The surface tension of the ink was determined to be 49.5 mN m^{-1} (23 °C) using a Bubble Pressure Analyser KSV BPA800[9] tensiometer.

The anionic dye-based ink sorption (in the case of PVOH there exists both absorption and adsorption) as studied with a PerkinElmer UV/VIS/NIR spectrometer (Lambda 900[10]). The ultraviolet–visible (UV–VIS) spectroscopy has been utilized in the study of adsorption by Shi et al. [6] and Backfolk et al. [16], but they concentrated on the sorption of inks with different salt-addition to the pigment surfaces, not how the addition of binder on the pigment particle surface affects the UV absorbance of inkjet ink colorant. The UV–VIS spectroscopy quantified the relation of the intensity of incident, I_0, and transmitted, I, radiation as a function of wavelength in the ultraviolet–visible spectral region. The idea was that the inkjet ink colorant ab/adsorbs in respect to the coating structure system during their mixing as ink is distributed amongst aqueous suspended pre-ground dried coating, and we can detect this as a change of colorant absorbance in the liquid phase with the UV–VIS.

Fig. 1 introduces the sample preparation and analysis procedure that we used. Coating color formulations were first formed into layers. The layers of studied pigment with different dispersing agents and/or different binders were produced in Teflon®[11] moulds by letting the slurry dry at room temperature (23 °C). This meant that all components of coating colors remained in the coating layer structure after drying. The dried coating layer was then ground for 2 min with a homogenizing mill (Retsch MM301 Mixer mill), adopting three grinding balls with diameter of 1 cm and at a rotation frequency of 30 s^{-1}. By grinding the pigment coating structure systems we wanted to avoid the extended pore network structure effect present in coating cakes or layers, which normally acts to limit accessibility to the constituent surfaces over time in respect to permeation, thus enabling the structure surface-related phenomena to be isolated. We assumed that the grinding effect was similar for each coating layer, and that this subsequent sample treatment was assumed to provide a sufficiently homogeneous distribution of structural components despite the potential for some soluble species migration during drying. The grinding of the pigment coating systems might also expose new surfaces of the pigment that

---

Table 1
The studied MCC and silica coating structure systems. Zeta-potential was measured with AcoustoSizer II[a].

Coating structure system	Dispersing agent, amount	Binder, amount	Zeta-potential, mV
MCC powder in water	–	–	21
Anionic MCC	Sodium polyacrylate, 0.5 pph	–	−37
Anionic MCC + 7 pph PVOH	Sodium polyacrylate, 0.5 pph	PVOH, 7 pph	−12
Anionic MCC + 7 pph SA	Sodium polyacrylate, 0.5 pph	SA latex, 7 pph	−37
Cationic MCC	polyDADMAC, 0.5 pph	–	24
Cationic MCC + 7 pph PVOH	polyDADMAC, 0.5 pph	PVOH, 7 pph	11
Silica	N/A	–	−22
Silica + 15 pph PVOH	N/A	PVOH, 7 pph	−19

[a] AcoustoSizer II is a product name of Colloidal Dynamics/Agilent, Technologies (Finland Oy), Linnoitustie 2B, FI-02600 Espoo, Finland.
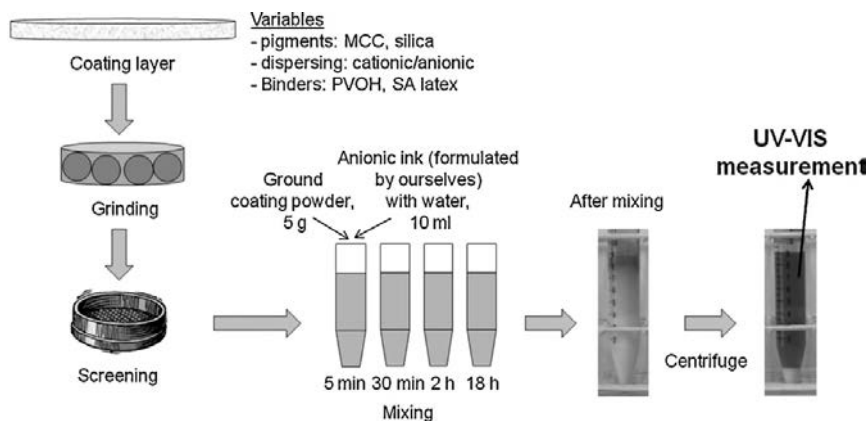
Fig. 1. The treatment of coating structure before UV–vis analysis in the UV absorbance study.

would otherwise be covered with binder polymer, or break the binder films, which in the porous coating system would have been unavailable for the colorant. However, given the relative low energy of homogenizing, this is expected to be minimal. The ground powder was screened through a 300 μm slit screen, to ensure that the coating powders did not contain inhomogeneous lumps and that the particles of the resulting coating "mini-structures" were as monosize as possible.

The anionic formulated ink was diluted with water (7 cm³ ink per dm³ water, the original ink contained 5 wt% dye colorant). 10 cm³ diluted ink was mixed with 5 g of the produced coating structure system powder, to produce a suspension of the powder particles in the diluted ink. The mixing was continued for a series of such samples over selected times (5 min, 30 min, 2 h and 18 h). Each mixture was centrifuged and the remaining dye concentration in the filtrate was analyzed in the UV–VIS spectrophotometer. The experiments were carried out at room temperature ($23 \pm 2\,°C$).

In the other part of this study, the connection between cationic charge of the paper coating surface, as it appears on the paper itself, and the print quality was assessed by surface application of polyDADMAC (Cartafix VXU[6]) with an Erichsen[12] film applicator (Model 288) followed by drying in an oven at 105 °C for 5 min. The applied polyDADMAC amount was 2.0–3.2 g m⁻². The polyDADMAC was applied on the same double-coated fine papers (pre-coating 7 g m⁻² and 8 g m⁻² top-coating, base paper 67 g m⁻²) as reported by Lamminmäki et al. [17]. The top-coating of double-coated paper contained 100 pph inkjet PCC (OMYAJET B5260[3]) and either PVOH (Mowiol 40-88[7]) or SA latex (Latexia 212 provided by

Table 2
The recipes and properties of top-coating colors.

Component	Coating color			
	7 pph PVOH	30 pph PVOH	7 pph SA	30 pph SA
Inkjet PCC	100	100	100	100
PVOH	7	30	–	–
SA	–	–	7	30
Polysalz S	–	–	6	6
Measured values				
Solids content, %	25.1	22.2	28.1	30.9
Zeta-potential[a], mV	2.4	2.6	−37.0	−32.8
pH	8.4	8.4	8.5	7.9

[a] Measured with AcoustoSizer II.

Ciba Specialty Chemicals[13]). The formulation of the top-coatings is shown in Table 2. The zeta-potentials of the coating colors were measured with an AcoustoSizer II by using a dilution ration of 1:1000 (de-ionized water). The pre-coating had 100 pph of ground calcium carbonate with a narrow particle size distribution having 60 wt% < 1 μm (Covercarb 60[3]), 12 pph styrene-butadiene latex (DL966[14]) and 0.6 pph carboxymethylcellulose (Finnfix 10[15]).

The sorption properties of the surfaces of cationically treated, and the same coating without treatment, were analyzed with a capacitance-based Clara device, as previously described by Lamminmäki et al. [17] using water (de-ionized) and the same formulated cyan dye-based ink that was used in the UV–VIS analyses. As the liquid permeates the pore structure, so the capacitance of the dielectric coating structure changes. The temperature of water was

---

23 °C. Two different temperatures of the ink were studied, 23 °C and 40 °C, to establish any effect that might occur in commercial inkjet printing presses, which can operate at elevated temperatures (40 °C is typical for an ink in a Versamark® press, for example). An ink at higher temperature may have different viscosity, dynamic surface tension and drying speeds. In the Clara measurement, the applied amount of liquid in the chamber of the device was 5 cm³. The measurements were made after equilibration under a relative humidity of 50%RH and 23 °C temperature. The result is expressed as a curve of capacitance change during time as the liquid penetrates through the sample in the z-direction. The resulting curve is an average of five parallel measurements. The external pressure was 0.10 bar, which is the calculated pressure that the 15 pl size droplet having a speed of 15 m s⁻¹ (density 1000 kg m⁻³) creates at the paper surface as the droplet hits to the paper surface (used in a Versamark® press). The pressure was estimated by utilizing the common pressure, density and speed formula.

The without and with polyDADMAC addition samples were printed with an HP DeskJet 3940 desk-top inkjet printer using constant settings (the substrate was kept as "plain paper" and the print quality "normal"). The printing was carried out at room temperature 23 ± 2 °C. The print quality was evaluated by print density (GretagMacbeth D196) as well as ink bleeding in respect to line width and raggedness, analyzed with a QEA personal IAS[16] system. The observed line width is defined in relation to an original target line width, where the extra width has been caused by the spreading and/or mixing of the inks as measured by the gray values following the standard ISO 13660. The raggedness describes the uniformity of the line edge area.

A water fastness test was used as an indication of colorant fixing properties to the paper coating surface. The printed single-color compact area was immersed for 5 min into de-ionized (23 °C) water. After that the samples were left hanging to dry in the dark at 23 °C temperature and 50%RH moisture content overnight (at least 17 h). Similar methods have been used in other studies [18–20]. The color change ΔE^* was measured with a GretagMacbeth SpectroEye[17] spectrophotometer. In the spectrophotometer we used a configuration of 2° measuring angle, D65 illuminant, UV-filter on and the coated unprinted paper defined as a white area. CIELab^* values and print densities were measured before and after the water-treatment. ΔE^* was calculated following the standard equation of SCAN-P 89:03.

3. Results and discussion

3.1. Anionic colorant absorption/adsorption in the coating structures

The zeta-potentials of the studied coating formulations are introduced in Table 1. The highest anionic charge was seen for the coating color formulations having anionically dispersed MCC or anionic MCC with SA latex. The addition of polyvinyl alcohol seems to decrease the anionic charge, although the PVOH has a non-ionic nature. This suggests that the PVOH is associating with the charged species. The highest cationic charge was observed with the MCC pigment with cationic dispersing.

The value of the UV–VIS absorbance peak was detected at a wavelength of 610 nm (Fig. 2), where the sorption maximum of cyan dye was located (actually, the "orange" region). The maximum absorbance ($A = -\log(I/I_0)$) value of colorant at 610 nm was about

---

3.7. Repetitive trials showed that the values varied between ±0.2 from the average value.

We did not calculate the adsorption amount of dye per sample surface area as, for example, Shi et al. [6] did, because the target was to define the differences between the coating structure systems as they would appear during the wetting regime, i.e. the pigment with cationic/anionic dispersing and the pigment with different dispersing system combined with different binder type addition at the ambient moisture condition. This was because the specific surface area of each coating structure system, which would have been required to define specific adsorption, could not be measured reliably using the BET method under the condition of application, due to loss of structural moisture during the evacuation necessary for sample preparation. The calculated theoretical greatest dye amount that the coating structure system could adsorb in our method was 0.698 mg (dye) g⁻¹ (coating structure system), assuming that the color change in the liquid phase is caused solely by the colorant adsorption into the coating structure system and not the other components in the ink. The calculation is based on the information that the original dye contained 5 wt% of colorant and 7 cm³ of ink was mixed into 1 dm³ water. In the UV–VIS analysis, 10 cm³ of this diluted ink was mixed with 5 g of the respective coating structure system. However, it is very likely that the other components of ink move into the filtrate, too, but they have probably a very small influence in the measured color because they were effectively transparent components in the color region. The effect of cationic polyDADMAC fixing to the coating pigment was clarified by washing the pigment with 0.5 pph polyDADMAC repeatedly, each with 20 cm³ de-ionized water (per washing time).

Fig. 3 shows how the anionic ink adsorbed amongst the different coating structure systems as a function of time. The absorbance of the filtrate from the MCC pigment powder (as received from the pigment manufacturer) was increased from 2.3 to 2.9 during the increase of mixing time, indicating some loss of sorption with time. When 0.5 pph of anionic dispersing agent was added, the absorbance value of the extracted filtrate rose to the level of 3.1 meaning that dispersing agent prevented colorant adsorption especially at the shorter time, below 2 h. The addition of 7 pph PVOH in the anionic dispersed MCC decreased the absorbance values showing that it supported the sorption process. Similar effects of PVOH were detected with silica. On the other hand, the SA latex containing coating structure mix had very similar results to that of the anionic dispersed MCC containing structure. Latex had no effect on absorbance, suggesting that it plays an inert role in respect to dye interaction. When the MCC pigment was dispersed with the cationic dispersing agent, the absorbance results were clearly lower, confirming the strong adsorptive tendency.

Fig. 3 shows that addition of anionic dispersing agent increased the light absorbance of the anionic colorant in the filtrate from the MCC pigment powder-in-ink suspension. The increase of light absorbance means that a reduced amount of colorant has adsorbed within the pigment coating structure system and so more colorant stays in the liquid phase. The result indicates that the MCC pigment powder has a surface chemistry, for example dispersing agent, already before dispersion in the ink which could attract, to some extent the colorant, whereas the anionic dispersing agent in the pigment system makes the pigment less attractive for the anionic colorant. However, the MCC pigment had quite similar zeta-potential (measured from the mixture where MCC pigment powder was mixed into water) as that of the cationically dispersed MCC, but still the colorant sorption remained on a higher level as in the case of cationic MCC or cationic MCC with PVOH. This indicates that in the case of MCC powder the cationic groups are not as available as in the cationically dispersed MCC systems. They could, therefore, be either in the pigment intra-particle pore space, and thus harder for the ink colorant to fix there as the colorant might need first of
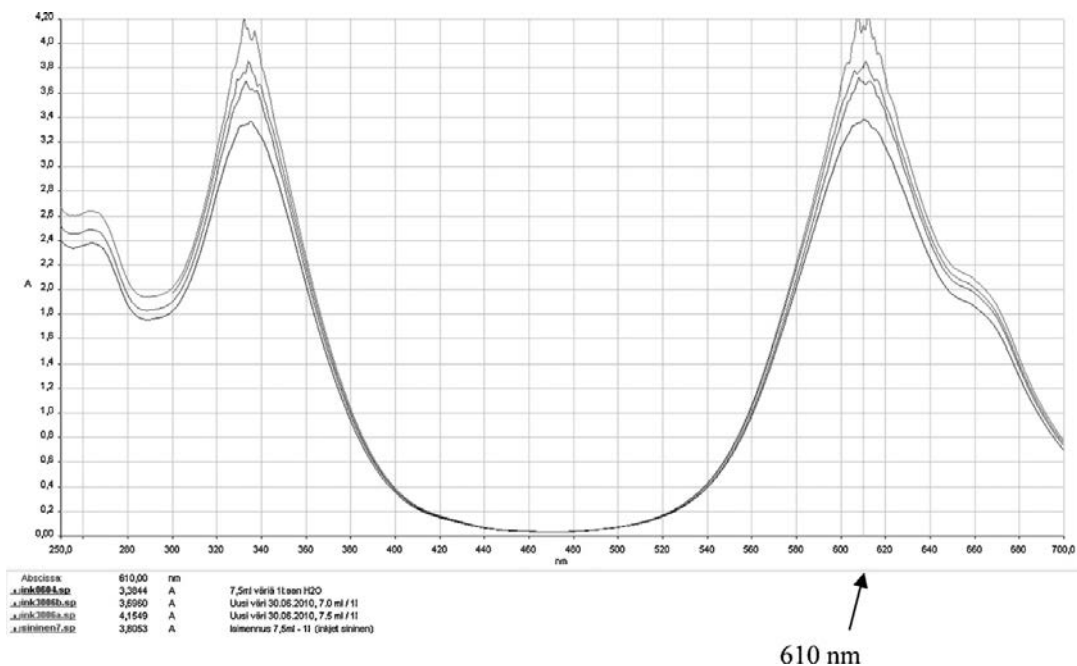
Fig. 2. An example of UV–vis result curves from different concentration of colorant dye.
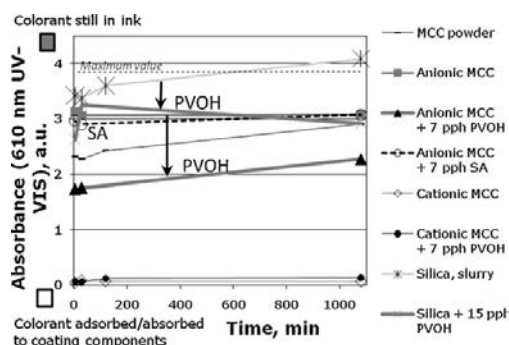

Fig. 3. The UV–vis light absorbance of liquid containing anionic cyan dye after the mixing procedure of different pigment systems. The absorbed liquid contained 7 cm³ ink which was diluted to 1 l water.
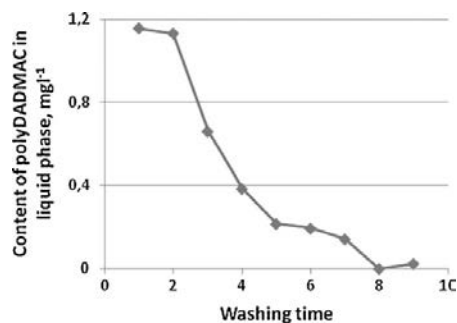

Fig. 4. The content of polyDADMAC in the filtrate after washing. At first, 5 g of pigment (dispersed with 0.5 pph of polyDADMAC) was mixed with de-ionized water (20 cm³) for 1 min, followed by transfer to a Büchner funnel and filtration. The filtrate was dried and the grammage was measured. After that a further 20 cm³ of water was added and the filtrate analyzed. The procedure of water addition was repeated eight times with analysis repeated after each dilution (call here washing). We assumed that the pigment remained on the filter paper (the filtrate was after each washing was transparent).

all to pass by anionically charged outer surfaces, or the cationic charge sites are distributed together with neighbouring anionic sites, which would act to repel the dye so making an approach to sorption sites also limited. In the case of cationically dispersed MCC the cationic additives and original cationic sites now locate all over the pigment surface and the anionic colorant can bind more easily without neighbouring charge repellancy.

Fig. 4 illustrates that not all the cationic polyDADMAC was fixed on the surface of MCC pigment. After the eight washings of the pigment coating structure system there was no further polyDADMAC extracted in the filtrate. This can indicate that during the inkjet ink imbibition in practice some excess may also be released away into the water phase. From the data in Fig. 4 it was possible to calculate that 15.7% of the originally added 24.9 mg g^{-1} was recovered during washing.

The addition of 7 pph PVOH in the anionically dispersed MCC pigment increased the colorant transfer into the pigment mixture (Fig. 3). A similar difference was noticed with the comparison of silica pigment and silica with PVOH. Both PVOH-containing coatings still had anionic charge, as the zeta-potential results indicated. The PVOH has non-ionic nature and so ionic interaction cannot explain the higher sorption. One explanation is that the diffusion of water molecules opens the PVOH polymer network so that the colorant can follow the water molecules into the amorphous part of the PVOH network and therefore this pigment coating structure system can take up more colorant. The colorant remains in the PVOH network (Fig. 5). However, when the added binder was anionic
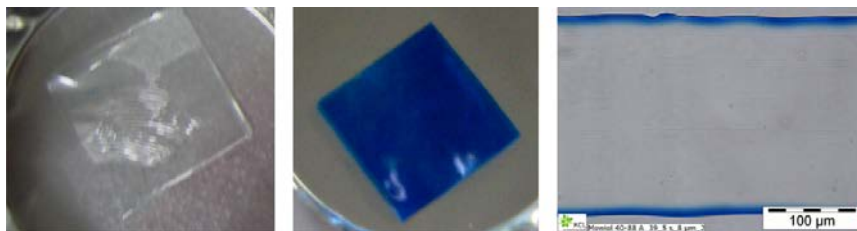
Fig. 5. The anionic colorant ink absorption is seen to occur into the PVOH film, but not into the SA latex film (thickness 205–260 µm): observation recorded after 5 s contact.

styrene acrylic latex the absorbance was very similar to the anionically dispersed MCC pigment. There are no opposite ionic charge groups which could bind the anionic colorant and the hydrophobic nature of SA latex prevents the diffusion of water molecules into the polymer network and so also the colorant diffusion into the binder polymer.

As the MCC pigment was dispersed with extra cationic dispersing agent and this pigment system was analyzed with UV–VIS spectrophotometer, the colorant sorption was clearly greater than in any anionic system and even in the original cationic pigment case. The UV–VIS results of additionally cationically dispersed MCC pigment after 2 h mixing time were on the level of 0.07 and the addition of 7 pph PVOH into this system increased it a little further to the level of 0.12. The addition of PVOH to the cationically dispersed MCC had a minimal effect on the results, and the added PVOH does not prevent the colorant sorption. The differences are not statistically significant. It seems that the cationic charge of the coating pigment system binds the anionic colorant effectively even in the lower zeta-potential area (11 mV) when the non-ionic PVOH polymer is either on the pigment surface, and/or within the intra-particle pores and/or distributed throughout the structure. This demonstrates the preferential action of Coulombic attraction over a distance rather than the contact-dependent diffusion into the binder polymer matrix. On the other hand, the water molecules diffuse into hydrophilic PVOH network and the colorant transfers into the polymer network in the same way as in the case of the anionic pigment coating structure system. The long mixing time did not significantly release the colorant from the pigment system, supporting the expected good water fastness.

The values of absorbance in Fig. 3 seem to increase somewhat in the cases of the anionic structures over time. The long time (18 h) of physical mixing releases some of the adsorbed colorant molecules back to the liquid. The non-permanence could be related to competitive adsorption between polyacrylate and the anionic dye. It may be assumed that simple addition of polyacrylate does not ensure complete adsorption within energetic mixing. Thus, the progressive adsorption of excess polyacrylate, its larger polymer structure displacing the dye competitively, could be responsible for dye release. The absorbance results of cationic structures, on the other hand, stayed very similar, also after the longest mixing time. The colorant has bound so fast to the pigment system that the long physical mixing time fails to release any more of the colorant.

The use of the organo silica, although not designed for inkjet application, allows us to assume that its surface is virtually inert in terms of charge-driven sorption – much like the polymer of the latex binder – and so makes an excellent control pigment for determining if there are any intrinsic charge properties of the MCC by means of comparison. The UV–VIS results of the filtrate extract from the mixes with anionically dispersed intrinsically hydrophobic silica pigment were on a higher level than the results of anionic MCC pigment, indicating that MCC pigment system adsorbed more ink colorant than the organo silica, even though the silica slurry had lower zeta-potential (less anionic, −22 mV) than MCC (−37 mV).

This indicates that the MCC pigment has some cationic components on the pigment surface that could attach the colorant molecules, which are clearly lacking in the case of the organo silica. The PVOH addition did not change the situation. In this case, there are also differences between the binder content. If we assume that binder forms a uniform layer on the pigment surface, we can calculate that the 15 pph PVOH addition could theoretically produce about 0.47 nm thickness of a uniform binder layer on the silica pigment surface, and the 7 pph PVOH on the MCC surface a 1.13 nm thick layer. In this calculation, we recall that the specific surface area of pigment was 220 m^2 g^{-1} for the silica and 46 m^2 g^{-1} for the MCC, and the specific gravity of PVOH was 1.26 g cm^{-3}. In the thicker PVOH layer, the swelling of binder permits the opening of the polymer network more. This kind of sorption difference in the results could be seen during the first 2 h. However, the binder content increase from 7 pph to 15 pph meant that the sorption properties of the coating layers were changed. In the case of the studied coatings, the sorption speed of the top-coatings applied on the precoated paper surface, as measured with drop penetration (CAM 200[9]) using a 6 µl water drop, decreased from 0.47 mm s$^{-0.5}$ to 0.17 mm s$^{-0.5}$, respectively. This can also have some effects on the studied formulation powders, especially for the larger particle size agglomerates or when soluble PVOH binder is itself adsorbed onto the coating pigment surfaces.

3.2. The effect on liquid ink penetration of cationic additive applied directly to the paper coating surface

The application of a few grams per square metre of polyDADMAC on the double-coated fine paper surface slowed down the speed of water and dye-based ink sorption into the structure (Fig. 6). The polymer acted to close up the surface layer, i.e. reduce permeability, so that it took more time for liquid to penetrate into the structure. The water produced the lowest capacitance values in the Clara equipment, then the anionic dye-containing ink at the temperature of 23 °C, and the quickest sorption was seen using the same ink at the higher temperature of 40 °C. Fig. 7 shows two examples of the variation of the Clara results.

Fig. 6 shows that cationic additive application on the anionic PCC coating, which had 7 pph of SA latex as a binder, has partially decreased the liquid penetration through the sample comparing to the penetration of the surface without the cationic additive. Clearly, the addition of polyDADMAC has dampened the capillary effect as the curve becomes monotonic. The difference exceeds the variations in the results. The 2.0–3.2 gm^{-2} polymer layer did not totally cover the coated paper surface, so that the liquid has possibilities to penetrate through "holes" into the structure. On the other hand, the ink vehicle can diffuse into the polymer layer, go through it and continue the penetration into the coating part of the structure by permeation flow. The polyDADMAC surface has a minimum at the 40 ms time. This could be the surface between the applied polymer and the coating layer. On the other hand, Fig. 4 shows that some of the polyDADMAC washed out from the MCC pigment coating
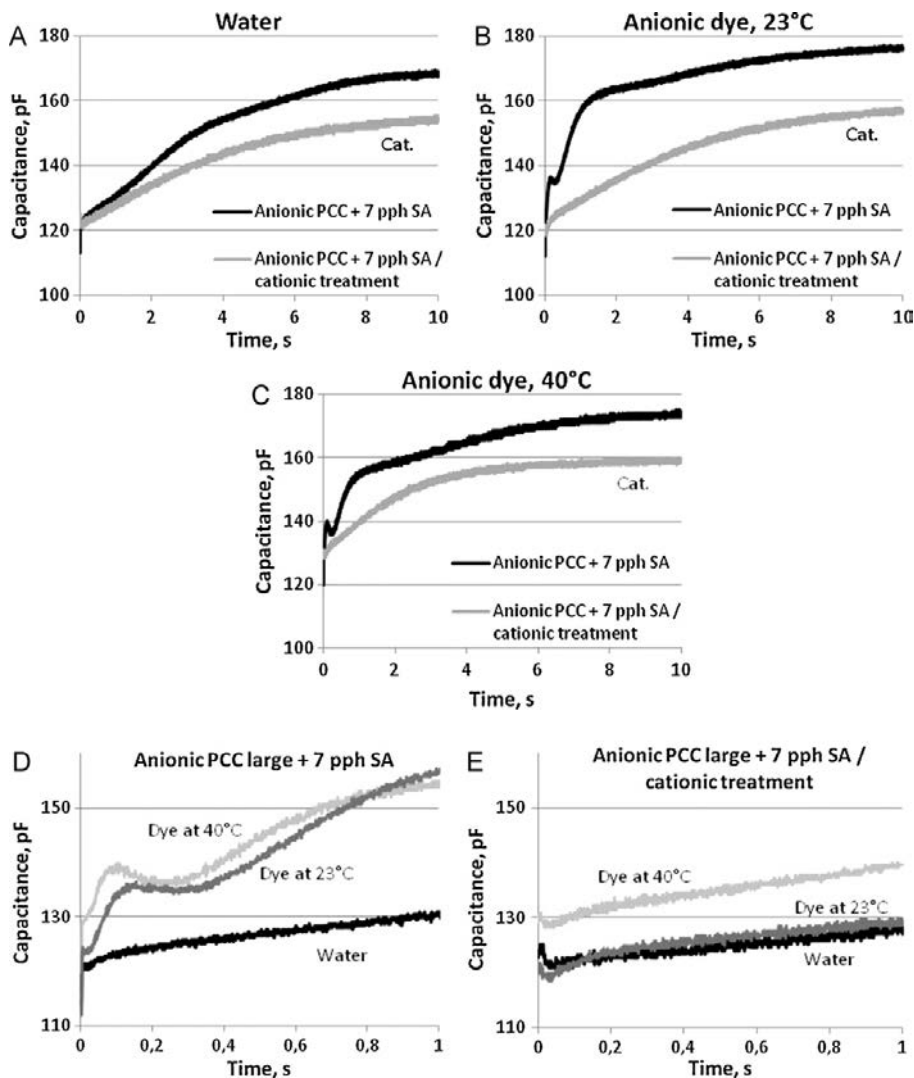
Fig. 6. The capacitance changes of a top-coated paper, having a top-coat of anionic PCC + 7 pph SA latex, and same surface with the added polyDADMAC (cationic) treatment plotted against the time. A, B, C – the liquids were water, anionic self-made cyan dye ink at 23 °C and the same ink at 40 °C, respectively. The penetration of water and dye-based inks (23 °C and 40 °C) into the anionic PCC coating (D) and polyDADMAC applied surface (E). The external pressure was 0.10 bar.

structure. Therefore, it is possible in this case of far excess polymer that some of the polymer transfers with ink vehicle into the coating layers and there affects the liquid penetration. The washing out can affect the properties of ink vehicle by increasing the viscosity, changing the surface tension or increasing the cationicity, and this could reflect in the location of local minimum. Additionally, the measurement method relies on the definition of capacitance under constant geometrical conditions, i.e. capacitance $C = \varepsilon A/d$, where ε is the dielectric constant and A and d are the geometrical parameters of planar area and sample thickness, respectively. Swelling of polymer dispersants and additives, as well as of the underlying fibrous matrix, clearly can affect the result strongly, especially in respect to increasing structural thickness.

The same 7 pph SA latex-containing coating layer was analyzed in our previous paper, Lamminmäki et al. [17], about two years ago.

In both measurement series, the same cyan dye-based commercial ink and same external pressure, 0.10 bar. The only difference was that the paper was stored for two years at a temperature 23 ± 2 °C and relative moisture content 50 ± 5 RH%. In the previous measurement, we did not notice a local minimum at 0.2–0.3 s. The reason behind this can be in the ageing of latex polymer and the weakening of fibre–fibre bonds.

Fig. 5 illustrates that the 40 °C ink penetrated quicker through the paper than the lower temperature ink. The velocity of particles and macromolecules depends on temperature, viscosity of the surrounding fluid and size of particle/macromolecule. The diffusional motion of macromolecules is greater with the 40 °C ink than with 23 °C ink. The ink imbibition is accelerated by use of a warmer ink, as viscosity also falls exponentially with temperature. Another advantage of using higher temperature ink is the possibility to speed up
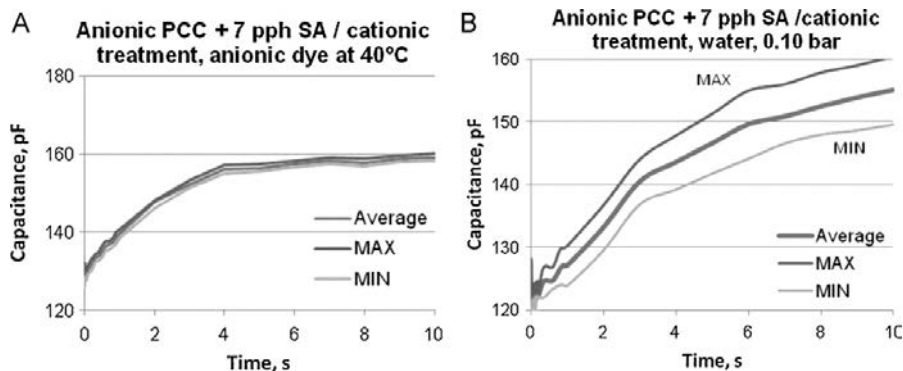
Fig. 7. The variation of the capacitance values of anionic PCC + 7 pph SA latex with the polyDADMAC (cationic) treated surface. External pressure was 0.10 bar and the liquid was anionic dye at 40 °C (A) and water (B).

the drying of the ink. In the real printing process, the ink amount is limited, and a warmer ink can start to evaporate/dry more quickly than a colder one. There may also be dependence of surface tension of the ink on temperature, especially if this is defined by surfactant action, which itself is diffusion dependent.

3.3. The effect of surface applied cationic additive on the inkjet print quality

The results of print densities are illustrated in Fig. 8. The pre-coating surface alone produced the lowest print density with both cyan and magenta dye-based ink because the colorant can penetrate through the pre-coating which is not designed for inkjet purpose (not enough pore volume, no suitable cationic charge). Otherwise, the print density results from the top-coated samples were on a high level, indicating that the applied ink amount was high and well distributed on and in the coating surface structure. On the anionic SA-containing coating, the cationic poly-DADMAC surface treatment produced a higher print density than the same coating layer without surface cationic additive (7 pph SA-containing coating). In the case of PVOH-containing coatings, the cationic additive application seems to decrease slightly the print density of cyan color, but the magenta surface remained similar. The higher amount of the soluble PVOH binder (30 pph) closed the coating layer structure. However, in this case there appeared places where the PVOH had formed film-like structures, as expected, but, in the middle of such localised film-like structures, a round hole was frequently observed. The colorant of the ink can penetrate through

this hole deeper into the coated paper, and therefore the print density became lower when using 30 pph PVOH than when using 7 pph PVOH despite the expected average decrease in permeability. The non-uniformity of the 30 pph PVOH coating was reflected also in the mottling values.

There are slight differences between the print densities of the cyan and magenta of cationic additive treated SA latex-containing surface and the same coating without cationic additive as well as on the 30 pph SA latex-containing coating layer. The difference behind these results can be the ionic charge contrast of dye and surface, but it is more likely that the printed surfaces have already so much dye-based ink that sufficient colorant remains on the top of the coating layer whatever the charge and the binder.

The bleeding was measured from the magenta line (Fig. 9), which was either printed as the first color laid on the paper surface (line spreading on the coating surface) or onto the pre-printed yellow surface (ink mixing). The magenta ink line width decreased as cationic additive was applied on the coated paper surface, both for the single color and the magenta on yellow cases. The cationic additive application did not decrease the raggedness of the magenta/yellow line, but the magenta line on the coated paper had less raggedness on the polyDADMAC treated surface than on the 7 pph SA-containing coating. However, the standard deviation of PCC + 7 pph SA with cationic additive was large indicating that there were some non-uniform areas in the polyDADMAC layer.

The results of line spreading and raggedness on the coating layer (Fig. 9: magenta/paper) show that cationic additive provides a narrower and sharper line than the anionic SA latex-containing coating. The opposite charge of the surface and ink (electrostatic forces) binds the anionic colorant effectively on the surface so that the colorant cannot spread in the x, y-direction of the surface although the polyDADMAC treated surface slowed the penetration of ink vehicle. Svanholm and Ström [21] showed that the addition of cationic additive into the coating color did not always diminish bleeding tendency of dye-based inkjet ink printed coatings. The cationic additive in the coating color does not necessarily locate in the top part of coating layer because, during the consolidation process, the additive can transfer deeper into the coating layer or even to the base paper, and so it cannot effectively take part in the fixing of colorant as it spreads on the surface. On the other hand, the porous properties of the coating layer affects the ink spreading by providing rapid sorption of the ink vehicle, and in the cationic additive containing coating layer the capillary and permeation flow competes more strongly with the ionic interactions than in the polyDADMAC surface treated coating layer. The only exception to the overall advantage of surface treating with cationic
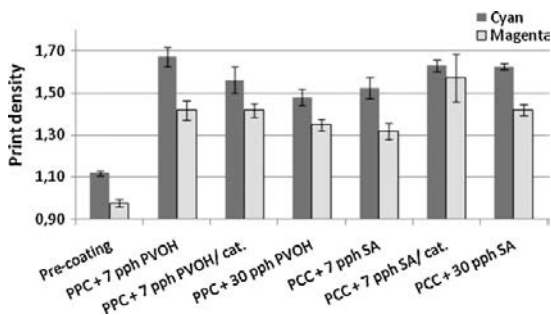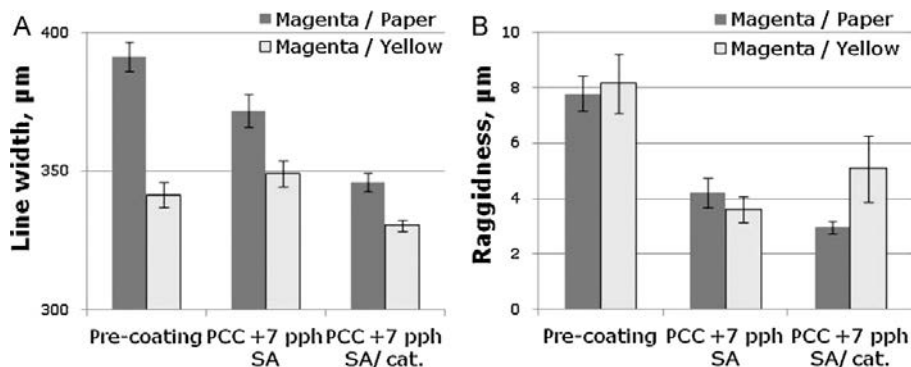

Fig. 8. Print density of cyan and magenta on the PCC coated surfaces and same surfaces, i.e. PVOH- versus SA latex-containing treated with cationic additive. Printed with HP DeskJet 3940 adopting dye-based inks.

Fig. 9. The line width (A) and raggedness (B) of magenta line on the plain coated paper surface and surface with yellow compact area. Printed with HP DeskJet 3940 adopting dye-based inks.

polymer could be detected with the magenta ink on the yellow surface, where the raggedness was higher with the cationically treated surface than with the SA containing coating. This clearly indicates that once the ink is isolated from the cationic layer by a previously applied color, and the sorption of ink vehicle is slowed by the presence of the polymer reducing the permeability, the dye can migrate more freely.

The water fastness (Fig. 10) was measured with print density changes and ΔE^* of 100% cyan surface after submersion in water. The print density difference between before and after water treatment was greater on the SA-containing surfaces than on the PVOH-containing surfaces. The water treatment of printed SA-containing coating releases the colorant out of the printed surface because there are no effective interactions between the colorant and the latex, whereas there is the diffusion absorption into the PVOH. The print density change was reduced by the cationic surface treatment of SA-containing coatings. The cationic additive application on the PVOH-containing coating, on the other hand, had quite minimal influence on the results of water fastness, indicating the adequate effect of PVOH alone. Similar trends could be noticed in the ΔE^* values. On the SA-containing coatings, the polyDADMAC treated surface produced the lowest ΔE^* value, and it had very similar results to those from the PVOH-containing coatings.

The water fastness results in Fig. 10 show that the cationic polyDADMAC treated SA-containing coating surface fixes the anionic colorant more permanently to the coating layer than the anionic SA latex-containing coating alone. The ionic interactions (electro-static Coulombic attraction) fix the colorant to the surface. The difference between the slightly cationic PVOH-containing coating and the cationic polyDADMAC surface treated PVOH-containing coating is small indicating that PVOH and polyDADMAC surface behaved very similarly in water fastness test and the cationicity does not bind anionic colorant there more effectively than polymer absorptive diffusion. The UV–VIS results, furthermore, showed that colorant can transfer into the PVOH-containing structure. The slightly cationic charge combining with the hydrophilic binder of the coating layer seems to be sufficient for an adequate inkjet ink colorant fixing, so that the colorant does not release out of the surface during the water fastness test used.

4. Conclusions

The sorption studies with the anionic dye-based ink and different coating component systems using UV–VIS spectrometry confirm that a cationic coating surface adsorbs anionic dye colorant more effectively than an anionic, as expected. The addition of 7 pph PVOH to an anionically dispersed pigment increases the sorption of colorant phase, whereas 7 pph SA latex has no effect on sorption. This indicates that colorant can absorb into the polyvinyl alcohol polymer network, even in the case when the polymer has not formed a uniform layer on the coating pigment surface, whereas it cannot undergo sorption in the SA polymer latex case.

The use of an ionically surface-inert organo silica pigment enabled a comparison to be made with an ionically surface-
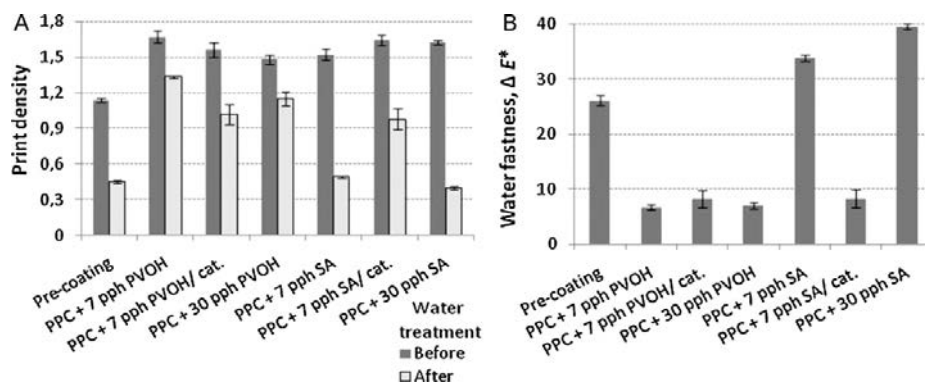
Fig. 10. The water fastness of surfaces: print density (A) and ΔE^* (B) of a 100% cyan print before and after water treatment. Printed with HP DeskJet 3940, adopting dye-based inks.

interactive modified calcium carbonate (MCC). Little to no adsorption of dye occurred in the case of the ionically surface-inert organo silica. In contrast, the limited sorption of anionic dye onto directly suspended MCC, however, indicated that the surface contained either shielded cationic sites or more likely a mixture of anionic and cationic sites, with probable nearest neighbour charge hindrance of anionic dye adsorption. Further studies of this phenomenon could reveal more precisely the charge distribution nature of the MCC surface by using selective charge interactive species.

The surface application of cationic polyDADMAC onto anionic coating layers slows down ink vehicle sorption but nonetheless reduces color spreading, due to the capture of anionic dye by the cationised surface. The opposite charge of the coating components and dye molecules binds the colorant most effectively to the top part of coating layer, producing less bleeding and improved water fastness. Ink-on-ink printing, however, acts to isolate the second laid-down ink from the surface coating charge, and combined with the reduced sorption speed of the ink vehicle, this leads to a deterioration of color-to-color bleed. Increasing the temperature of the dye ink was seen to speed up the penetration.

References

[1] G. Morea-Swift, H. Jones, The use of synthetic silicas in coated media for ink-jet printing, in: Tappi Coating Conference and Trade Fair, Washington, DC, USA, Tappi Press, Atlanta GA, USA, 1–4 May, 2000, pp. 317–328.
[2] K. Vikman, T. Vuorinen, (a): Light fastness of ink jet prints on modified conventional coatings, Nordic Pulp and Paper Research Journal 19 (4) (2004) 481–488.
[3] P.B. Malla, S. Devisetti, Novel kaolin pigment for high solids ink jet coatings, Paper Technology 46 (8) (2005) 17–27.
[4] E. Svanholm, Printability and Ink-Coating Interactions in Inkjet Printing, Doctoral thesis, Karlstad University, Faculty of Technology and Science, Chemical Engineering, 2007, 2, Karldstad 2007, 48.
[5] H.L. Lee, J.W. Jang, S.G. Lee, Role of cationic additives and binders on color development in ink jet printing, in: 61st Appita Annual Conference and Exhibition, Gold Coast, Australia, 6–9 May, 2007, p. 7 p.
[6] J. Shi, T.P. Schuman, J.O. Stoffer, Ink-jet printing paper with improved water-fastness, Journal of Coating Technology Research 1 (3) (2004) 225–234.
[7] J. Sreekumar, M. Sain, R. Farnood, W. Dougherty, Influence of styrene maleic anhydride imide on ink-jet print quality and coating structure, Nordic Pulp and Paper Research Journal 22 (3) (2007) 307–313.
[8] D. Glittenberg, A. Voigt, Economic formulations for improved quality ink-jet papers, Paper Technology 42 (9) (2001) 25–29.
[9] M.S. Saraiva, J.A.F. Gamelas, A.P. Mendes de Sousa, B.M. Reis, J.L. Amaral, P.J. Ferreira, A new approach for the modification of paper surface properties using polyoxometalates, Materials 3 (1) (2010) 201–215, Available at: www.mdpi.com/journal/materials.
[10] K.C. Nguyen, C.N. Ke, R.J. Adamic, S. Ganapathiappan, Preparation of permanent color inks from water-soluble colorants using specific phosphonium salts, U.S. Patent 6,248,161B, June 19, 2001.
[11] T. Kallio, J. Kekkonen, P. Stenius, Acid/base properties and adsorption of an azo dye on coating pigments, Journal of Dispersion Science and Technology 27 (2006) 825–834.
[12] T. Hartus, Adsorption and desorption behaviour of ink jet dye on paper, Graphic Arts in Finland 27 (3) (1998) 3–9.
[13] P.A.C. Gane, C.J. Ridgway, Moisture pickup in calcium carbonate coating structure: role of surface and pore structure geometry, in: Tappi 10th Advanced Coating Fundamentals Symposium, Montreal, Canada, Tappi press, Atlanta, GA, USA, 11–13 June, 2008, p. 24.
[14] D.W. Donigian, P.C. Wernett, M.G. McFadden, J.J. McKay, Ink jet dye fixation and coating pigments, in: Tappi Coating/Papermakers Conference, New Orleans, LA, USA, 4–6 May, 1998, pp. 393–412.
[15] D. Glittenberg, A. Voigt, D. Donigian, Neuartige Pigment-Stärke-Kombination zum Online- und Offline-Streichen höherwertiger Inkjet-Papiere, Wochenblatt für Papierfabrikation 130 (19) (2002) 1279–1285.
[16] K. Backfolk, J.B. Rosenholm, J. Husband, D. Eklund, The influence of surface chemical properties of kaolin surfaces on the adsorption of poly(vinyl alcohol), Colloids and Surfaces A: Physicochemical and Engineering Aspects 275 (2006) 133–141.
[17] T. Lamminmäki, J. Kettle, P. Puukko, J. Ketoja, P. Gane, The role of binder type in determining inkjet print quality, Nordic Pulp and Paper Research Journal 25 (3) (2010) 380–390.
[18] R.Y. Ryu, R.D. Gilbert, S.A. Khan, Influence of cationic additives on the rheological, optical and printing properties of ink jet coatings, Tappi Journal 82 (11) (1999) 128–134.
[19] K Khoultchaev, T. Graczyk, Influence of polymer–polymer interaction on properties of ink jet coatings, Journal of Imaging Science and Technology 45 (1) (2001) 16–23.
[20] K. Vikman, T. Vuorinen, (b): Water fastness if ink jet prints on modified conventional coatings, Journal of Imaging Science and Technology 48 (2) (2004) 138–147.
[21] E. Svanholm, G. Ström, Influence of polyvinyl alcohol on inkjet printability, in: Tappi International Printing and Graphic Arts Conference, Vancouver, Canada, 4–6 October, 2004, pp. 187–209.

Title	**The comparative dynamics of bulk liquid flow and interpolymer diffusion during inkjet ink imbibition in porous coating structures**
Author(s)	Taina Lamminmäki
Abstract	The focus of this thesis is to establish the timescale of interactions, physical and chemical, during dye-based inkjet ink imbibition into calcium carbonate ($CaCO_3$) pigmented coatings. Comparison is made between conventional offset quality $CaCO_3$, and special inkjet qualities in the form of either modified or precipitated $CaCO_3$ combined with swelling diffusion driving or non-swelling diffusion-inert binder. The selection of pigment is based on the control of pore volume, pore size distribution and connectivity of the coating layer. Pigments with nano-size pores (intra-particle) are primarily exemplified. The final coating layers display discrete pore size bimodality in relation to the intra-particle and inter-particle pores. Polyvinyl alcohol (PVOH) is used as the diffusion sensitive binder and styrene acrylate latex (SA) as the bulk diffusion-inert binder. By changing the coating structures and using the contrasting binders, the roles of liquid diffusion, capillary pressure and permeation flow are clarified both in the short and long timescale imbibition. The wetting force within the finest capillaries drives the ink into the porous structure, whilst the viscous drag within the structure resists the movement. The nano-size capillaries initiate absorption of the ink vehicle, though typical impact pressure of an inkjet droplet is shown to provide forced wetting. During the flow, the hydrophilic binder swells, acting to close the smallest pores and reduce the remaining pore diameters. The total pore volume decrease competes with the initial capillarity. The diffusion is shown to have a marked effect on the polar liquid absorption rate into the PVOH-containing coatings over different timescales. The swelling opens the polymer matrix so that the colorant fits into the binder structure and can either hydrogen bond or become mechanically trapped. The diffusion coefficient of water in PVOH and on SA latex films is shown to be similar, despite the difference in geometry. Colorant fixing is enhanced mainly by the ionic interaction between the colorant and surface, and there is an optimal rate beyond which the colorant has insufficient time to translate under the Coulombic attraction toward the cationic adsorption sites or to respond to the binder matrix diffusion potential. The competing mechanisms of liquid flow and ab/adsorption are seen as crucial to developing a high quality print. High speed inkjet print density depends on the colorant location in the structure and the optical properties of the whole coated paper. Intercolour bleeding is also dependent on the coating absorption capacity at an adequately high rate in competition with colorant spreading.
ISBN, ISSN	
Date	March 2012
Language	English, Finnish abstract
Pages	187 p. + app 89 p.
Name of the project	
Commissioned by	
Keywords	Diffusion, absorption, permeability, porosity, ionic charge, coating binder, coating, inkjet printing
Publisher	

Nimeke	**Liuoksen virtausdynamiikka ja polymeerien diffuusio mustesuihkuvärin asettumisessa huokoisiin päällysterakenteisiin**
Tekijä(t)	Taina Lamminmäki
Tiivistelmä	Tämän väitöskirjan tavoitteena on selvittää liukoisen inkjet-värin asettumisessa vallitsevien vuorovaikutusten, sekä fyysisten että kemiallisten, aikaskaaloja kalsiumkarbonaattipigmenttipäällysteissä ($CaCO_3$). Pigmentteinä on käytetty sekä perinteistä offset-laadun että erityisiä inkjet-laadun $CaCO_3$-pigmenttejä, jotka ovat joko modifioituja tai saostettuja $CaCO_3$-pigmenttejä ja näihin on yhdistetty turpoava, diffundoiva tai ei-turpoava, diffundoimaton sideaine. Pigmentit on valittu siten, että päällysteisiin saadaan erilaisia huokostilavuuksien ja -kokojakaumien rakenteita. Inkjet-päällysteissä käytetään usein pigmenttejä, joissa itse pigmenttipartikkelissa on nanokoon huokosia (sisäisiä huokosia). Lopullisessa päällystekerroksessa on sekä pigmentin sisäisiä että ulkoisia huokosia. Polyvinyylialkoholia (PVOH) käytetään työssä diffuusioherkkänä sideaineena ja styreeni-akrylaatti-lateksia (SA) diffundoimattomana sideaineena. Päällysteen diffuusion, kapillaari- ja permeaatiovirtauksen merkityksiä lyhyen ja pitkän aikajakson värin asettumisessa selvitetään käyttämällä erilaisia päällysterakenteita ja sideaineita. Pienimpien kapillaarien kastumisvoimat ajavat värin huokoiseen rakenteeseen, kun taas viskoottiset hidastusvoimat rakenteessa vastustavat nesteen liikettä. Nanokoon kapillaarit käynnistävät värin liuotinosan absorption, kun taas inkjet-pisaran iskeytymisen aikaansaama voima lisää kastelevuutta. Virtauksen aikana hydrofiilinen sideaine turpoaa sulkien pienimpiä huokosia ja pienentäen huokosten halkaisijoita. Koko huokostilavuuden pieneneminen kilpailee alkuperäisen kapillaarisuuden kanssa. Työssä osoitetaan, että diffuusiolla on merkittävä vaikutus polaarisen nesteen absorptionopeuteen PVOH-sisältävissä päällysteissä eri ajanhetkinä. Lisäksi turpoaminen avaa polymerimatriisia niin, että värin väriaine mahtuu sideaineen rakenteen sisään ja joko muodostaa vetysidoksia tai jäädä rakenteeseen värin kuivuttua. PVOH- tai SA-lateksi-filmin veden diffuusiokerroin on samaa suuruusluokkaa, tosin polymeerien diffuusiotyypit ovat erit (massa- ja pintadiffuusio). Ioniset vuorovaikutukset väriaineen ja pinnan välillä vaikuttavat väriaineen kiinnittymiseen. Väriaineen kiinnittymiselle on löydettävissä optimaalinen absorptionopeus, jossa väriaineelle jää riittävästi aikaa sitoutua Coulombisilla attraktiovoimilla ja kationisilla vuorovaikutuksilla tai siirtyä diffuusiolla sideainematriisiin. Hyvä painojälki saadaan vain, jos päällysterakenteeseen syntyy värin virtausta sekä absorptiota ja adsorptiota. Korkeanopeuksisen mustesuihkukutulostuksen painojäljen densiteetti riippuu väriaineen lopullisesta sijainnista rakenteessa sekä koko päällystetyn paperin optisista ominaisuuksista. Eri värien sekoittuminen keskenään (bleeding) riippuu päällysteen absorbtionopeudesta ja siitä, miten värit leviävät päällysteen pinnalla.
ISBN, ISSN	
Julkaisuaika	Maaliskuu 2012
Kieli	Suomi, englanninkielinen tiivistelmä
Sivumäärä	187 s. + liitt. 89 s.
Projektin nimi	
Toimeksiantajat	
Avainsanat	Diffusion, absorption, permeability, porosity, ionic charge, coating binder, coating, inkjet printing
Julkaisija	

The comparative dynamics of bulk liquid flow and interpolymer diffusion during inkjet ink imbibition in porous coating structures

The focus of this thesis is to establish the timescale of interactions, physical and chemical, during dye-based inkjet ink imbibition into calcium carbonate ($CaCO_3$) pigmented coatings. Comparison is made between conventional offset quality $CaCO_3$, and special inkjet qualities in the form of either modified or precipitated $CaCO_3$ combined with swelling diffusion driving or non-swelling diffusion-inert binder. Polyvinyl alcohol (PVOH) is used as the diffusion sensitive binder and styrene acrylate latex (SA) as the bulk diffusion-inert binder. The nano-size capillaries initiate absorption of the ink vehicle, though typical impact pressure of an inkjet droplet is shown to provide forced wetting. During the flow, the hydrophilic binder swells, acting to close the smallest pores and reduce the remaining pore diameters. The total pore volume decrease competes with the initial capillarity. The diffusion is shown to have a marked effect on the polar liquid absorption rate into the PVOH-containing coatings over different timescales. The swelling opens the polymer matrix so that the colorant fits into the binder structure and can either hydrogen bond or become mechanically trapped. The diffusion coefficient of water in PVOH and on SA latex films is shown to be similar, despite the difference in geometry. The competing mechanisms of liquid flow and ab/adsorption are seen as crucial to developing a high quality print. High speed inkjet print density depends on the colorant location in the structure and the optical properties of the whole coated paper.